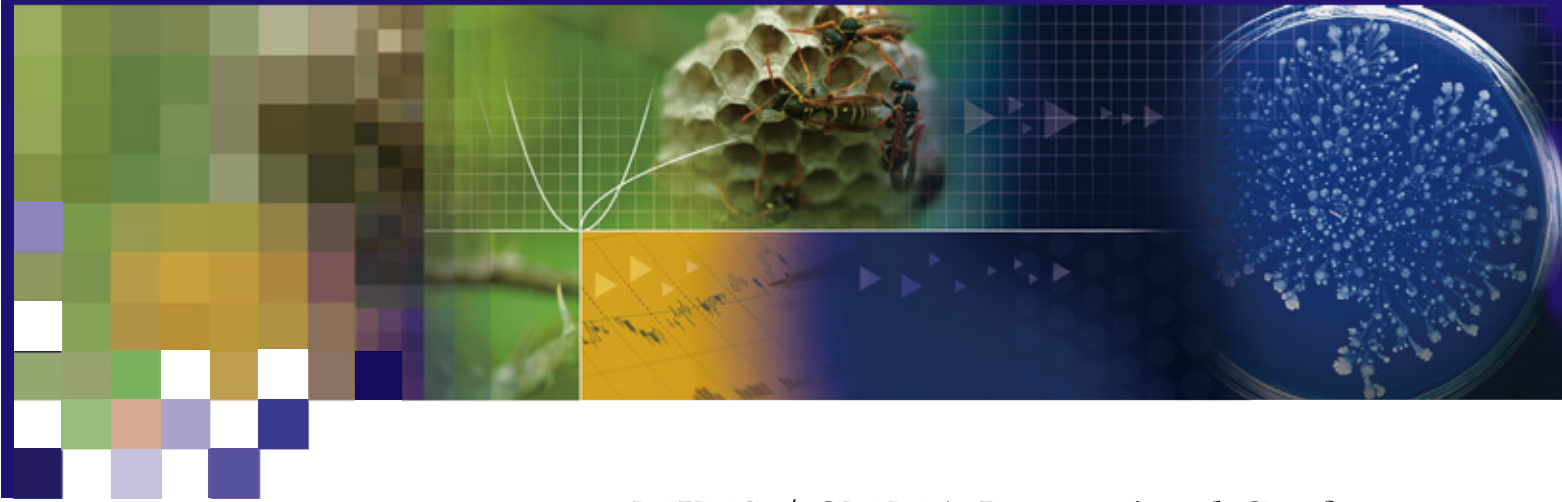


# Lecture Note Series

in Mathematical Sciences  
Based on Modeling and Analysis



ICMMA 2024 MIMS / CMMA International Conference on  
"Self-organization in Life and Matter"





## Lecture Note Series

2024 MIMS / CMMA International Conference on  
"Self-organization in Life and Matter"  
(ICMMA 2024)

©Copyright 2024 Meiji University, All rights reserved.  
Meiji University,  
1-1 Kanda-Surugadai, Chiyoda-ku, Tokyo 101-8301, Japan

Supported by:  
Meiji Institute for Advanced Study of Mathematical Sciences (MIMS),  
Center for Mathematical Modeling and Applications, Meiji University(CMMA)

Meiji Institute for Advanced Study of Mathematical Sciences (MIMS)  
8F High-Rise Wing, Nakano Campus, Meiji University,  
4-21-1 Nakano, Nakanoku, Tokyo, Japan, 164-8525

## Organizing Committee of ICMMA 2024

Chair: Nobuhiko J. Suematsu (Meiji University)  
Members: Takahiro Nakamura (Meiji University)  
Kota Ikeda (Meiji University)  
Hiraku Nishimori (Meiji University)  
Ken-Ichi Nakamura (Meiji University)  
Masashi Shiraishi (Meiji University)





# ICMMA 2024

**International Conference  
on  
Self-organization in  
Life and Matter**

**9th - 11th September, 2024**

**Nakano Campus, Meiji University**





## Preface

The International Conference on “Self-Organization in Life and Matter” was part of the International Conference on Mathematical Modeling and Applications (ICMMA) series. It took place from September 9 to 11, 2024, at the Nakano campus of Meiji University.

Self-organizing phenomena are widely observed in nature, and many of these processes have been artificially reproduced in physicochemical systems. Additionally, the fundamental mechanisms of self-organization have been clarified using mathematical models. These theoretical insights often inspire new biological experiments that aim to uncover the mysteries of life. Physicochemical systems also play a critical role in supporting such processes, collectively referred to as “mathematical modeling.”

During the conference, twelve invited speakers, recognized as leading researchers in their fields, presented comprehensive reviews and shared their recent insights. The topics covered a wide range of areas, such as rhythmic behavior in biochemical reactions and insights into circadian rhythms—drawing from molecular biology, the behaviors of individual animals and plants, and mathematical models. Additionally, it included pattern formation in physicochemical systems and the dynamics of self-propelled particles. The overlap among these diverse self-organization systems provided hints for further research. Despite the varied backgrounds of the attendees, including the invited speakers, lively discussions occurred regarding these differences. This interdisciplinary dialogue has significant potential to generate new research fields.

The recordings of these insightful presentations are expected to enhance future research. This lecture note is compiled from the presentation slides of the invited speakers. We hope that it will serve as a milestone for fostering new interdisciplinary studies.

The conference was organized by Takahiro Nakamura, Kota Ikeda, Nobuhiko J. Suematsu, Hiraku Nishimori, Ken-ichi Nakamura, and Masashi Shiraishi. The diverse backgrounds of the organizers contributed to the interdisciplinary nature of the conference. Finally, we express our gratitude to MIMS, Meiji University, for their generous support of this conference.

February 20, 2025.  
Nobuhiko J. Suematsu









September 9, 2024

\* Please click on the speaker's name to jump to the lecture slides.

	●	Opening
13:00~14:00	●	István Lagzi (Budapest University of Technology and Economics, Hungary) "Material design and engineering using reactions and mass transport processes"
14:00~15:00	●	Jae Kyoung Kim (Korea Advanced Institute of Science and Technology (KAIST), Republic of Korea) "Mastering Noise in Rhythm Generation: Strategies for Utilization and Avoidance"
15:00	●	Coffee Break
15:15~16:15	●	Akiko Satake (Kyushu University, Japan) "Synchrony from genes to ecosystems"
16:15~17:15	●	Hiroya Nakao (Tokyo Institute of Technology, Japan) "Dynamical reduction approach to the analysis and control of rhythmic systems"
17:15	●	Coffee Break
17:30~18:30	●	Takashi Miura (Kyushu University, Japan) "Self-organization of cell-cell boundary structures in kidney cells"







September 10, 2024

\* Please click on the speaker's name to jump to the lecture slides.


10:00~12:00  Poster presentation

12:00~13:00  Lunch

13:30~14:30  [Aneta Stefanovska \(Lancaster University, UK\)](#)  
"Imperfect clocks that govern mammalian physiological functions – an overview from circadian to milliseconds scales"

14:30~15:30  [Haruna Fujioka \(Okayama University, Japan\)](#)  
"Individual activity-rest rhythms of ants under laboratory colony conditions"

15:30  Coffee Break

16:00~17:00  [Daisuke Ono \(Nagoya University, Japan\)](#)  
"Cytosolic circadian rhythms in the mammalian central circadian clock"

17:00~18:00  [Federico Rossi \(University of Siena, Italy\)](#)  
"Synthesis and Application of Giant Unilamellar Vesicles for Cellular Modeling and Advanced Materials"






18:00~  Banquet



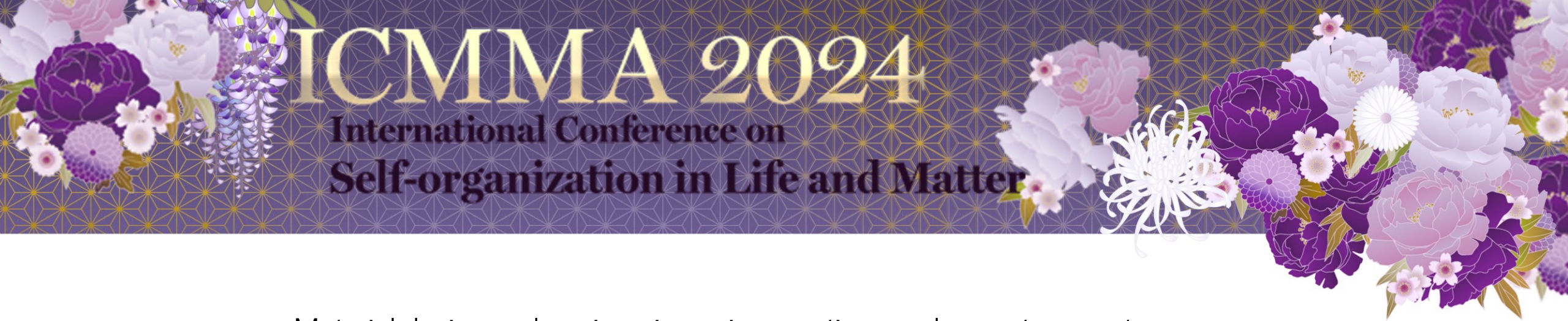


# September 11, 2024

\* Please click on the speaker's name to jump to the lecture slides.

- |             |   |  |
|-------------|---|--|
| 9:00~10:00  |  | Hiroshi Ito (Kyushu University, Japan)<br>"Cellular circadian rhythm can be more precise through output"   |
| 10:00~11:00 |  | Gisele Oda (Universidade de São Paulo, Brasil)<br>"Biological Clocks of Subterranean Rodents: Field Work meets Mathematical Modeling in South America" |
| 11:00       |  | Coffee Break   |
| 11:15~12:15 |  | Hiroyuki Kitahata (Chiba University, Japan)<br>"Relation between motion and shape in self-phoretic motions"  |
| 12:15~12:20 |  | Closing  |





## Material design and engineering using reactions and mass transport processes

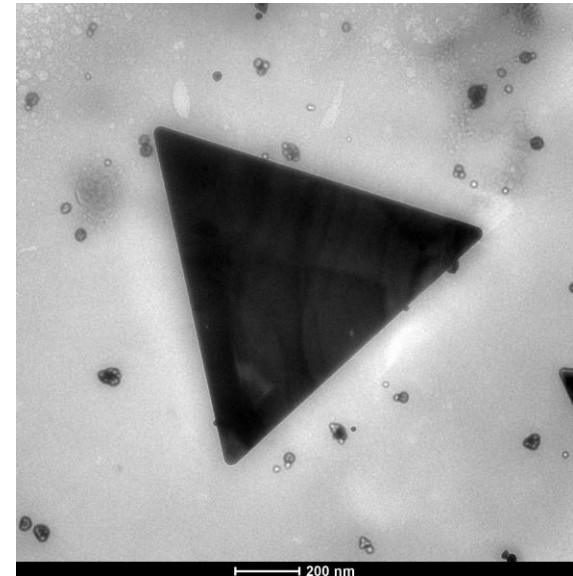
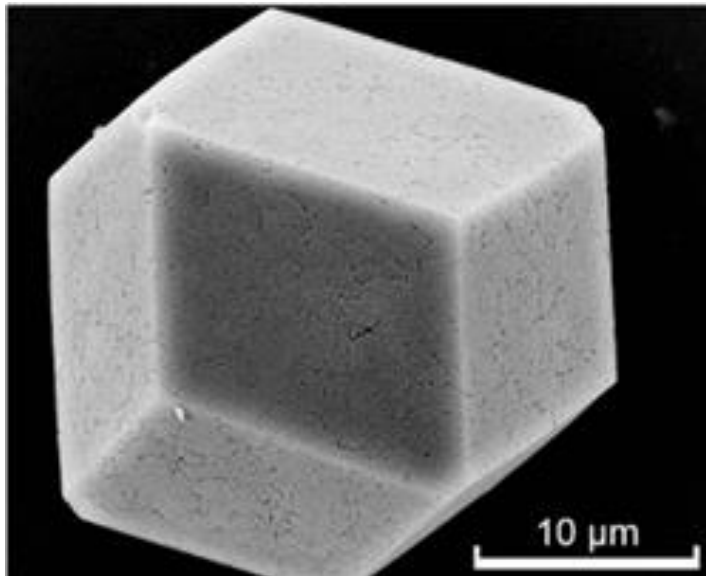
István Lagzi (Budapest University of Technology and Economics)

Wet synthesis is one of the most widely used techniques for generating crystalline materials. The reagents are mixed in this procedure, and crystals form due to the nucleation and growth processes. In crystal growth and engineering, the most crucial is the temporal control of the processes over time to obtain samples with a desired average size and dispersity. In the lecture, recently developed alternative methods will be presented and discussed for synthesizing various crystalline materials, such as inorganic precipitate particles, zeolitic imidazolate frameworks, and gold nanoparticles. We highlight the advantage of applying a gel reactor utilizing diffusion and ionic migration driven by a direct electric field. Additionally, we show that cell-sized microcompartments (giant unilamellar vesicles) can act as reactors for the synthesis of crystals. In these techniques, the mass transport affects the mass flux of chemical species in the system, influencing nucleation and crystal growth. Therefore, control of mass transport of the chemical species can be used to tune the morphology, average size, and size distribution of crystalline materials.

### References

- [1] N. Német, G. Holló, G. Schusztér, D. Horváth, Á. Tóth, F. Rossi, I. Lagzi, *Chem. Commun.*, 58 38 (2022) 5777–5780.
- [2] S. Farkas, M. S. Fónyi, G. Holló, N. Német, N. Valletti, Á. Kukovecz, G. Schusztér, F. Rossi, I. Lagzi, *J. Phys. Chem. C*, 126, 22, (2022) 9580–9586.
- [3] N. Német, G. Holló, N. Valletti, S. Farkas, B. Dúzs, Á. Kukovecz, G. Schusztér, I. Szalai, F. Rossi, I. Lagzi, *Mater. Adv.*, 5 (2024) 1199–1204.

# Material design and engineering using reactions and mass transport processes



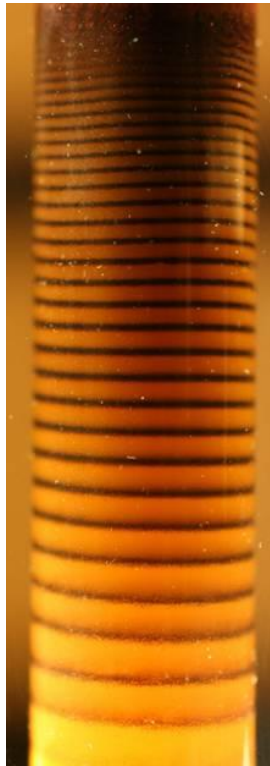
**István Lagzi**

Budapest University of Technology and Economics  
Department of Physics

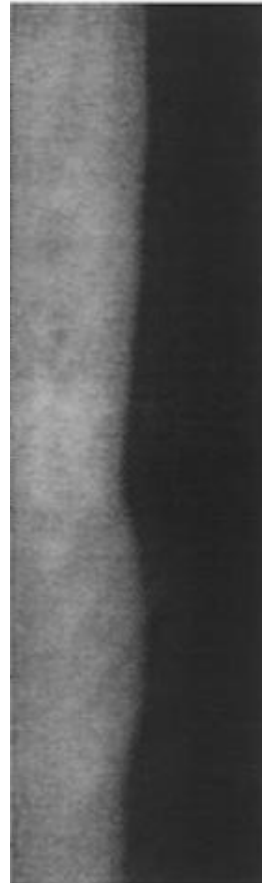
International Conference on Self-organization in Life and Matter  
Meiji University  
09-11/September/2024

# General introduction

## Reaction-diffusion systems



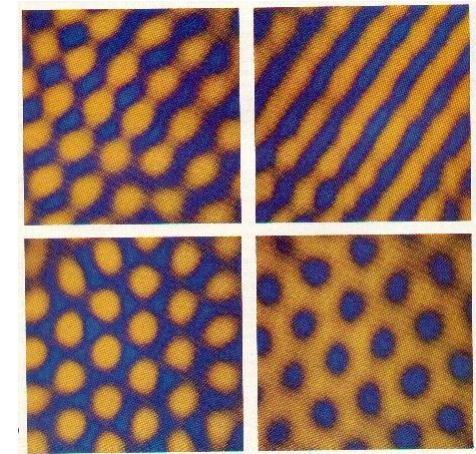
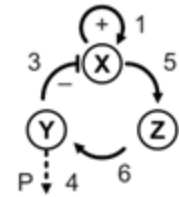
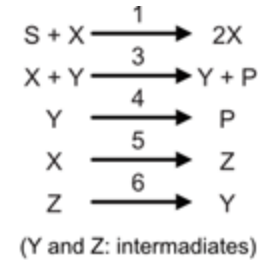
Liesegang phenomenon  
**1896**



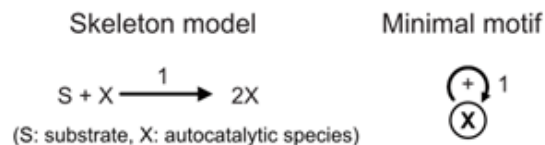
Autocatalytic  
fronts  
**1906**



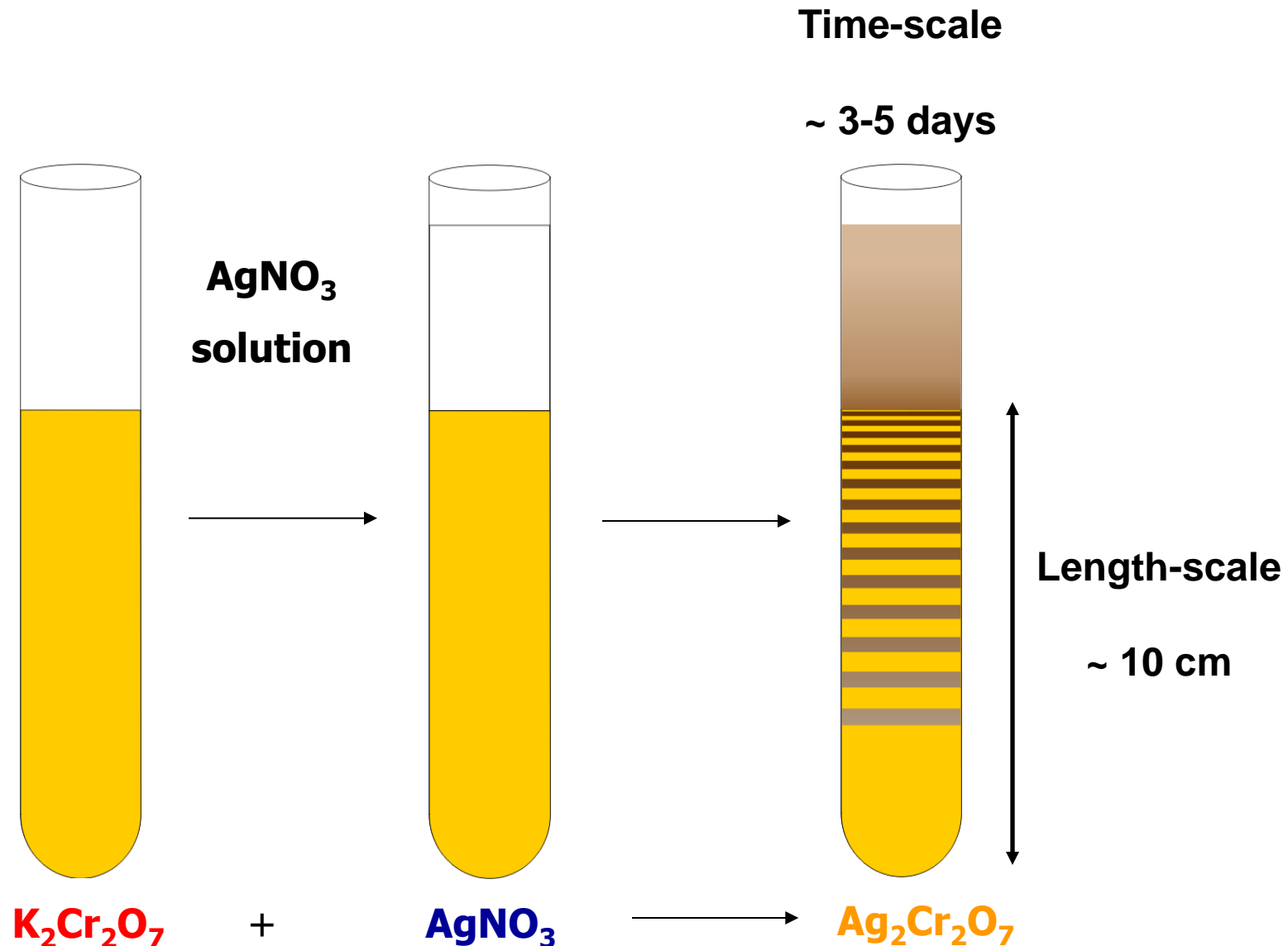
BZ waves  
**1970**



Turing pattern  
**1990**



# Periodic precipitation – proof of concept

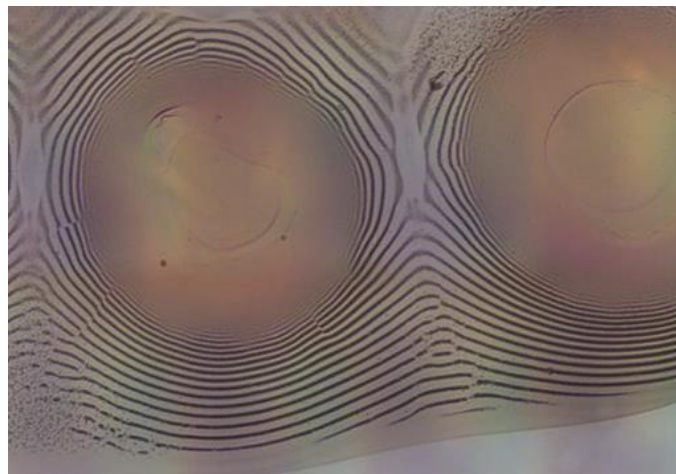
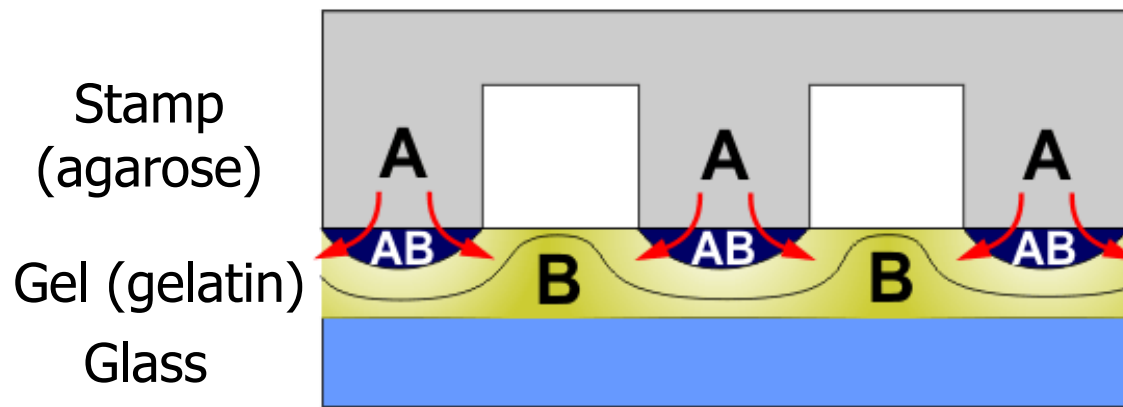




# Experimental system

Outer  
electrolyte

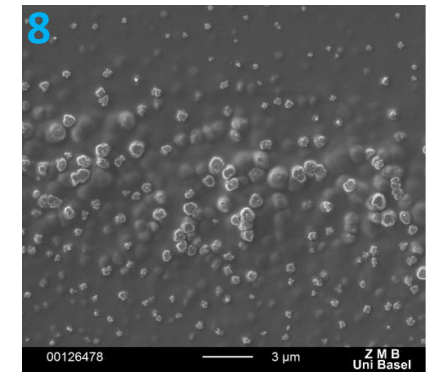
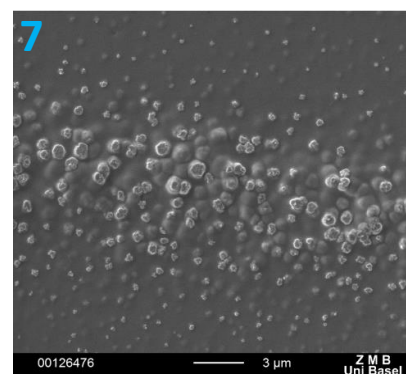
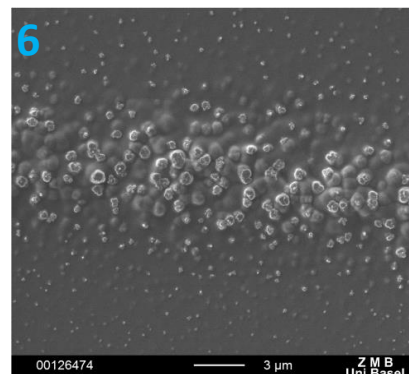
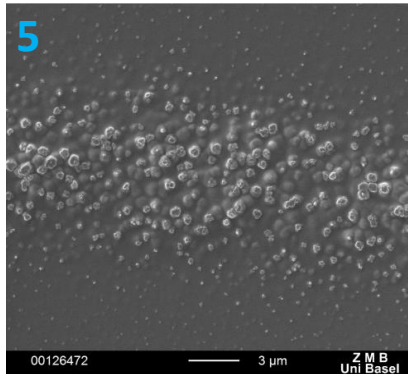
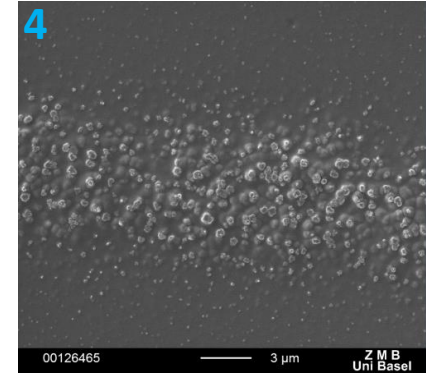
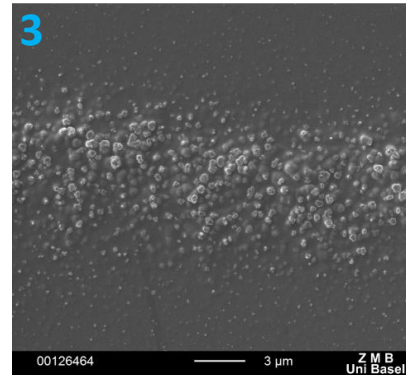
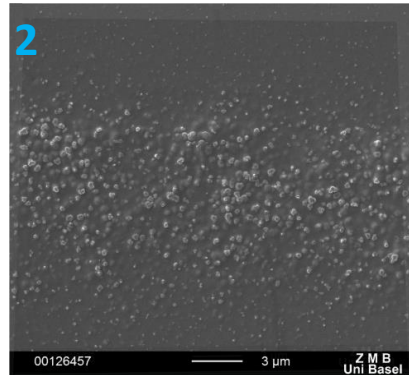
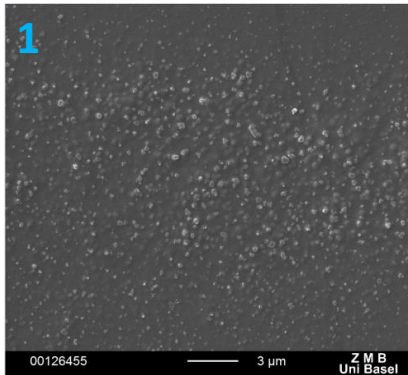
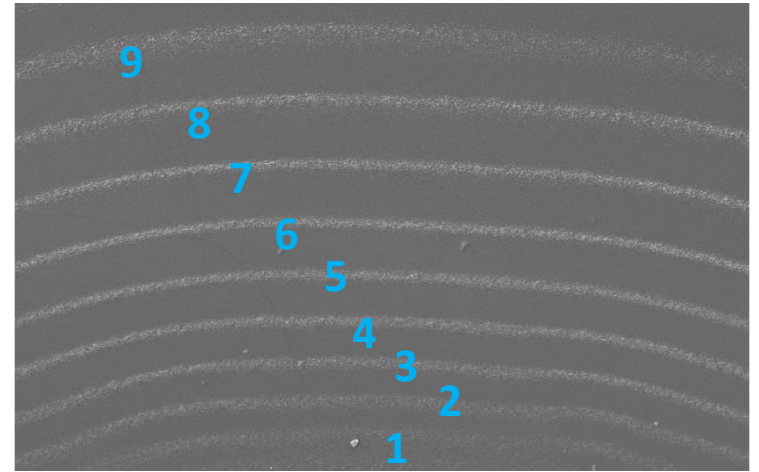
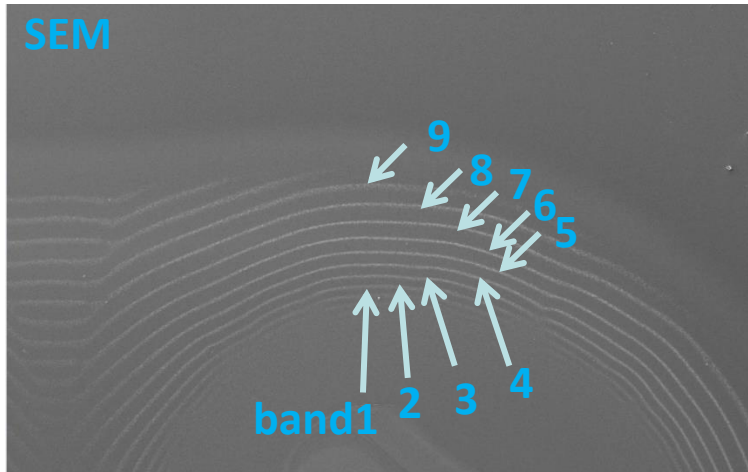
Inner  
electrolyte



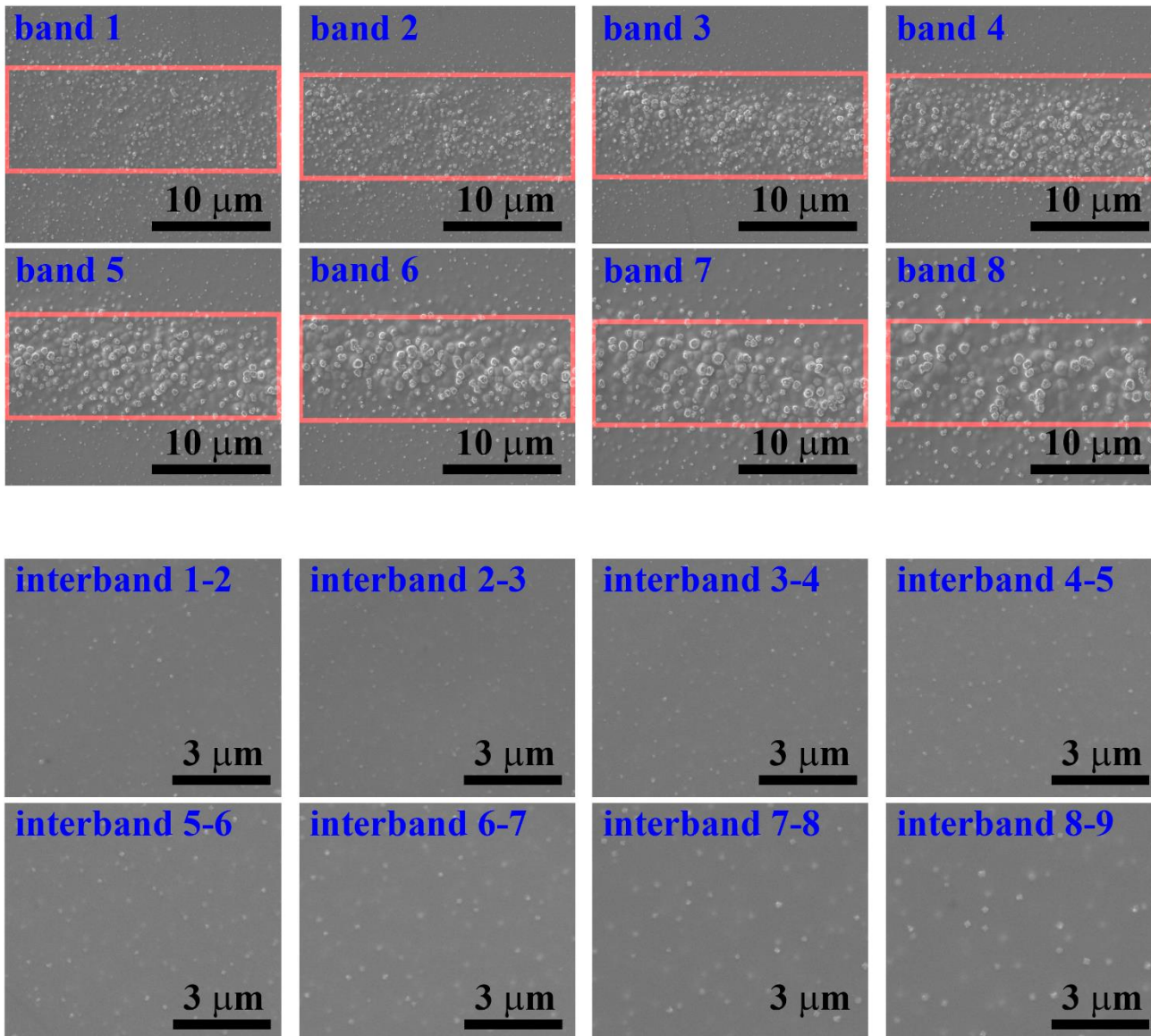
500  $\mu\text{m}$



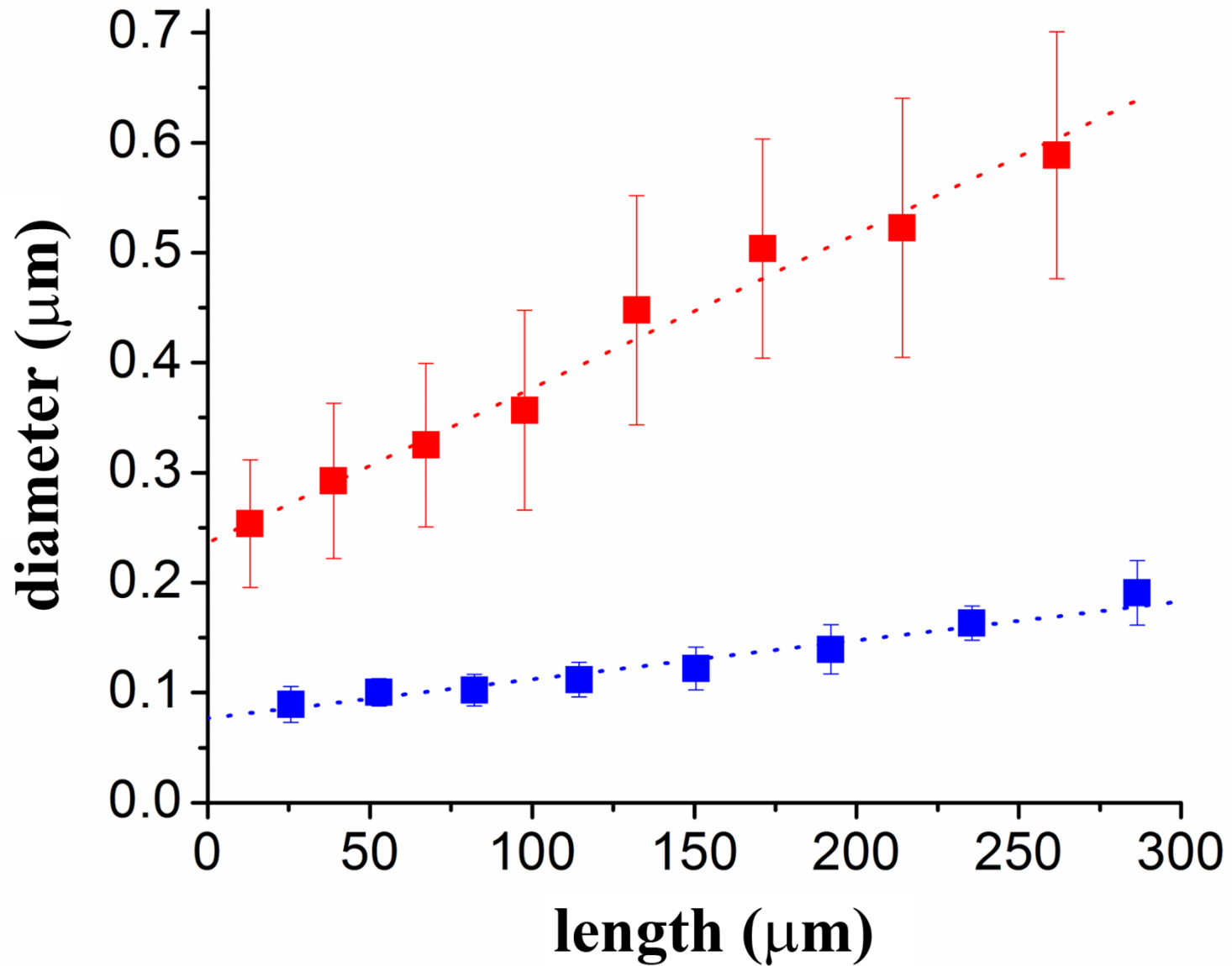
# Results



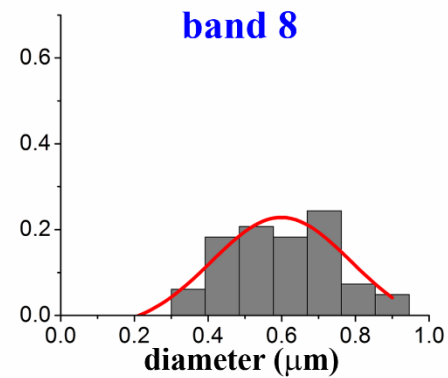
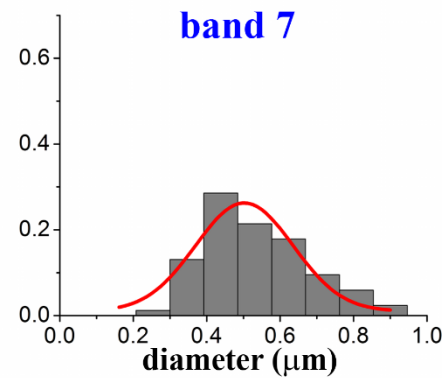
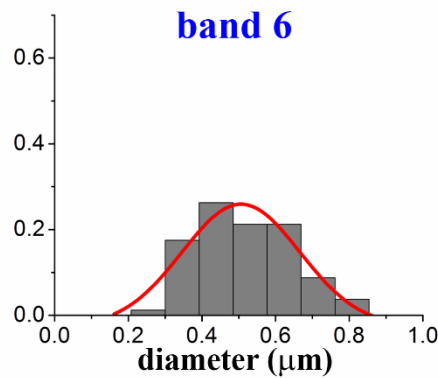
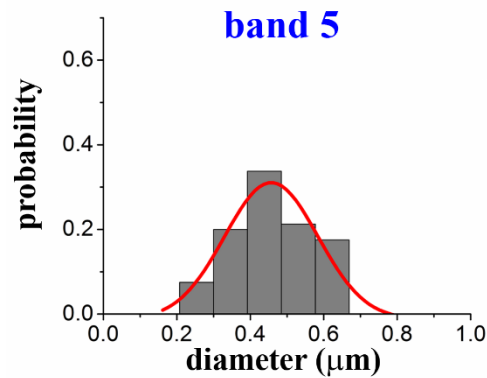
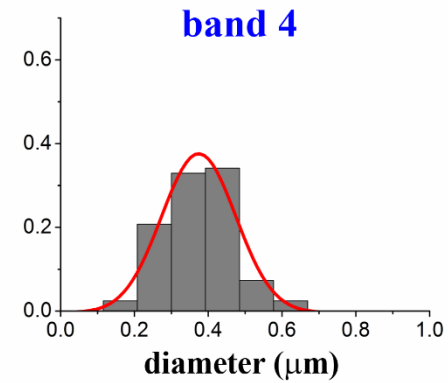
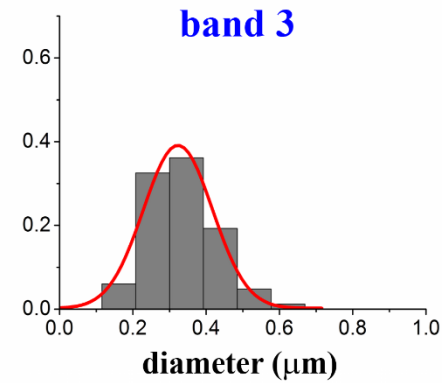
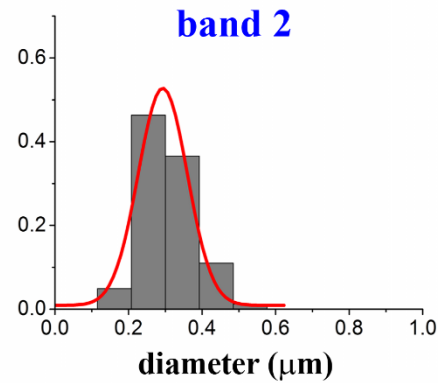
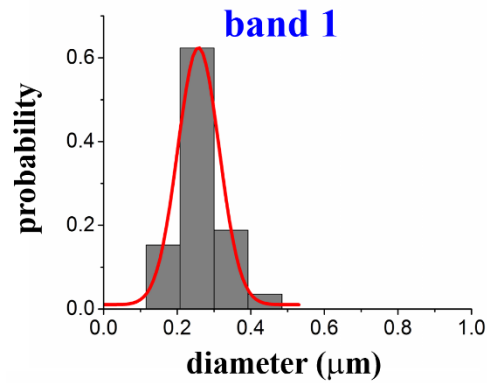
# Results



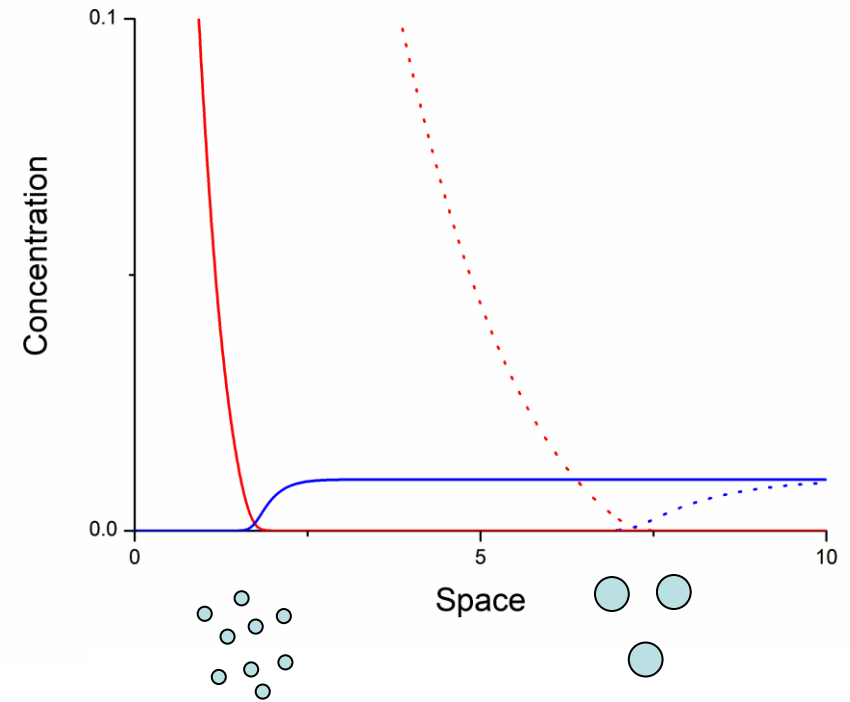
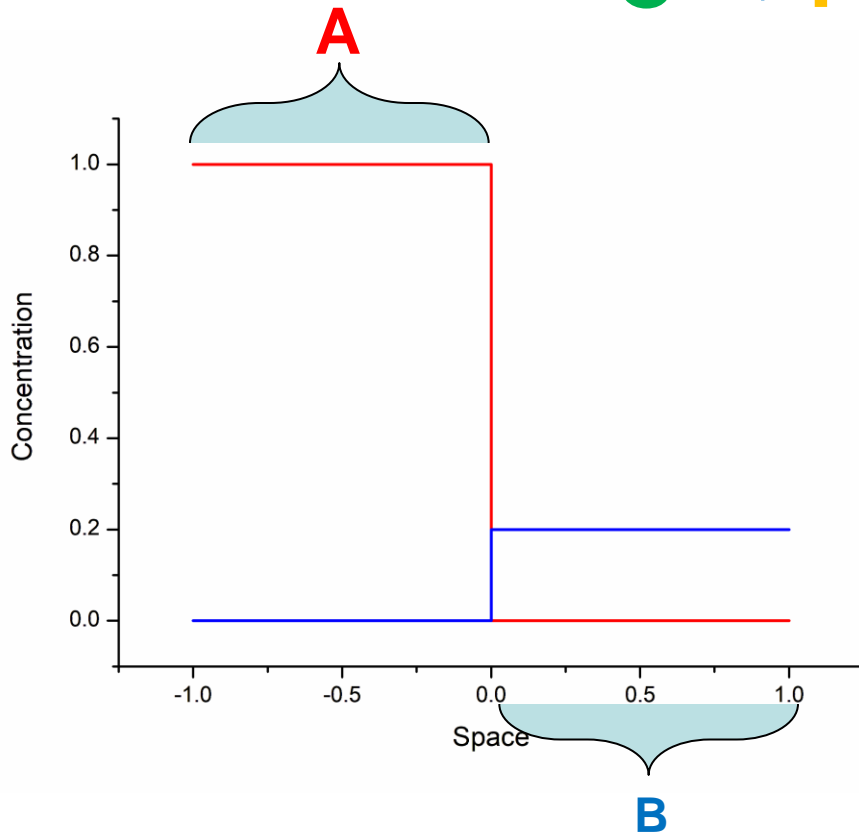
# Results



# Results

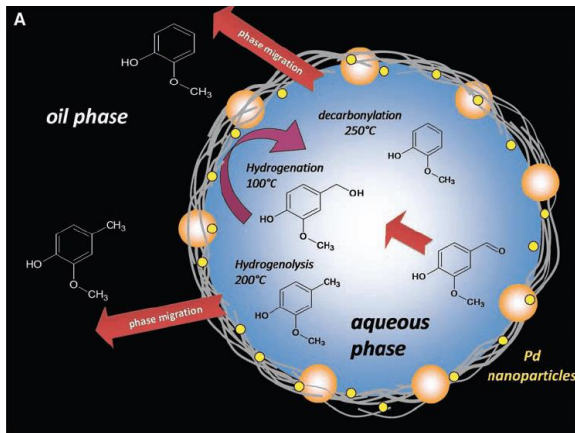


# Periodic precipitation – proof of concept

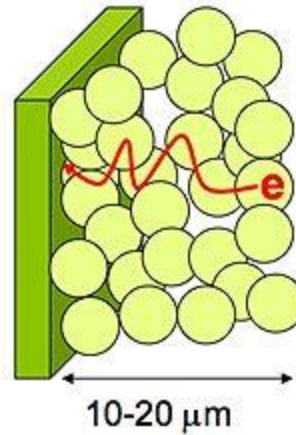




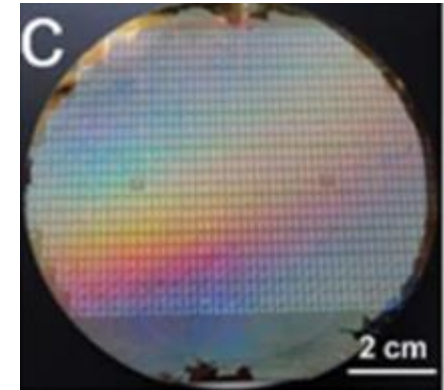
# Nano- and microparticles



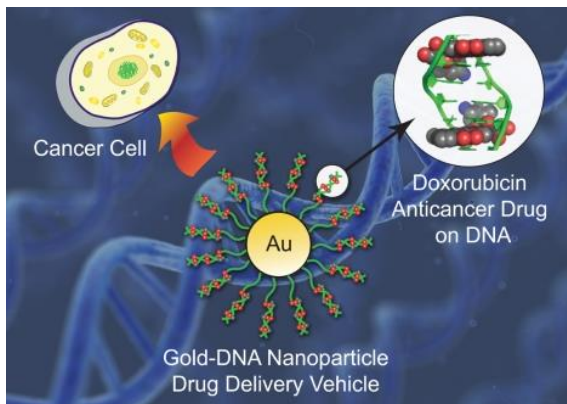
**Catalysis**



**Electronics**



**Sensorics**



**Nanomedicine**

## Important:

(i) Size of particles

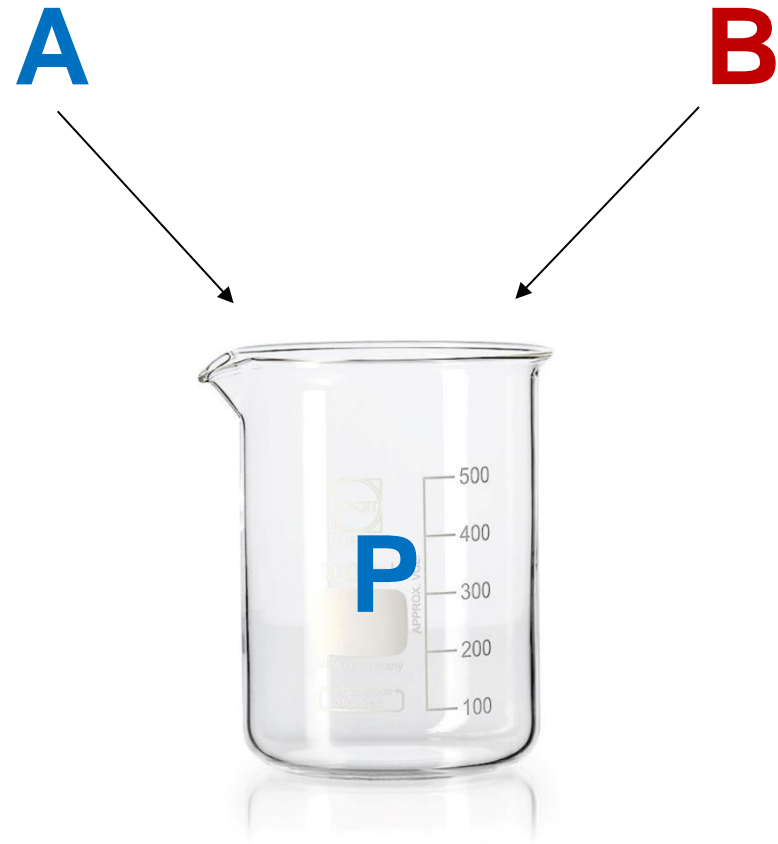
(ii) Particle size distribution



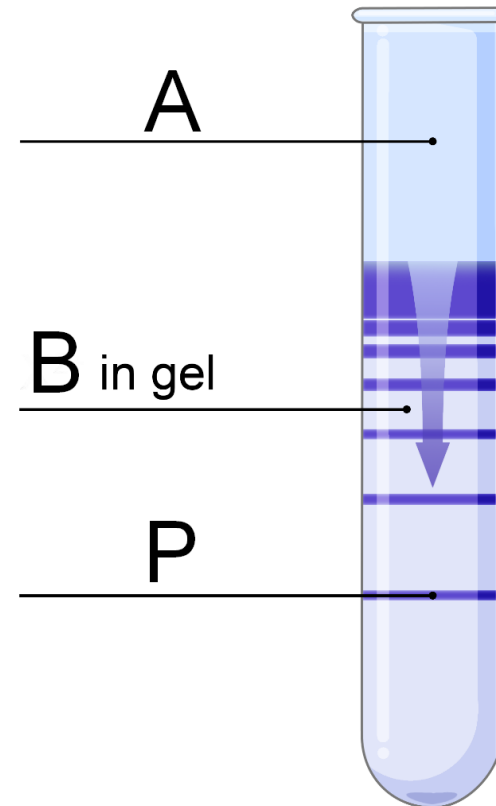
# Wet synthesis



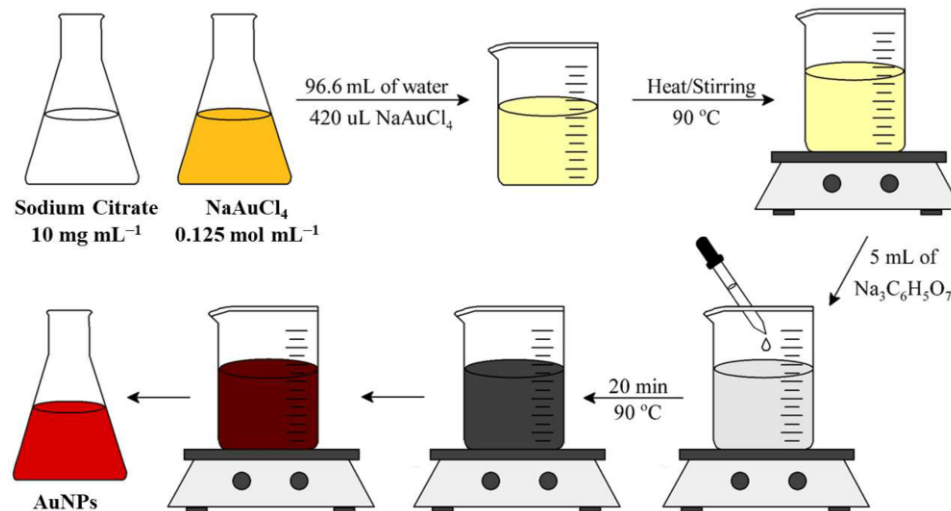
**Bulk**



**Reaction-diffusion**

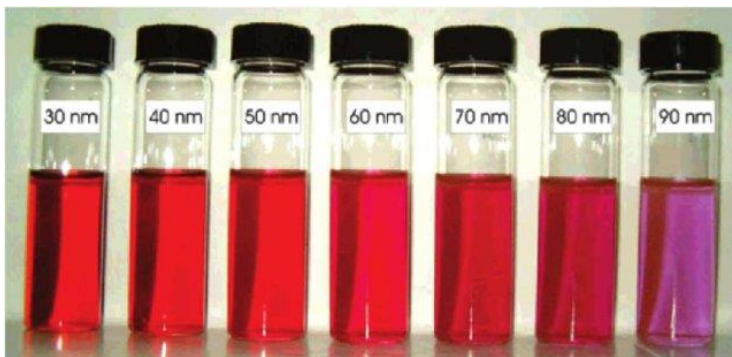


# I. GOLD NANOPARTICLES



**Turkevich method**

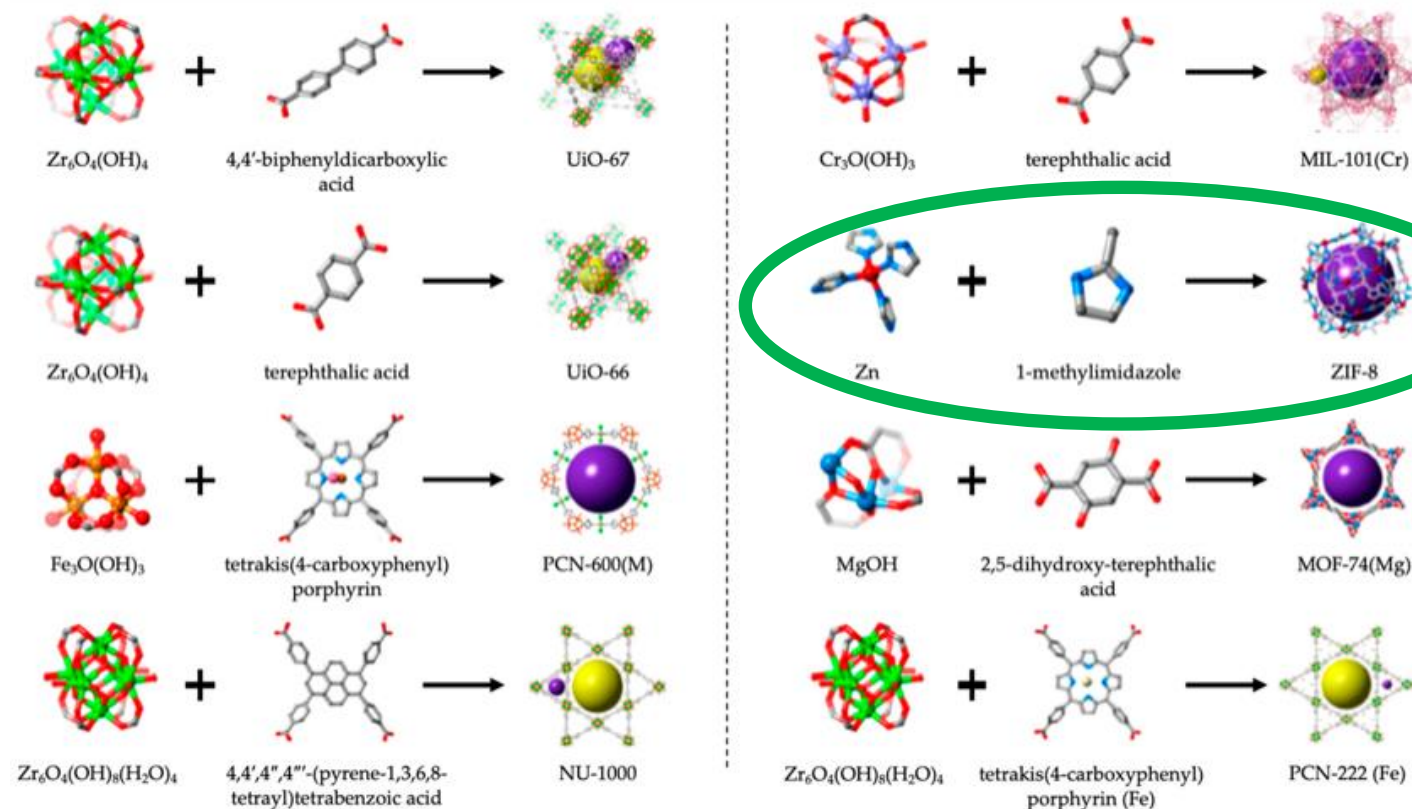
Oliveira, A.E.F.; Pereira, A.C.; Resende, M.A.C.; Ferreira, L.F. Gold Nanoparticles: A Didactic Step-by-Step of the Synthesis Using the Turkevich Method, Mechanisms, and Characterizations. *Analytica* 2023, 4, 250-263. <https://doi.org/10.3390/analytica4020020>



**Color: surface plasmon resonance (SPR)**

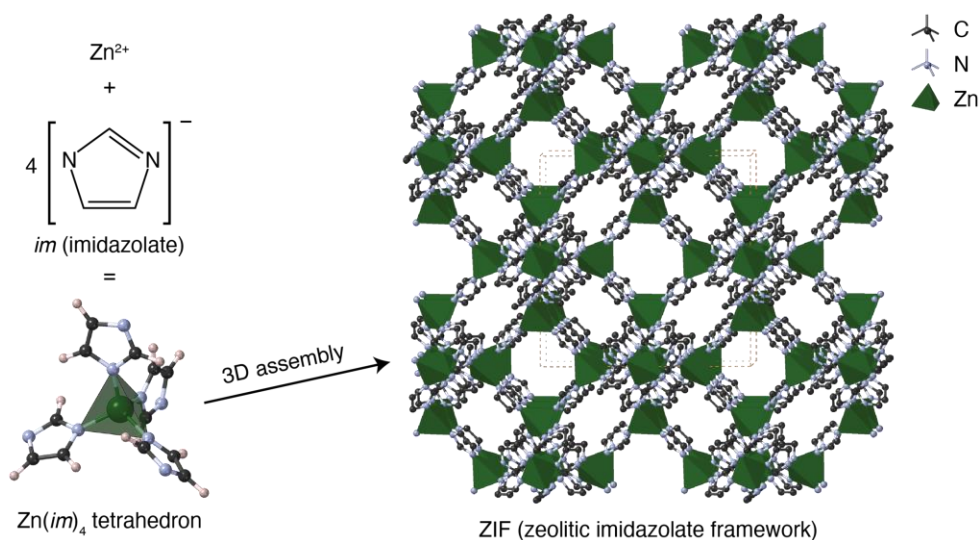
Subara, Deni, and Irwandi Jaswir. 2018. "Gold Nanoparticles: Synthesis and Application for Halal Authentication in Meat and Meat Products". *International Journal on Advanced Science, Engineering and Information Technology* 8 (4-2):1633-41. <https://doi.org/10.18517/ijaseit.8.4-2.7055>.

# II. METAL-ORGANIC FRAMEWORKS (MOFs)



Gutiérrez-Serpa, A.; Pacheco-Fernández, I.; Pasán, J.; Pino, V. Metal–Organic Frameworks as Key Materials for Solid-Phase Microextraction Devices—A Review. *Separations* **2019**, *6*, 47. <https://doi.org/10.3390/separations6040047>

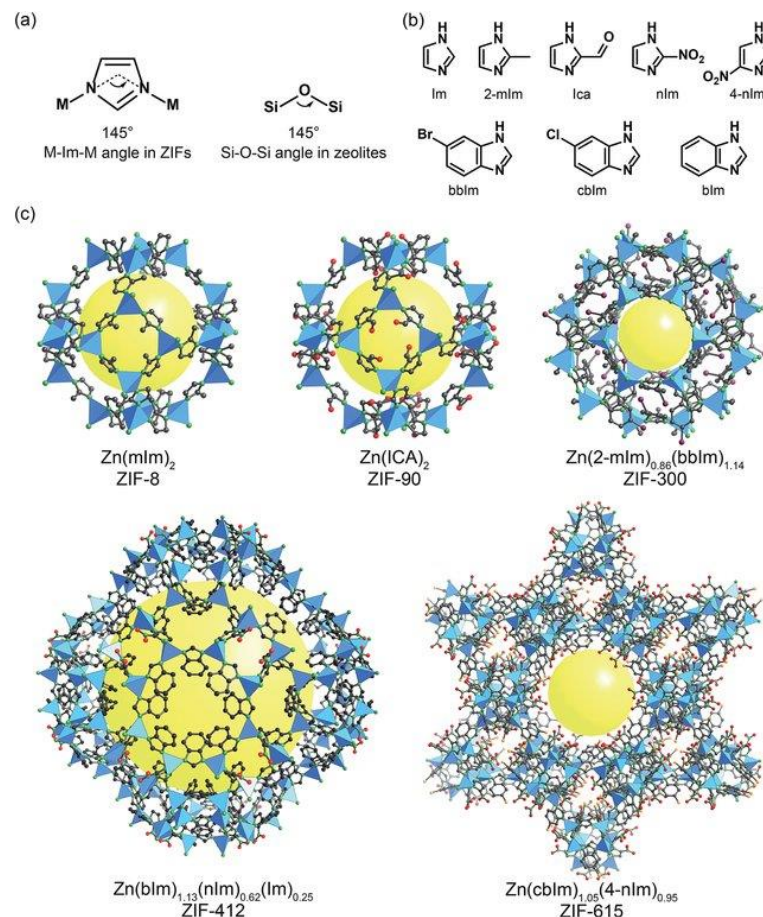
# II. METAL-ORGANIC FRAMEWORKS (MOFs)



[https://en.wikipedia.org/wiki/Zeolitic\\_imidazolate\\_framework](https://en.wikipedia.org/wiki/Zeolitic_imidazolate_framework)

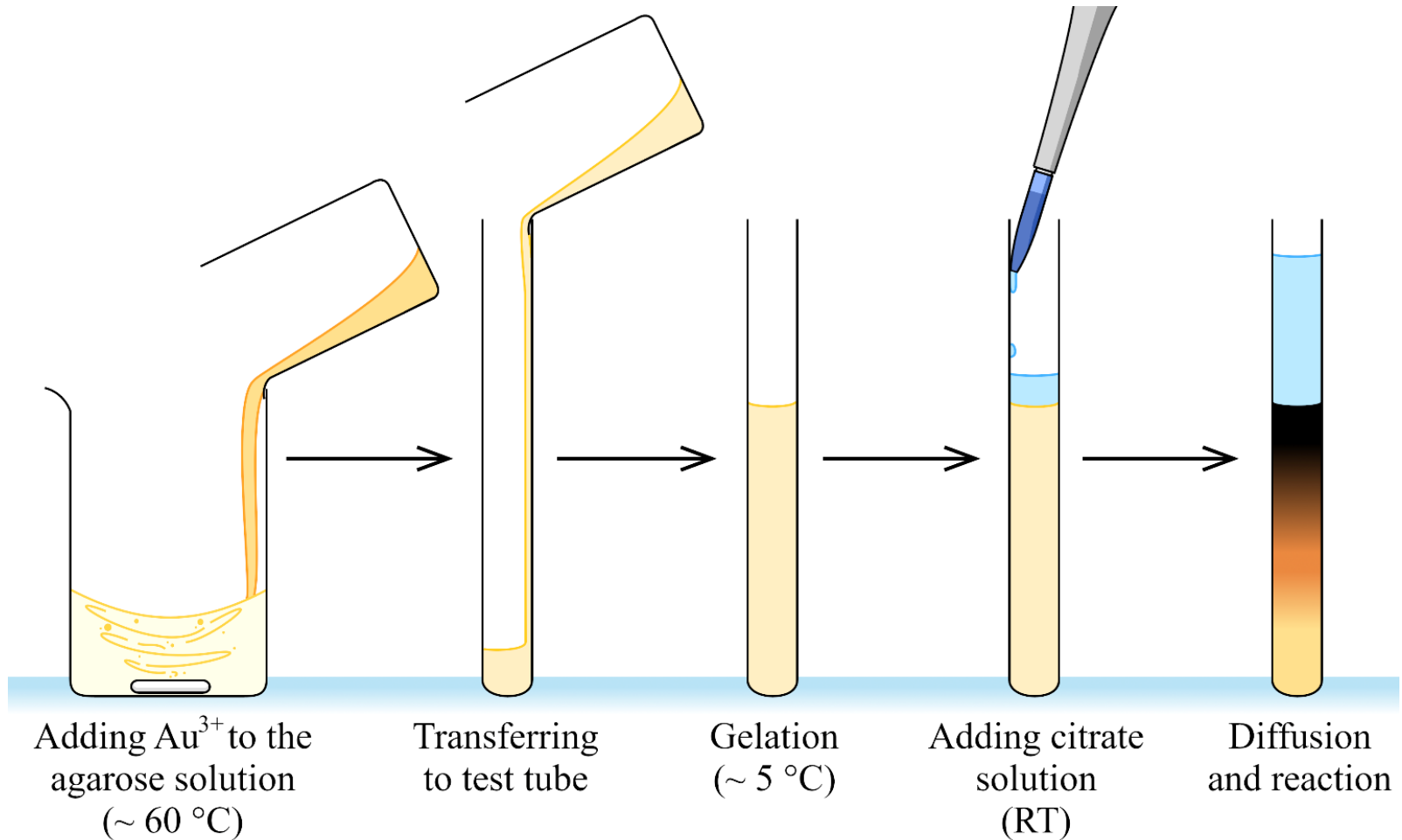
## Application:

- Gas separation/storage
- Catalysis
- Electronic devices
- Drug delivery system



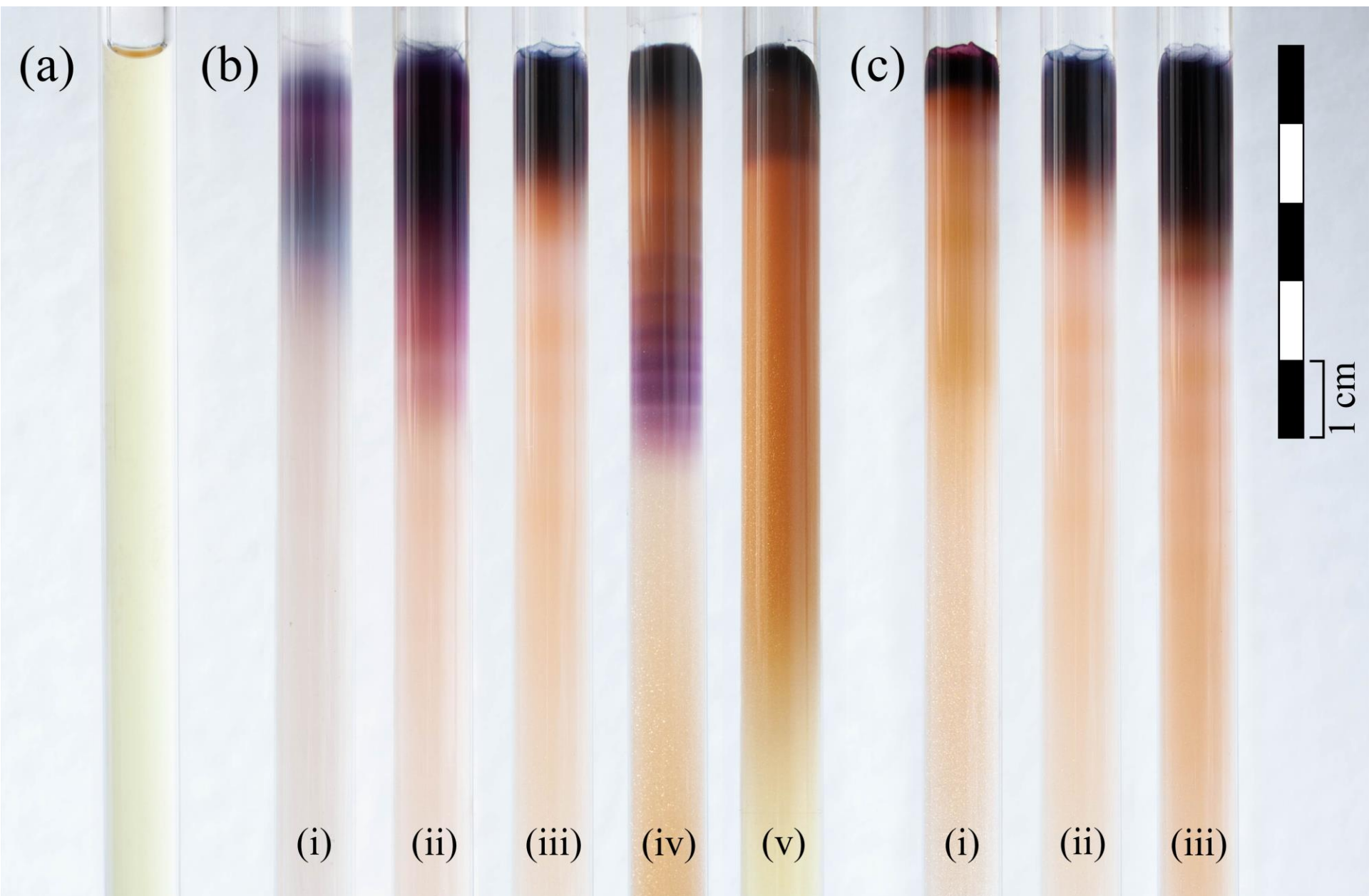
B. Rungtaweeworanit *et al.*, *Faraday Discuss.*, 201, 9–45 (2017).

# I. Synthesis of gold particles using reaction-diffusion



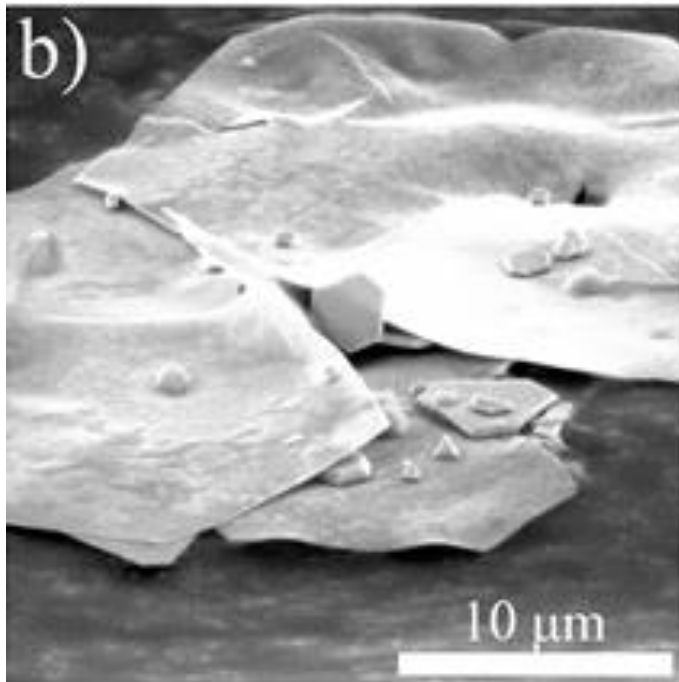
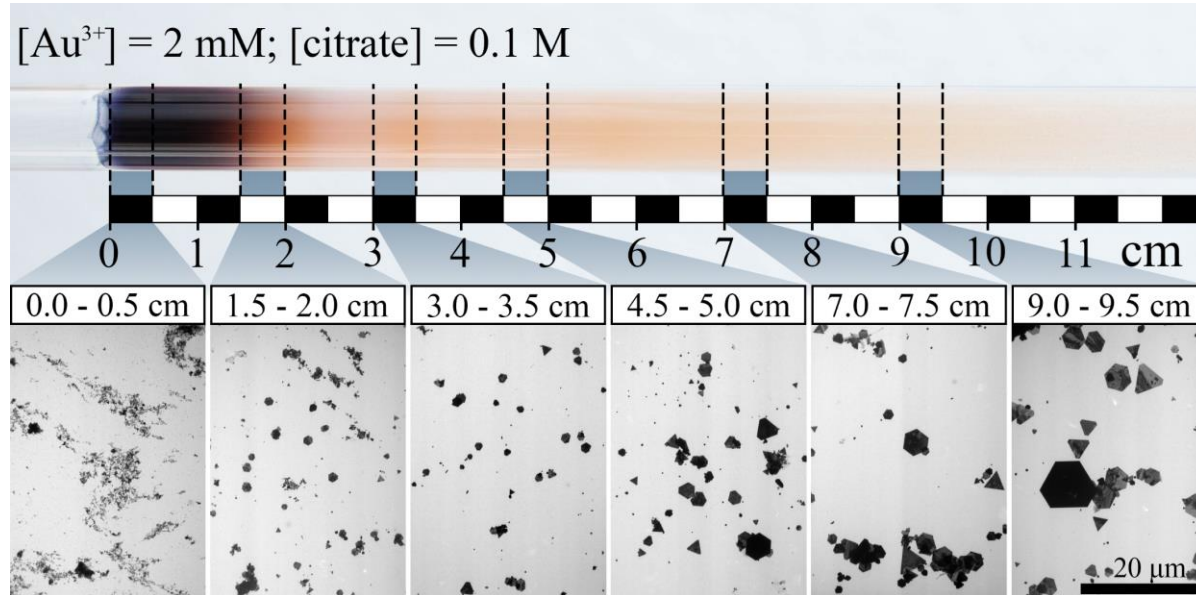


# Gold Nanoparticles





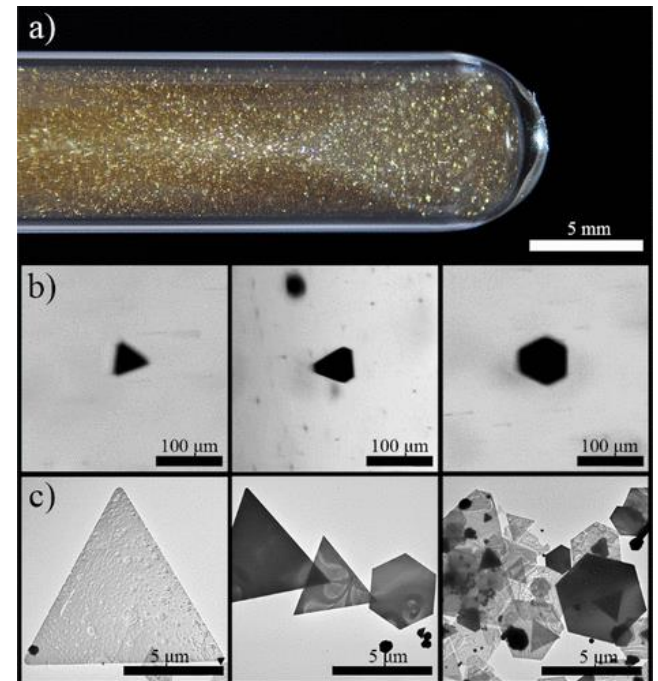
# Gold Nanoparticles



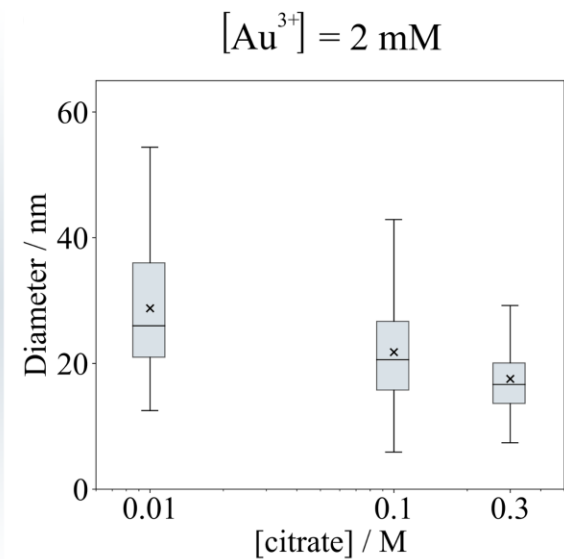
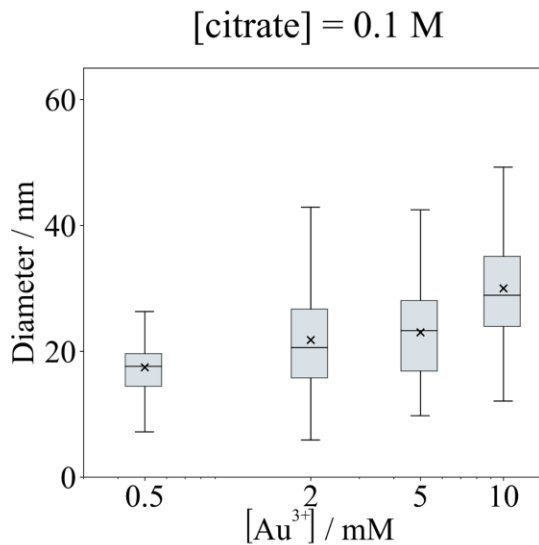
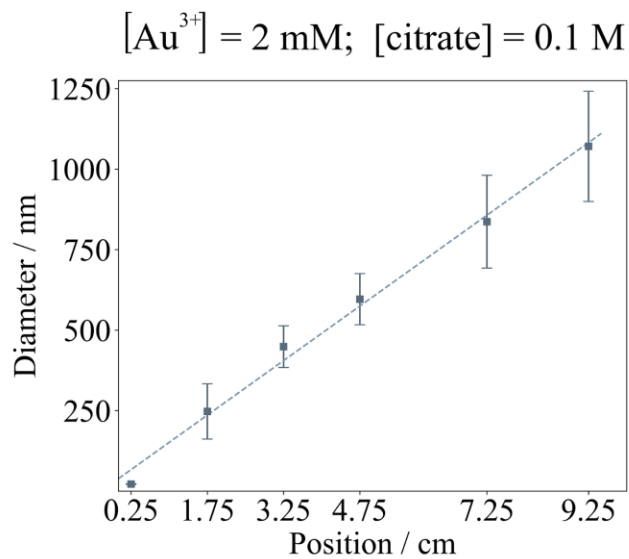
Aspect ratio:

(50 nm : 80  $\mu\text{m}$ )

1 : 1600



# Gold Nanoparticles



near the liquid-gel interface

**Effect of the agarose:**

**(i) Gel: convection-free environment**

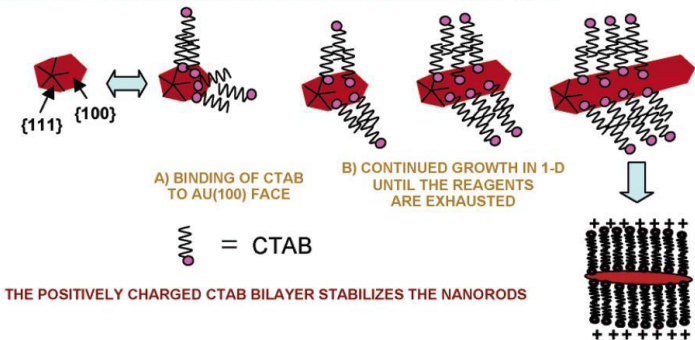
**(ii) Acting as “surfactant”**

**(iii) One-step synthesis**

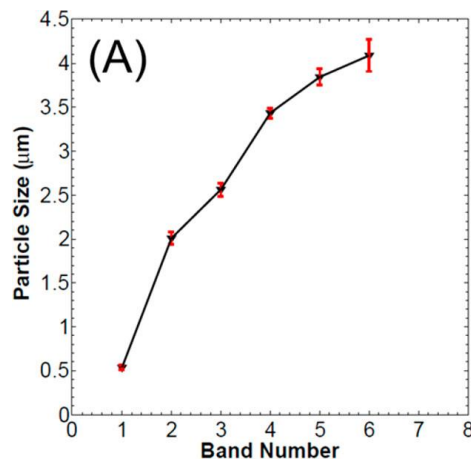
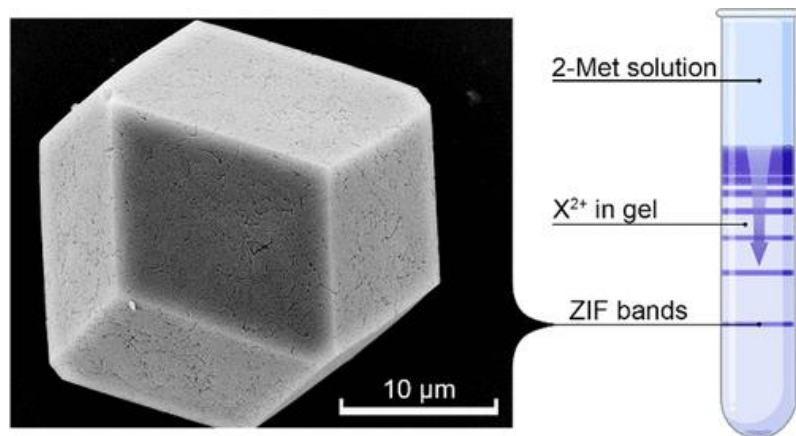
STEP 1: SYMMETRY BREAKING IN FCC METALS



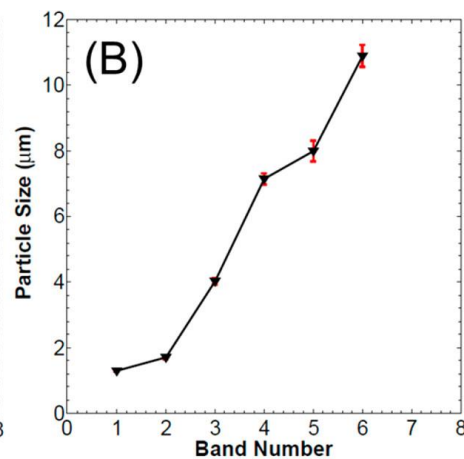
STEP 2: PREFERENTIAL SURFACTANT BINDING TO SPECIFIC CRYSTAL FACES



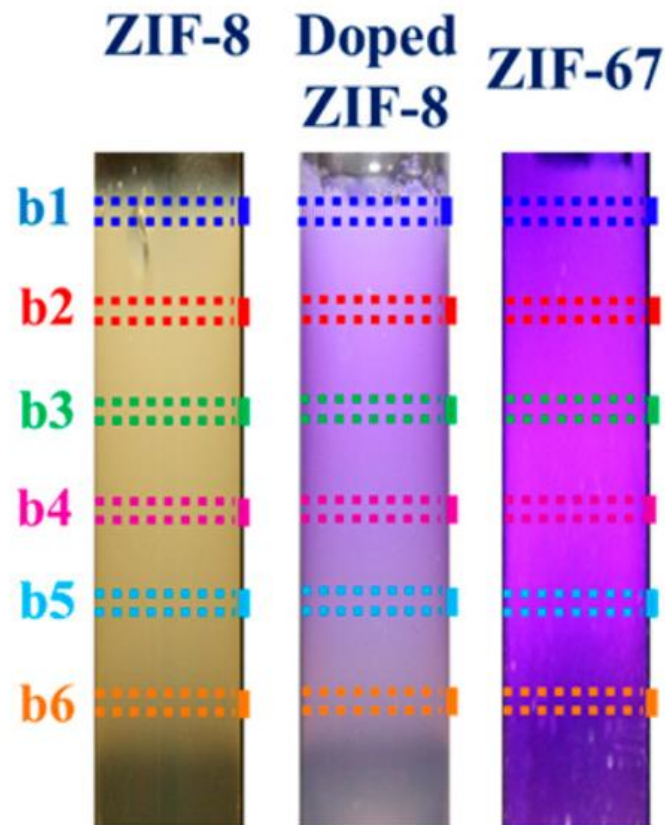
## II. Synthesis of zeolitic imidazolate frameworks (ZIFs) using reaction-diffusion



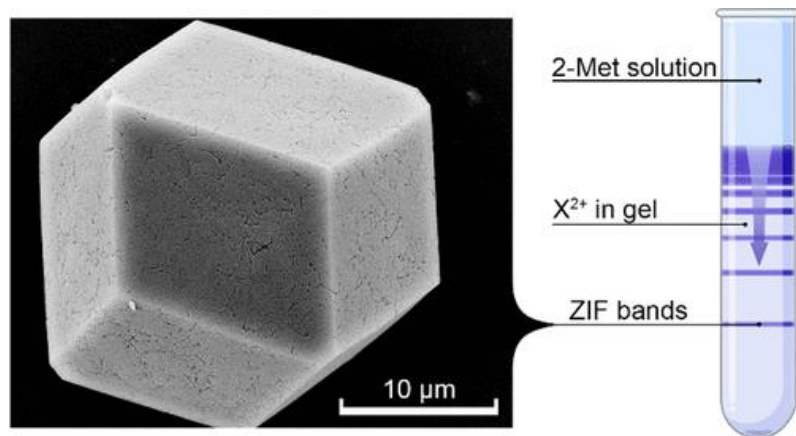
**ZIF-8**



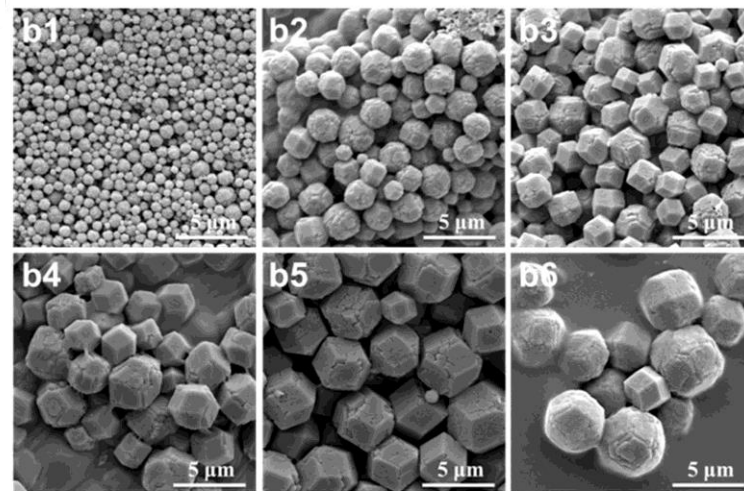
**ZIF-67**



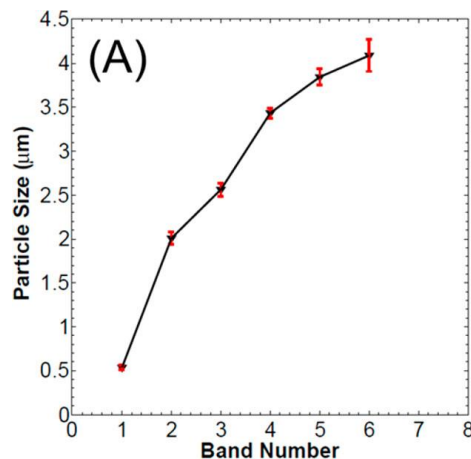
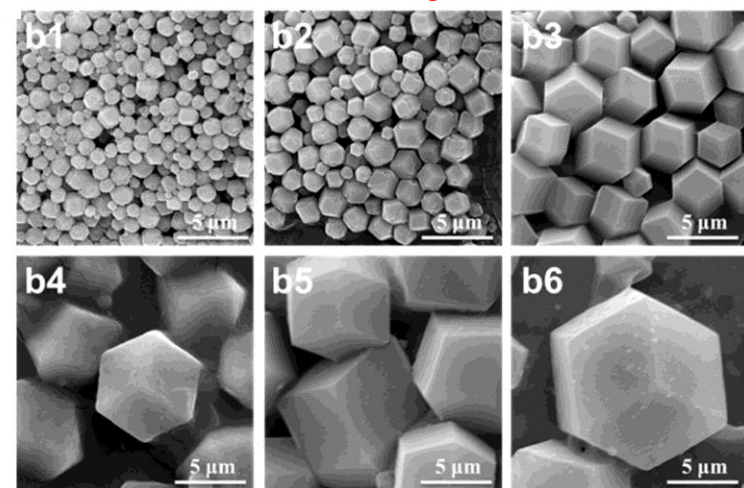
## II. Synthesis of zeolitic imidazolate frameworks (ZIFs) using reaction-diffusion



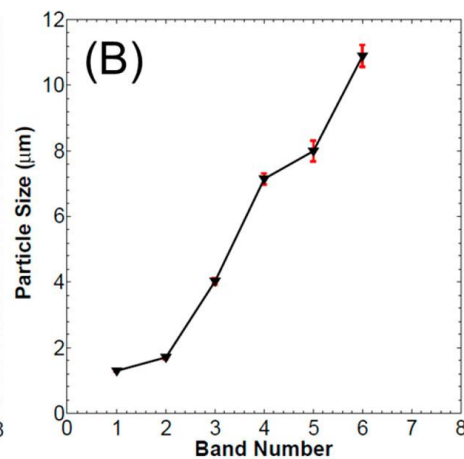
**ZIF-8**



**ZIF-67**



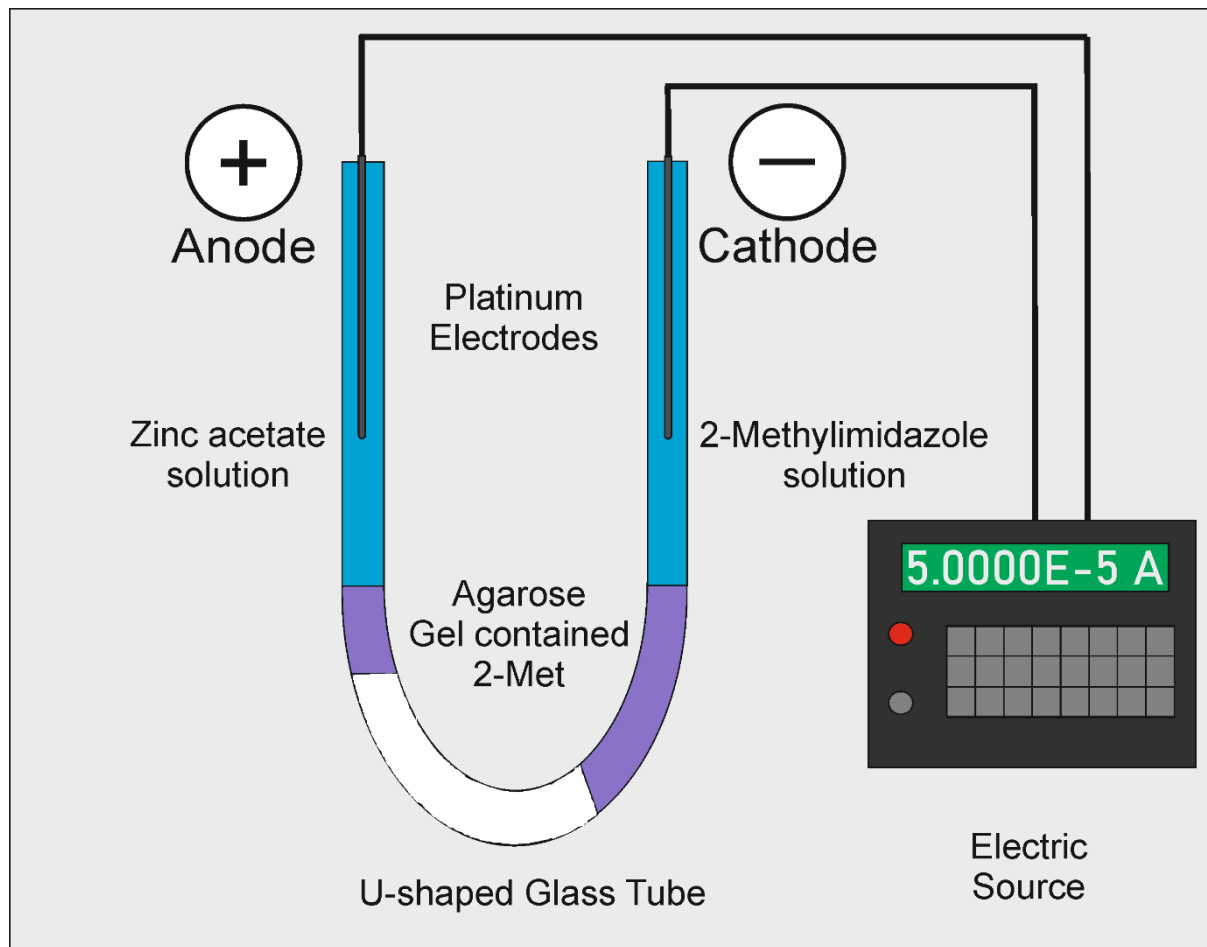
**ZIF-8**



**ZIF-67**



### III. Synthesis of zeolitic imidazolate frameworks (ZIFs) in an electric field

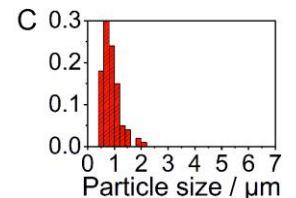
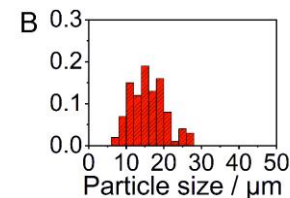
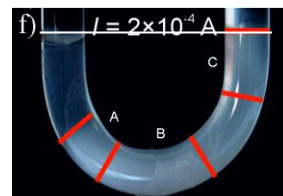
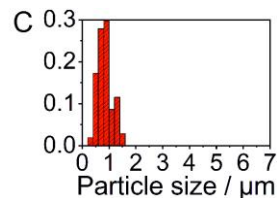
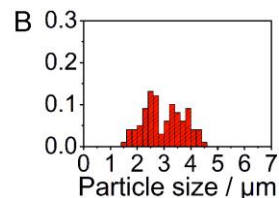
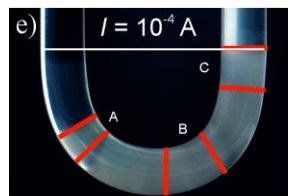
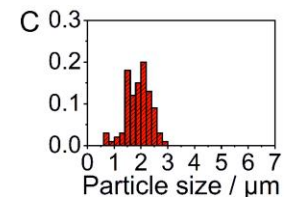
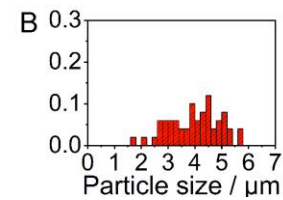
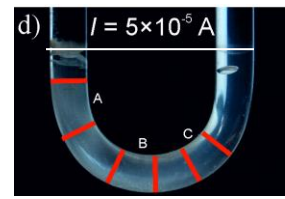
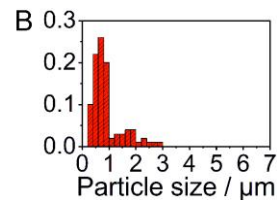
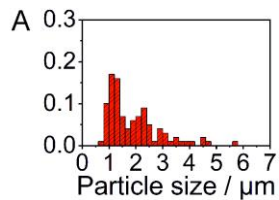
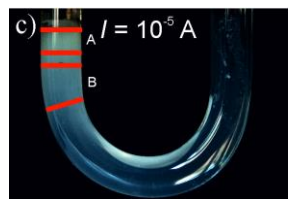
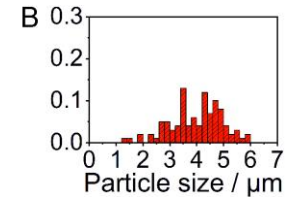
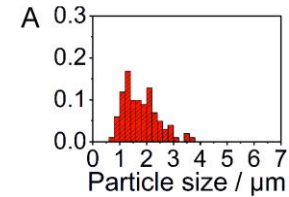
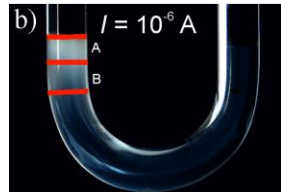
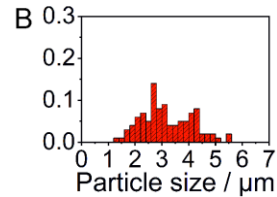
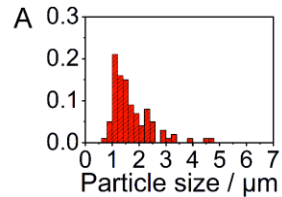
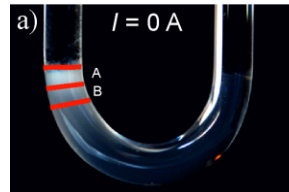


**Experimental setup**



# III. Synthesis of zeolitic imidazolate frameworks (ZIFs) in an electric field

## Experimental results



# III. Synthesis of zeolitic imidazolate frameworks (ZIFs) in an electric field

## Kinetic model



$$k_1 = 10^{-4} \text{ M}^{-2}\text{s}^{-1}$$

$$r_1 = k_1 [\text{L}]^2 [\text{M}^{2+}]$$



$$k_2 = 10^{-3} \text{ M}^{-1}\text{s}^{-1}$$

$$r_2 = k_2 [\text{C}^{2+}]^2$$



$$k_3 = 10^{-2} \text{ M}^{-1}\text{s}^{-1}$$

$$r_3 = k_3 [\text{C}^{2+}] [\text{nMOF}]$$



$$k_4 = 10^{-4} \text{ s}^{-1}$$

$$r_4 = k_4 [\text{nMOF}] [\text{L}] / [\text{L}^+]$$



$$K = 1.4125 \times 10^6$$

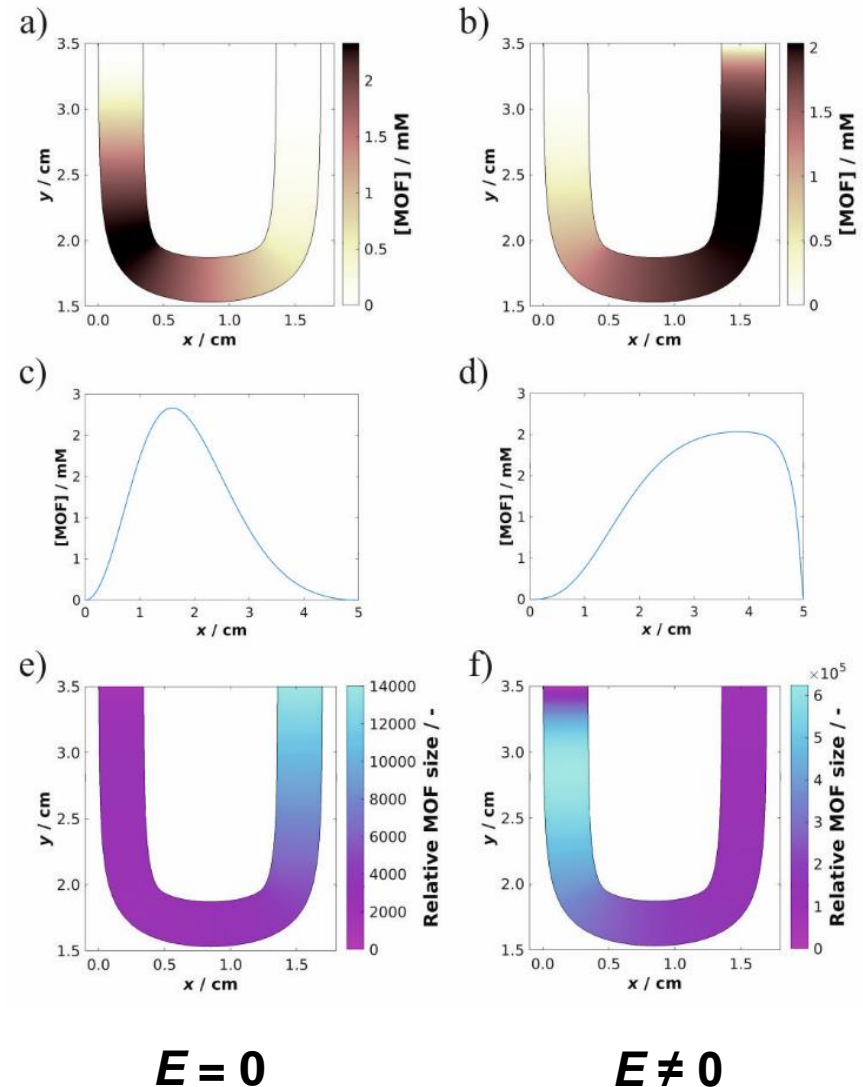
# III. Synthesis of zeolitic imidazolate frameworks (ZIFs) in an electric field

## Numerical results

$$\frac{\partial c_i}{\partial t} = D_i \frac{\partial^2 c_i}{\partial x^2} - \frac{D_i z_i F}{RT} \frac{\partial c_i E(x, t)}{\partial x} + R_i(c)$$

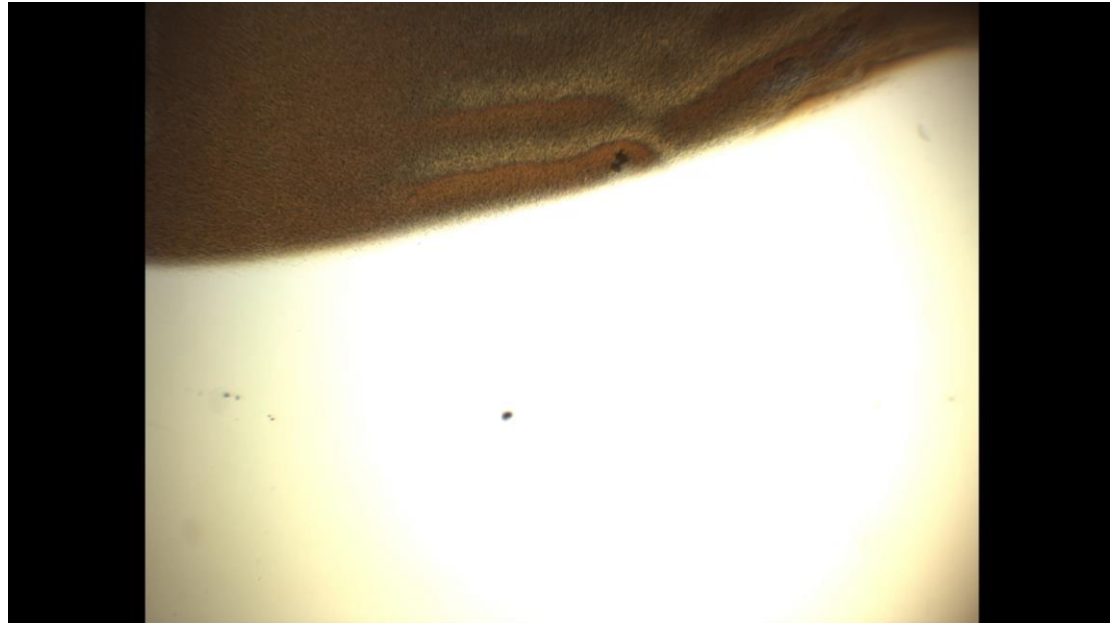
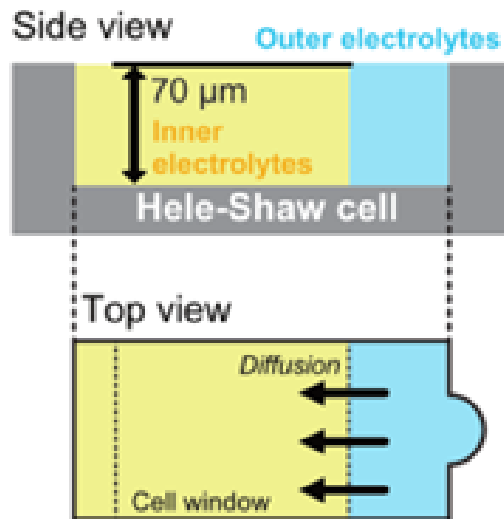
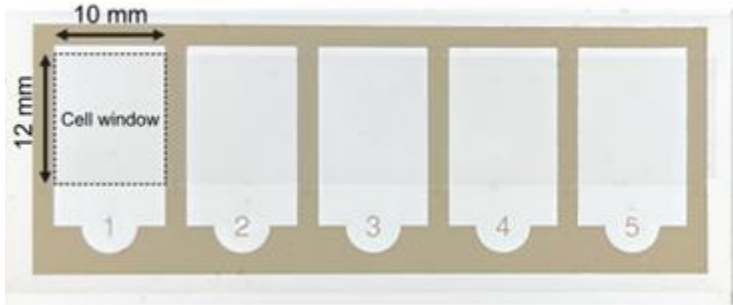
$$E(x, t) = \frac{\frac{I}{AF} + \sum_i D_i z_i \frac{\partial c_i}{\partial x}}{\frac{F}{RT} \sum_i D_i z_i^2 c_i}$$

Galvanostatic conditions, *i.e.*,  $I = \text{const}$



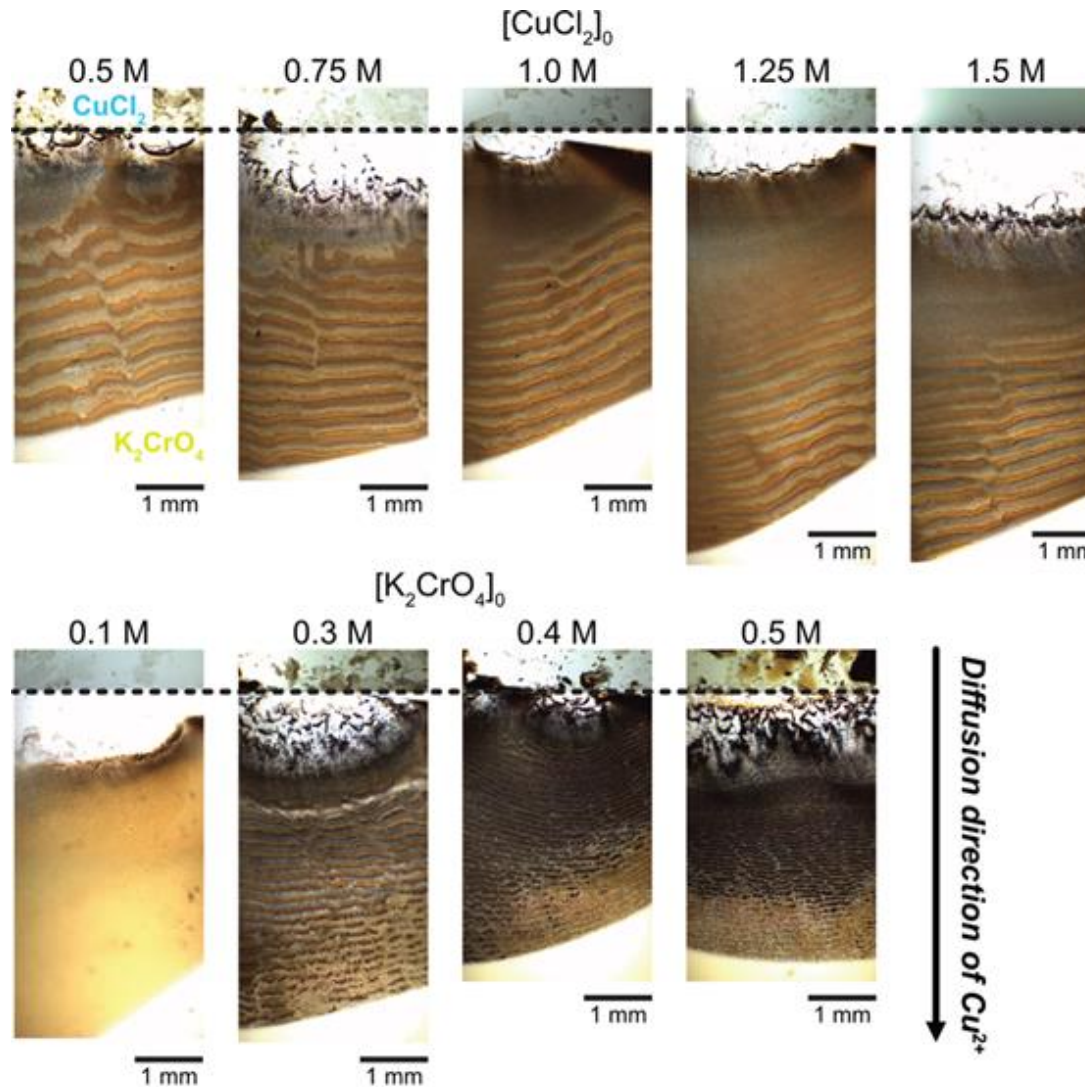
# Further directions – reaction with mass transport

## I. Periodic precipitation – gel-free environment



# Further directions – reaction with mass transport

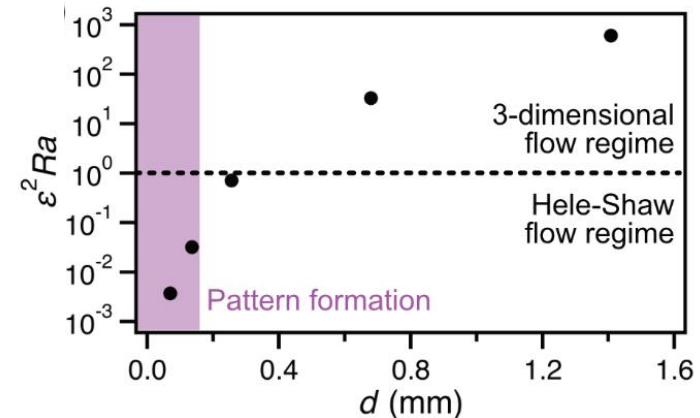
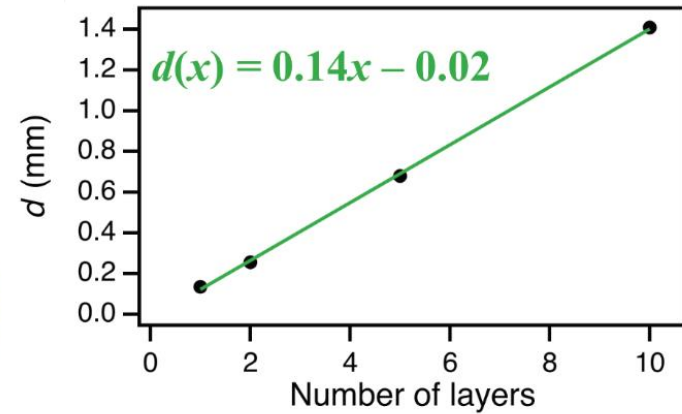
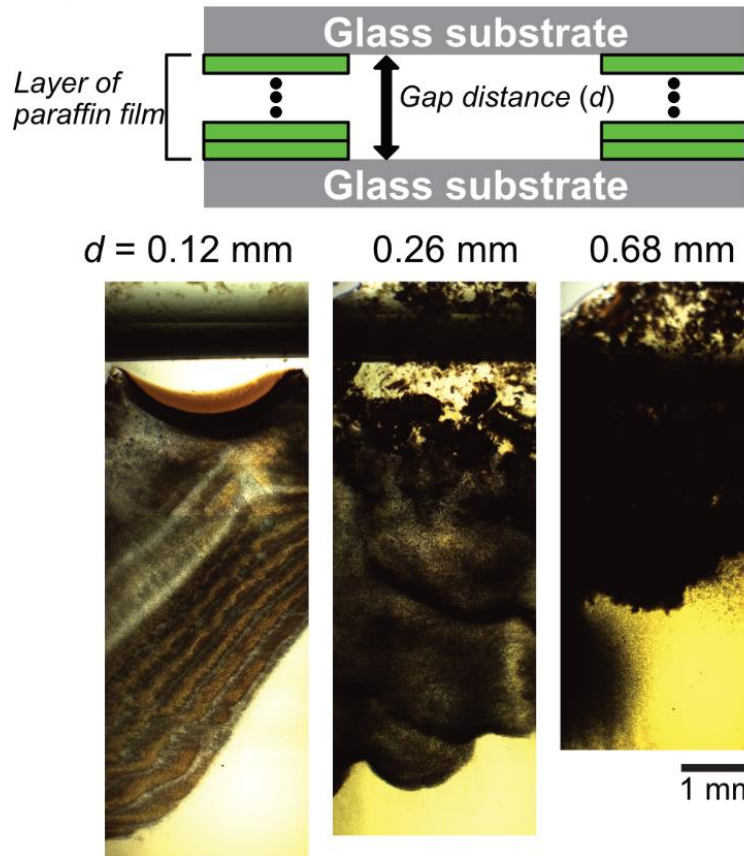
## I. Periodic precipitation – gel-free environment





# Further directions – reaction with mass transport

## I. Periodic precipitation – gel-free environment



$$Ra = \frac{g\Delta\rho_s d^2 L}{12\mu D} \text{ Rayleigh-Darcy number}$$

$$\epsilon = \frac{d}{L\sqrt{12}} \text{ geometry parameter}$$

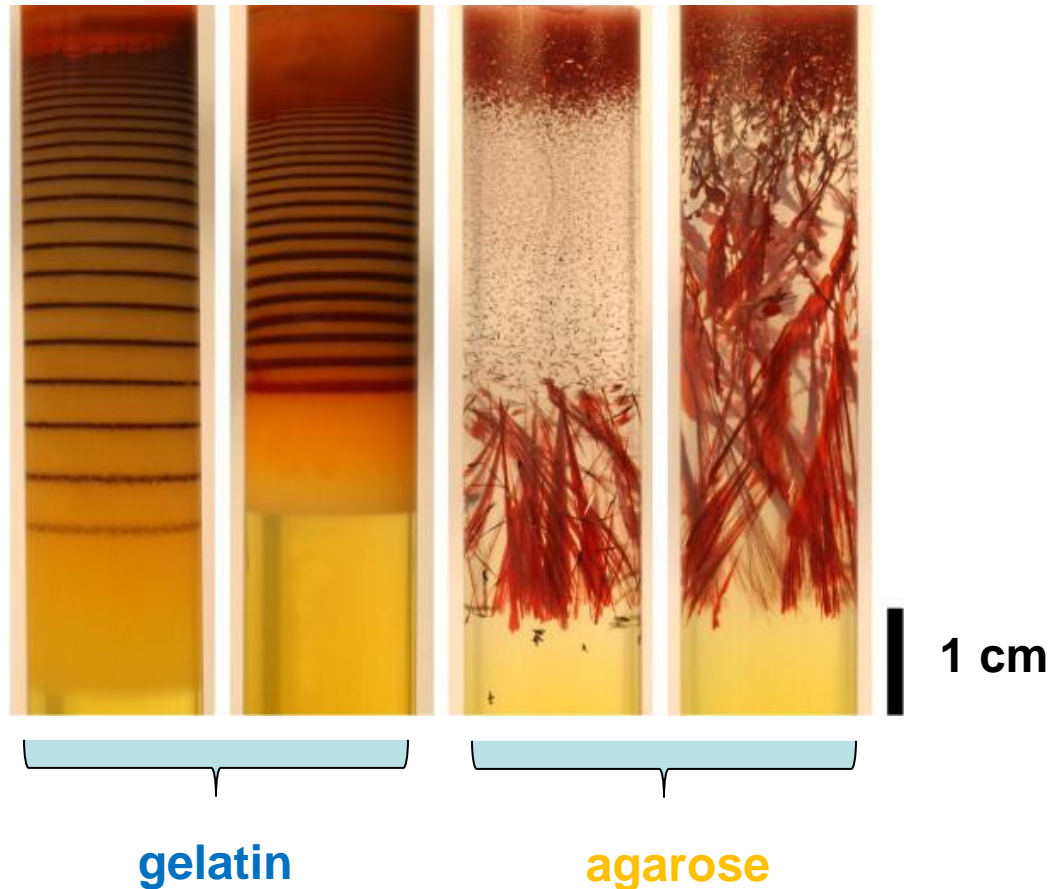
$$\epsilon^2 Ra$$

**Hele-Shaw regime ( $\epsilon^2 Ra < 1$ )**

**flow regime ( $\epsilon^2 Ra \geq 1$ )**

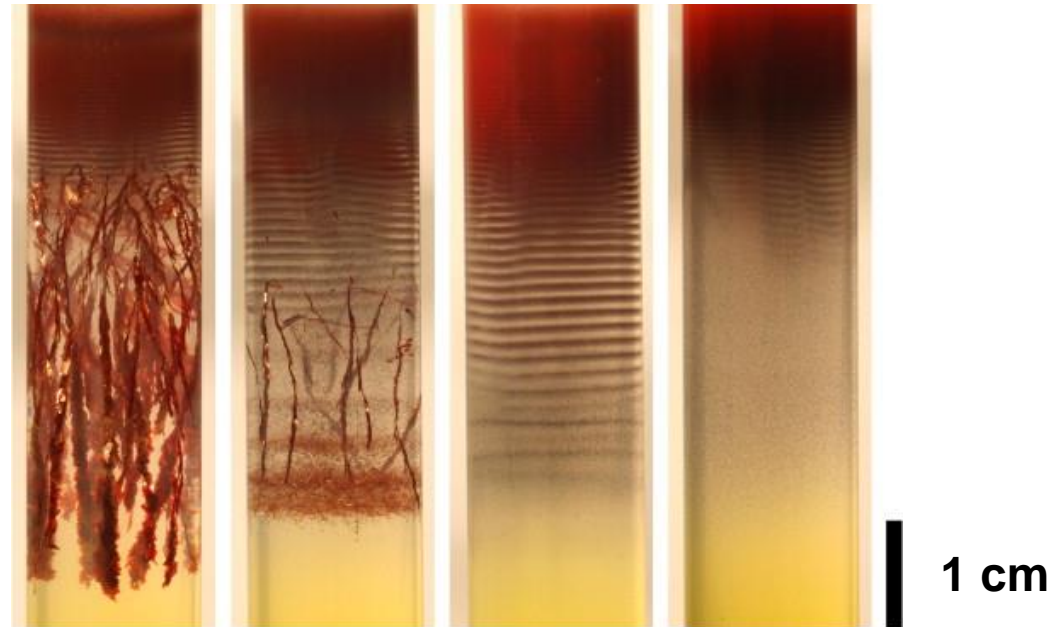
# Further directions – reaction with mass transport

## I. Periodic precipitation – gel-free environment



# Further directions – reaction with mass transport

## I. Periodic precipitation – gel-free environment



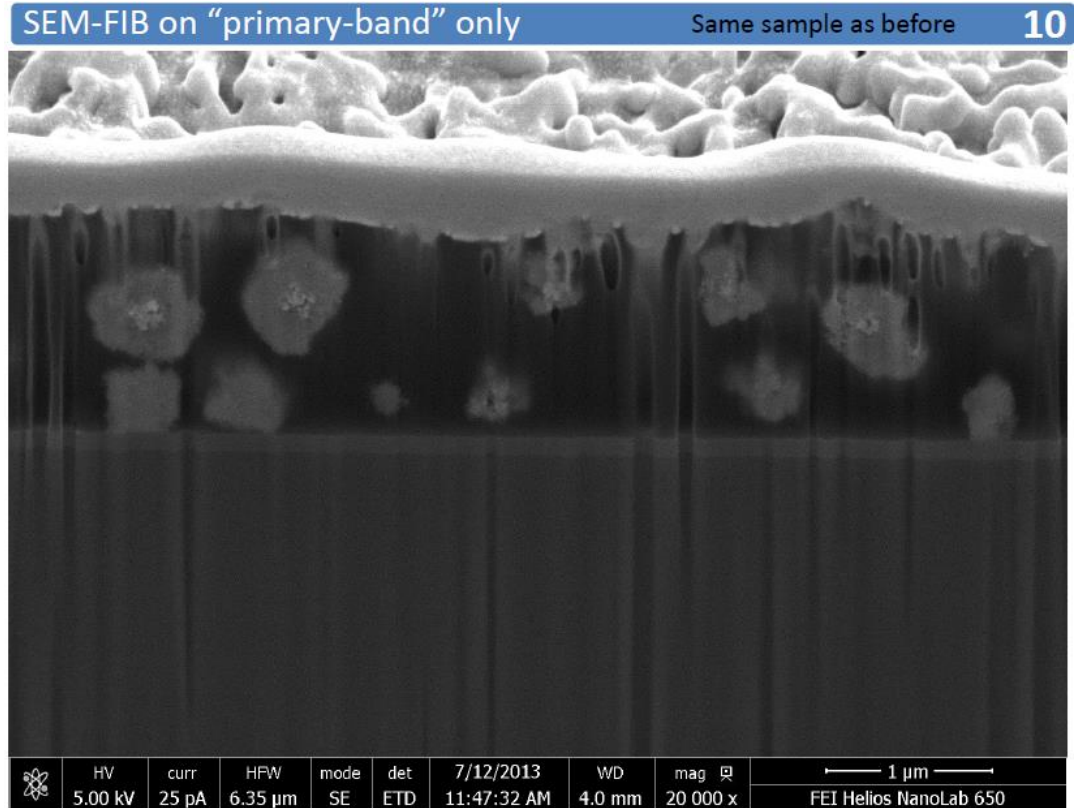
gelatin (w/w %) :      0.001      0.005      0.01      0.1

agarose gel: 0.5 w/w %



# Further directions – reaction with mass transport

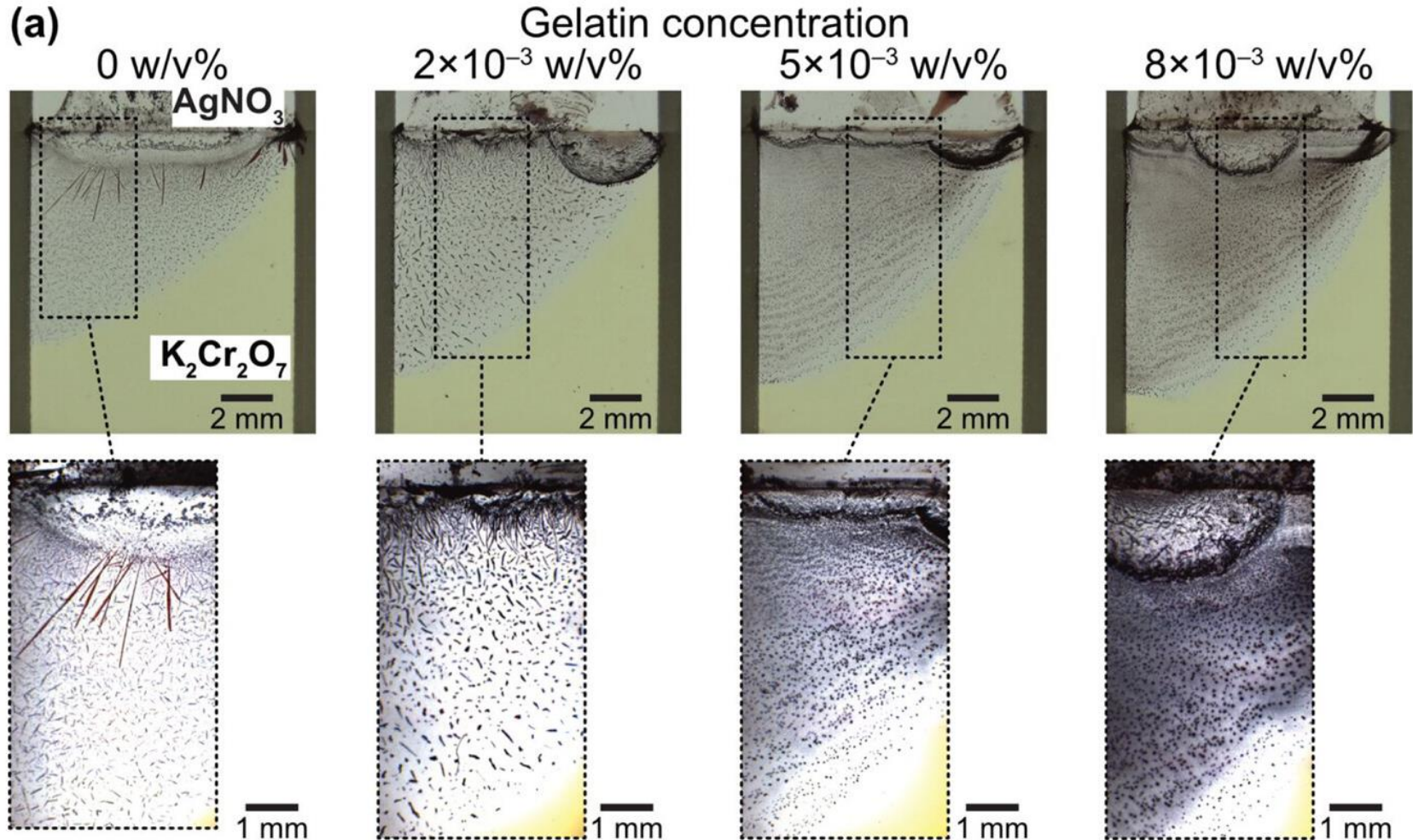
## I. Periodic precipitation – gel-free environment





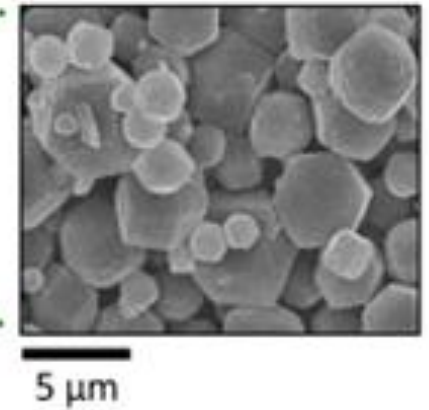
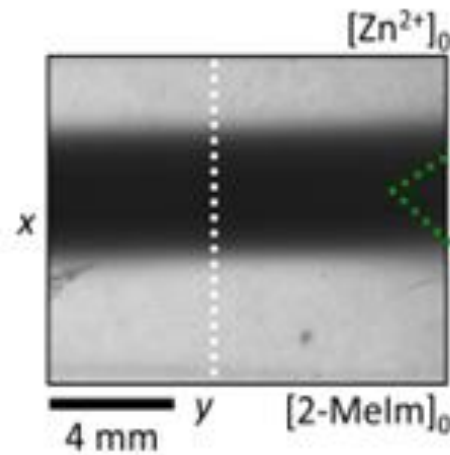
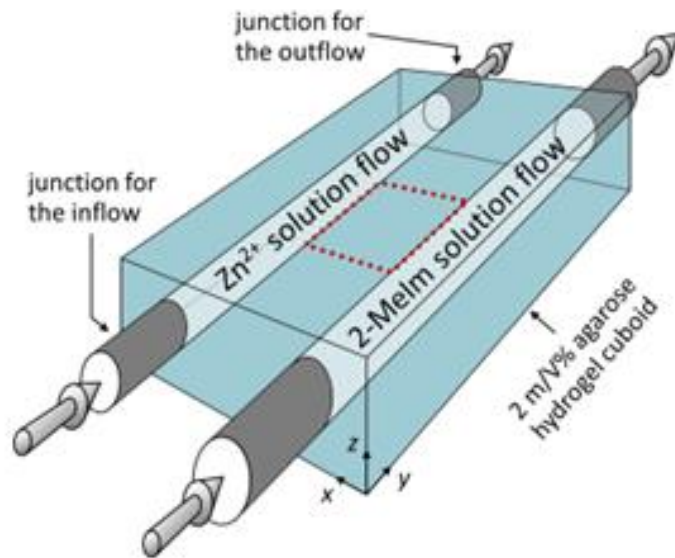
# Further directions – reaction with mass transport

## I. Periodic precipitation – gel-free environment



# Further directions – reaction with mass transport

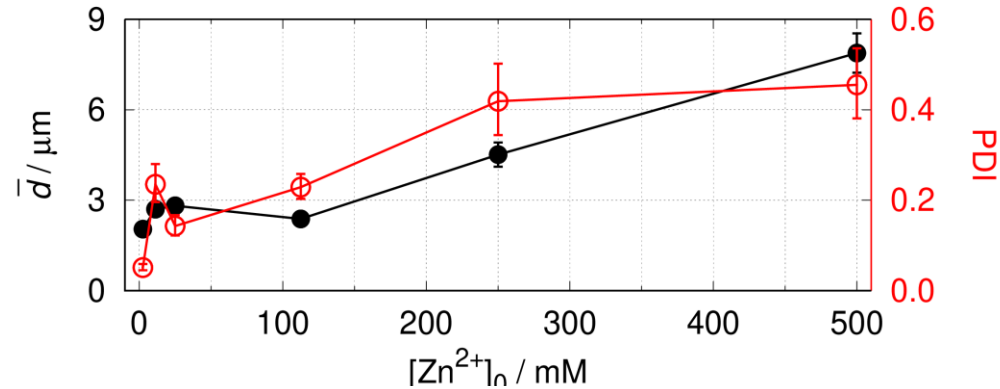
## II. Antagonistic mass fluxes



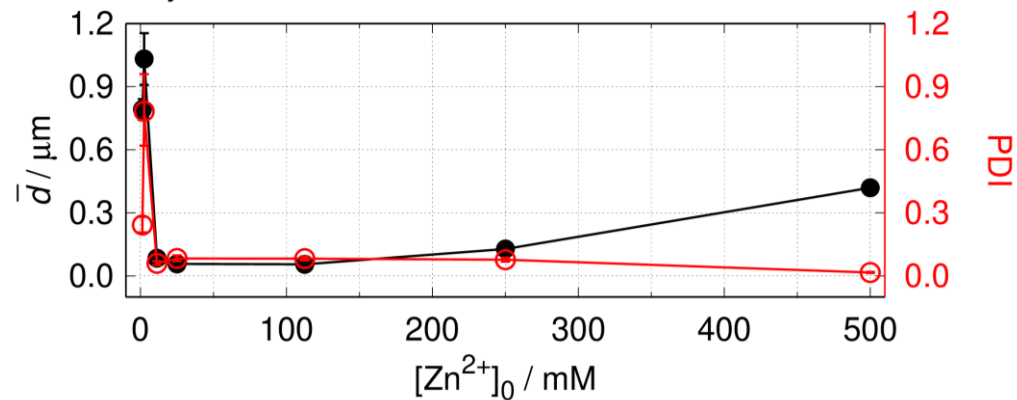
# Further directions – reaction with mass transport

## II. Antagonistic mass fluxes

(a) Out-of-equilibrium synthesis

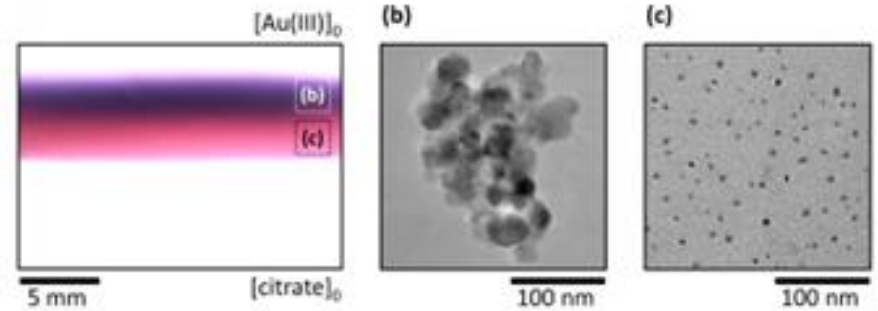
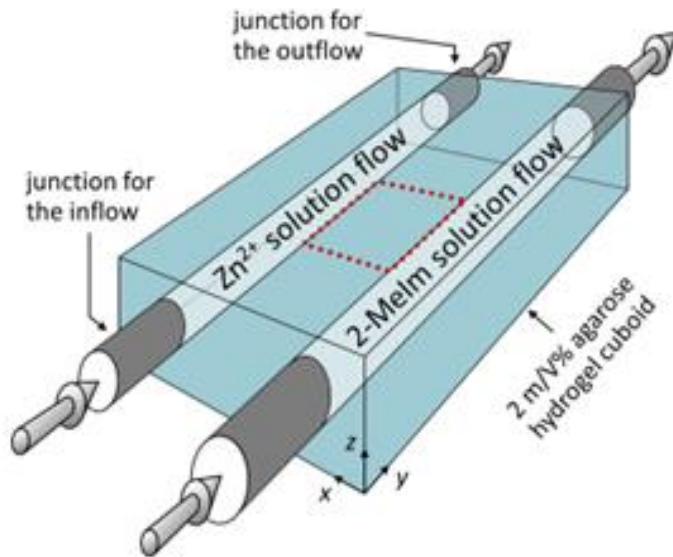


Bulk synthesis



# Further directions – reaction with mass transport

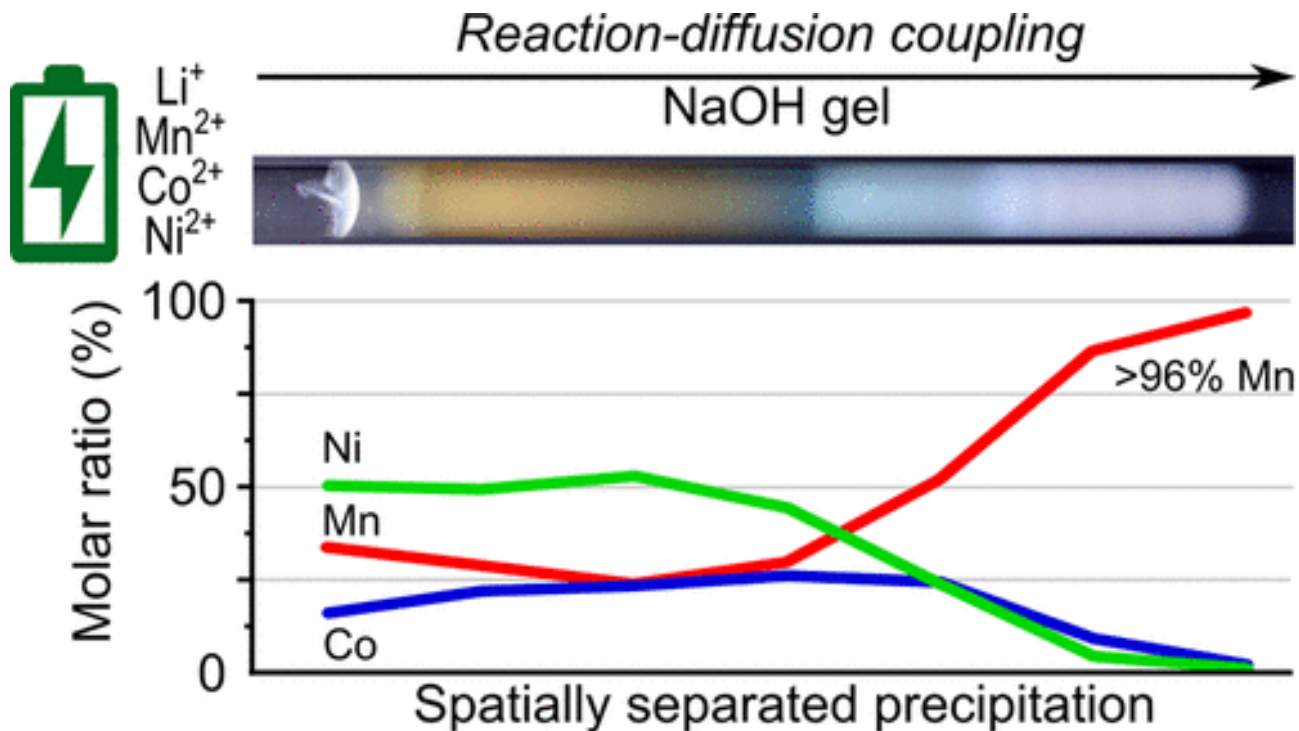
## II. Antagonistic mass fluxes





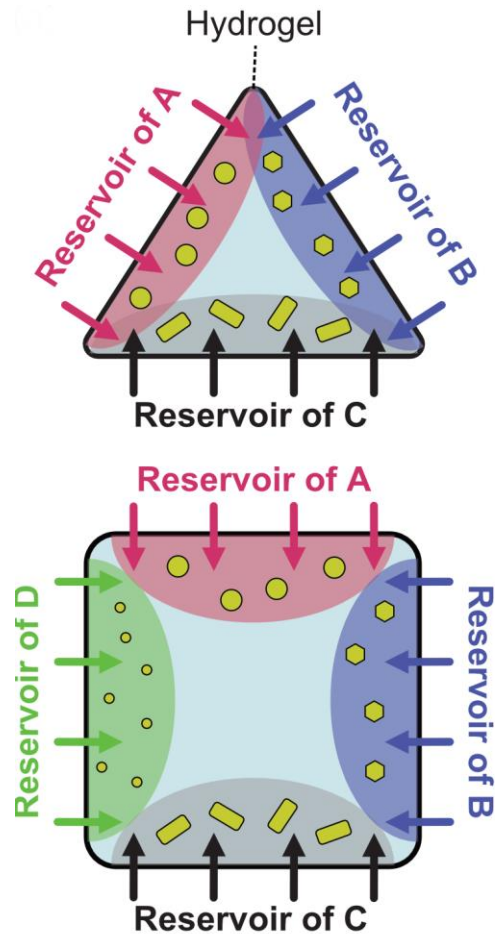
# Further directions – reaction with mass transport

## III. Separation of metal cations



# Further directions – reaction with mass transport

## IV. Hydrogel reactors



- A: Metal ion
- B: Linker or reducing agent
- C: Additives (e.g. surfactant)
- D: Additives (e.g. another reducing agent)

# Acknowledgments

## ■ Special thanks

- Norbert Német (Budapest University of Technology and Economics)
- Dr. Masaki Itatani (Hokkaido University)
- Prof. Federico Rossi, Dr. Paola Albanese, Ms. Nadia Valletti (University of Siena, Italy)
- Prof. Ágota Tóth, Prof. Dezső Horváth, Dr. Gábor Schusztar, Dr. Paszkál Papp (University of Szeged, Hungary)
- Prof. Robert Horvath, Dr. Sándor Kurunczi, (Center for Energy Research, Hungary)
- Dr. Gábor Holló (University of Lausanne, Switzerland)
- Prof. Nobuhiko J Suematsu (Meiji University, Japan)
- Prof. István Szalai (Eötvös University)

## ■ Grants

- The National Research, Development, and Innovation Office of Hungary
- The National Research, Development, and Innovation Fund of Hungary



北海道大学  
HOKKAIDO UNIVERSITY

UNIVERSITÀ  
DI SIENA  
1240



Centre for  
Energy Research

Unil

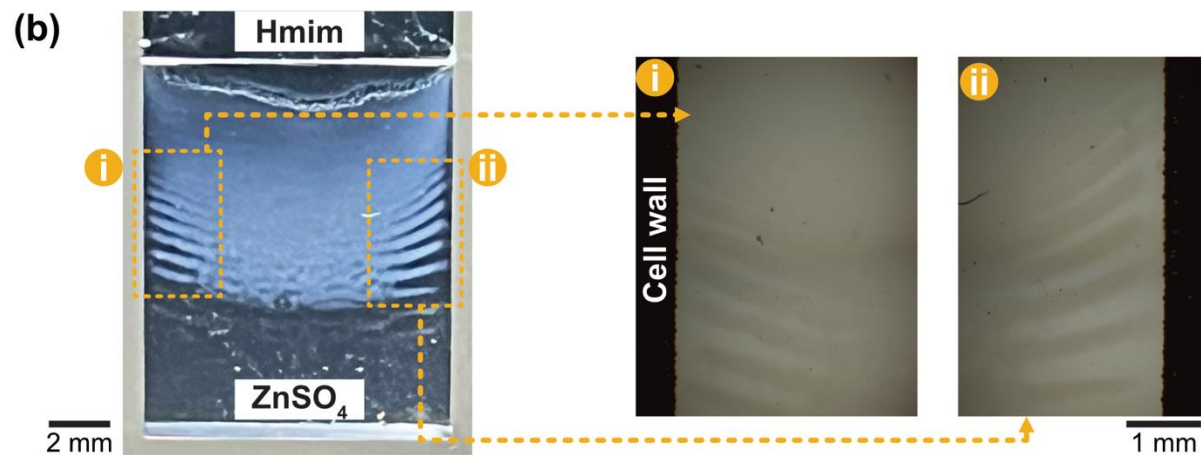
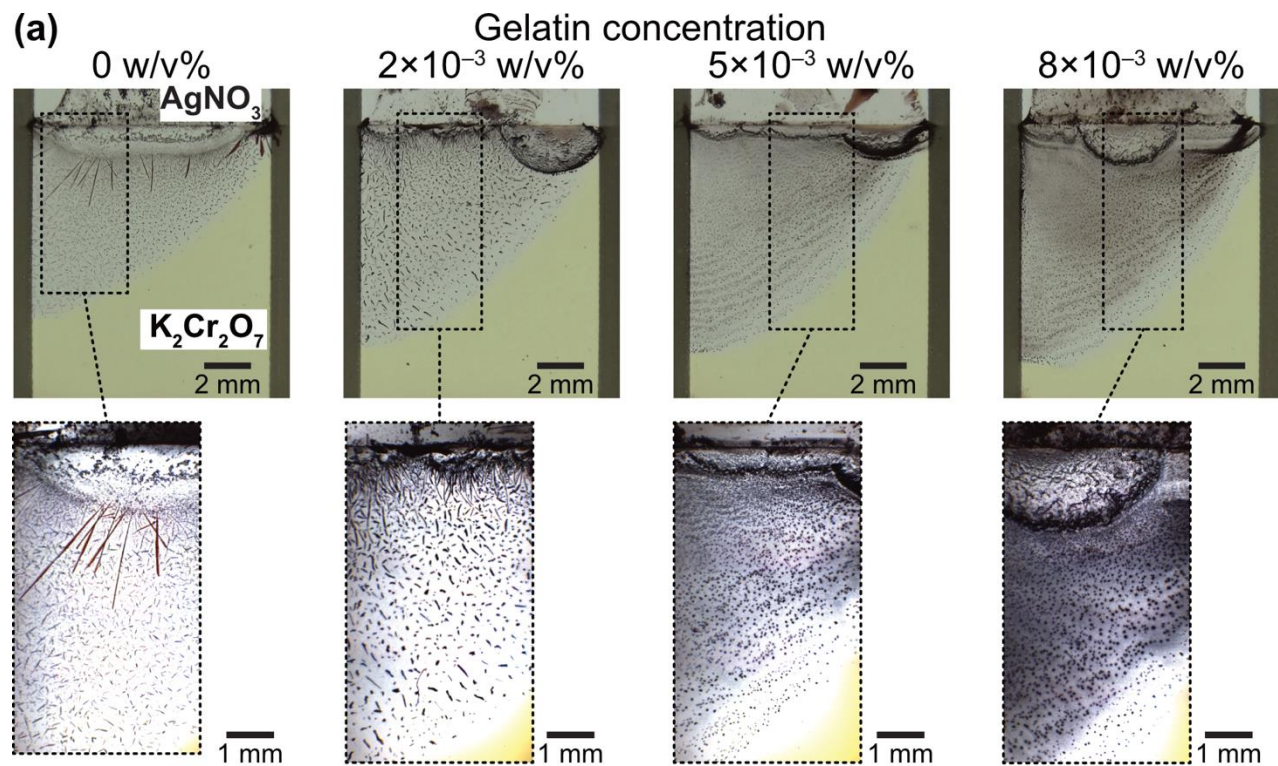
UNIL | Université de Lausanne

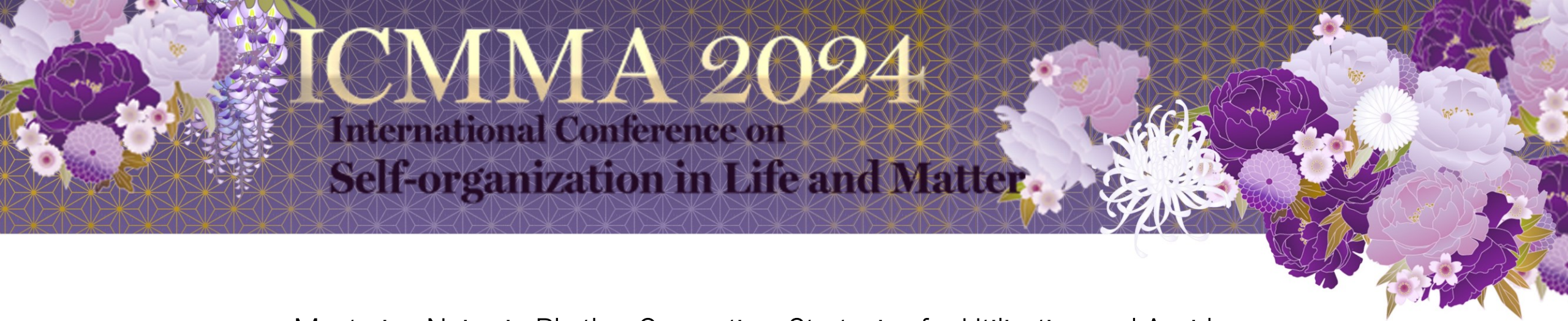


Thank you for your attention









## Mastering Noise in Rhythm Generation: Strategies for Utilization and Avoidance

Jae Kyoung Kim (KAIST & IBS)

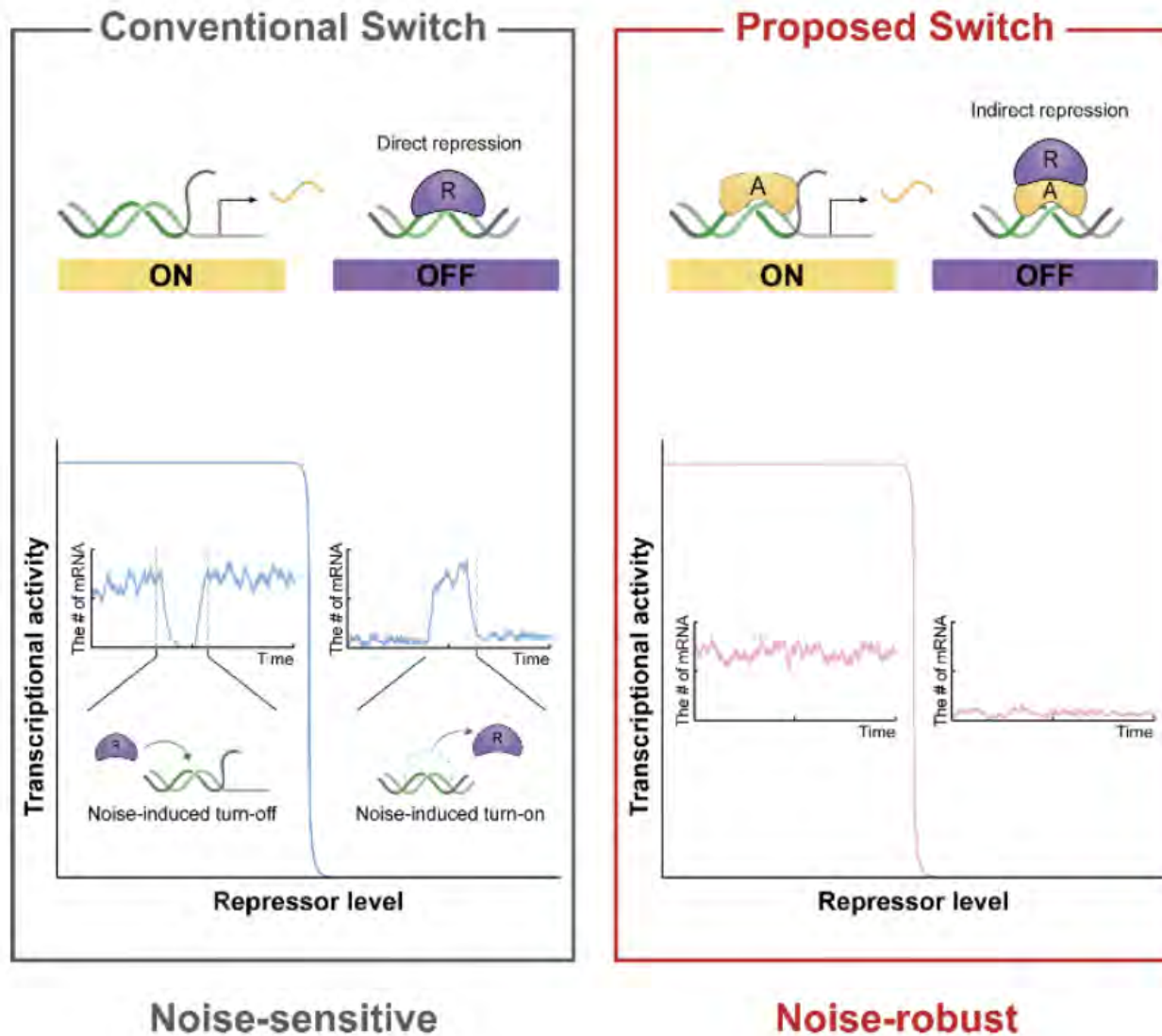
Circadian rhythms, despite being enveloped in inevitable biological noise, exhibit remarkable resilience, maintaining precise 24-hour cycles. This presentation delves into the sophisticated mechanisms by which circadian clocks navigate the challenges of noise, ensuring timely transcriptional regulation. We explore the orchestration of multiple repression strategies —encompassing sequestration, displacement, and blocking of PER proteins—employed by circadian systems to achieve robust transcriptional repression and activation amidst environmental and intrinsic fluctuations. A focal point is the utilization of photoswitches, a pivotal adaptation allowing PER proteins to accurately time their nuclear entry for transcriptional regulation, overcoming the heterogeneity in their perinuclear arrival times caused by spatiotemporal noise. Moreover, we shed light on the counterintuitive benefits of noise within this biological context. Specifically, we discuss how a controlled degree of noise can sharpen the circadian rhythm's waveform and enhance the signal-to-noise ratio, offering insights into the adaptive significance of noise in biological systems. This talk aims to underscore the intricate balance between noise utilization and avoidance, highlighting its role in the resilience and precision of circadian rhythms.

### References

- [1]Otohe Y, Jeong EM, Ito S, Fukada Y\* Kim JK\* and Yoshitane H\*, Phosphorylation of DNA-binding domains of CLOCK-BMAL1 complex is essential for mammalian circadian clockwork,PNAS (2024)
- [2]Jeong EM, Kim JK, Robust Ultrasensitive Transcriptional Switch in Noisy Cellular Environments,NPJ Syst Biol & Appl (2024)
- [3]Song YM, Campbell S, Shiau L, Kim JK\*, Ott W\*, Noisy delay denoises biochemical oscillators,Physical Review Letters (2024)
- [4]Chae S, Kim DW, Igoshin OA, Lee S, Kim JK, Beyond microtubule: Cellular environment at the endoplasmic reticulum attracts proteins to the nucleus, essential for nuclear transport, iScience(2024)
- [5]Chae SJ, Kim DW, Lee S, Kim JK, Spatially coordinated collective phosphorylation filters spatiotemporal noises for precise circadian timekeeping, iScience (2023)
- [6]Beesley S\*, Kim DW\*, DAlessandro M, Jin Y, Lee K, Joo H, Young Y, Tomko R, Kim JK †, Lee C+, Wake-sleep cycles are severely disrupted by diseases affecting cytoplasmic homeostasis,PNAS (2020)



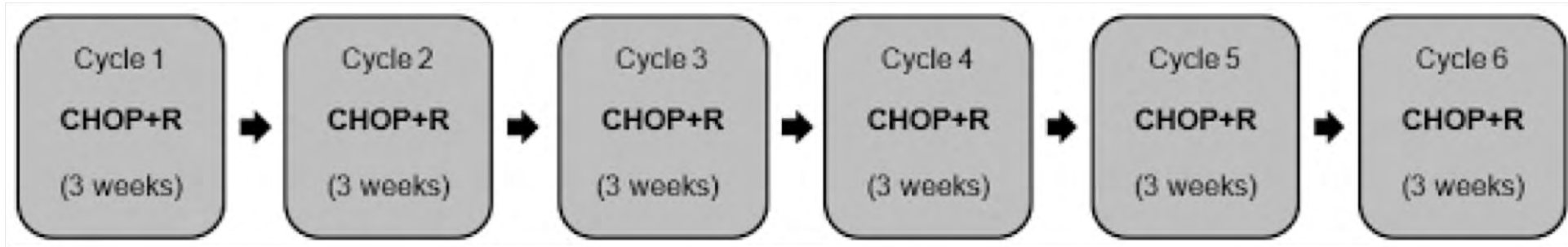
# Mastering noise in rhythm generation: strategies for utilization and avoidance



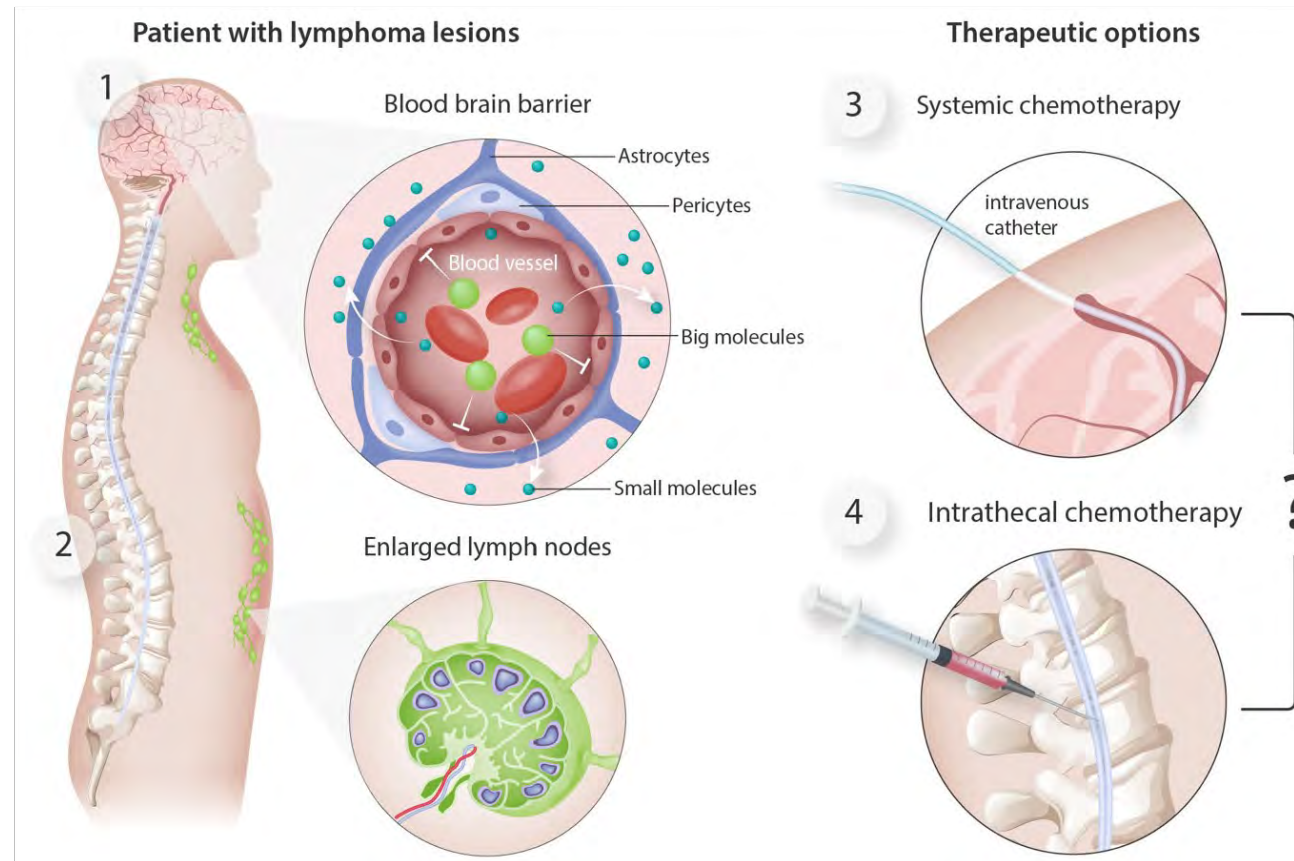
Jae Kyoung Kim

Mathematical Sciences, KAIST  
Biomedical Mathematics Group, IBS

# Anti-cancer therapy for DLBCL: **Morning** vs **Afternoon** ?



With Yungil Koh  
(Seoul Nat Medical Center)

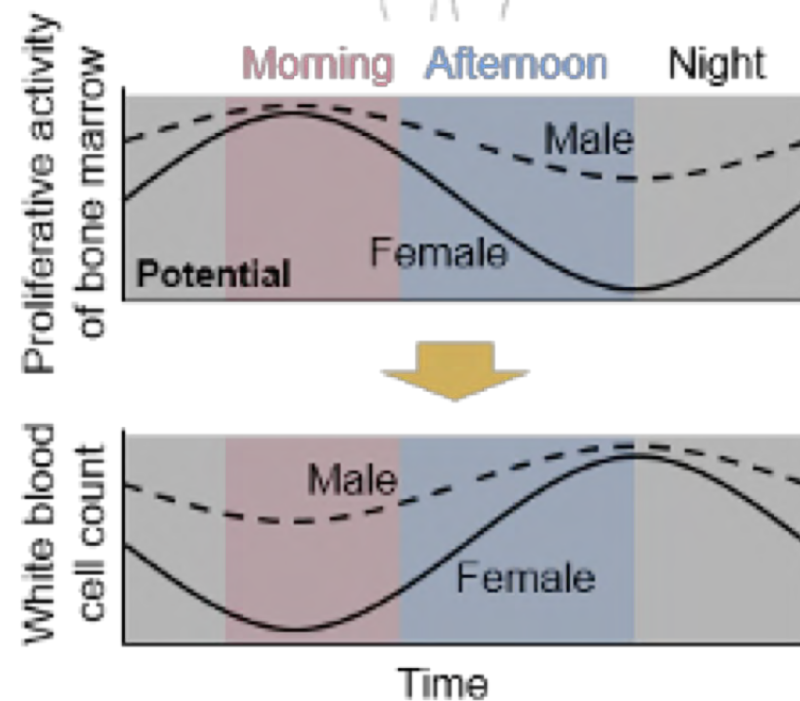
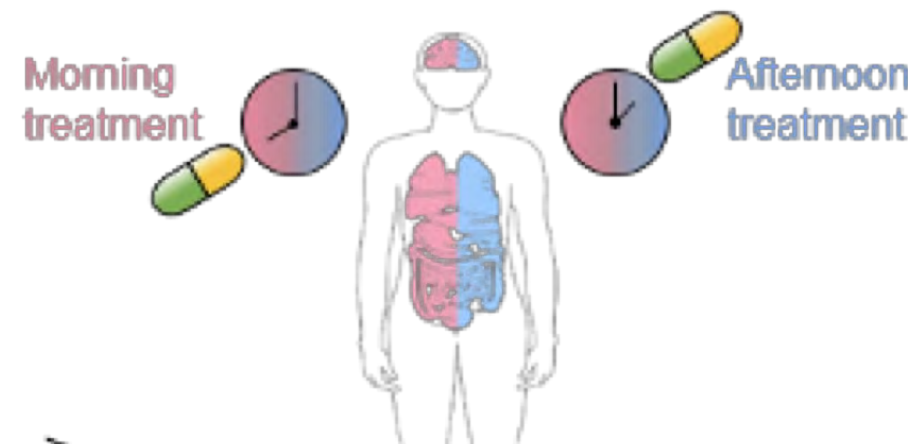
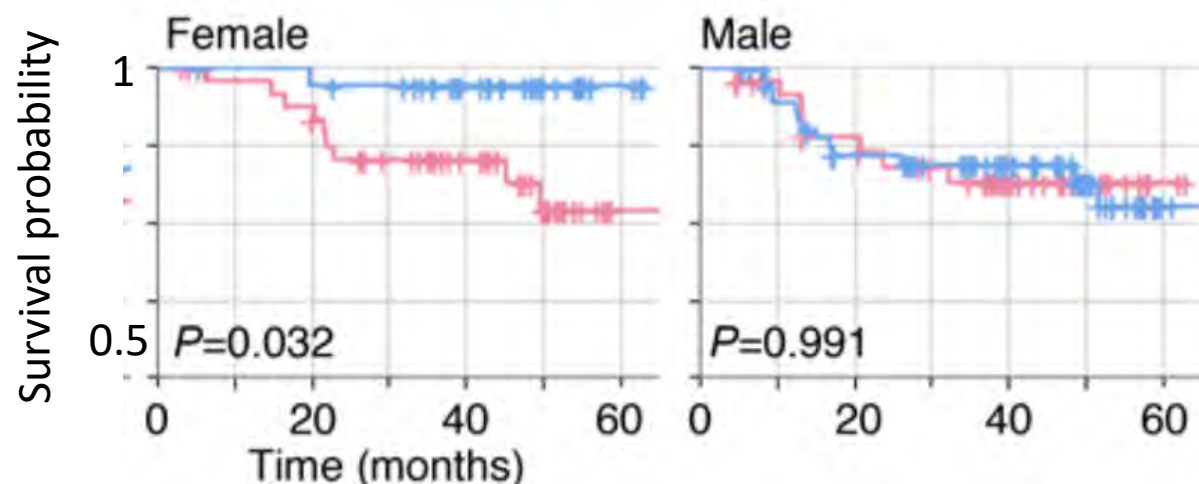




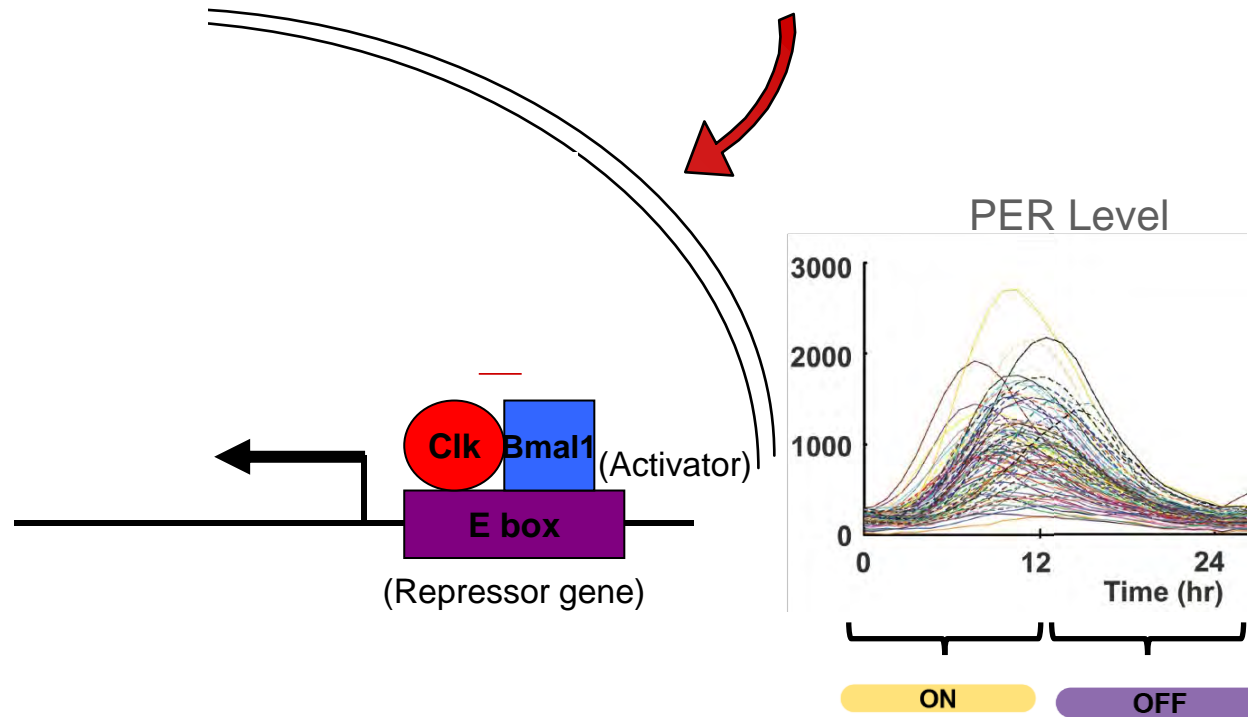
# Outcomes for R-CHOP Worse in Morning for Female Patients With Lymphoma

By Elana Gotkine HealthDay Reporter

Overall survival

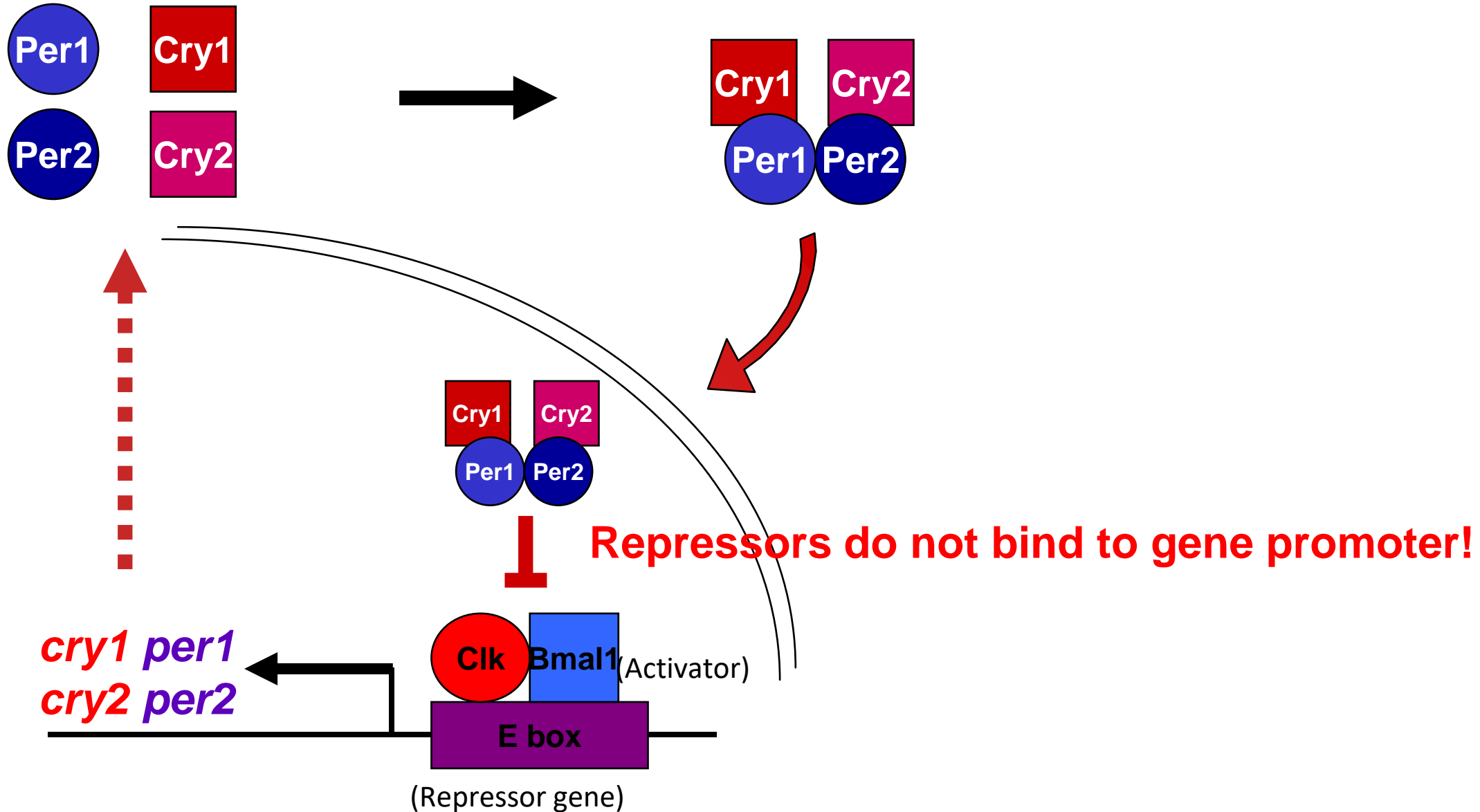


# Transcriptional negative feedback loop generates circadian rhythms



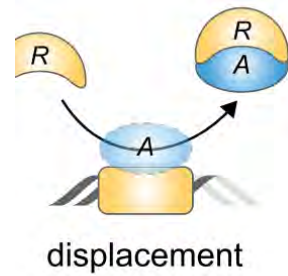
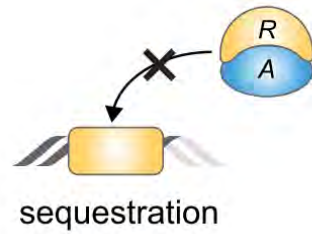
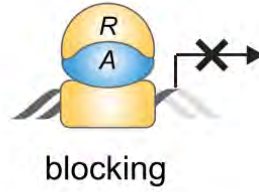
**How to turn on and off transcription for 12h everyday despite noise?**

# Indirect transcriptional repression

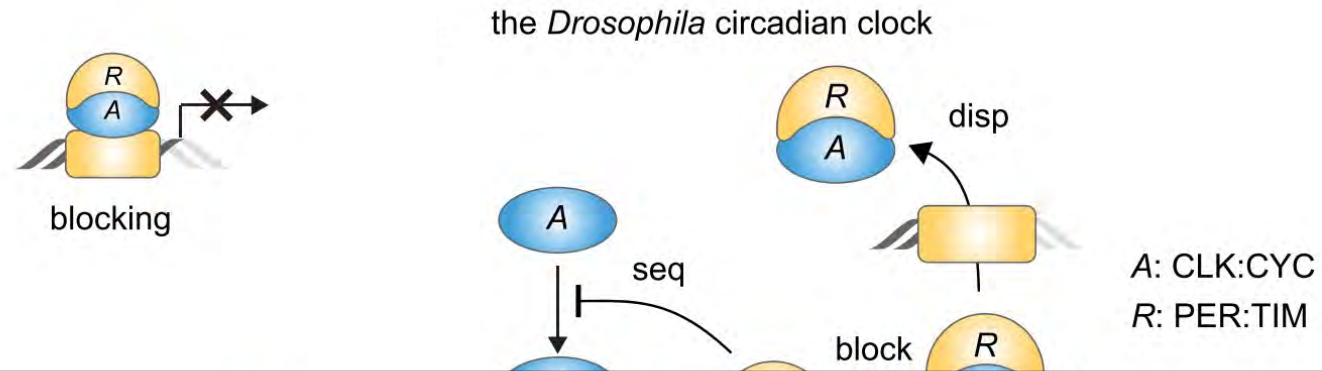




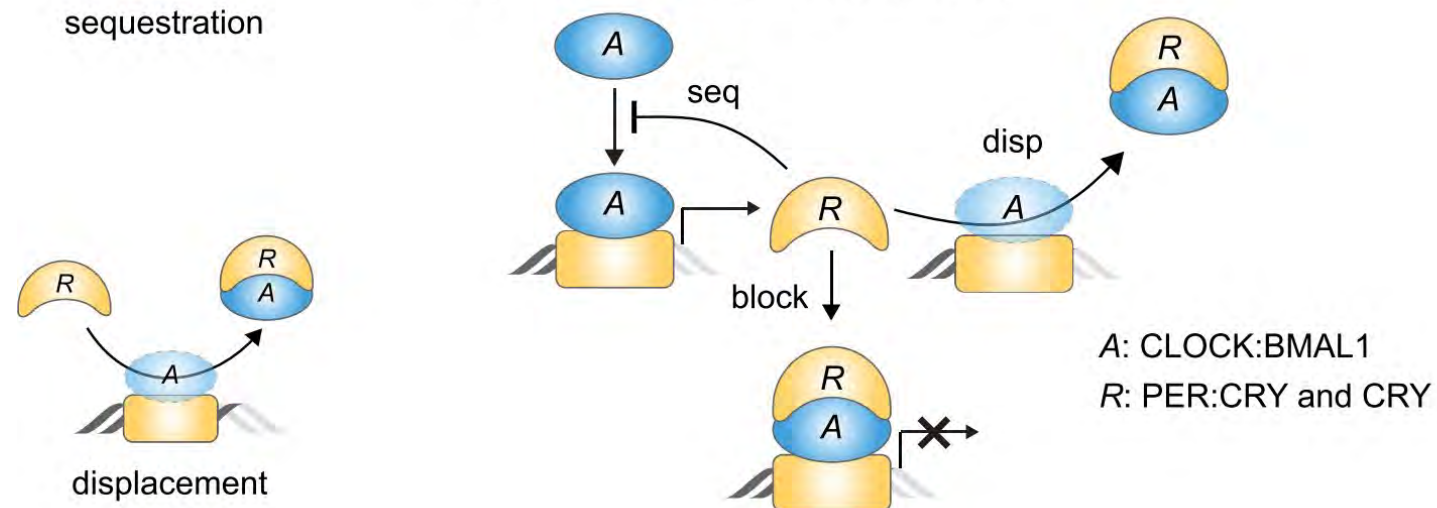
# What kind of repression mechanism is used?



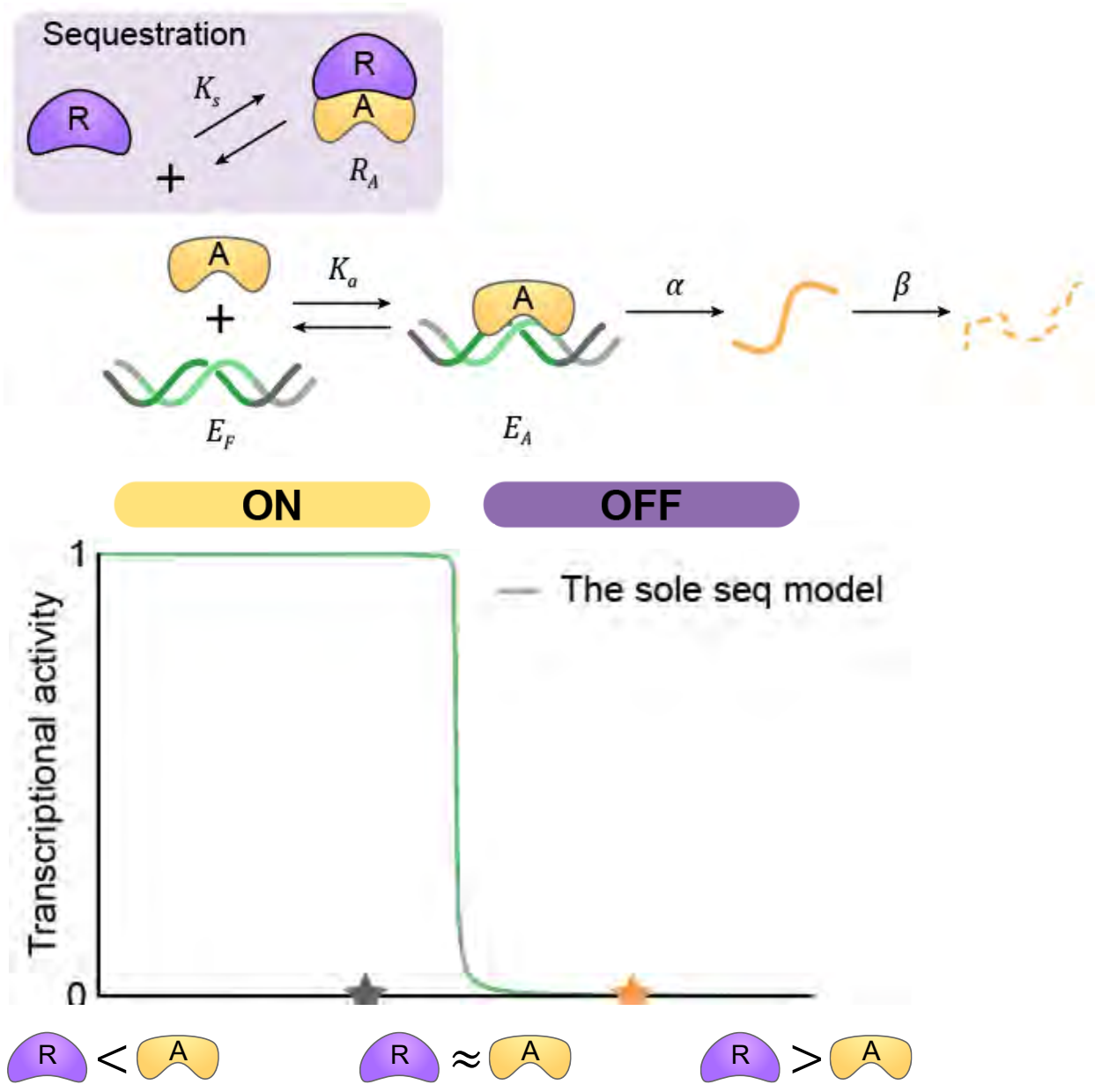
What kind of repression mechanism is used? All of them!!



**Using all of them together seems redundant!  
Why do all of them are used?**



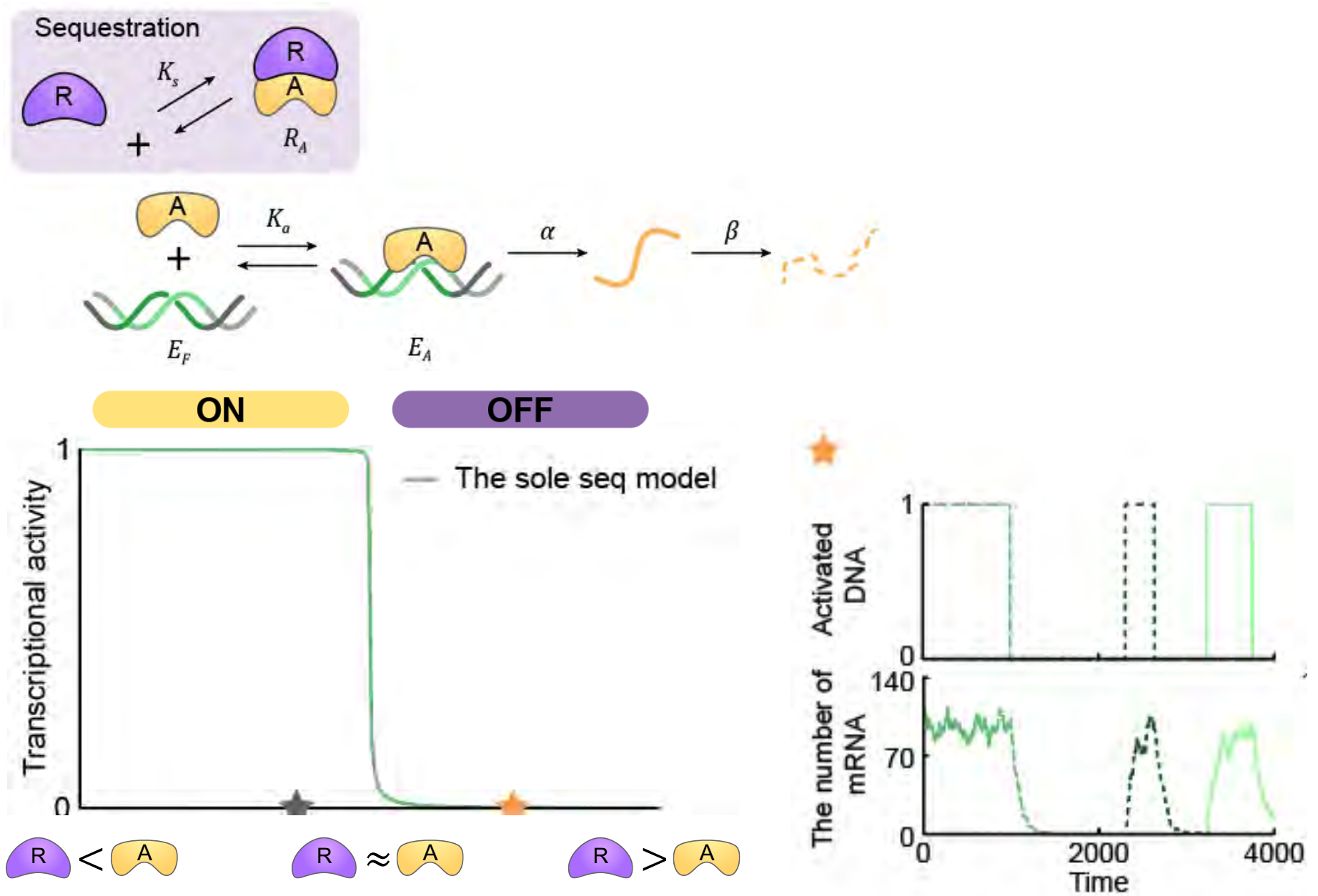
# Sequestration can generate on and off switch depending on R:A



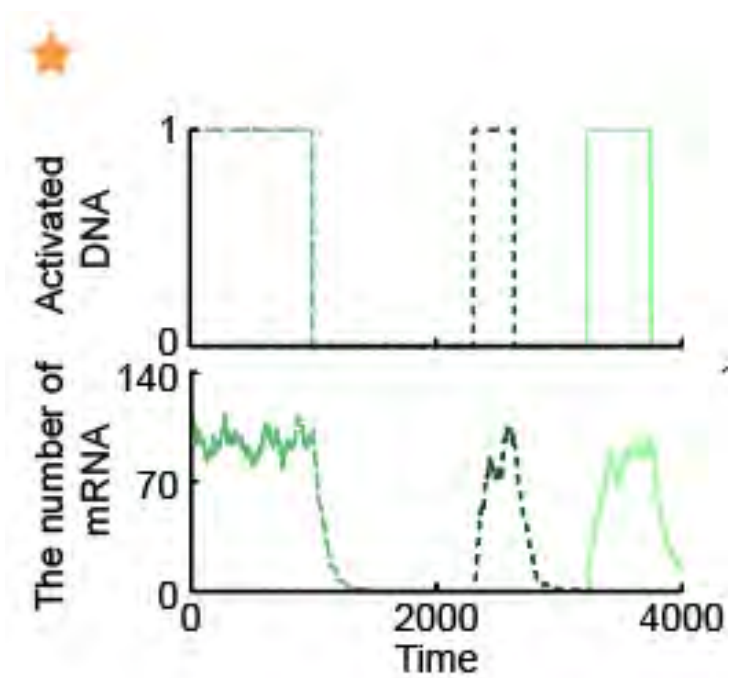
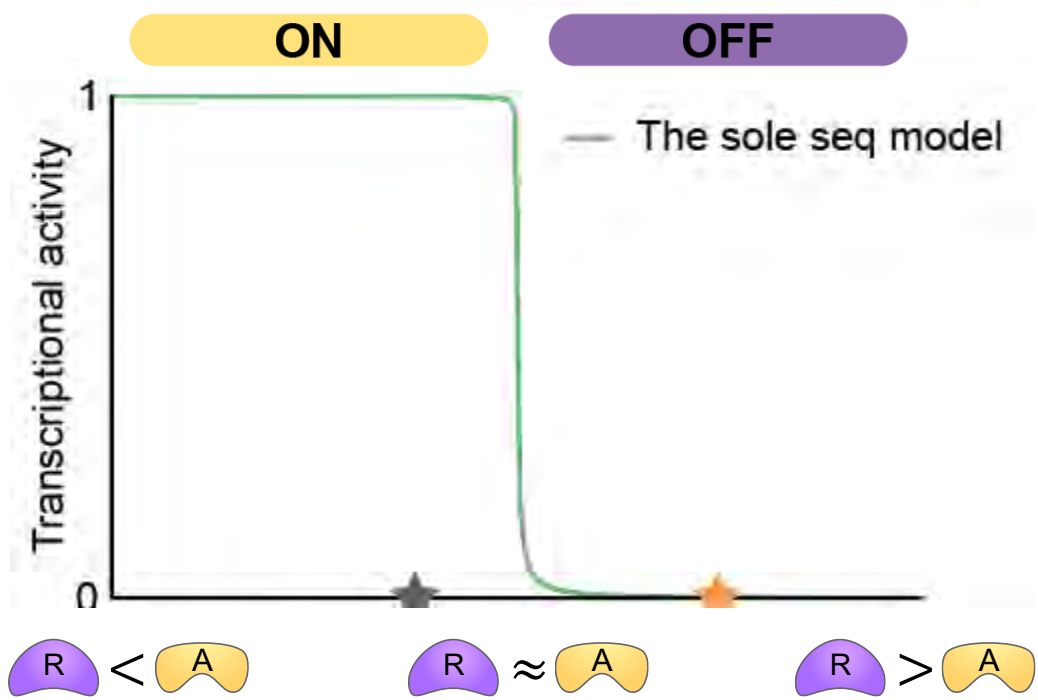
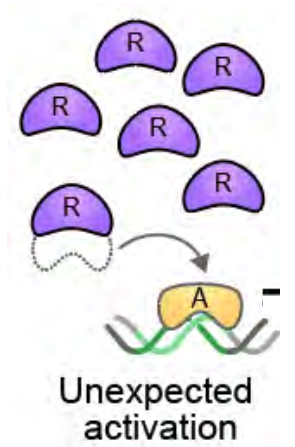
Euimin Jeong  
(IBS)



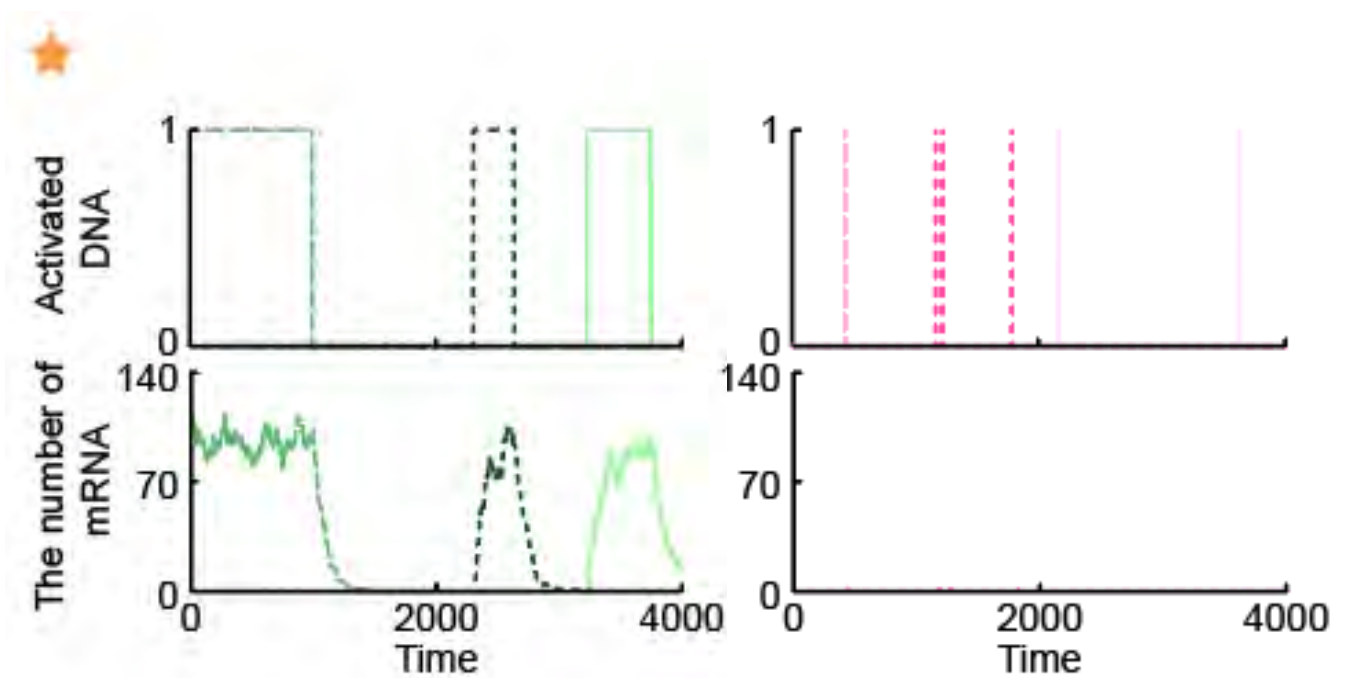
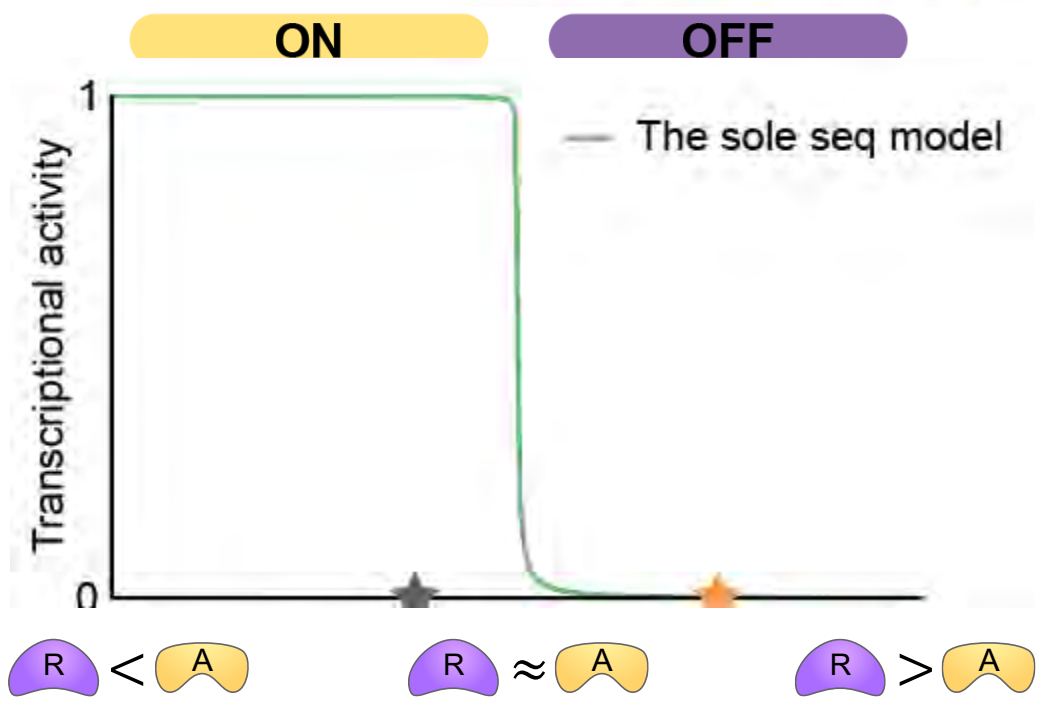
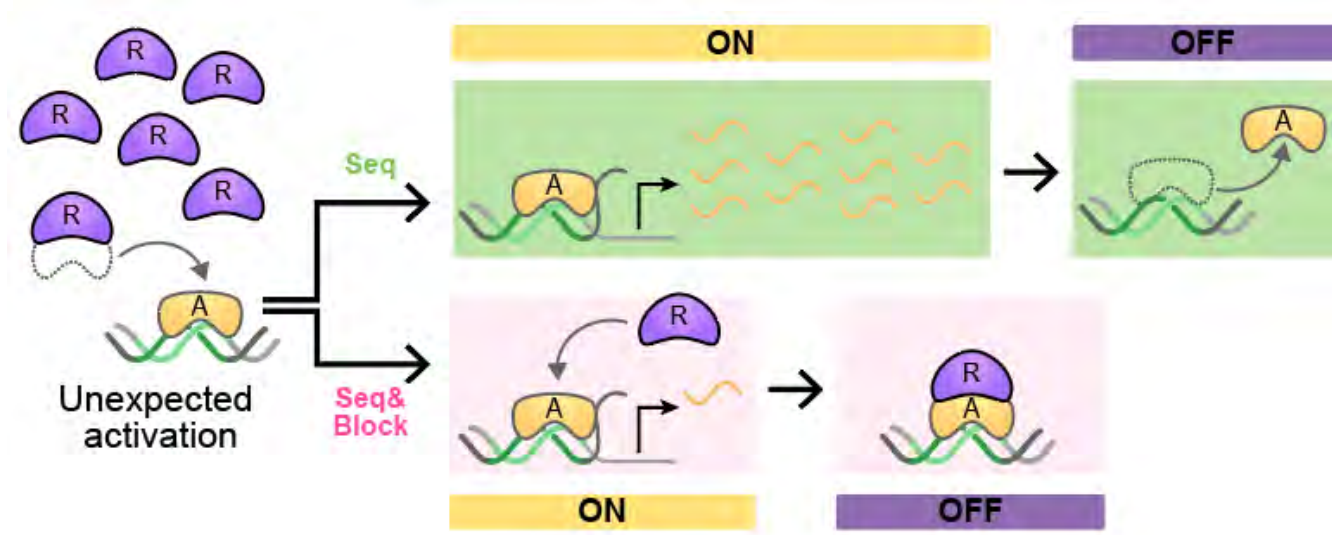
However, undesired activation occurs during repression phase to noise!



# Unexpected activation persists during the repression phase!

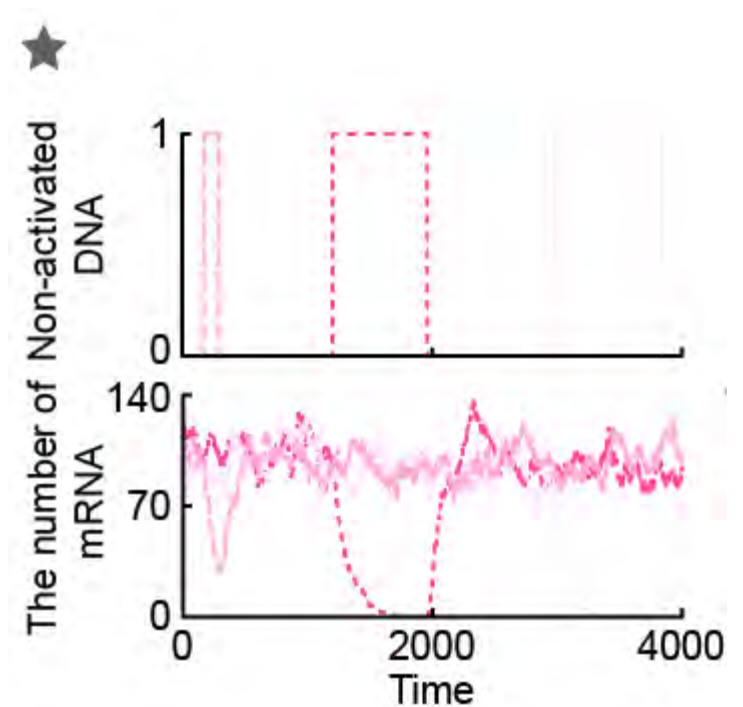
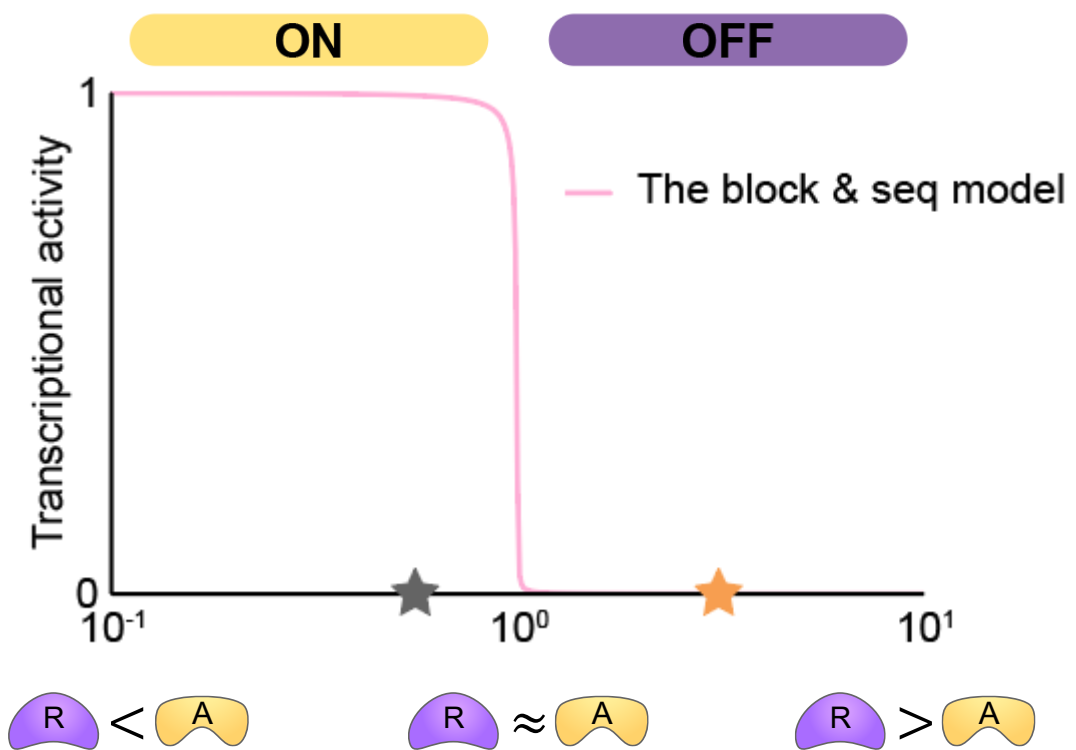


With the blocking, the unexpected activation is rapidly restored to repression.

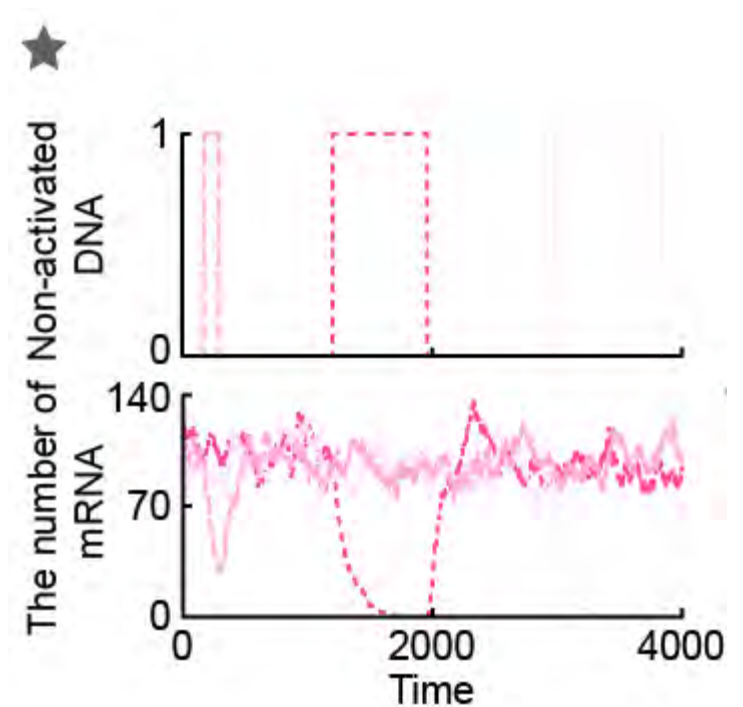
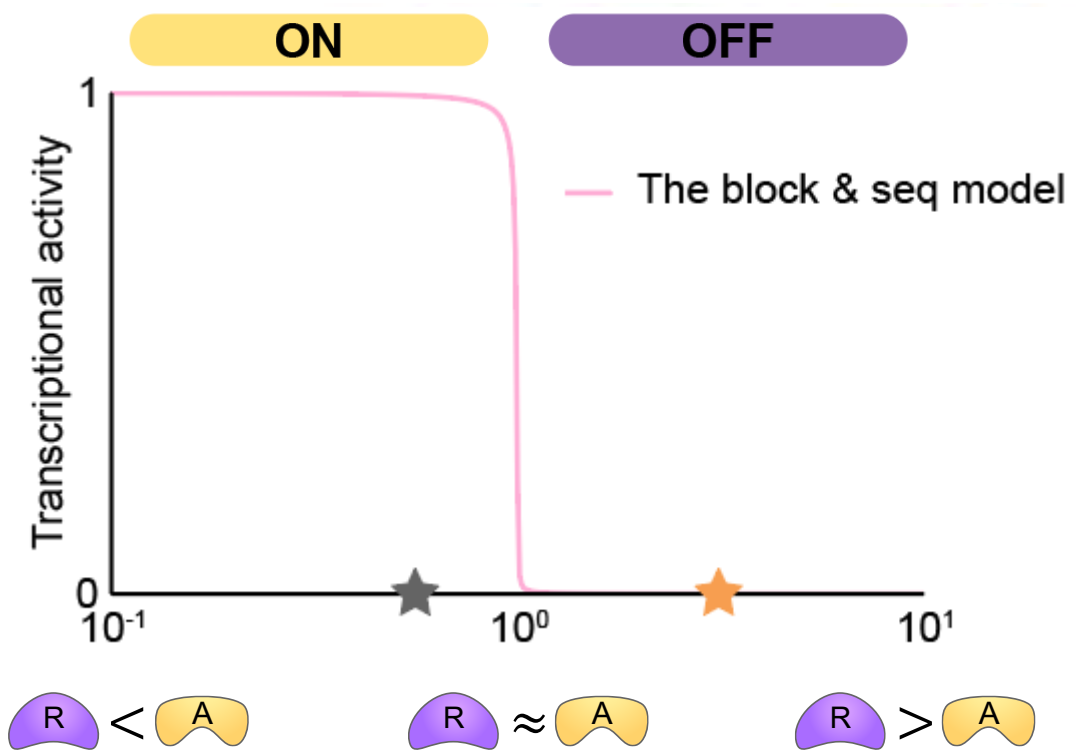
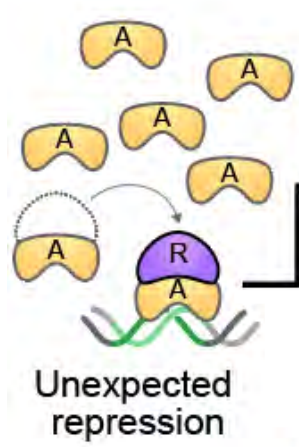




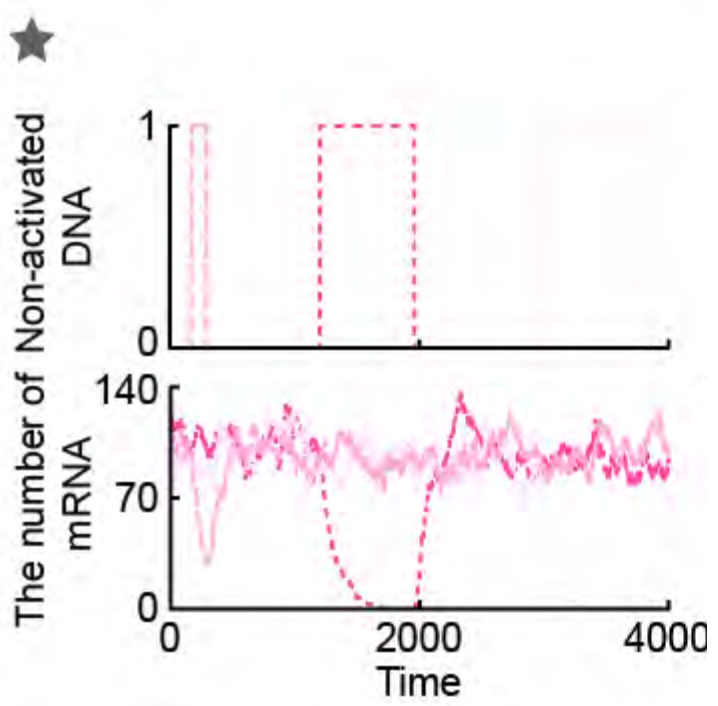
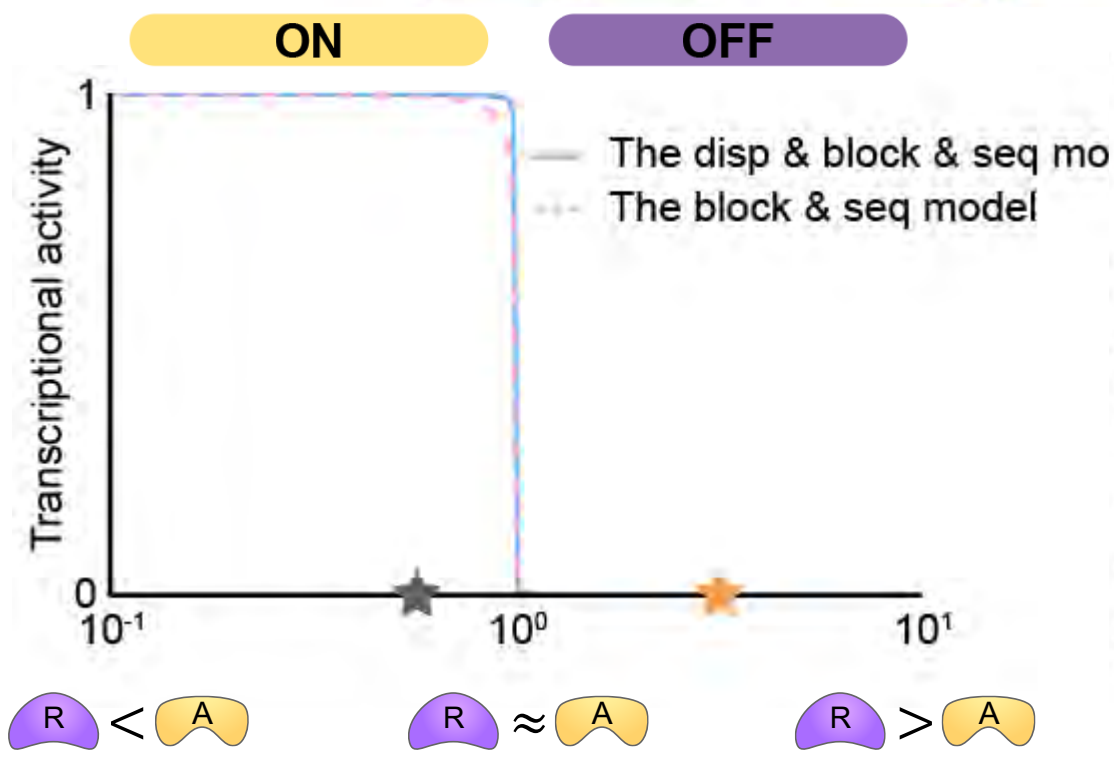
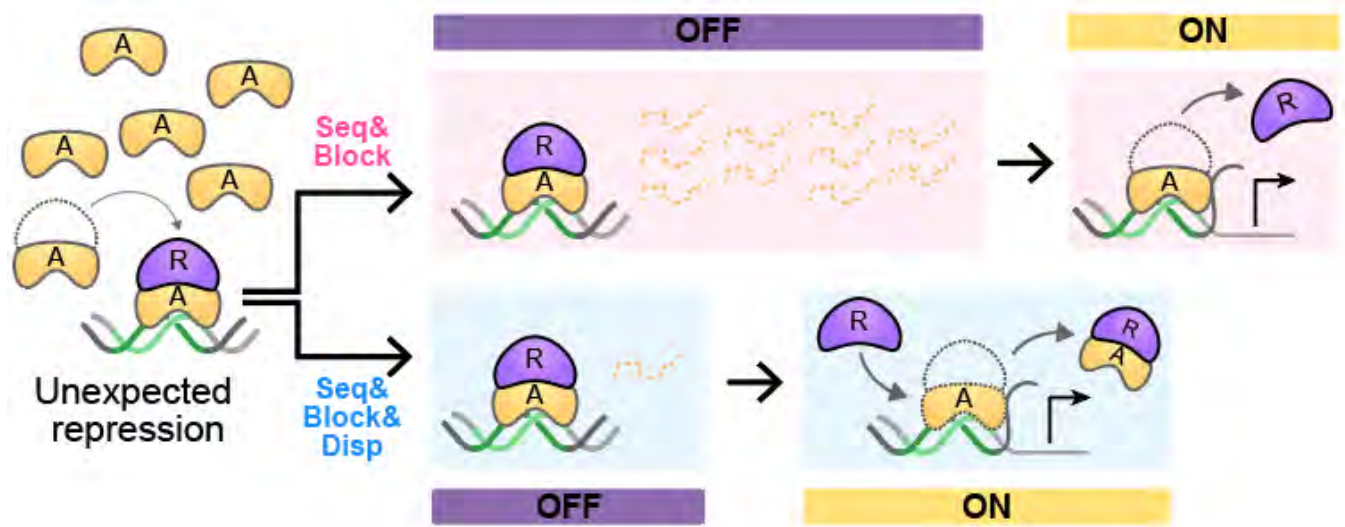
However, with the blocking, undesired repression occurs during activation phase!



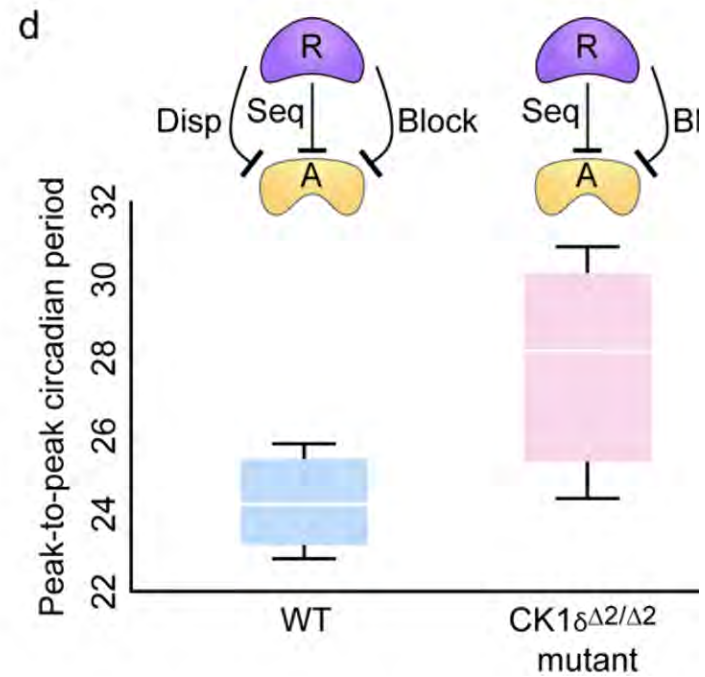
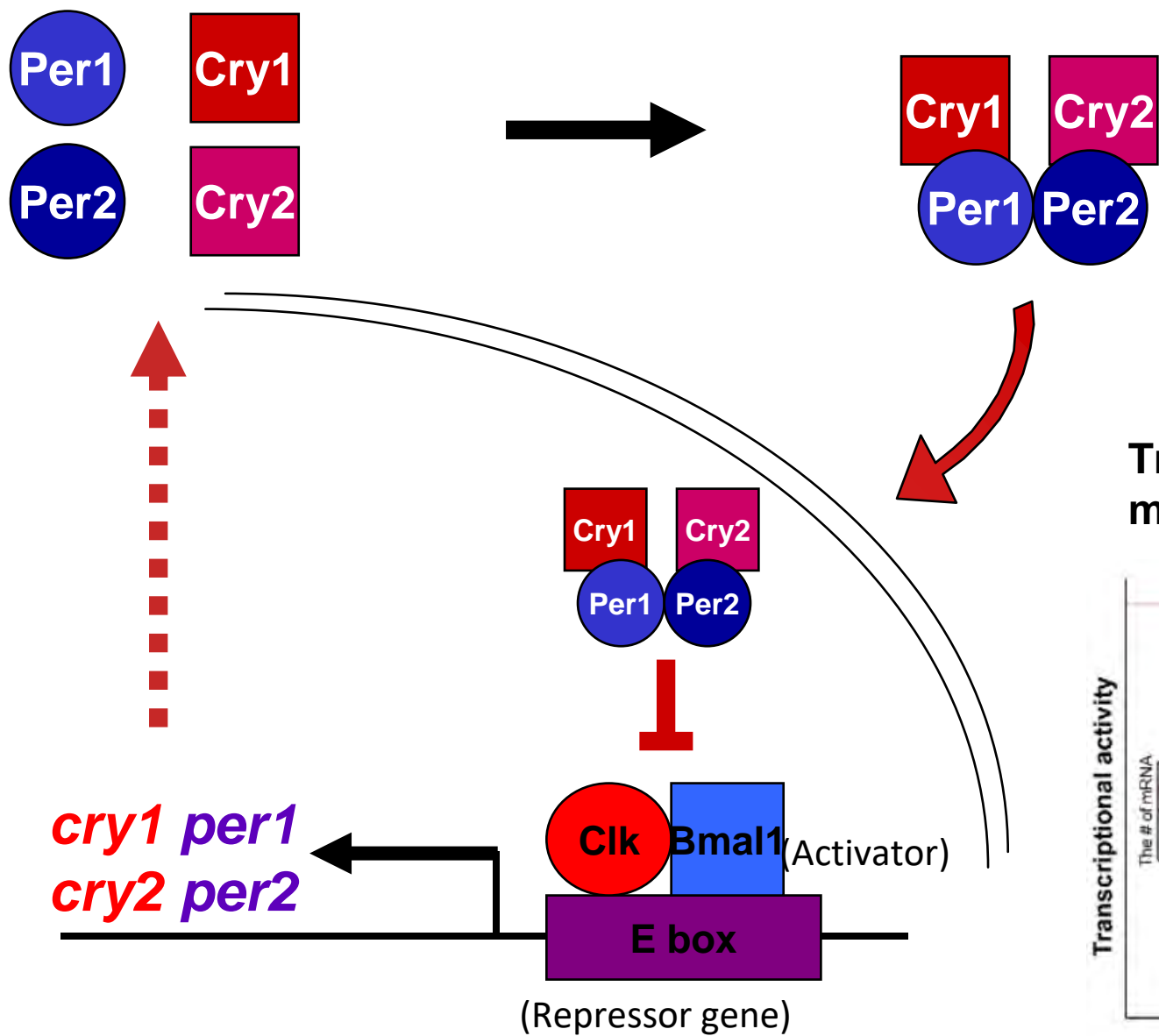
# Unexpected repression persists for a long time during activation phase



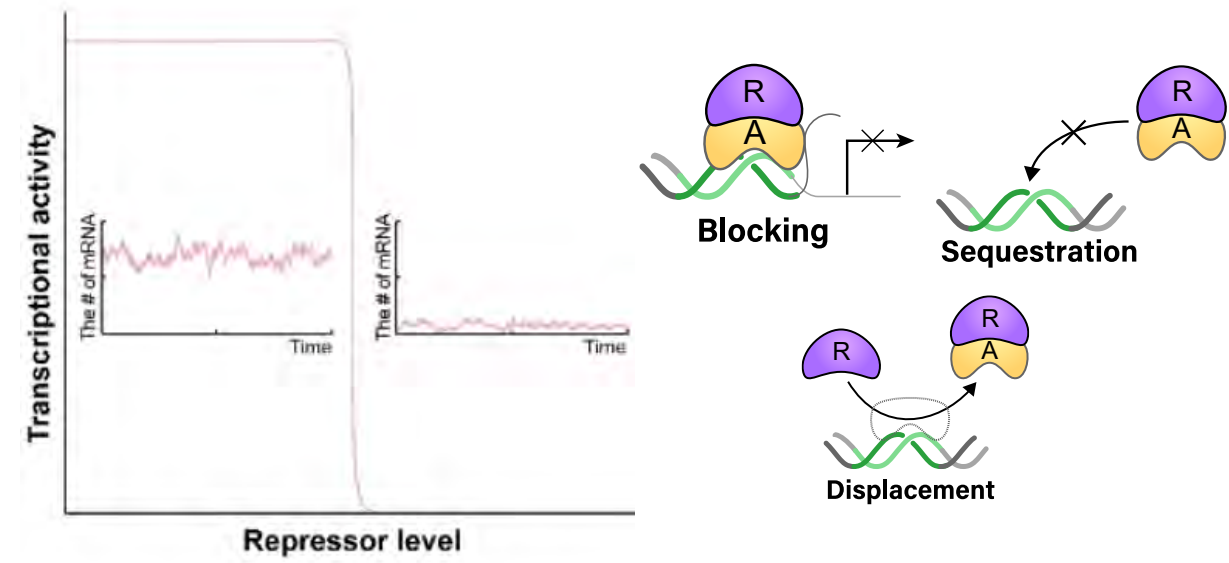
With displacement, the unexpected repression is rapidly restored to the activation.



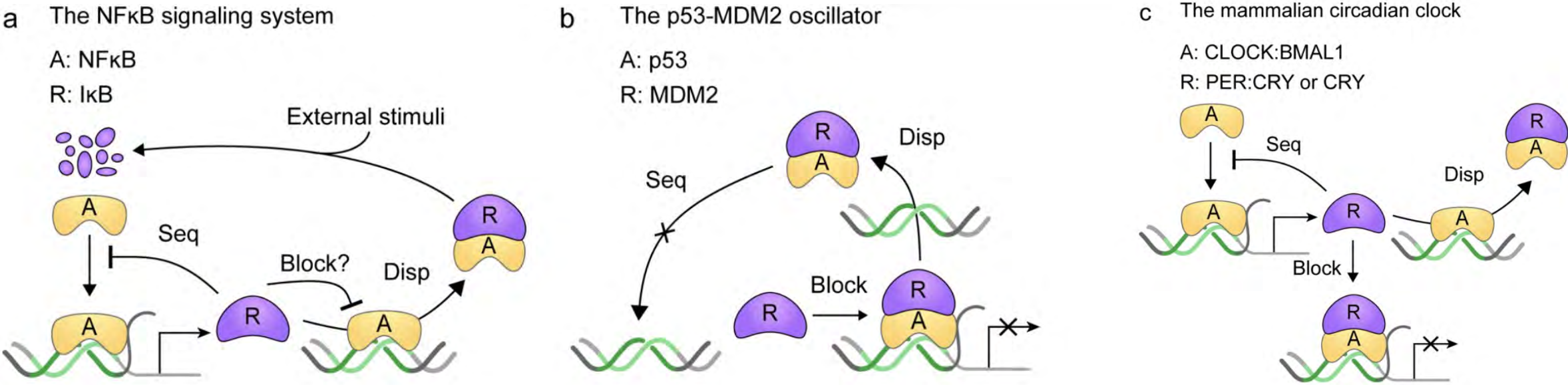




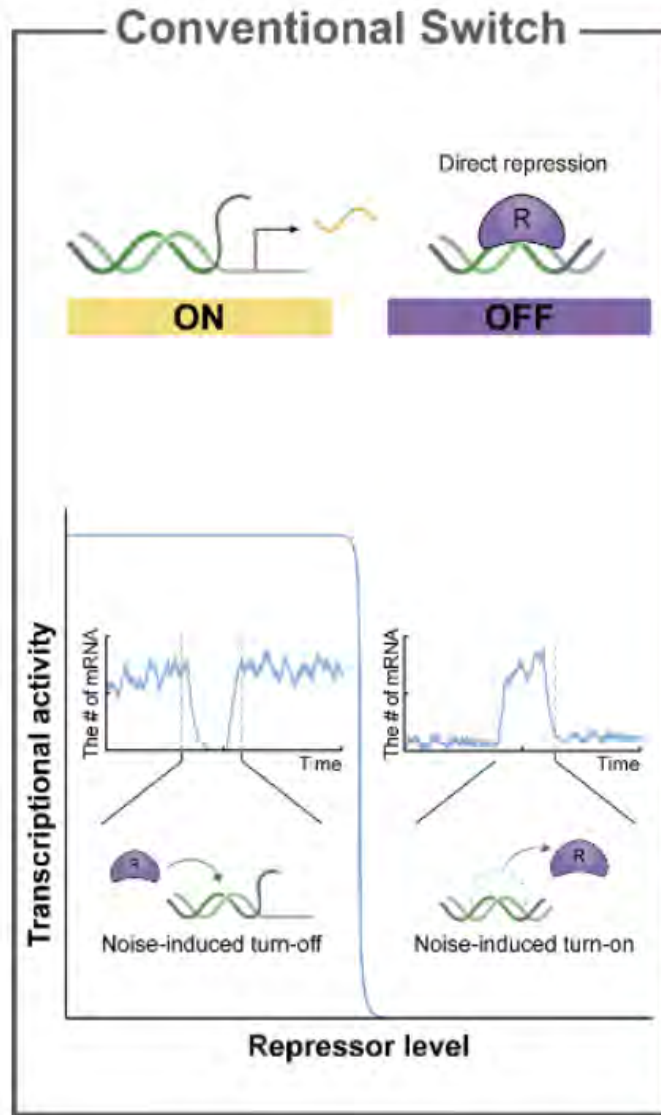
Transcriptional regulation noise is filtered by multiple repression mechanisms



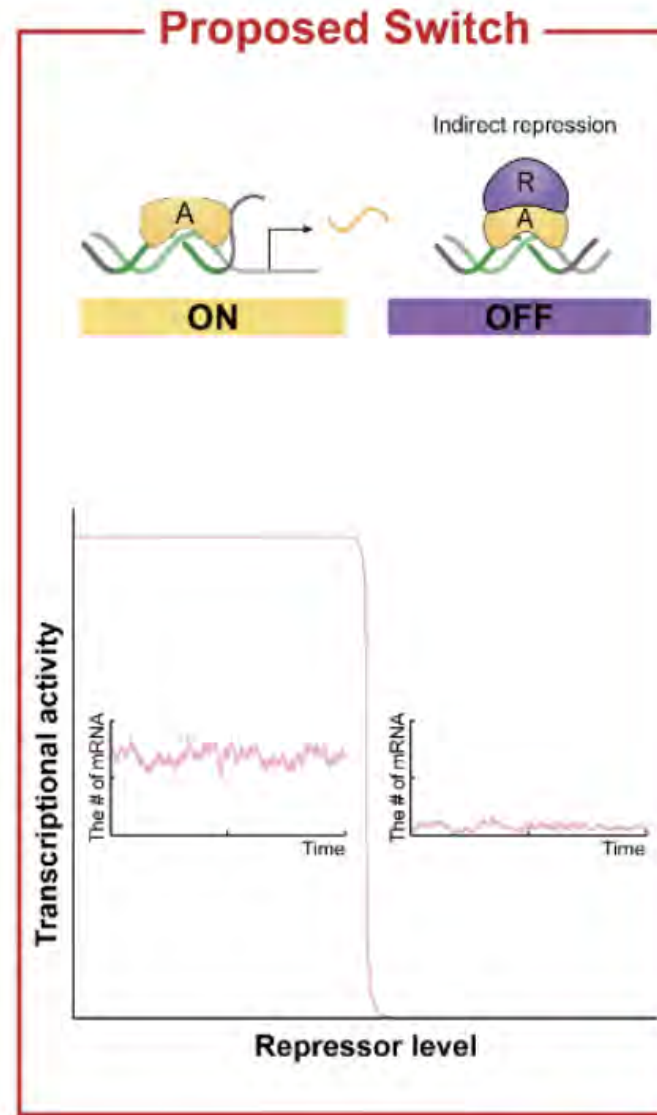
Blocking + sequestration + displacement, seemingly redundant, is commonly used.



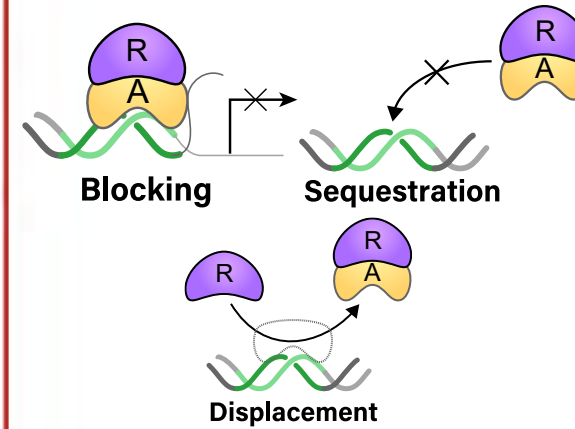
# 1<sup>st</sup> mechanism leading to “sensitive” response & ”robust” to noise



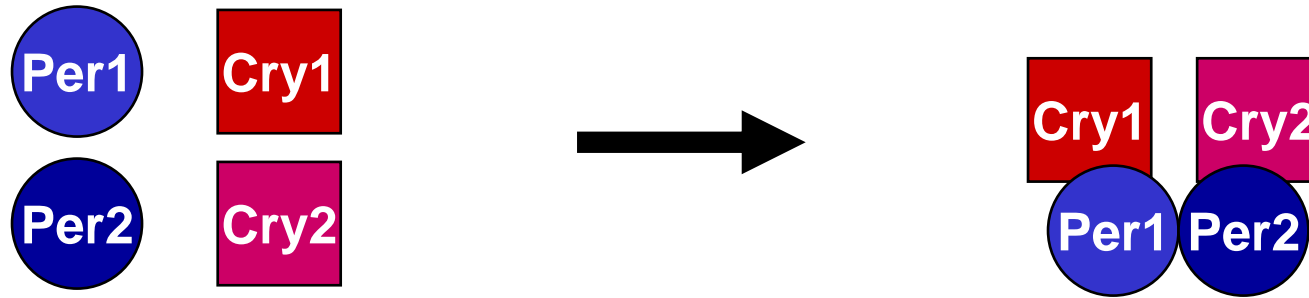
Noise-sensitive



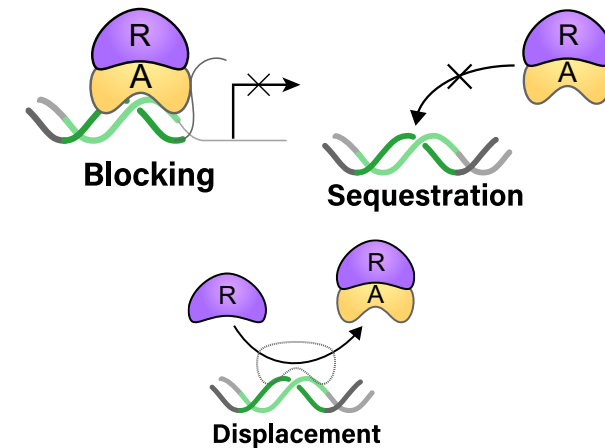
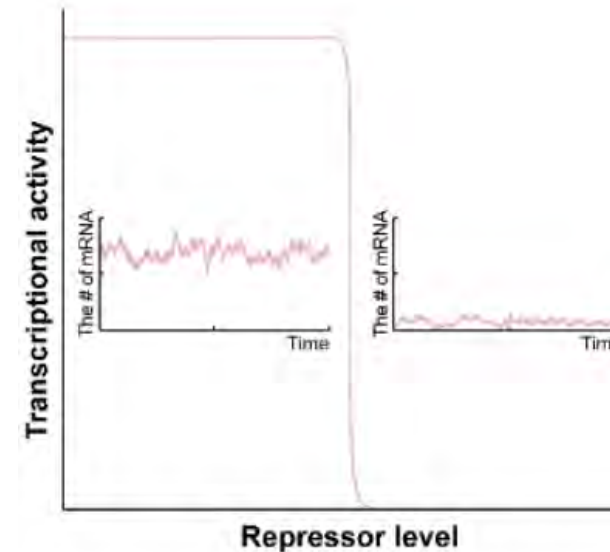
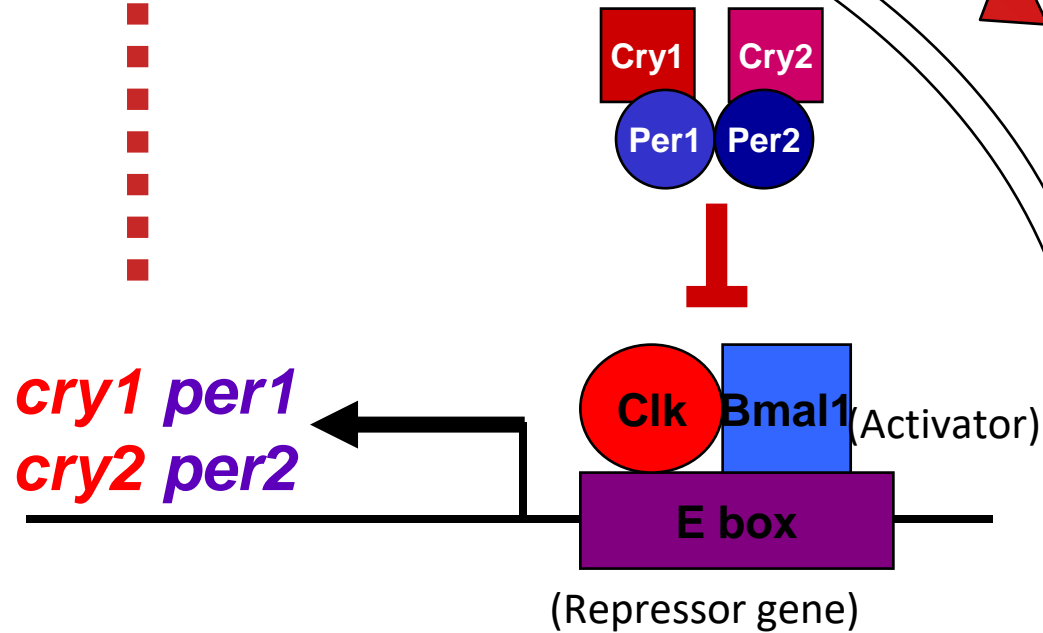
Noise-robust



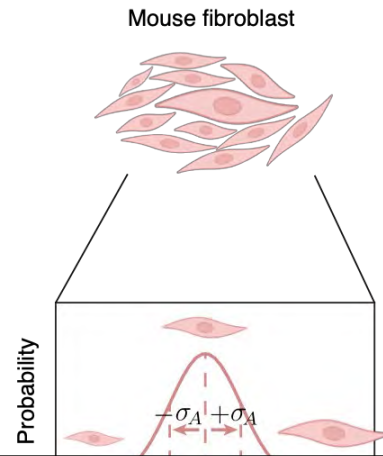




**PER need to enter at the right time of day!**

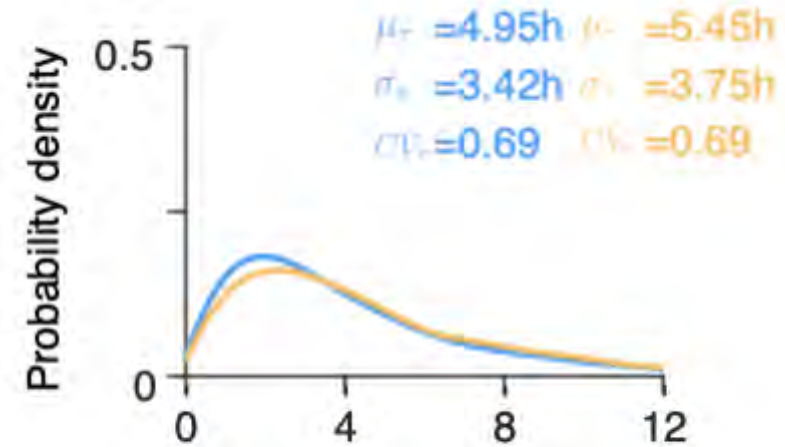


# Travel time of molecules is calculated by agent-based modeling



Cell size:  $2346 \pm 558 \mu\text{m}$

PER Diffusion coefficient  
 $D=0.25 \mu\text{m}^2/\text{s}$   
Koch et al, eLife (2020)



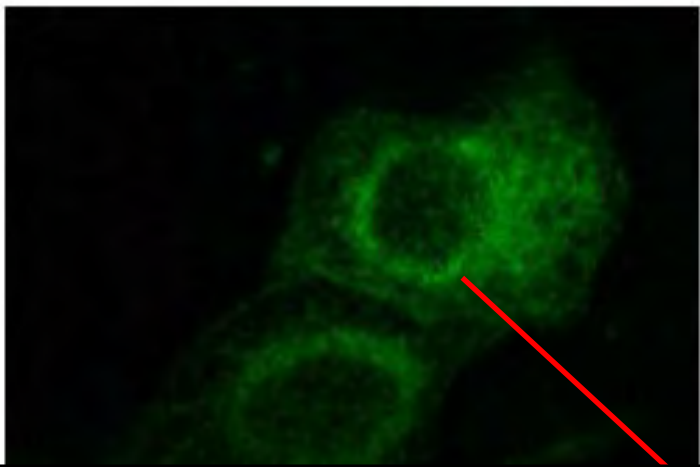
Travel time of PER molecules vary from 0h to 12h.

How do PER molecules enter nucleus at the right time to turn off transcription?



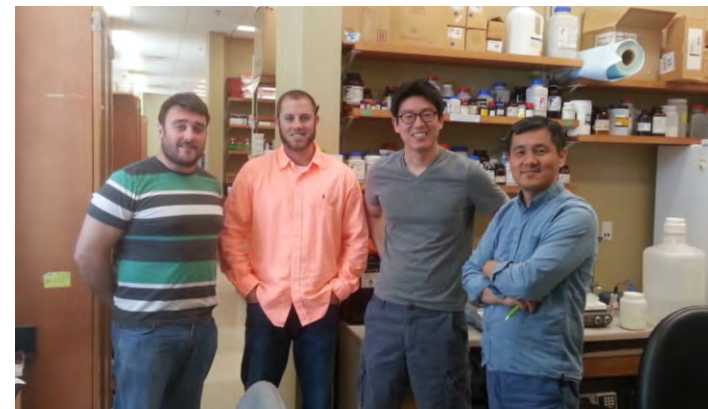
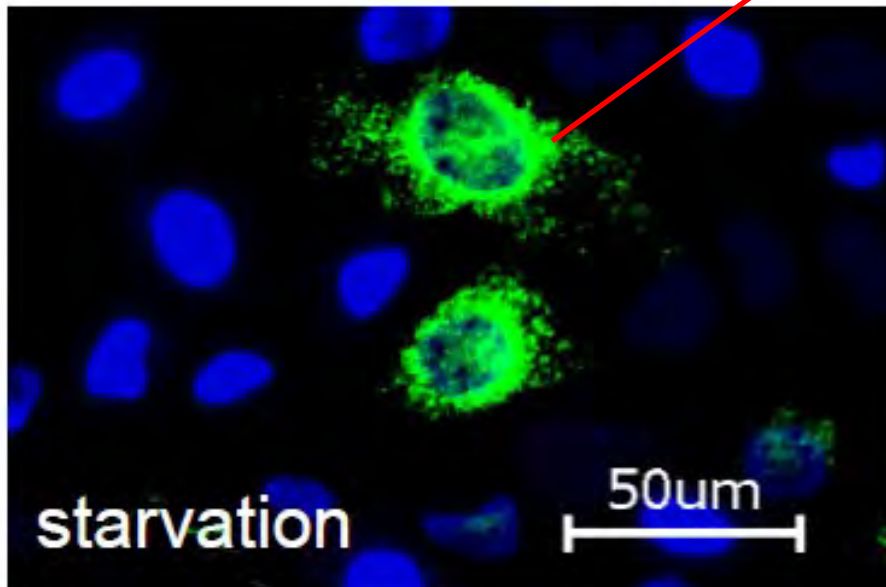
Seokjoo Choe  
(KAIST)





**Mechanism for such collective behaviors of molecules?**

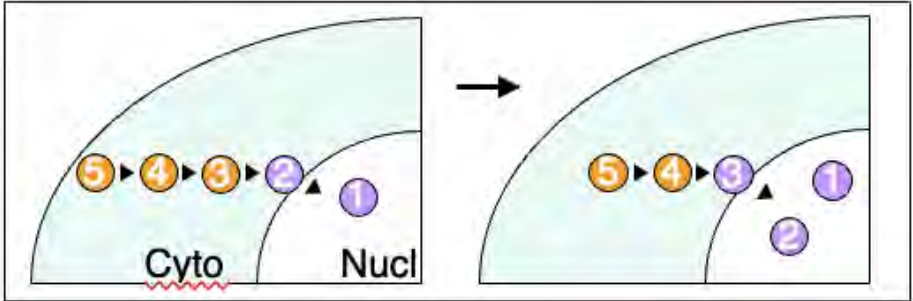
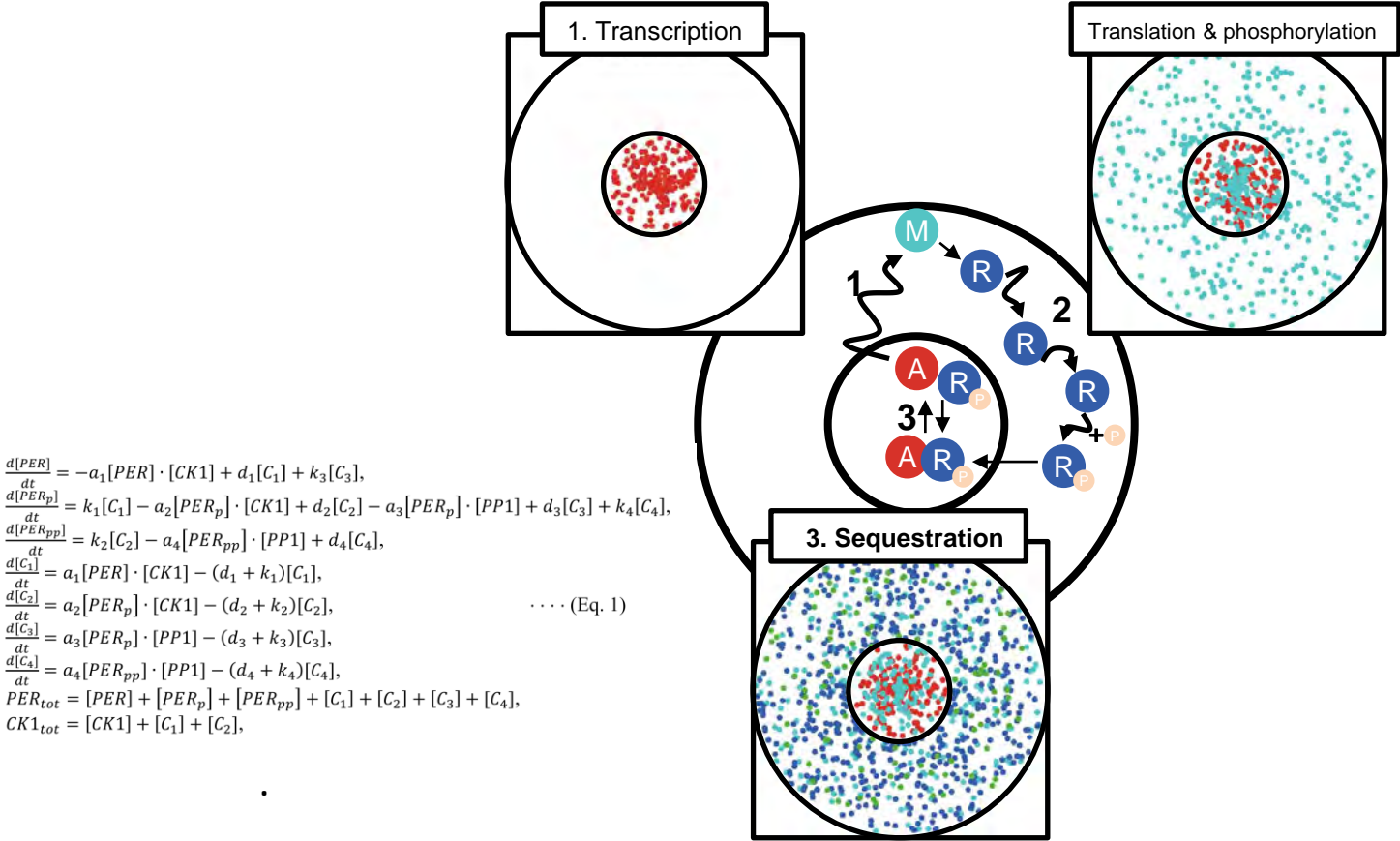
molecules at the perinucleus.



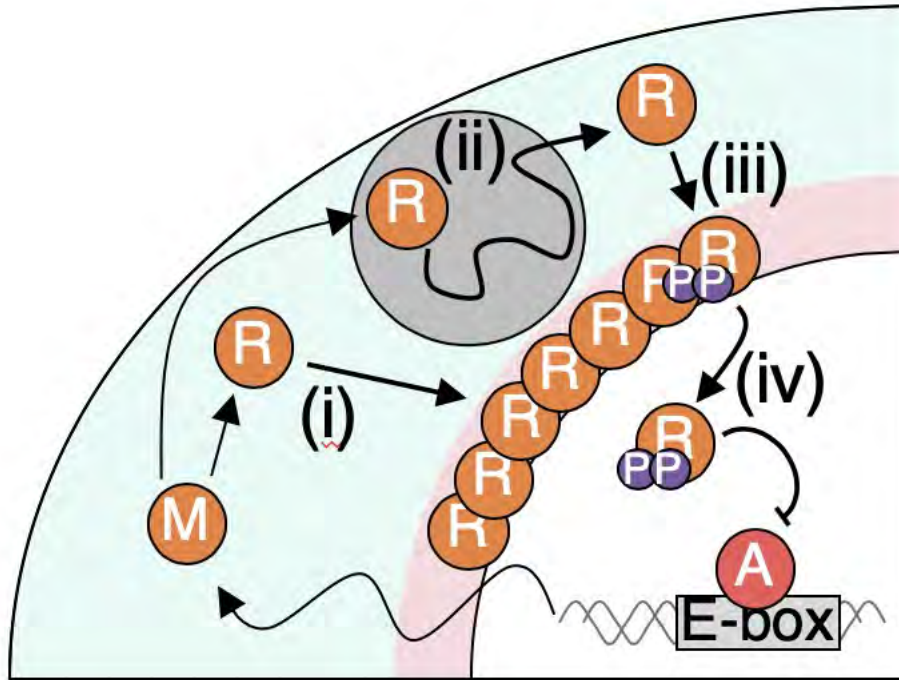
Choogon Lee Lab (Florida State U)



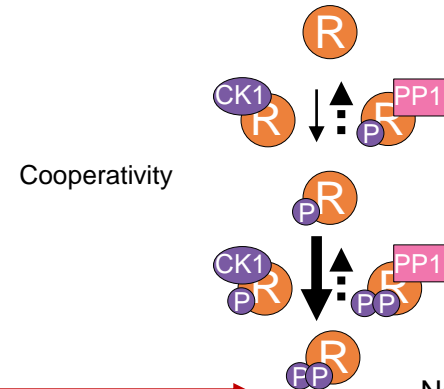
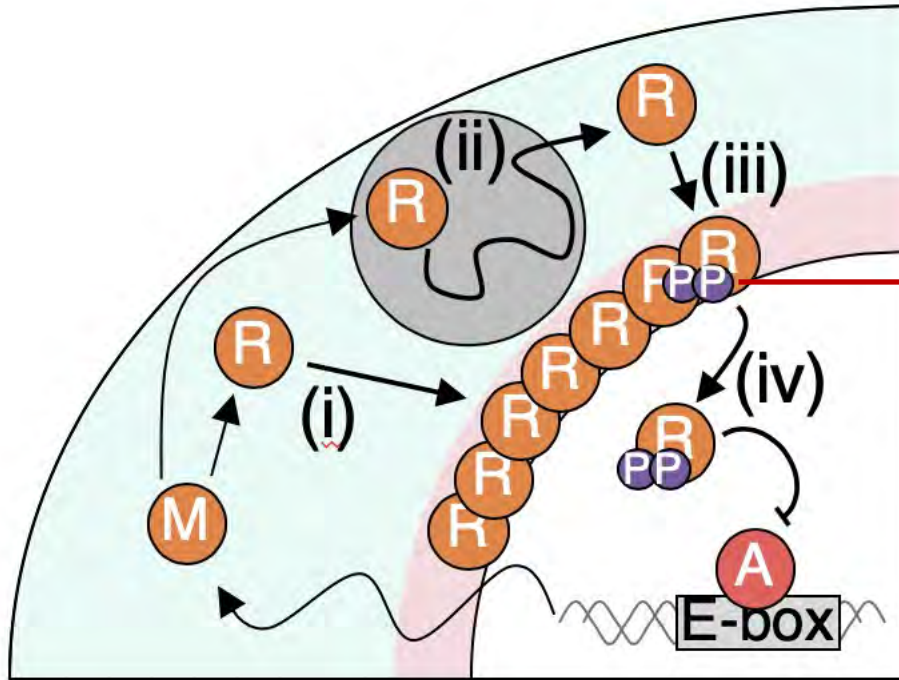
# Mathematical model for spatio-temporal dynamics of PER



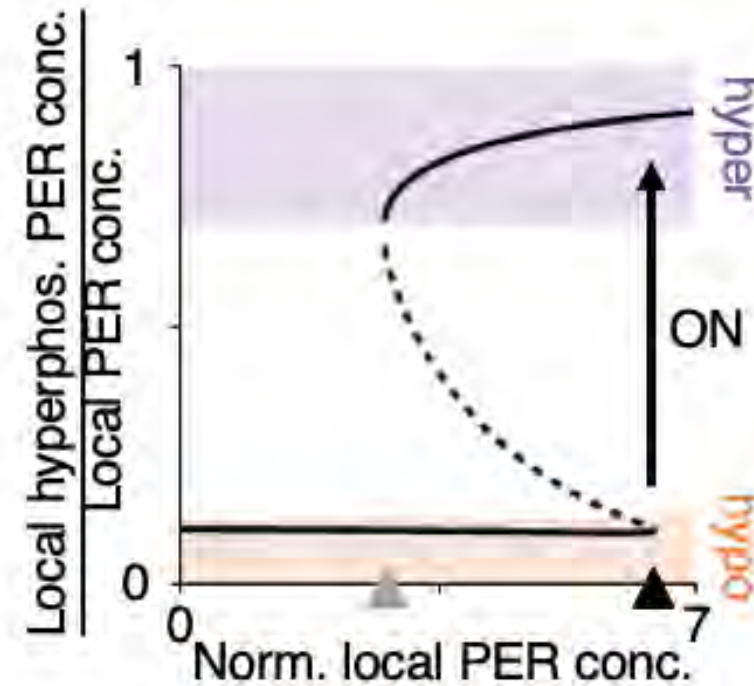
Multi-Phosphorylation is required for nuclear entry of PER



# Switch-like PER phosphorylation



Narasimamurthy et al, PNAS (2018)

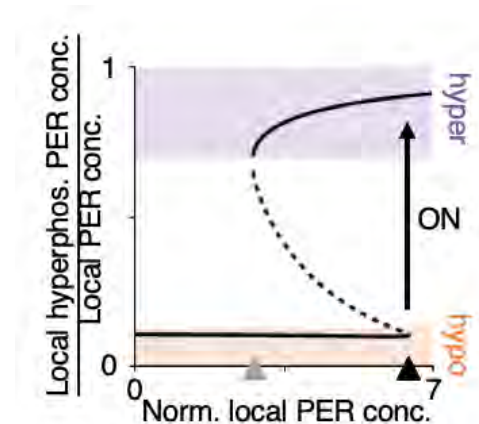
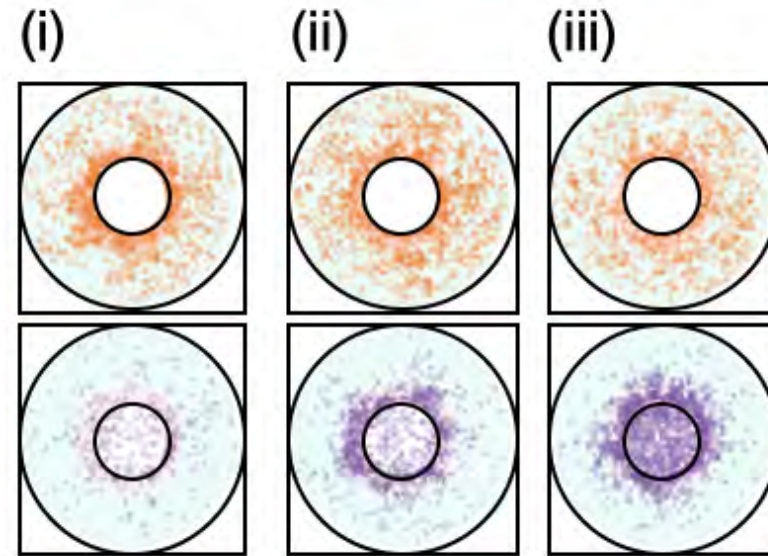
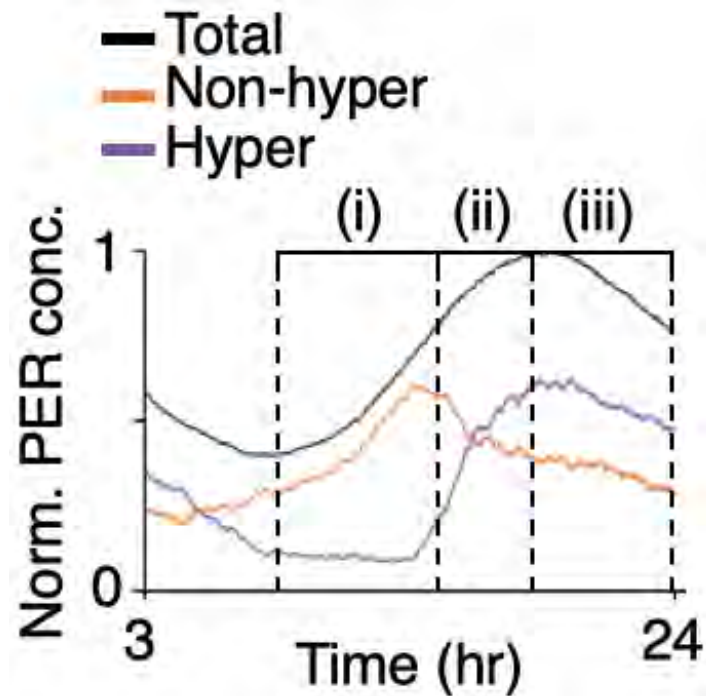


David Virshup  
(DUKE-NUS)



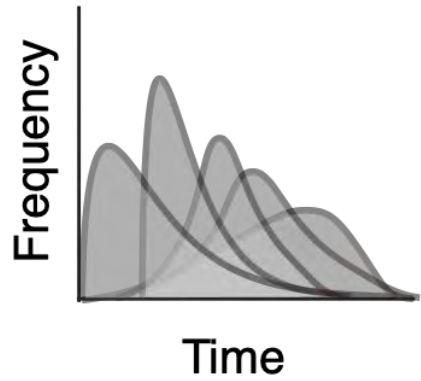


Switch-like PER phosphorylation+ Advection simulates sharp increase of phosphorylated PER and nucleus entry

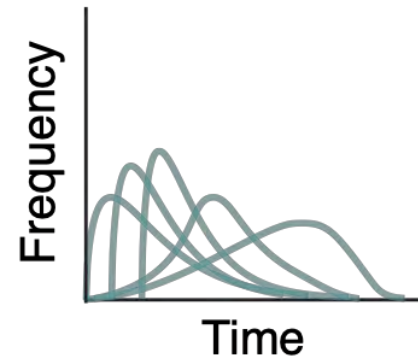


# Phosphoswitch maintains circadian rhythms despite heterogenous PER arrival time

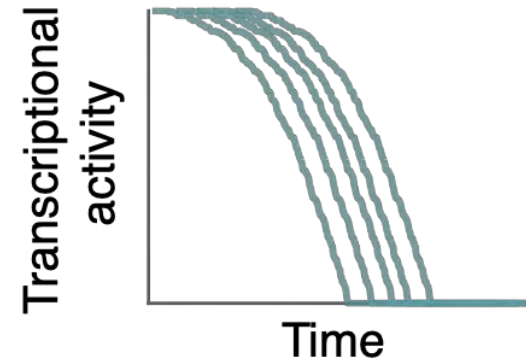
(i) Protein arrival time ( $t_p$ )



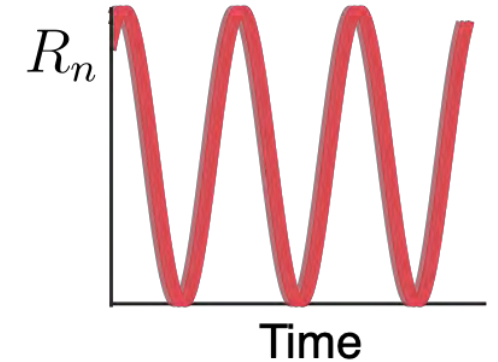
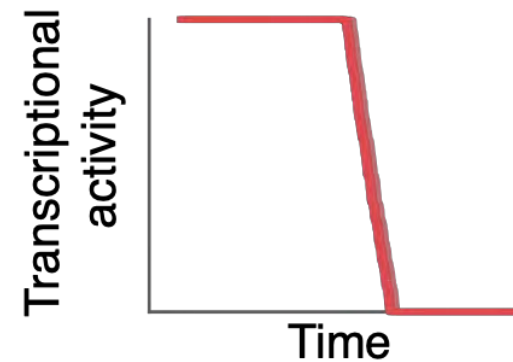
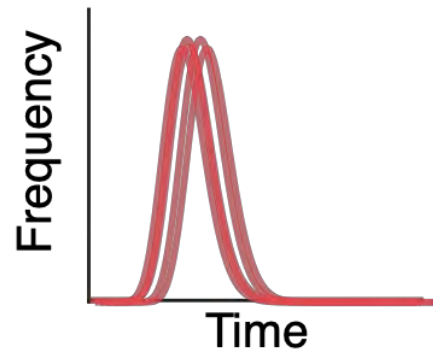
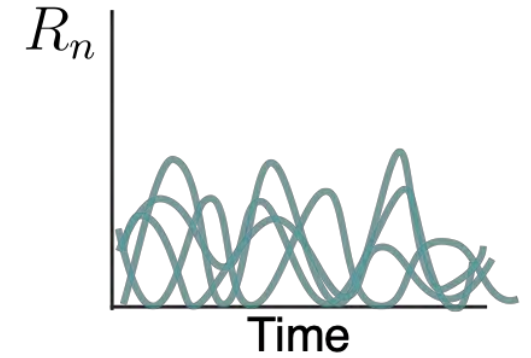
(ii) Nuclear entry time ( $t_n$ )



(iii) Transcriptional repression

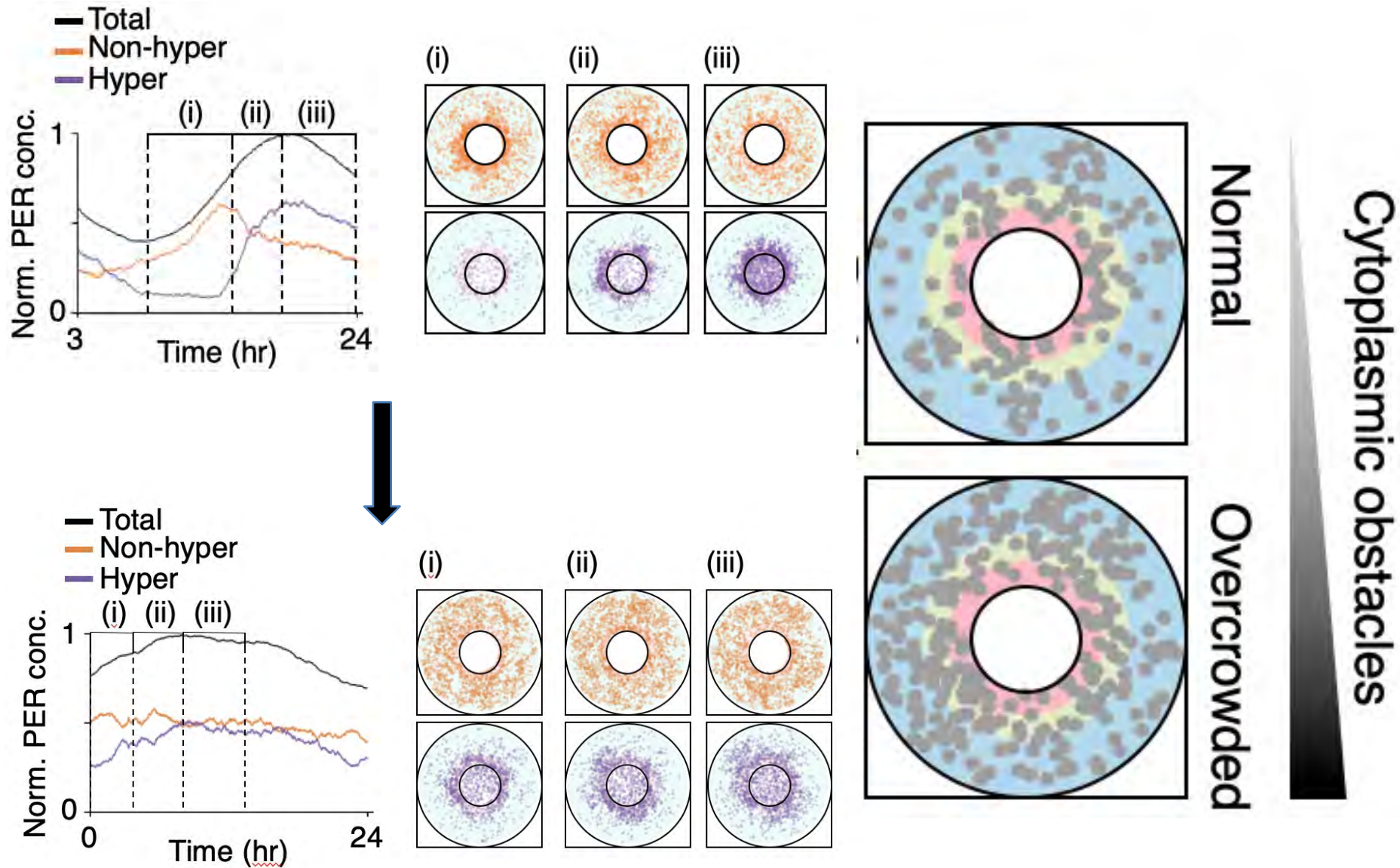


(iv) Circadian oscillation



Seokjoo Choe  
(KAIST)

In extremely overcrowded cell, phosphoswitch does not work and circadian rhythms become unstable...





HOME > SCIENCE TRANSLATIONAL MEDICINE > VOL. 12, NO. 569 > CYTOPLASMIC TRAFFIC JAMS AFFECT CIRCADIAN TIMING



**EDITORS' CHOICE** | CIRCADIAN CLOCK

## Cytoplasmic traffic jams affect circadian timing

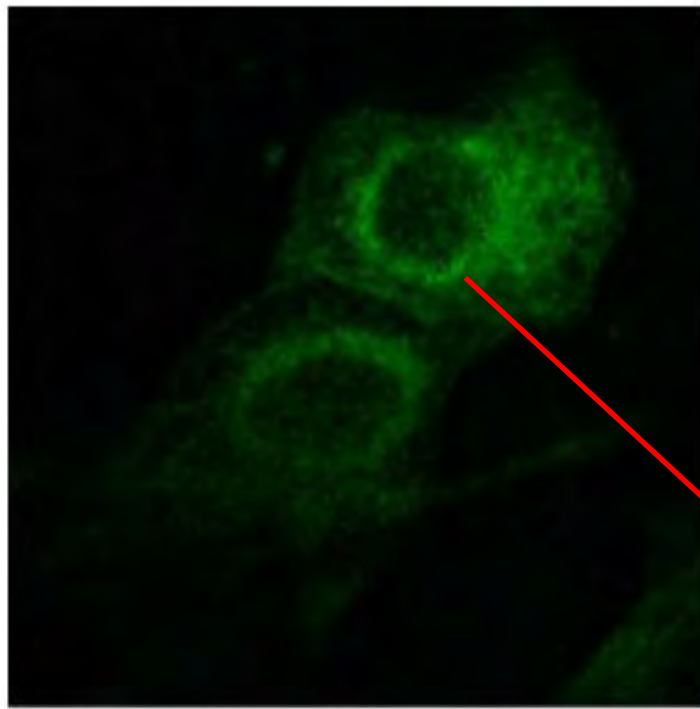
JENNIFER M. HURLEY

**What else does cause cytoplasmic congestion?**

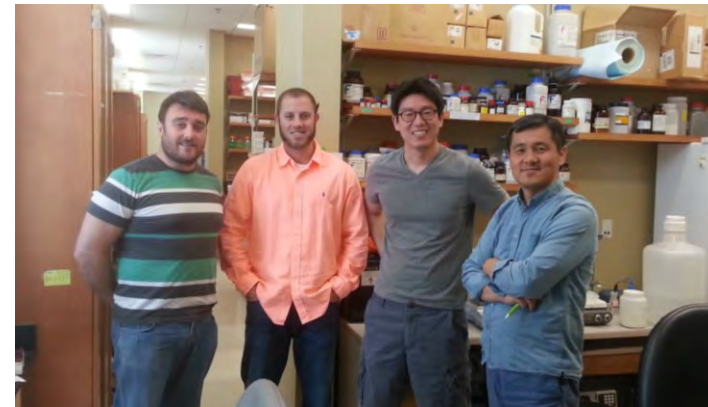
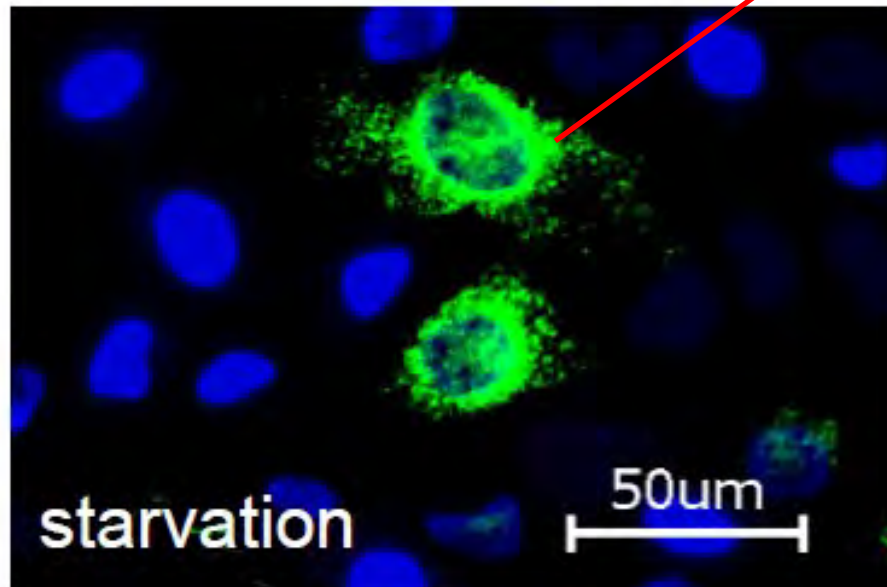
**Aging, Autophagy mal-function, and Alzheimer's disease.**

**Indeed, they cause unstable sleep-wake cycle.**

**This explains why do obesity, aging and Az cause unstable sleep-wake cycle.**



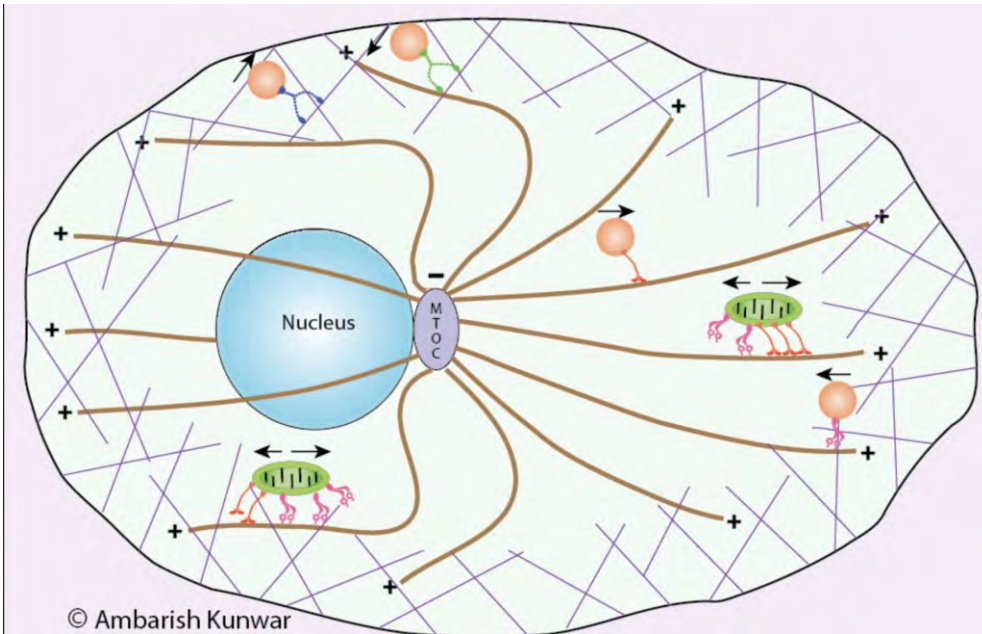
**How PER moves toward to perinucleus?**



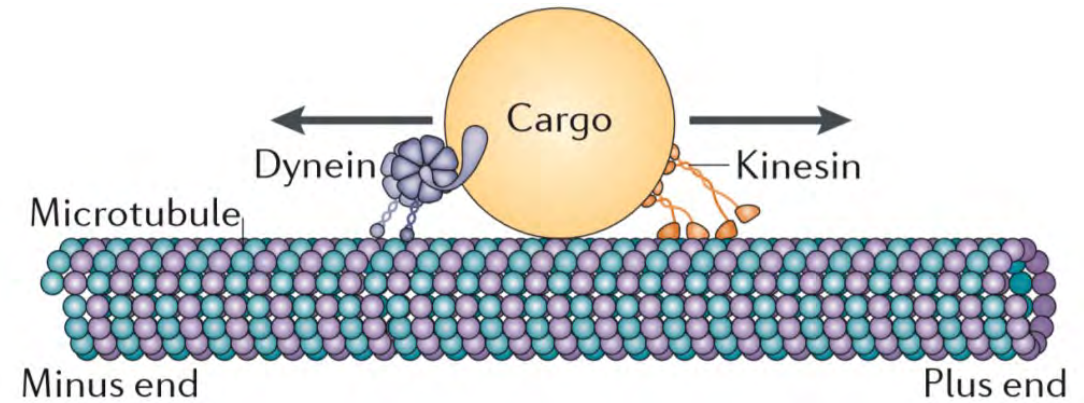
Choogon Lee Lab (Florida State U)

Transport to perinucleus is mainly based on microtubules and molecular motors

Microtubule: road heading to nucleus

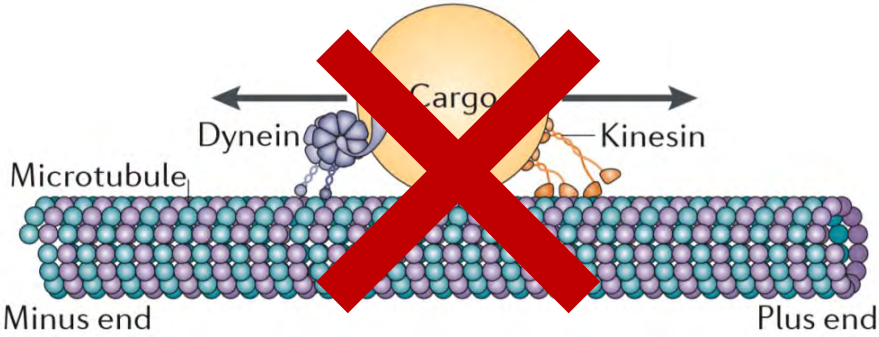


Motor proteins: truck transporting proteins

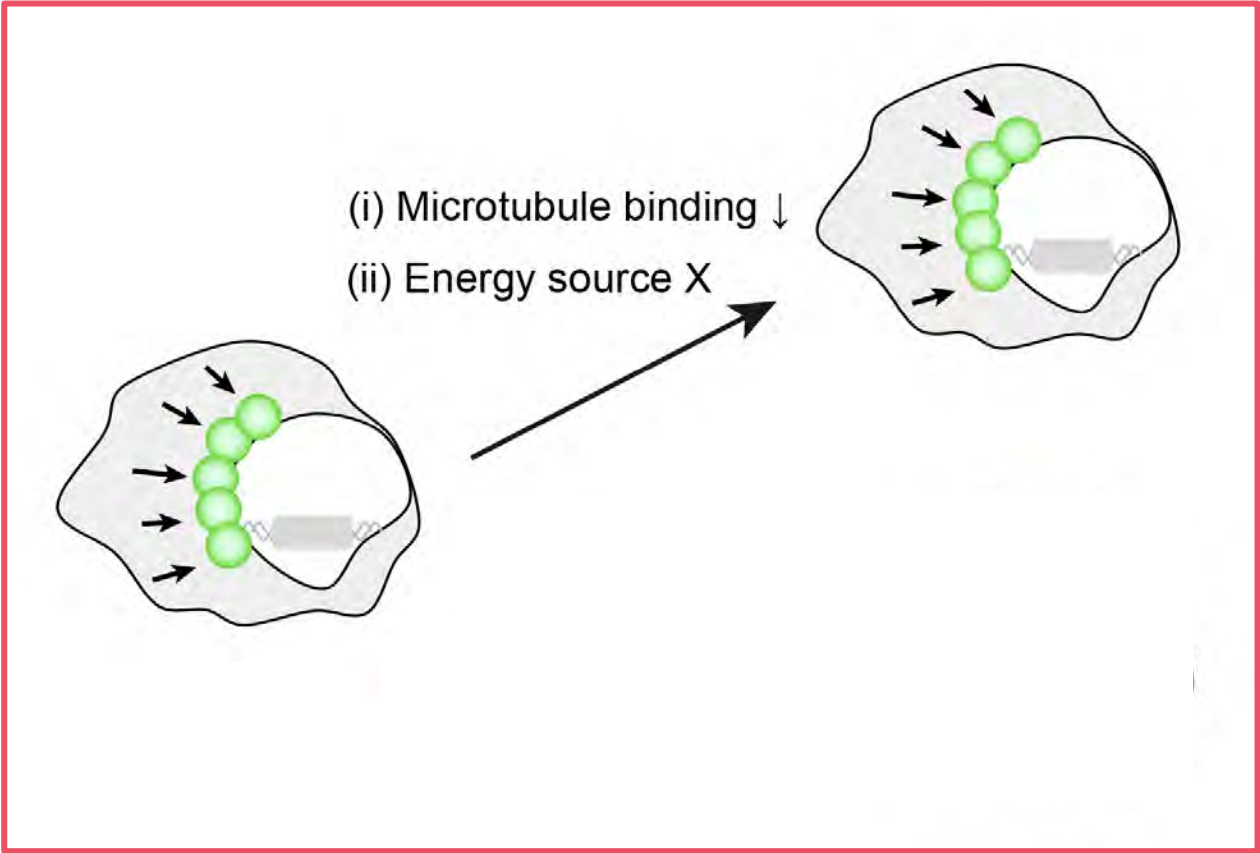
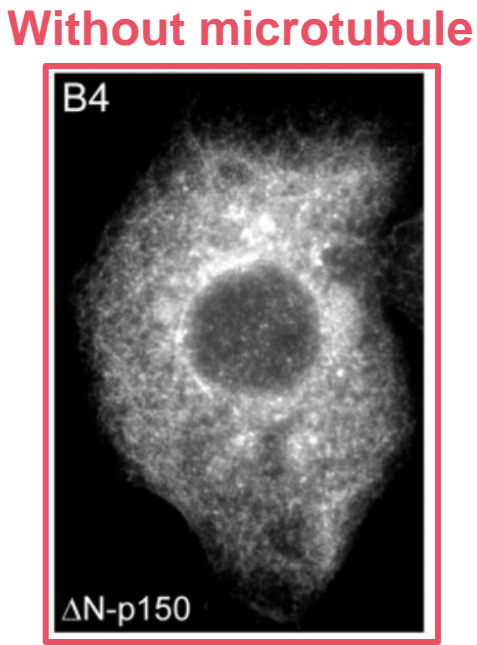
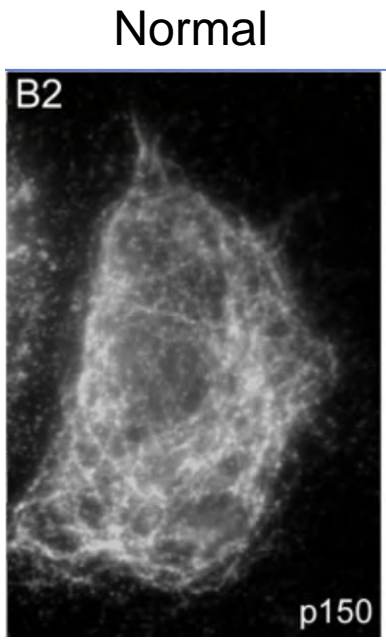




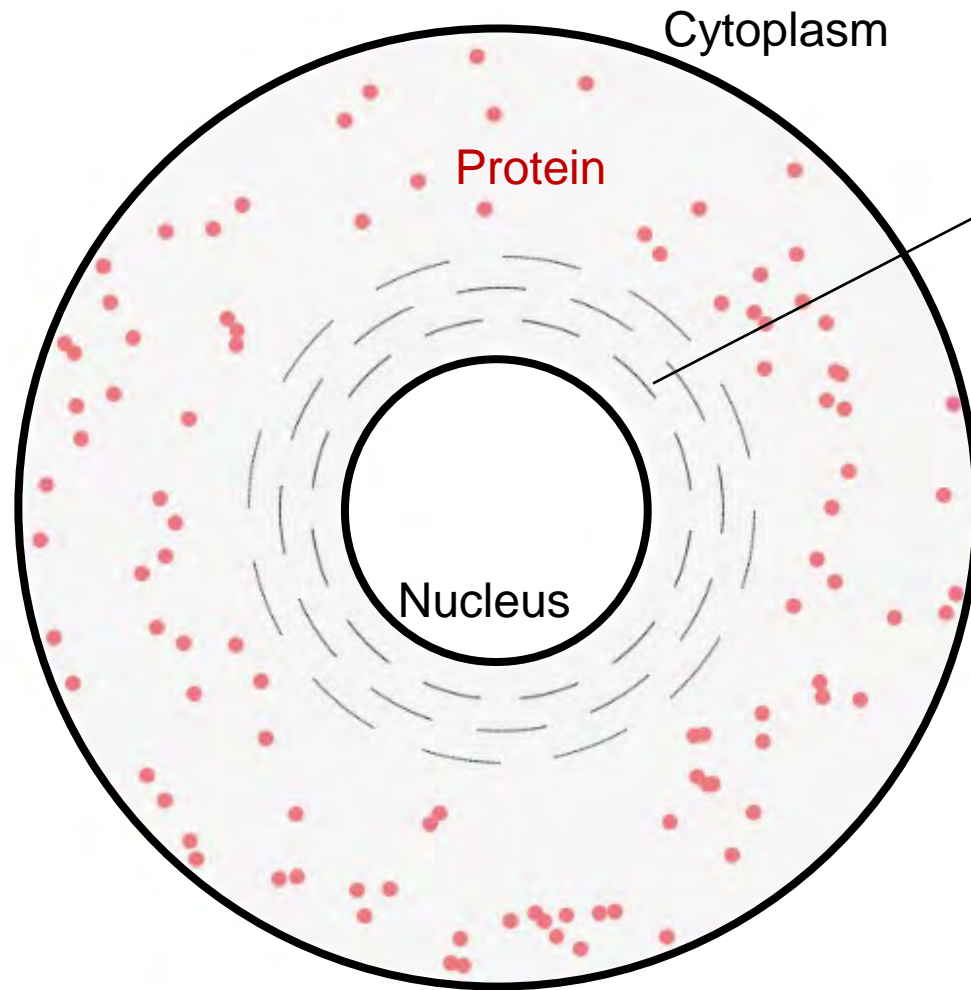
However, **even without microtubule**, protein can be transported to perinucleus!



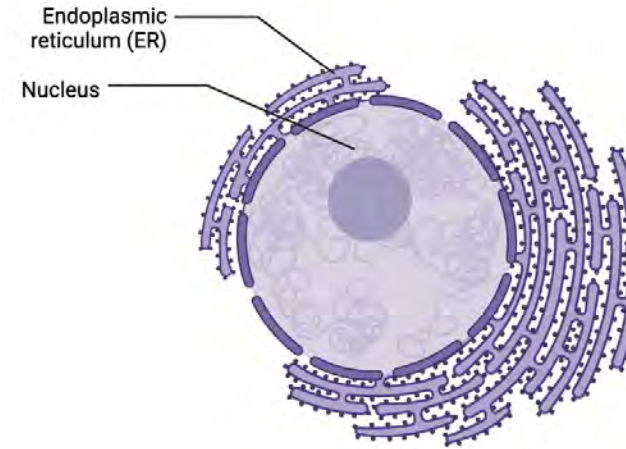
Such protein transport may have diffusive character!



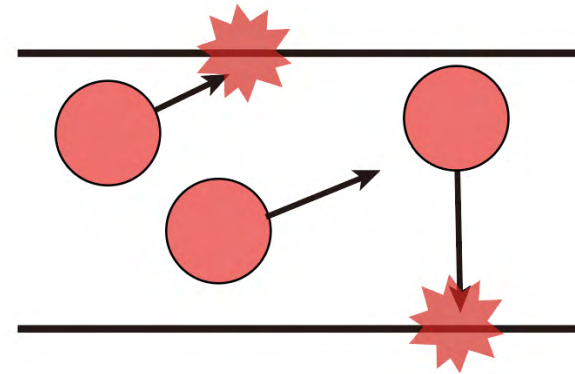
To investigate the role of diffusive character, we developed an agent-based model mimicking protein diffusion in a cell with ER.



Endoplasmic reticulum (ER)



Protein movement is hampered in the ER



Seok Joo Chae  
(KAIST & IBS)



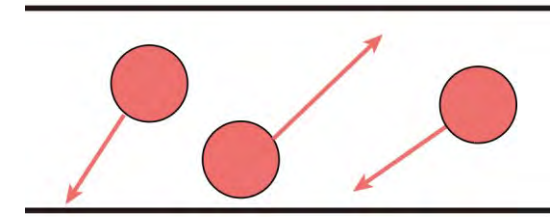
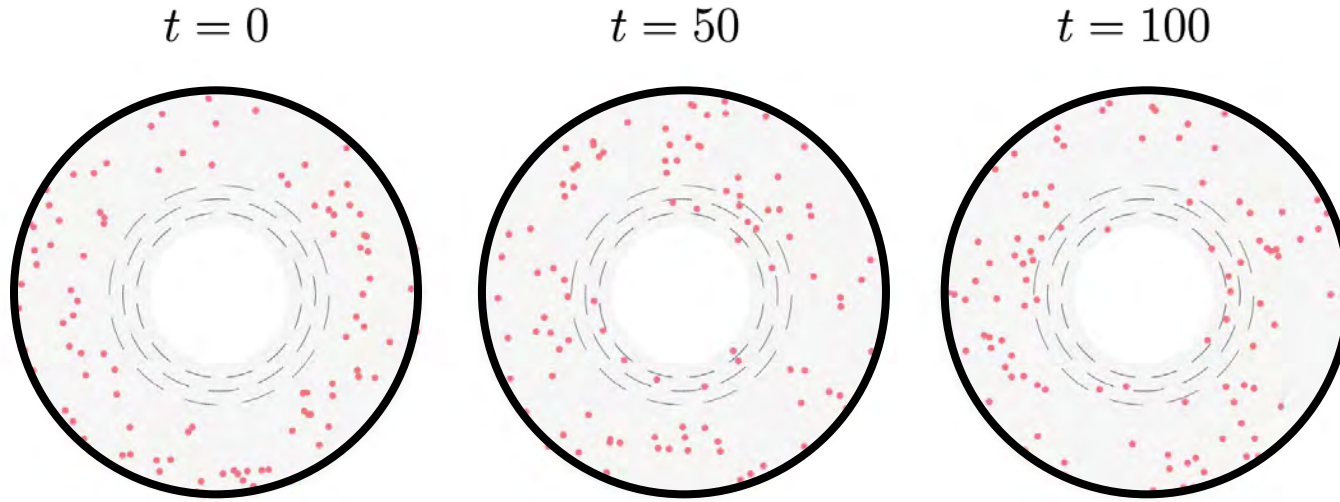
Dae Wook Kim  
Seogang U



Oleg Igoshin, Rice U

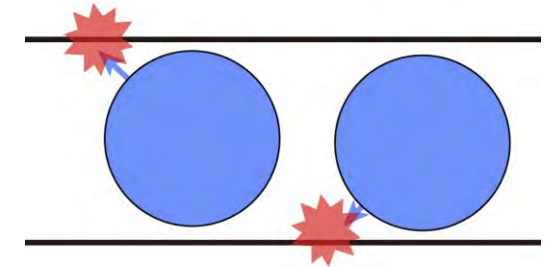
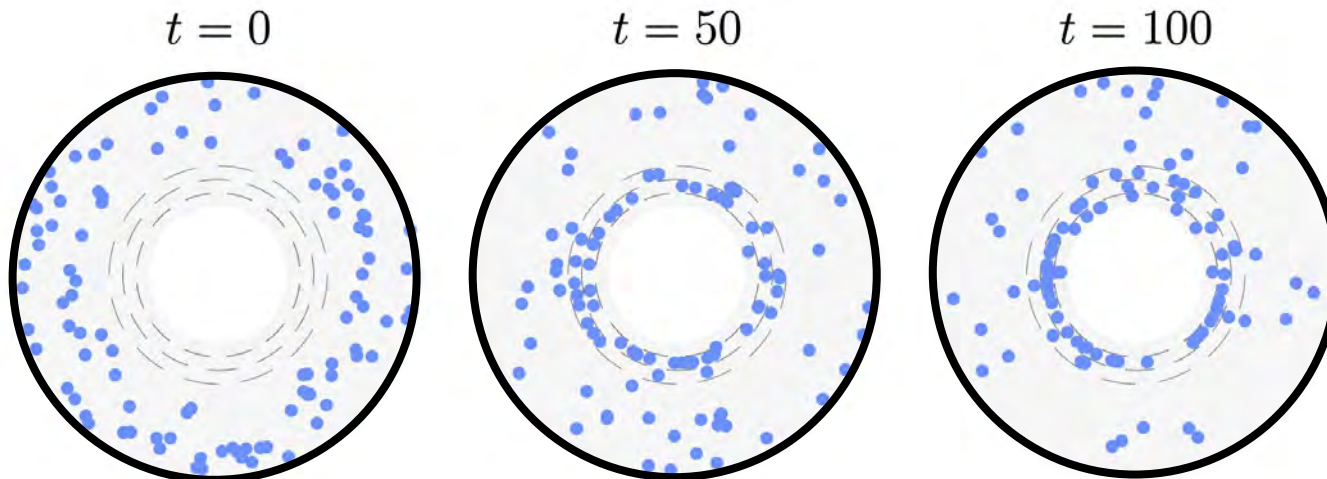
# Diffusion within the cell with the ER structure results in perinuclear accumulation

**Smaller sized** proteins does not accumulate near the nucleus



Low collision frequency with the ER

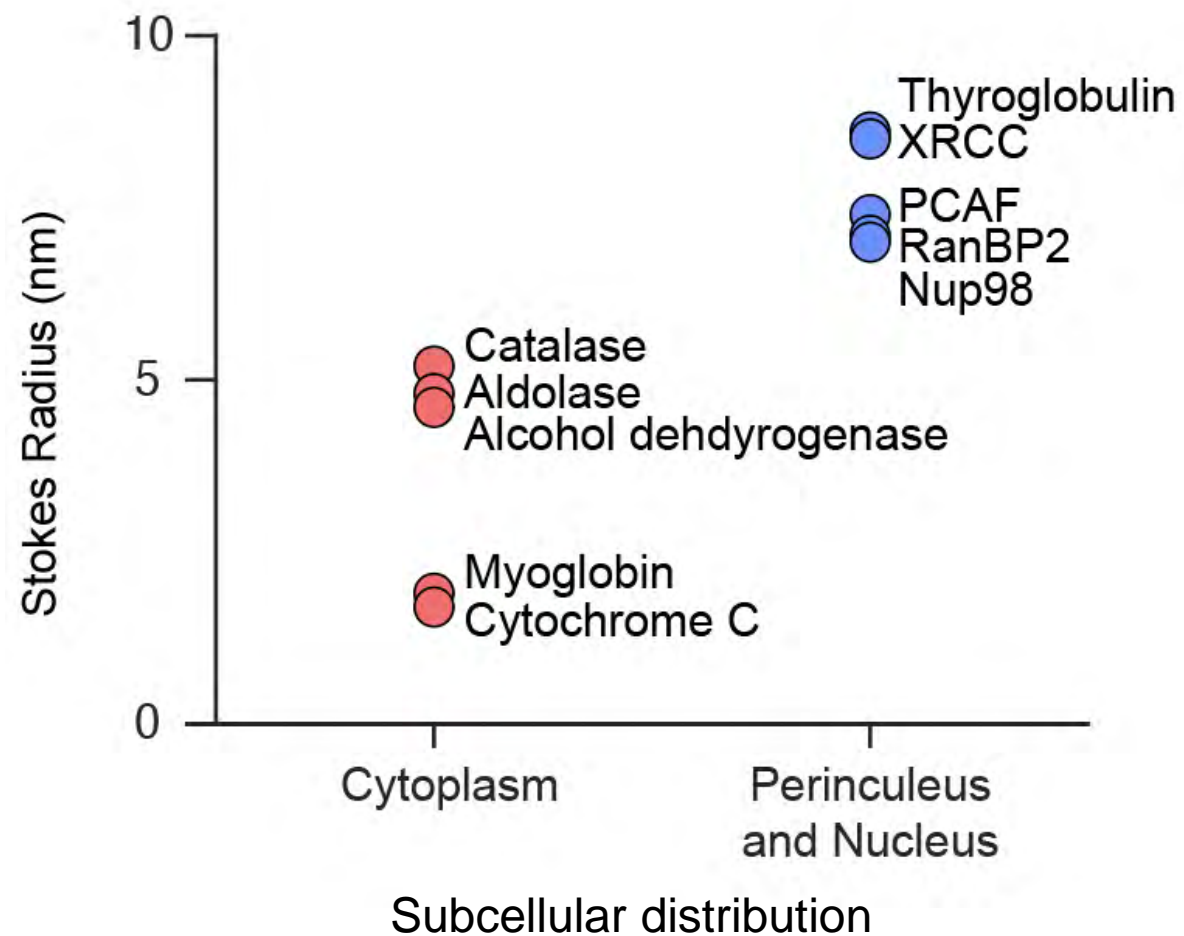
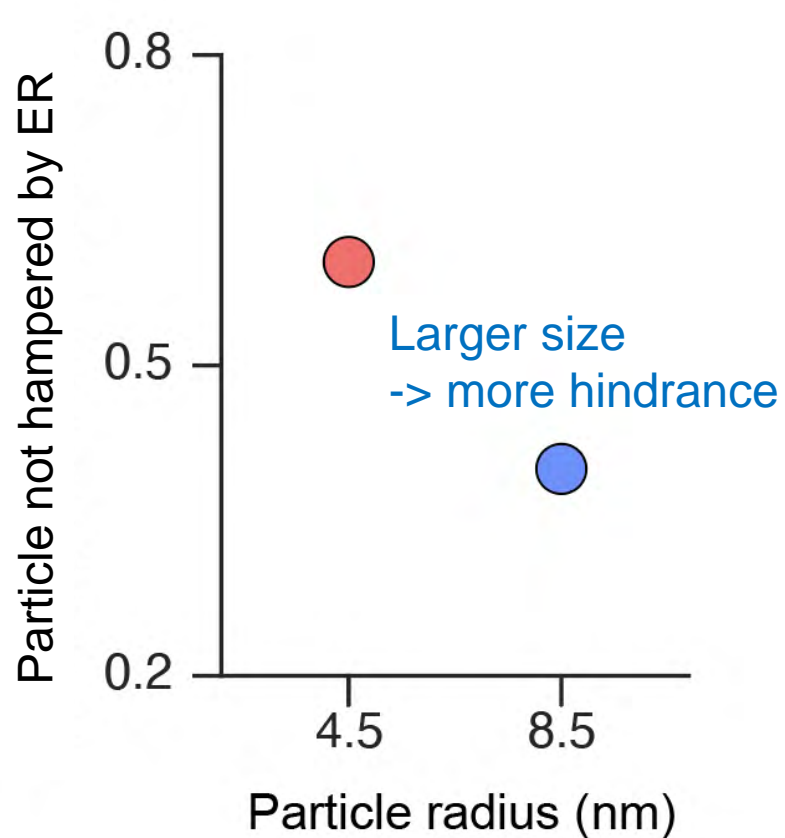
However, **larger sized** proteins do accumulate



High collision frequency with the ER

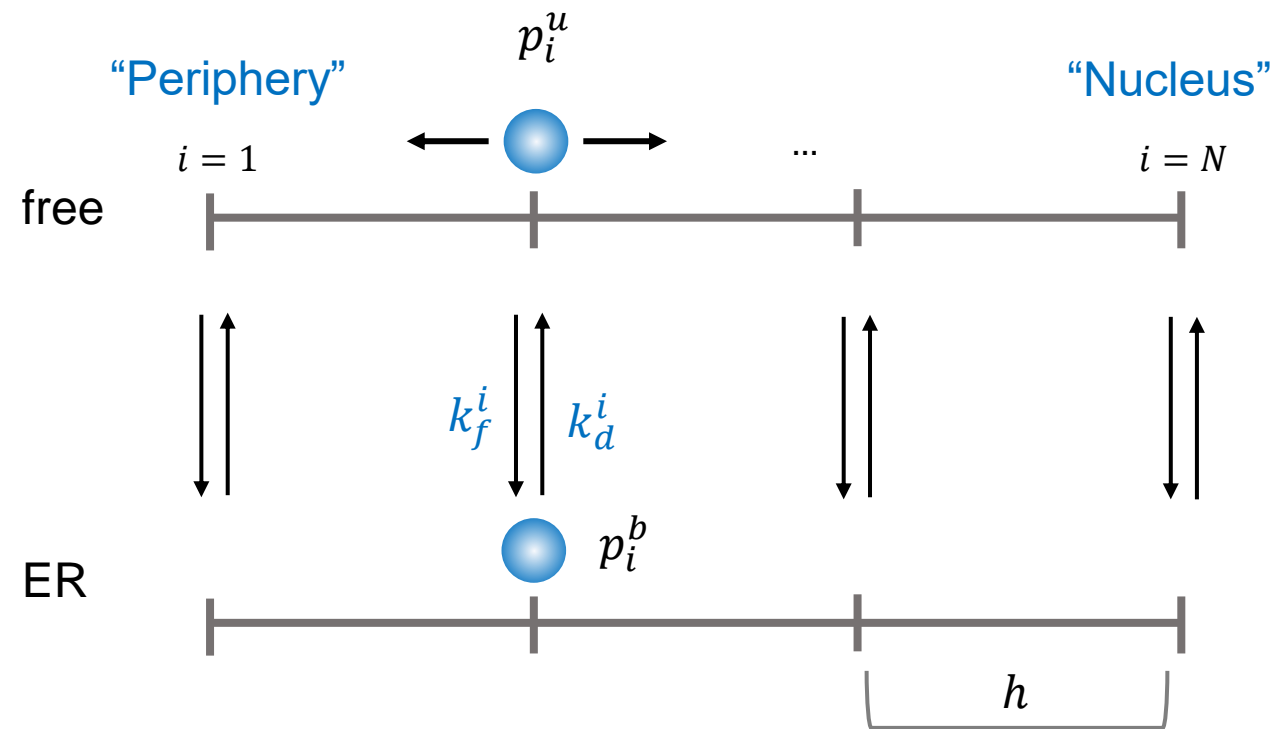


Larger proteins are prone to diffusion hindrance and tend to accumulate near the nucleus!



How can we understand heterogeneous diffusion mathematically?

# Microscopic model for diffusion + the collision (binding) of ER



- $p_i^u$ : probability of finding unbounded protein at  $i$ -th grid
- $p_i^b$ : probability of finding bounded protein at  $i$ -th grid
- $p_i^T$ : probability of finding protein at  $i$ -th grid (bounded + unbounded)

Diffusion + Binding/unbinding

$$\frac{dp_i^u}{dt} = \frac{\delta}{h^2} (-2p_i^u + p_{i-1}^u + p_{i+1}^u) + k_d^i p_i^b - k_f^i p_i^u$$
$$\frac{dp_i^b}{dt} = -k_d^i p_i^b + k_f^i p_i^u$$
$$\frac{dp_i^T}{dt} = \frac{\delta}{h^2} (-2p_i^u + p_{i-1}^u + p_{i+1}^u)$$

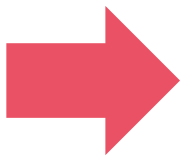
# One step further: heterogeneous diffusion of protein can be effectively described by Chapman's law

Microscopic model for **diffusion** + the **binding/unbinding** with ER

$$\frac{\partial p_i^u}{\partial t} = \frac{\delta}{h^2} (-2p_i^u + p_{i-1}^u + p_{i+1}^u) + k_d^i p_i^b - k_f^i p_i^u$$

$$\frac{\partial p_i^b}{\partial t} = -k_d^i p_i^b + k_f^i p_i^u$$

$$\frac{\partial p_i^T}{\partial t} = \frac{\delta}{h^2} (-2p_i^u + p_{i-1}^u + p_{i+1}^u)$$



Fast binding/unbinding  
 $h \rightarrow 0$

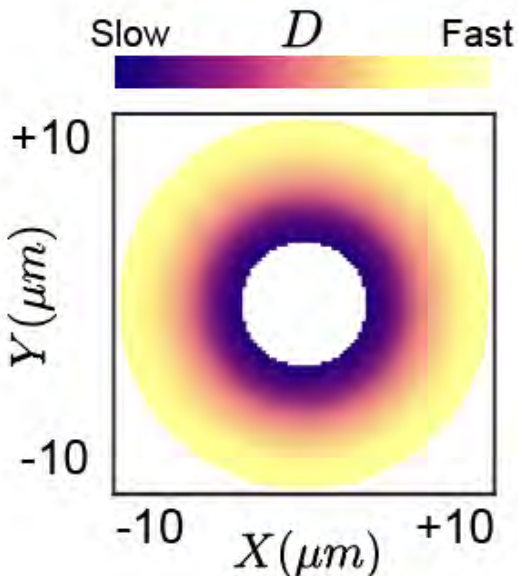
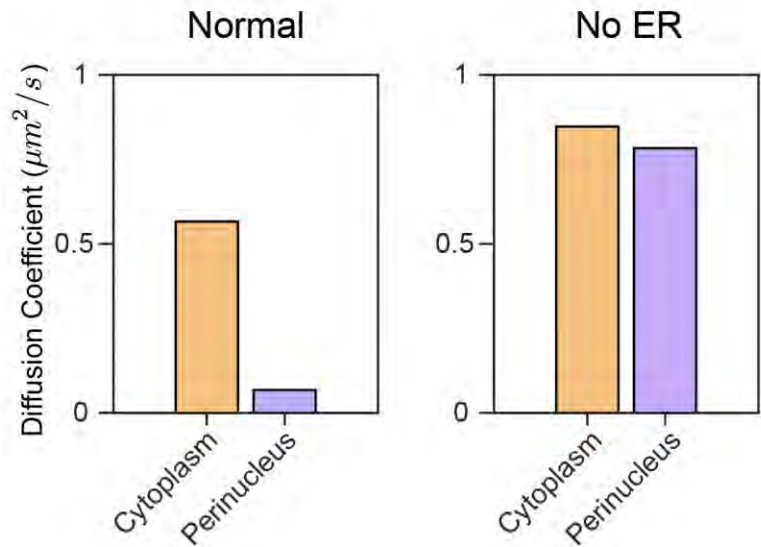
Chapman's Law

$$\frac{\partial p(x, t)}{\partial t} = \Delta(D(x)p(x, t))$$

$p(x, t)$  : prob. finding a protein at  $x$  and  $t$

$$D(x) = \frac{\delta}{\left(1 + \frac{k_f(x)}{k_b(x)}\right)}$$

Denser ER  $\rightarrow$  Larger  $k_f$   $\rightarrow$  Smaller  $D(x)$





A drift term in Chapman's law can account for perinuclear accumulation in heterogeneous environment!

Chapman's Law

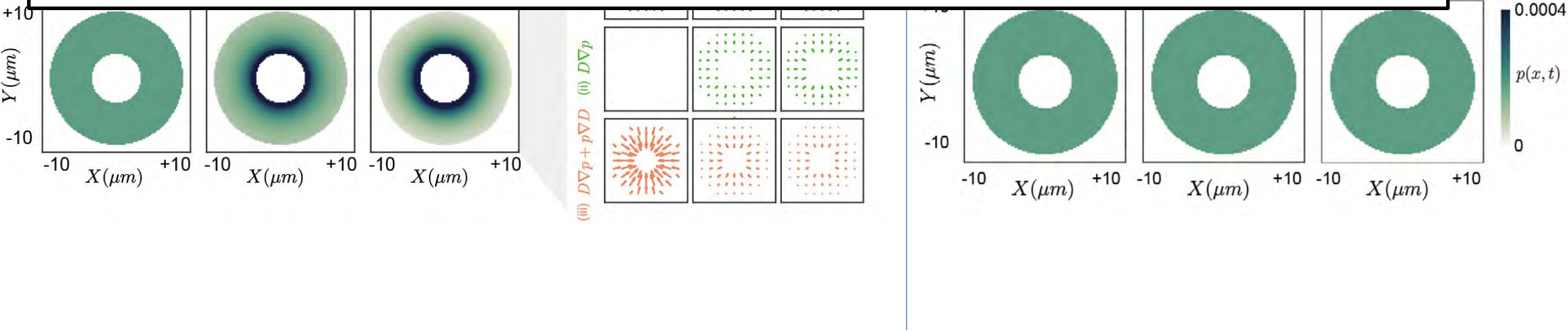
$$\frac{\partial p(x, t)}{\partial t} = \Delta(D(x)p(x, t))$$

$$\frac{\partial p}{\partial t} = -\nabla \cdot J$$
$$J = -(D\nabla p + p\nabla D)$$

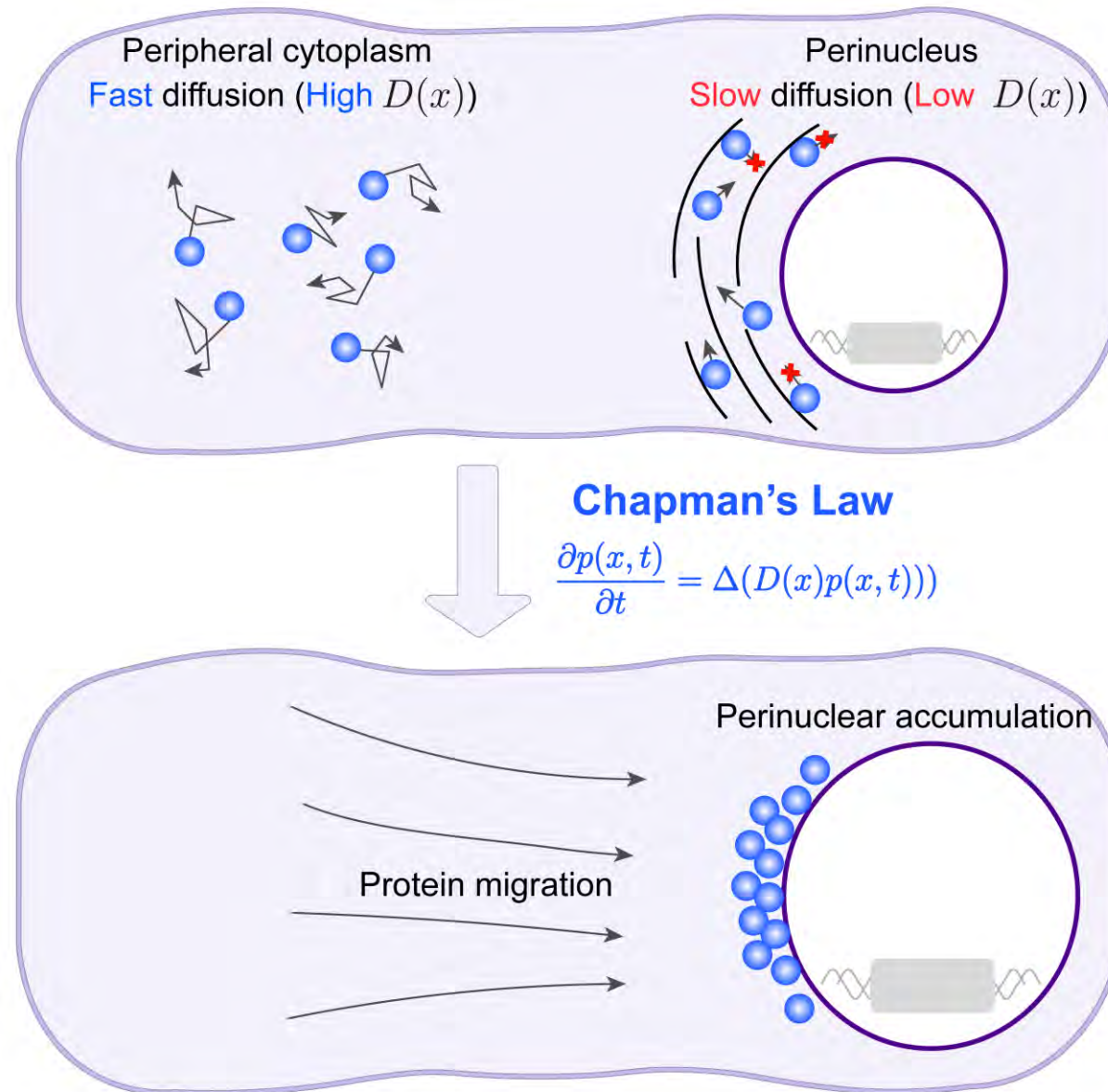
$D\nabla p$ : Fickian (diffusive) flow

$p\nabla D$ : Drift due to the heterogeneous environment

Chapman's law seems the way to go to describe intracellular diffusion of molecules!



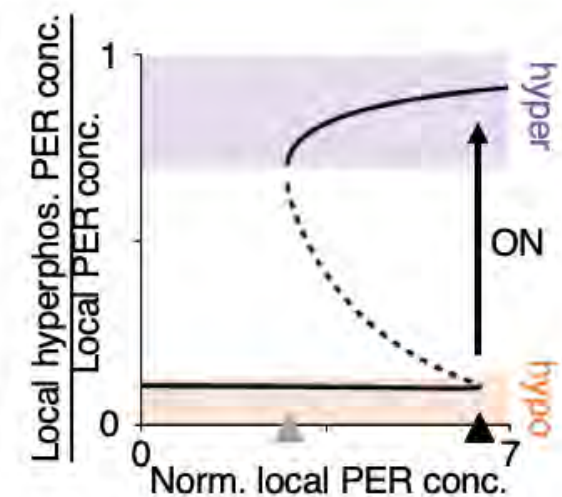
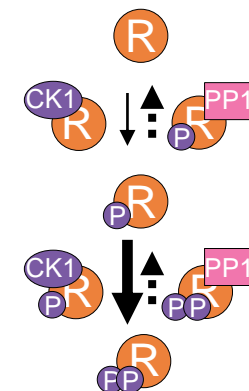
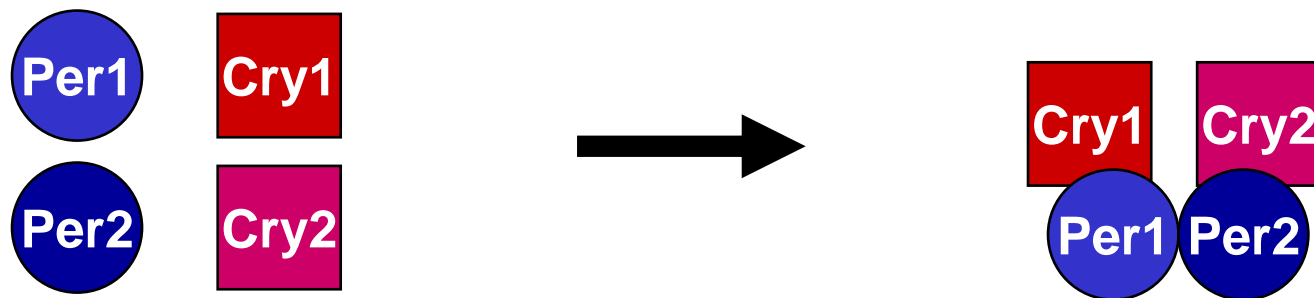
# Beyond microtubules: The cellular environment at the endoplasmic reticulum attracts proteins to the nucleus, enabling nuclear transport



Seek postdoc this fall!



Seokjoo Choe  
(KAIST)

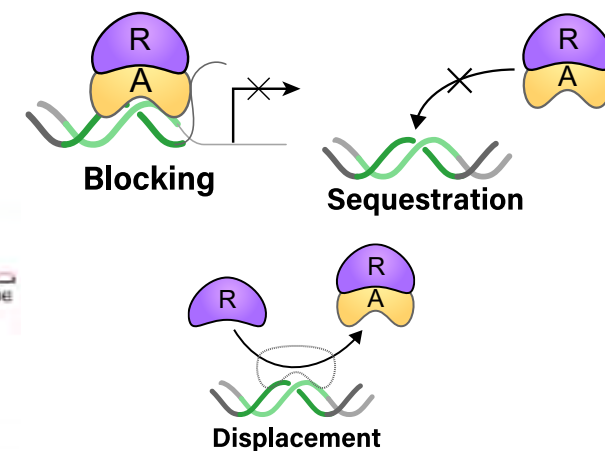
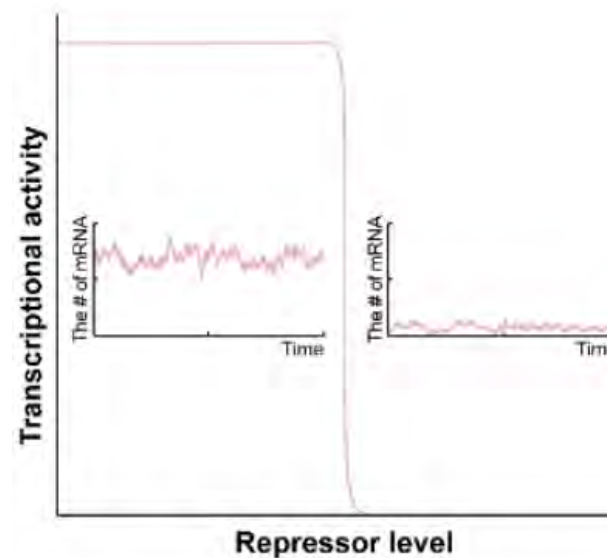
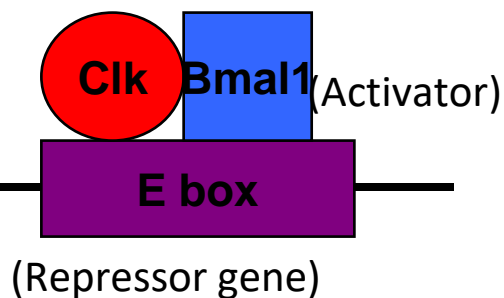


**Noise is always bad?**

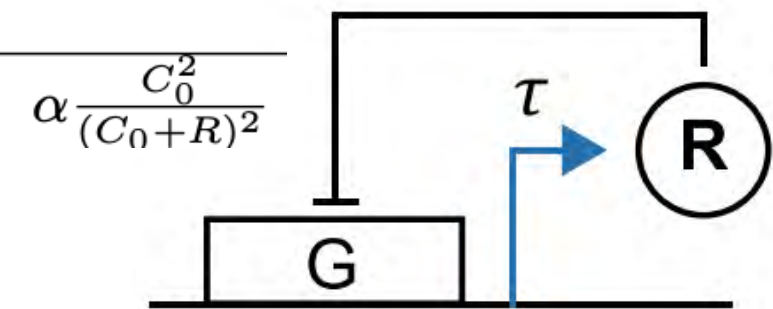
Travel time noise is filtered by phosphoswitch

Transcriptional regulation noise is filtered by multi-repression

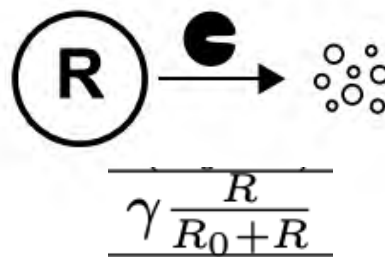
*cry1 per1*  
*cry2 per2*







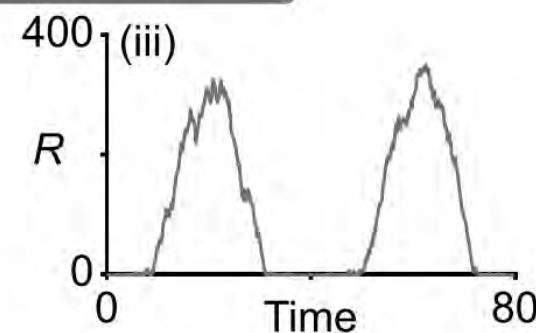
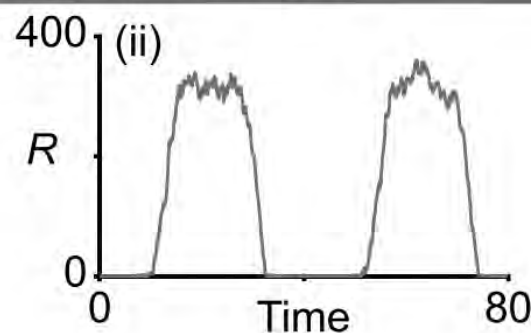
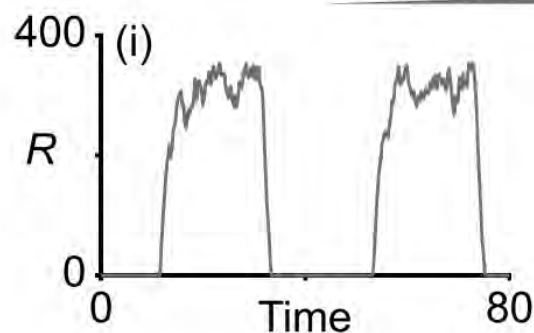
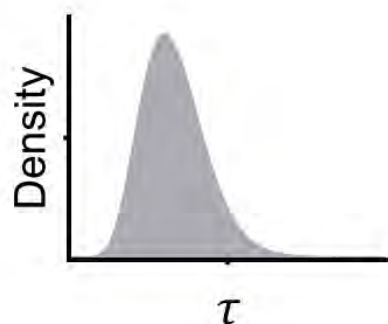
## Mather oscillator



$$\frac{dR(t)}{dt} = \frac{\alpha}{(C_0 + R(t - \tau))^2} - \beta R(t) - \frac{\delta R(t)}{R_0 + R(t)}$$



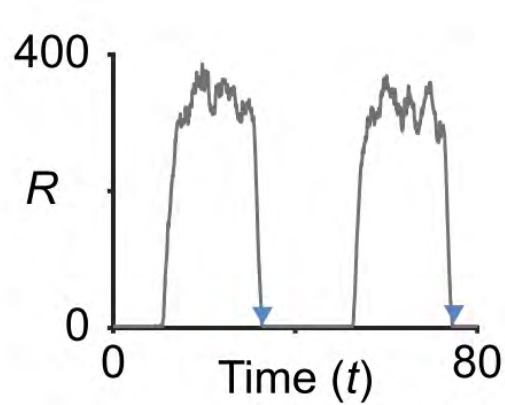
Yumin Song  
(KAIST)



$cv[\tau]$

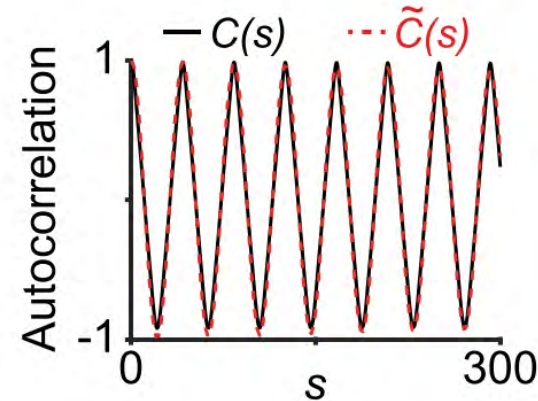
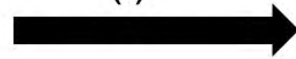
Larger variance in time delay leads to shaper oscillation

# Period, Amplitude, Sharpness and Signal-to-noise ratio (SNR)



$$C(s) = \frac{\int (R(t) - \bar{R})(R(t+s) - \bar{R}) dt}{\int (R(t) - \bar{R})^2 dt}$$

(i)



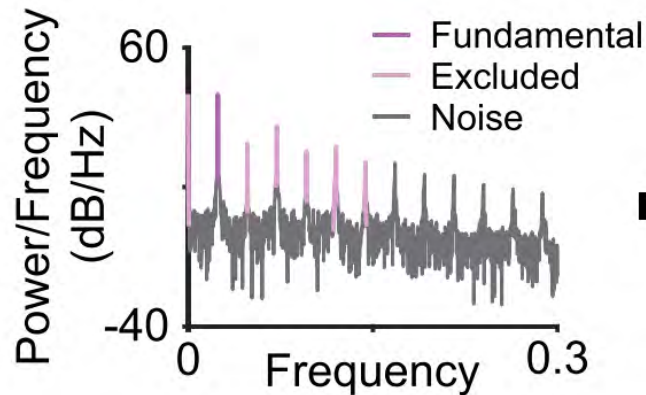
$$C(s) \approx \tilde{C}(s) = e^{-s/\eta} \cos\left(\frac{2\pi s}{T}\right)$$



**Period =  $T$**

Splitting into multiple trajectories with 10 cycles

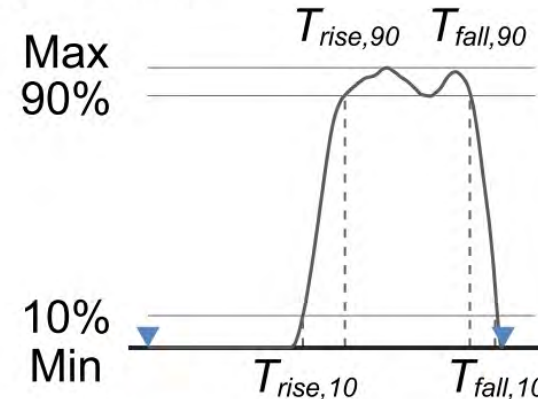
(iii)



**Signal-to-noise ratio (SNR)**



Smoothing with 10% neighborhood

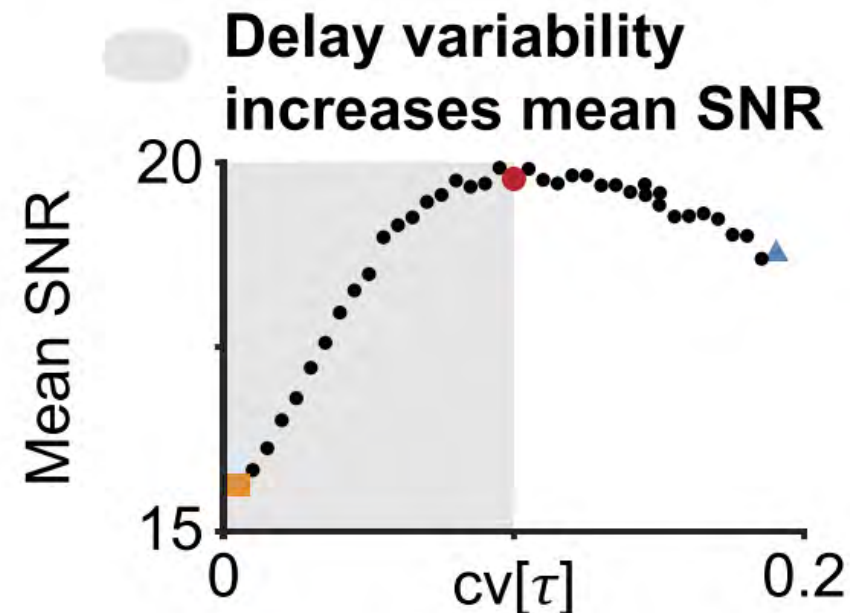
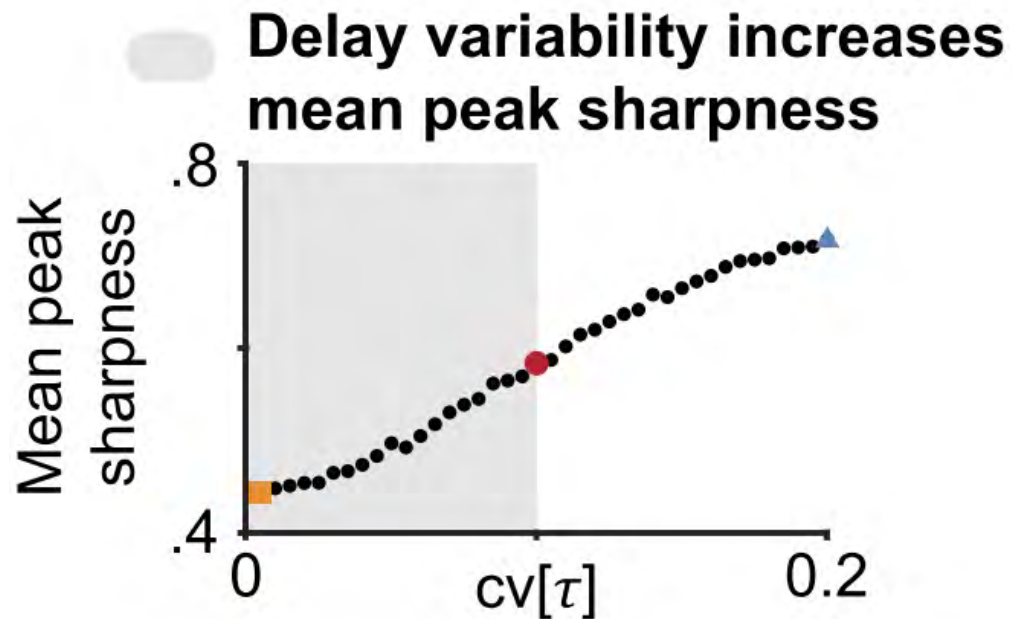
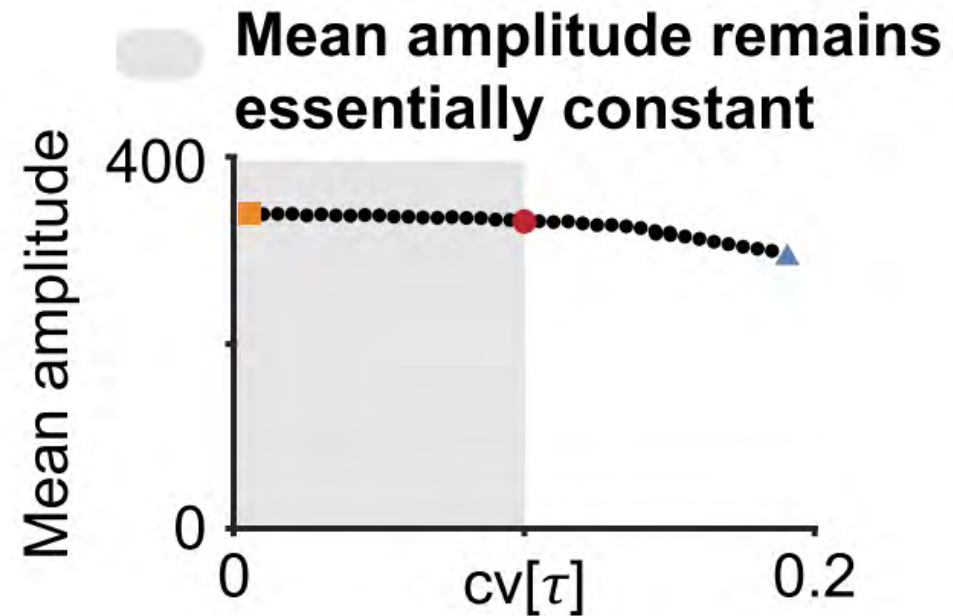
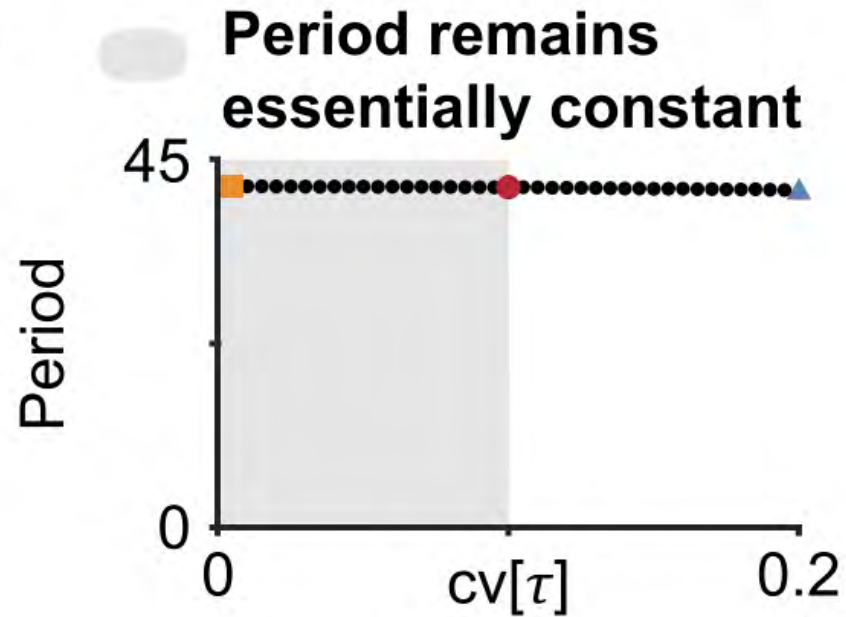


**Amplitude**  
= Max - Min

**Peak sharpness**

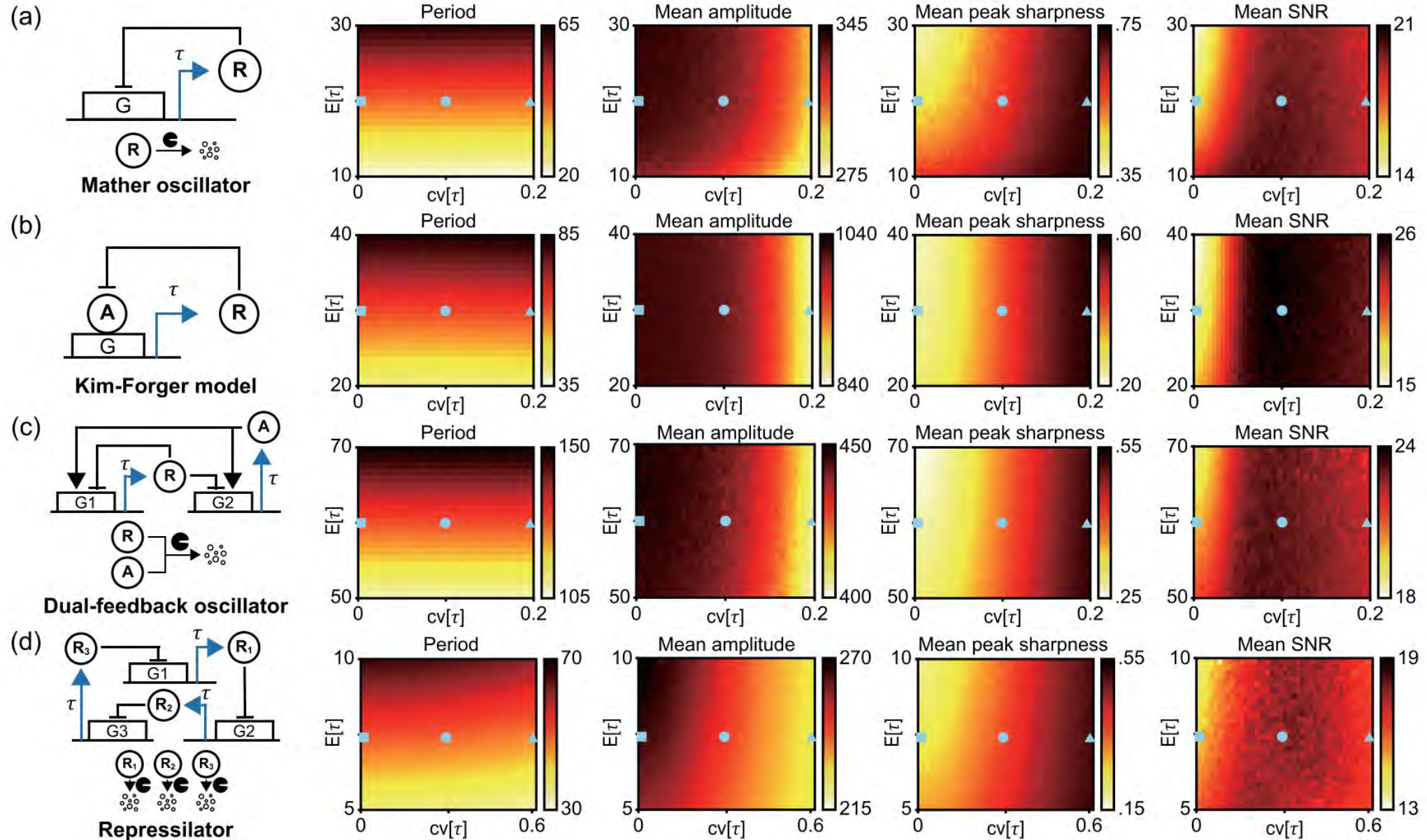
$$= 1 - \frac{T_{fall,90} - T_{rise,90}}{T_{fall,10} - T_{rise,10}}$$

Modest noise in time delay leads to sharp oscillation with high SNR!



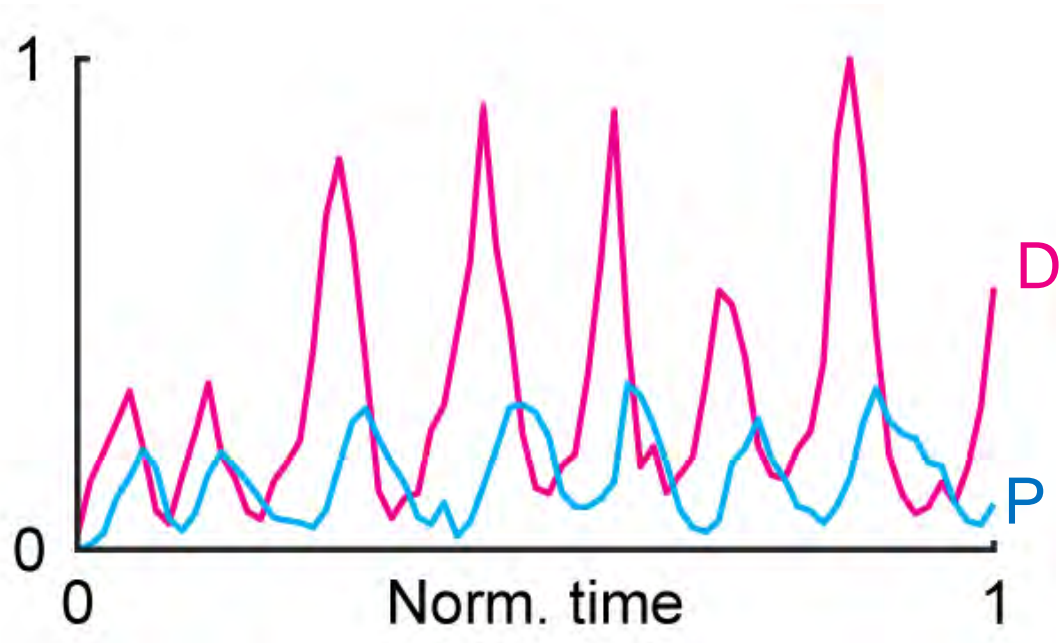


# Modest noise in time delay leads to sharp oscillation with high SNR for various models!



# Can we infer the regulatory network from timeseries data alone?

## Dynamic data



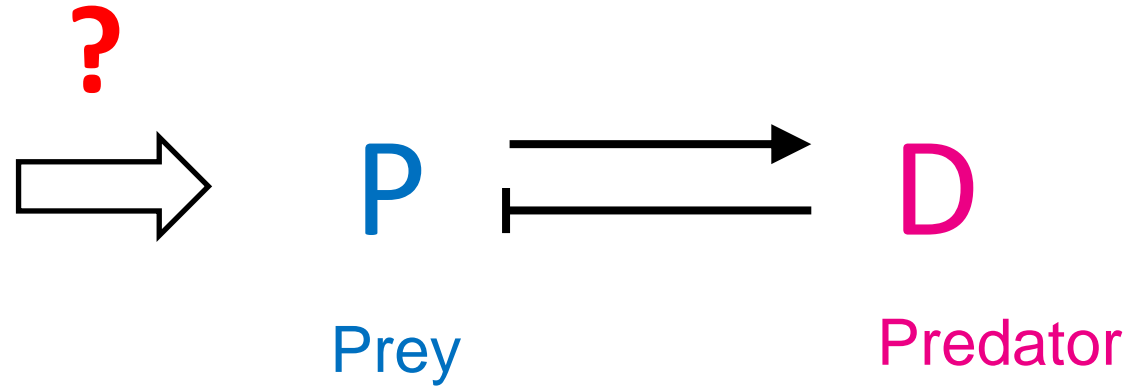
Paramecium



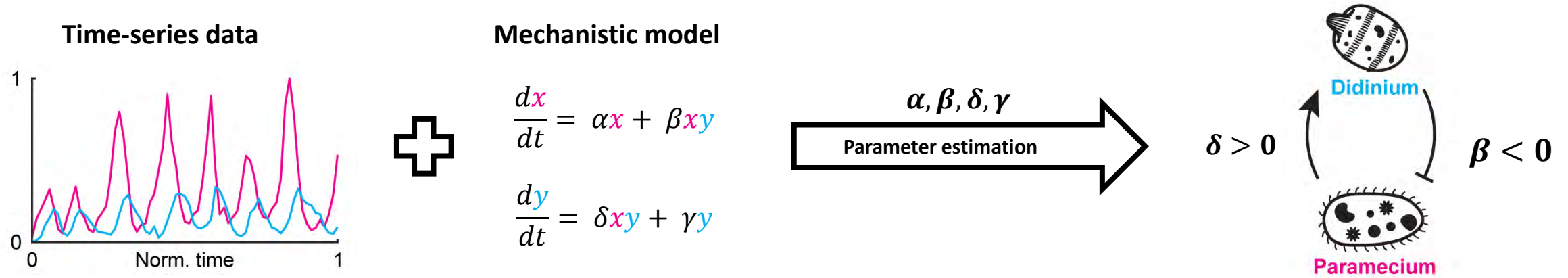
Didinium



## Regulatory Network



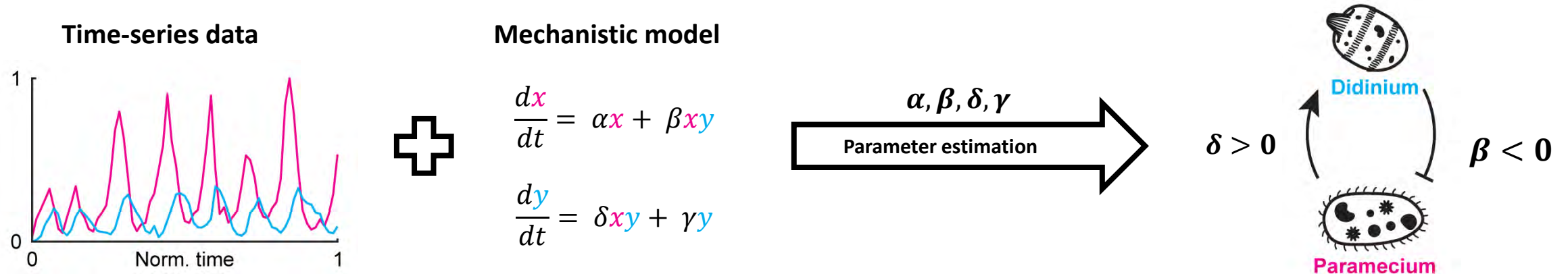
# Model based methods are popular, but have a serious limit!



**How do we know this model is correct?**

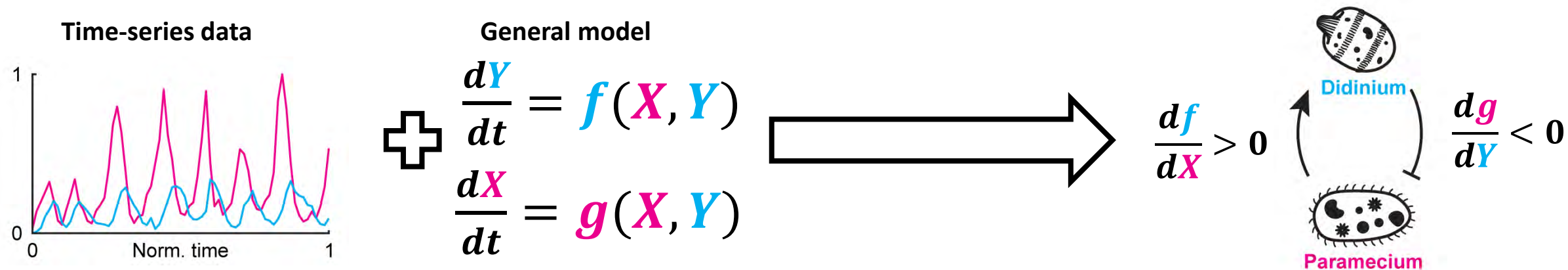


# General Model-based Inference can overcome the limit of model choice



How do we know this model is correct?

Infer the regulatory type from general ODE



Which models do describe the positive regulation?

X



Y

$$\dot{Y} = X \quad \text{V}$$

$$\dot{Y} = X^2 + 1 \quad \text{V}$$

$$\dot{Y} = 2\sqrt{X} + 3 \quad \text{V}$$

$$\dot{Y} = -X + 3 \quad \text{Negative}$$

$$\dot{Y} = X^2 - X \quad \text{Mixed}$$

$$\dot{Y} = \frac{X}{X+2} - 1 \quad \text{V}$$

# What is the common rule of the positive regulations?

(X)

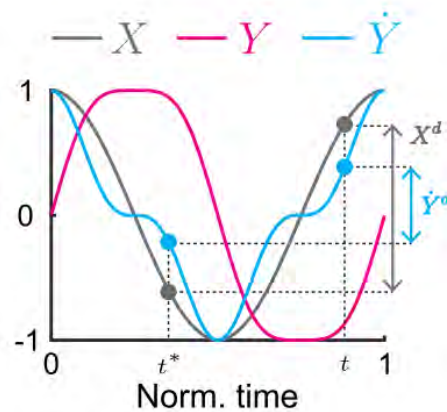
$$\dot{Y} = X$$



(Y)

$$\dot{Y} = X^2 + 1$$

$$\dot{Y} = 2\sqrt{X} + 3$$



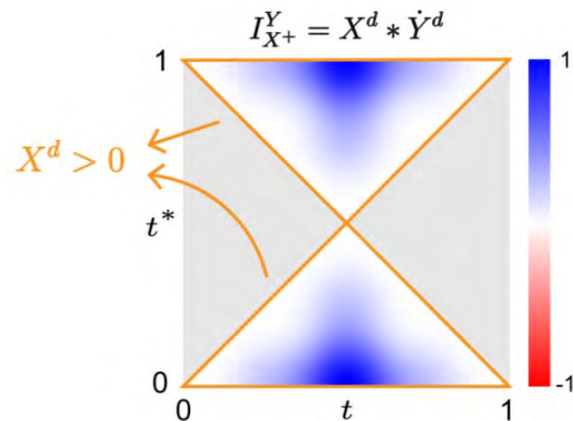
When  $X$  increases,  $\dot{Y}$  always increases.

Translate into the context of time series

If  $X^d = X(t) - X(t^*) > 0$ , then  $\dot{Y}^d = \dot{Y}(t) - \dot{Y}(t^*) > 0$

**Regulation detection function**

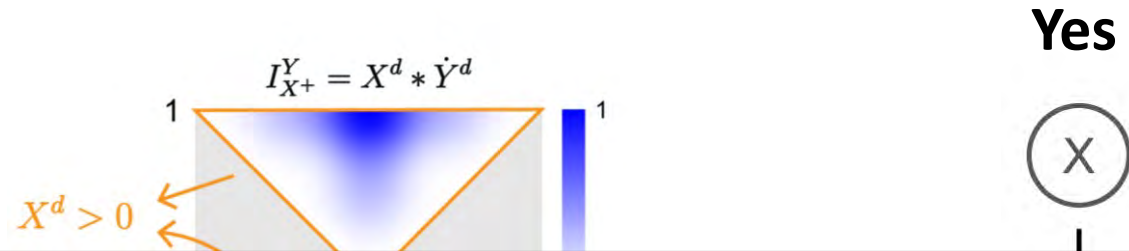
$I_{X+}^Y := X^d \times \dot{Y}^d > 0$  for  $t$  and  $t^*$  with  $X^d > 0$



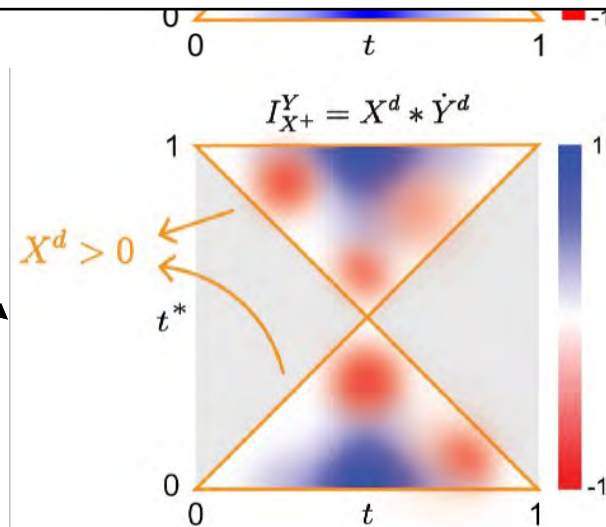
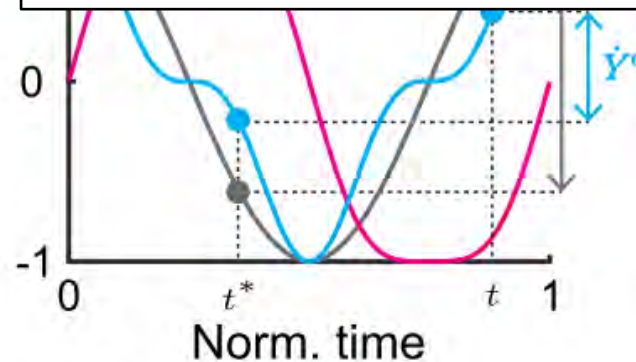


We can infer positive regulation from time-series with **regulation detection function**

$$I_{X^+}^Y := X^d \times \dot{Y}^d > 0 \text{ for } t \text{ and } t^* \text{ with } X^d > 0$$



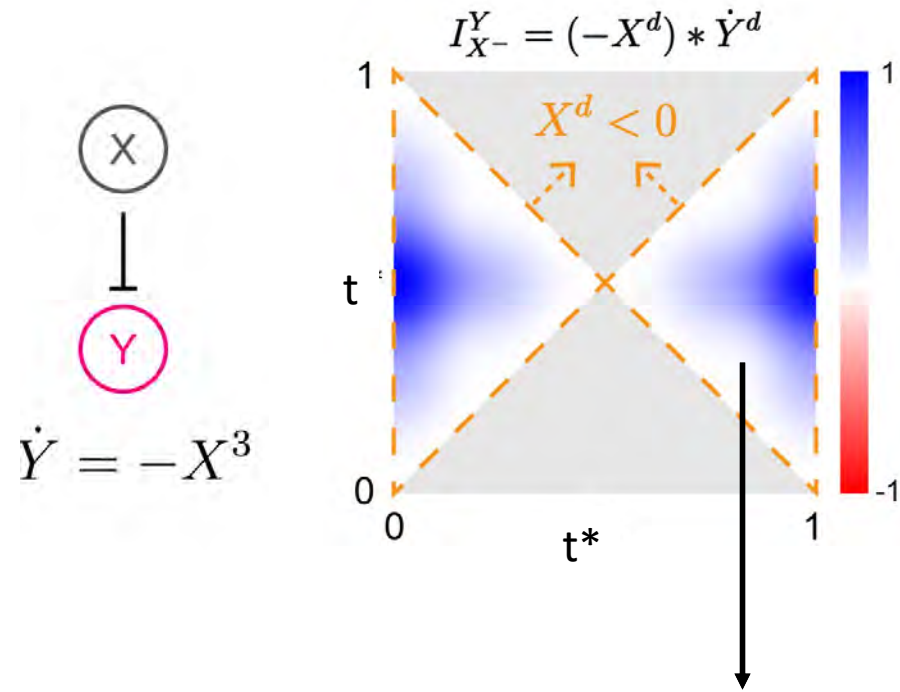
**What about negative regulation?**



No



We can also infer negative regulation from time-series!



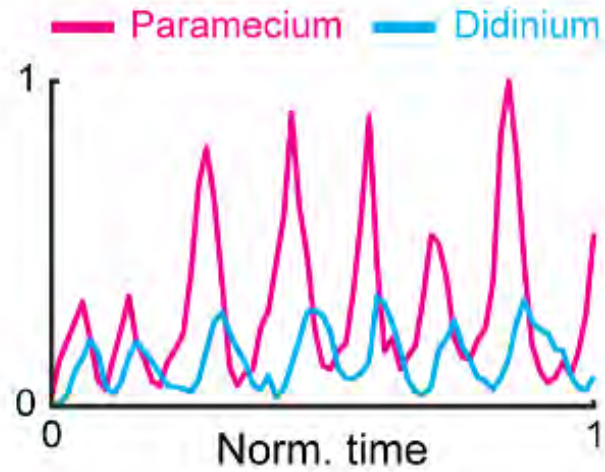
When  $X$  **decreases**,  $\dot{Y}$  always increases.

If  $X^d = X(t) - X(t^*) < 0$ , then  $\dot{Y}^d = \dot{Y}(t) - \dot{Y}(t^*) > 0$

Regulation detection function:  $I_{X-}^Y := (-X^d) \times \dot{Y}^d > 0$  for  $X^d < 0$

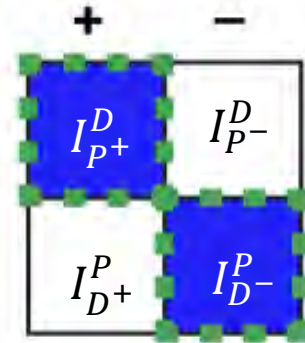
The positiveness of  $I_{X-}^Y$  obtained with time-series implies the negative regulation

Positiveness of regulation detetion function



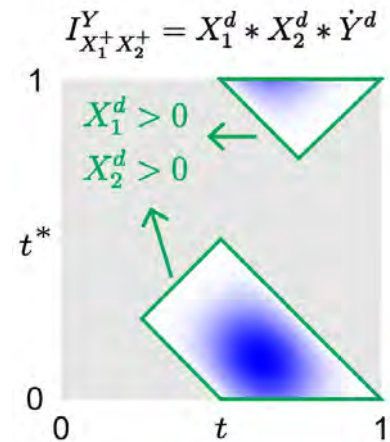
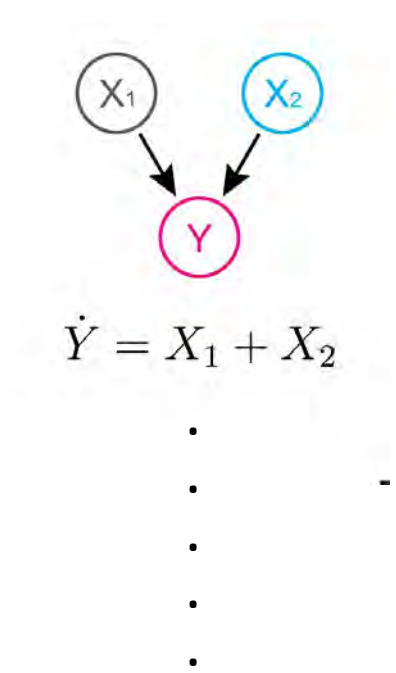
P to D

D to P



**What about multi-regulations?**

# Extension to multi-regulation is easy!

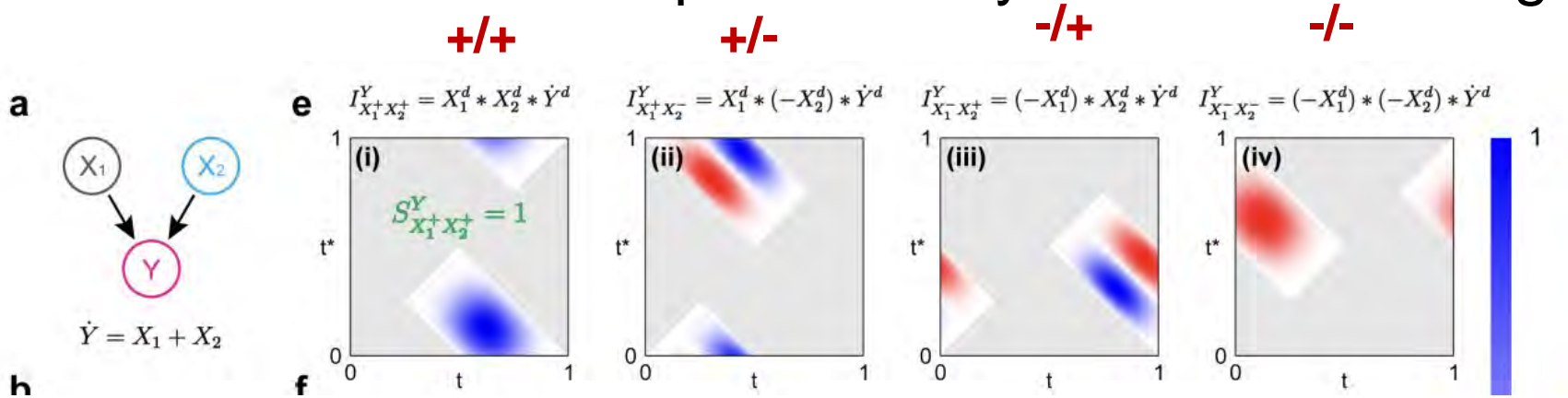


When both  $X_1$  and  $X_2$  increase,  $\dot{Y}$  always increases.

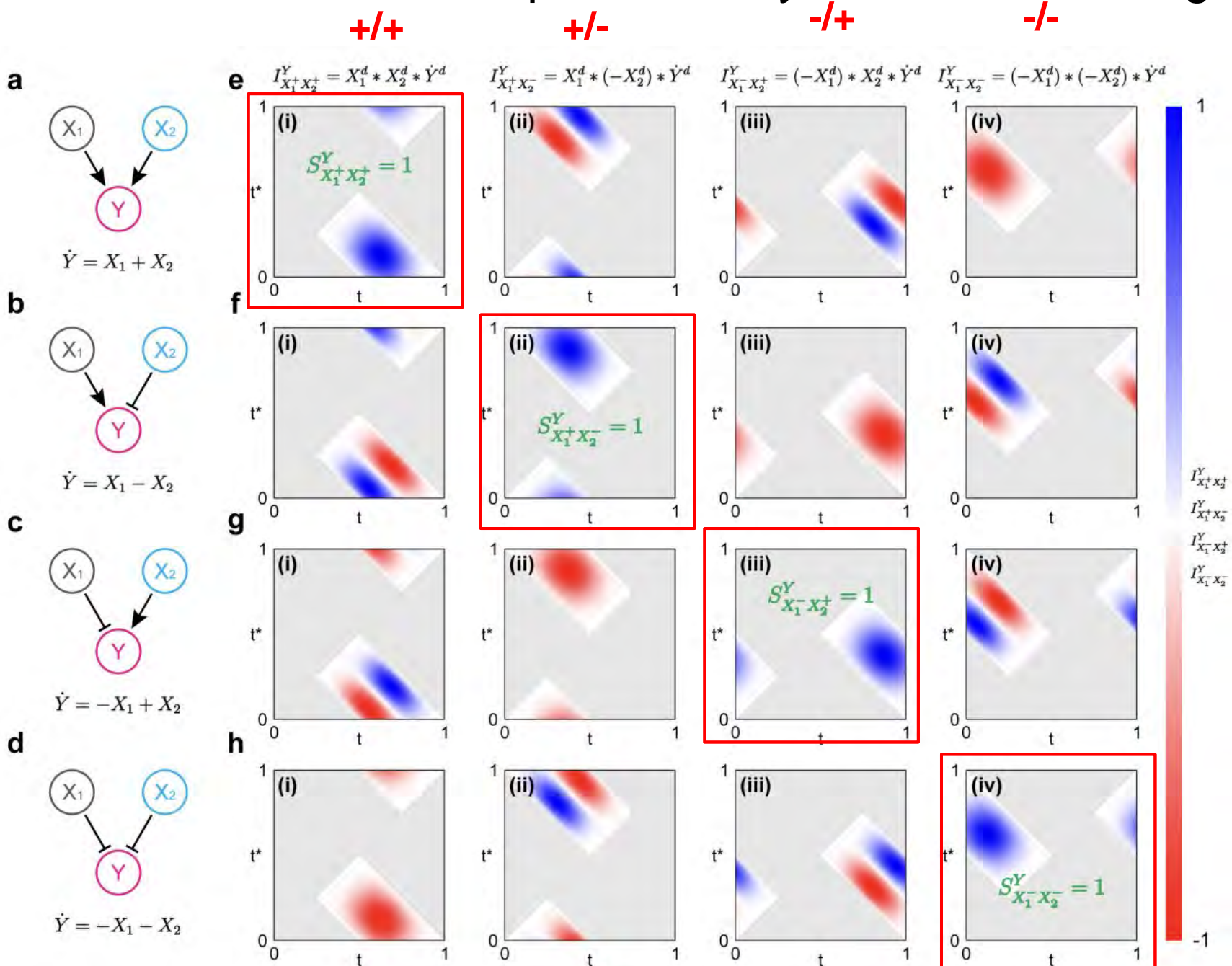
If  $X_1^d, X_2^d > 0$ , then  $\dot{Y}^d > 0$  for  $t$  and  $t^*$ .



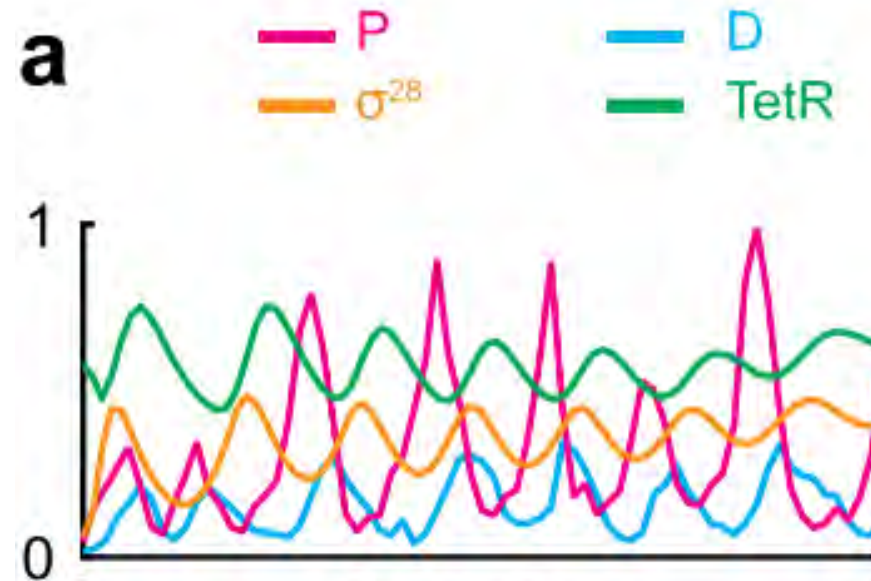
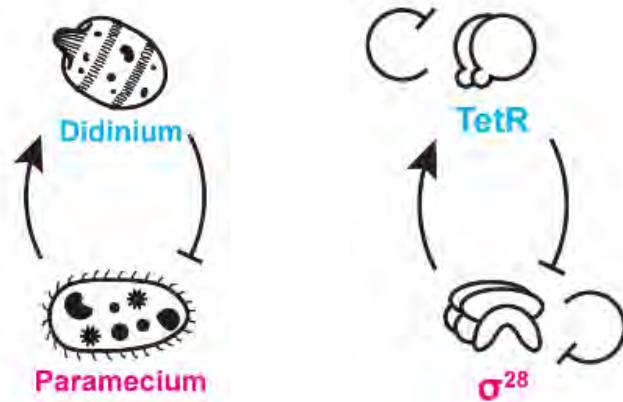
# Regulation detection function is positive only for the correct regulation type!



# Regulation detection function is positive only for the correct regulation type!

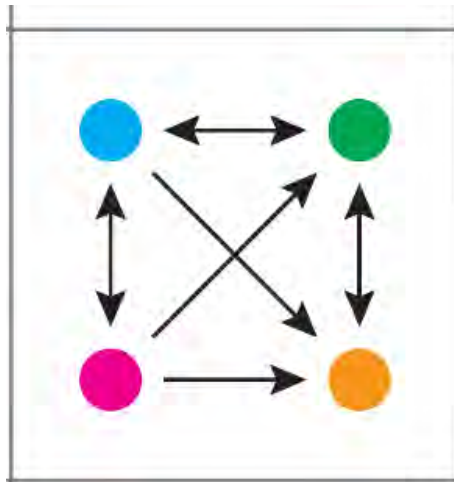


Ecology + Intracellular data

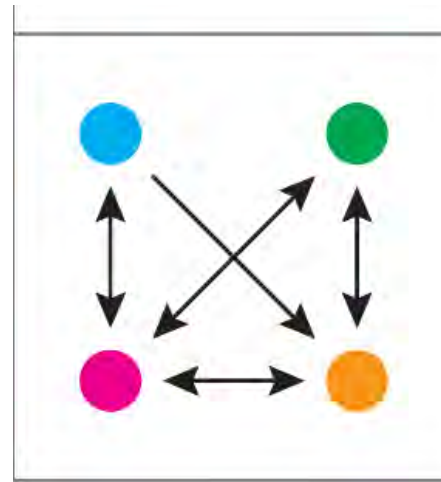


**For real noisy data, we need to incorporate statistical approach!**

(Statistical theory)

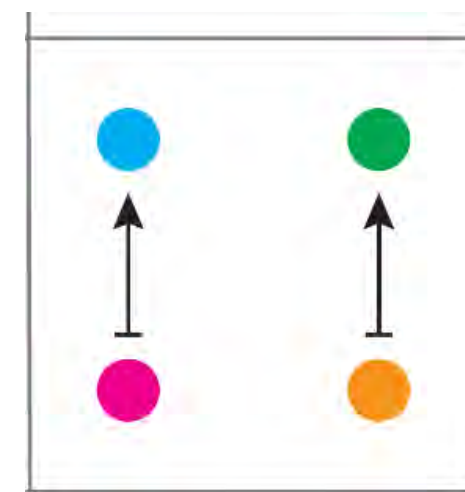


(Taken's theorem)



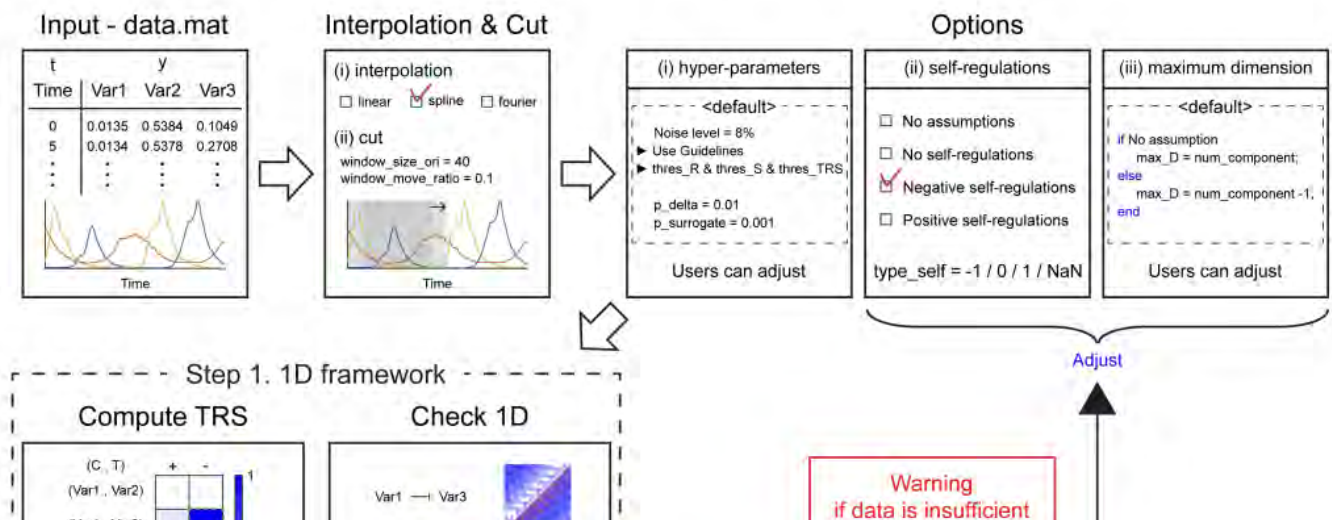
Sugihara, Science (2012)

(General model-based)



Park, Ha, Kim, Nature Communications (2023)

# General-ODE-Based Inference (GOBI)



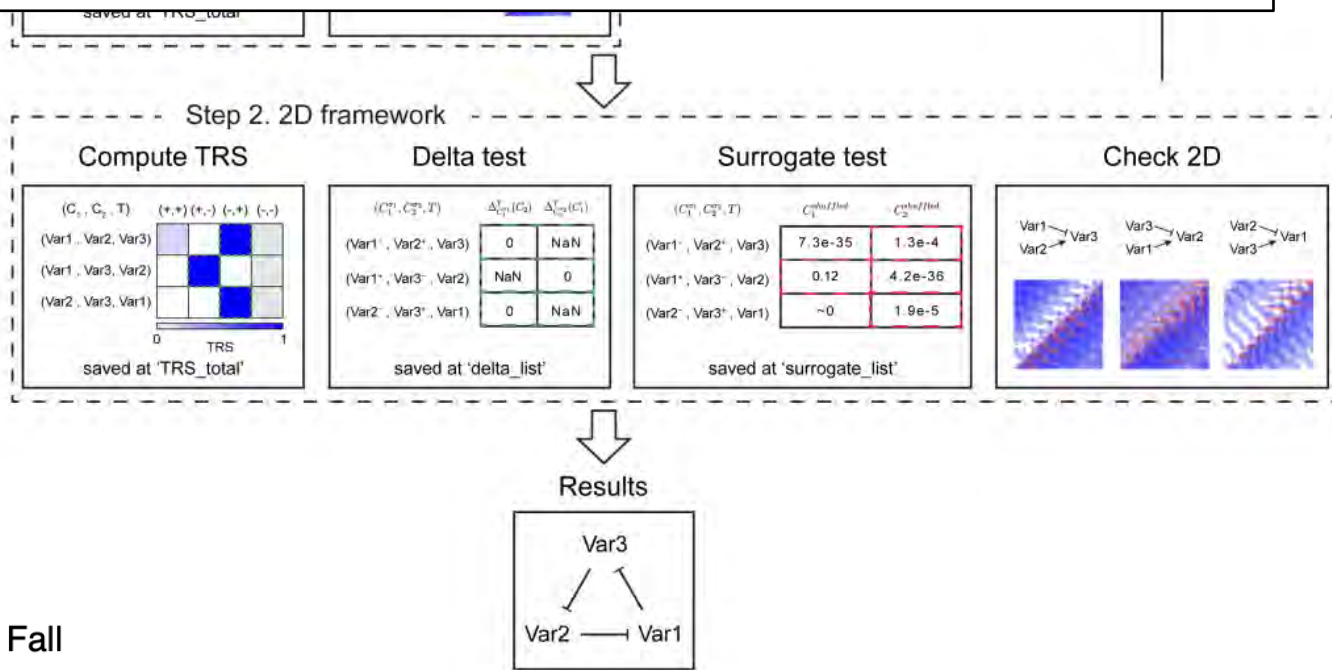
Let's apply GOBI to solve real-world problem!

Park, Ha, Kim, Nature Communications (2023)



Seokmin Ha (KAIST Undergrad)  
MIT Graduate Student, 2023 Fall

Seho Park (KAIST Undergrad)  
U Wisconsin Graduate Student, 2023 Fall





# Dengue outbreak even with the active prevention and control program!

APRIL 17, 2024 | 3 MIN READ

## A Dengue Fever Outbreak Is Setting Records in the Americas

At least 2.1 million cases of dengue fever have been reported in North and South America, and this year 1,800 people have died from the mosquito-borne disease

BY FRANCISCO "A.J." CAMACHO & E&E NEWS



Health

Life, But Better

Fitness

Food

Sleep

Mindfulness

Relationships

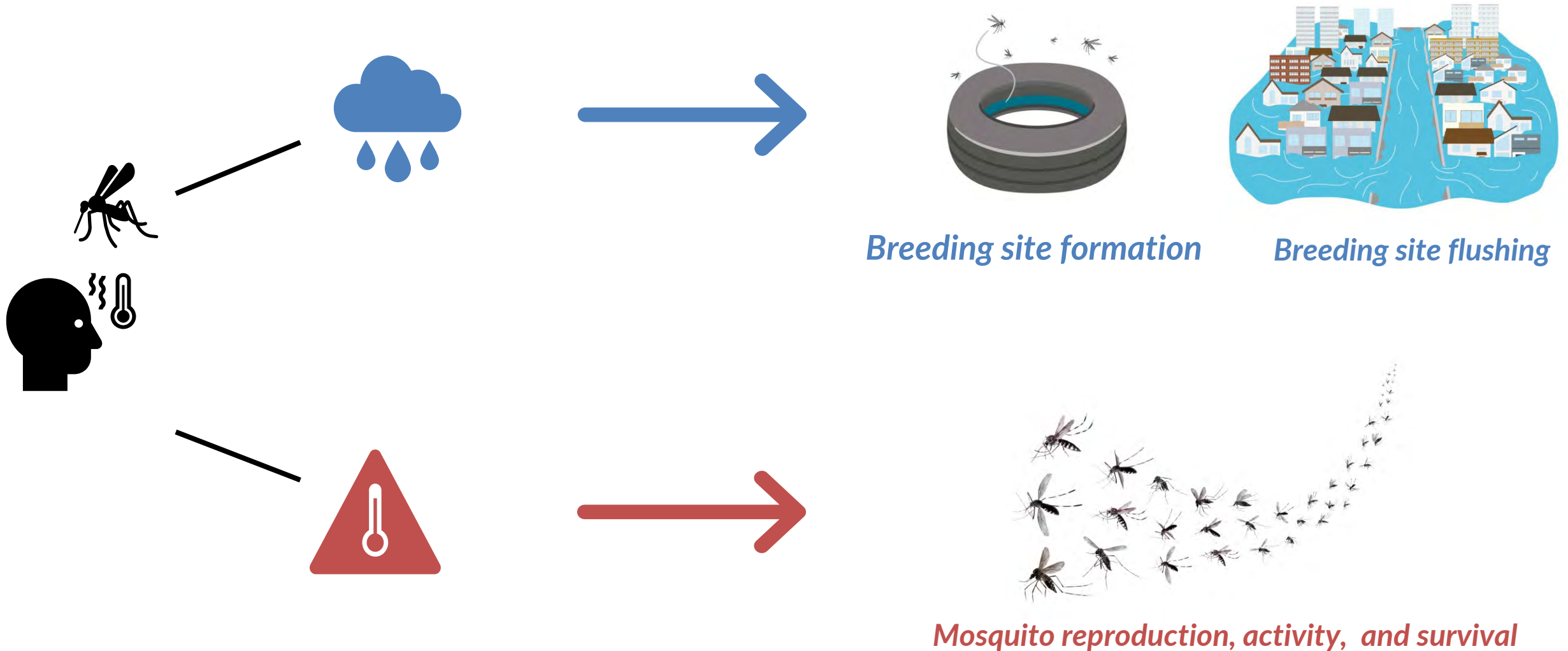
## How the Paris Olympics could become a super-spreader event for dengue

THE  
CONVERSATION















Analysis by Mark Booth

🕒 4 minute read · Published 6:31 AM EDT, Fri June 14, 2024

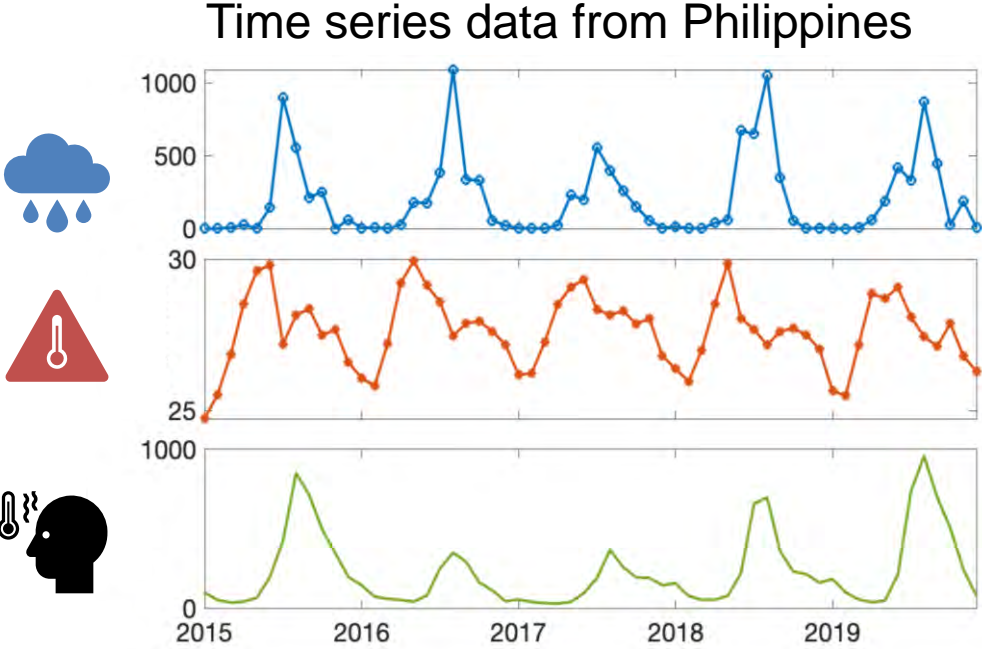
This increasing trend of Dengue cases could be due to weather changes.



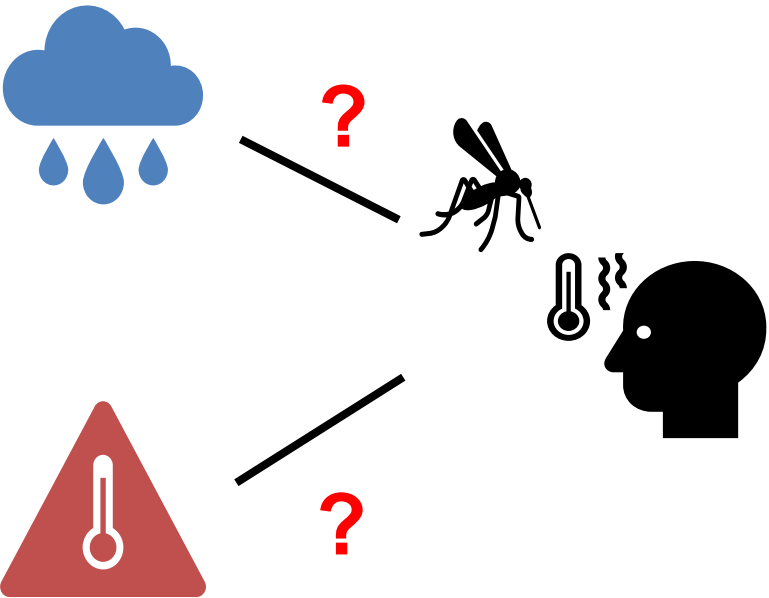
# The effects of weather variables to dengue incidence is unclear

			
<p>Spatiotemporal dynamics of dengue in Colombia in relation to the combined effects of local climate and ENSO</p> <p>Estefanía Muñoz <sup>a, b, c</sup>, Germán Poveda <sup>b</sup>, M. Patricia Arbeláez <sup>a, c</sup>, Iván D. Vélez <sup>a, c</sup></p> <p><sup>a</sup> World Mosquito Program, Colombia <sup>b</sup> Departamento de Geociencias y Medio Ambiente, Universidad Nacional de Colombia, Medellín, Colombia <sup>c</sup> PECET, Universidad de Antioquia, Medellín, Colombia</p>			 <b>Controversial</b>
<p>Choi et al. BMC Public Health (2016) 16:241 DOI 10.1186/s12889-016-2923-2</p> <p>BMC Public Health</p> <p>RESEARCH ARTICLE Open Access CrossMark</p> <p>Effects of weather factors on dengue fever incidence and implications for interventions in Cambodia</p> <p>Youngjo Choi<sup>1*</sup>, Choon Siang Tang<sup>1</sup>, Lachlan McIver<sup>2</sup>, Masafiro Hashizume<sup>3</sup>, Vibol Chan<sup>1</sup>, Rabintra Romauld Abeyesinghe<sup>1</sup>, Steven Iddings<sup>1</sup> and Rekol Huy<sup>1</sup></p>			
<p>PLOS NEGLECTED TROPICAL DISEASES</p> <p>OPEN ACCESS PEER-REVIEWED RESEARCH ARTICLE</p> <p>Local and Global Effects of Climate on Dengue Transmission in Puerto Rico</p> <p>Michael A. Johansson , Francesca Dominici, Gregory E. Glass</p> <p>Published: February 17, 2009 • <a href="https://doi.org/10.1371/journal.pntd.0000382">https://doi.org/10.1371/journal.pntd.0000382</a></p>		 	
<p>Extreme weather conditions and dengue outbreak in Guangdong, China: Spatial heterogeneity based on climate variability</p> <p>Jian Cheng <sup>a, b</sup>, Hilary Bambrick <sup>a</sup>, Laith Yakob <sup>c</sup>, Gregor Devine <sup>d</sup>, Francesca D. Frentiu <sup>e</sup>, Gail Williams <sup>f</sup>, Zhongjie Li <sup>g</sup>, Weizhong Yang <sup>a, b</sup>, Wenbiao Hu <sup>a, *</sup></p>	 		

# Casual relationship between weather variables and dengue incidence?



**GOBI**



**Jeon, Saebom (전세봄)**

Visiting Research Fellow (2023.01-2024.02)  
Associate Professor, Department of Marketing Big Data, Mokwon University



**Aurelio A. de los Reyes V**

Senior Researchers (2021.10 – 2023.01)



**Olive Cawiding**

Graduate Student  
Graduate student at Dept. of Mathematical Sciences, KAIST.  
Office: B223  
Email: orcawiding\_at\_kaist.ac.kr



Both R+/T+ & R-/T+ are inferred!

Rain  
Temp

Dengue

Rain

Dengue

Rain  
Temp

Dengue

Rain

Dengue

Rain  
Temp

Dengue

Temp

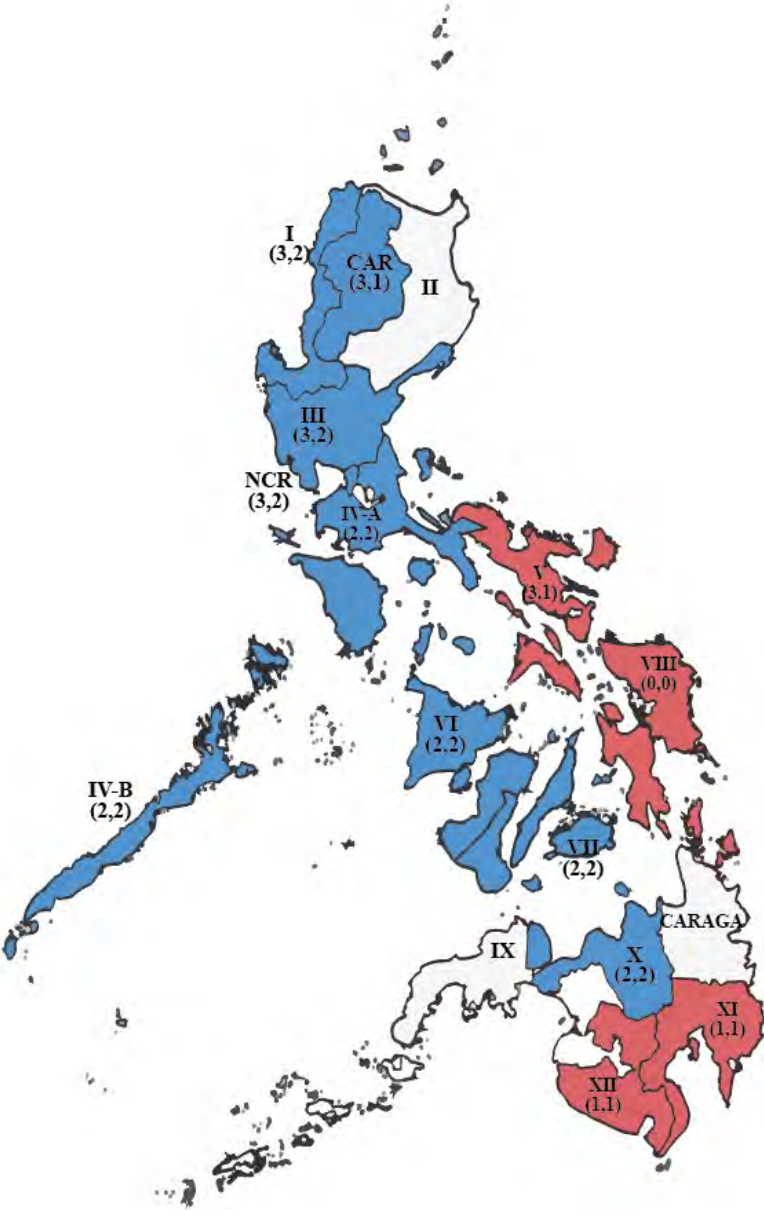
Dengue

Rain  
Temp

Dengue

Temp

Dengue

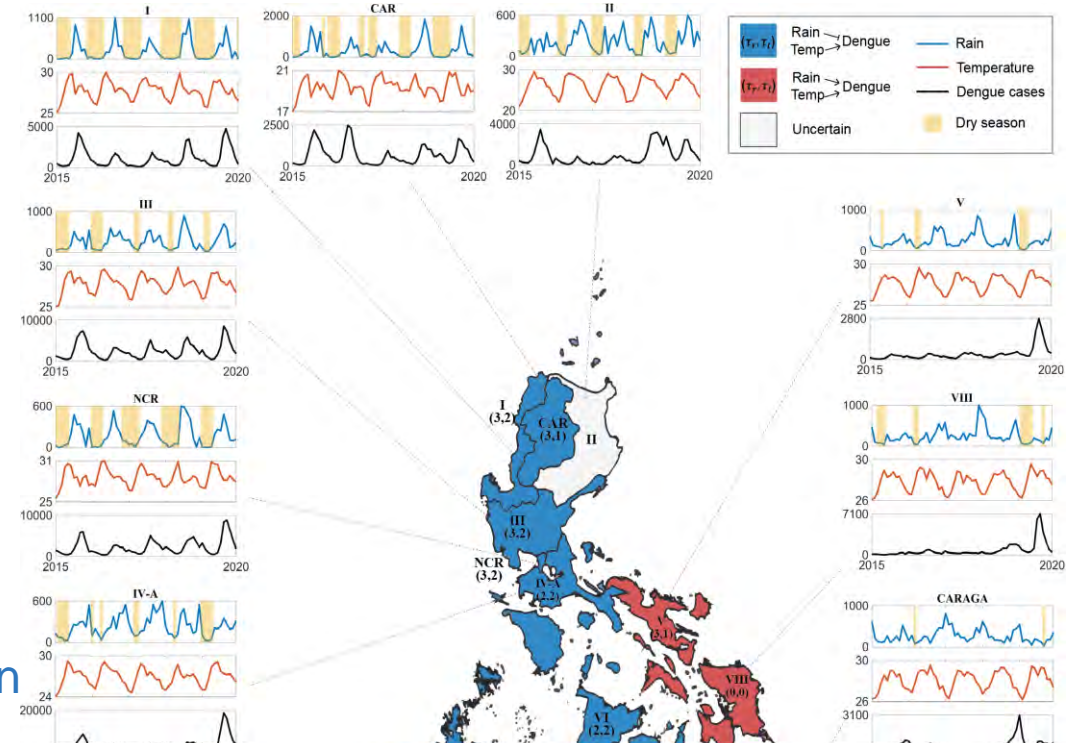


Regions with the same regulation type are located next to each other.

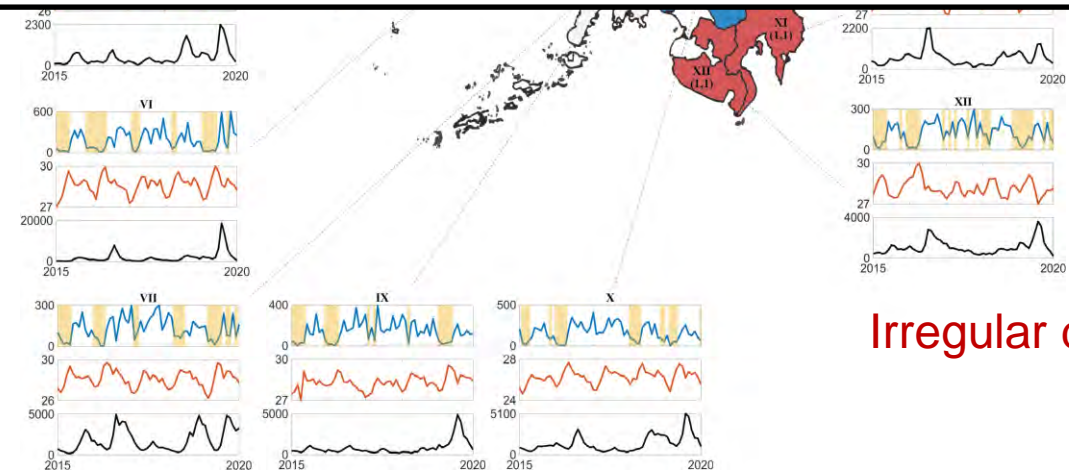
What climate conditions distinguish the western and eastern regions?

Dry season length variability is the key!

Regular dry season

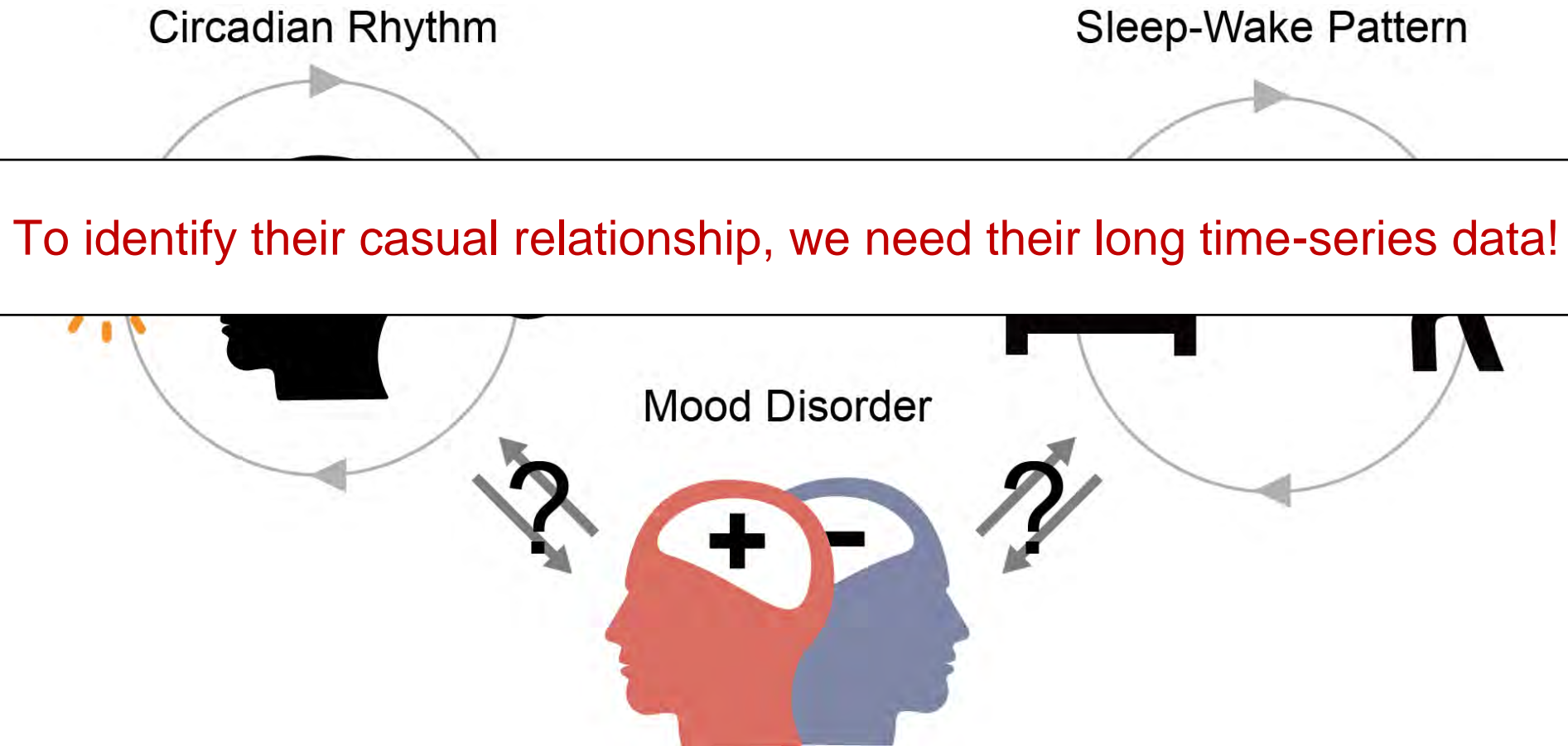


Another approach to infer network



Irregular dry season

Causal relationships b/w sleep, circadian rhythm, and mood are still unknown



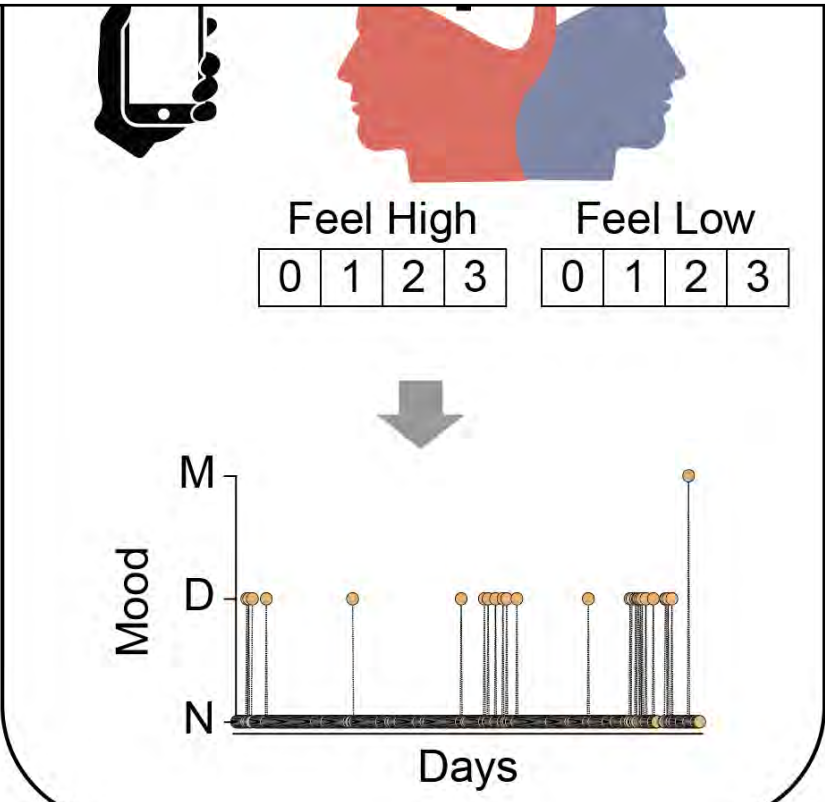
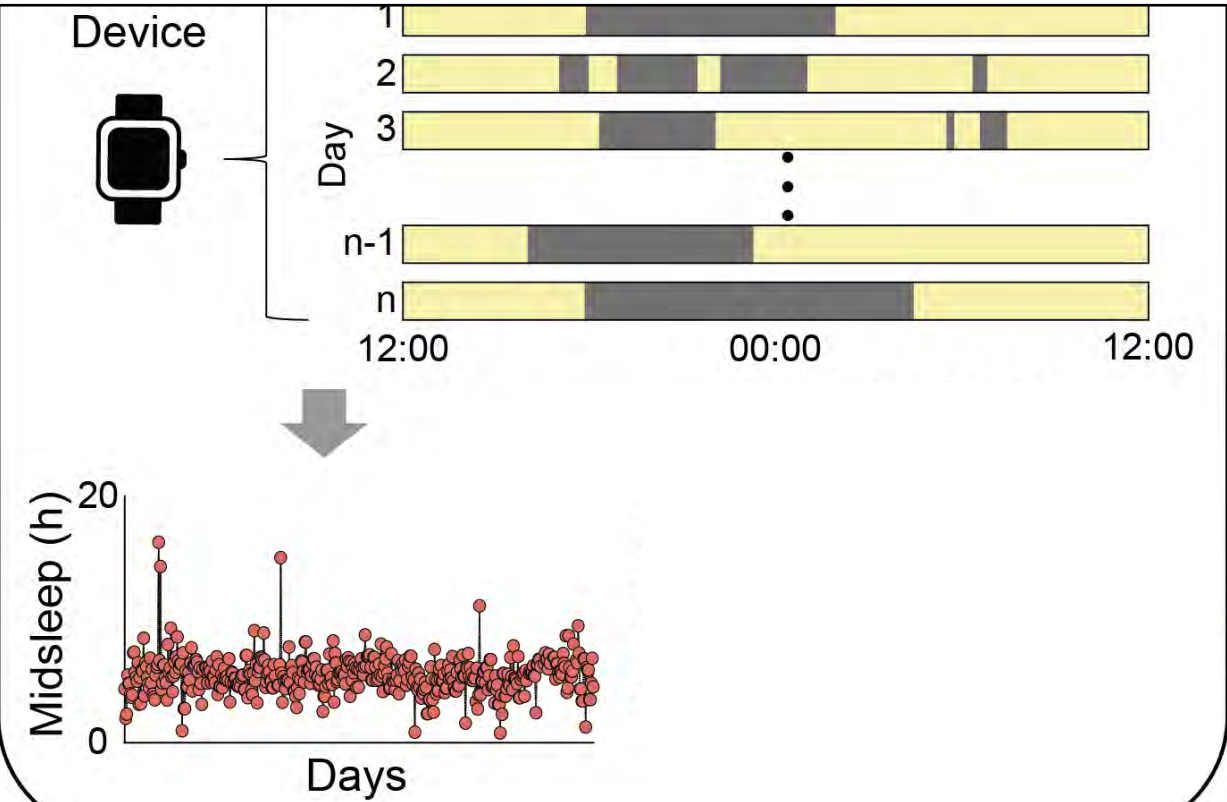
“Current evidence supports the **existence of associations** between sleep/circadian rhythm disturbances and depression **but the direction of causality remains elusive**”

# Collect sleep data and mood changes of patients with mood disorders

(a) 139 patients (29~1457 days for each patient)

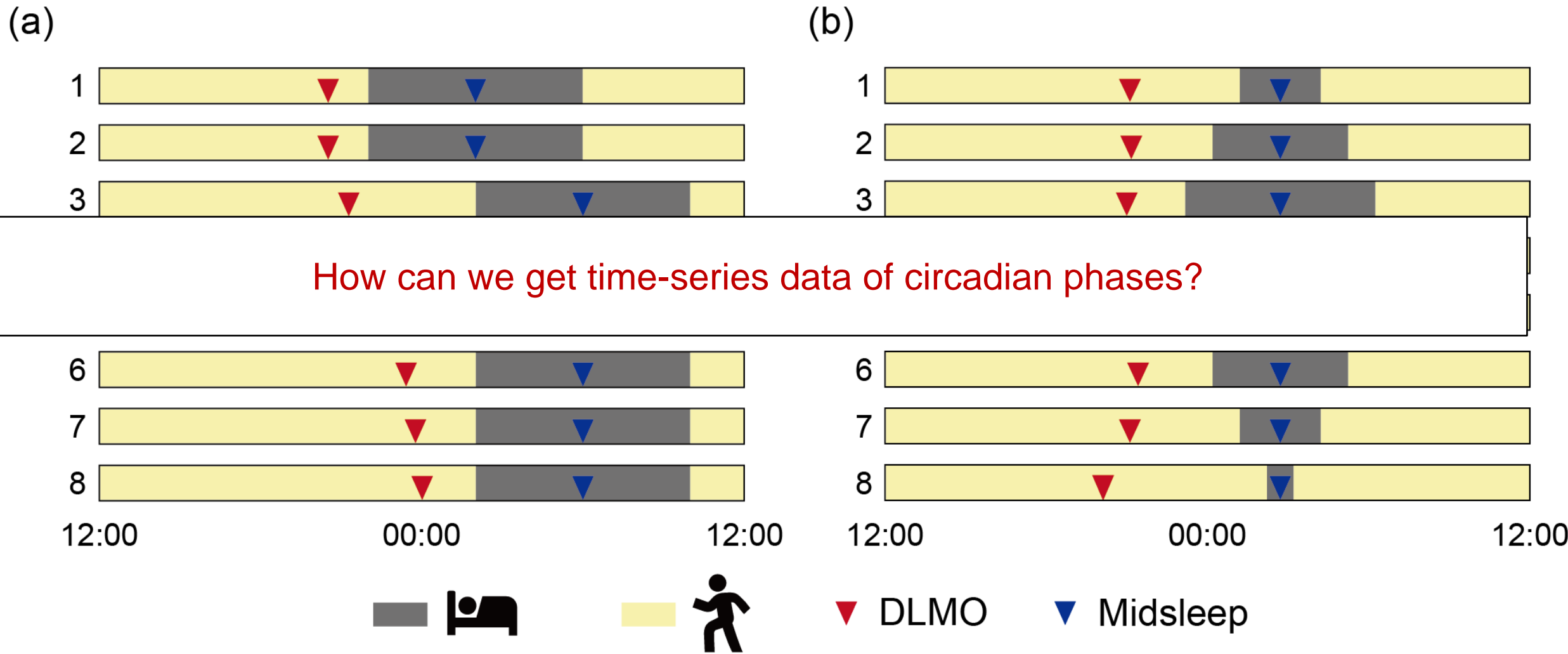
(b)

What about circadian phases? How can we get time-series data of circadian phases?





# Mid sleep phase is different from circadian phase!

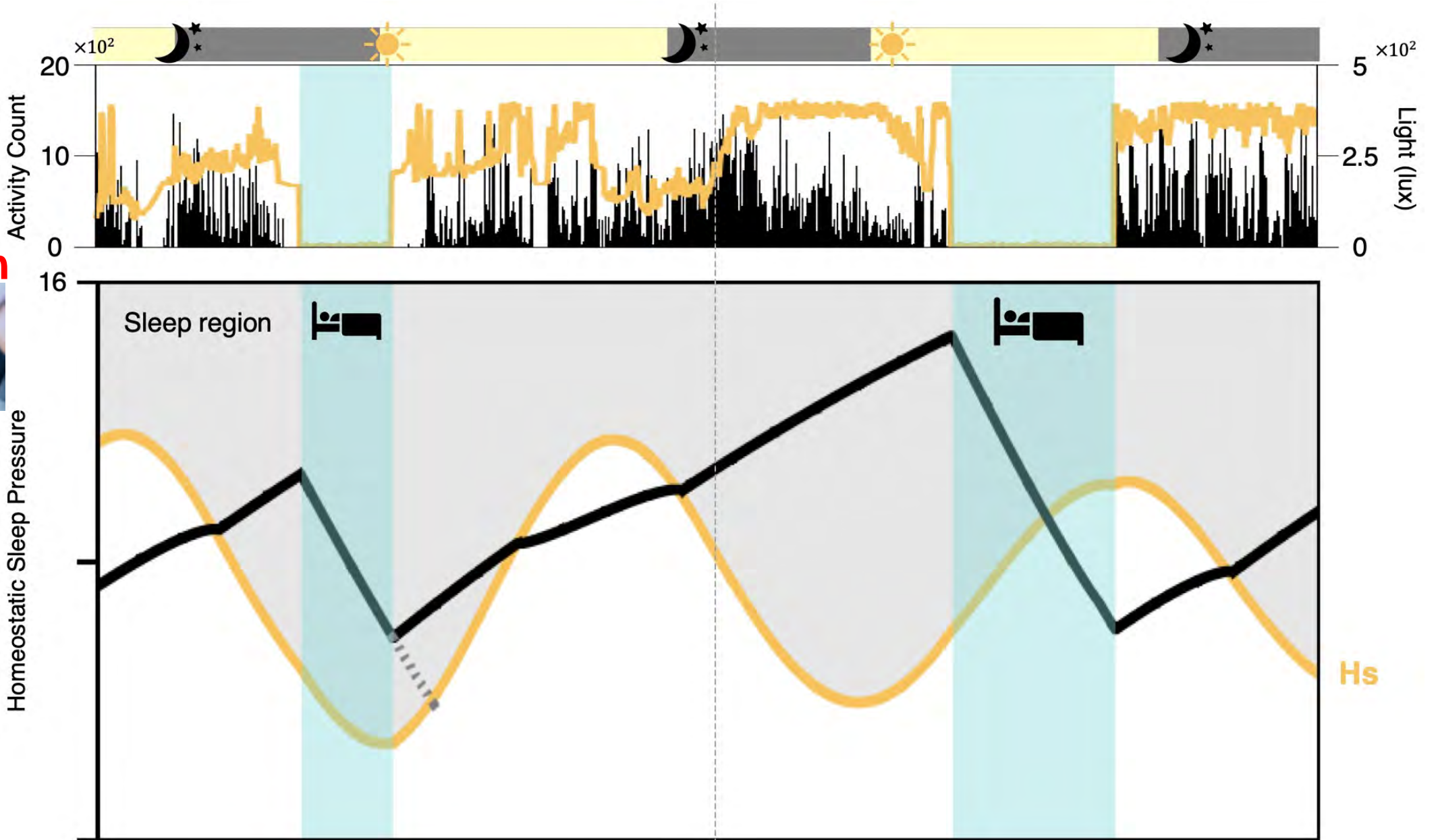


# Sleep pressure & Circadian rhythm can be estimated with math modeling!

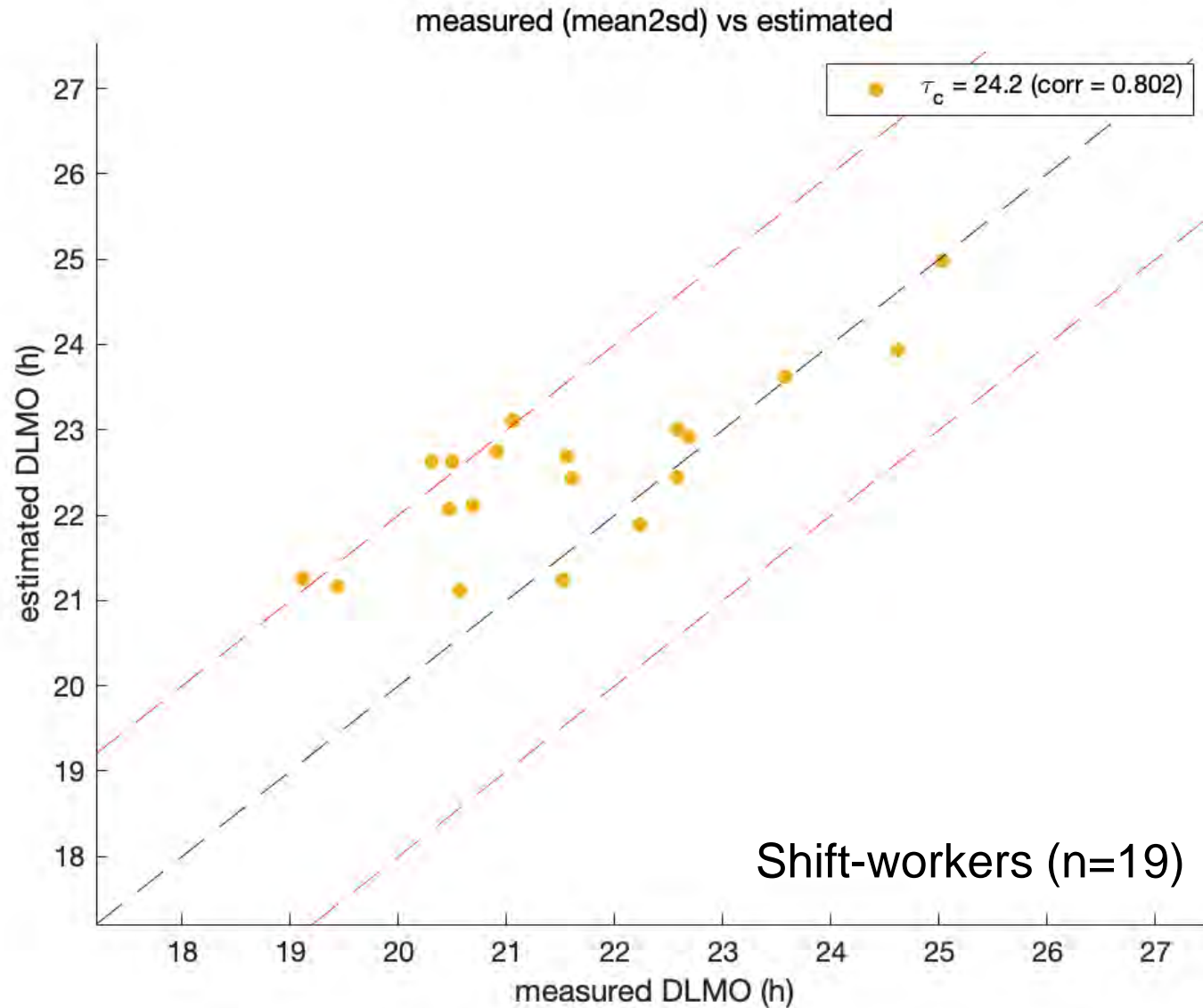
Data



Simulation



Even for rotating shift workers, math model can accurately predict DLMO!  
For regulator workers, much more accurate (<1hr)



Eun Yeon Joo  
(Samsung Medical Center)



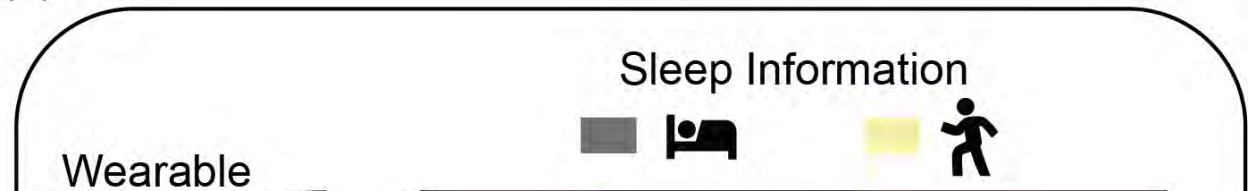
Su Jung Choi  
(SKKU)



Dong Ju, Lim  
(KAIST Grad)

# Collect sleep data and mood changes of patients with mood disorders

(a) 139 patients (29~1457 days for each patient)

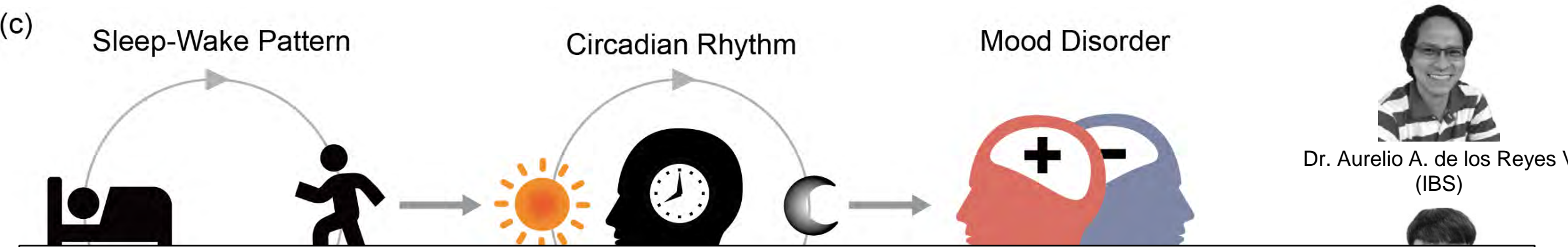


(b)



Transfer Entropy is applied to timeseries data to identify causal relationship!





Dr. Aurelio A. de los Reyes V  
(IBS)

Can we predict mood episodes with only sleep-wake data measured with wearables?

Yumin Song  
(KAIST grad)



Jaegwon Jeong  
(Korea U Medical School)



Dr. Hunjung Lee  
(Korea U Medical School)

Current issue

eBioMedicine  
Part of THE LANCET Discovery Science

Editorial

Articles

Review

Endometrial cancer: improving management among increasing incidence rates

Endogenous circadian rhythm expression in the gut: misrecognition of people living with IBS

Advances in soft and porous organosynthetic catalysis

May 2024  
Volume 103

Song, Jung et al., *Ebiomedicine* (2024)

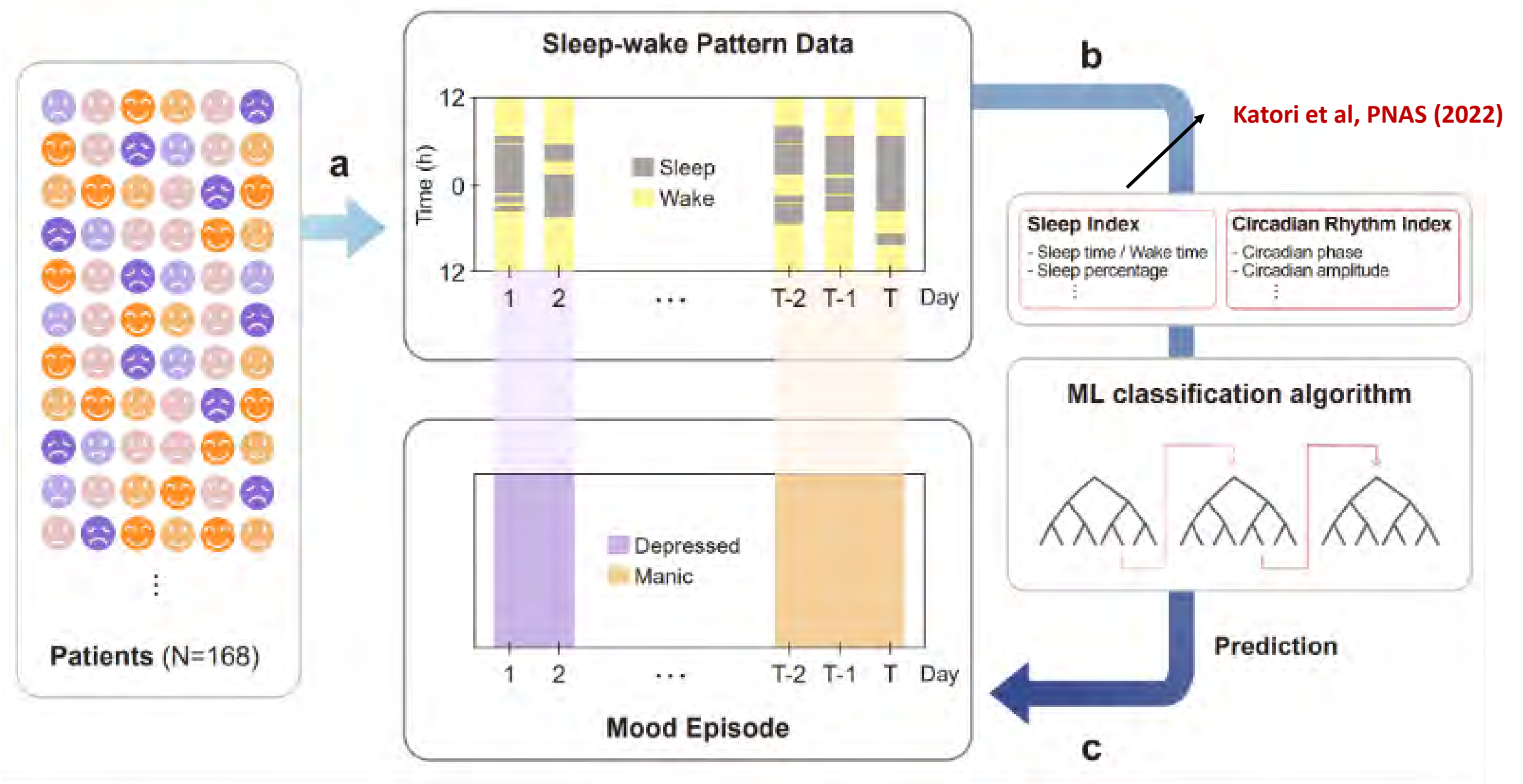
ARTICLES

Causal dynamics of sleep, circadian rhythm, and mood symptoms in patients with major depression and bipolar disorder: insights from longitudinal wearable device data

Song et al.

image ©

# Can we predict mood episodes with only sleep-wake data measured with wearables?



# We can accurately predict mood episodes with only sleep-wake data



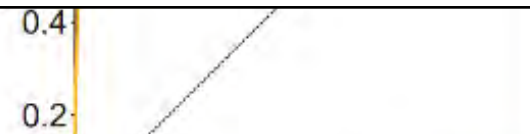
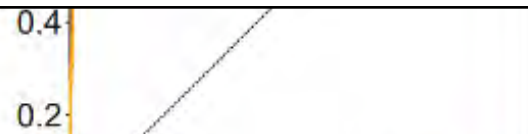
Depressive episode

Manic episode

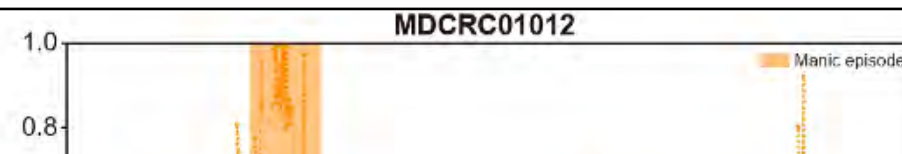
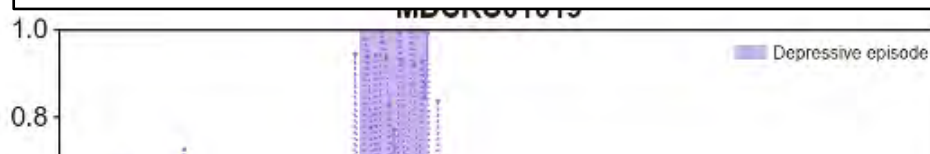
Hypomanic episode



**Most important feature for prediction is “Circadian phase”**

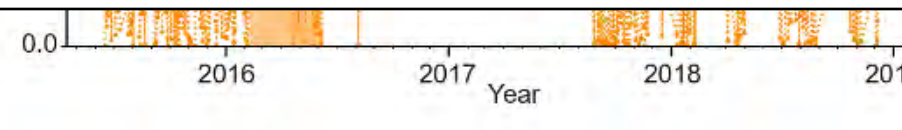
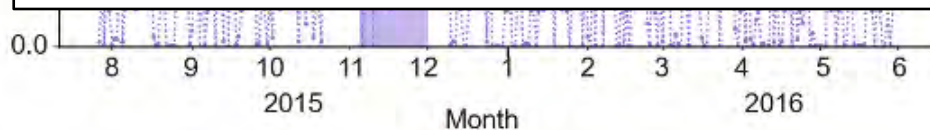


**Math + AI + Circadian Rhythms = Happiness!**



Jaegwon Jeong  
(Korea U Medical School)

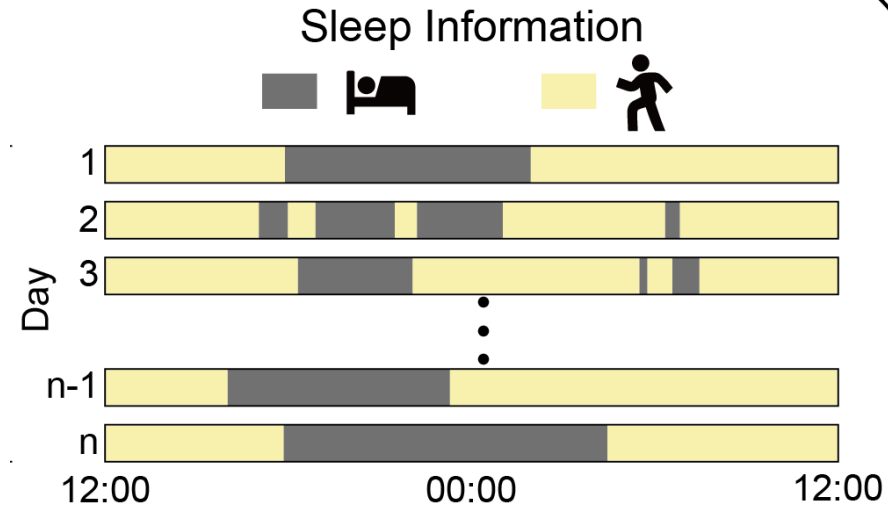
**This framework can be used to identify the other diseases caused by circadian rhythms disruption!**



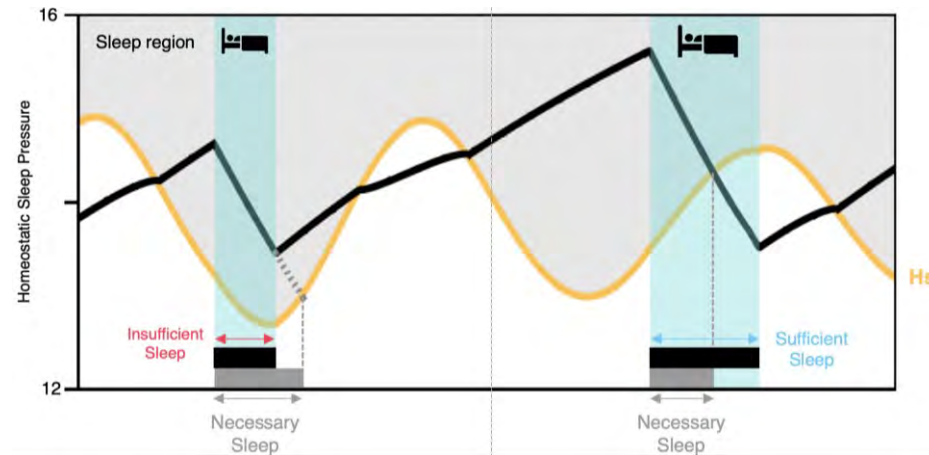
Dr. Hunjung Lee  
(Korea U Medical School)

Lim, Jung at al (Under review)

## Wearables



## Math modeling



## Past!

Sleep Time

REM/Non-REM  
Sleep

Sleep Scoring

## AI

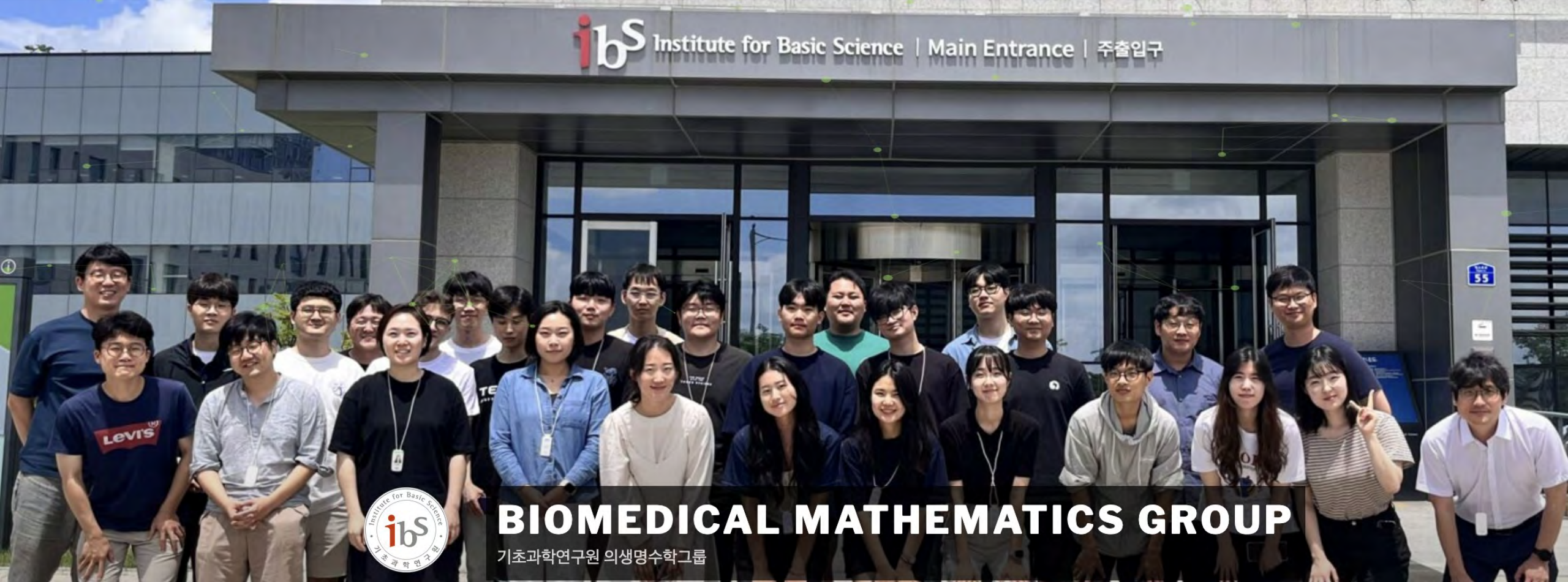
## Future!

Predict mood episodes  
Song et al, eBiomedicine (2024)

Predict sleep sufficiency  
Hong et al, iScience (2021)

Predict alertness  
Song et al, Sleep (2024)





Cancer Chrono



Dae Wook Kim  
Assistant Prof. Seogang Univ

Multiple repressions



Euimin Jeong  
(IBS)

Phosphoswitch



Seokjoo Choe  
(KAIST)

Time delay noise



Yumin Song  
(KAIST)

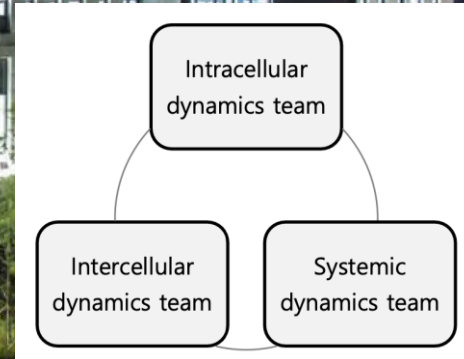


At BIMAG, researchers from mathematics, biology and medicine work together to develop mathematical theories and apply them to solve biomedical puzzles.



## BIOMEDICAL MATHEMATICS GROUP

기초과학연구원 의생명수학그룹



### News of BIMAG events



ibsbimag



bimagibs

### Visiting scholar program!


### Senior researcher and post-doc positions!

### BIMAG public online Colloquium






# Everyone: Public & Online colloquium



**2022 FALL**  
**BIOMEDICAL MATHEMATICS COLLOQUIUM**


**ibS** Institute for Basic Science  
Biomedical Mathematics Group



**ZOOM**  
ID: 997 8258 4700 (IBSBIMAG) PW: 1234


	DATE	TIME (KST)	TITLE	SPEAKER
Sep.	- 2	11:00 am	Cell signaling in 2D vs. 3D	James Ferrell Stanford U
	Oct.	- 7	10:30 am	A Dynamic Paradigm for Molecular Cell Biology
- 7		11:00 am	Time-keeping and Decision-making in the Cell Cycle	John Tyson Virginia Tech
- 21		10:30 am	A Brief Introduction to Stochastic Reaction Networks.	David Anderson U of Wisconsin-Madison
- 21		11:00 am	Stationary distributions and positive recurrence of chemical reaction networks	David Anderson U of Wisconsin-Madison
- 26		4:00 pm	Mathematical modelling of the sleep-wake cycle: light, clocks and social rhythms	Anne Skeldon U of Surrey
Nov.	- 9	4:00 pm	Modeling cell-to-cell heterogeneity from a signaling network	Mariko Okada Osaka U
	- 18	11:00 am	Quantifying dynamical changes in sparse, noisy, high-dimensional data	Rosemary Braun Northwestern U
	- 23	4:00 pm	TBD	Edda Klipp Humboldt-Universität
	- 30	4:00 pm	Brain dynamics during shiftwork: from maths and codes to real-world applications.	Svetlana Postnova U of Sydney
Dec.	- 2	11:00 am	Mammalian synthetic biology by controller design	Domitilla Del Vecchio MIT
	- 9	11:00 am	TBD	George Sugihara Scripps Institution

Before/After daylight saving time: W 16:00 (KST) = W 8:00/7:00 (UK) = W 3:00/2:00 (NY) & F11:00 (KST) = F 3:00/2:00 (UK) = Th 22:00/21:00 (NY)  
All the colloquium is online and public. Anyone can participate in the colloquium via the ZOOM link provided in the BIMAG homepage.  
Homepage <https://www.ibs.re.kr/bimag> | Contact [bimag@ibs.re.kr](mailto:bimag@ibs.re.kr)



**2022 SPRING**  
**BIOMEDICAL MATHEMATICS ONLINE COLLOQUIUM**

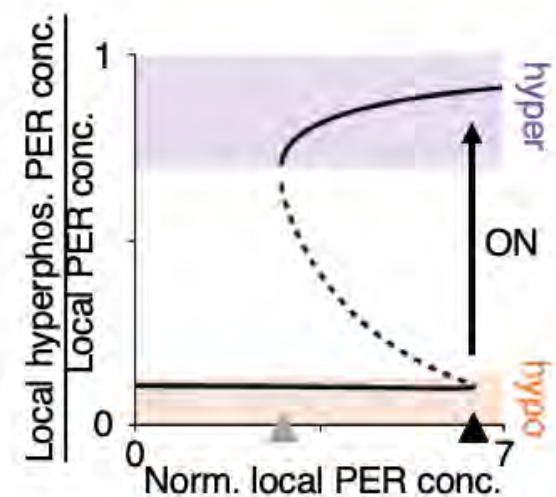
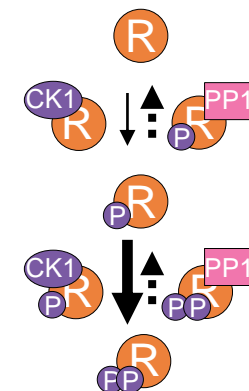
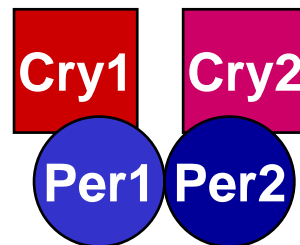
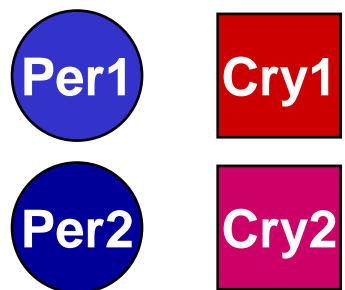
**ibS** Institute for Basic Science  
Biomedical Mathematics Group



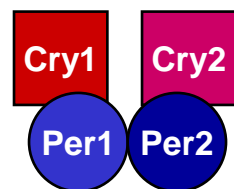
**ZOOM**  
ID: 997 8258 4700 (IBSBIMAG) PW: 1234

	DATE	TIME (KST)	TITLE	SPEAKER
March	- 3	11:00 ~ 12:00	Spatiotemporal reconstruction of static single-cell genomics data	Qing Nie University of California, Irvine
	- 24	10:30 ~ 10:55 11:00 ~ 12:00	Introduction to topological data analysis Topological data analysis of spatial systems	Mason Porter UCLA
	- 31	11:00 ~ 12:00	TBD	Uri Alon Weizmann Institute of Science
April	- 7	11:00 ~ 12:00	Universal biology in adaptation and evolution: Dimensional reduction, and fluctuation-response relationship	Kunihiko Kaneko The University of Tokyo
	- 14	10:30 ~ 10:55 11:00 ~ 12:00	An overview of methods used for multi-scale modeling and analysis A systems biology approach using multi-scale modeling to understand the immune response to tuberculosis infection and treatment	Denise Kirschner University of Michigan
	- 28	11:00 ~ 12:00	Scaling behaviors in physiological fluctuations: Relevance to circadian regulation and insights into the development of Alzheimer's disease	Kun Hu Harvard University
	May	- 12	10:30 ~ 10:55 11:00 ~ 12:00	Introduction to balanced networks Plasticity and balance in neuronal networks
- 25		16:30 ~ 16:55 17:00 ~ 18:00	Stochastic modelling of reaction-diffusion processes Multi-resolution methods for modelling intracellular processes	Radek Erban University of Oxford
June	- 1	17:00 ~ 18:00	From live cell imaging to moment-based variational inference	Heinz Koeppl TU Darmstadt

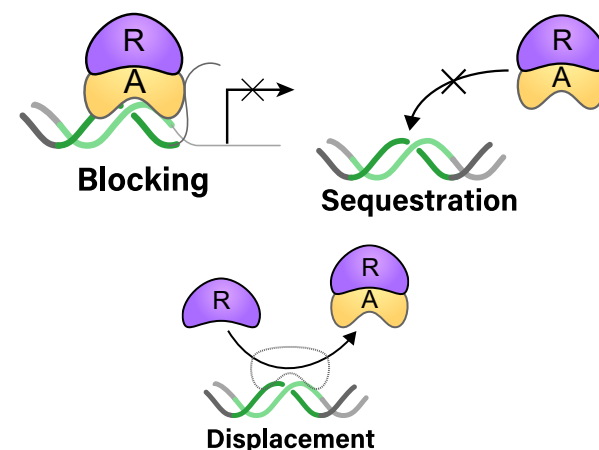
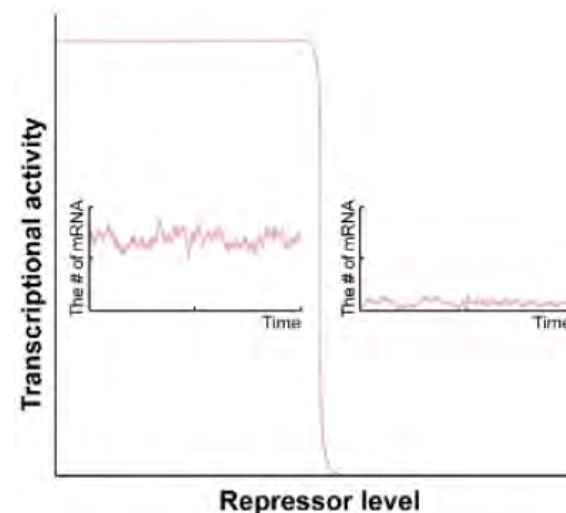
After March 13: W 16:30 (KST) = W 8:30 (UK) = W 3:30 (NY) & Th 10:30 (KST) = Th 2:30 (UK) = W 21:30 (NY)  
All the colloquium is online and public. Anyone can participate in the colloquium via the ZOOM link provided in the BIMAG homepage.  
Homepage <https://www.ibs.re.kr/bimag> | Contact [bimag@ibs.re.kr](mailto:bimag@ibs.re.kr)



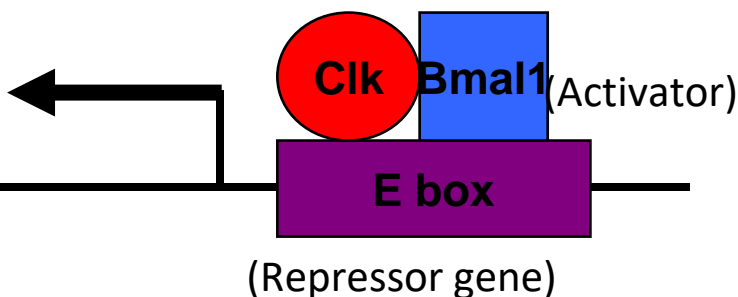
Travel time noise is filtered by phosphoswitch, leading to nucleus entry of repressors at right time



Transcriptional regulation noise is filtered by multi-repression, leading to repression and activation at right time.



*cry1 per1*  
*cry2 per2*



(Repressor gene)

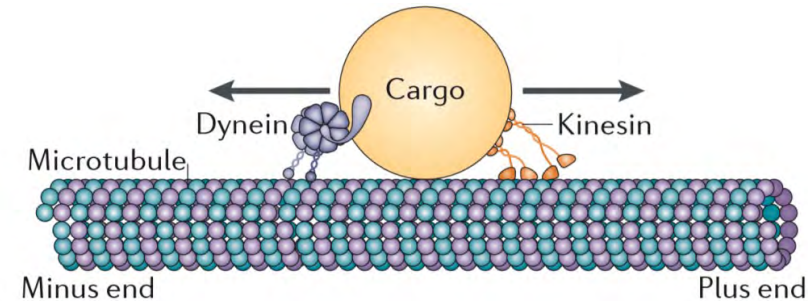
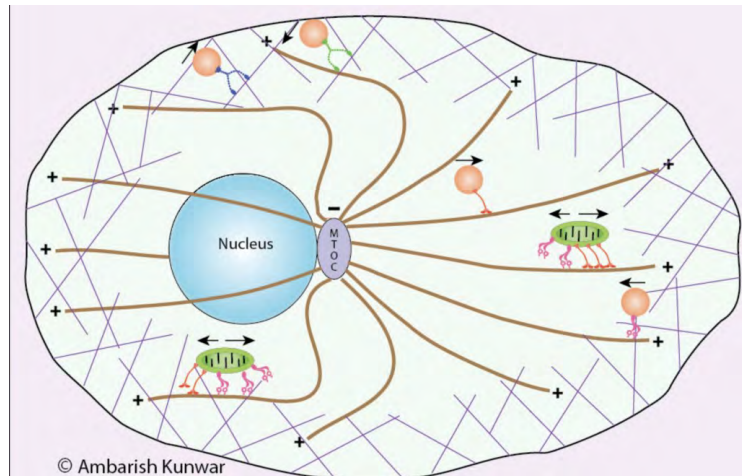




# Transport to perinucleus is mainly based on microtubules and molecular motors

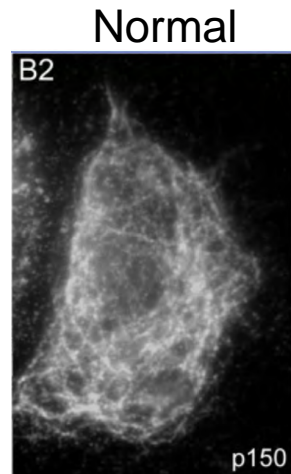
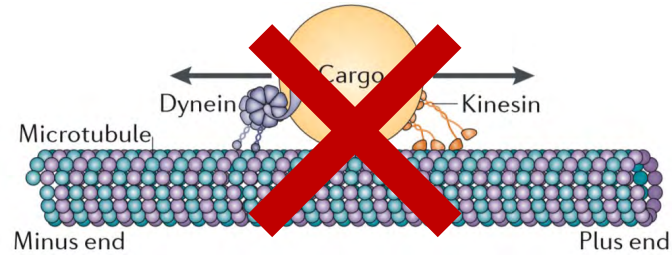
Microtubule: road heading to nucleus

Motor proteins: truck transporting proteins

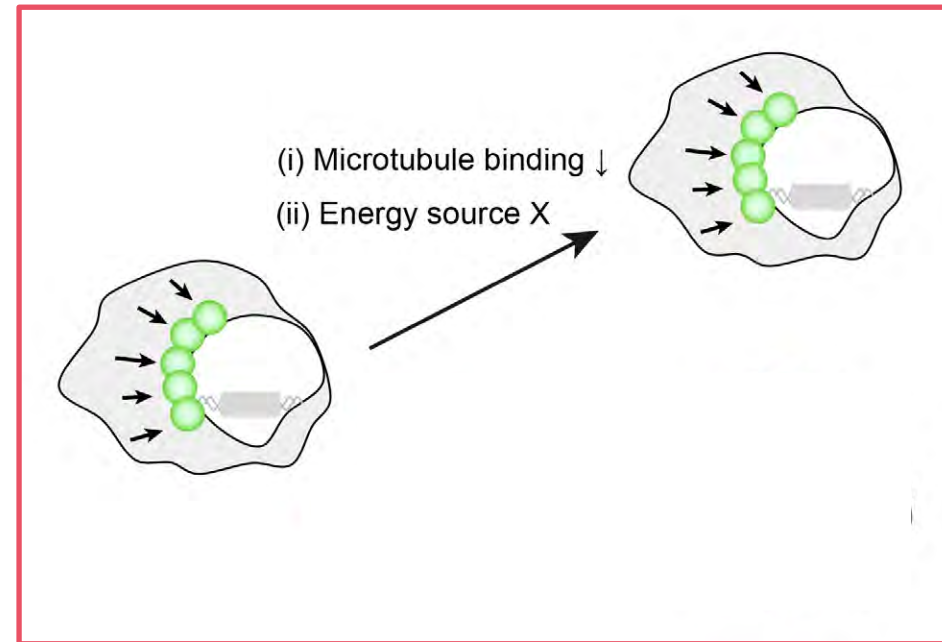
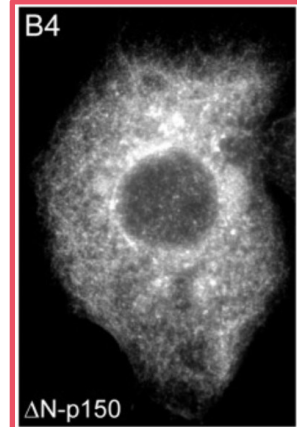


**However, PER do not move along microtubule!**

However, **even without microtubule**, protein can be transported to perinucleus!



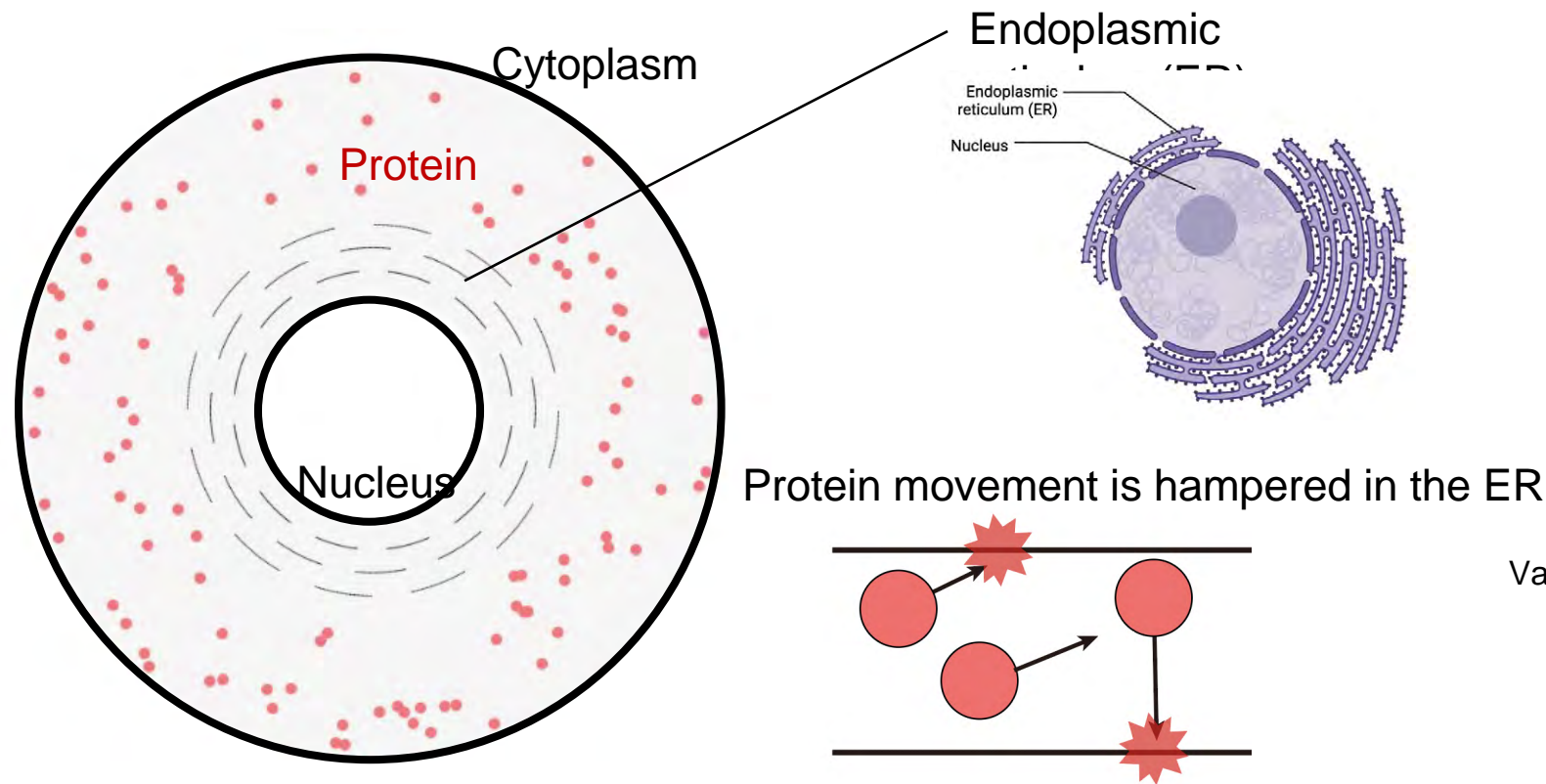
**Without microtubule**



Retrieved from Hancock Lab  
Kim et al. (2007)

**Such protein transport may have diffusive character!**

To investigate the role of diffusive character, we developed an agent-based model mimicking protein diffusion in a cell with ER.



Seok Joo Chae  
(KAIST & IBS)



Dae Wook Kim  
Van Loo Postdoc Fellow  
U Michigan

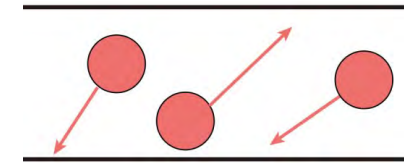
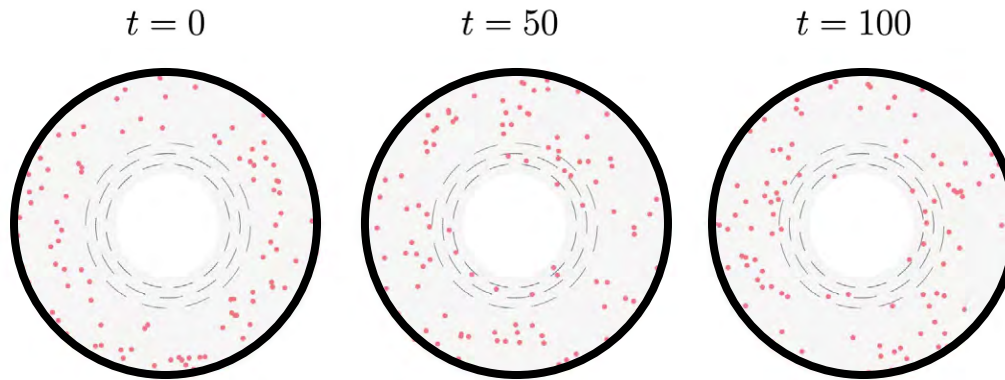


Oleg Igoshin, Rice U



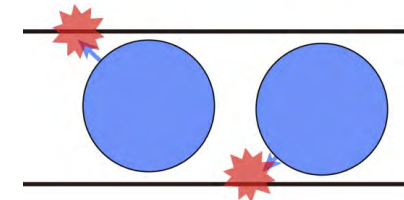
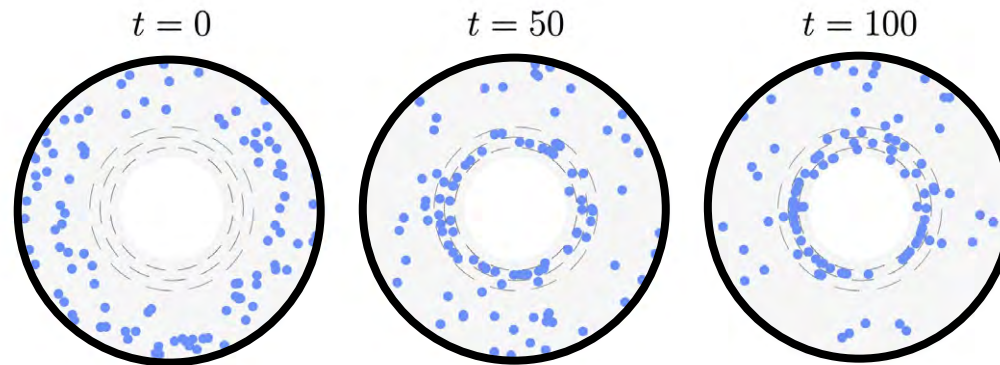
# Diffusion within the cell with the ER structure results in perinuclear accumulation

**Smaller sized proteins does not accumulate near the nucleus**



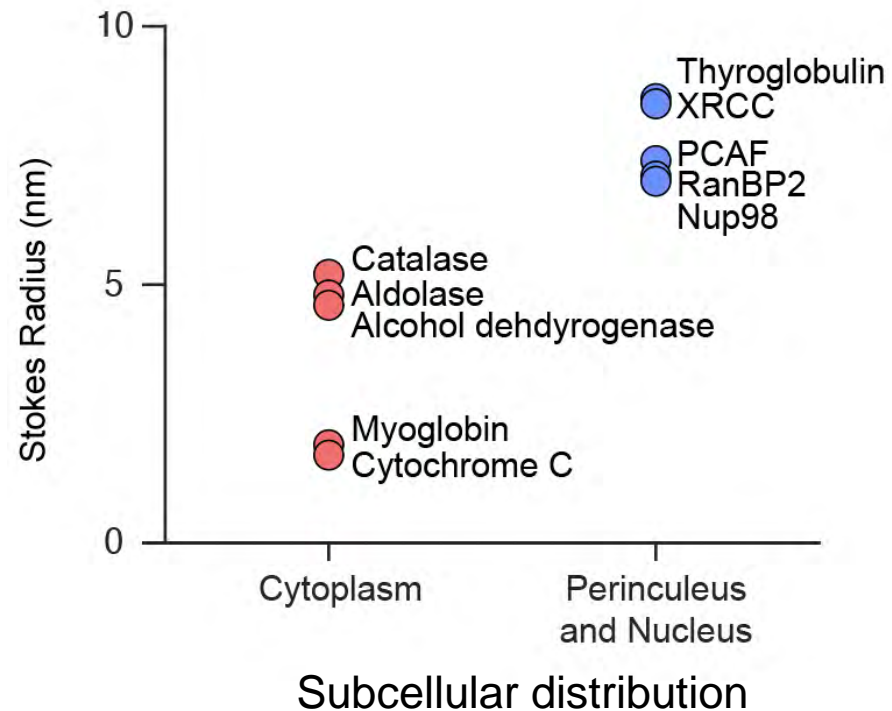
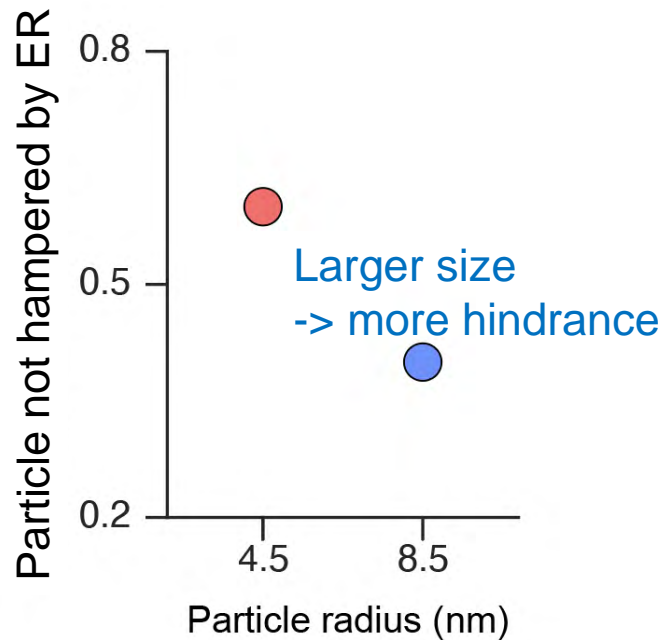
Low collision frequency with the ER

**However, larger sized proteins do accumulate**

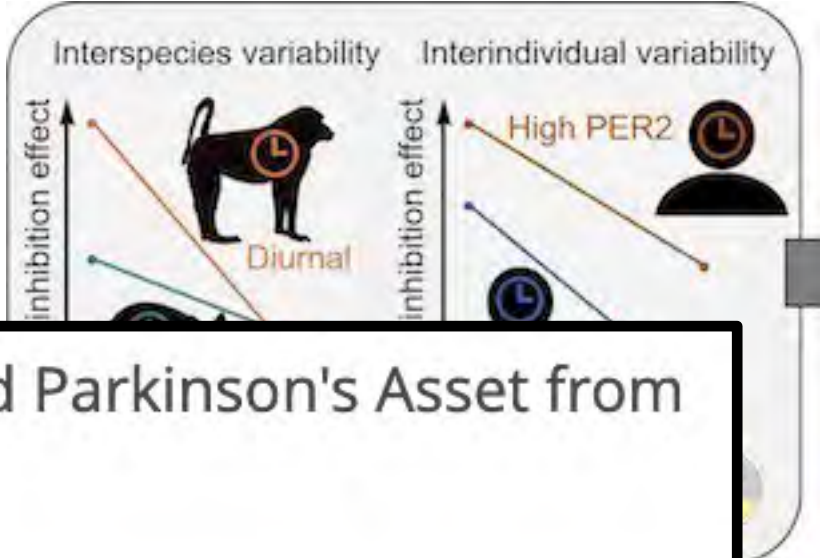


High collision frequency with the ER

Larger proteins are prone to diffusion hindrance and tend to accumulate near the nucleus!



# PER phosphorylation has been target for circadian regulation



## Biogen Acquires Alzheimer's and Parkinson's Asset from Pfizer in \$710 Million Deal

Published: Jan 13, 2020 | By Mark Terry



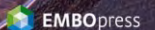
Rel. Conc. of  
Bmal mRNA / PF-670

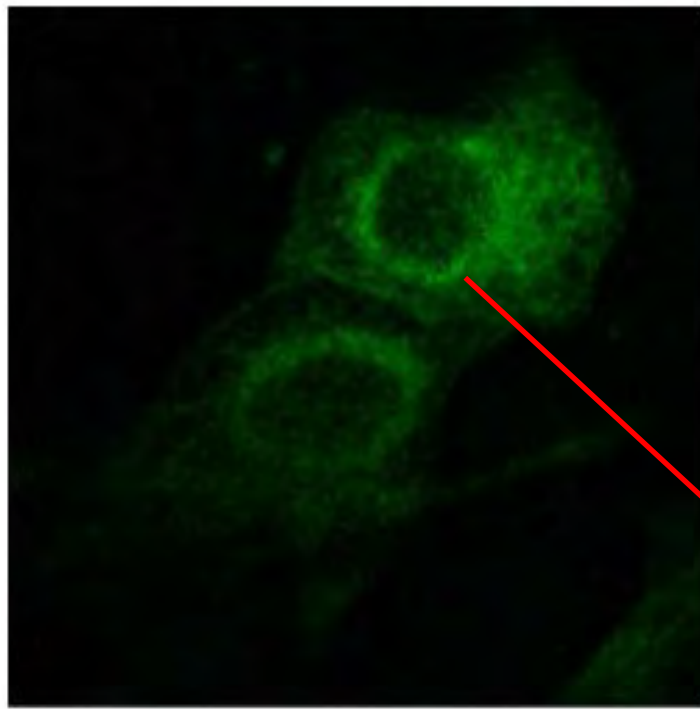


Strong

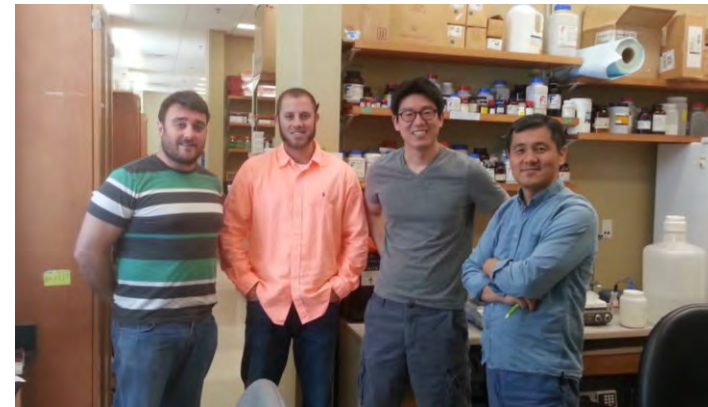
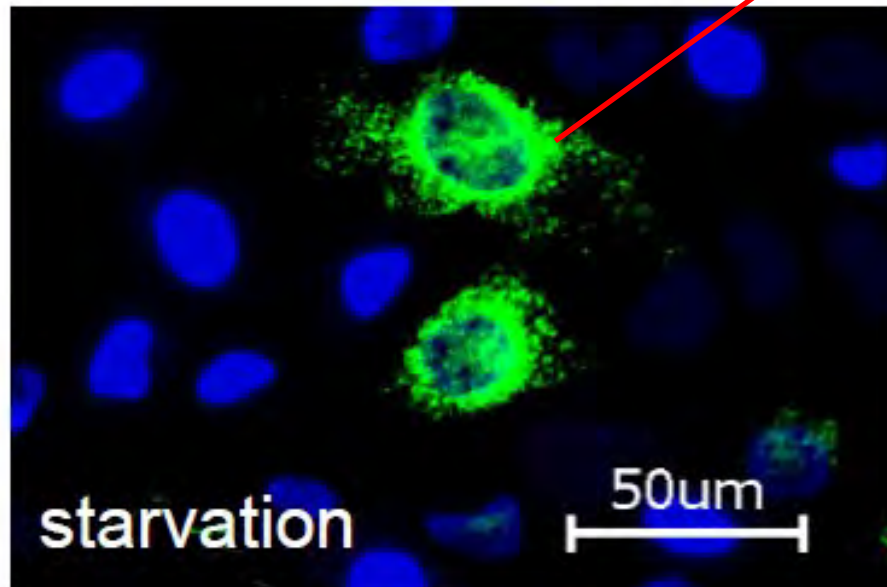


Determinants of clock  
modulating drug efficacy





**How PER moves toward to perinucleus?**

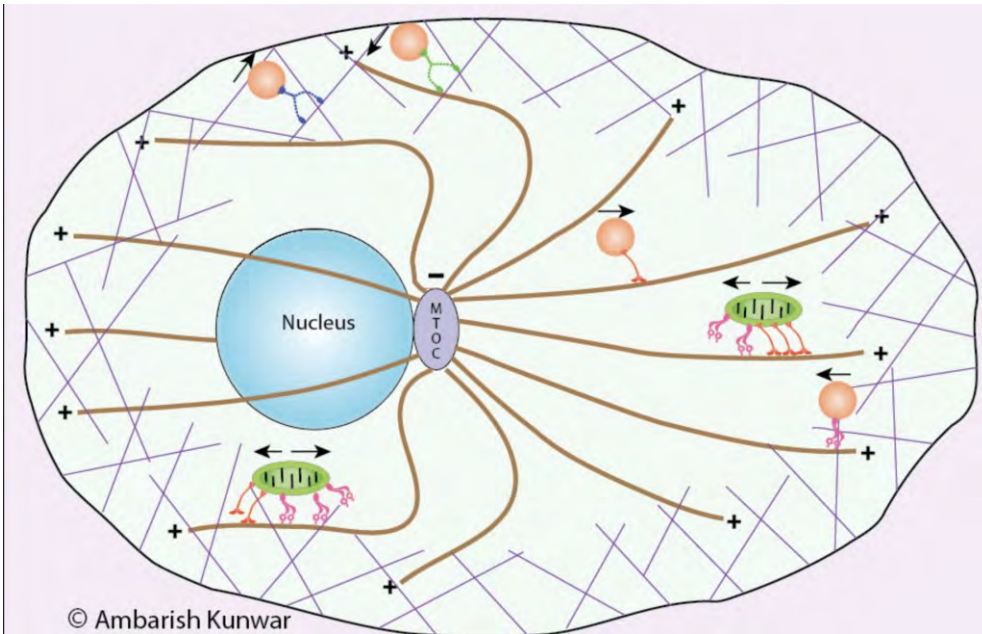


Choogon Lee Lab (Florida State U)

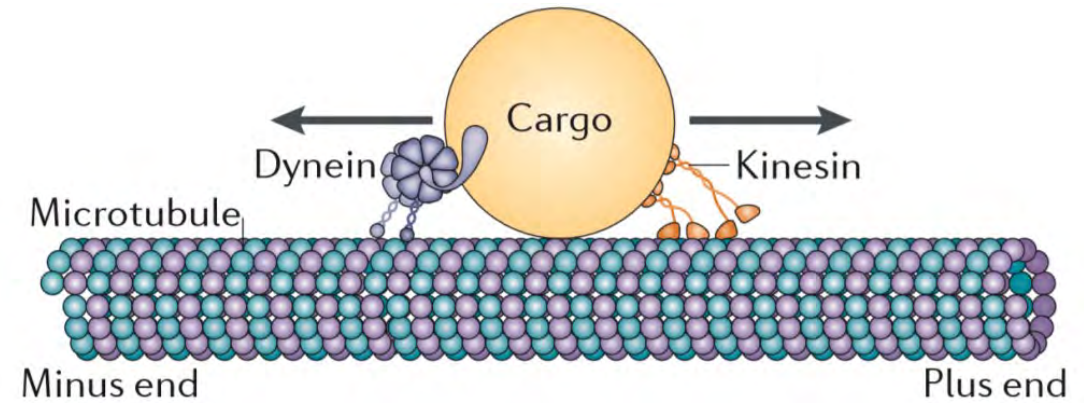


# Transport to perinucleus is mainly based on microtubules and molecular motors

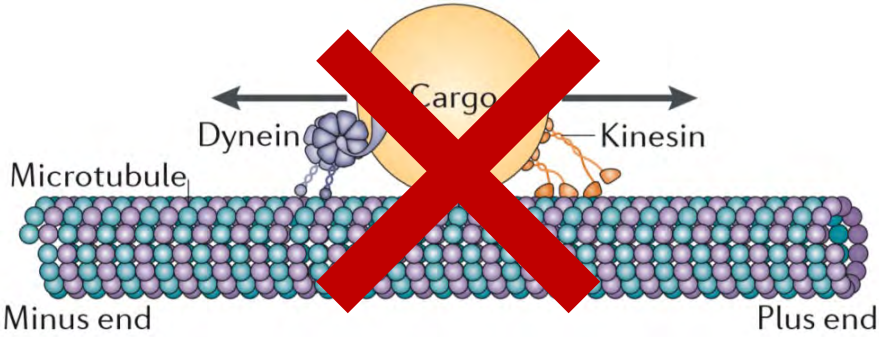
Microtubule: road heading to nucleus



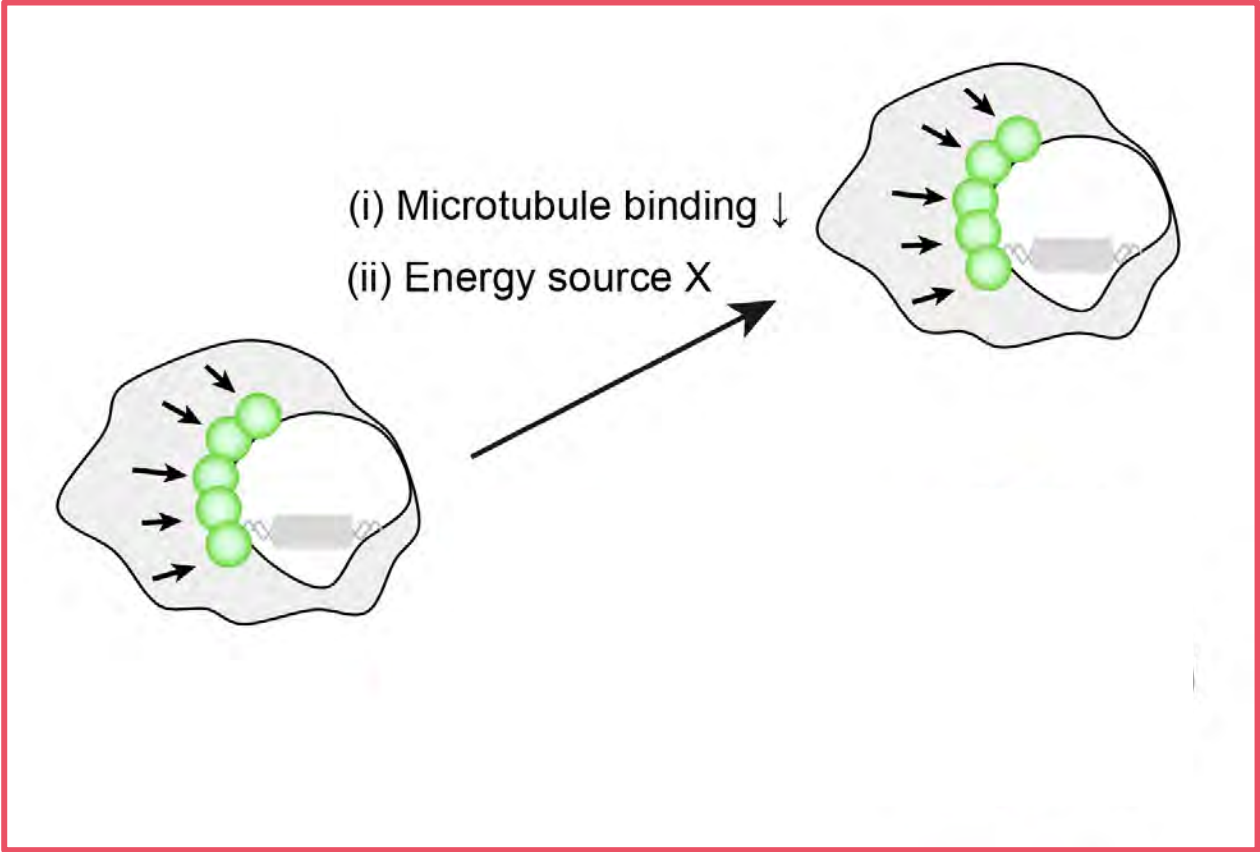
Motor proteins: truck transporting proteins



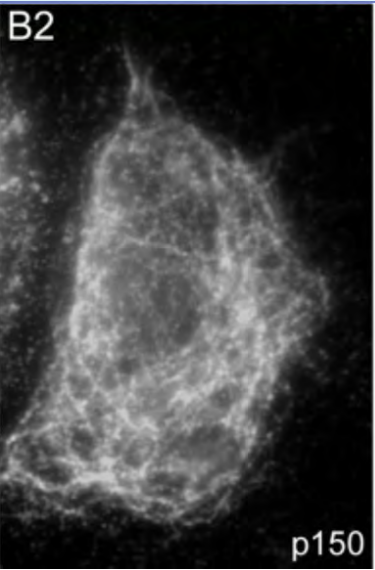
However, **even without microtubule**, protein can be transported to perinucleus!



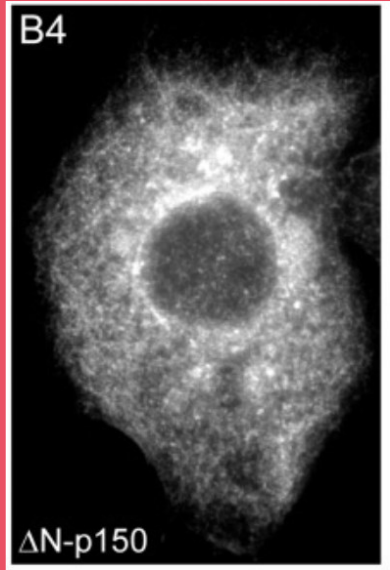
Such protein transport may have diffusive character!



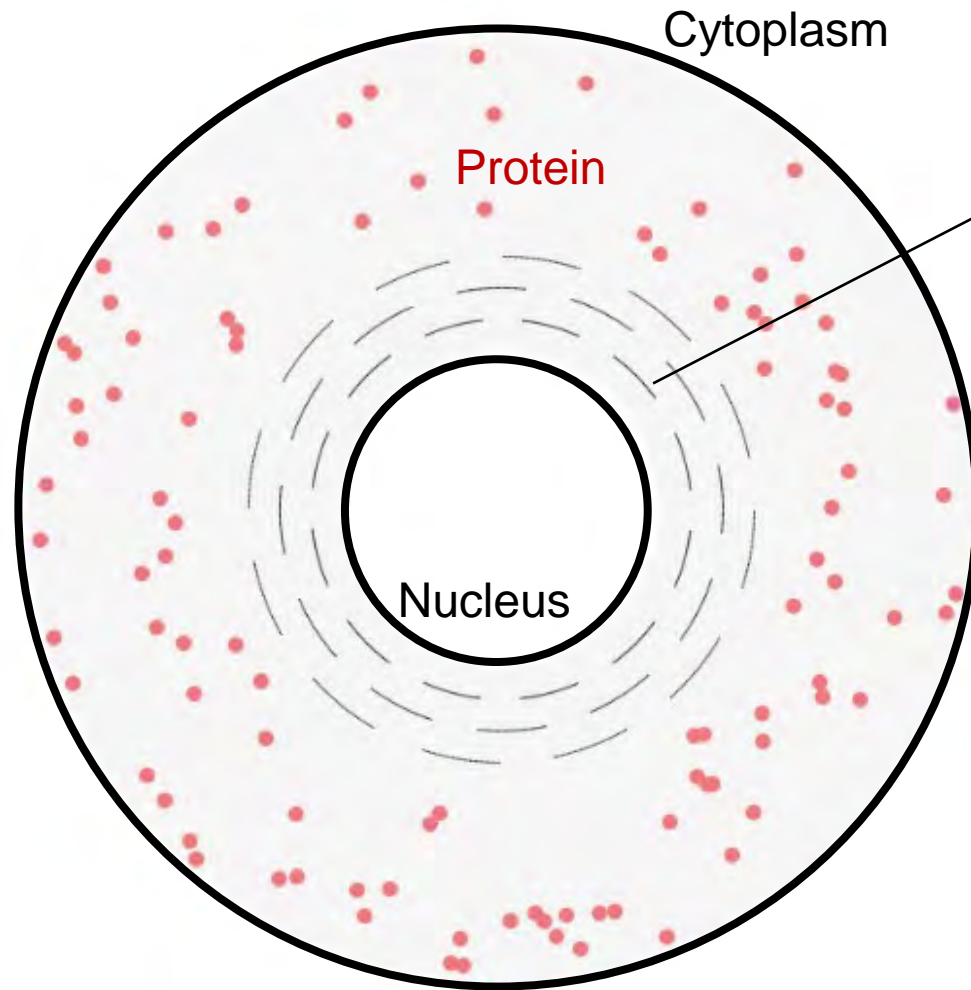
Normal



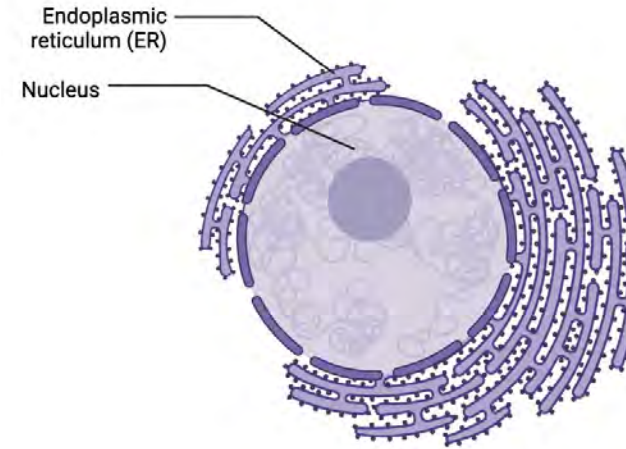
Without microtubule



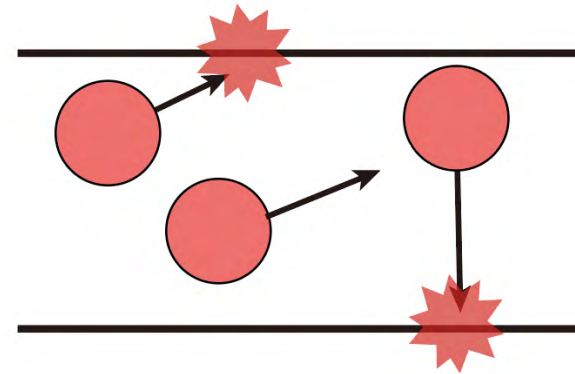
To investigate the role of diffusive character, we developed an agent-based model mimicking protein diffusion in a cell with ER.



Endoplasmic reticulum (ER)



Protein movement is hampered in the ER



Seok Joo Chae  
(KAIST & IBS)



Dae Wook Kim  
Seogang U

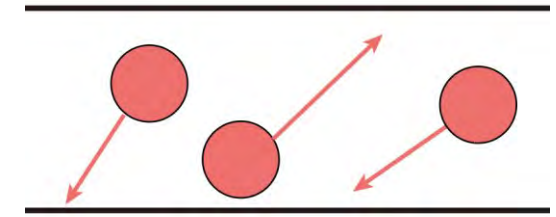
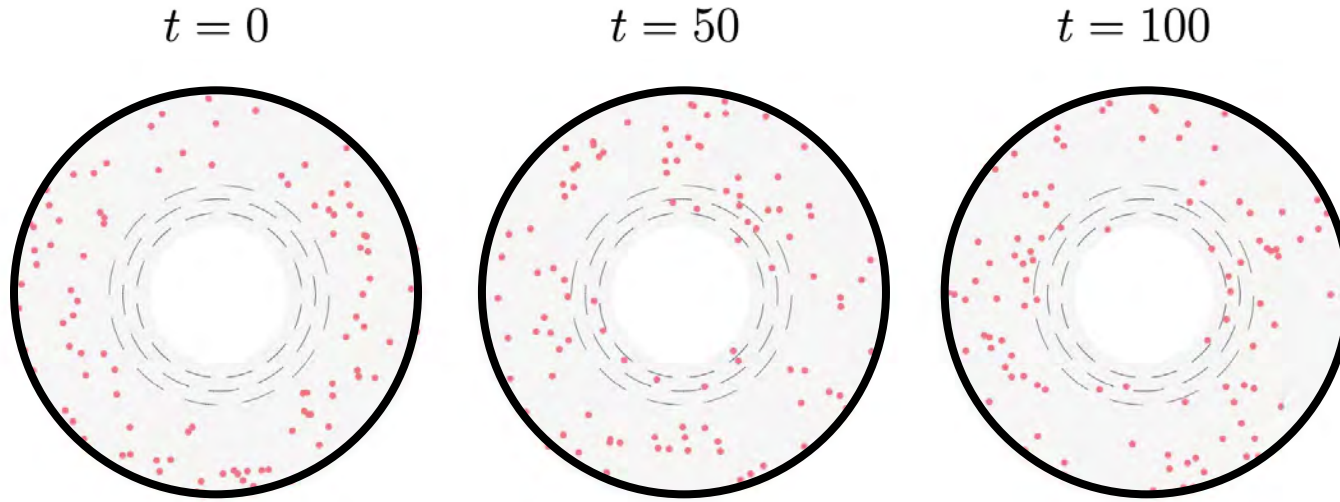


Oleg Igoshin, Rice U



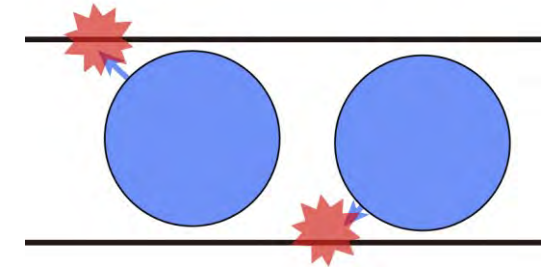
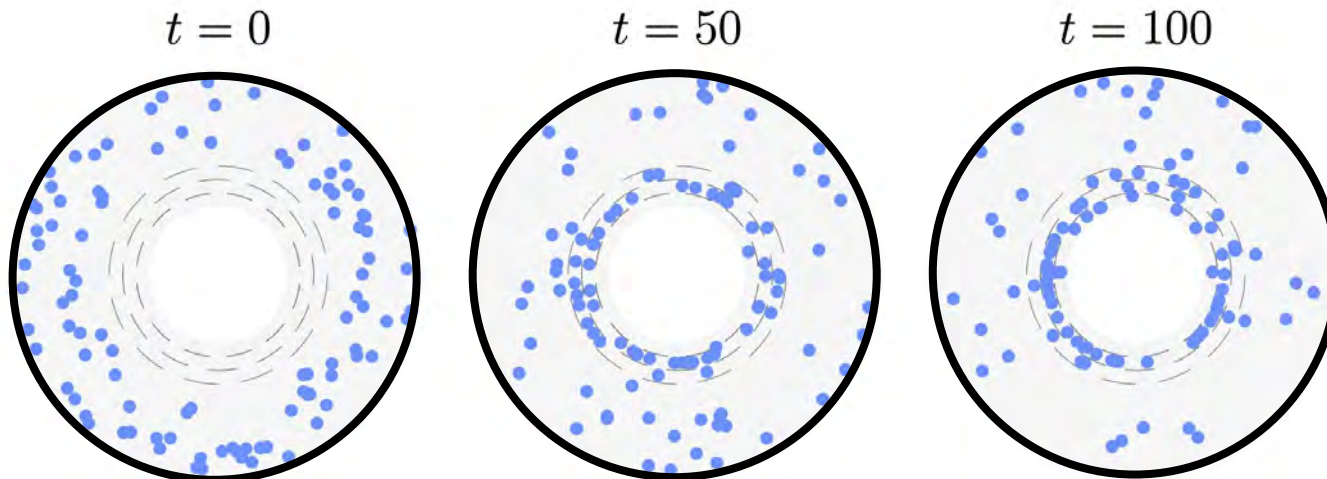
# Diffusion within the cell with the ER structure results in perinuclear accumulation

**Smaller sized** proteins does not accumulate near the nucleus



Low collision frequency with the ER

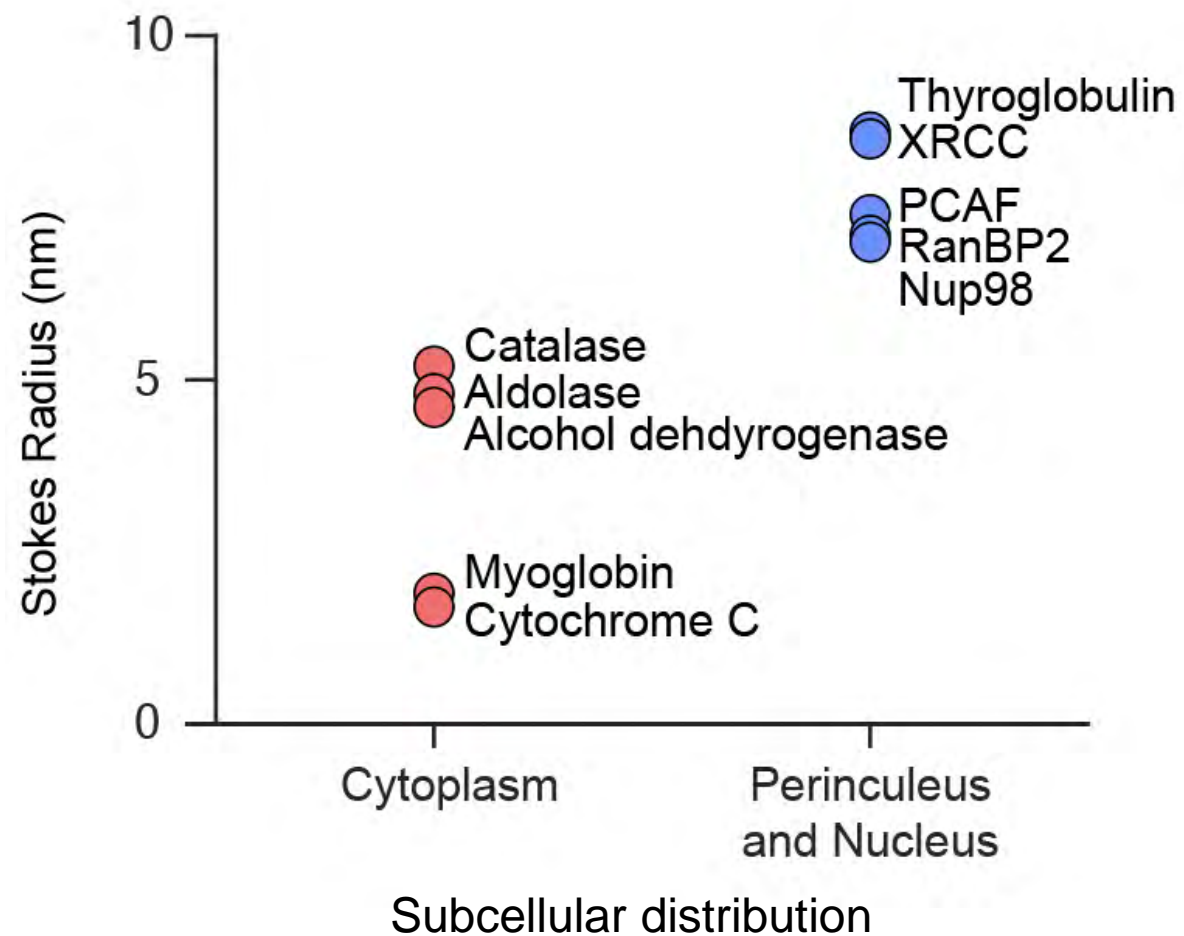
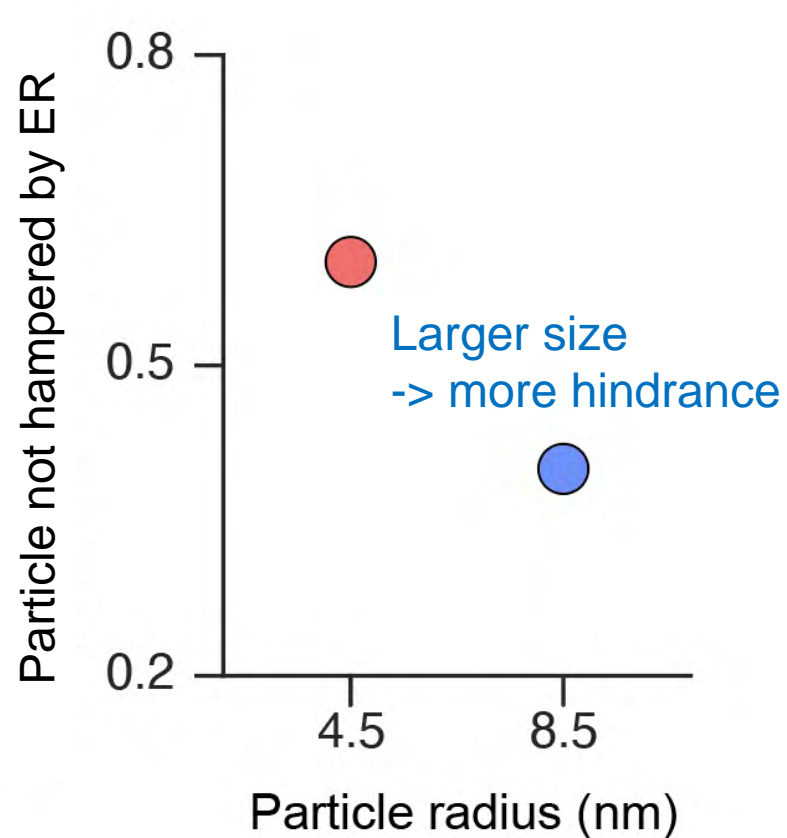
However, **larger sized** proteins do accumulate



High collision frequency with the ER

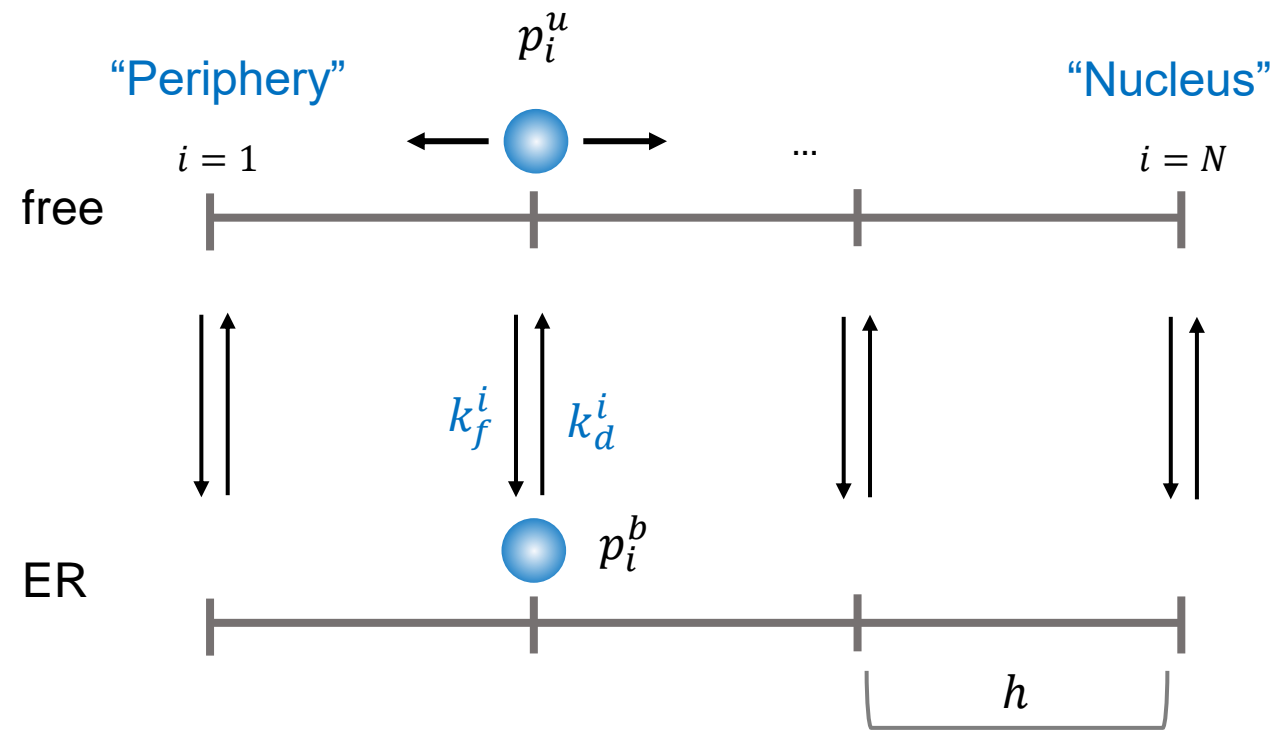


Larger proteins are prone to diffusion hindrance and tend to accumulate near the nucleus!



How can we understand heterogeneous diffusion mathematically?

# Microscopic model for diffusion + the collision (binding) of ER



- $p_i^u$ : probability of finding unbounded protein at i-th grid
- $p_i^b$ : probability of finding bounded protein at i-th grid
- $p_i^T$ : probability of finding protein at i-th grid (bounded + unbounded)

Diffusion + Binding/unbinding

$$\frac{dp_i^u}{dt} = \frac{\delta}{h^2} (-2p_i^u + p_{i-1}^u + p_{i+1}^u) + k_d^i p_i^b - k_f^i p_i^u$$
$$\frac{dp_i^b}{dt} = -k_d^i p_i^b + k_f^i p_i^u$$
$$\frac{dp_i^T}{dt} = \frac{\delta}{h^2} (-2p_i^u + p_{i-1}^u + p_{i+1}^u)$$

# One step further: heterogeneous diffusion of protein can be effectively described by Chapman's law

Microscopic model for **diffusion** + the **binding/unbinding** with ER

$$\frac{\partial p_i^u}{\partial t} = \frac{\delta}{h^2} (-2p_i^u + p_{i-1}^u + p_{i+1}^u) + k_d^i p_i^b - k_f^i p_i^u$$

$$\frac{\partial p_i^b}{\partial t} = -k_d^i p_i^b + k_f^i p_i^u$$

$$\frac{\partial p_i^T}{\partial t} = \frac{\delta}{h^2} (-2p_i^u + p_{i-1}^u + p_{i+1}^u)$$



Fast binding/unbinding  
 $h \rightarrow 0$

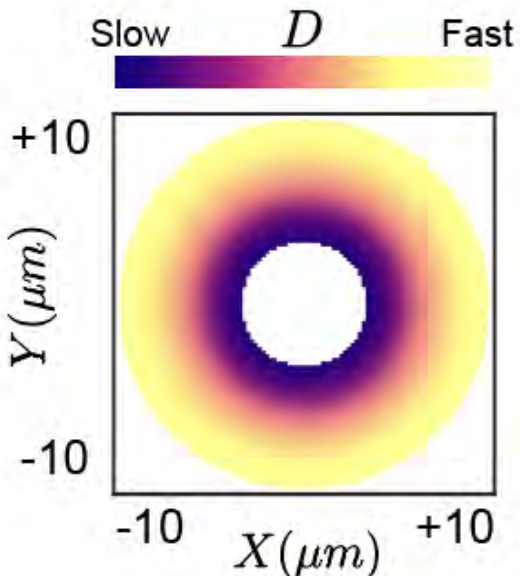
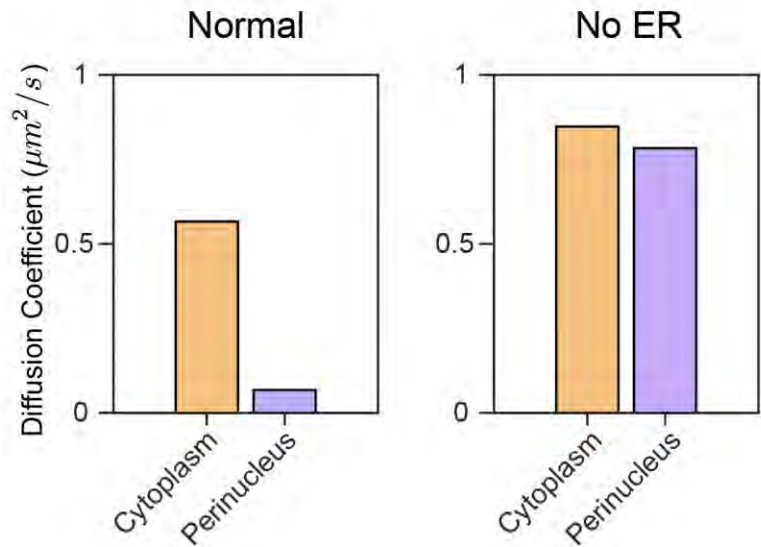
Chapman's Law

$$\frac{\partial p(x, t)}{\partial t} = \Delta(D(x)p(x, t))$$

$p(x, t)$  : prob. finding a protein at  $x$  and  $t$

$$D(x) = \frac{\delta}{\left(1 + \frac{k_f(x)}{k_b(x)}\right)}$$

Denser ER  $\rightarrow$  Larger  $k_f$   $\rightarrow$  Smaller  $D(x)$



A drift term in Chapman's law can account for perinuclear accumulation in heterogeneous environment!

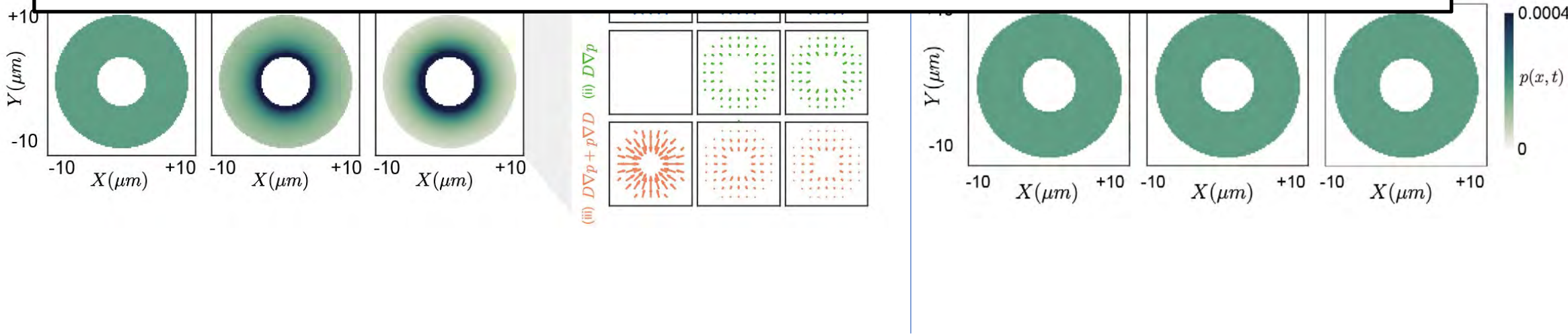
Chapman's Law

$$\frac{\partial p(x, t)}{\partial t} = \Delta(D(x)p(x, t))$$

$$\frac{\partial p}{\partial t} = -\nabla \cdot J$$
$$J = -(D\nabla p + p\nabla D)$$

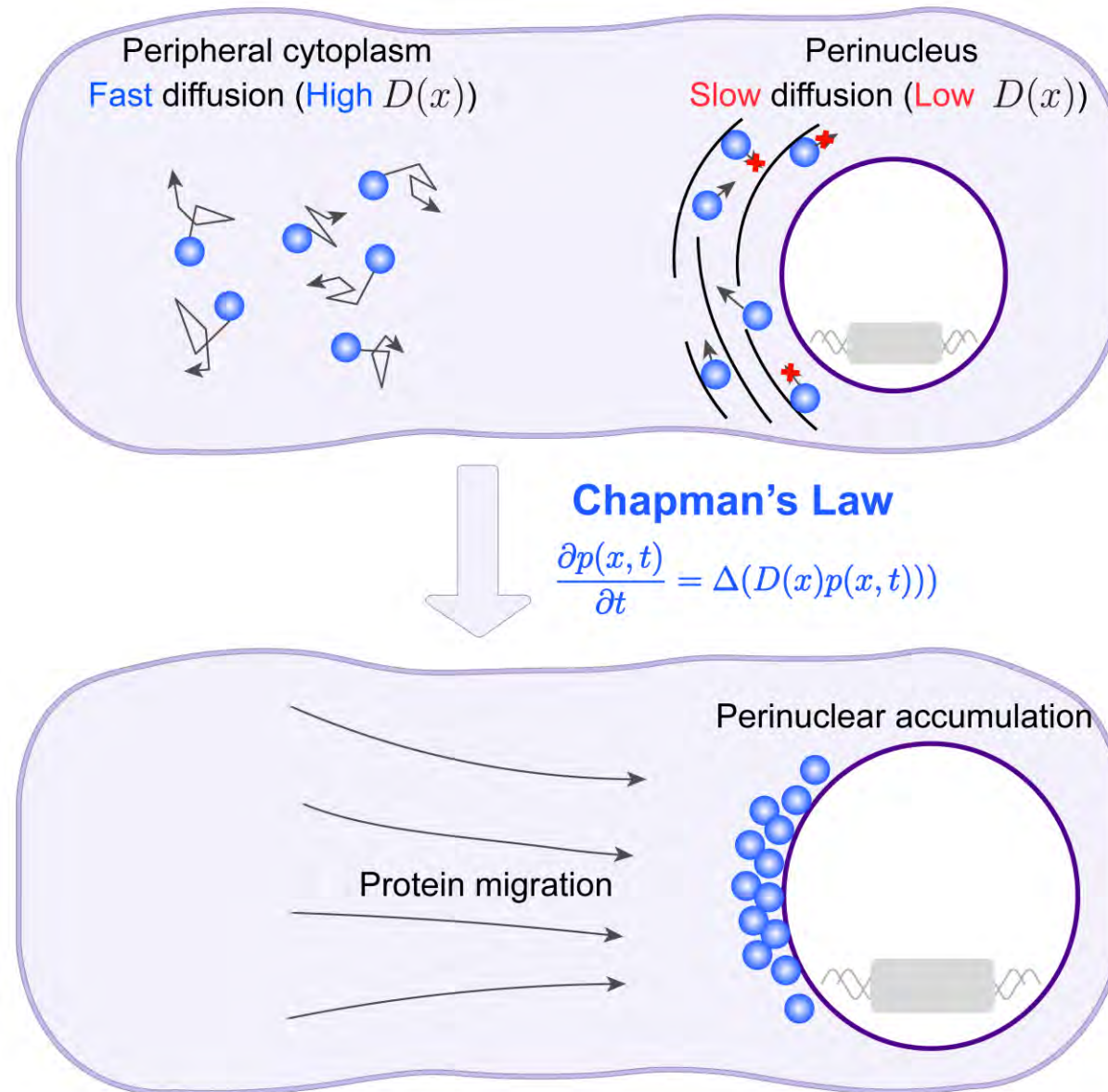
$D\nabla p$ : Fickian (diffusive) flow  
 $p\nabla D$ : Drift due to the heterogeneous environment

**Chapman's law seems the way to go to describe intracellular diffusion of molecules!**





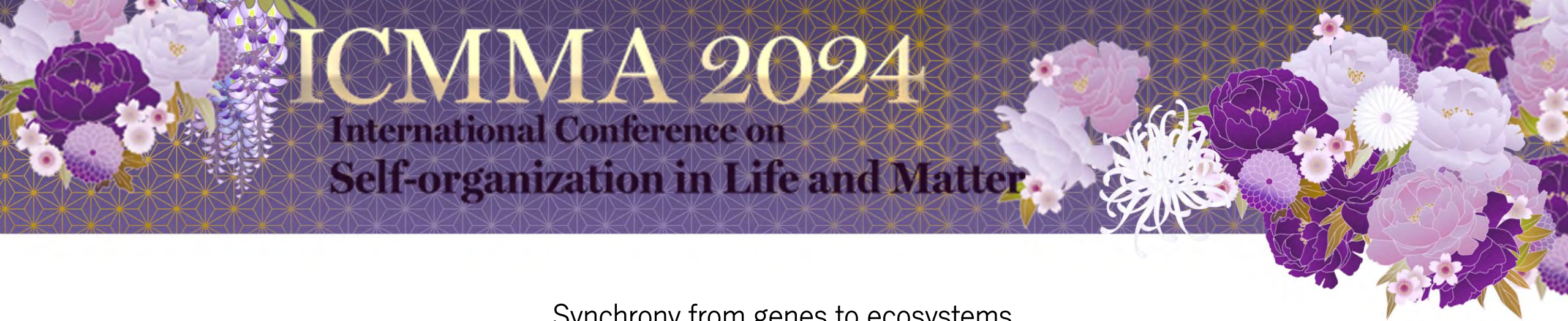
# Beyond microtubules: The cellular environment at the endoplasmic reticulum attracts proteins to the nucleus, enabling nuclear transport



Seek postdoc this fall!



Seokjoo Choe  
(KAIST)



## Synchrony from genes to ecosystems

Akiko Satake (Kyushu University)

Self-organized synchrony among diverse biological components has been identified in many biological systems. The synchronized flowering and fruiting observed in temperate and tropical rainforests represent one of the most mysterious and large-scale events in ecosystems. Occurring at irregular intervals spanning several years, a remarkable phenomenon unfolds where nearly all tree individuals within a population, sometimes alongside species from other families, simultaneously burst into flower. The proposed explanation posits that an internal nutrient cycle, coupled with an external water-stress signal, orchestrates this synchrony, drawing parallels to the intricate mechanisms of molecular circadian clocks (1). However, in contrast with the extensive theoretical and ecological analysis of phenotypic observation, little is known about the molecular mechanisms underlying the synchrony, since dominant tree species in forest ecosystems are non-model species in terms of molecular and genome biology. Leveraging the progress in genome sequencing and information technologies, we can generate genome-wide transcriptomic data at the ecosystem level under naturally fluctuating conditions (2). Our spatiotemporal gene expression data revealed a hierarchical synchrony that manifests within the genome, tissues, individual trees, and populations. We found distinctive gene expression profiles in leaf tissues as opposed to buds and flowers, and parallel expression profiles between different species during both summer and winter. When coherence in gene expression at the individual level aligns at the forest level, it induces feedback effects on the atmosphere and climate. This feedback loop, in turn, influences the reproductive success and survival of plants, a topic we'll delve into further. (3)

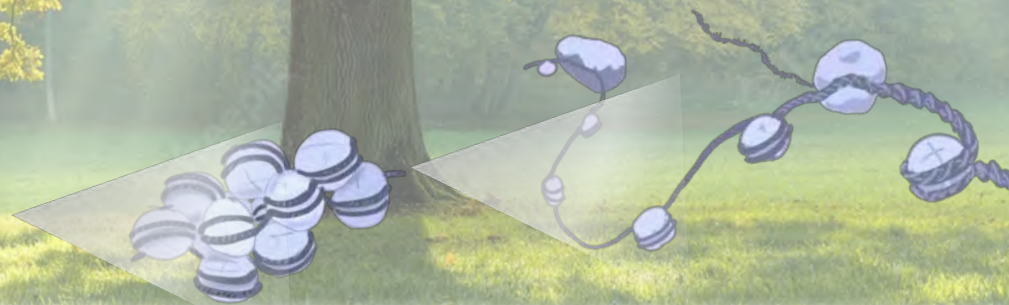
### References

- [1] Satake, A. & Iwasa, Yoh. (2000). Pollen coupling of forest trees: forming synchronized and periodic reproduction out of chaos. *Journal of theoretical biology*, 203(2), 63-84.
- [2] Satake, A. et al. (2013). Forecasting flowering phenology under climate warming by modelling the regulatory dynamics of flowering-time genes. *Nature communications*, 4(1), 2303.
- [3] Satake et al. (2024). Plant molecular phenology and climate feedbacks mediated by BVOCs. *Annual Review of Plant Biology*, 75.





# Synchrony from genes to ecosystems



**Akiko Satake**

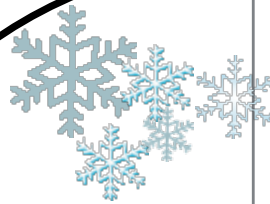
**(Laboratory of Mathematical Biology, Kyushu University)**



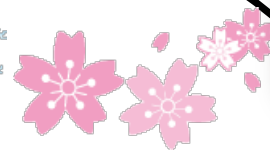
# Cyclic seasonal activities of plants and animals



*Camellia japonica*



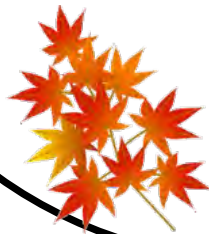
Winter



Spring



**Phenology: Nature's calendar**



*Spider lily*  
*Lycoris radiate*



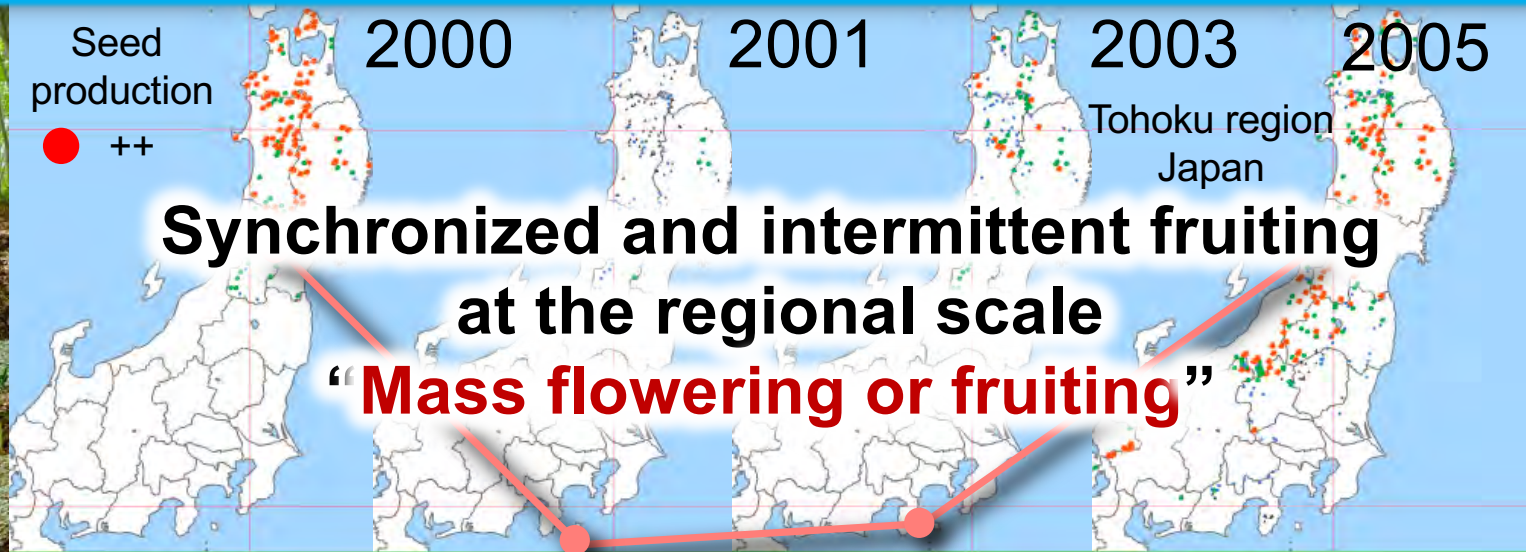
*Morning glory*  
*Ipomoea tricolor*



# Mass flowering: synchronized reproduction with supra-annual periodicity

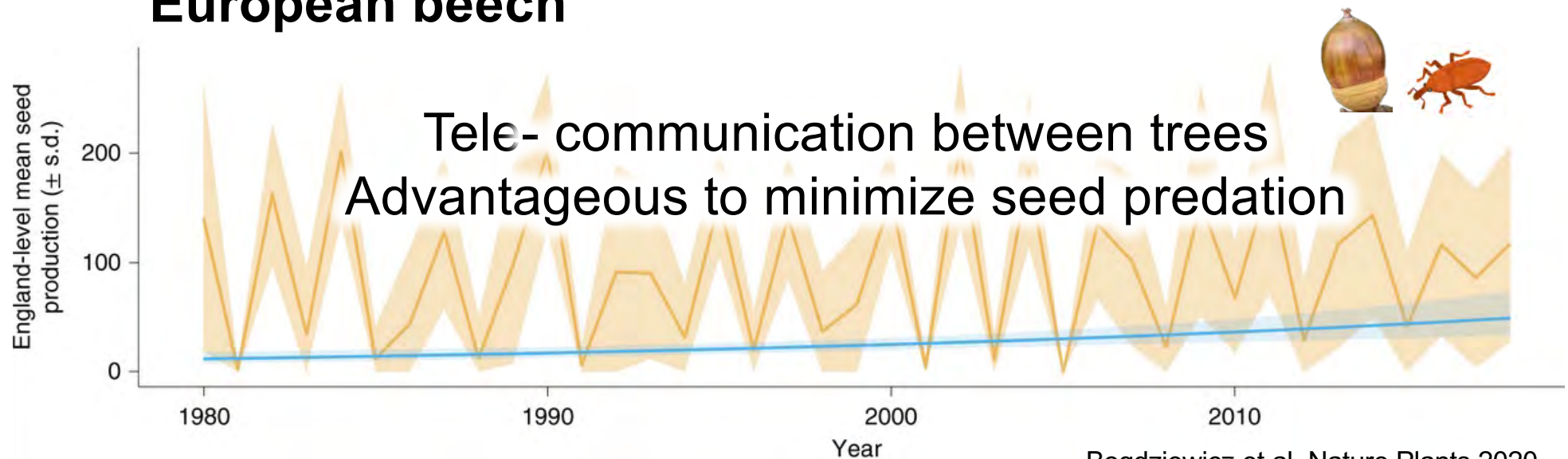


**Japanese beech**



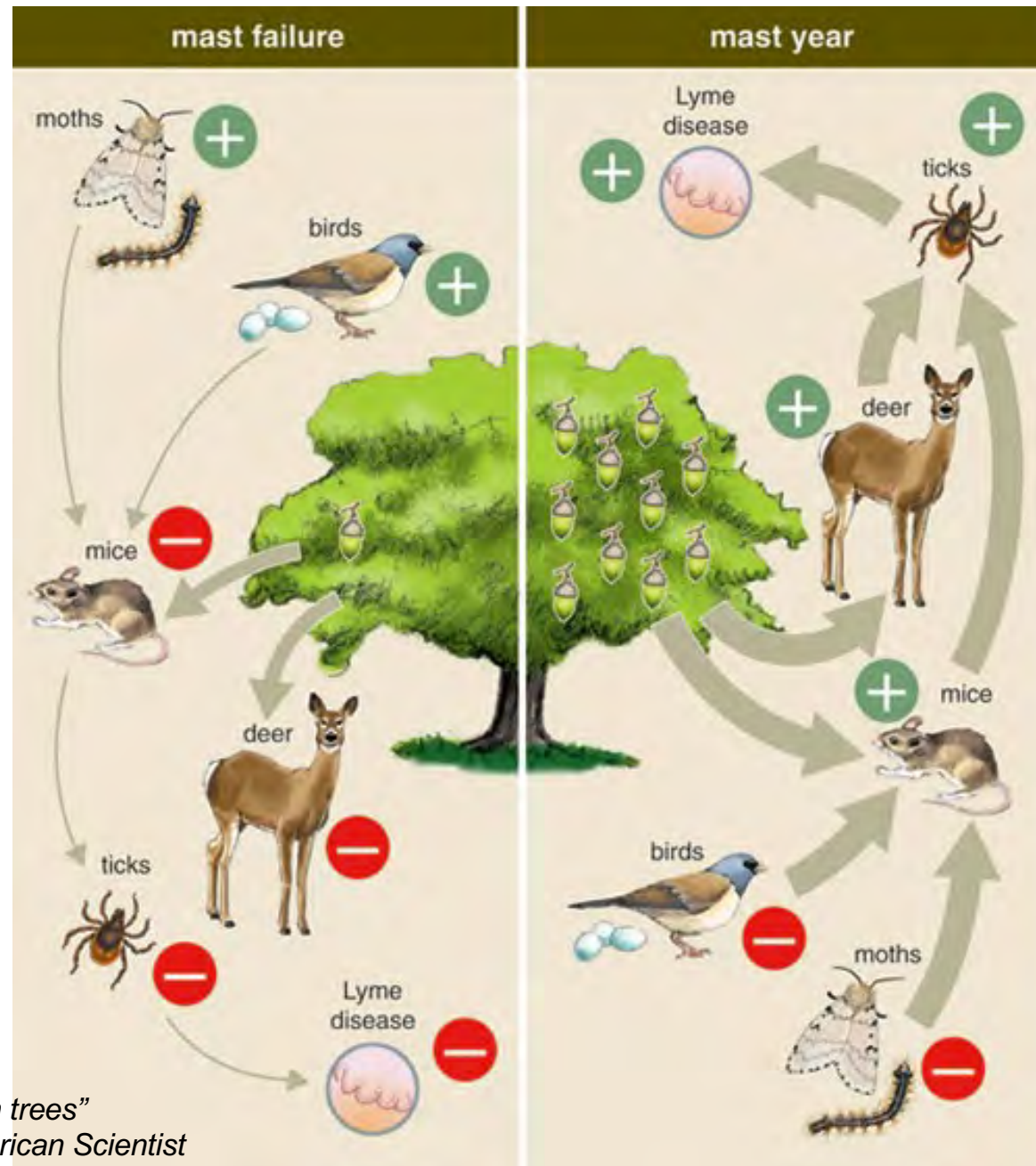
Forest and Forest Products Research Institute  
Satake et al. 2021 New Phytol

## European beech



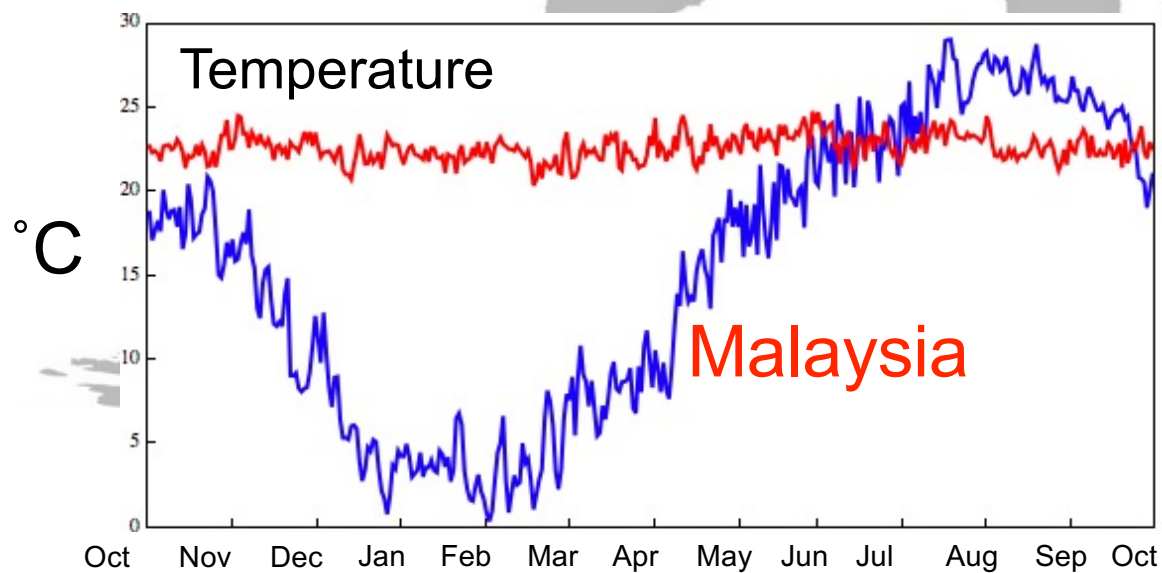
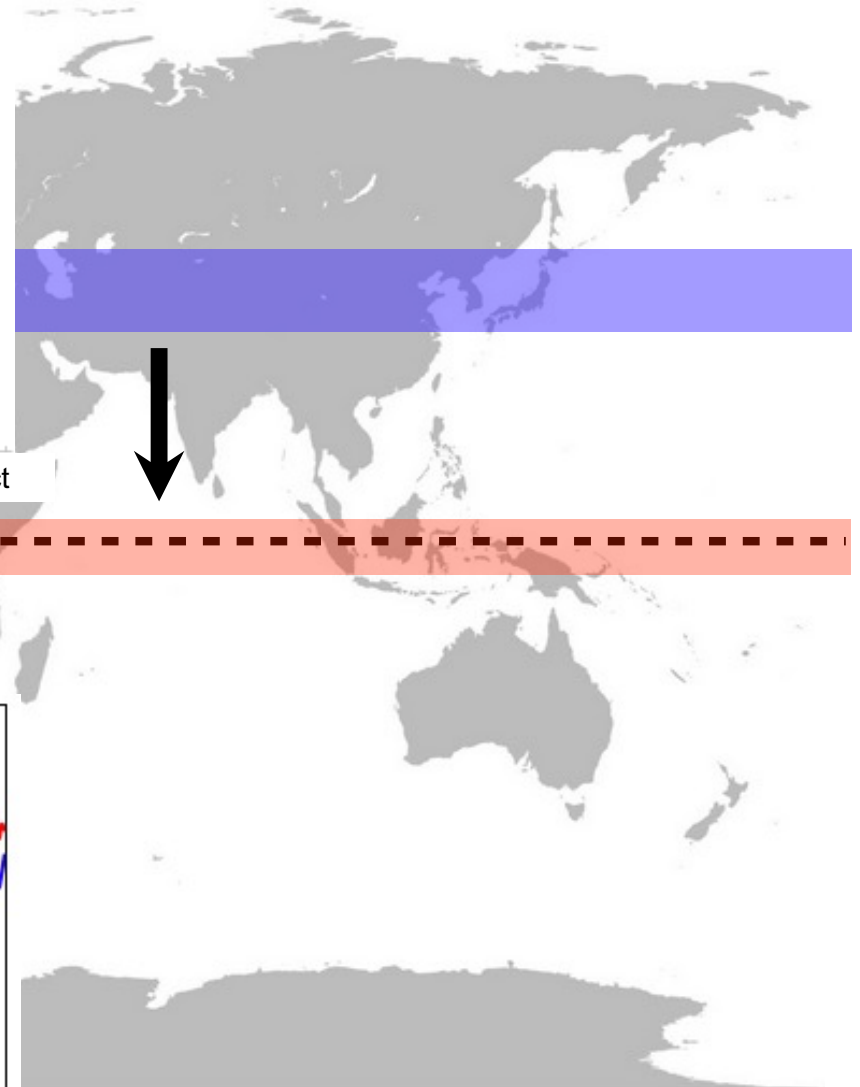
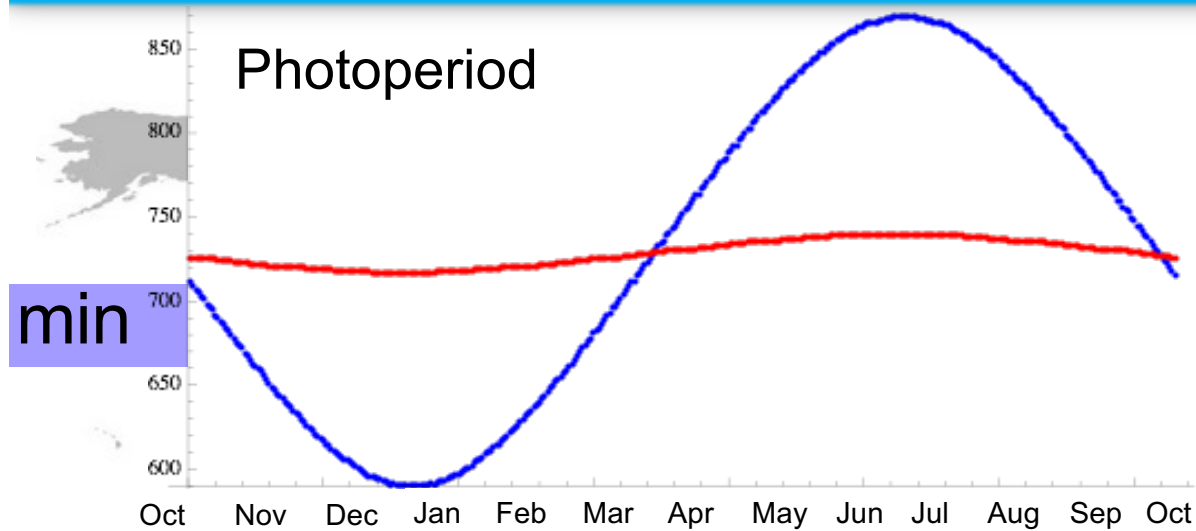
Bogdziewicz et al. Nature Plants 2020

# Ramifying effect of masting on ecosystems



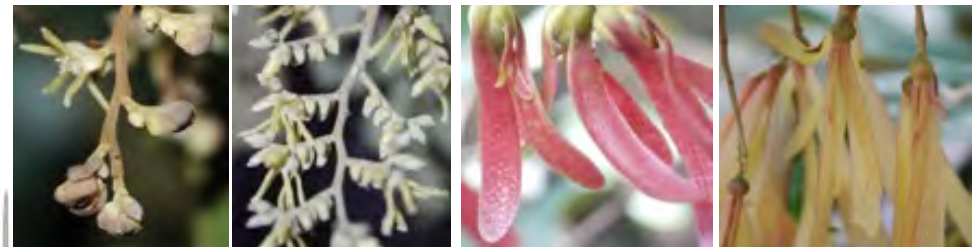
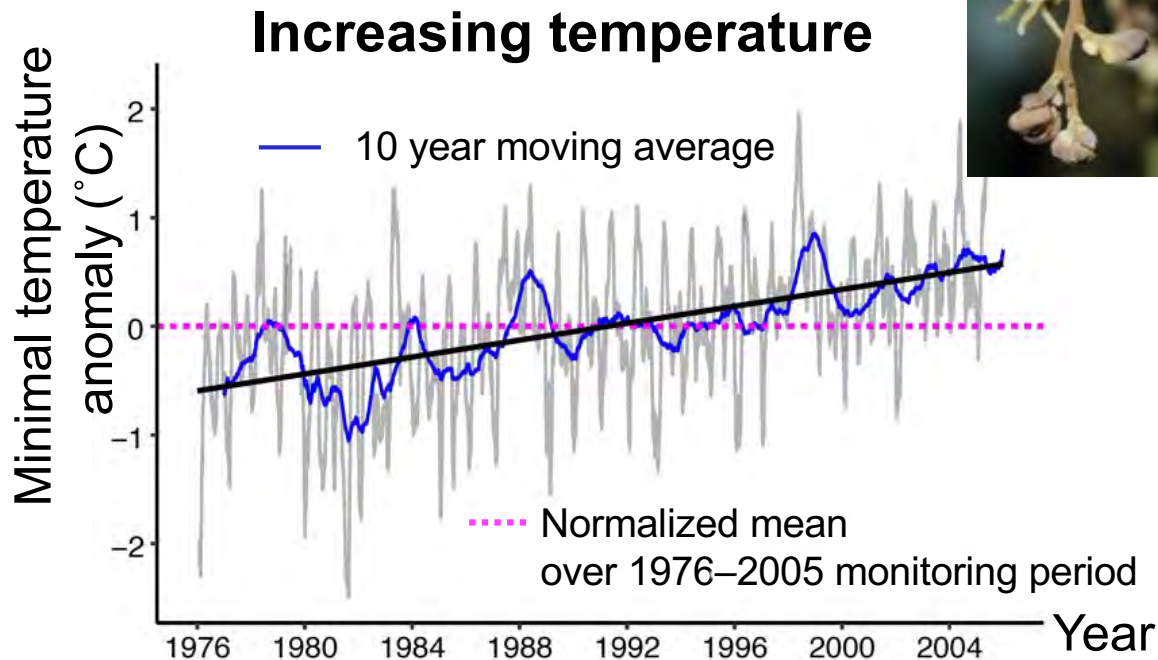
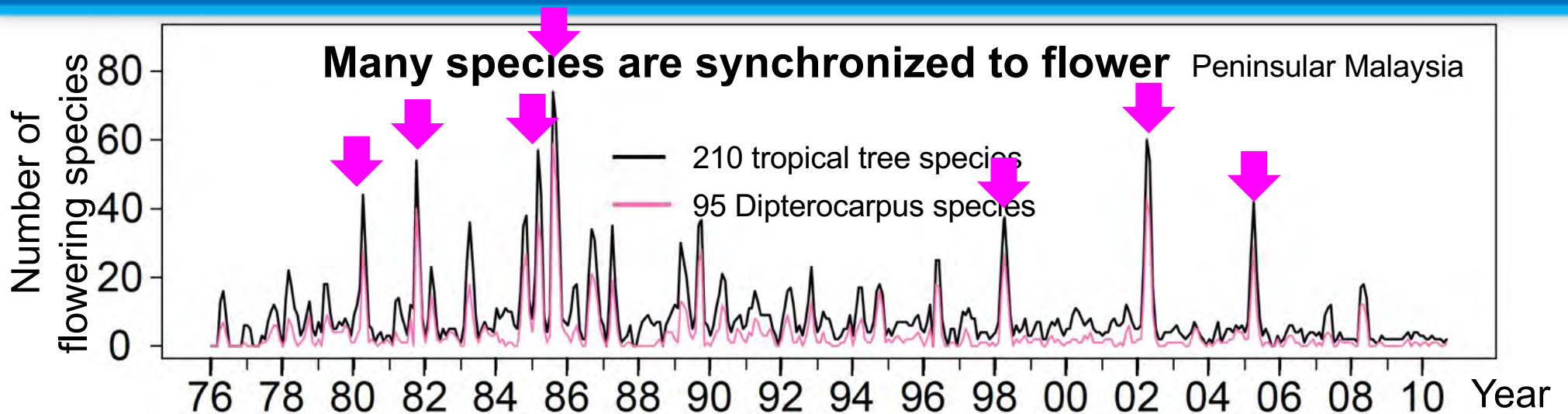
*"The Mystery of masting in trees"*  
Koenig & Knops 2005 *American Scientist*

# How about in tropics?





# Highly synchronized flowering in tropics



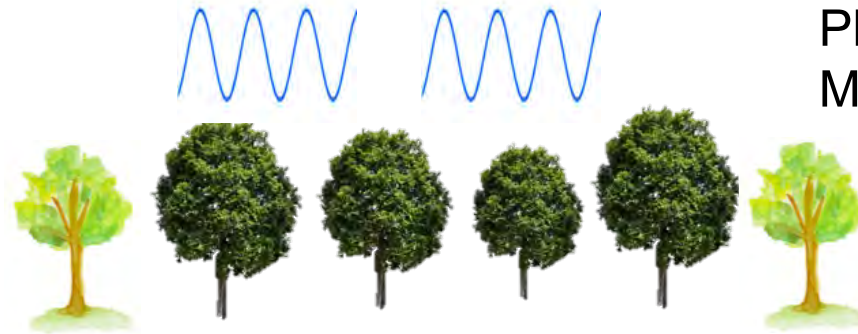
**Mass flowering events are decreasing due to increasing temperature**



# Multi-scale synchrony

Ecosystem  
Population

Synchrony at the **population/ecosystem** level



Phenology  
Mass flowering or fruiting

Individual

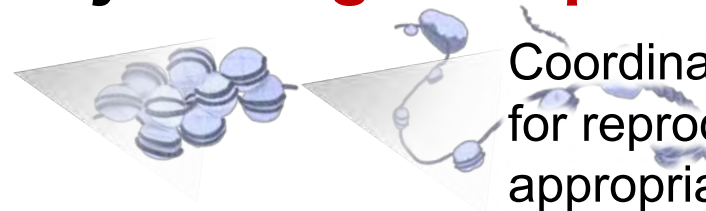
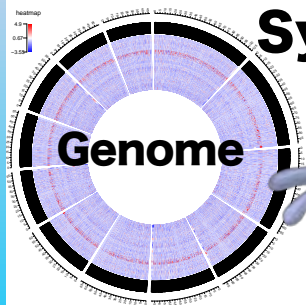
Synchrony at the **individual** level



Modular branching structure  
Synchrony across branches

Gene

Synchrony at the **gene expression** level



Coordinated gene expression  
for reproduction at an  
appropriate timing



**Dominant tree species  
in forest ecosystems are “non-model”  
for molecular and genetic studies**

Tropical rainforest in 西双版纳



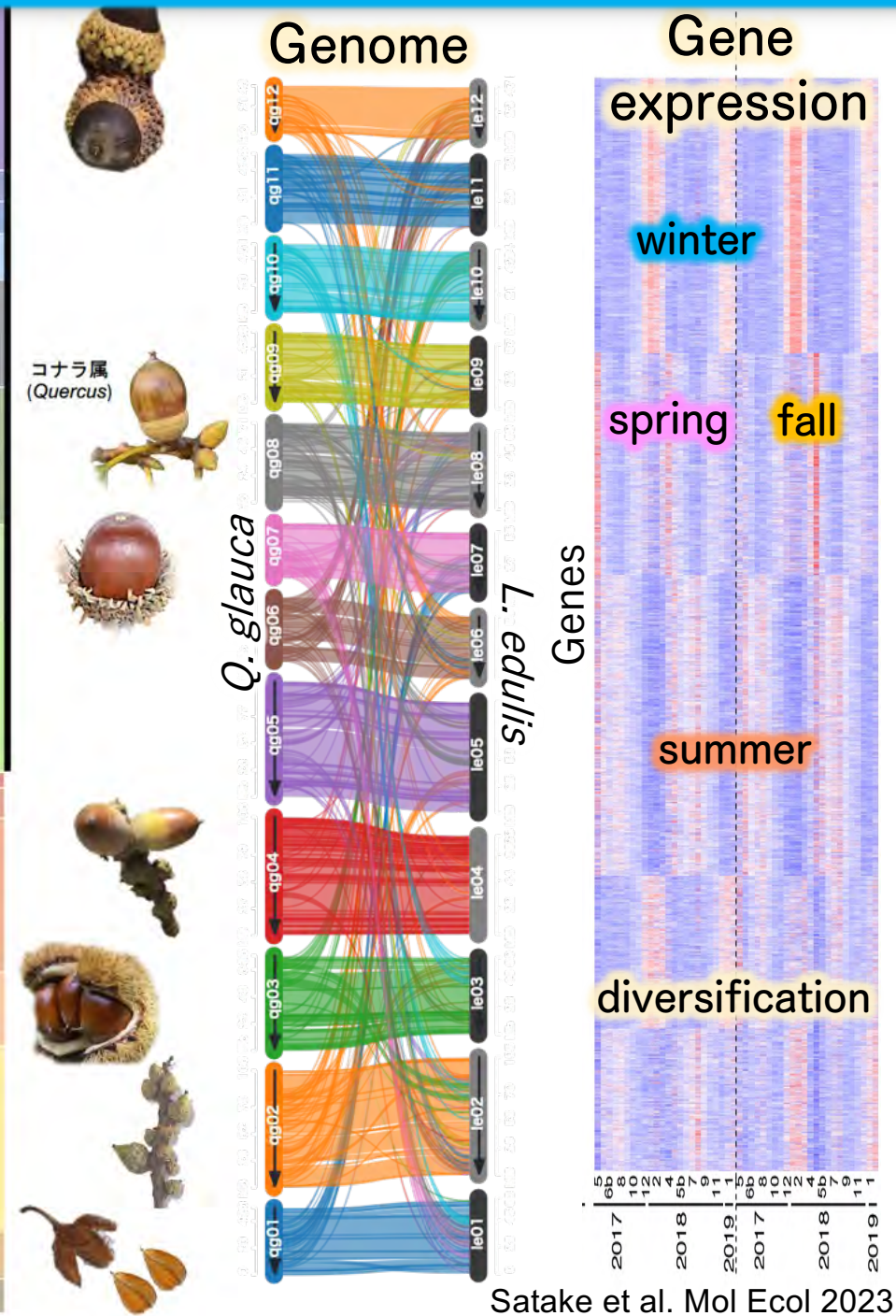
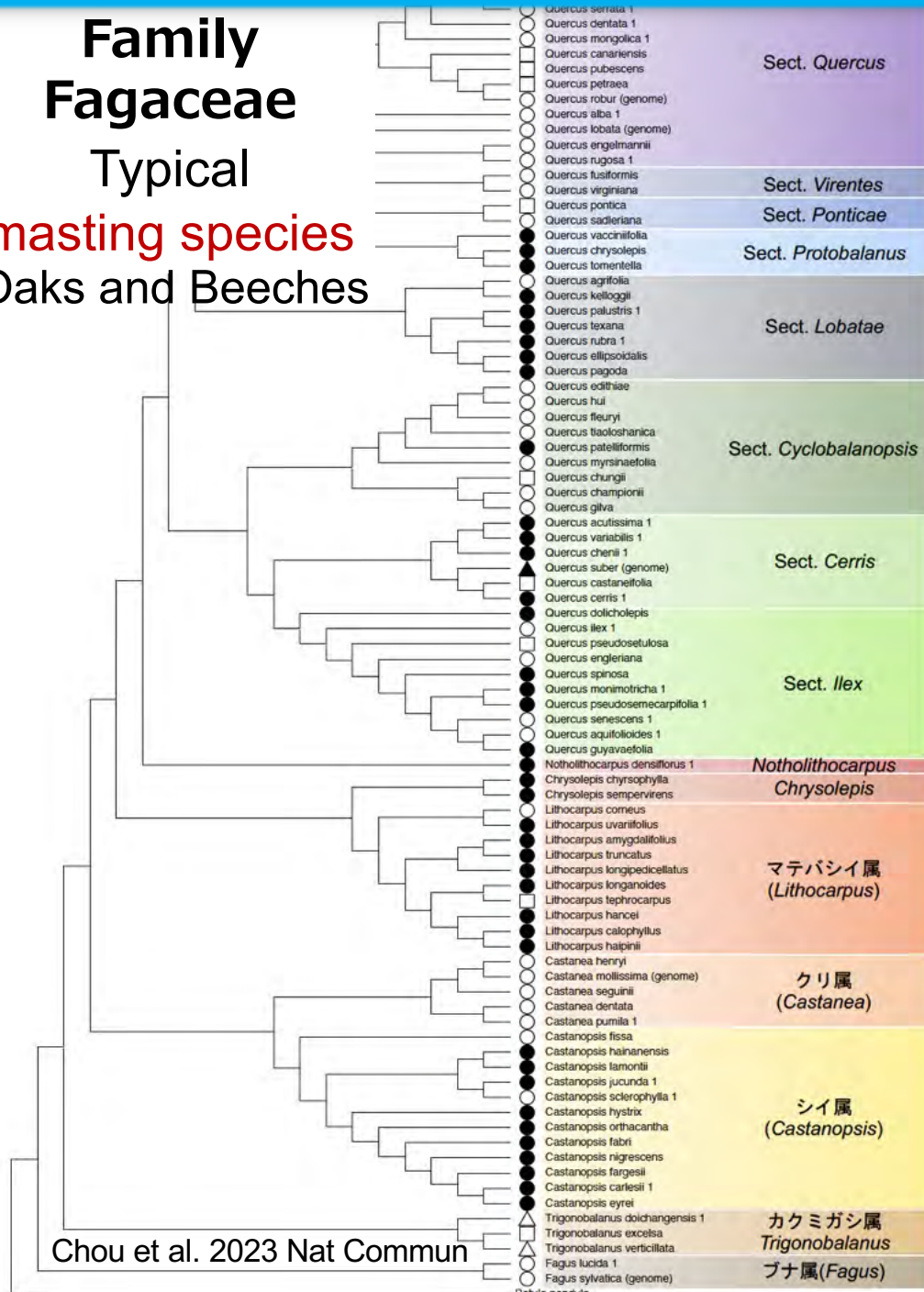
# Genomic resources become available in trees

# Family Fagaceae

# Typical

## maisting species

### Oaks and Beeches



Satake et al. Mol Ecol 2023



# Synchrony from genes to ecosystems

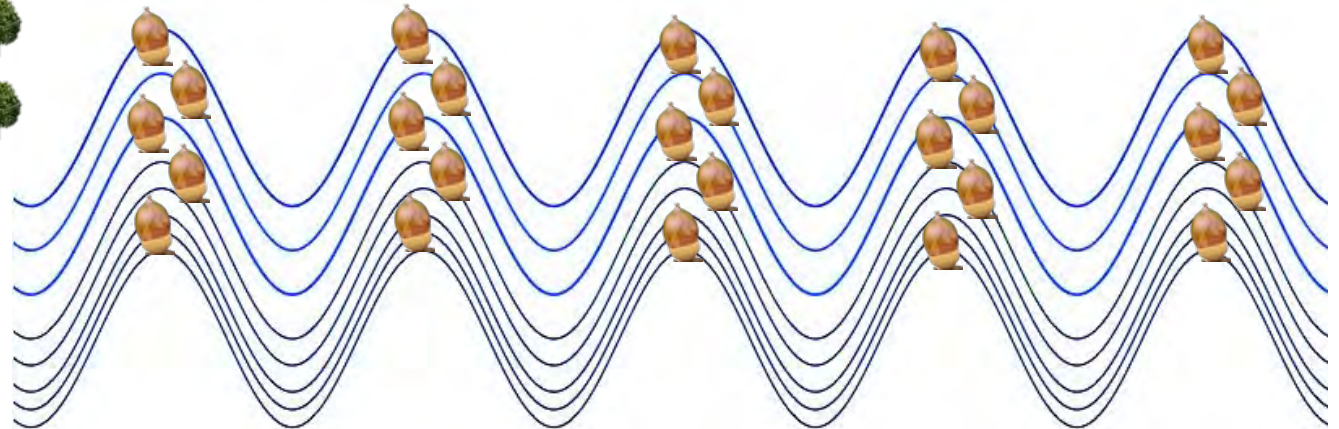
Ecosystem

Population

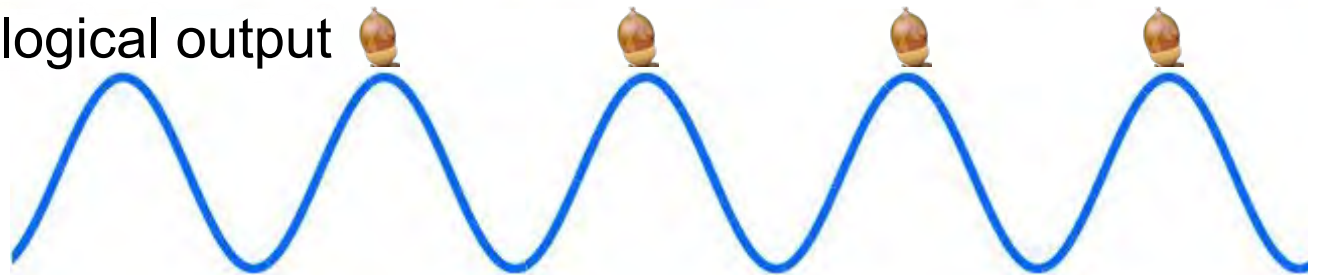
Individual

Gene

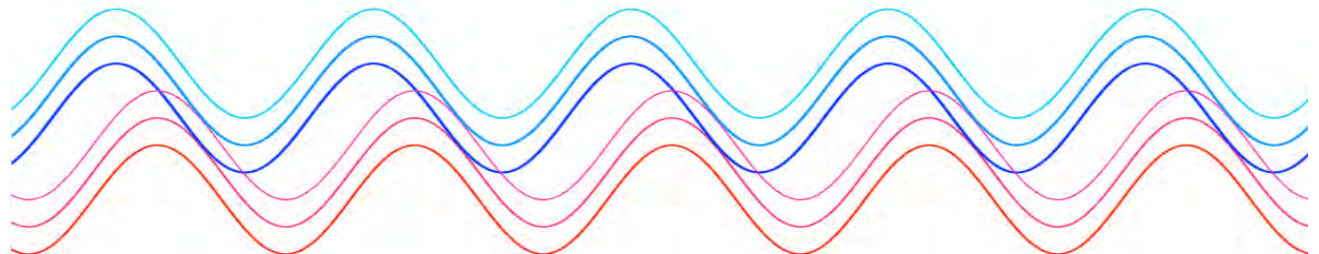
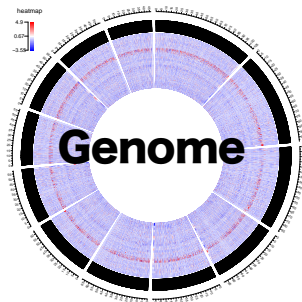
Output at the forest ecosystem level



Phenological output

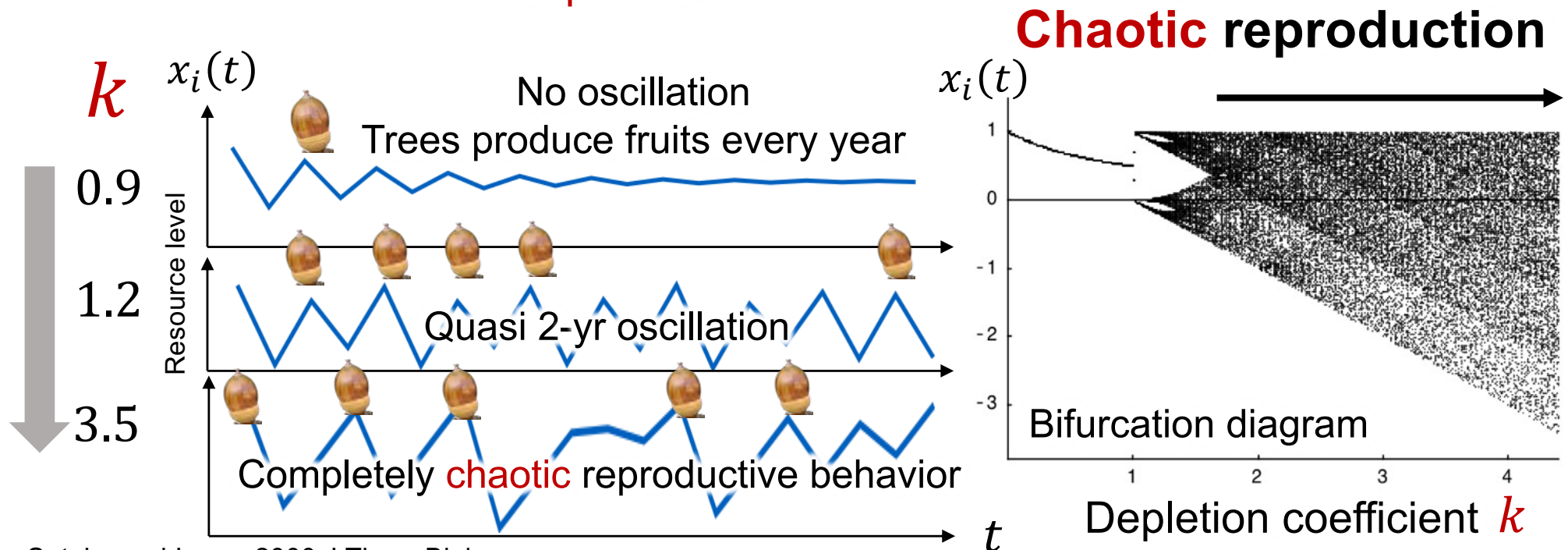
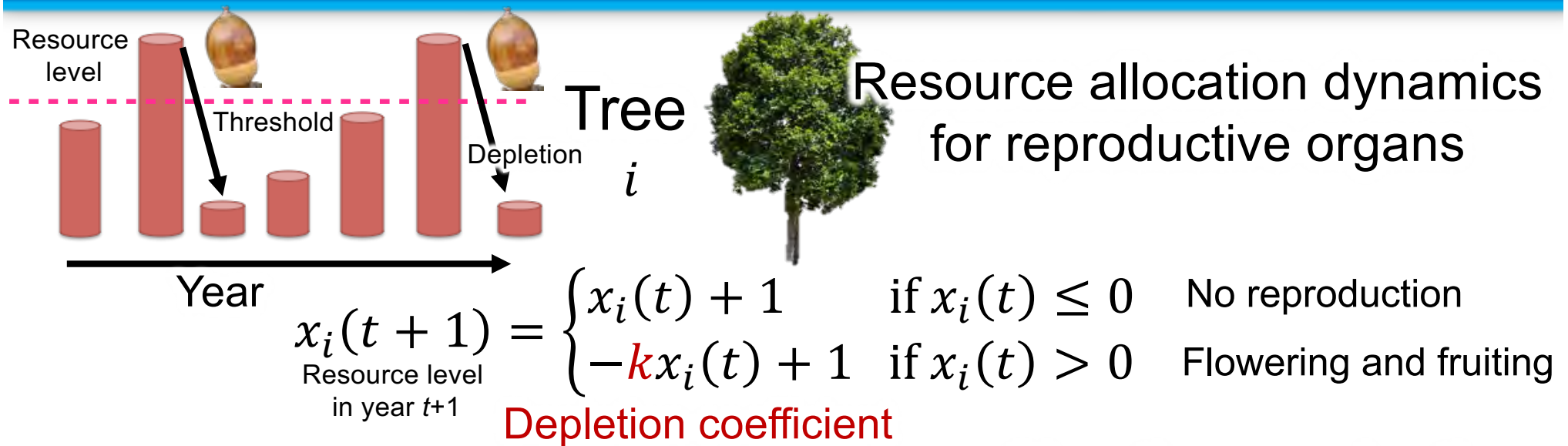


Molecular phenology: genome - wide gene expression in nature





# A mathematical model explaining the emergence of population synchrony





A diagram showing eight stylized green trees arranged in a loose circle. Blue double-headed arrows connect each tree to its immediate neighbors, forming a ring. Yellow dots are scattered around the trees, representing seeds or resources. The background is a photograph of a dense green forest under a blue sky with light clouds.

How are trees synchronized?

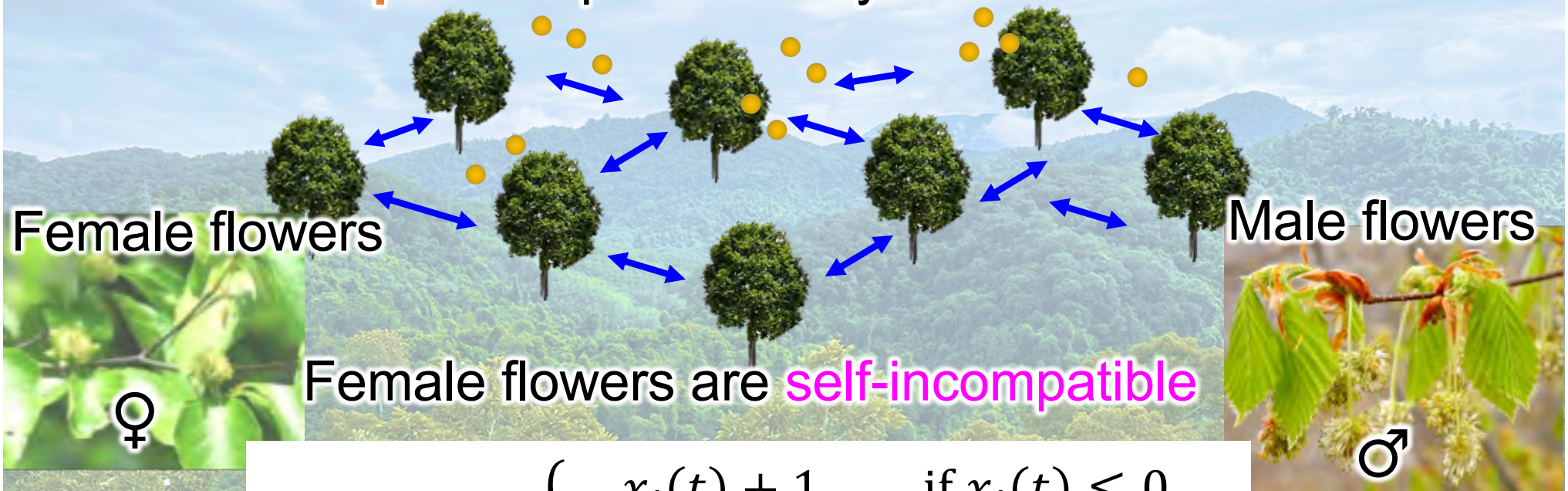


When individual tree exhibits **chaotic** reproduction, slight difference in resource levels between trees **expand exponentially**.



# Pollen coupling

Pollination success depends on abundance of **pollens** produced by other trees



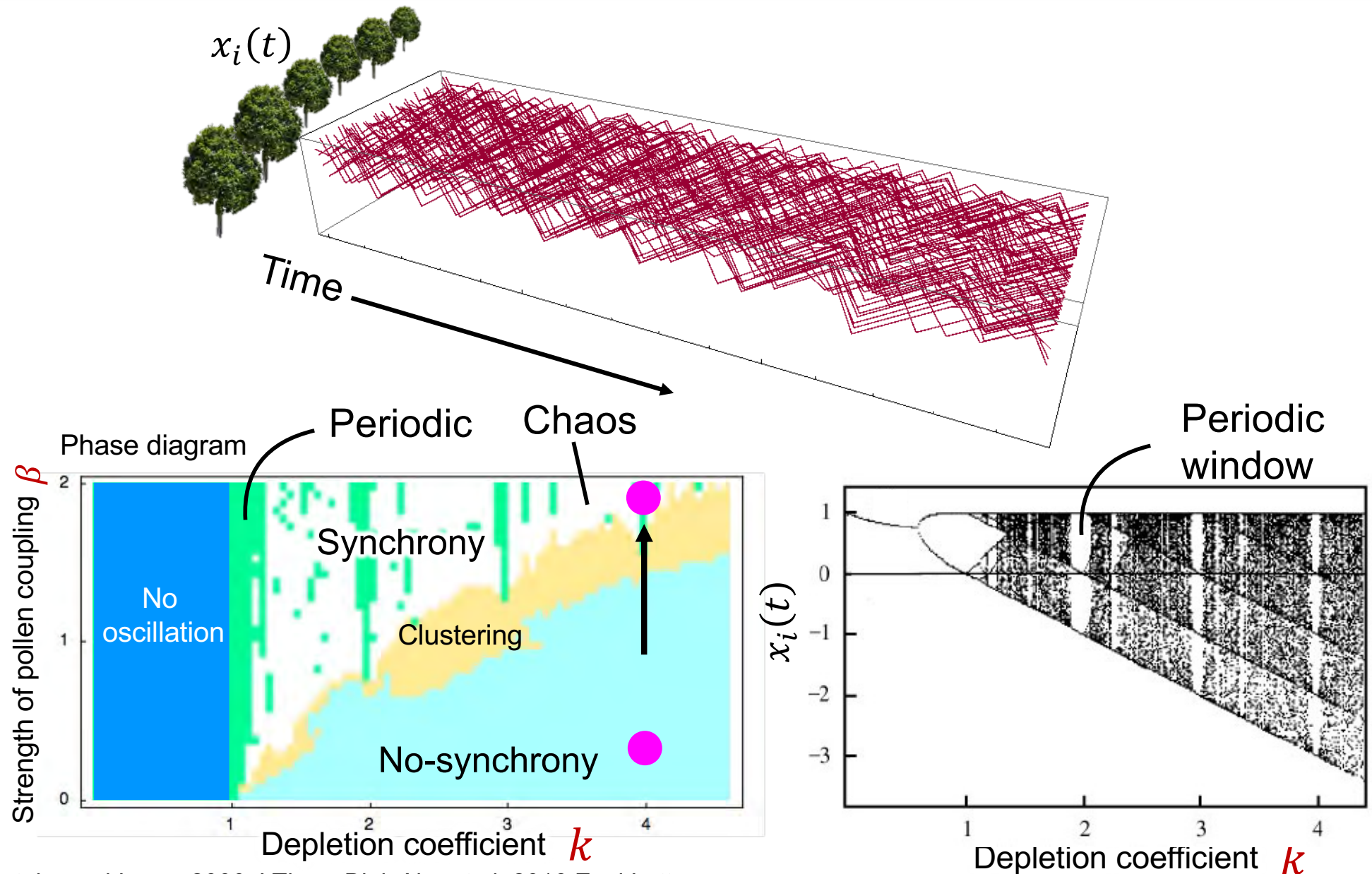
Female flowers are **self-incompatible**

$$x_i(t+1) = \begin{cases} x_i(t) + 1 & \text{if } x_i(t) \leq 0 \\ -kP_i(t)x_i(t) + 1 & \text{if } x_i(t) > 0 \end{cases}$$

Pollination success  $P_i(t) = \left( \frac{1}{N-1} \sum_{j \neq i} [x_j(t)]_+ \right)^\beta$

$\beta$  : Coupling strength

# Emergence of periodic reproduction out of chaos





# Synchrony from genes to ecosystems

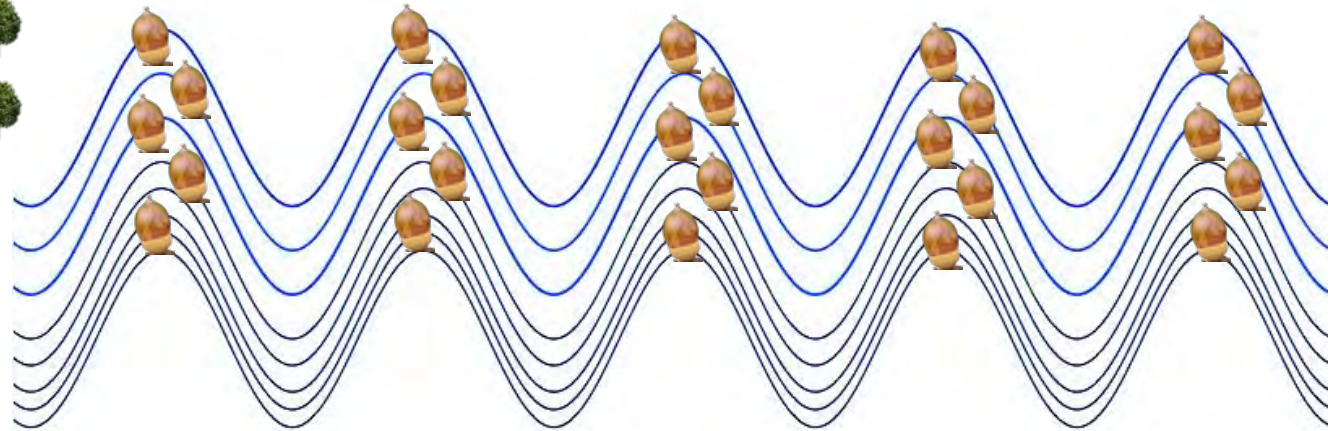
Ecosystem

Population

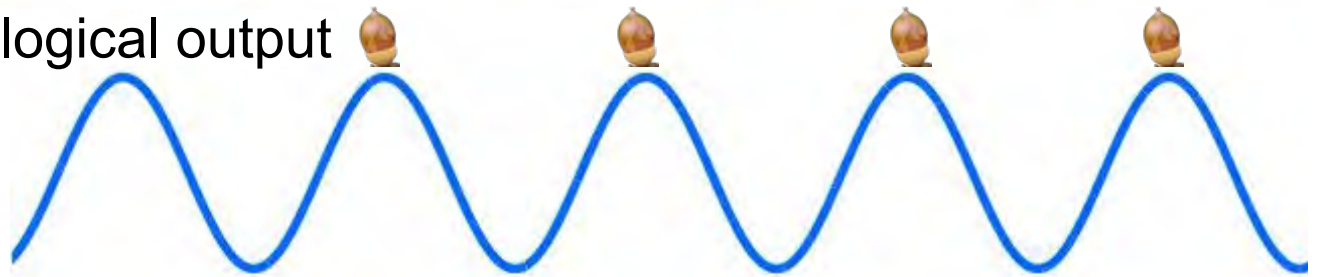
Individual

Gene

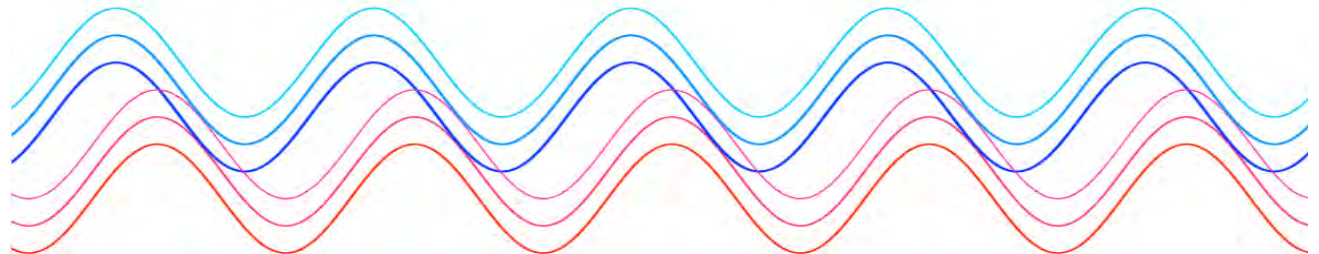
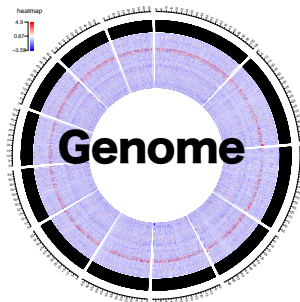
Output at the forest ecosystem level



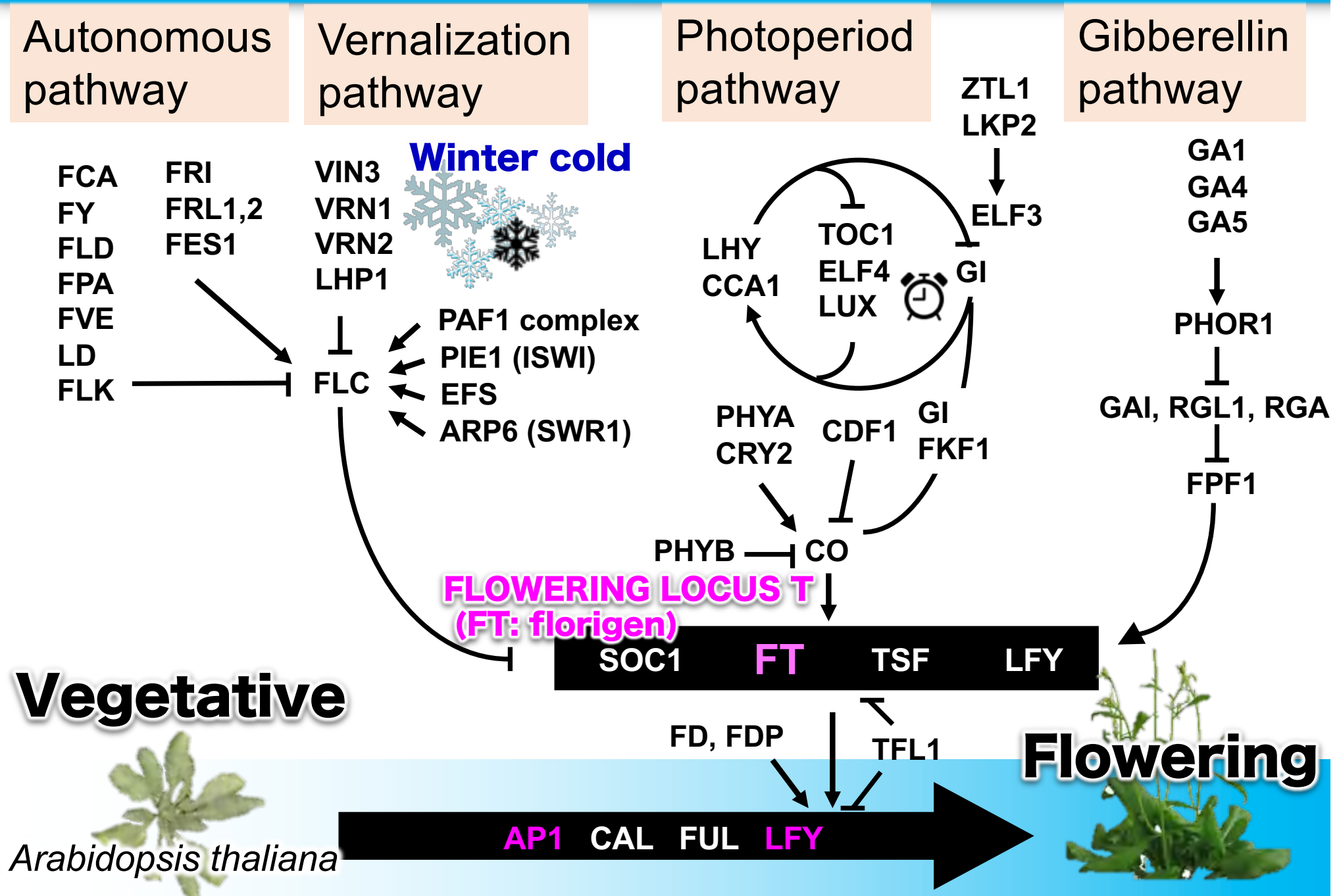
Phenological output



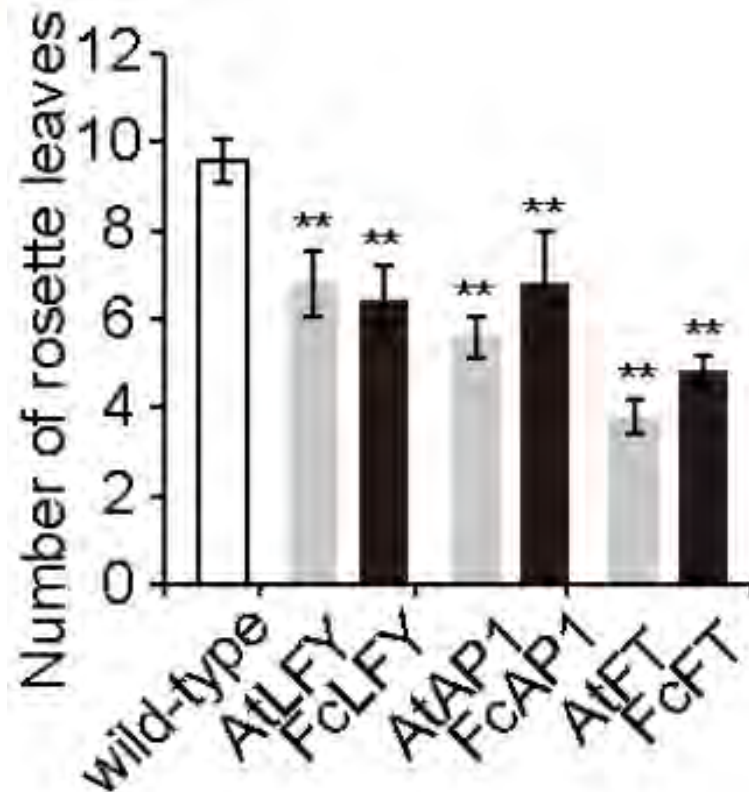
Molecular phenology: genome-wide gene expression in natural c



# Genes encoding when to flower



# Transformation using *A. thaliana*



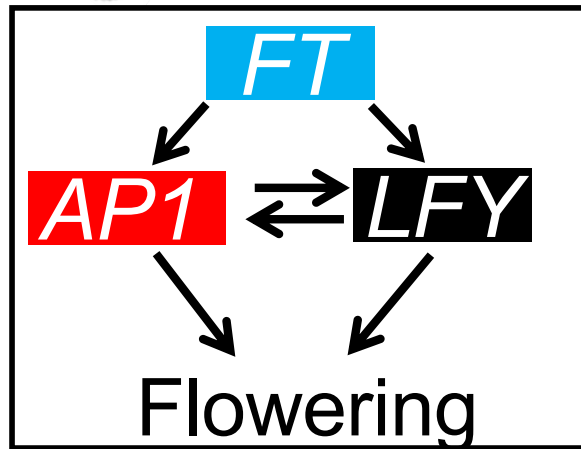
Isolation of *FT*, *AP1*, and *LFY* in *Fagus crenata* (Japanese beech).

Overexpression of *Fagus* flowering genes resulted in early flowering.

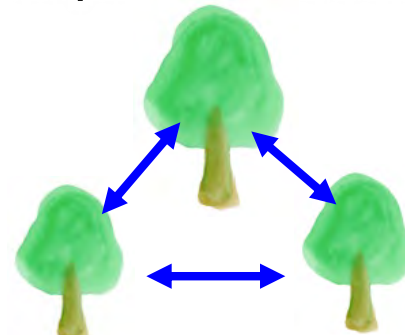


# 7-yr monitoring of *FT* expression revealed intra- and inter-individual synchrony

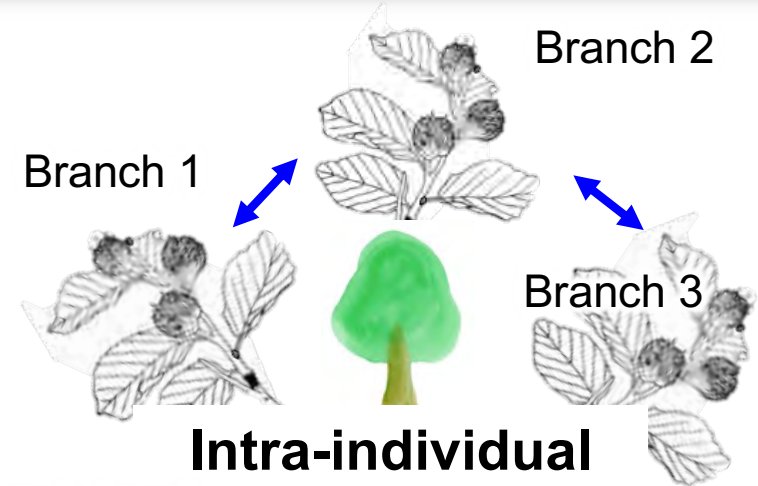
leaf bud → qPCR



Japanese beech

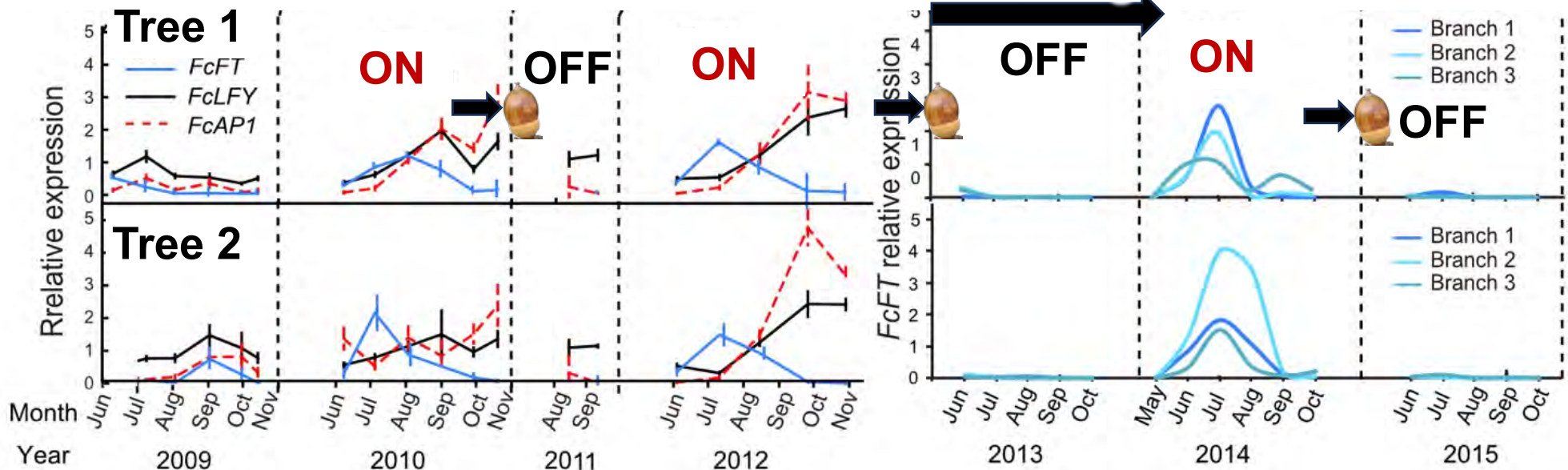


Inter-individual Synchrony



Intra-individual Synchrony

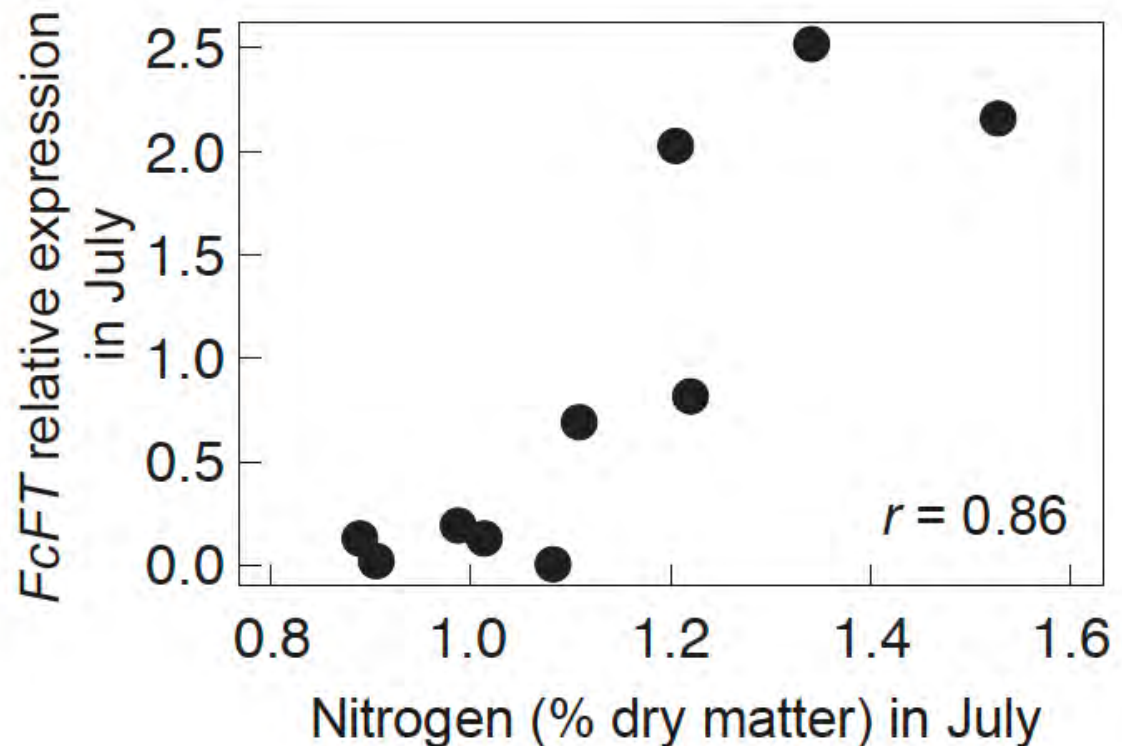
Branch-level monitoring



# What drives interannual fluctuation in flowering gene expression?

Between year variations in internal nutrient states?

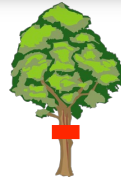
We measured nutrient (C and N) concentration in current-year shoots.



# Nitrogen fertilization experiments confirmed the role of nitrogen on mass flowering

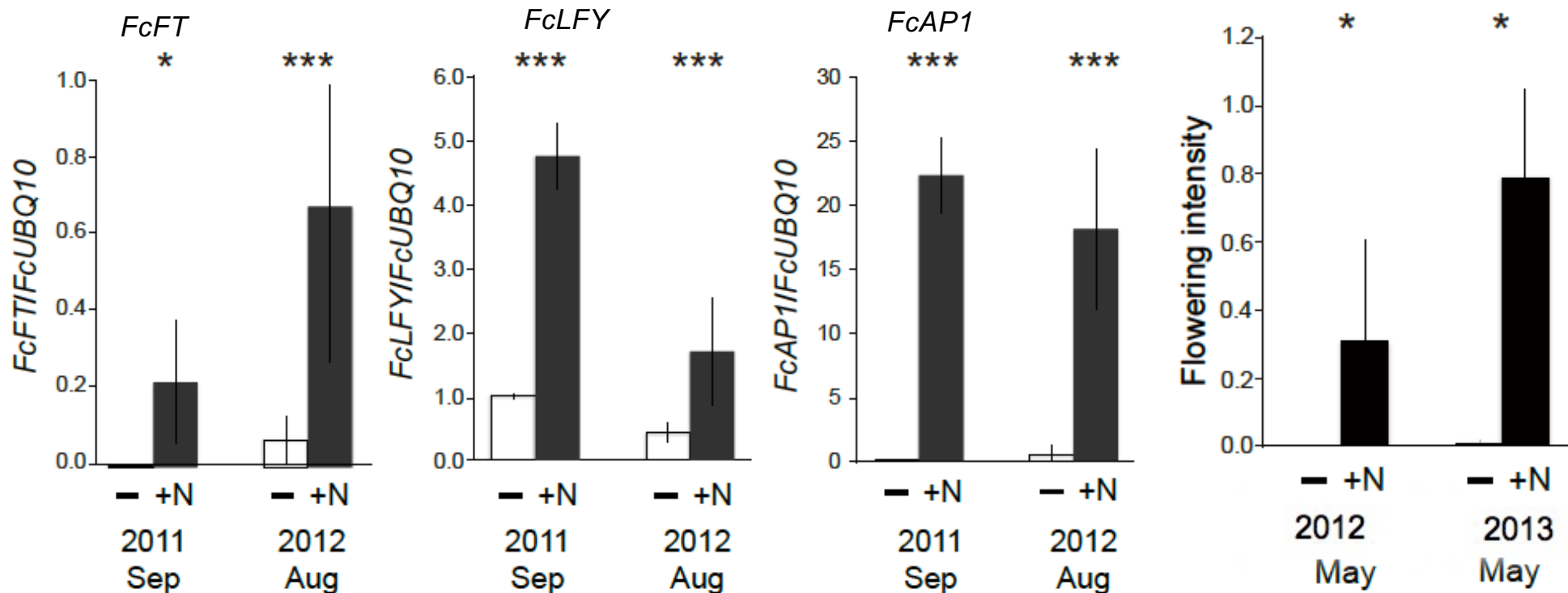
fertilization  
(+N)  
Once per month  
from April to Aug

control  
(-)

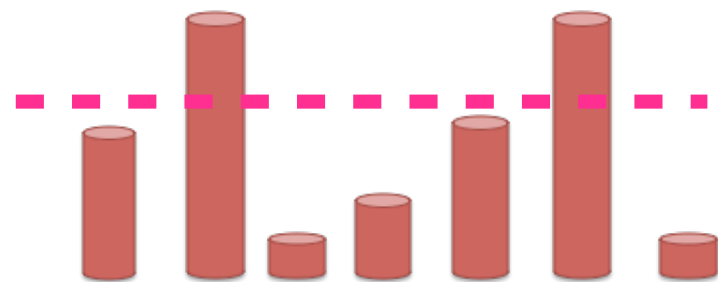


2011, September

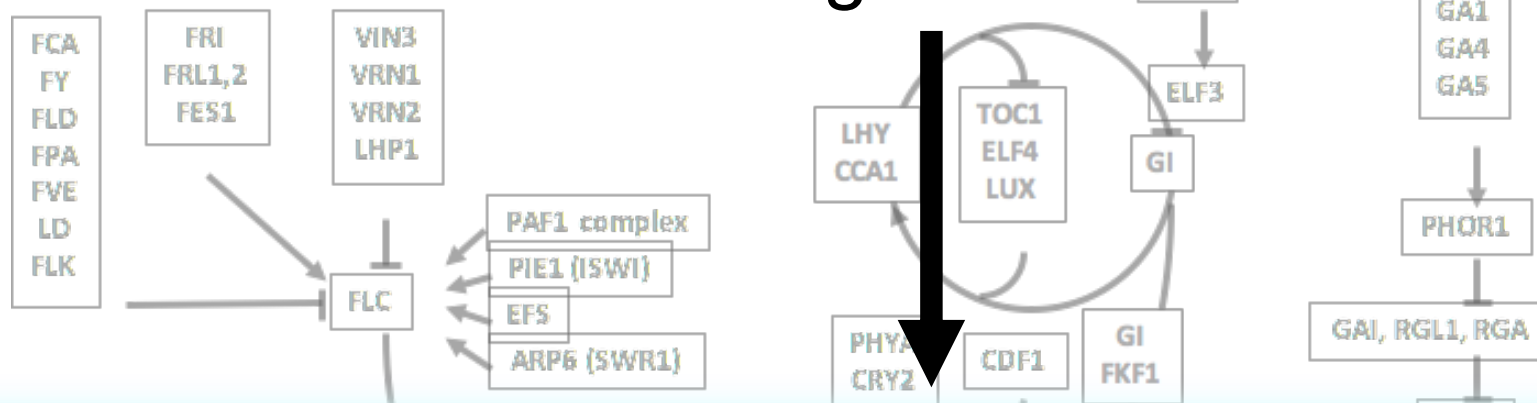
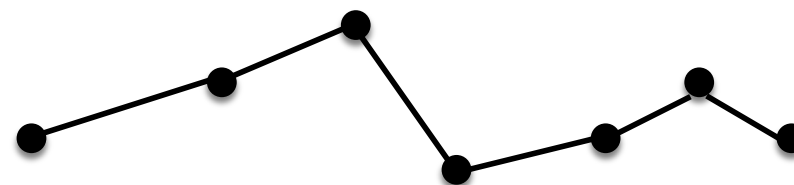
Masting can be manipulated by nitrogen fertilization.





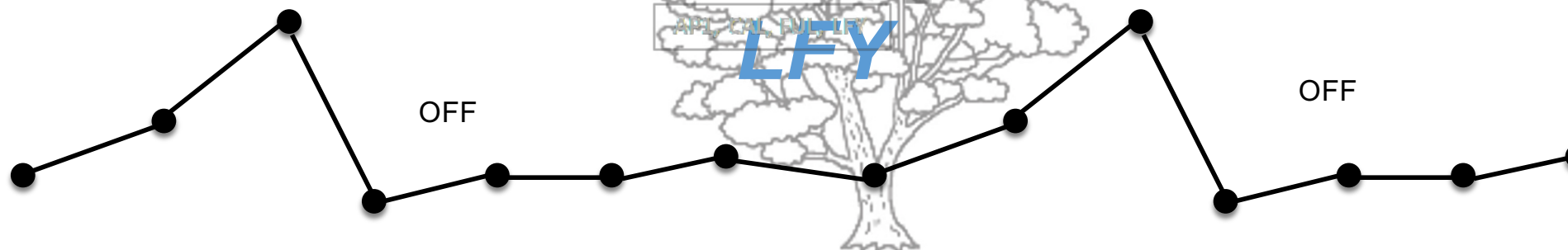


Nitrogen



Target gene analyses → Transcriptome analyses

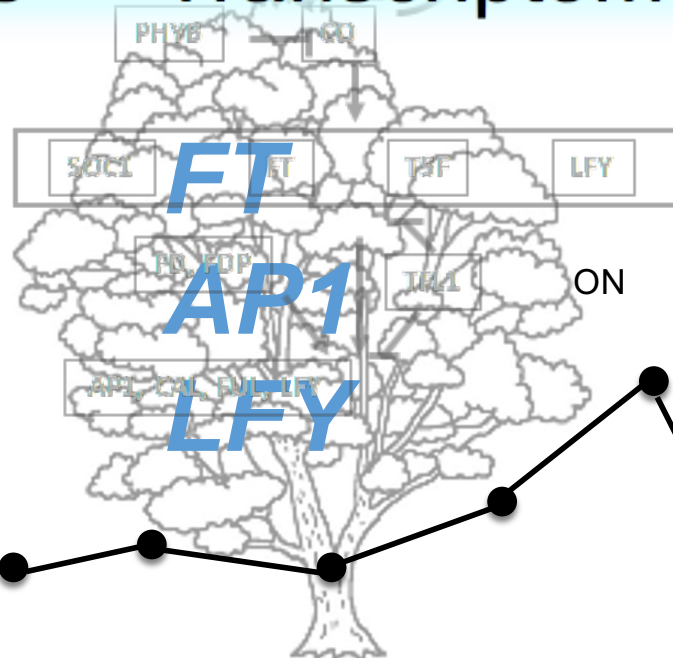
ON



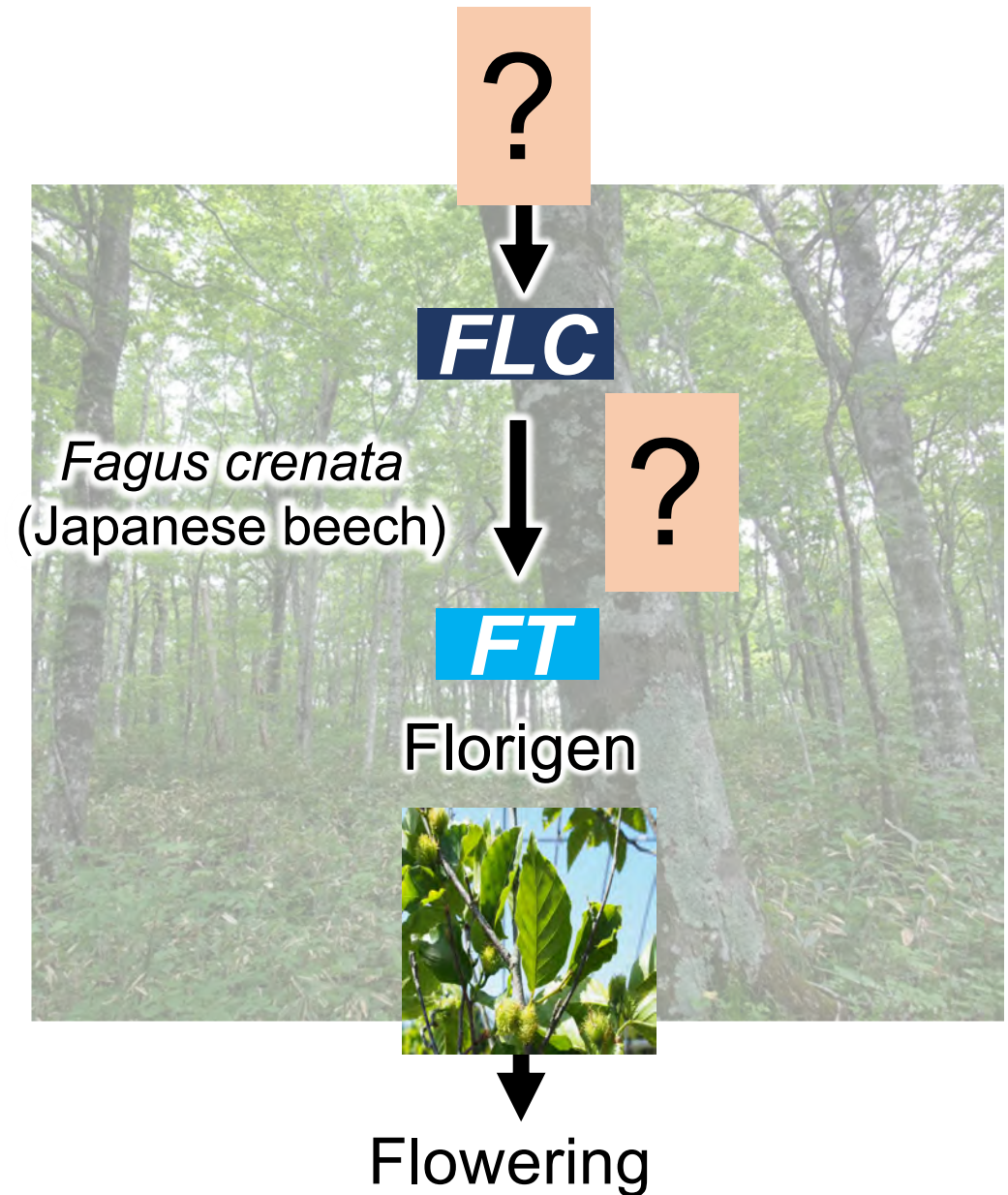
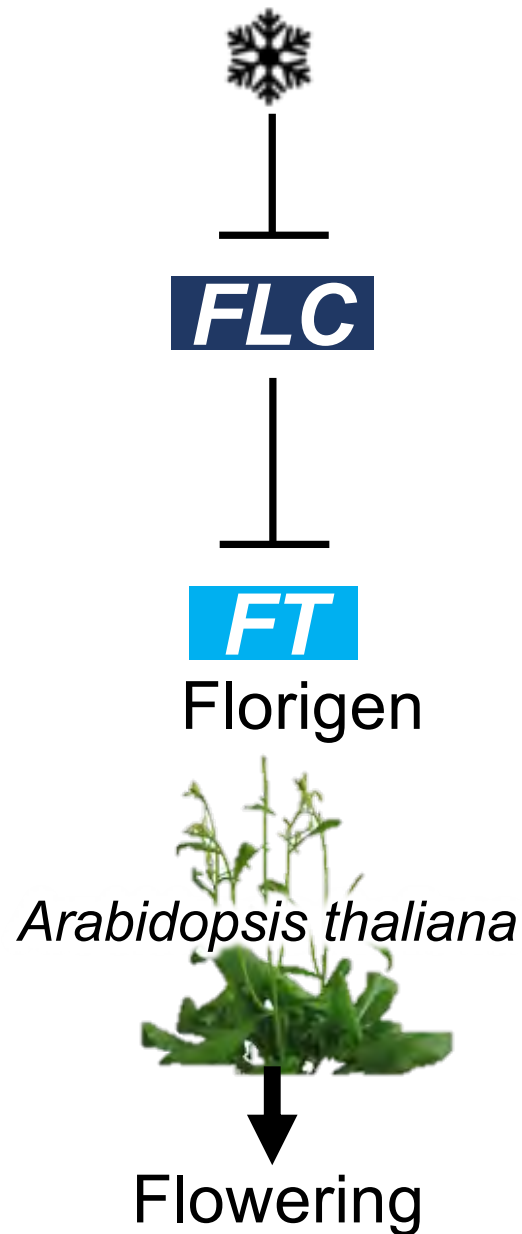
OFF

ON

OFF



# Comparison between *A. thaliana* and *F. crenata*



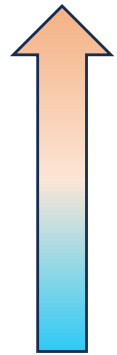
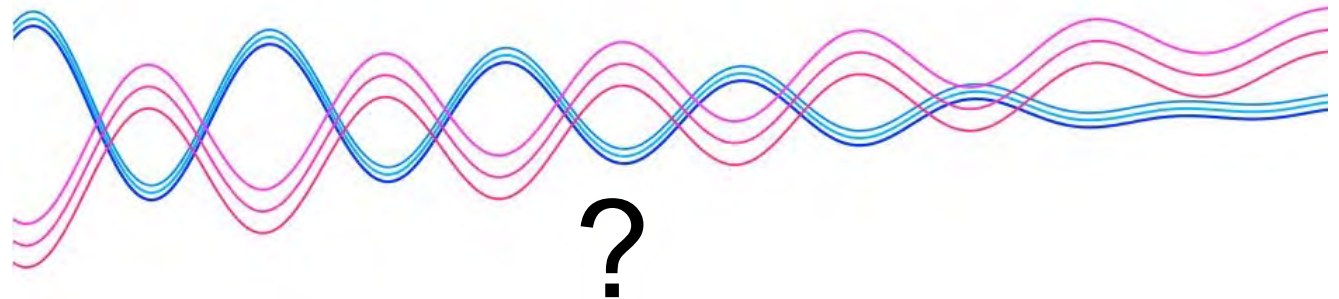
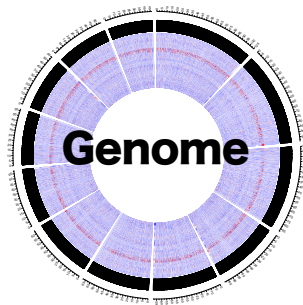
# How organisms in nature respond to climate warming?



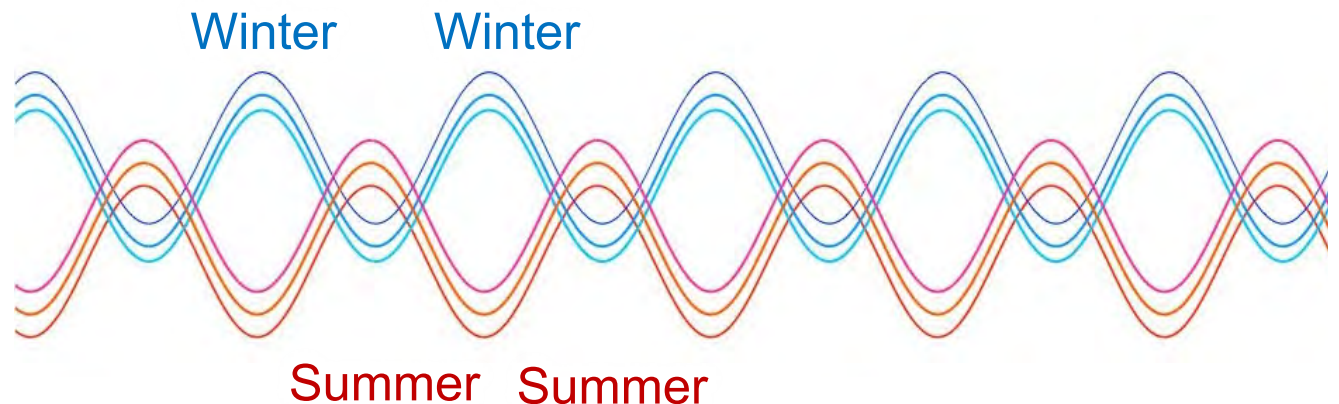
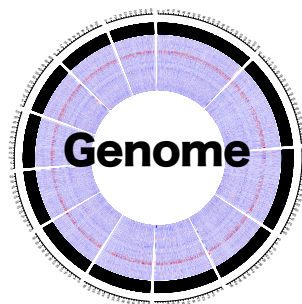
## Seasonal gene expression pattern may be affected by climate change

Winter will become milder in future

Future



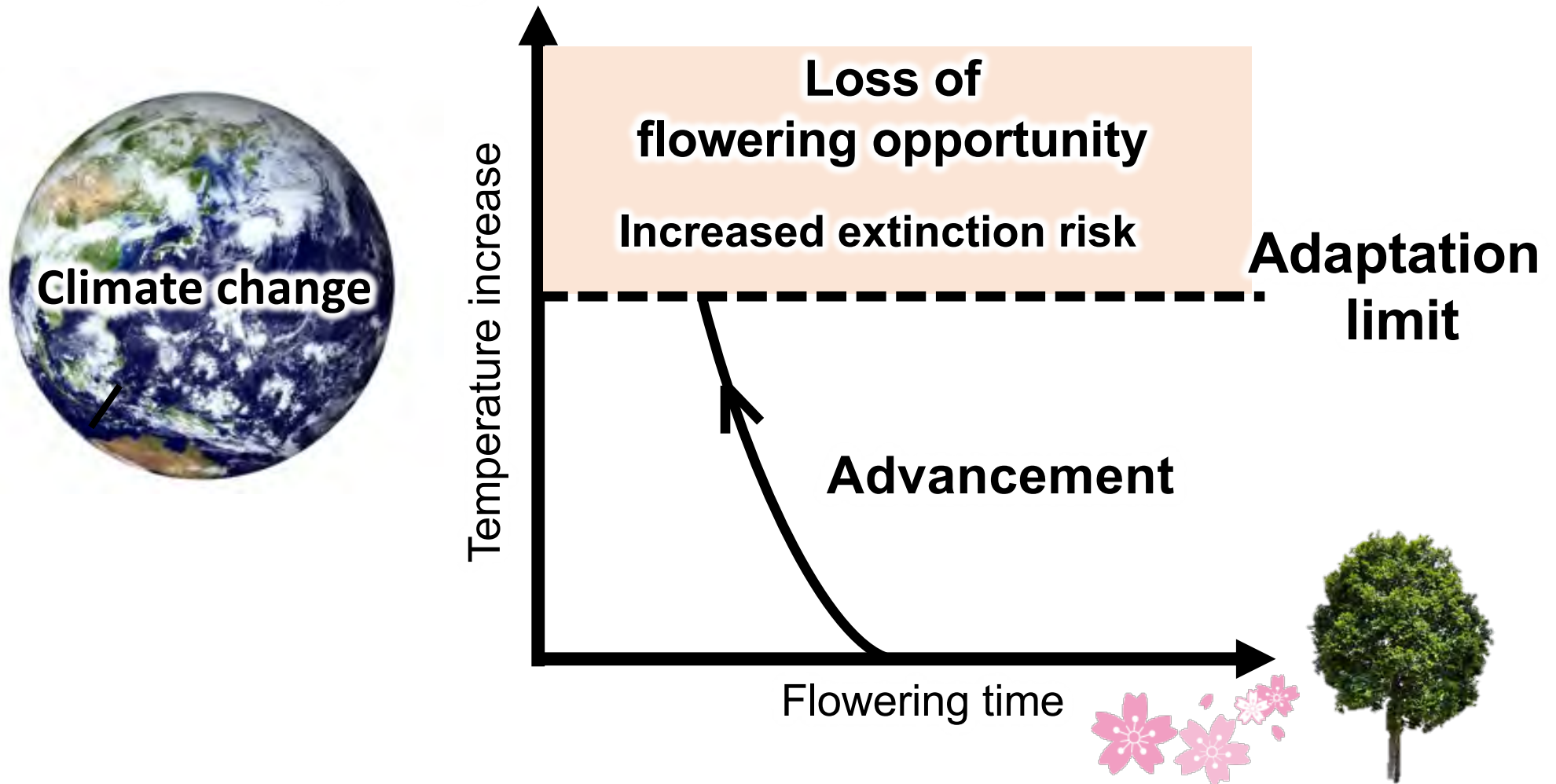
Present





# To what extent can plants adapt to global warming?

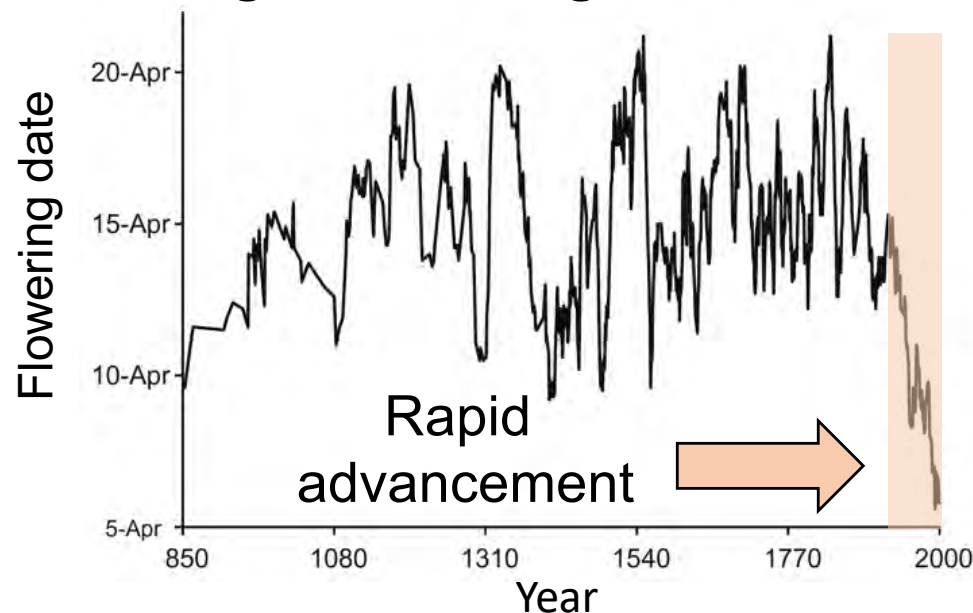
The adaptation limit above which flowering opportunity is completely lost and extinction risk increases



# Flowering phenology and climate change

Historical record of  
cherry blossom blooming in Kyoto  
1,200 years

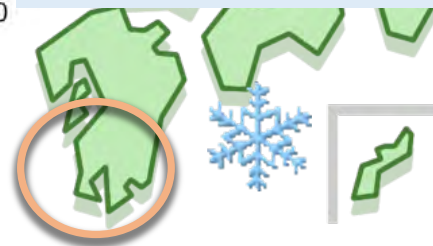
**Timing of flowering has advanced**



Primack et al. 2009 Biol Conserv  
Aono and Kazui 2008 Int J Climatol



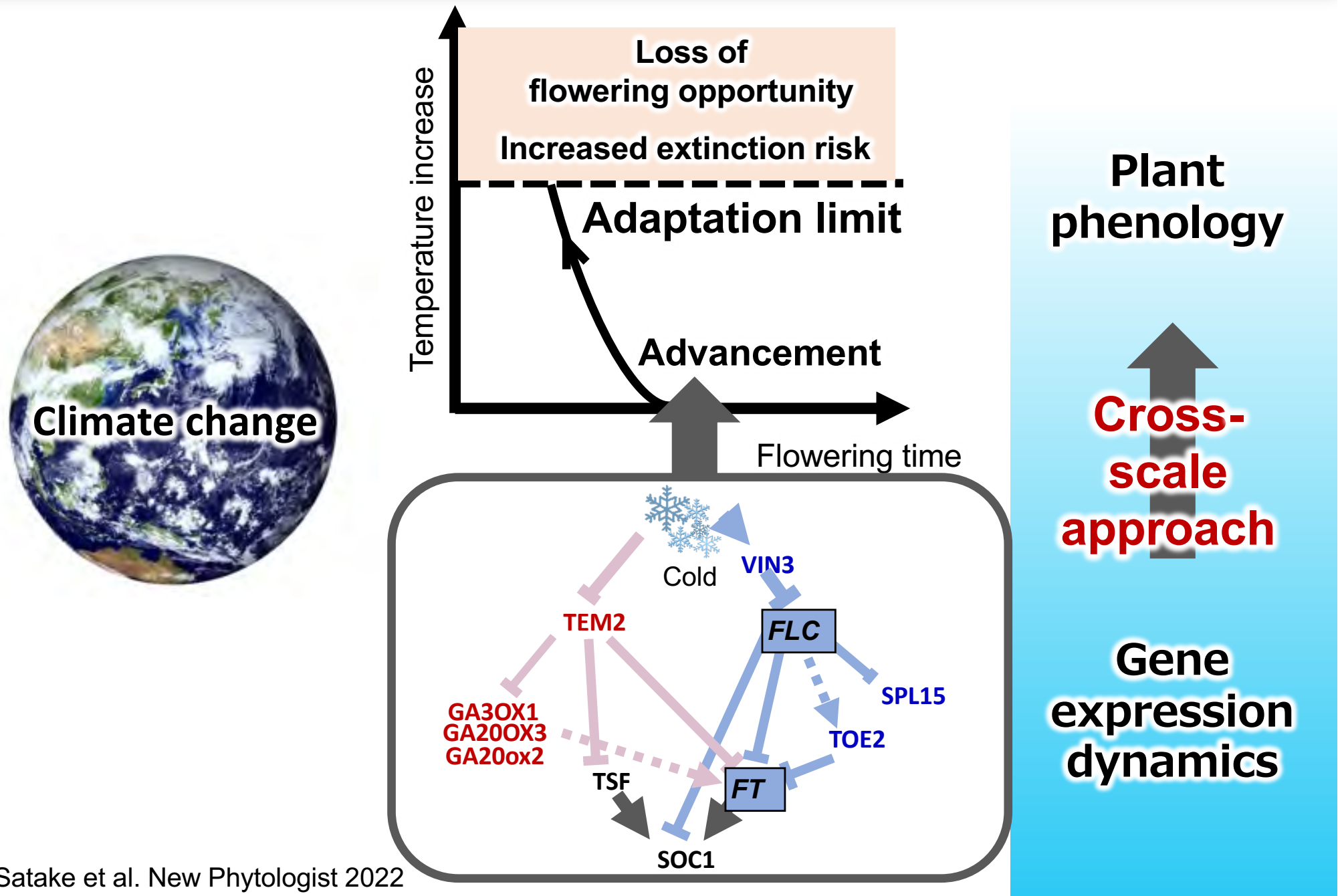
**Low temperature necessary for  
buds to break dormancy will be  
unavailable**



Maruoka and Ito 2009

**Blooming events may disappear in future**

# Estimating adaptation limits at the genetic level



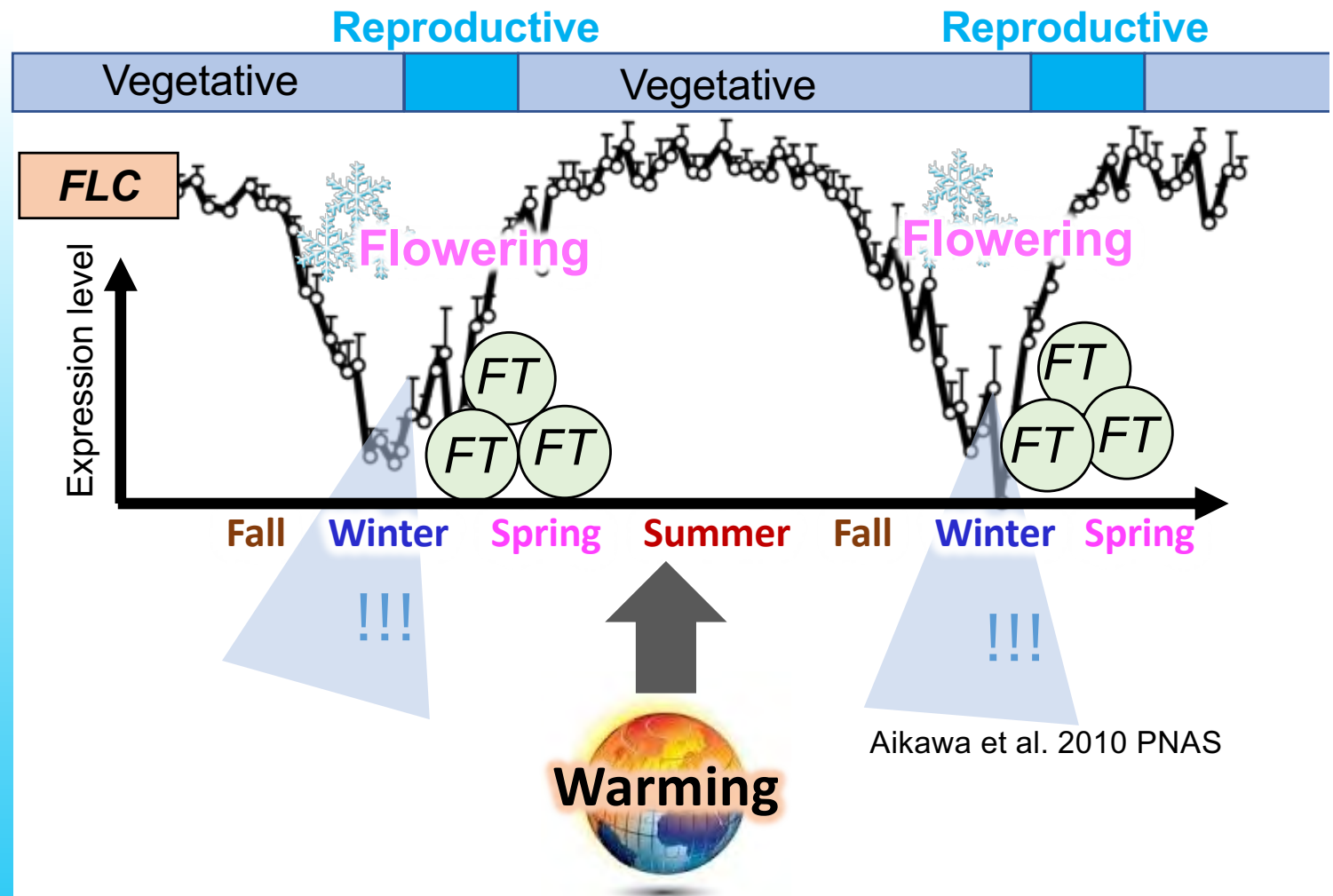
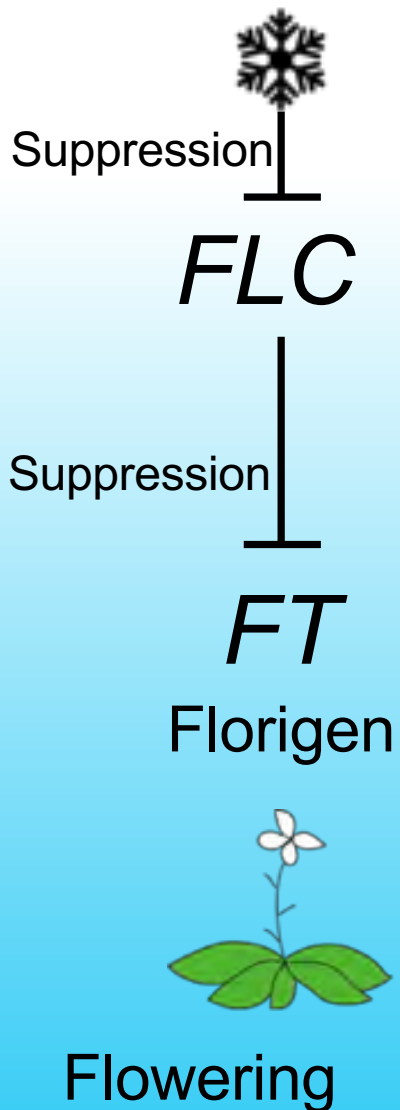


## ***FLC* plays a critical role in cold responses**

# Cold

## Winter cold suppresses *FLC* expression

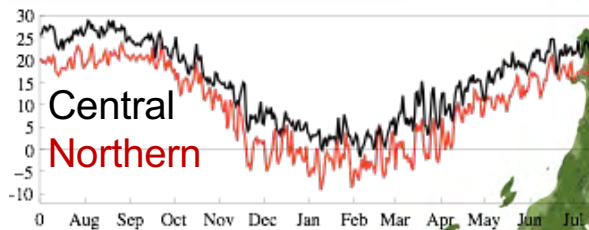
## Seasonal expression profile of *FLC* in perennial *Arabidopsis*



# Evaluation of adaptation limits based on gene expression analysis



*Arabidopsis helleri* subsp. *gemmifera*  
a perennial herb



Northern and Central  
populations in Japan

Prediction

Experiment

Field  
monitoring

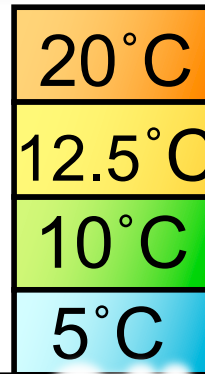
Modelling

# Temperature control experiments

Long day condition  
(16h light/8h dark)

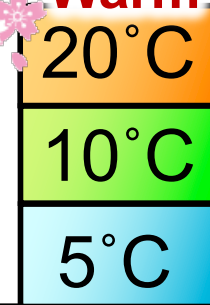


8 weeks

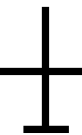
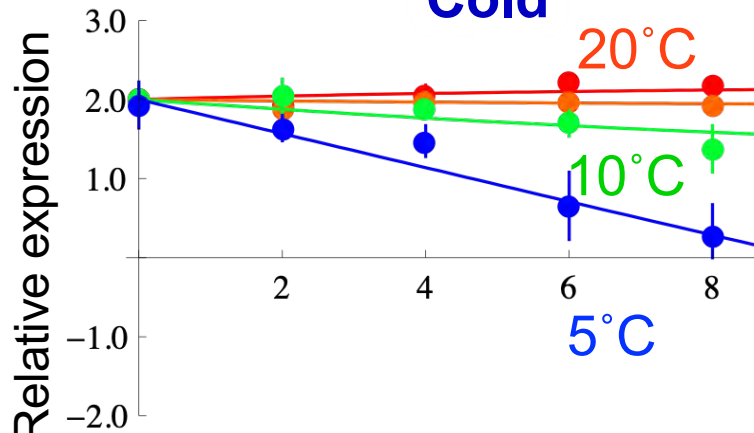


34 weeks

Warm



*FLC*

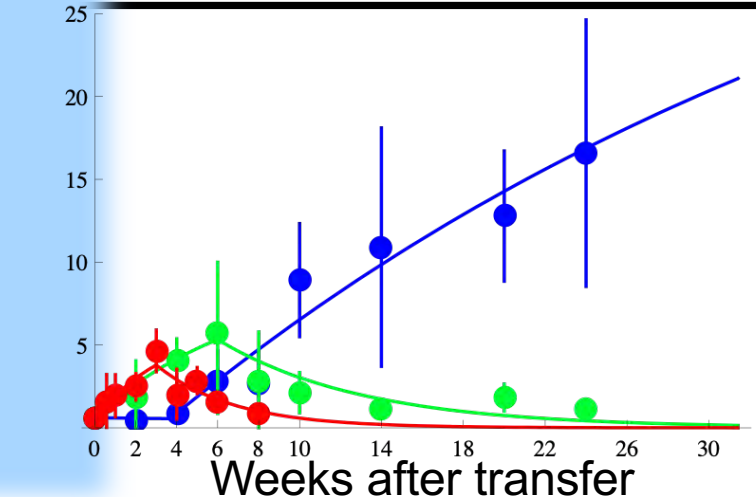
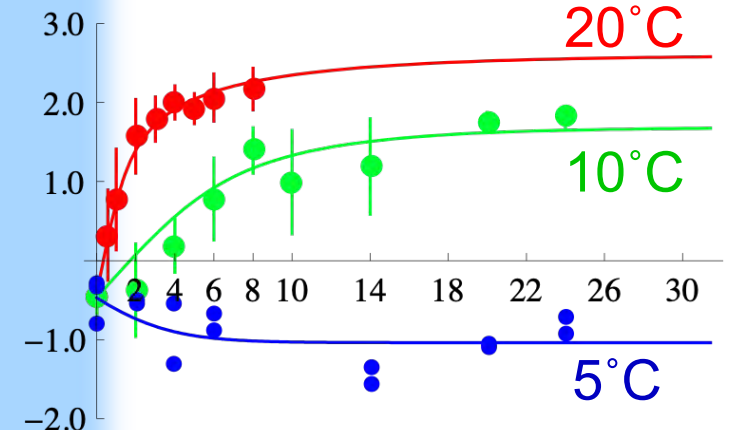
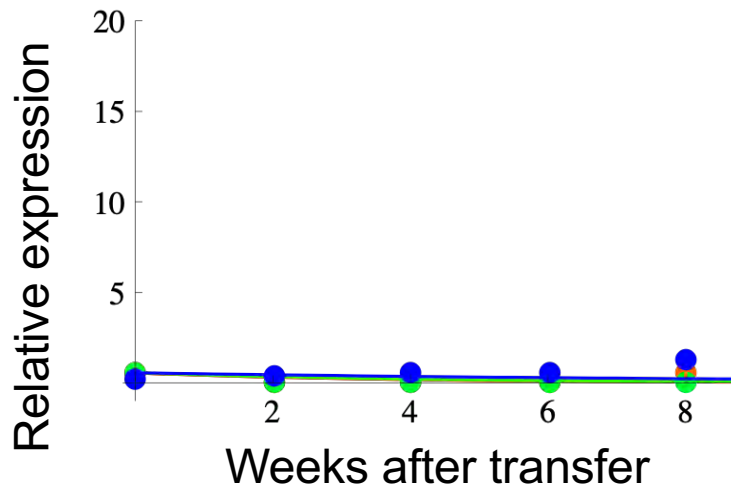


*FT*

Florigen



flowering



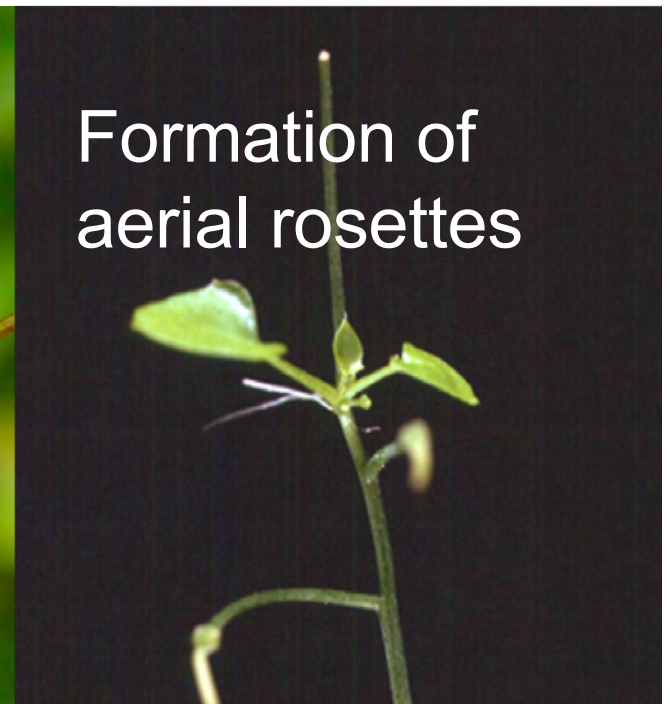


# Start and end of flowering in *A. halleri*

Bolting

Flowering

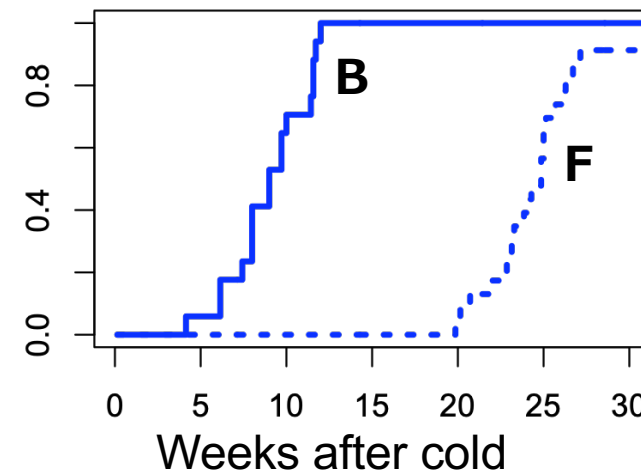
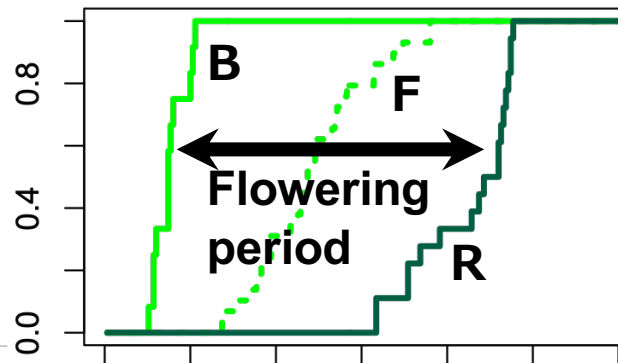
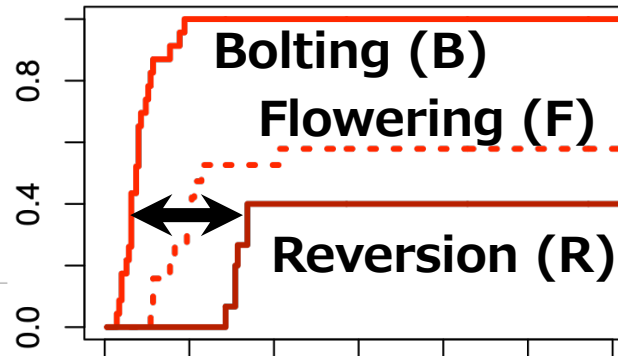
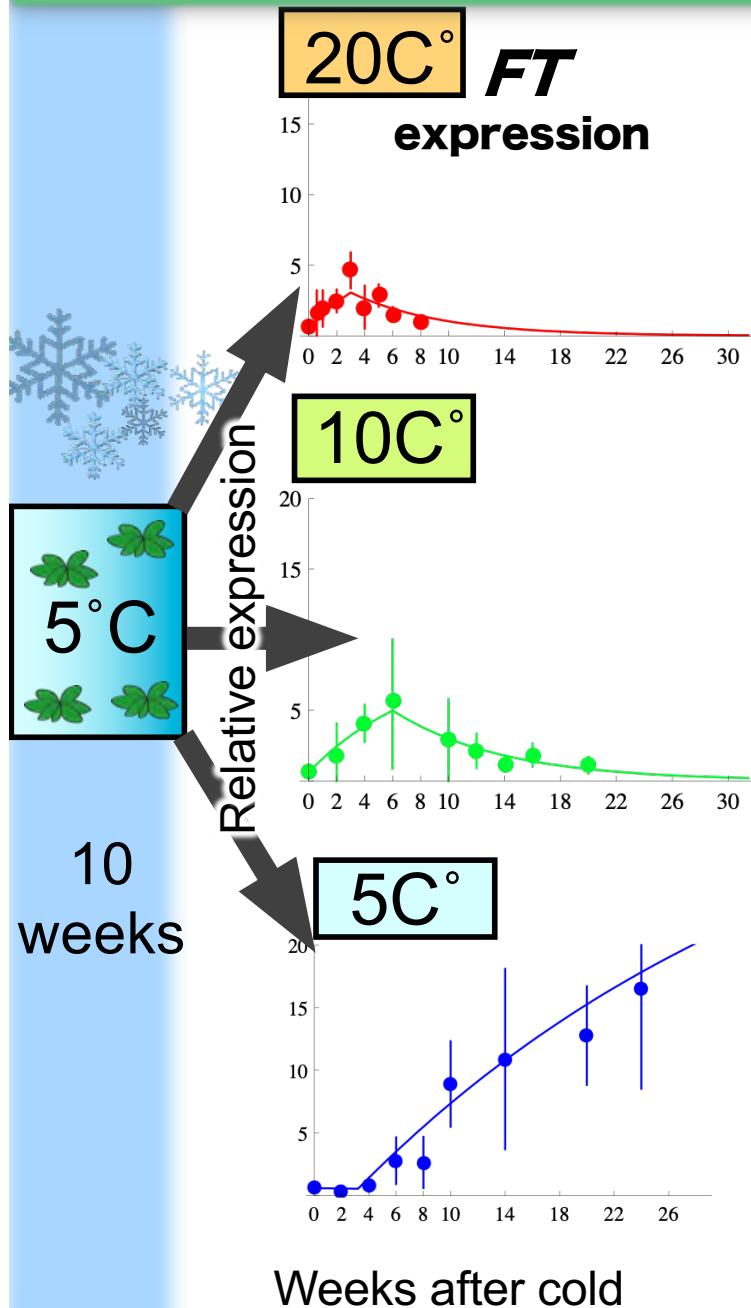
Reversion to  
vegetative  
growth



Start

End

# Systematic responses to temperature



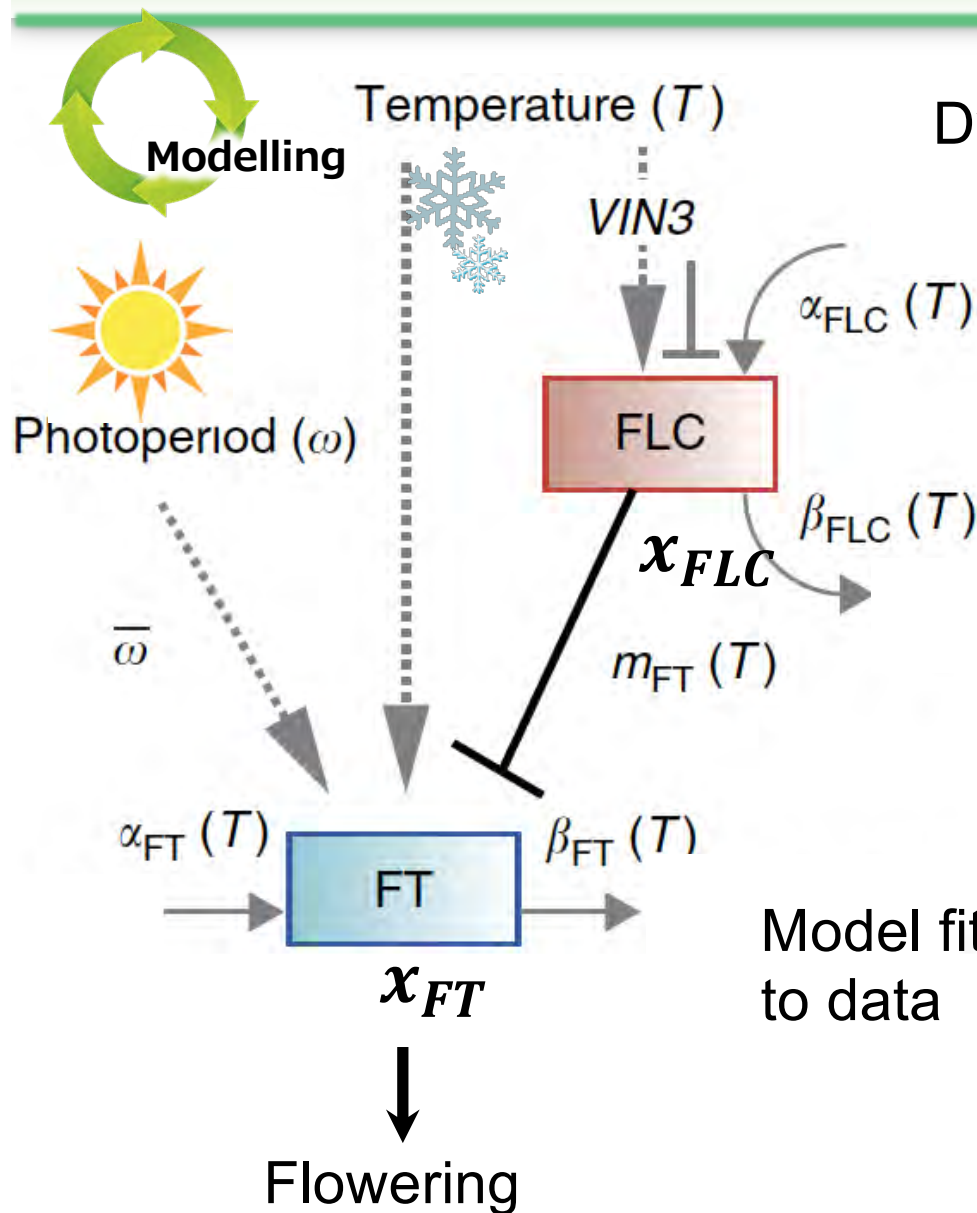
## Phenological shift

Bolting and Flowering times were advanced at warmer temperature.

Flowering period became shorter at warmer temperature.

Reversion did not occur at 5°C.  
Plants continued flowering.

# Modelling gene expression dynamics



Dynamics for  $FLC$  and  $FT$  expression

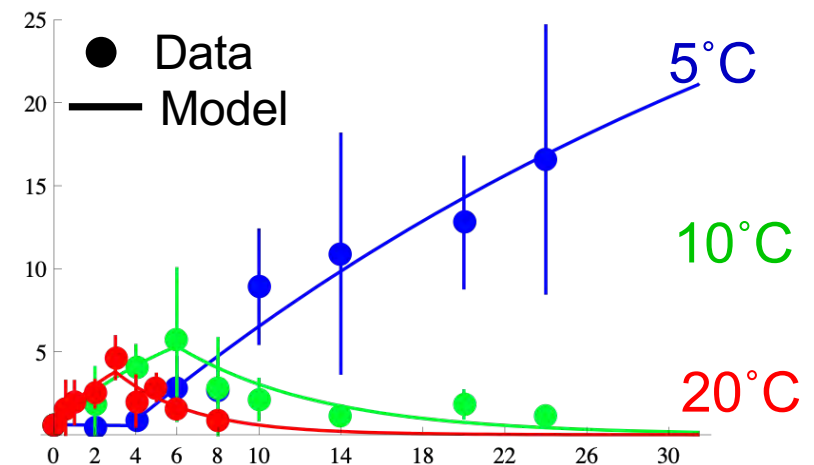
$$\frac{dx_{FLC}}{dt} = \underset{\text{Production}}{\alpha_{FLC}(T)} - \underset{\text{Degradation}}{\beta_{FLC}(T)} x_{FLC}$$

$$\frac{dx_{FT}}{dt} = \alpha_{FT}(T) g(x_{FLC}) h(\omega) - \beta_{FT}(T) x_{FT}$$

Temperature ( $T$ ) dependent

$$g(x_{FLC}) = \frac{1}{1 + \frac{x_{FLC}^H}{m_{FT}(T)}} \quad h(\omega) = \begin{cases} 1 & \text{if } \omega \geq \bar{\omega} \\ 0 & \text{if } \omega < \bar{\omega} \end{cases}$$

$\bar{\omega}$  : critical photoperiod



## Estimation of temperature response functions



# From laboratory to natural environments



- Natural Habitat
- Common Garden

Can our model predict flowering phenology in natural conditions?

## Transplant experiments

September



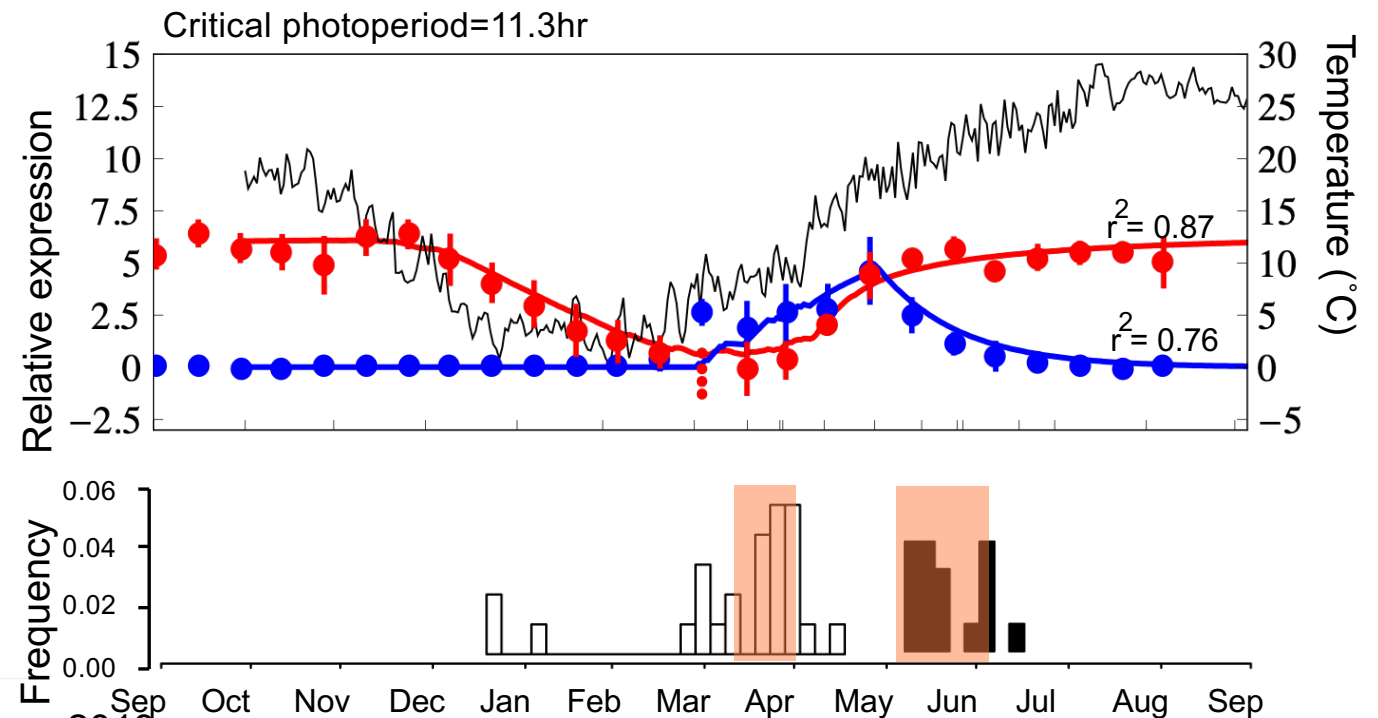
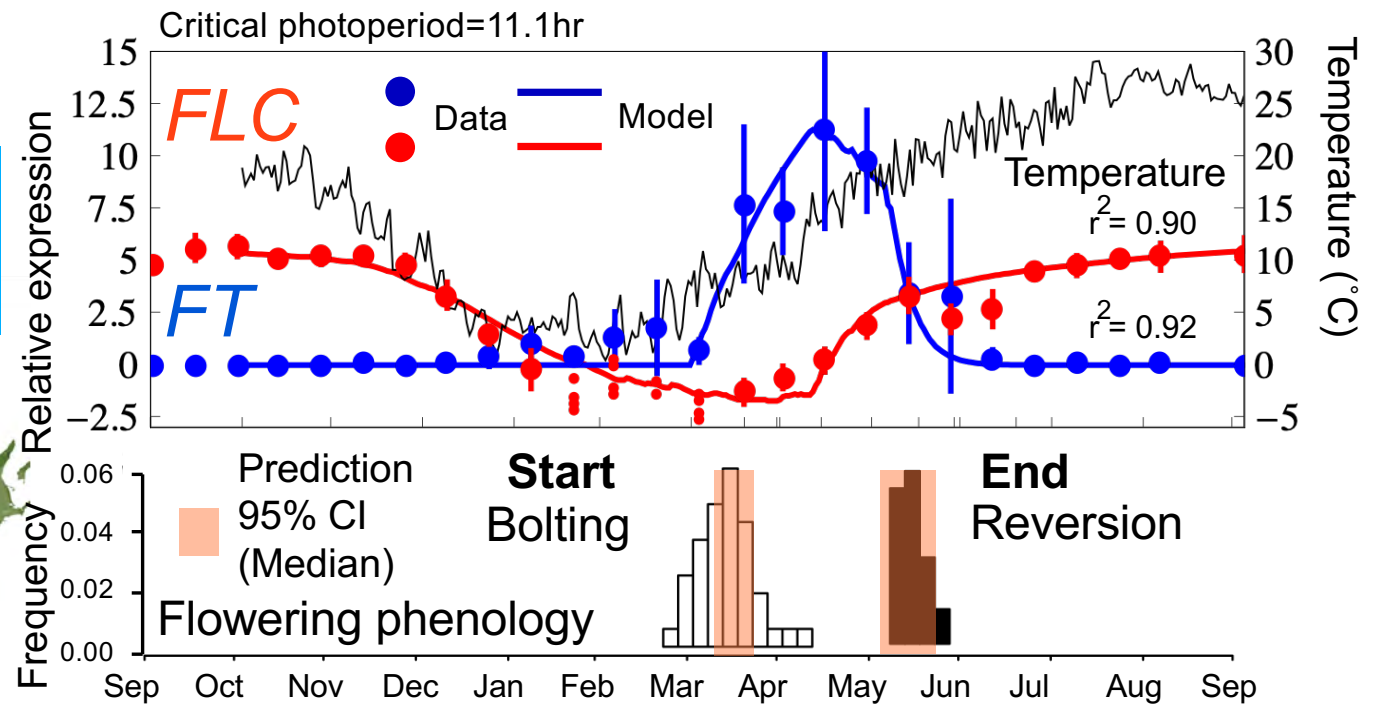
May



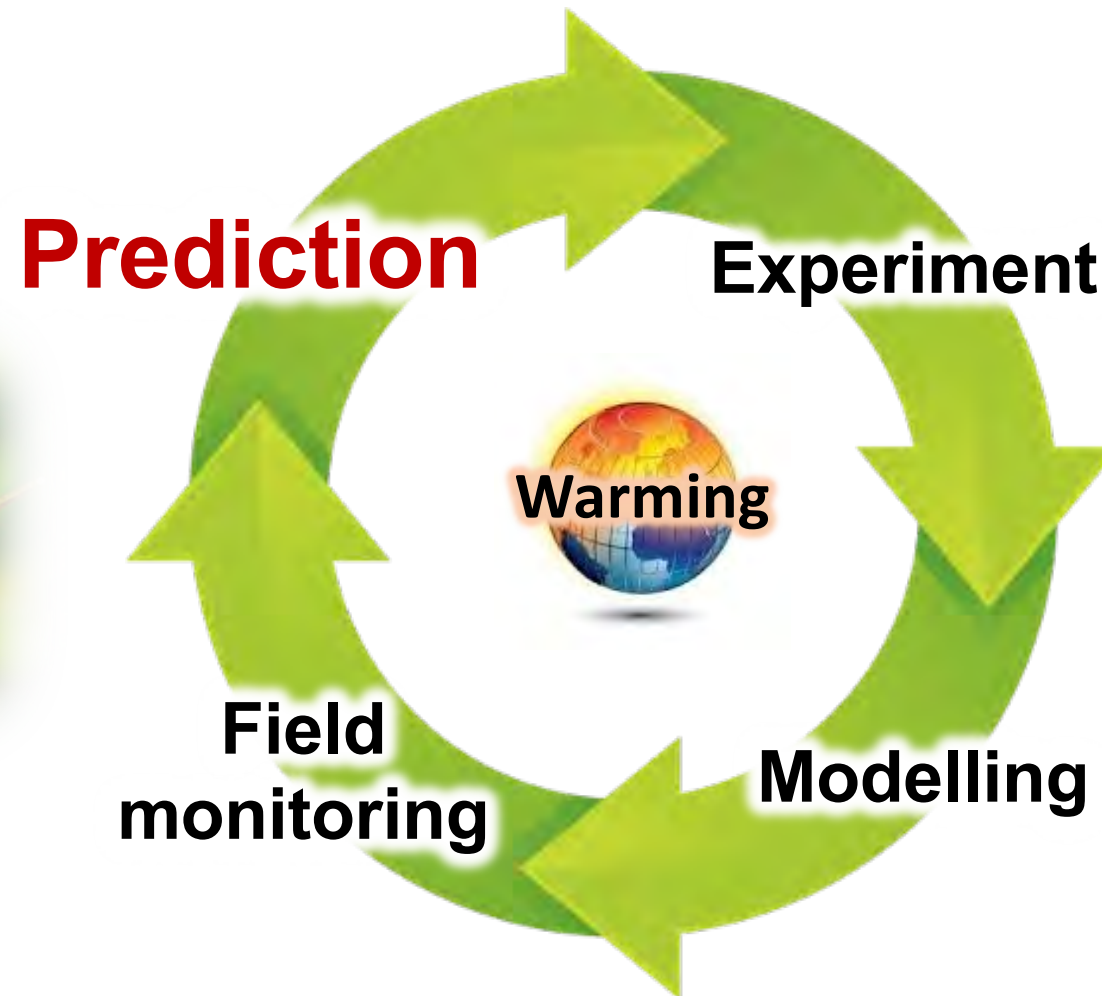
Northern population



Central population



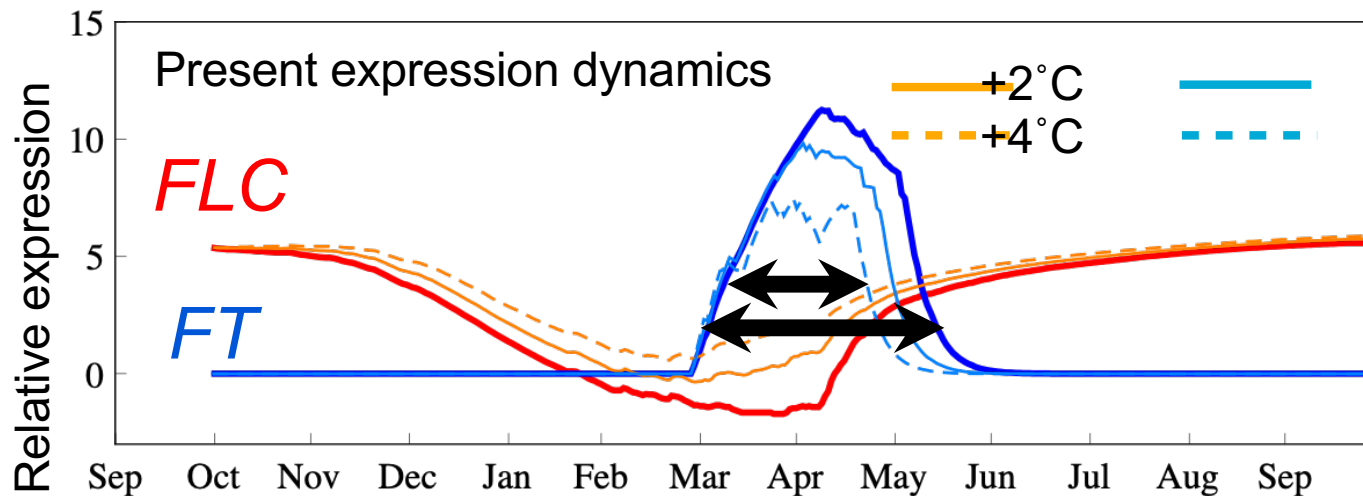
# Predicting future flowering phenology





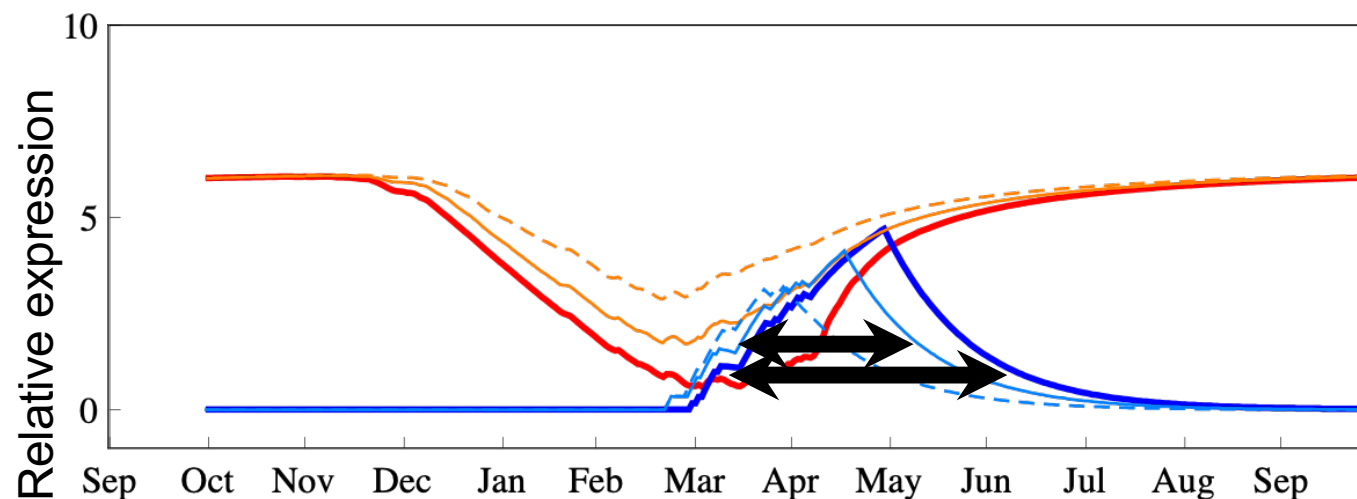
# What will happen with climate warming?

Northern population



*FLC* suppression in winter becomes milder.  
The period when *FT* is activated becomes shorter.

Central population

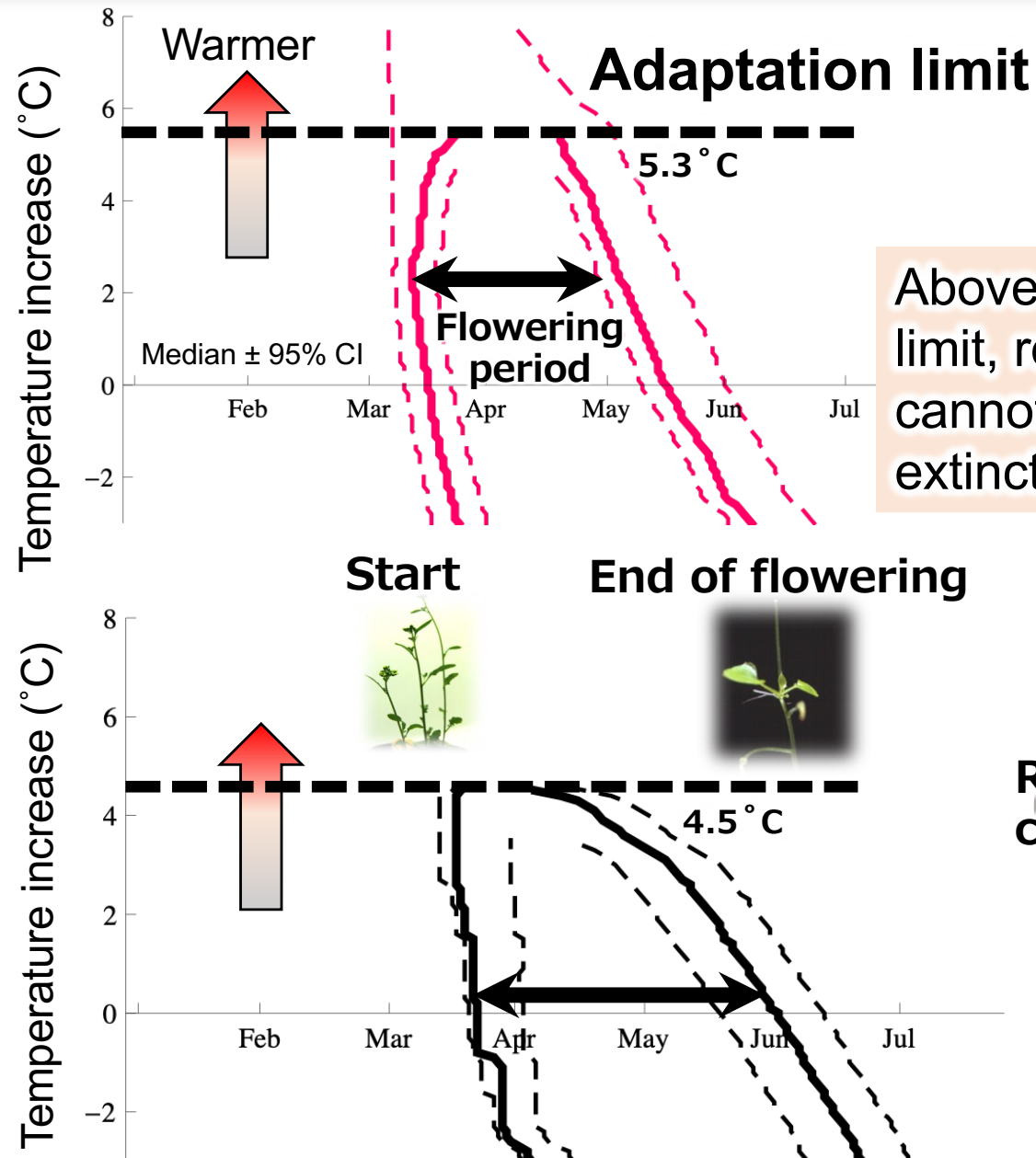


# The adaptation limit of *A. halleri* is 4.5–5.3°C

Northern population



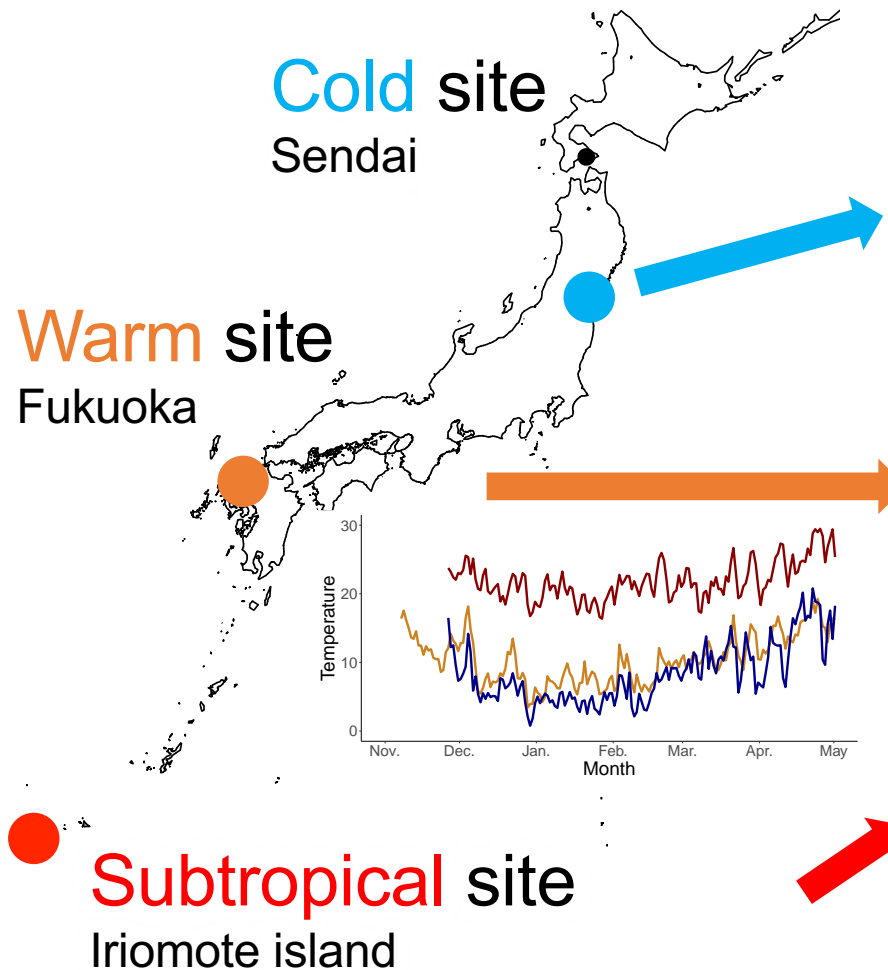
Central population



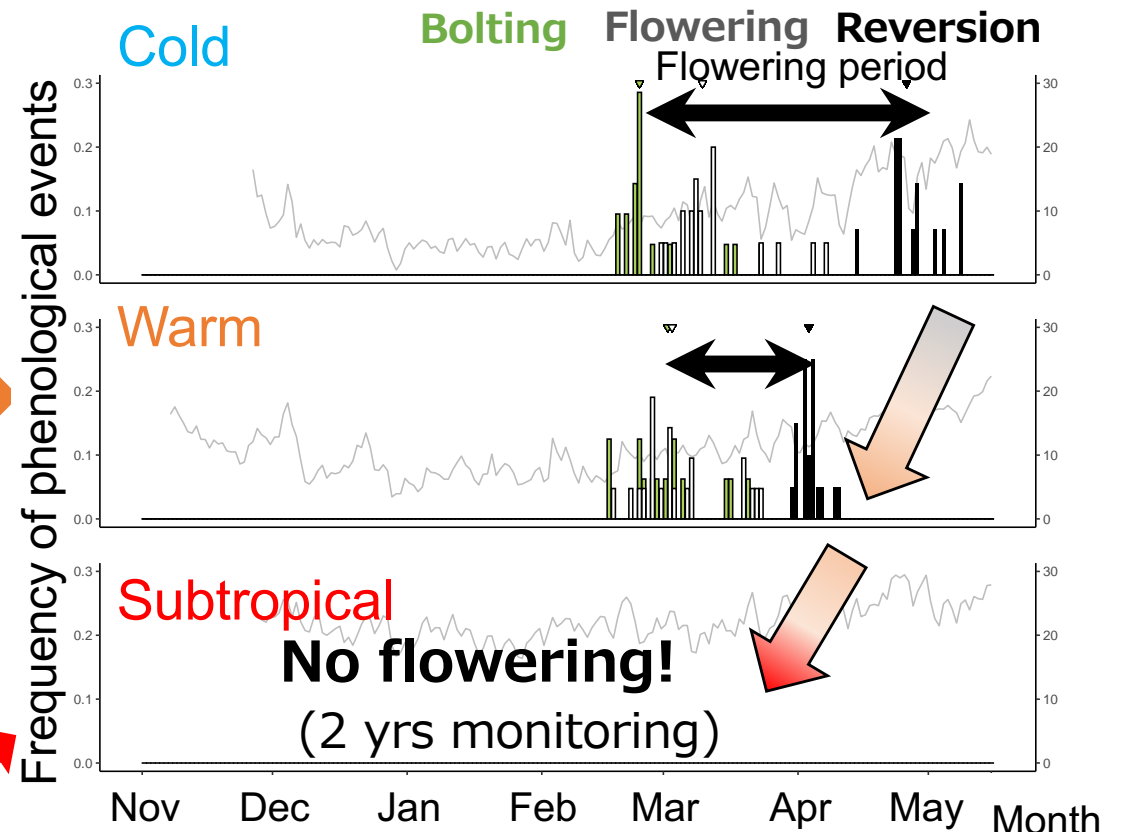
Above the adaptation limit, reproductive cycle cannot be sustained and extinction risk increases.

# Testing the adaptation limit

## Transplant experiments



## Shortening of flowering period due to warming

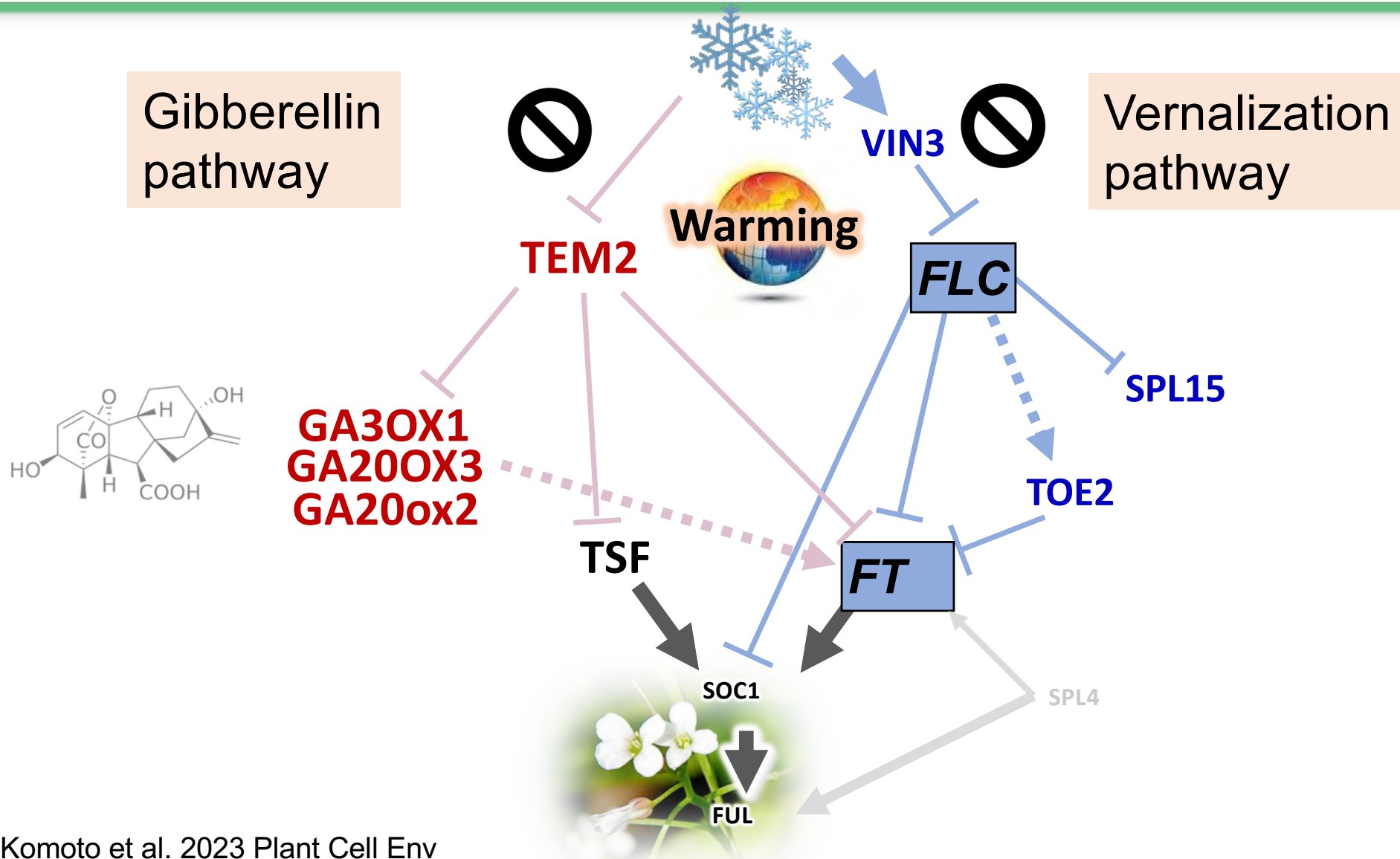


Komoto et al. 2023 Plant Cell Env

Flowering opportunity was lost at the subtropical site



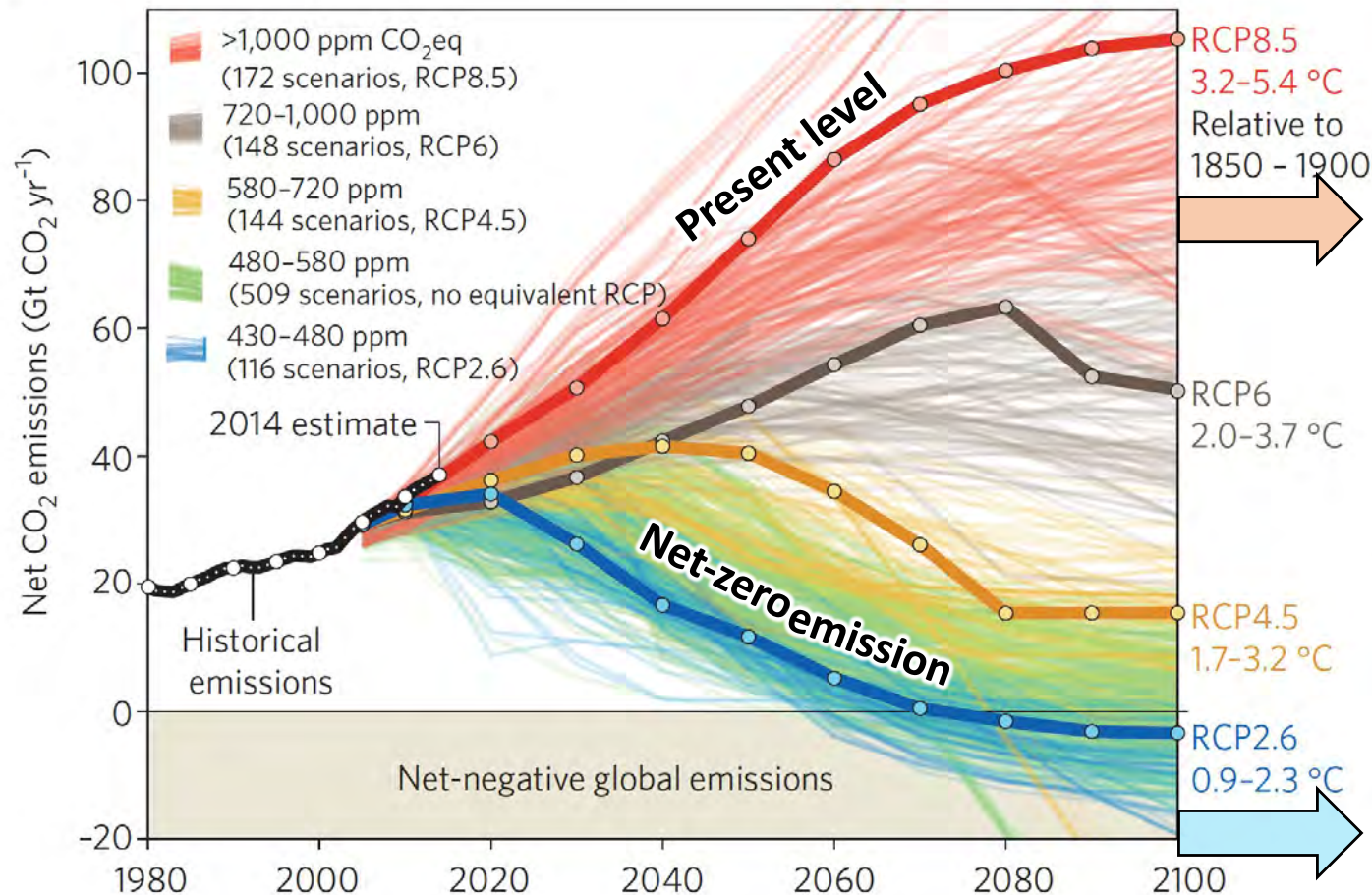
# Comparison of genome-wide transcriptional profiles



Komoto et al. 2023 Plant Cell Env

## Two pathways that regulate adaptation limits

# CO<sub>2</sub> emission scenarios and temperature outcome



Fuss et al. Nature Climate Change 2014

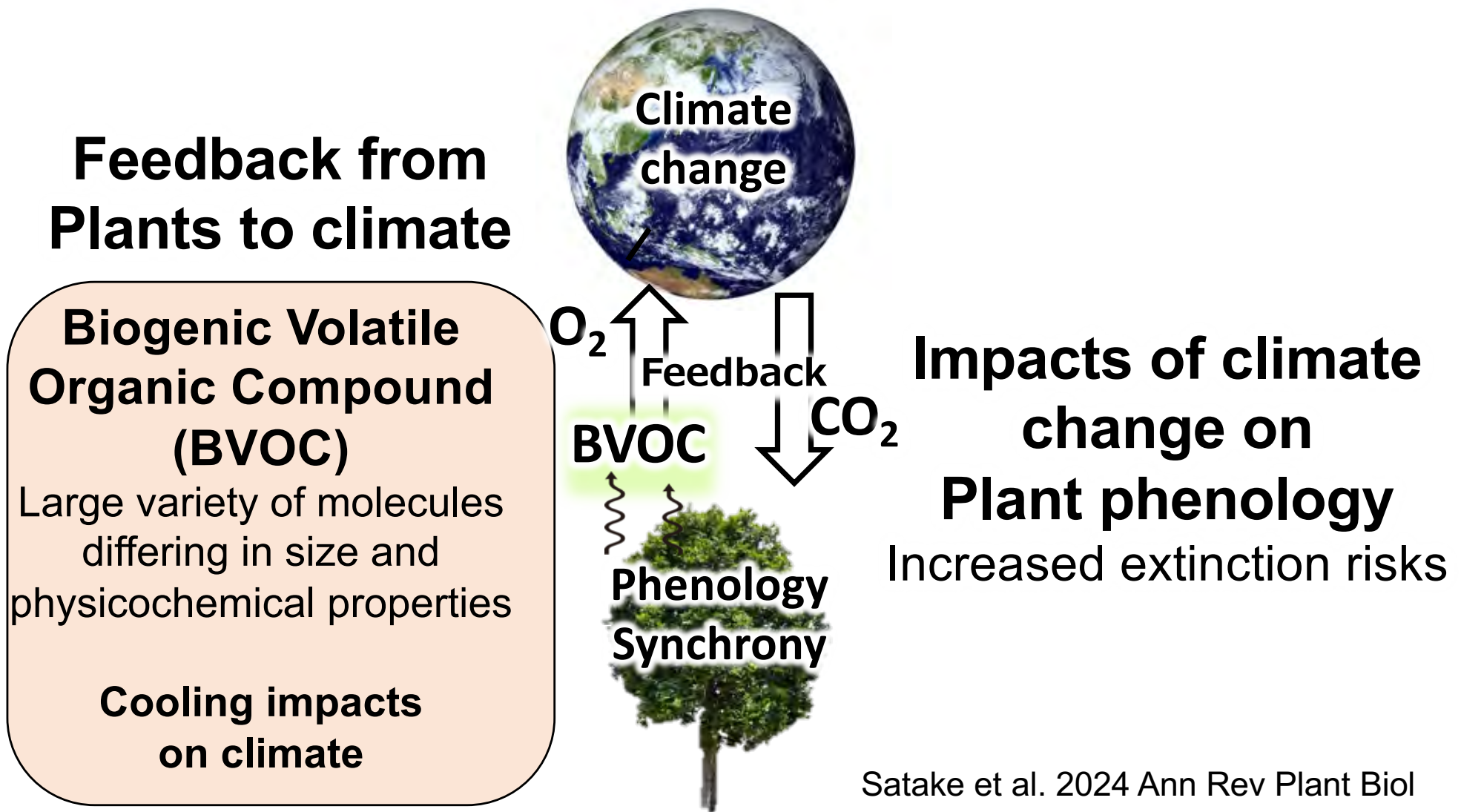
**3.2-5.4°C  
temperature  
increase**

Close to  
the adaptation limit  
of *A. halleri*

**0.9-2.3°C  
temperature  
increase**

**Further studies needed to estimate  
adaptation limits in other species**

# Plants are not only affected by climate

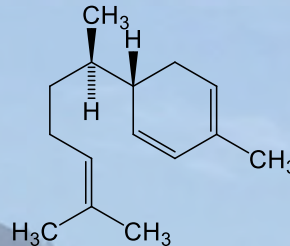
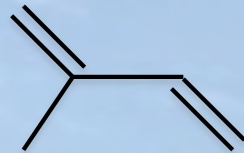
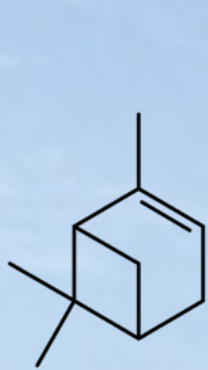


**Plants alter atmospheric composition and climatic processes**



# Plants release enormous amount of BVOCs

**BVOCs**  
biogenic volatile organic compounds



**BVOC**

**CO<sub>2</sub>**

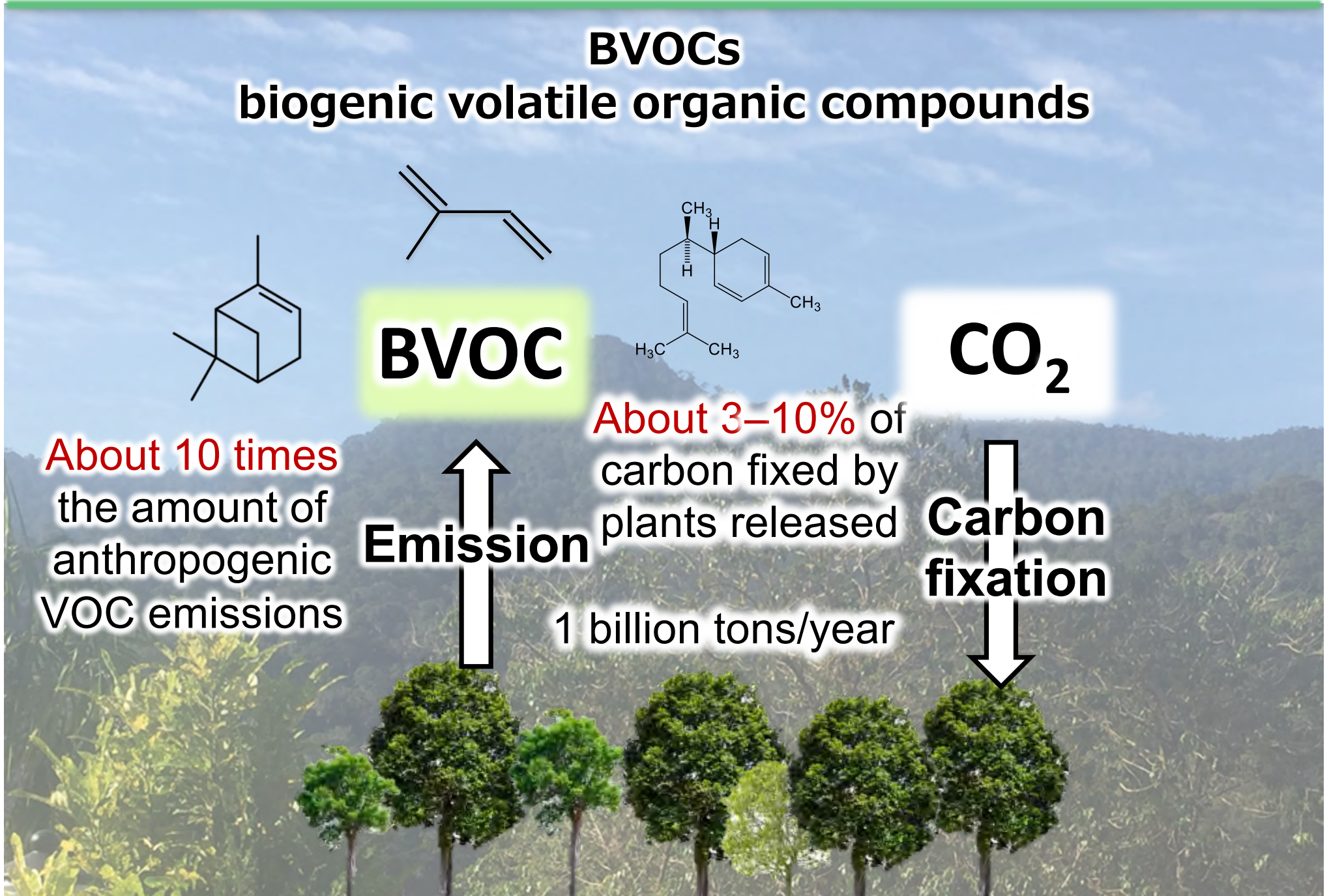
About 10 times  
the amount of  
anthropogenic  
VOC emissions

**Emission**

About 3–10% of  
carbon fixed by  
plants released

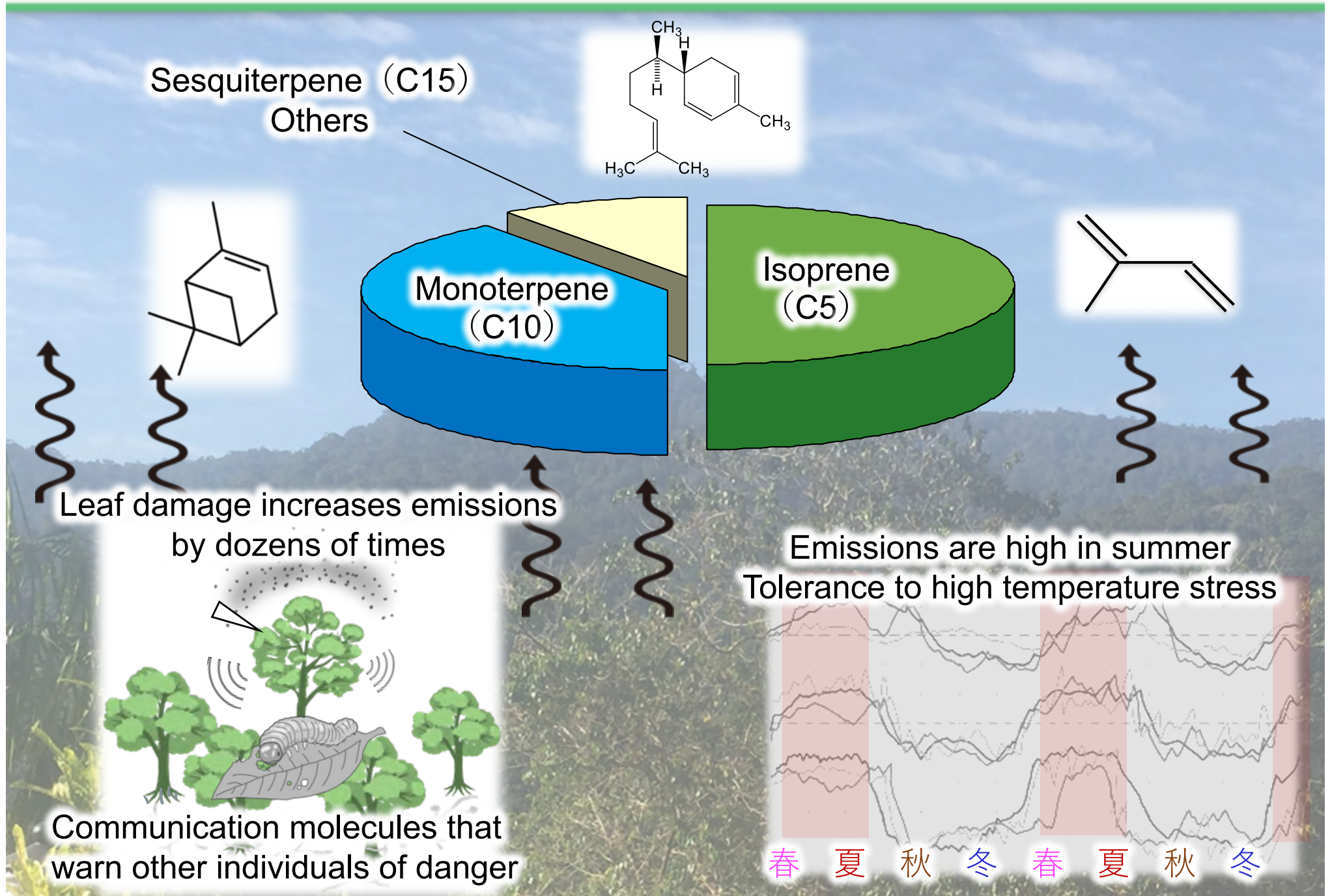
**Carbon  
fixation**

1 billion tons/year

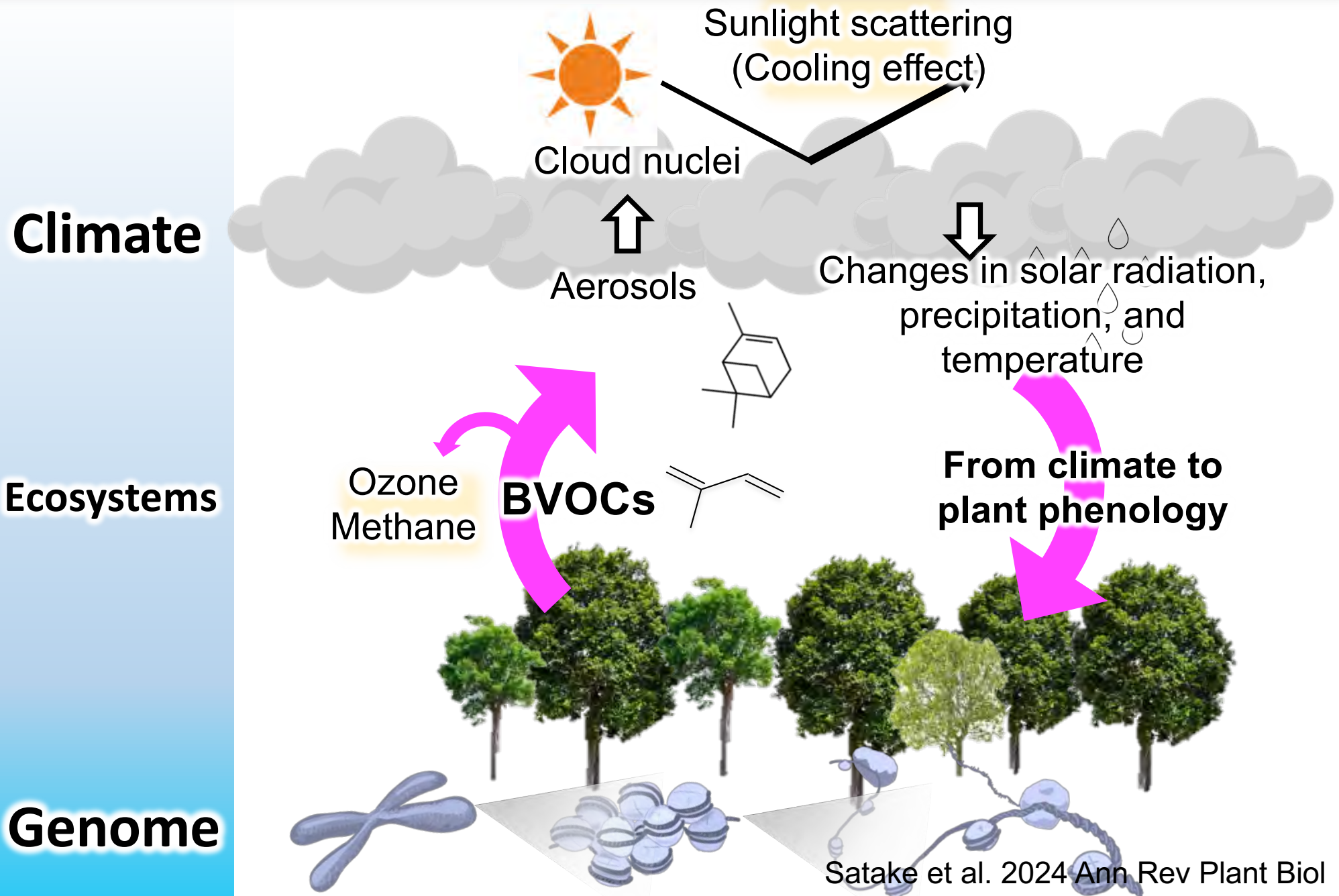




# BVOC composition and emission phenology



# BVOC-mediated climate feedbacks





# Large scale monitoring of molecular phenology and BVOC emission



# Synchrony from genes to ecosystems

Climate

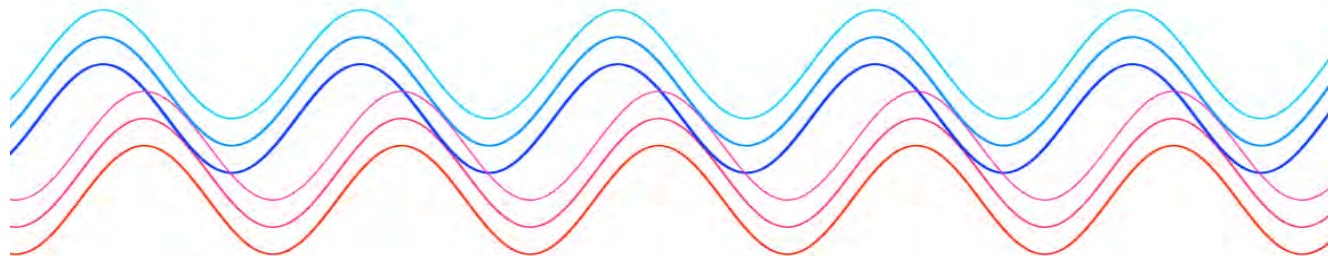
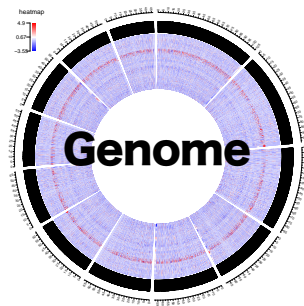
Ecosystem



and climate!

Interdisciplinary research is needed  
to scale up molecular knowledge to  
population, regional, and global scales

Gene





# Acknowledgements to Collaborators

Yoh Iwasa (Kyushu Univ.)  
Yuko Miyazaki (Okayama Univ.)  
Tsutomu Hiura (Tokyo Univ.)  
Qingmin Han (FFPRI)  
Valantin Journé  
(Adam Mackewicz University)

Yukako Chiba (Hokkaido Univ.)  
Yukari Saburi (Hokkaido Univ.)  
Tetsuhiro Kawagoe (Kyoto Univ.)  
Hiroshi Kudoh (Kyoto Univ.)

Hideyuki Komoto (Kyushu Univ.)  
Ai Nagahama (Kyushu Univ.)  
Hiroyuki Toyama (NIES)  
Junko Kyozyuka (Tohoku Univ.)  
Yuki Hata (Tohoku Univ.)  
Yui Kaji (Ryukyu Univ.)

Shuichi Kudo  
Yuka Ikezaki  
Junko Kusumi  
Hideki Hirakawa  
(Kyushu Univ.)

Sachiko Isobe  
(Kazusa DNA Research Institute)

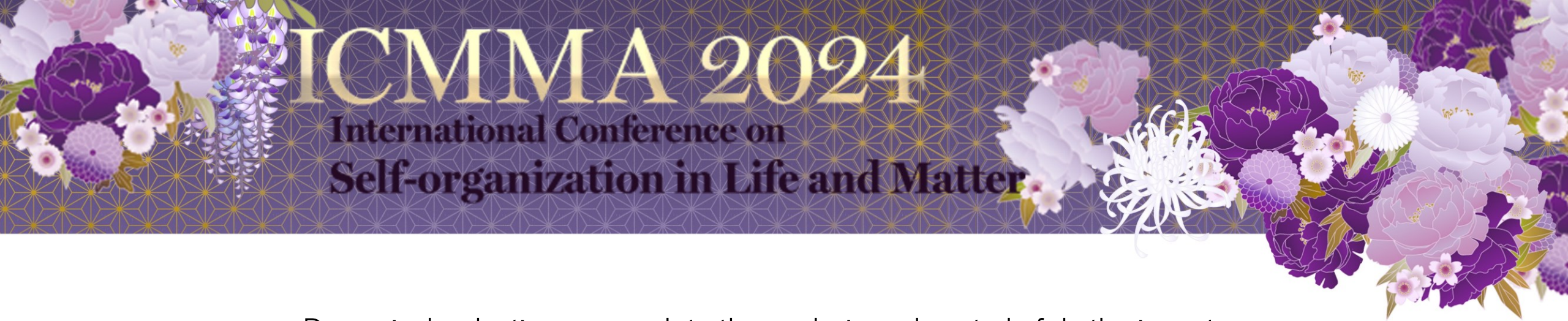
Thanks to  
our lab members too!



JSPS

科研費  
KAKENHI





## Dynamical reduction approach to the analysis and control of rhythmic systems

Hiroya Nakao (Tokyo Institute of Technology)

Dynamical reduction provides a powerful approach to the analysis and control of nonlinear oscillators. In this talk, three recent topics illustrating the use of such dynamical reduction will be briefly presented.

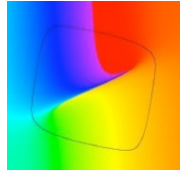
(i)Koopman operator and phase-amplitude reduction. The relationshipbetween Koopman operator theory and phase reduction theory for limit-cycle oscillators has recently become clear. This has led to a generalization of classical phase reduction to phase-amplitude reduction, which incorporates deviations from the limit cycle as amplitudes. The theoretical framework and a simple application to optimal entrainment with amplitude suppression are briefly explained.

(ii)Phase-reduction approach to noise-induced coherent oscillations. Noise can induce stochastic oscillations in excitable systems without limit cycles. It is shown that, for some fast-slow systems, we can construct hybrid (piecewise-continuous) dynamical systems approximating their stochastic oscillations. As an example, entrainment and synchronization of a noisy fast-slow excitable system is discussed.

(iii)Design of nonlinear oscillators based on phase reduction. Using the reduced phase equation, we can develop a method to design a dynamical system with a prescribed trajectory and phase response characteristics. As an example, an artificial star-shaped oscillator that exhibits multi-stable entrainment to high-frequency periodic input is designed.

### References

- [1]S Shirasaka, W Kurebayashi, and H Nakao, In: A. Mauroy, I. Mezić, Y. Susuki (eds.) *TheKoopman Operator in Systems and Control*. Springer (2020).
- [2]J Zhu, Y Kato, and H Nakao, *Physical Review Research* 4, L022041 (2022).
- [3]N Namura, T Ishii, and H Nakao, *IEEE Transactions on Automatic Control*, 69 (2024).



# **Dynamical reduction approach to the analysis and control of rhythmic systems**

**Hiroya Nakao**

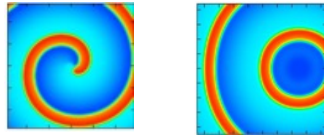
**Tokyo Institute of Technology**

Collaborators:

S. Shirasaka, W. Kurebayashi, J. Zhu, T. Ishii, and N. Namura

# Phase reduction approach to rhythmic systems

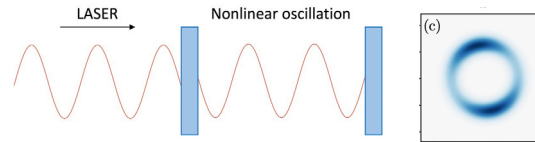
## Physical chemistry



$$\frac{\partial}{\partial t} \mathbf{X}(\mathbf{r}, t) = \mathbf{F}(\mathbf{X}) + D \nabla^2 \mathbf{X}$$

Oscillatory chemical reaction

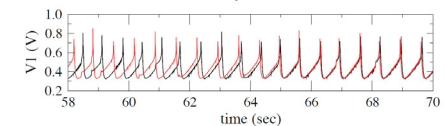
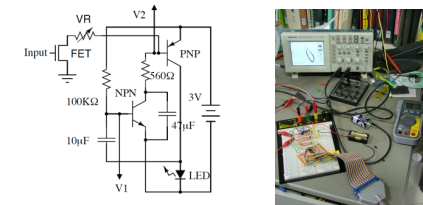
## Open quantum systems



$$\dot{\rho} = -i[-\Delta a^\dagger a + iE(a - a^\dagger) + i\eta(a^2 e^{-i\theta} - a^{\dagger 2} e^{i\theta}), \rho] + \gamma_1 \mathcal{D}[a^\dagger] \rho + \gamma_2 \mathcal{D}[a^2] \rho$$

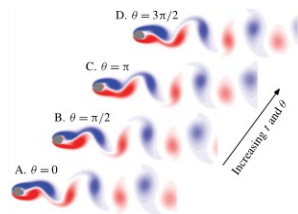
Quantum synchronization

## Electrical engineering



Noise-induced synchronization

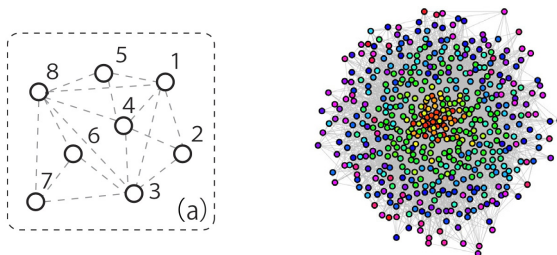
## Fluid mechanics



Synchronization of vortices

$$\frac{\partial \mathbf{u}}{\partial t} + \mathbf{u} \cdot \nabla \mathbf{u} = -\nabla p + Re^{-1} \nabla^2 \mathbf{u} + \varepsilon \mathbf{f}$$

## Network science

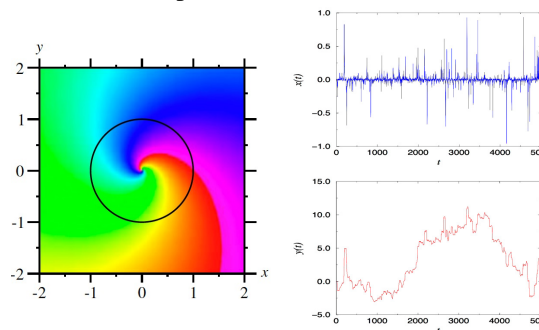


Sensor networks

Self-organization

$$\dot{\mathbf{X}}_i(t) = \mathbf{F}_i(\mathbf{X}_i) + \sum_j L_{ij} \mathbf{X}_j$$

## Nonlinear oscillations and synchronization



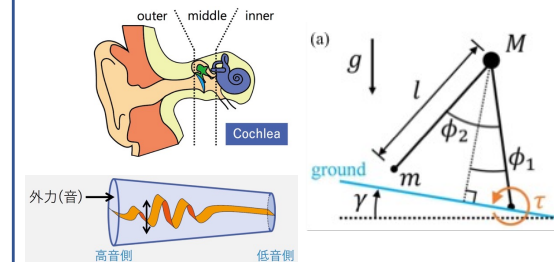
$$\dot{\mathbf{X}}(t) = \mathbf{F}(\mathbf{X}(t))$$

$$dX(t) = f(X, t)dt + g(X, t)dW(t)$$

Dynamical systems

Stochastic processes

## Biomechanics



Hearing

Walking

Neuroscience

Non-eq. physics

Machine learning

...



# Today's topics

- Dynamical reduction provides a powerful approach to the analysis and control of synchronizing nonlinear oscillators.
- Today's topics:
  1. Koopman operator and phase-amplitude reduction of limit-cycle oscillators
  2. Phase-reduction approach to noise-induced coherent oscillations
  3. Design of nonlinear oscillators based on phase reduction theory

# Topic 1

## **Koopman operator and phase-amplitude reduction of limit-cycle oscillators**

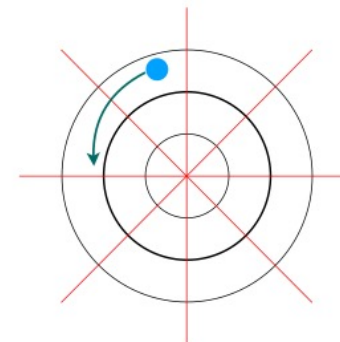
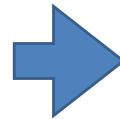
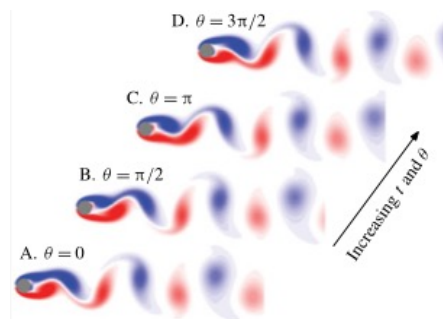
**Joint work with**

**S. Shirasaka (Osaka), W. Kurebayashi (Hirosaki),**

**Y. Kato (Hakodate), S. Takata (Toshiba), P. Mirceski (Tokyo Tech)**

# Dimensionality reduction in dynamical systems

- In dissipative systems, the state is often attracted to a low-dimensional manifold in the phase space (or state space).
- Deriving simple equations for "key variables" representing the low-dimensional dynamics provides us with much insights.
- *Phase reduction theory* for limit-cycle oscillations is a typical example of such dimensionality reduction.
- Recently developing Koopman-operator approach gives a new viewpoint and leads to generalized *phase-amplitude reduction theory*.



$$\frac{\partial \mathbf{u}}{\partial t} + \mathbf{u} \cdot \nabla \mathbf{u} = -\nabla p + Re^{-1} \nabla^2 \mathbf{u} + \varepsilon \mathbf{f}$$

$$\dot{\theta} = \omega + \varepsilon \mathbf{Z}(\theta) \cdot \mathbf{f}$$

Phase-response analysis of synchronization for periodic flows  
K. Taira (UCLA) & HN (Tokyo Tech), J. Fluid. Mech. 2018



# Example: global linearization via Koopman

- 2D system with a stable fixed point at (0,0)

$$\frac{d}{dt} \begin{pmatrix} x \\ y \end{pmatrix} = \begin{pmatrix} \mu x \\ \lambda(y - x^2) \end{pmatrix} \quad \mu, \lambda < 0$$

- Jacobi matrix at (0,0)

$$J = \begin{pmatrix} \mu & 0 \\ 0 & \lambda \end{pmatrix} \quad \text{Eigenvalues : } \mu, \lambda$$

- Infinitesimal “Koopman” operator (generator)

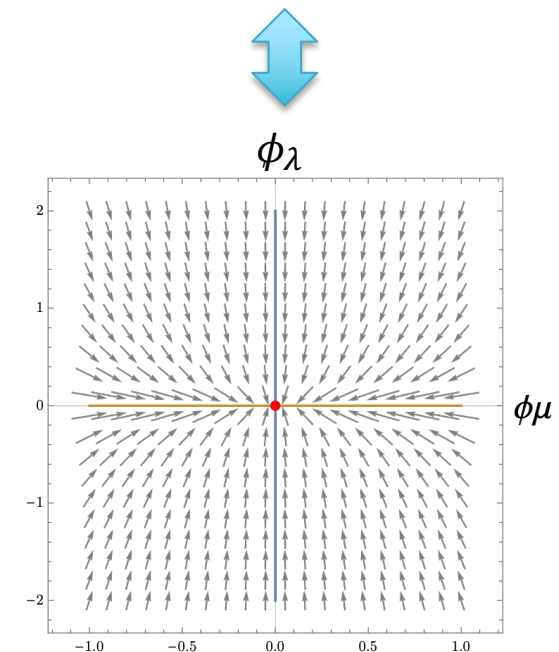
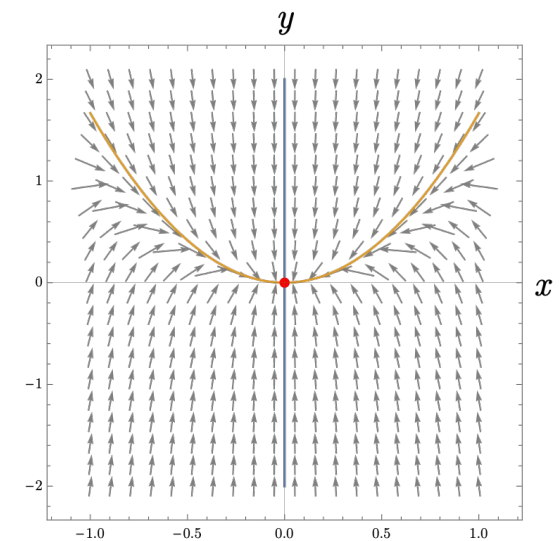
$$A = \mu x \frac{\partial}{\partial x} + \lambda(y - x^2) \frac{\partial}{\partial y}$$

- Principal “Koopman” eigenfunctions of  $A$

$$\phi_\mu(x, y) = x, \quad \phi_\lambda(x, y) = y - \frac{\lambda}{\lambda - 2\mu} x^2$$

- Using  $\phi_{\mu,\nu}$  as new variables, the system is linearized:

$$\frac{d}{dt} \begin{pmatrix} \phi_\mu \\ \phi_\lambda \end{pmatrix} = \begin{pmatrix} \mu & 0 \\ 0 & \lambda \end{pmatrix} \begin{pmatrix} \phi_\mu \\ \phi_\lambda \end{pmatrix}$$



# Example: reduction of the linearized system

- In the new variables, the system is linearized:

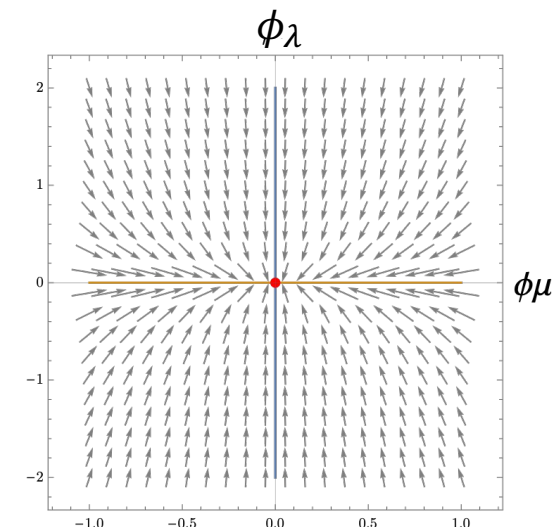
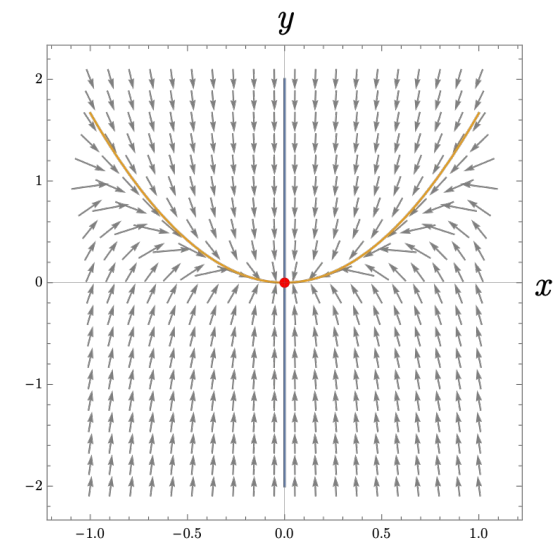
$$\frac{d}{dt}\phi_\mu = \mu\phi_\mu \quad \frac{d}{dt}\phi_\lambda = \lambda\phi_\lambda$$

$$x = \phi_\mu, \quad y = \phi_\lambda + \frac{\lambda}{\lambda - 2\mu}\phi_\mu^2$$

- Now, if  $\lambda \ll \mu < 0$ , the variable  $\phi_\lambda$  converges to 0 much faster than  $\phi_\mu$ .
- In the limit  $\lambda \rightarrow -\infty$ , we can adiabatically eliminate  $\phi_\lambda$ , i.e., we can approximately assume  $\phi_\lambda = 0$ .
- This gives a **reduced 1-dim. equation for  $\phi_\mu$** :

$$\frac{d}{dt}\phi_\mu = \mu\phi_\mu$$

- Slow (inertial) manifold:  $y = \frac{\lambda}{\lambda - 2\mu}x^2$



# Koopman operator and generator

- Dynamical system (autonomous)

$$\frac{d\mathbf{x}}{dt} = \mathbf{F}(\mathbf{x})$$

$\mathbf{x} \in \mathbb{R}^N$  : system state

$\mathbf{F}$  : smooth dynamics

- Flow  $S^\tau : \mathbb{R}^N \rightarrow \mathbb{R}^N$

$$\mathbf{x}(t + \tau) = S^\tau \mathbf{x}(t)$$

Evolution of state

- Observable  $f \in \mathcal{F} : \mathbb{R}^N \rightarrow \mathbb{C}$

- Koopman operator  $U^\tau : \mathcal{F} \rightarrow \mathcal{F}$

Evolution of observable

$$(U^\tau f)(\mathbf{x}) = f(S^\tau \mathbf{x})$$

Linear operator!

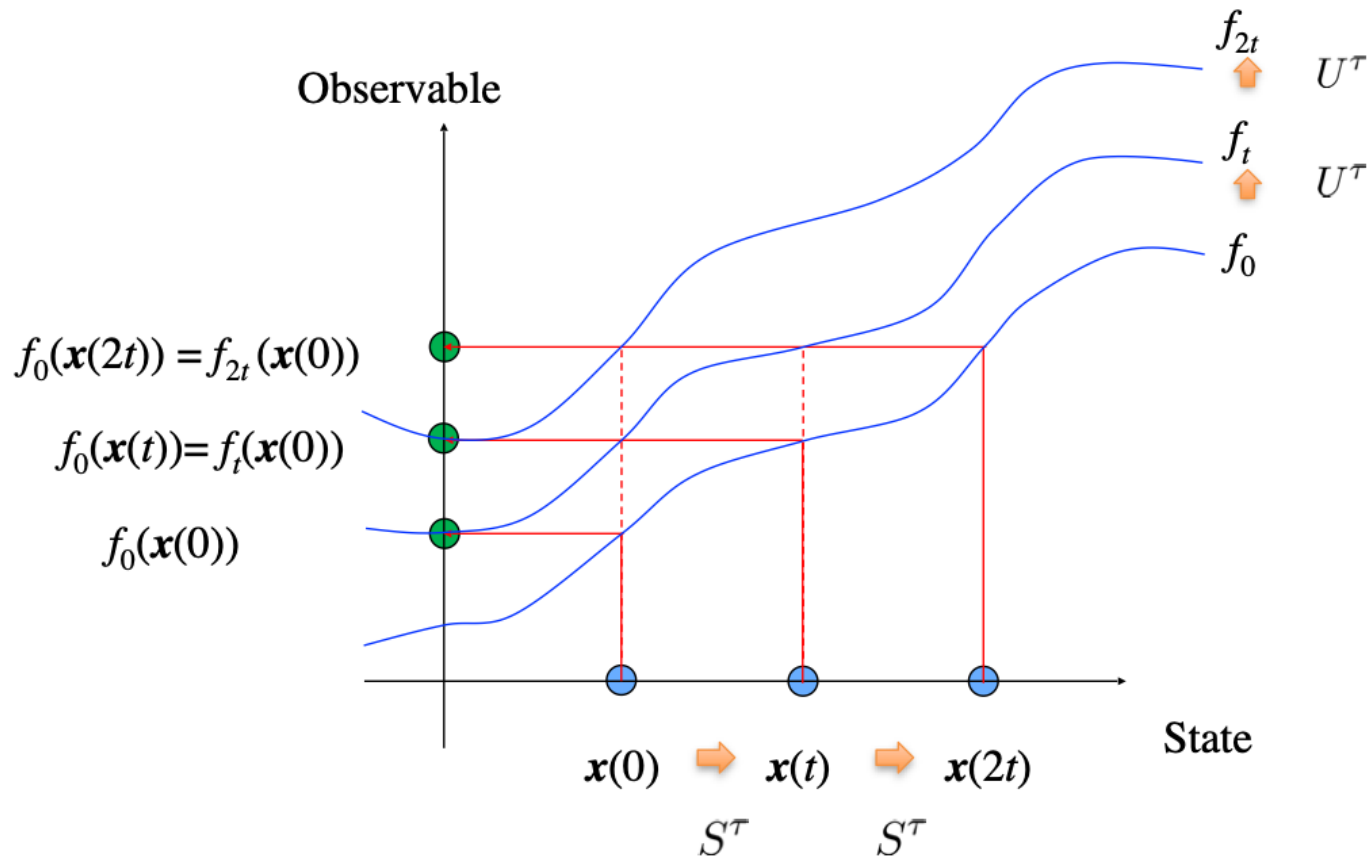
- Generator of the Koopman operator

$$Af(\mathbf{x}) = \lim_{\tau \rightarrow 0} \frac{U^\tau f(\mathbf{x}) - f(\mathbf{x})}{\tau} = \mathbf{F}(\mathbf{x}) \cdot \nabla f(\mathbf{x})$$



# Evolution of state vs. evolution of observable

Constant observable & evolving state vs. constant state & evolving observable



Observed value of  $x(t)$  by  $f_0$  at time 0 = observed value of  $x(0)$  by  $f_t$  at time  $t$

$$f_t(x(0)) = (U^t f_0)(x(0)) = f_0(S^t x(0)) = f_0(x(t))$$

# Koopman eigenvalues and eigenfunctions

- Eigenfunctions of the Koopman generator  $A$  :

$$A\phi_\lambda(\mathbf{x}) = \lambda\phi_\lambda(\mathbf{x}) \quad \lambda : \text{eigenvalue} \quad \phi_\lambda(\mathbf{x}) : \text{eigenfunction}$$

- There are infinitely many Koopman eigenvalues. If the system has a fixed point or limit cycle, the stability exponents are included in them.
- Koopman mode expansion of the observable  $f$  :

$$f(\mathbf{x}) = \sum_{i=1}^{\infty} c_i \phi_{\lambda_i}(\mathbf{x}) \quad \{c_i\} : \text{coefficients}$$

$\{\lambda_i\} : \text{eigenvalues}$

- Linear time evolution of the observable :

$$U^t f(\mathbf{x}) = e^{tA} f(\mathbf{x}) = \sum_{i=1}^{\infty} c_i e^{\lambda_i t} \phi_{\lambda_i}(\mathbf{x}) \quad \{\phi_{\lambda_i}\} : \text{eigenfunctions}$$

# Linearization by Koopman eigenfunctions

- System with a linearly (exponentially) stable fixed point or limit cycle

$$\dot{\mathbf{x}} = \mathbf{F}(\mathbf{x})$$

- Linear stability or Floquet exponents are the 'principal' Koopman eigenvalues

$$\lambda_1, \dots, \lambda_N$$

- Principal Koopman eigenfunctions

$$\psi_1(\mathbf{x}), \dots, \psi_N(\mathbf{x})$$

- Introduction of new coordinates using principal Koopman eigenfunctions

$$y_i = \psi_i(\mathbf{x}) \quad (i = 1, \dots, N)$$

- In the new coordinates  $y_1, \dots, y_N$ , the system dynamics is linearized:

$$\dot{y}_i = \lambda_i y_i \quad (i = 1, \dots, N)$$

$$\left( \frac{d\psi_i(\mathbf{x})}{dt} = \nabla \psi_i(\mathbf{x}) \cdot \frac{d\mathbf{x}}{dt} = \mathbf{F}(\mathbf{x}) \cdot \nabla \psi_i(\mathbf{x}) = A\psi_i(\mathbf{x}) = \lambda_i \psi_i(\mathbf{x}) \right)$$

- By retaining only slow variables, dimensionality of the system can be reduced.



# Reduction of weakly perturbed systems

- Weakly driven system by a small perturbation  $\mathbf{p}(t)$

$$\dot{\mathbf{x}} = \mathbf{F}(\mathbf{x}) + \mathbf{p}(t)$$

- Change of variables using Koopman eigenfunctions  $\psi_1(\mathbf{x}), \dots, \psi_N(\mathbf{x})$

$$y_i = \psi_i(\mathbf{x}) \quad (i = 1, \dots, N)$$

- Semi-linear system evolution in the new variables

$$\begin{aligned} \dot{y}_i &= \nabla \psi_i(\mathbf{x}) \cdot \dot{\mathbf{x}} = \nabla \psi_i(\mathbf{x}) \cdot \mathbf{F}(\mathbf{x}) + \nabla \psi_i(\mathbf{x}) \cdot \mathbf{p}(t) \\ &= \lambda_i y_i + \mathbf{Z}_i(y_1, \dots, y_N) \cdot \mathbf{p}(t) \end{aligned}$$

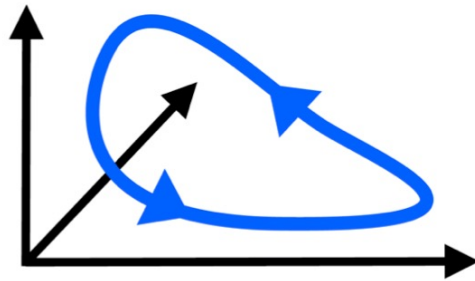
$$\mathbf{Z}_i(y_1, \dots, y_N) = \nabla \psi_i(\mathbf{x}): \text{ sensitivity (response) functions}$$

- Eliminating the fast-decaying variables  $y_{M+1}, \dots$  yields reduced equations:

$$\dot{y}_i \simeq \lambda_i y_i + \mathbf{Z}_i(y_1, \dots, y_M, 0, \dots, 0) \cdot \mathbf{p}(t) \quad (i = 1, \dots, M)$$

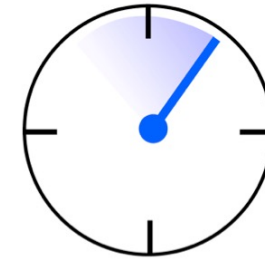
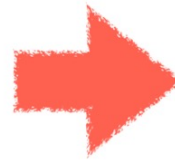
# Phase reduction analysis of limit-cycle oscillators

High-dim  
Nonlinear  
ODE



$$\dot{X} = F(X) + p(t)$$

Weakly perturbed oscillator

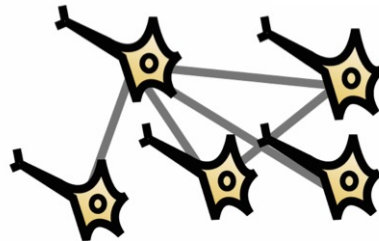


1-dim  
semi-linear  
ODE

$$\dot{\theta} = \omega + Z(\theta) \cdot p(t)$$

Simple 1-dim. phase equation

Reduction



Analysis

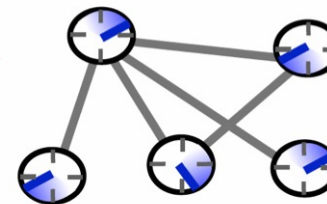


Figure by  
Wataru  
Kurebayashi

$$\dot{X}_j = F(X_j) + \sum_{k=1}^N G(X_j, X_k)$$

Network of weakly coupled oscillators

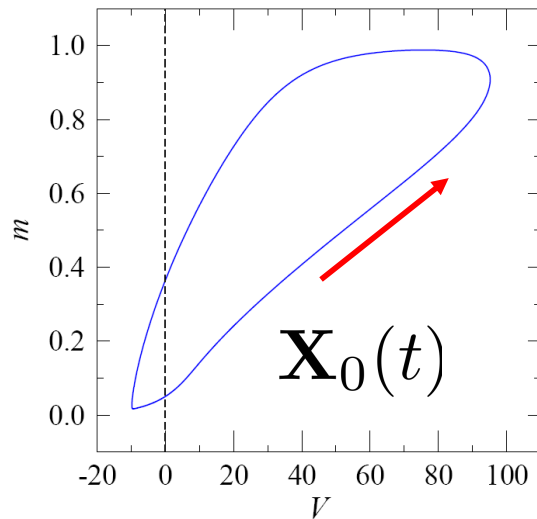
$$\dot{\theta}_j = \omega_j + \sum_{k=1}^N g(\theta_j, \theta_k)$$

Coupled phase oscillators

Winfree (1967), Kuramoto (1984), Hoppensteadt & Izhikevich (1997), Ermentrout (2000), ...

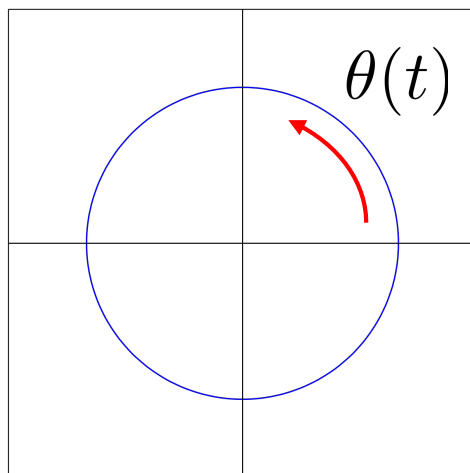
# Phase along a limit cycle

- We can introduce a *phase*  $\theta$  along the limit-cycle (LC) orbit that increases with a *constant frequency*  $\omega$  with time.



$$\dot{\mathbf{X}}(t) = \mathbf{F}(\mathbf{X})$$

$$\mathbf{X}(t) \in \mathbb{R}^N$$



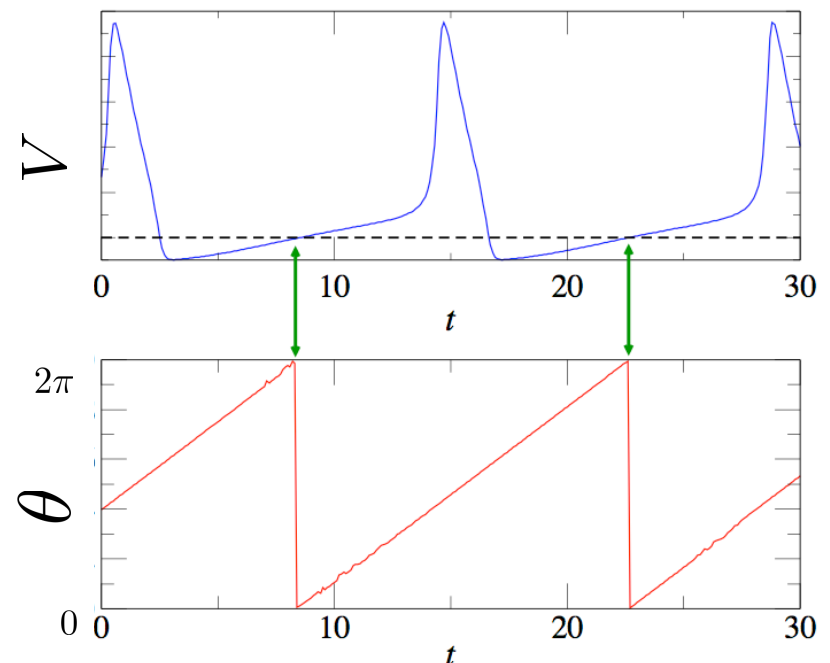
$$\dot{\theta}(t) = \omega$$

$$\theta(t) \in [0, 2\pi]$$

$$\mathbf{X}_0(t) = \mathbf{X}_0(t + T) : \text{LC orbit}$$

$$T = 2\pi/\omega : \text{period}$$

$$\omega : \text{frequency}$$



Phase = (rescaled) time



# Asymptotic phase

- For an exponentially stable LC, we can introduce the "*asymptotic phase*" that increases with a constant frequency  $\omega$  in the basin of the LC.

- An "*asymptotic phase function*"

$$\Theta(\mathbf{X}) : \mathbb{R}^N \rightarrow [0, 2\pi)$$

satisfying

$$\dot{\Theta}(\mathbf{X}) = \nabla \Theta(\mathbf{X}) \cdot \dot{\mathbf{X}} = \mathbf{F}(\mathbf{X}) \cdot \nabla \Theta(\mathbf{X}) = \omega$$

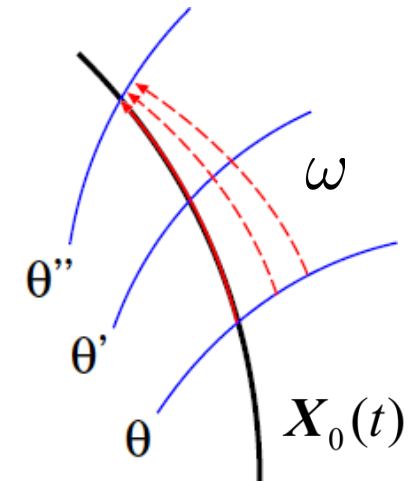
can be defined in the basin of the LC, which maps the  $N$ -dim. system state to a phase value.

- The phase  $\theta = \Theta(\mathbf{X})$  of the oscillator state obeys

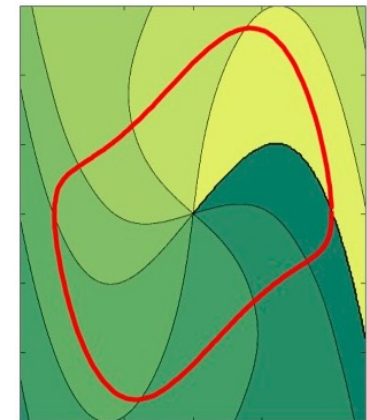
$$\dot{\theta}(t) = \omega$$

- The oscillator state on the LC can be represented as

$$\mathbf{X}_0(\theta) \quad (0 \leq \theta < 2\pi)$$



Isochrons  
(Level sets of phase)



Phase function  $\Theta(\mathbf{X})$   
(van der Pol oscillator)

# (Asymptotic) amplitudes

- For an exponentially stable LC, we can also introduce the "*amplitudes*" that exponentially decays with a *constant rate* (Floquet exponent  $\mu$  with  $\text{Re } \mu < 0$ ).
- An "*amplitude function*" (we focus on the slowest mode)

$$R(\mathbf{X}) : \mathbb{R}^N \rightarrow \mathbb{C}$$

satisfying

$$\dot{R}(\mathbf{X}) = \nabla R(\mathbf{X}) \cdot \dot{\mathbf{X}} = \mathbf{F}(\mathbf{X}) \cdot \nabla R(\mathbf{X}) = \mu R(\mathbf{X})$$

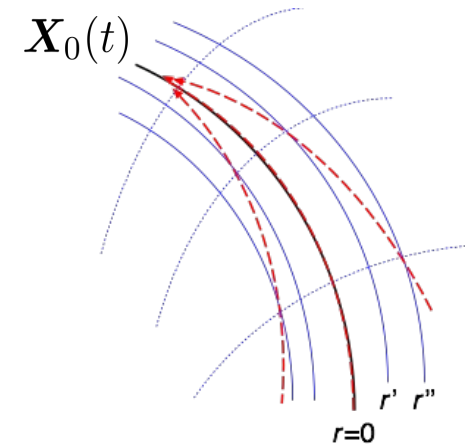
can be defined in the basin of the LC, which maps the  $N$ -dim. system state to a complex amplitude.

- The amplitude  $r = R(\mathbf{X})$  of the oscillator obeys

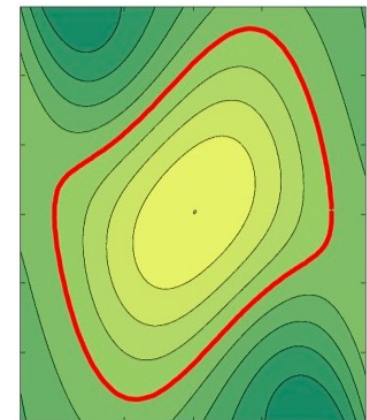
$$\dot{r}(t) = \mu r(t)$$

- The amplitude vanishes on the LC :

$$R(\mathbf{X}_0(\theta)) = 0$$



Isostables  
(Level sets of amplitude)



Amplitude function  
(van der Pol oscillator)

# Koopman eigenfunctions of a limit cycle

- System with an exponentially stable limit cycle

$$\frac{dx}{dt} = F(x)$$

- Limit cycle with period  $T$  and frequency  $\omega = 2\pi/T$

$$x_0(t) = x_0(t + T)$$

- Eigenvalues and eigenfunctions of the Koopman generator  $A$

$$A\phi_j(x) = \lambda_j\phi_j(x)$$

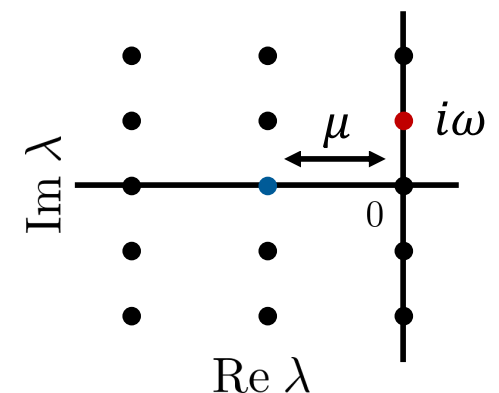
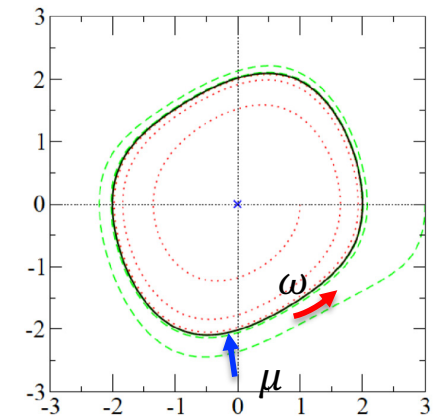
- Principal eigenvalues of Koopman generator = Floquet exponents

$$\lambda_1 = i\omega, \lambda_2 = \mu, \lambda_3, \dots, \lambda_N$$

$$0 > \operatorname{Re} \lambda_2 \geq \dots \geq \operatorname{Re} \lambda_N$$

- Associated principal Koopman eigenfunctions satisfy

$$\frac{d}{dt}\phi_j(x) = A\phi_j(x) = \lambda_j\phi_j(x) \quad (j = 1, \dots, N)$$





# Koopman eigenfunctions of a limit cycle

- Koopman generator of the limit-cycle oscillator

$$\frac{d\mathbf{x}}{dt} = \mathbf{F}(\mathbf{x}) \quad \Rightarrow \quad A = \mathbf{F}(\mathbf{x}) \cdot \nabla$$

- By definition, the asymptotic phase satisfies

$$\mathbf{F}(\mathbf{x}) \cdot \nabla \Theta(\mathbf{x}) = \omega$$

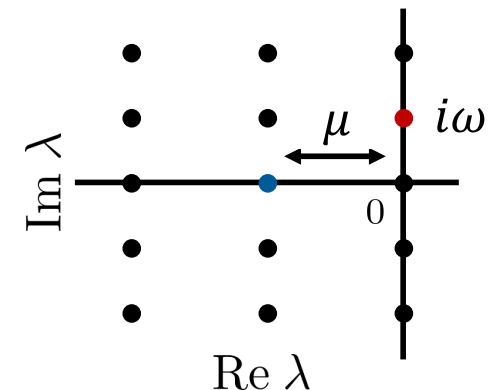
- Complex exponential  $\Psi(\mathbf{x}) = \exp[i\Theta(\mathbf{x})]$  of the asymptotic phase  $\Theta(\mathbf{x})$  is a Koopman eigenfunction with eigenvalue  $\lambda_1 = i\omega$ , i.e.,  $\Psi(\mathbf{x}) = \phi_1(\mathbf{x})$ :

$$A\Psi(\mathbf{x}) = \mathbf{F}(\mathbf{x}) \cdot \nabla \Psi(\mathbf{x}) = i\omega \Psi(\mathbf{x}) \quad \omega : \text{natural frequency}$$

- Similarly, the amplitude  $R(\mathbf{x})$  is the Koopman eigenfunction with the eigenvalue  $\lambda_2 = \mu$ , i.e.,  $R(\mathbf{x}) = \phi_2(\mathbf{x})$ :

$$AR(\mathbf{x}) = \mathbf{F}(\mathbf{x}) \cdot \nabla R(\mathbf{x}) = \mu R(\mathbf{x}) \quad \mu < 0 : \text{2nd Floquet}$$

- Koopman eigenfunction gives an operator-theoretic definition of the *asymptotic phase* and *amplitude(s)* originally defined geometrically.



# Phase-amplitude reduction of limit cycles

- Weakly perturbed limit-cycle oscillator

$$\dot{\mathbf{x}} = \mathbf{F}(\mathbf{x}) + \epsilon \mathbf{p}(t)$$

Mauroy *et al.* (2013)  
Wilson & Moehlis (2016)  
Shirasaka *et al.* (2017)

- Phase and amplitude functions = the first two Koopman eigenfunctions

$$\Theta(\mathbf{x}) = \arg \psi_1(\mathbf{x}), \quad R(\mathbf{x}) = \psi_2(\mathbf{x})$$

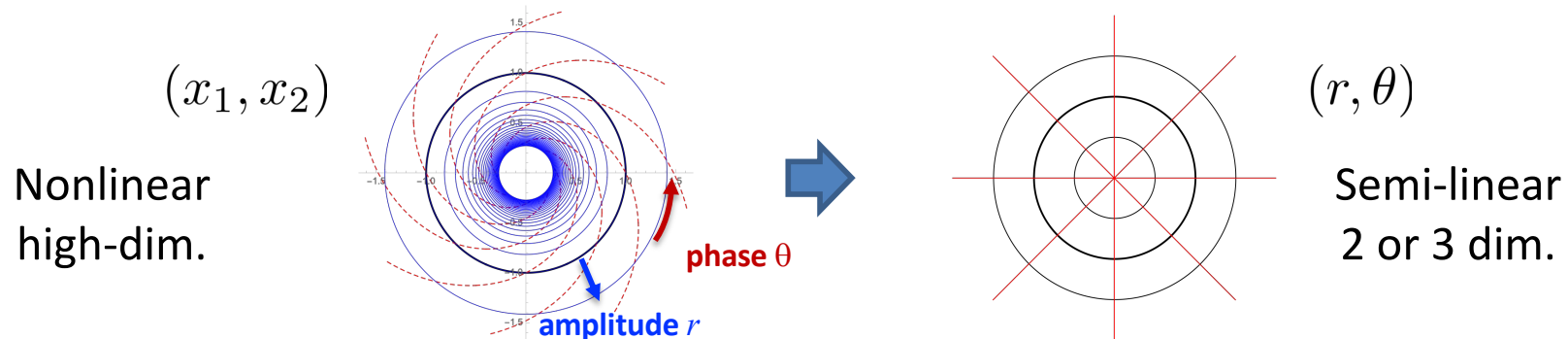
- Phase and amplitude of the oscillator state :  $\theta = \Theta(\mathbf{x})$ ,  $r = R(\mathbf{x})$

- Approximate phase-amplitude equations (correct up to  $O(\epsilon)$ )

$$\dot{\theta} = \omega + \epsilon \mathbf{Z}(\theta) \cdot \mathbf{p}(t), \quad \dot{r} = \mu r + \epsilon \mathbf{I}(\theta) \cdot \mathbf{p}(t)$$

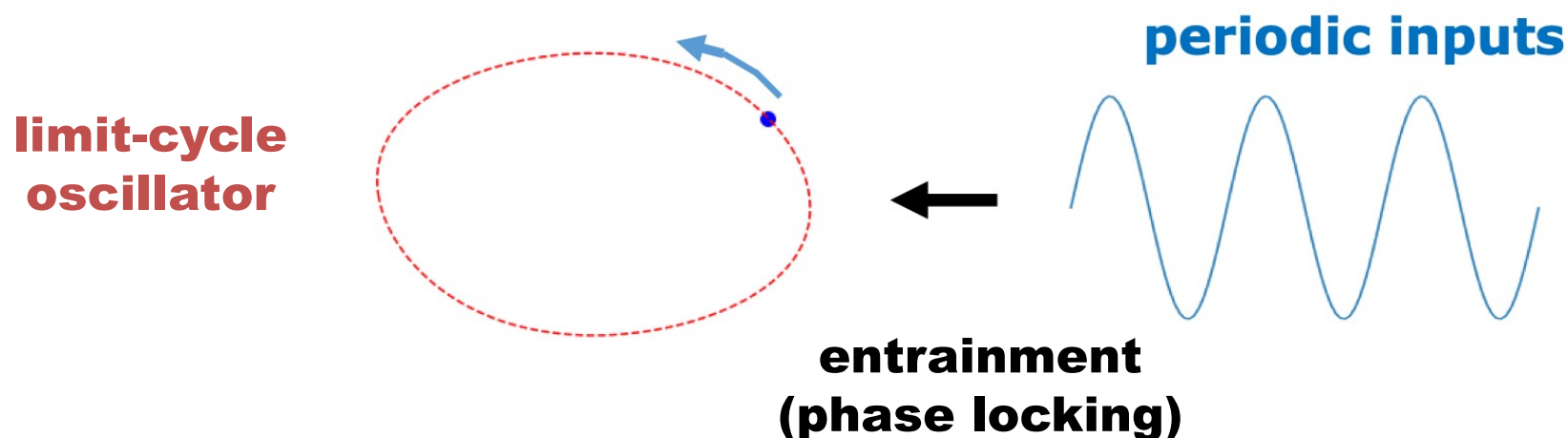
- Phase and amplitude (or isochron and isostable) sensitivity functions

$$\mathbf{Z}(\theta) = \nabla \Theta(\mathbf{x})|_{\mathbf{x}=\mathbf{x}_0(\theta)}, \quad \mathbf{I}(\theta) = \nabla R(\mathbf{x})|_{\mathbf{x}=\mathbf{x}_0(\theta)}$$



# Example: optimal entrainment by a periodic input

Entrainment (phase locking) of rhythmic dynamics to a periodic input



Optimal input signal for entrainment?

Using phase-amplitude reduction, we can easily derive the optimal signal.



# Optimal entrainment via phase-only reduction

- Optimal periodic signal for entrainment of oscillators based on phase reduction.

- Oscillator driven by a weak periodic input  $\mathbf{q}(\Omega t)$  of frequency  $\Omega = 2\pi/T_e$

$$\dot{\mathbf{X}} = \mathbf{F}(\mathbf{X}) + \mathbf{q}(\Omega t)$$

- Reduced phase equation for the oscillator phase  $\theta$

$$\dot{\theta} = \omega + \mathbf{Z}(\theta) \cdot \mathbf{q}(\Omega t)$$

- Phase difference  $\phi(t) = \theta(t) - \Omega t$  between the oscillator and the input obeys

$$\dot{\phi} = \Delta + \Gamma(\phi), \quad \Gamma(\phi) = [\mathbf{Z}(\phi + \Omega t) \cdot \mathbf{q}(\Omega t)]_t$$

where  $[g(s)]_t = \frac{1}{T_e} \int_0^{T_e} g(t) dt$  is the time average over one period  $T_e$ .

- If  $\phi$  has a stable phase-locking point  $\phi^*$ , its linear stability is

$$-\Gamma'(\phi^*) = -[\mathbf{Z}'(\phi^* + \Omega t) \cdot \mathbf{q}(\Omega t)]_t$$

- Optimal periodic input  $\mathbf{q}$  for the linear stability of the entrainment?

# Optimal entrainment via phase-only reduction

- Optimization problem for the linear stability of the phase-locked point:

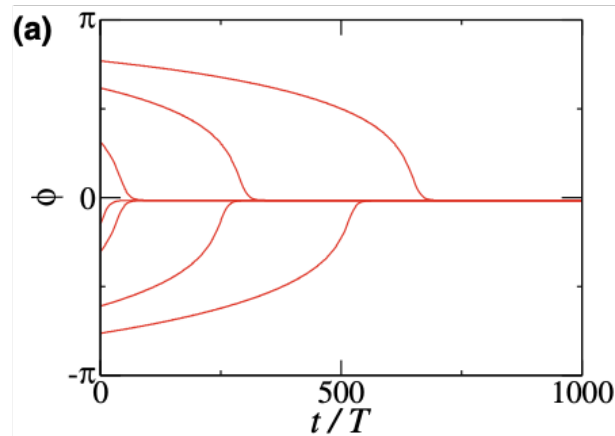
$$\max_{\mathbf{q}} -\Gamma'(\phi^*) \text{ s.t. } \Delta + \Gamma(\phi^*) = 0, [|\mathbf{q}(t)|^2]_t = P$$

where the constraints are (i)  $\phi^*$  is a fixed point and (ii) the power of  $\mathbf{q}$  is  $P > 0$ .

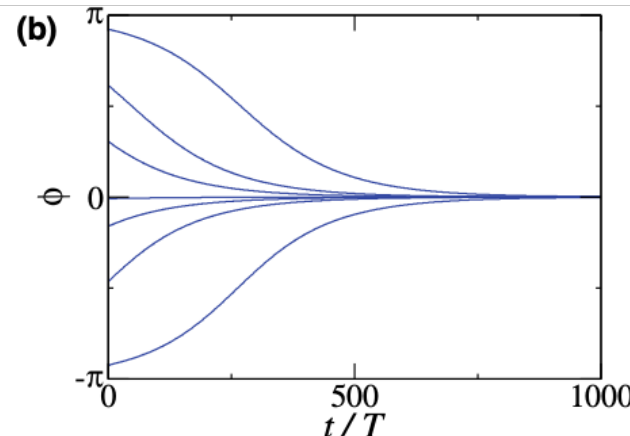
- Solution:  $\mathbf{q}(\Omega t) = -\frac{1}{2\nu} \mathbf{Z}'(\phi^* + \Omega t) + \frac{\mu}{2\nu} \mathbf{Z}(\phi^* + \Omega t)$

$$\mu = -\frac{2\nu\Delta}{[|\mathbf{Z}(t)|^2]_t}, \nu = \frac{1}{2} \sqrt{\frac{[|\mathbf{Z}(t)|^2]_t}{P - \Delta^2/[|\mathbf{Z}(t)|^2]_t}}$$

- Example:



Optimal  $\mathbf{q}$



Sinusoidal  $\mathbf{q}$

Faster phase locking!

Zlotnik *et al.*, PRL (2013)

# Optimal entrainment via phase-amplitude reduction

- Phase reduction approximation can easily break down for strong inputs.

- We introduce feedback of the amplitude deviation to the input

$$\mathbf{q}(t) \rightarrow \mathbf{q}'(t) = \mathbf{q}(t) - \alpha\{\mathbf{X}(t) - \mathbf{X}_0(\theta(t))\}$$

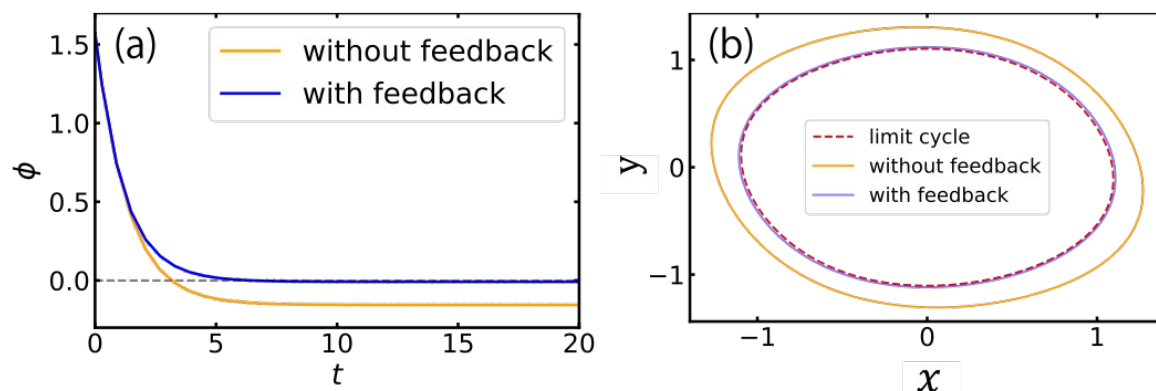
- Phase equation remains the same at the lowest order in  $\mathbf{q}$  ( $\alpha > 0$  : gain)

$$\dot{\theta}(t) = \omega + \langle \mathbf{Z}(\theta), \mathbf{q}'(t) \rangle = \omega + \langle \mathbf{Z}(\theta), \mathbf{q}(t) \rangle$$

- Amplitude decay rate changes from  $\mu$  to  $\mu - \alpha$  : faster relaxation to the LC

$$\dot{r}(t) = \mu r(t) \rightarrow \dot{r}(t) = (\mu - \alpha)r(t)$$

- Faster entrainment with stronger inputs can be realized.



S. Takata, Y. Kato and HN, "Fast optimal entrainment of limit-cycle oscillators by strong periodic inputs via phase-amplitude reduction and Floquet theory", Chaos 31, 093124 (2021)



# Summary

- Phase reduction theory for limit-cycle oscillators has historically been developed from a geometrical viewpoint.
- Recent developments in the Koopman operator theory enabled us a systematic, operator-theoretic formulation of phase reduction.
- Moreover, via Koopman operator theory, we can naturally introduce the amplitudes and generalize the phase-reduction theory to phase-amplitude reduction theory.
- These theories can further be developed for networked or spatially-extended systems in a straightforward manner.

## Topic 2

# **Phase-reduction approach to noise-induced coherent oscillations**

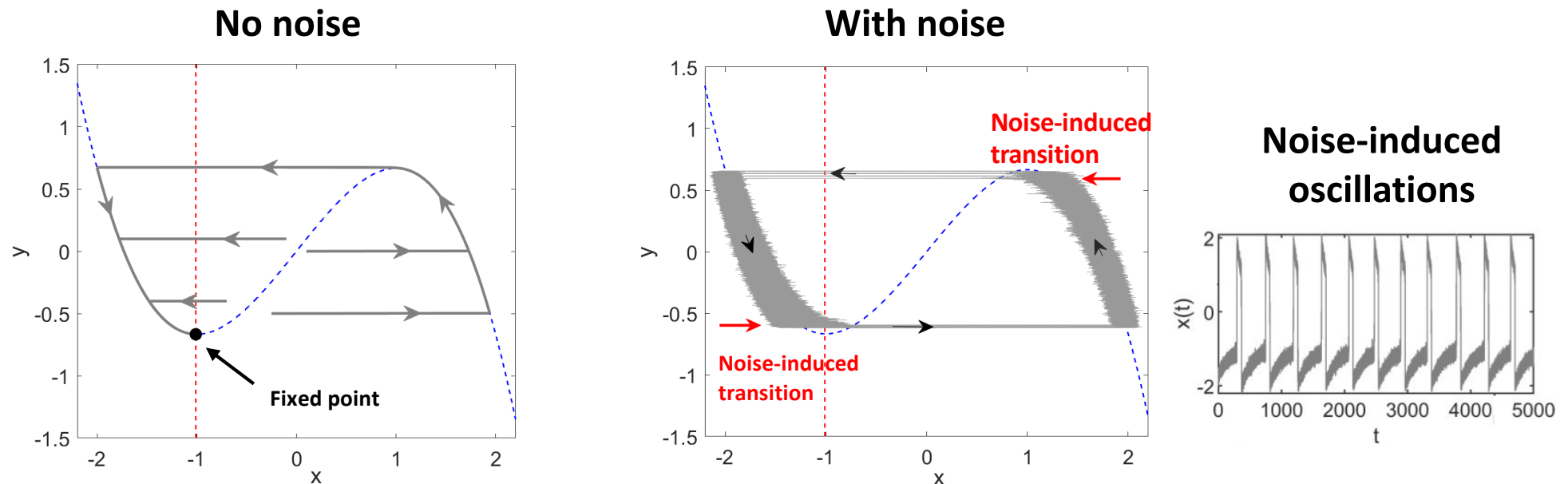
**Jinjie Zhu (Nanjing University of Aeronautic and Astronautics)**  
**Yuzuru Kato (Future University Hakodate)**  
**Hiroya Nakao (Tokyo Tech)**

# Background

## Noise-induced coherent oscillations

- Noise can induce coherent oscillations in fast-slow excitable systems.
- Such noise-induced oscillatory systems can also exhibit synchronization.
- The system has no limit-cycle solution – phase reduction is not applicable.
- Can we develop an approximate phase reduction method for such systems?

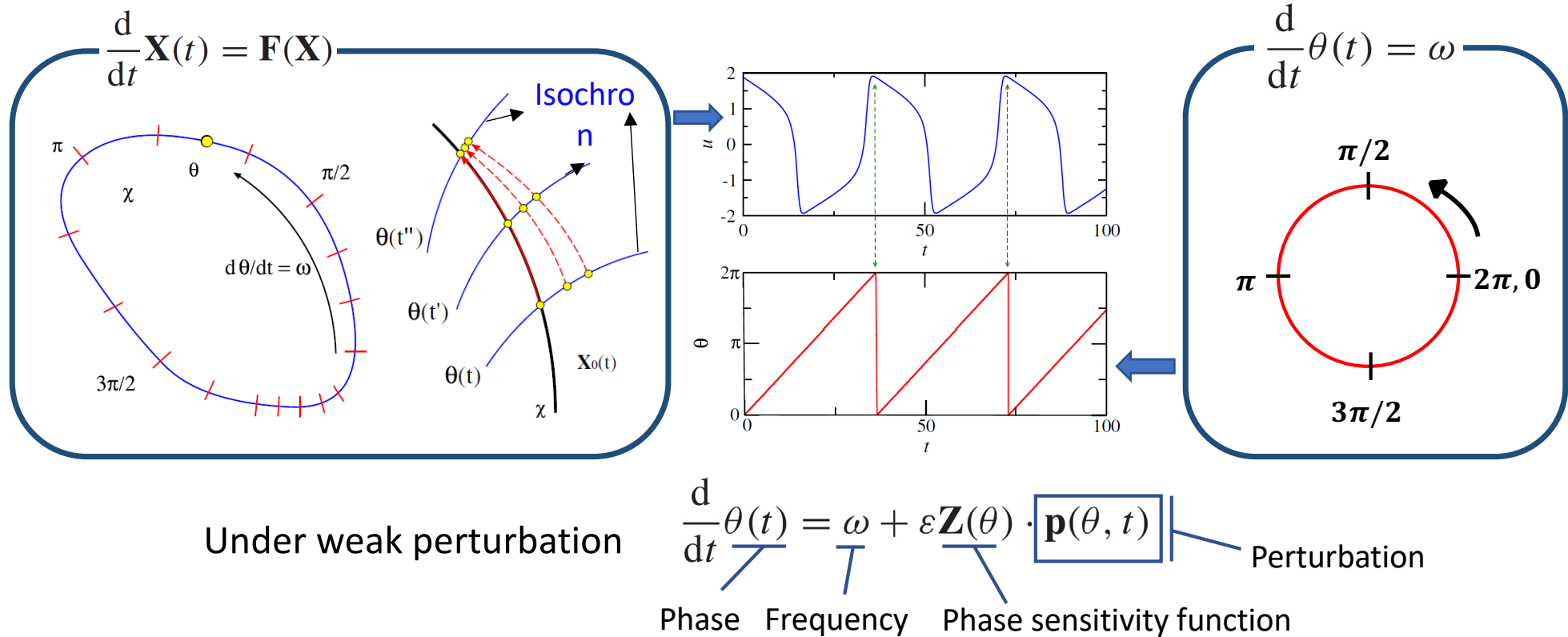
## Excitable system



Jinjie Zhu, Yuzuru Kato, and Hiroya Nakao, "Phase dynamics of noise-induced coherent oscillations in excitable systems", Phys. Rev. Research 4, L022041 (2022)

## Phase reduction theory

For **deterministic** limit-cycling system



Under weak perturbation



### Phase reduction theory

For **stochastic coherent** systems?

#### Aim

- Finding the **reference orbit** as the limit cycle in deterministic oscillatory cases
- Establishing an approximate **hybrid system** for calculating **phase sensitivity function**
- Constructing the **effective phase equation** and giving some examples

# Phase reduction of noise-induced coherent system

## Noise induced coherent excitable FitzHugh-Nagumo system

$$\varepsilon \dot{x} = f(x) - y + \sqrt{D_\nu} \nu(t),$$

$$\dot{y} = x + a,$$

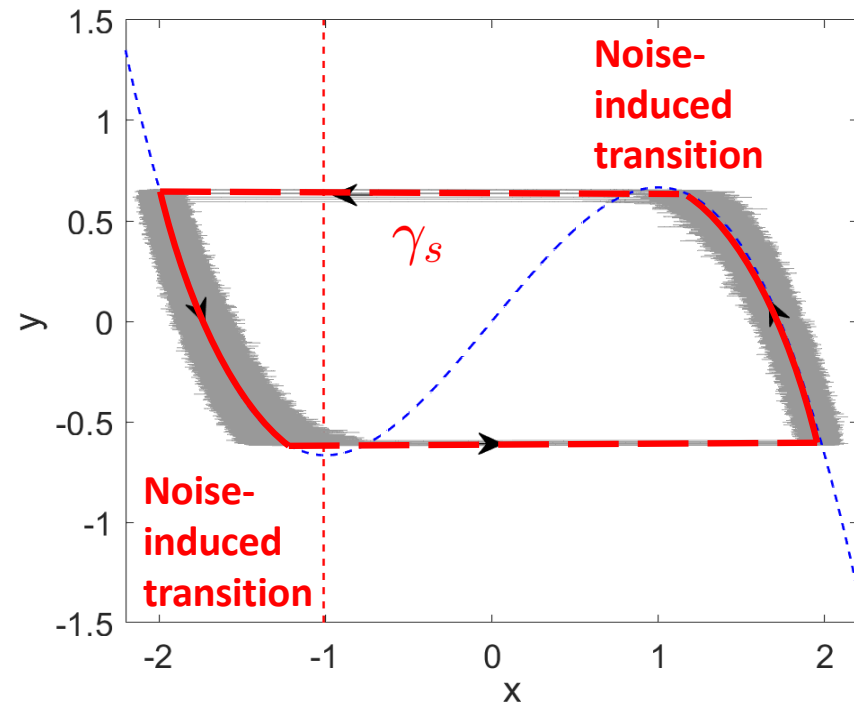
$$f(x) = x - \frac{x^3}{3}$$

### Parameters

$$D_\nu = 0.01, \varepsilon = 0.0001 \text{ and } a = 1.01$$

### Gaussian White noise

$$\langle \nu(t) \rangle = 0 \text{ and } \langle \nu(t) \nu(\tau) \rangle = \delta(t - \tau)$$

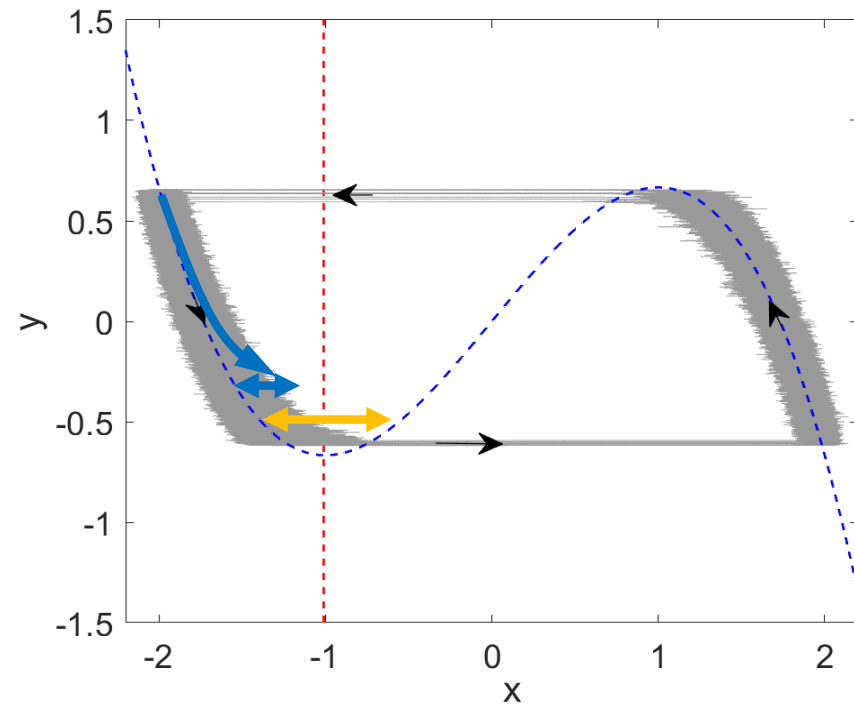


## Distance matching condition

$$\boxed{\int_{y_0}^{y_l} \frac{S(y)}{\varepsilon (f_l^{-1}(y) + a) T_e(y)} dy} = \boxed{S(y_l)}$$

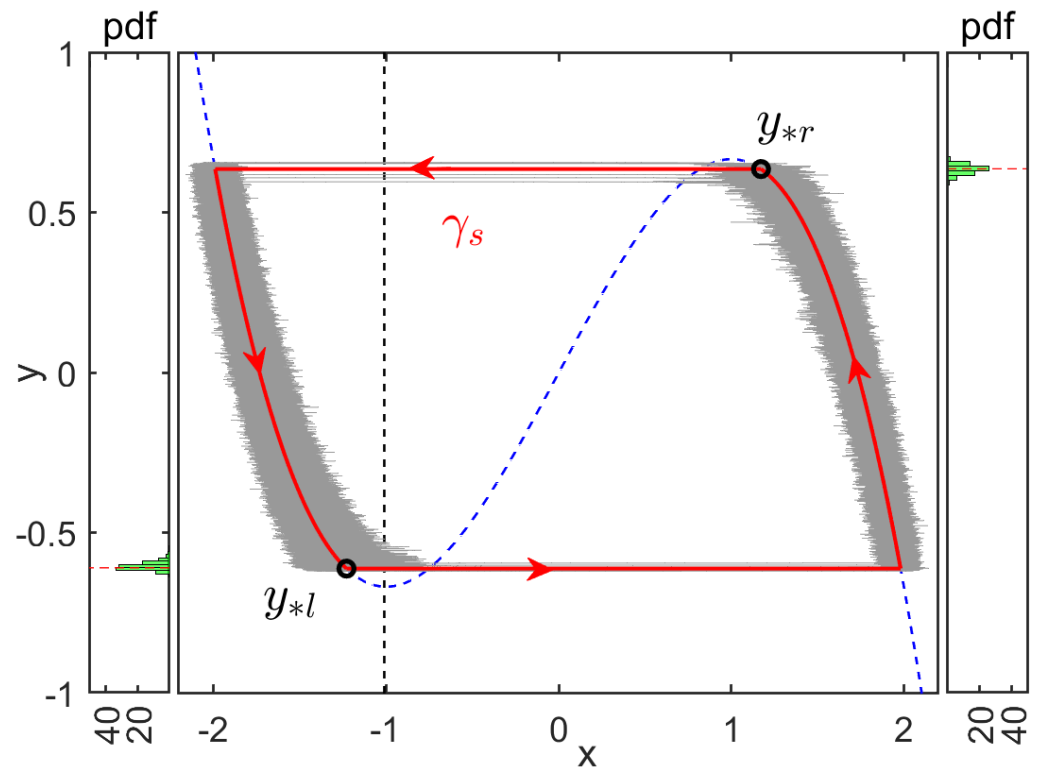
LHS RHS

$$T_e(y) = \frac{2\pi}{\sqrt{|U''(x_m)|U''(x_l)}} \exp\left(\frac{2(U(x_m) - U(x_l))}{D_\nu}\right)$$



## Distance matching condition

$$\underbrace{\int_{y_0}^{y_l} \frac{S(y)}{\varepsilon (f_l^{-1}(y) + a) T_e(y)} dy}_{\text{LHS}} = \underbrace{S(y_l)}_{\text{RHS}}$$

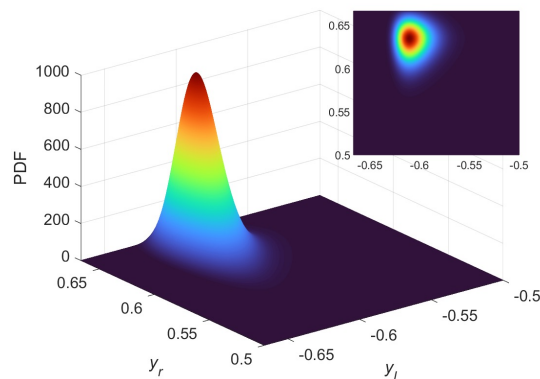




## First passage time distribution

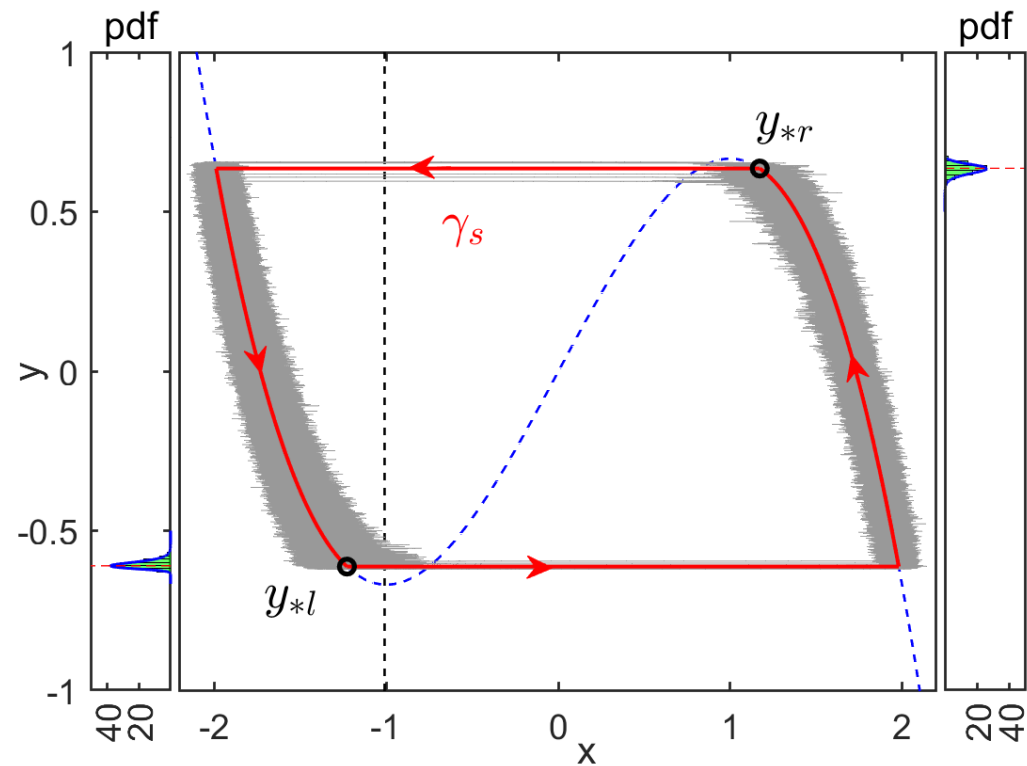
$$\rho_l(t) = \frac{1}{T_e(t)} \exp \left( - \int_{-\infty}^t \frac{1}{T_e(t')} dt' \right)$$

$$\rho_l(y) = \frac{\exp \left( - \int^y \frac{1}{\varepsilon (f_l^{-1}(y') + a) T_e(y')} dy' \right)}{\varepsilon |f_l^{-1}(y) + a| T_e(y)}$$



$$\rho(y_l, y_r) = \rho_l(y_l) \rho_r(y_r)$$

Zhu et al. 2022.



## Hybrid system

$$\dot{\mathbf{X}} = \mathbf{F}(\mathbf{X}), \text{ if } \mathbf{X} \notin \Pi_i,$$

$$\mathbf{X}(t+0) = \Phi_i(\mathbf{X}(t)), \text{ if } \mathbf{X} \in \Pi_i, i = l, r$$

Switching surfaces  $\Pi_i = \{\mathbf{X} | L(\mathbf{X}) = y_i\}$   
 $L(\mathbf{X}) = y$

Transition function

$$\Phi_l(\mathbf{X}) = [2 \cos(\varphi), y]^\top, \Phi_r(\mathbf{X}) = [2 \cos(\varphi + \frac{2\pi}{3}), y]^\top$$

(solving the cubic equation by using trigonometric functions)

$$x - \frac{x^3}{3} - y = 0$$

Zhu et al. 2022.

## Phase reduction

$$\dot{\theta}(t) = \omega + \mathbf{Z}(\theta) \cdot \mathbf{P}(\theta, t)$$

Adjoint method for  
Phase sensitivity function

$$\omega \frac{d}{d\theta} \mathbf{Z}(\theta) = -\mathbf{J}(\theta)^\top \mathbf{Z}(\theta), \text{ if } \mathbf{X}(\theta) \notin \Pi_i,$$

$$\mathbf{Z}(\theta(t)) = \mathbf{C}_i^\top \mathbf{Z}(\theta(t+0)), \text{ if } \mathbf{X}(\theta) \in \Pi_i,$$

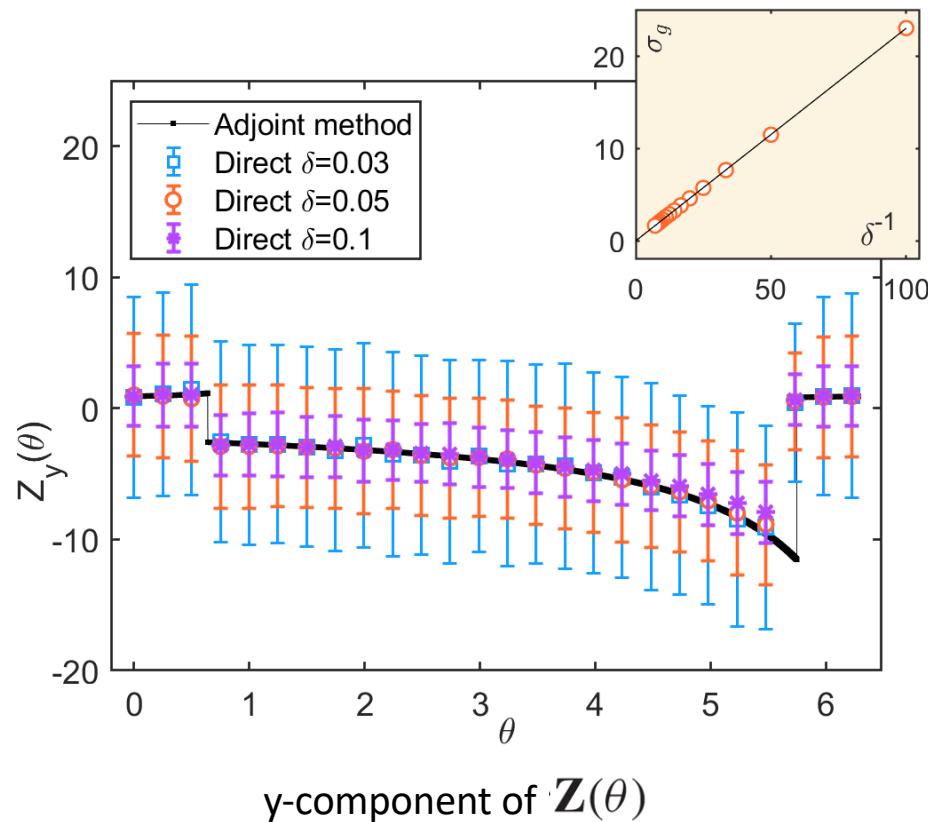
Salutation matrix

with normalization condition:

$$\mathbf{Z}(\theta) \cdot \mathbf{F}(\mathbf{X}(\theta)) = \omega$$

Shirasaka et al. 2017. Ermentrout 1996.

# Phase reduction of noise-induced coherent system



## Phase reduction

$$\dot{\theta}(t) = \omega + \mathbf{Z}(\theta) \cdot \mathbf{P}(\theta, t)$$

**Adjoint method for**  
Phase sensitivity function

$$\omega \frac{d}{d\theta} \mathbf{Z}(\theta) = -\mathbf{J}(\theta)^\top \mathbf{Z}(\theta), \text{ if } \mathbf{X}(\theta) \notin \Pi_i,$$

$$\mathbf{Z}(\theta(t)) = \mathbf{C}_i^\top \mathbf{Z}(\theta(t+0)), \text{ if } \mathbf{X}(\theta) \in \Pi_i,$$

Saltation matrix

with normalization condition:

$$\mathbf{Z}(\theta) \cdot \mathbf{F}(\mathbf{X}(\theta)) = \omega$$

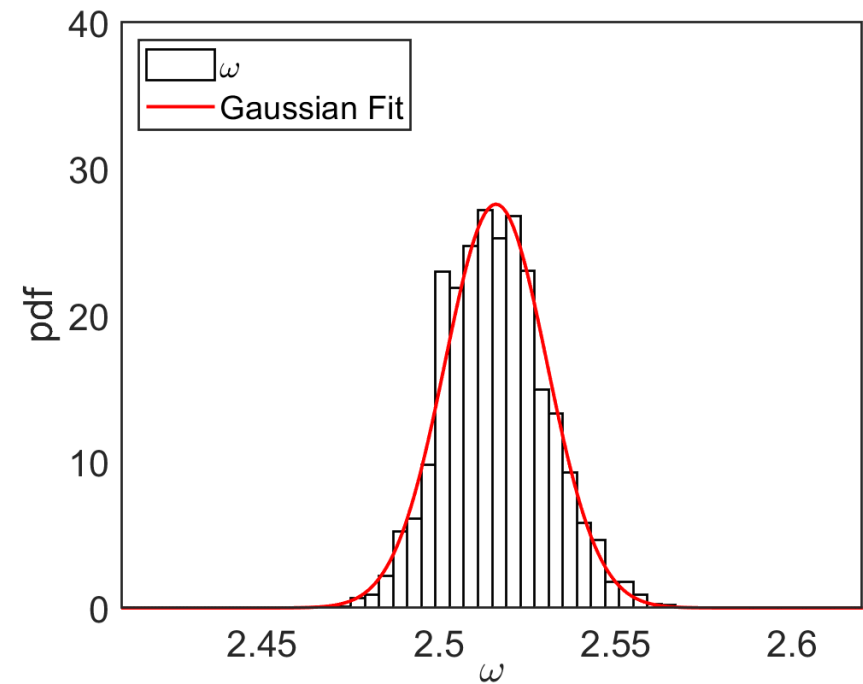
Shirasaka et al. 2017. Ermentrout 1996.

## Effective phase equation

$$\dot{\theta}(t) = \underbrace{\omega}_{\text{Effective frequency}} + \mathbf{Z}(\theta) \cdot \mathbf{P}(\theta, t) + \sqrt{\underbrace{D_e}_{\text{Effective noise intensity}}} \xi(t)$$

$$\omega_e = \langle [\theta(t) - \theta(0)]/t \rangle$$

$$D_e = \left\langle ([\theta(t) - \theta(0)]/t - \omega_e)^2 \right\rangle t$$





## Effective phase equation

$$\dot{\theta}(t) = \omega_e + \mathbf{Z}(\theta) \cdot \mathbf{P}(\theta, t) + \sqrt{D_e} \xi(t)$$

$\omega_e$

$$T_h = \int_{y_r}^{y_l} \frac{dy}{\varepsilon(f_l^{-1}(y) + a)} + \int_{y_l}^{y_r} \frac{dy}{\varepsilon(f_r^{-1}(y) + a)}$$

$$\omega_h = 2\pi T_h^{-1}$$

1

$$\langle \omega_h \rangle = \int \int \omega_h(y_l, y_r) \rho(y_l, y_r) dy_l dy_r$$

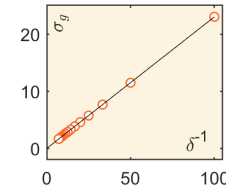
2

$$\rho(y_l, y_r) = \rho_l(y_l) \rho_r(y_r)$$

$D_e$

1

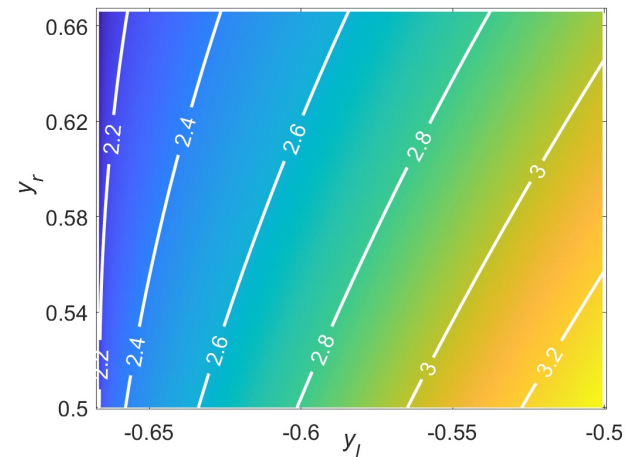
$$\sigma_g = \delta^{-1} \sqrt{2D_e t}$$



2

$$\sigma_{\omega_h} = \int \int \omega_h(y_l, y_r)^2 \rho(y_l, y_r) dy_l dy_r - \langle \omega_h \rangle^2$$

$$D_e = \frac{2\pi \sigma_{\omega_h}}{\langle \omega_h \rangle}$$



## Example: Periodic forcing

$$\begin{aligned} \varepsilon \dot{x} &= f(x) - y + \sqrt{D_\nu} \nu(t), \\ \dot{y} &= x + a + \underline{\mu \sin(\Omega t)}, \end{aligned} \quad \text{Phase reduction} \quad \longrightarrow \quad \dot{\theta} = \omega_e + \sqrt{D_e} \xi(t) + \mu Z_y(\theta) \sin(\Omega t)$$

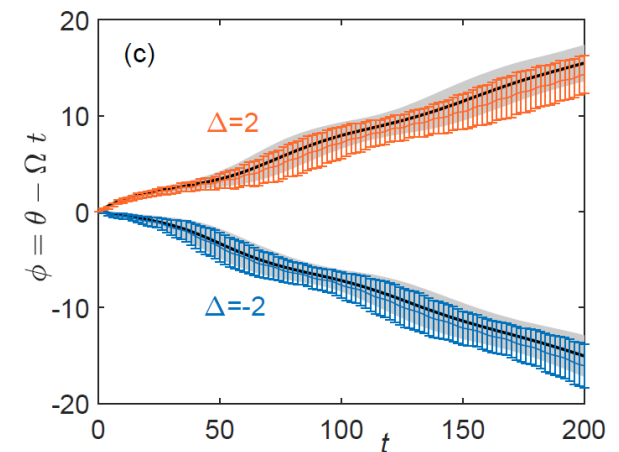
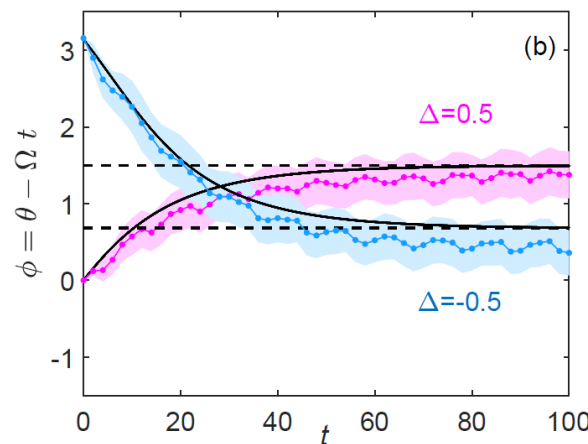
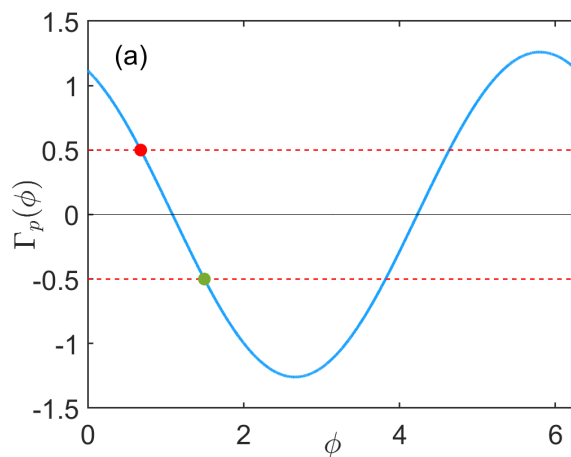
$$\dot{\phi} = \mu (\Delta + \Gamma_p(\phi)) + \sqrt{D_e} \xi(t)$$

Averaging

$$\Gamma_p(\phi) = \frac{1}{2\pi} \int_0^{2\pi} Z_y(\phi + \psi) \sin(\psi) d\psi$$

$$\phi(t) = \theta(t) - \Omega t$$

$$\omega_e - \Omega = \mu \Delta$$



# Example: Two-coupled oscillators

$$\varepsilon \dot{x}_i = x_i - \frac{x_i^3}{3} - y_i + \sqrt{D_\nu} \nu_i(t),$$

$$\dot{y}_i = (x_i + a) + \mu \underline{G_y(y_i, y_j)}, \quad G_y(y_i, y_j) = y_j - y_i$$

Phase reduction

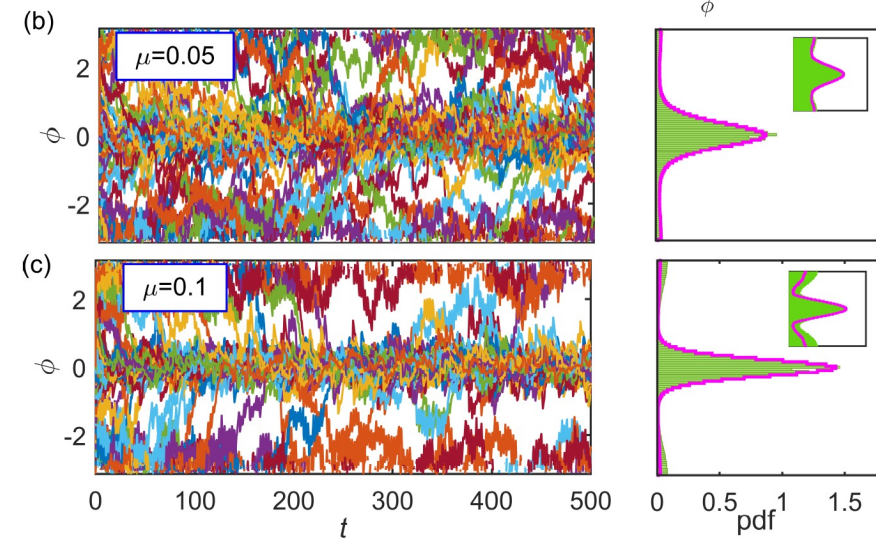
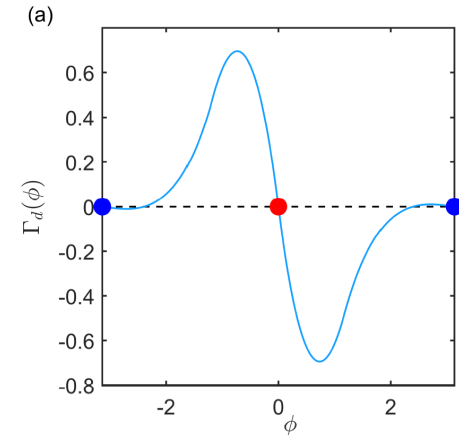
$$\dot{\theta}_i = \omega_e + \sqrt{D_e} \xi_i(t) + \mu Z_y(\theta_i) G_y(\theta_i, \theta_j)$$

Averaging

$$\dot{\phi} = \sqrt{2D_e} \xi(t) + \mu \Gamma_d(\phi)$$

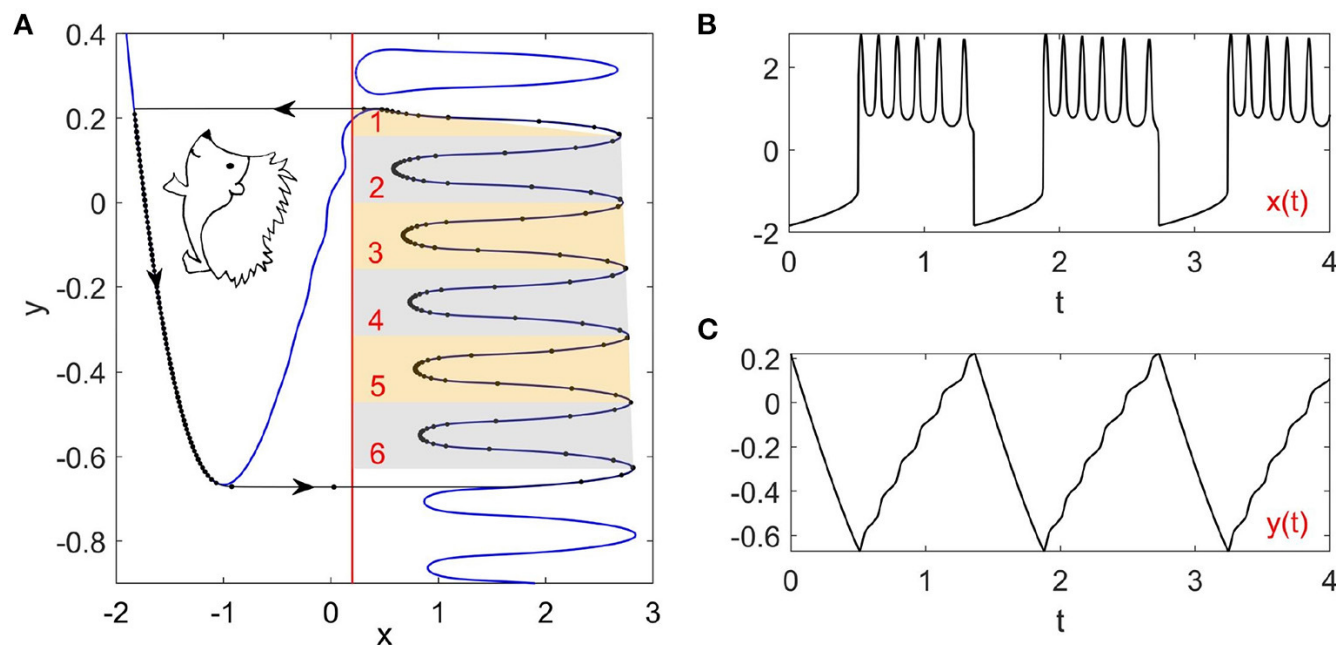
$$\Gamma(\phi) = \frac{1}{2\pi} \int_0^{2\pi} Z_y(\phi + \psi) G_y(\phi + \psi, \psi) d\psi$$

$$\Gamma_d(\phi) = \Gamma(\phi) - \Gamma(-\phi) \quad \phi = \theta_1 - \theta_2$$



## Conclusions

- Established the effective phase equation for coherent excitable systems
- Applied to a periodically forced and mutually coupled oscillators
- More complex stochastic oscillations may also be analyzed
- Extension to networks?



Jinjie Zhu and Hiroya Nakao, "Noise-tuned bursting in a Hedgehog burster", *Front. Comput. Neurosci.* 16:970643 (2022).



## Topic 3

# **Design of nonlinear oscillators based on phase reduction**

**Joint work with**

**Norihisa Namura, Tsubasa Ishii (Tokyo Tech)**

# Design of limit-cycle oscillators

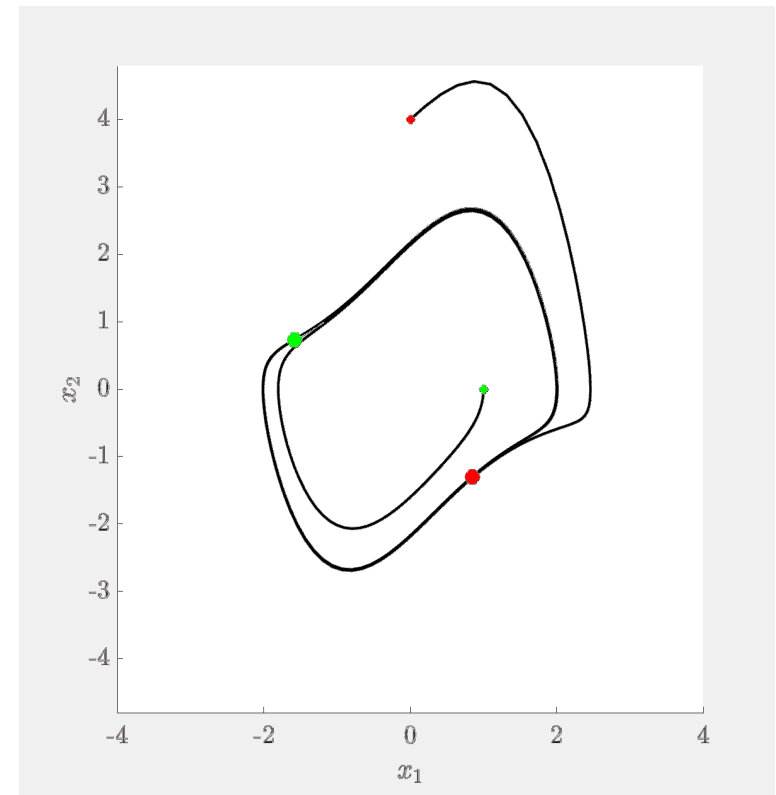
- For engineering applications of limit-cycle oscillations, methods to design dynamical systems with given periodic orbits have been proposed<sup>1, 2 3</sup>.
- For synchronization, not only the periodic orbit but the phase response property of the oscillator is also important.
- We propose a method to design a stable oscillator with a given phase response property in addition to a given periodic orbit.

# Research objective

- Dynamical system describing a limit-cycle oscillator.

$$\frac{d\mathbf{X}}{dt} = \mathbf{F}(\mathbf{X}), \quad \mathbf{X} \in \mathbb{R}^d.$$

- The vector field  $\mathbf{F}$  is assumed to possess a stable limit-cycle solution  $\mathbf{X}_0(t)$  of period  $T$ , satisfying  $\mathbf{X}_0(t) = \mathbf{X}_0(t + T)$ .
- We design the vector field  $\mathbf{F}$  so that the system has a stable limit cycle with a prescribed periodic orbit and phase response property.



# Asymptotic phase and phase function

- For an exponentially stable limit cycle (LC), the phase can be extended to the basin of the LC.
- We can introduce an asymptotic phase function

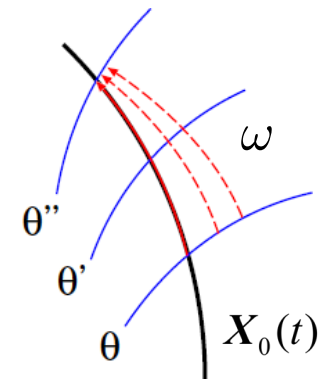
$$\Theta(\mathbf{X}) : \mathbf{R}^d \rightarrow [0, 2\pi]$$

such that

$$\dot{\Theta}(\mathbf{X}) = \nabla \Theta(\mathbf{X}) \cdot \dot{\mathbf{X}} = \mathbf{F}(\mathbf{X}) \cdot \nabla \Theta(\mathbf{X}) = \omega$$

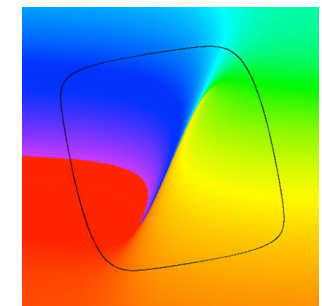
in the basin of the LC, which maps the  $d$ -dimensional system state  $\mathbf{X}$  to a phase value<sup>4</sup>.

- The phase  $\theta = \Theta(\mathbf{X})$  of the oscillator obeys  $\dot{\theta} = \omega$ .
- The oscillator state on the LC is represented as  $\mathbf{X}_0(\theta)$  as a function of  $\theta$ .



Isochrons

(Level sets of the phase)



Phase function  $\Theta(\mathbf{X})$   
(FitzHugh-Nagumo)

<sup>4</sup> A. T. Winfree (J. Theor. Biol. 1967) / J. Guckenheimer (J. Math. Biol. 1975) / Y. Kuramoto (Springer 1984).



# Phase reduction and phase sensitivity function

- A limit-cycle oscillator subjected to a weak input  $q(\mathbf{X}, t)$ .

$$\frac{d\mathbf{X}}{dt} = \mathbf{F}(\mathbf{X}) + \varepsilon \mathbf{q}(\mathbf{X}, t), \quad 0 \leq \varepsilon \ll 1.$$

- The phase  $\theta = \Theta(\mathbf{X})$  of the oscillator approximately obeys

$$\frac{d\theta}{dt} = \omega + \varepsilon \mathbf{Z}(\theta) \cdot \mathbf{q}(\mathbf{X}_0(\theta), t),$$

where the phase sensitivity function (PSF) is defined as

$$\mathbf{Z}(\theta) = \nabla \Theta(\mathbf{X})|_{\mathbf{X}=\mathbf{X}_0(\theta)}.$$

- The PSF  $\mathbf{Z}(\theta)$  obeys the following adjoint equation and normalization condition:

$$\omega \frac{d}{d\theta} \mathbf{Z}(\theta) = -\mathbf{J}(\mathbf{X}_0(\theta))^\top \mathbf{Z}(\theta), \quad \mathbf{Z}(\theta) \cdot \mathbf{F}(\mathbf{X}_0(\theta)) = \omega,$$

where  $\mathbf{J}(\mathbf{X}_0(\theta))$  is the Jacobian matrix of  $\mathbf{F}(\mathbf{X})$  at  $\mathbf{X}_0(\theta)$ .

---

<sup>5</sup> Y. Kuramoto (Springer 1984) / G. B. Ermentrout and N. Kopell (J. Math. Biol. 1991) / E. Brown, J. Moehlis, & P. Holmes (Neural Comput. 2004)

# Design of a 2D oscillator with given properties

- Our aim: design of a 2D oscillator with a given periodic orbit and PSF.
- We approximate the vector field  $F(\mathbf{X})$  of the oscillator by polynomials.

$$\mathbf{F}(\mathbf{X}) = \begin{bmatrix} F_1(\mathbf{X}) \\ F_2(\mathbf{X}) \end{bmatrix} \simeq \begin{bmatrix} \mathbf{U}^\top(\mathbf{X})\zeta_1 \\ \mathbf{U}^\top(\mathbf{X})\zeta_2 \end{bmatrix}.$$

Here,  $\mathbf{X} = [x_1 \ x_2]^\top$ ,  $\zeta_1$ ,  $\zeta_2$  are the expansion coefficients, and

$$\mathbf{U}(\mathbf{X}) = \left[ 1 \quad \overline{x_1} \quad \overline{x_2} \quad \overline{x_1^2} \quad \overline{x_1 x_2} \quad \overline{x_2^2} \quad \cdots \quad \overline{x_2^n} \right]^\top,$$

where  $n$  is the order of polynomials and the overline represents standardization.

- We estimate the coefficients  $\zeta_1$ ,  $\zeta_2$  so that  $\mathbf{F}(\mathbf{X})$  has a linearly stable limit cycle with a given periodic orbit  $\mathbf{X}_0(t)$  and PSF  $\mathbf{Z}(\theta)$ .

# Condition for the periodic orbit

- The vector field  $F \approx [U^\top(\mathbf{X}_0(t))\zeta_1 \quad U^\top(\mathbf{X}_0(t))\zeta_2]^\top$  of the designed oscillator should satisfy

$$F(\mathbf{X}_0(t)) = \frac{d}{dt}\mathbf{X}_0(t)$$

- To realize this condition as much as possible, we seek  $\zeta_1$  and  $\zeta_2$  that minimize the error of the following equations for  $\mathbf{X}_0(t) = [p_1(t) \ p_2(t)]^\top$ :

$$U^\top(\mathbf{X}_0(t))\zeta_1 \simeq \frac{d}{dt}p_1(t), \quad U^\top(\mathbf{X}_0(t))\zeta_2 \simeq \frac{d}{dt}p_2(t).$$

- Introducing  $\xi = [\zeta_1^\top \ \zeta_2^\top]^\top$  and discretizing the time as  $\{t_k\}_{k=1}^L$ , the above equations can be expressed as

$$\begin{bmatrix} U^\top(\mathbf{X}_0(t_k)) & \mathbf{0} \\ \mathbf{0} & U^\top(\mathbf{X}_0(t_k)) \end{bmatrix} \xi \simeq \begin{bmatrix} \dot{p}_1(t_k) \\ \dot{p}_2(t_k) \end{bmatrix}.$$

# Condition for the PSF

- The PSF  $\mathbf{Z}(\theta) = \mathbf{Z}(\omega t) := \tilde{\mathbf{Z}}(t) = [\tilde{Z}_1(t) \ \tilde{Z}_2(t)]^\top$  of the designed oscillator should satisfy the following adjoint equation.

$$\tilde{\mathbf{Z}}(t) = -\mathbf{J}^\top(t) \tilde{\mathbf{Z}}(t) = -[\nabla \mathbf{F}(\mathbf{X}_0(t))]^\top \tilde{\mathbf{Z}}(t).$$

- We seek  $\zeta_1$  and  $\zeta_2$  that minimize the error of the following approximation:

$$\begin{aligned} \tilde{Z}_1(t) \mathbf{U}_1^\top(\mathbf{X}_0(t)) \zeta_1 + \tilde{Z}_2(t) \mathbf{U}_1^\top(\mathbf{X}_0(t)) \zeta_2 &\simeq -\frac{d}{dt} \tilde{Z}_1(t), \\ \tilde{Z}_1(t) \mathbf{U}_2^\top(\mathbf{X}_0(t)) \zeta_1 + \tilde{Z}_2(t) \mathbf{U}_2^\top(\mathbf{X}_0(t)) \zeta_2 &\simeq -\frac{d}{dt} \tilde{Z}_2(t), \end{aligned}$$

where  $\mathbf{U}_{1,2}(\mathbf{X}) = (\nabla \mathbf{U}(\mathbf{X}))_{1,2}$ .

- Introducing  $\boldsymbol{\xi} = [\zeta_1^\top \ \zeta_2^\top]^\top$  and  $\{t_k\}_{k=1}^L$ , we can express them as

$$\begin{bmatrix} \tilde{Z}_1(t_k) \mathbf{U}_1^\top(\mathbf{X}_0(t_k)) & \tilde{Z}_2(t_k) \mathbf{U}_1^\top(\mathbf{X}_0(t_k)) \\ \tilde{Z}_1(t_k) \mathbf{U}_2^\top(\mathbf{X}_0(t_k)) & \tilde{Z}_2(t_k) \mathbf{U}_2^\top(\mathbf{X}_0(t_k)) \end{bmatrix} \boldsymbol{\xi} \simeq \begin{bmatrix} -\dot{\tilde{Z}}_1(t_k) \\ -\dot{\tilde{Z}}_2(t_k) \end{bmatrix}.$$



# Objective function

- The conditions for the periodic orbit and PSF are summarized as

$$\mathbf{A}\boldsymbol{\xi} \approx \mathbf{b}$$

where  $\boldsymbol{\xi} = [\boldsymbol{\zeta}_1^\top \ \boldsymbol{\zeta}_2^\top]^\top$  is the coefficient vector and  $\mathbf{A}$  and  $\mathbf{b}$  are

$$\mathbf{A} = \begin{bmatrix} \vdots & \vdots \\ \mathbf{U}^\top(\mathbf{X}_0(t_k)) & \mathbf{0} \\ \mathbf{0} & \mathbf{U}^\top(\mathbf{X}_0(t_k)) \\ \vdots & \vdots \\ \tilde{Z}_1(t_k)\mathbf{U}_1^\top(\mathbf{X}_0(t_k)) & \tilde{Z}_2(t_k)\mathbf{U}_1^\top(\mathbf{X}_0(t_k)) \\ \tilde{Z}_1(t_k)\mathbf{U}_2^\top(\mathbf{X}_0(t_k)) & \tilde{Z}_2(t_k)\mathbf{U}_2^\top(\mathbf{X}_0(t_k)) \\ \vdots & \vdots \end{bmatrix}, \quad \mathbf{b} = \begin{bmatrix} \vdots \\ \dot{p}_1(t_k) \\ \dot{p}_2(t_k) \\ \vdots \\ -\dot{\tilde{Z}}_1(t_k) \\ -\dot{\tilde{Z}}_2(t_k) \\ \vdots \end{bmatrix}.$$

- We seek  $\boldsymbol{\xi} = [\boldsymbol{\zeta}_1^\top \ \boldsymbol{\zeta}_2^\top]^\top$  that minimizes the error  $\|\mathbf{A}\boldsymbol{\xi} - \mathbf{b}\|^2$ .

# Stability condition

- From Floquet theory<sup>6</sup>, the Floquet exponents  $\lambda_1$  and  $\lambda_2$  characterizing the linear stability of the limit cycle satisfy

$$\lambda_1 + \lambda_2 = \frac{1}{T} \int_0^T \text{tr}(\mathbf{J}(\mathbf{X}_0(t))) dt.$$

- For limit cycles, the first exponent  $\lambda_1 = 0$ , so we get

$$\lambda = \lambda_2 \simeq \frac{1}{L} \sum_{k=1}^L (U_1^\top(\mathbf{X}_0(t_k))\zeta_1 + U_2^\top(\mathbf{X}_0(t_k))\zeta_2) := \mathbf{C}\boldsymbol{\xi}.$$

- We require that the periodic orbit is sufficiently linearly stable by imposing

$$\lambda = \mathbf{C}\boldsymbol{\xi} \leq \lambda_{\text{tol}}$$

for some tolerance value  $\lambda_{\text{tol}} < 0$ .

---

<sup>6</sup>J. Guckenheimer and P. Holmes, Nonlinear oscillations, dynamical systems, and bifurcations of vector fields (Springer, 1983).

# Optimization problem for the coefficients

- The coefficient vector  $\xi = [\zeta_1^\top \ \zeta_2^\top]^\top$  is obtained by solving the following optimization problem.

## Optimization

The vector field of a 2D oscillator is obtained by the following quadratic programming with a linear constraint.

$$\begin{aligned} \xi^* = \operatorname{argmin}_{\xi} \quad & \frac{1}{2} \|A\xi - b\|^2 + \gamma \|\xi\|^2 \\ \text{s.t.} \quad & C\xi \leq \lambda_{\text{tol}}. \end{aligned}$$

- We added a regularization term with a weight  $\gamma$  to prevent the coefficient values from becoming unnecessarily large.
- This problem is convex and can easily be solved.

# Ex1: Reconstruction of the FHN oscillator

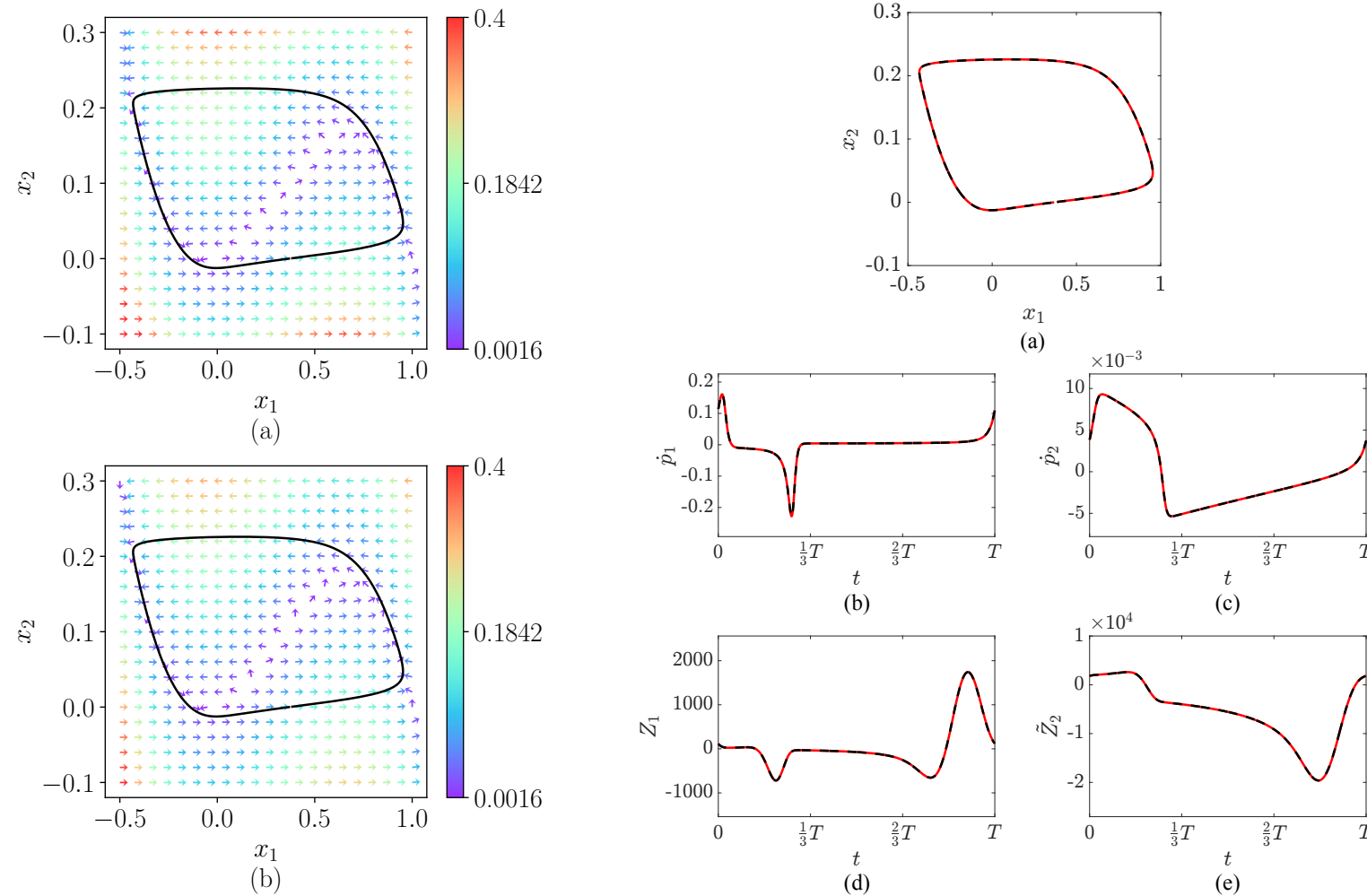
- Example 1: We (re)construct a 2D oscillator possessing the periodic orbit and PSF of the FitzHugh-Nagumo (FHN) oscillator.

$$\frac{d}{dt} \begin{bmatrix} x_1 \\ x_2 \end{bmatrix} = \begin{bmatrix} x_1(x_1 - a)(1 - x_1) - x_2 \\ c(x_1 - bx_2) \end{bmatrix}, \quad a = -0.1, \quad b = 0.5, \quad c = 0.01.$$

- This FHN oscillator has the following properties:
  - Period:  $T = 126.5$ .
  - Natural frequency:  $\omega = 0.0497$ .
  - Second Floquet exponent:  $\lambda = -0.4586$ .
- We try to design **a more stable oscillator** with the same periodic orbit but with a smaller second Floquet exponent:  $\lambda_{\text{tol}} = -0.5$ .
- We set the polynomial degree as  $n = 10$  and the regularization parameter as  $\gamma = 1.0 \times 10^{-3}$ .



# Results: reconstruction of the FHN oscillator



(a) Phase plane and vector field, (b,c) periodic orbit, (d,e) PSF.

- We could design a vector field with the same periodic orbit and PSF as the FHN with enhanced stability than the original.

## Ex2: Design of a star-shaped oscillator

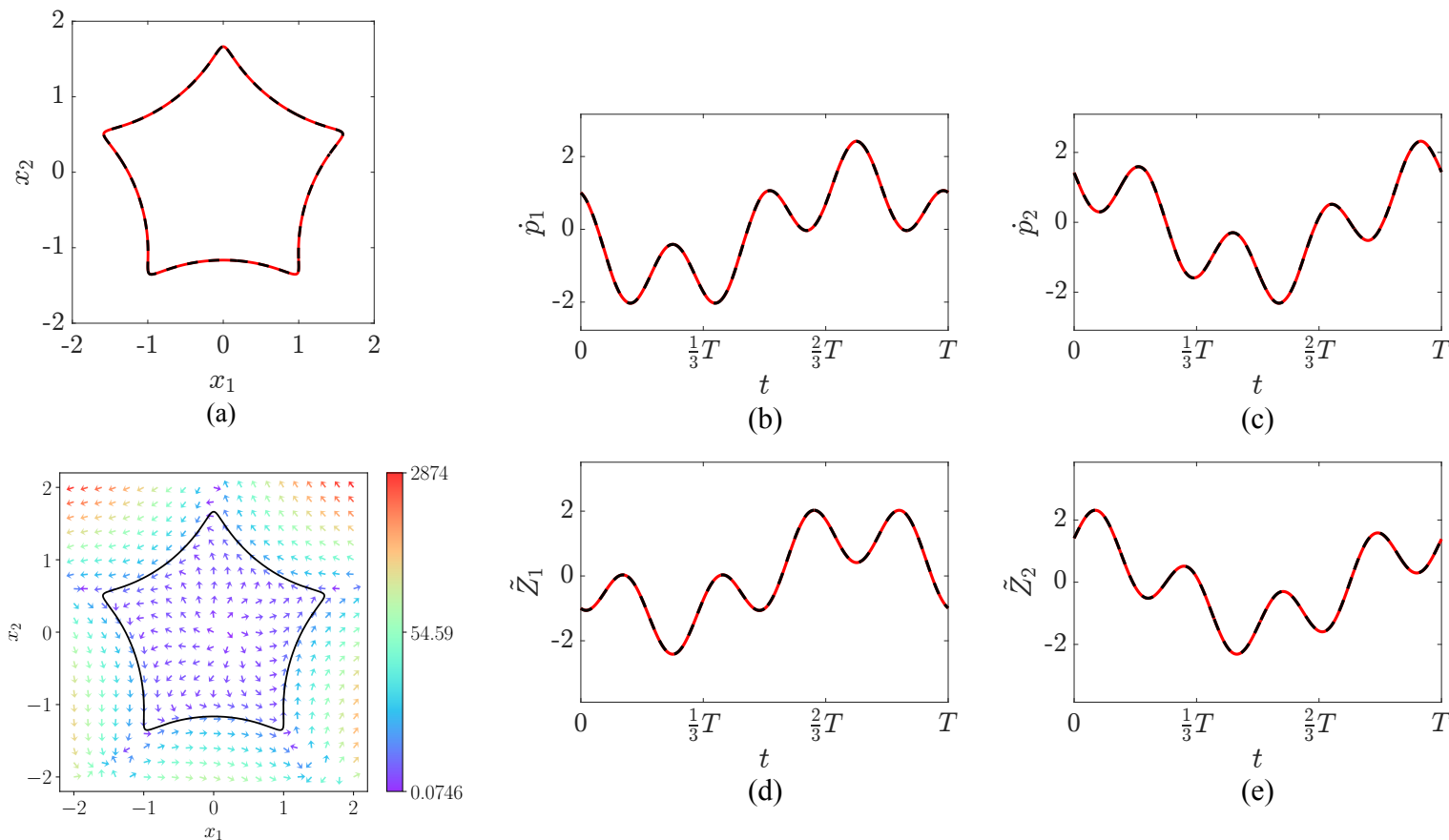
- Example 2: We design an artificial oscillator with a star-shaped periodic orbit and PSF with the 1st and 4th harmonics:

$$\mathbf{X}_0(t) = \begin{bmatrix} \sqrt{2} \cos(t) + \frac{1}{4} \sin(4t) \\ \sqrt{2} \sin(t) + \frac{1}{4} \cos(4t) \end{bmatrix},$$

$$\tilde{\mathbf{Z}}(t) = \begin{bmatrix} -\sqrt{2} \sin(t) - \cos(4t) \\ \sqrt{2} \cos(t) + \sin(4t) \end{bmatrix}.$$

- This oscillator has a period  $T = 2\pi$  and natural frequency  $\omega = 1$ .
- We set the stability tolerance value as  $\lambda_{\text{tol}} = -1$ , the polynomial degree as  $n = 10$ , and the weight parameter as  $\gamma = 1.0 \times 10^{-3}$ .

# Results: star-shaped oscillator



(a) Phase plane and vector field, (b,c) periodic orbit, (d,e) PSF.

- We could design a star-shaped oscillator with the given PSF and stability.

## Ex3: Design of a circular oscillator with a high-harmonic PSF

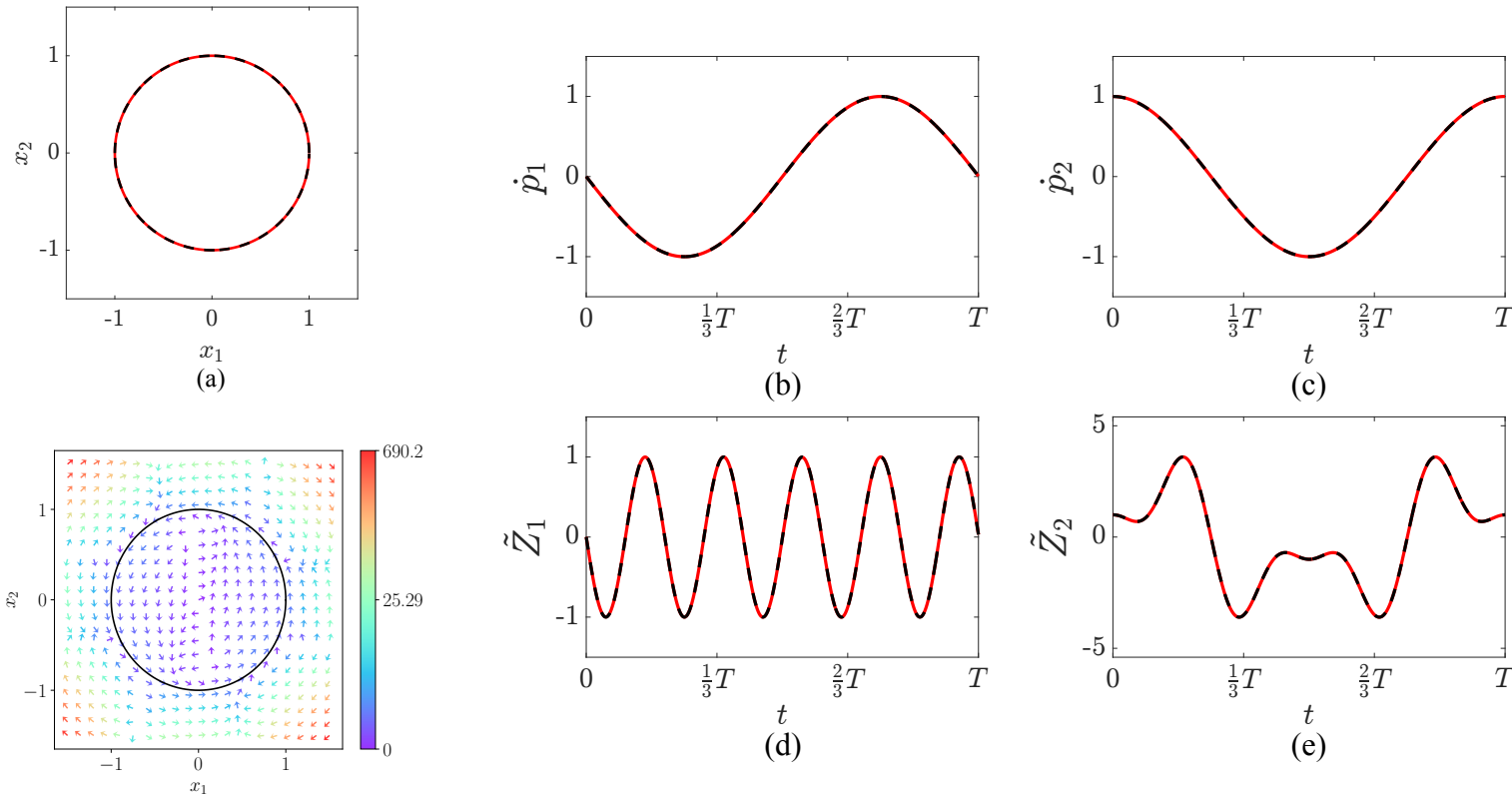
- Example 3: We design an artificial oscillator whose periodic orbit is a unit circle but PSF has high-harmonic components:

$$\mathbf{X}_0(t) = \begin{bmatrix} \cos(t) \\ \sin(t) \end{bmatrix},$$
$$\tilde{\mathbf{Z}}(t) = \begin{bmatrix} -\sin(5t) \\ 2\cos(t) - 2\cos(3t) + \cos(5t) \end{bmatrix}.$$

- This oscillator has a period  $T = 2\pi$  and natural frequency  $\omega = 1$ .
- We set the stability tolerance value as  $\lambda_{\text{tol}} = -1$ .
- We set the polynomial degree as  $n = 7$  and the weight parameter as  $\gamma = 1.0 \times 10^{-2}$ .



# Results: circular oscillator with a high-harmonic PSF



(a) Phase plane and vector field, (b,c) periodic orbit, (d,e) PSF.

- The oscillator has a high-harmonic PSF despite the periodic orbit is a unit circle.

# Multi-stable synchronization by a periodic input

- We apply a weak periodic input with a frequency  $\Omega = 5\omega$  to the designed oscillator with the high-harmonic harmonic PSF:

$$\frac{d\theta}{dt} = \omega + \varepsilon \mathbf{Z}(\theta) \cdot \mathbf{q}(t), \quad \mathbf{q}(t) = [\sin(\Omega t) \ 0]^\top.$$

- After averaging, the phase difference  $\phi = \theta - \Omega t/5$  between the oscillator and the periodic input obeys<sup>7</sup>

$$\frac{d\phi}{dt} \simeq -\frac{\varepsilon}{2} \cos(5\phi),$$

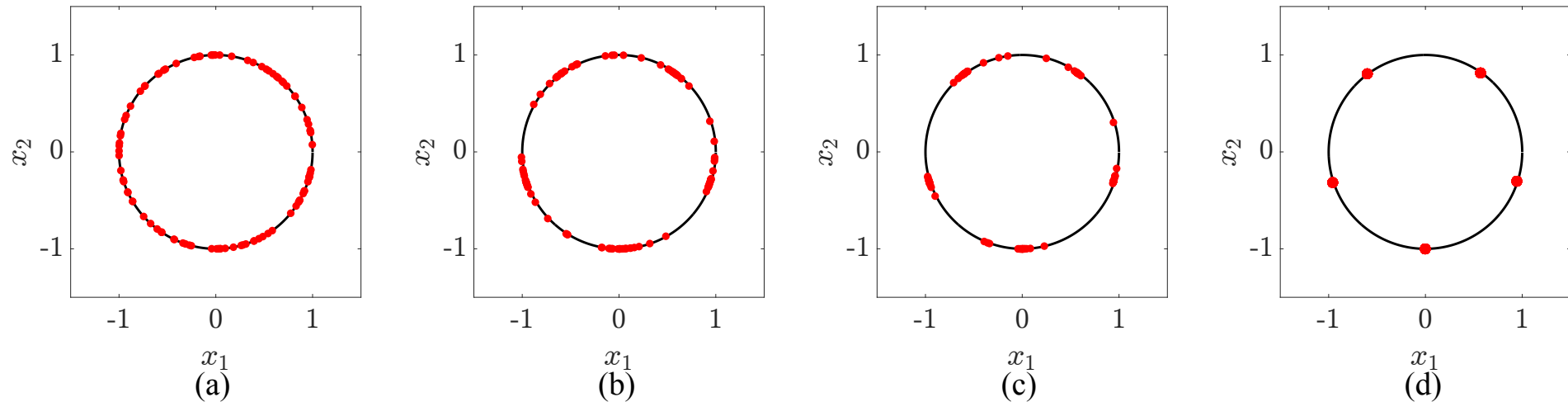
which has 5 stable fixed points satisfying  $\dot{\phi} = 0$  within  $\phi \in [0, 2\pi)$ .

- Population of these oscillators are expected to exhibit 5-cluster states when driven by the periodic input of  $\Omega = 5\omega$ .

---

<sup>7</sup>F.C. Hoppensteadt and E. Izhikevich, Weakly Connected Neural Networks, Springer, 1997.

# Multi-stable synchronization dynamics



Entrainment of 100 independent designed oscillators to the periodic input with multiple stable phase differences. (a)  $t = 0$ . (b)  $t = 2\pi$ . (c)  $t = 4\pi$ . (d)  $t = 16\pi$ .  $\epsilon = 0.01$ .

# Summary

- We proposed a method for designing 2D oscillators that possess stable prescribed periodic orbits and PSFs.
- We could reconstruct the dynamics of the FitzHugh-Nagumo oscillator.
- We were also able to design oscillators with an artificial periodic orbits and PSFs.

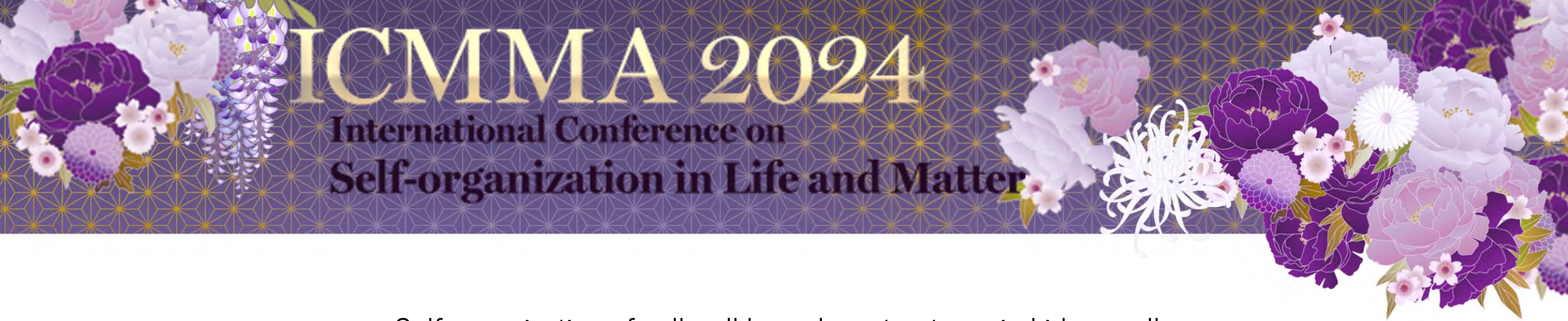
## References:

N. Namura, T. Ishii, and HN, Designing two-dimensional limit-cycle oscillators with prescribed trajectories and phase-response characteristics, IEEE Trans. Automatic Control, 69, 3144 (2024).

N. Namura and HN, Design of Limit-Cycle Oscillators with Prescribed Trajectories and Phase-Response Properties via Phase Reduction and Floquet Theory, Proc. 2023 62nd IEEE CDC, 3962 (2024).



**Thank you very much for your kind attention!**



## Self-organization of cell-cell boundary structures in kidney cells

Takashi Miura (Kyushu University)

Recently, the multicellular structure in biological systems has been extensively studied by combining experimental and theoretical approaches. On the other hand, shapes within cells have not received much attention. Individual cells show very complex structures, and understanding the mechanism of subcellular pattern formation should facilitate cell biology.

The kidney is a highly specialized organ for generating urine. Cells in the kidney have various unique shapes to implement their function. For example, Podocytes have numerous intricate secondary processes that act as filters to generate urine from blood. The cell-cell junction of renal tubules sometimes shows an intricate shape to facilitate paracellular transport. We formulated mathematical models of self-organization of these two cell-cell junctions and tried to verify the models experimentally.

### References

[1] Mechanism of interdigitation formation at apical boundary of MDCK cell. [Miyazaki S](#), Otani T, Sugihara K, Fujimori T, Furuse M, Miura T. *iScience*. 2023 Apr 21;26(5):106594. doi: 10.1016/j.isci.2023.106594. PMID: 37250331

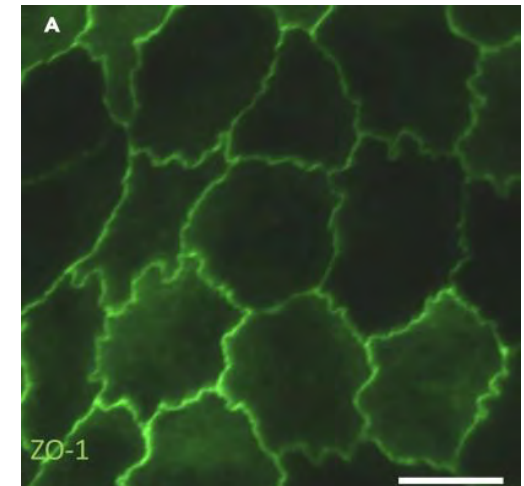


**Figure 1.** Interdigitation of cell-cell junction in MDCK cell sheet.

# Self-organization of cell-cell boundary structures in kidney cells

A fluorescence microscopy image of kidney cells. The image shows a complex network of green fluorescent structures, likely representing cell-cell boundary structures, against a dark background. The structures are highly branched and interconnected, forming a dense, web-like pattern. The fluorescence is bright and clear, highlighting the intricate details of the cell boundaries.

Takashi Miura  
Department of Anatomy and Cell Biology  
Kyushu University Graduate School of Medical Sciences



# Interdigitation of skull suture



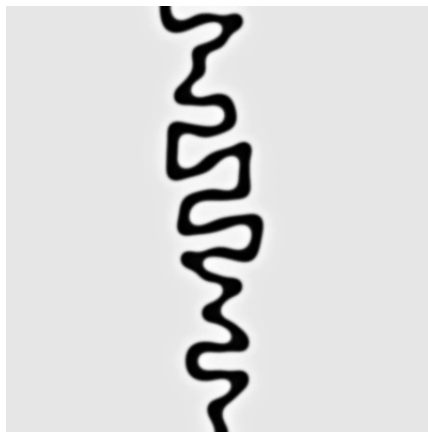
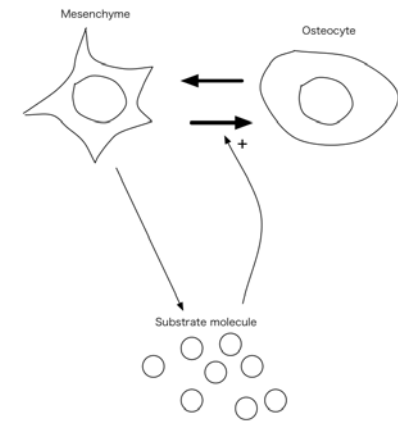
Newborn



Adult

u: 組織の分化度

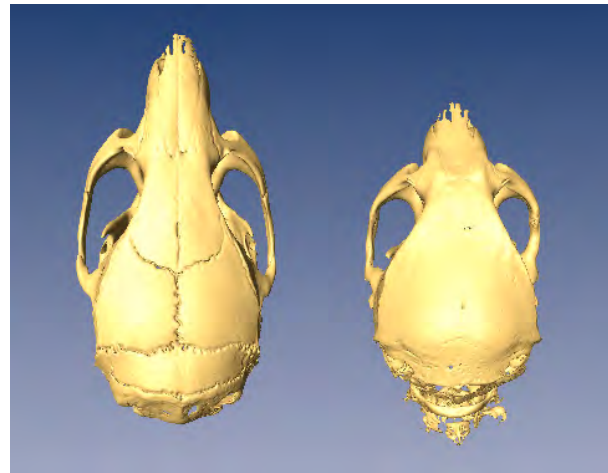
v: 基質因子



u: tissue  
differentiation state

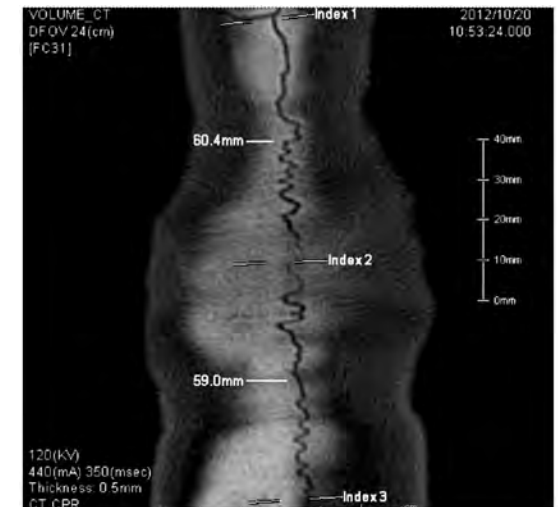


v: substrate



Wt

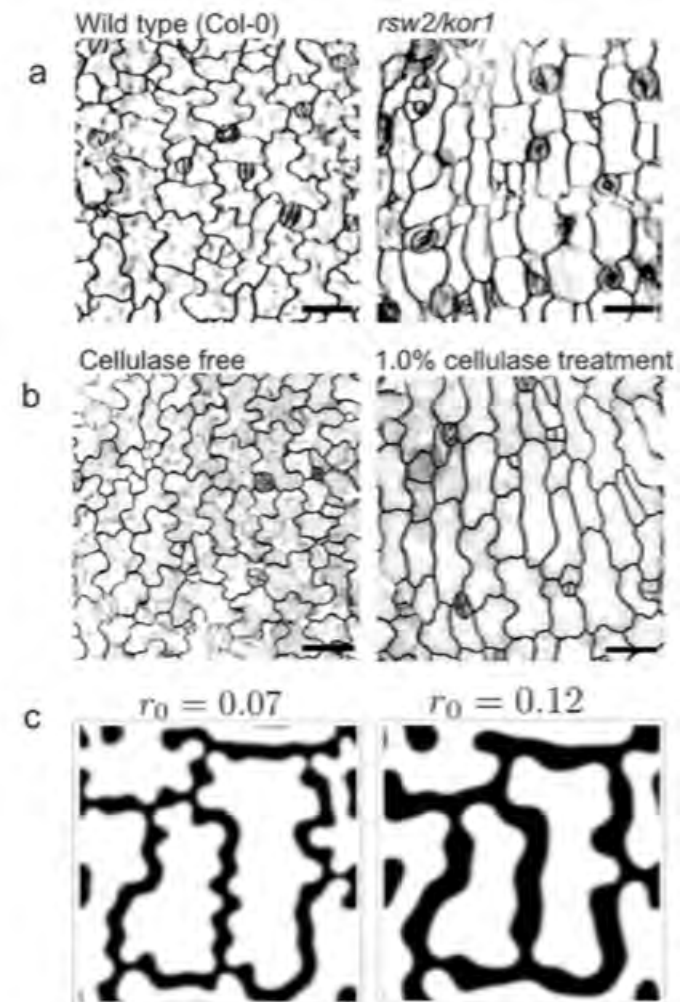
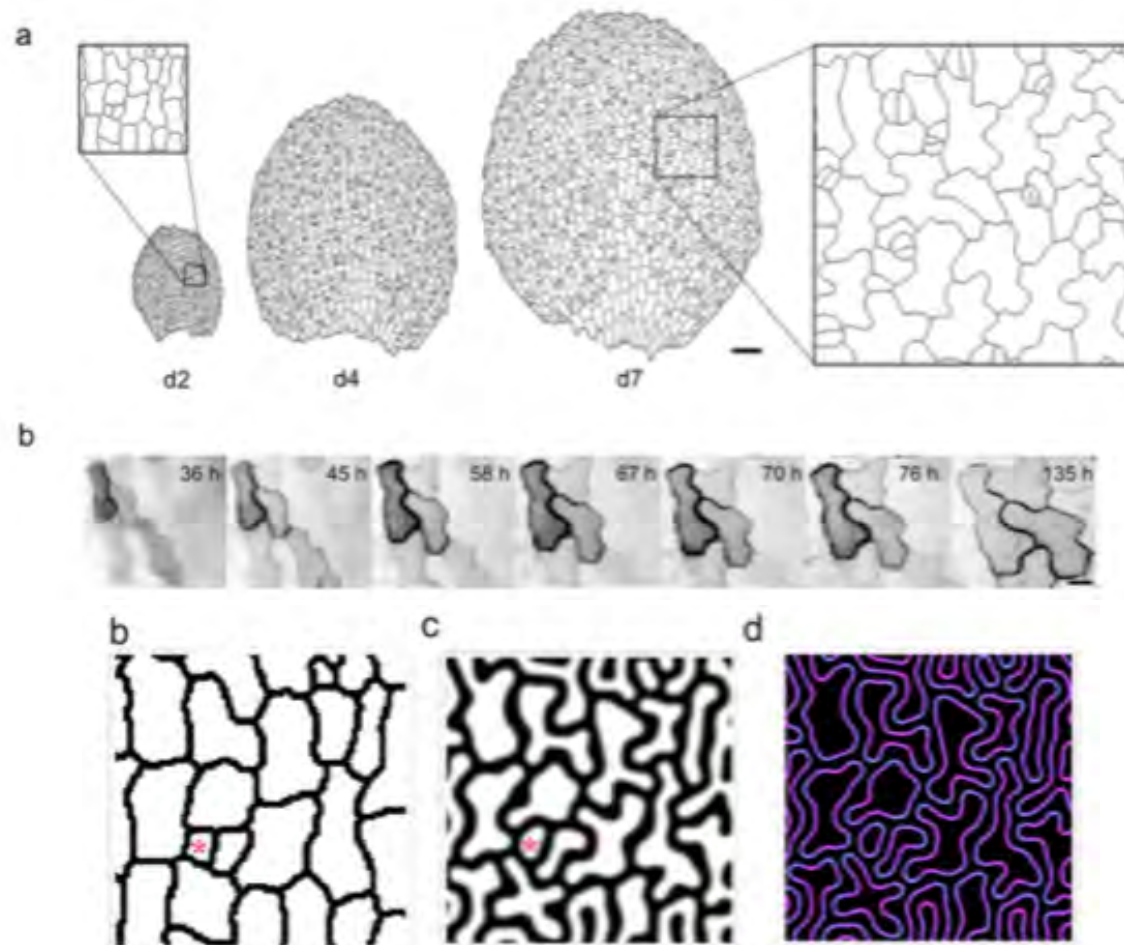
FGFR2c GOF Het





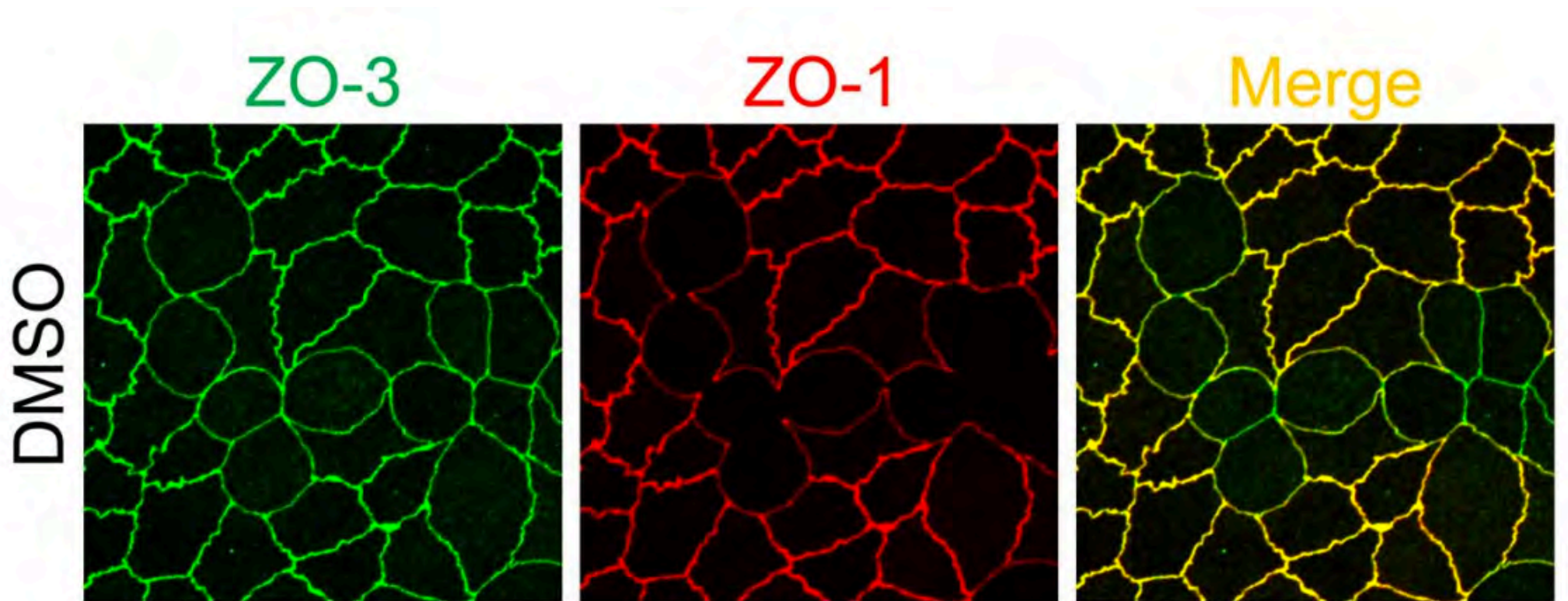


# Interdigitation of plant cell





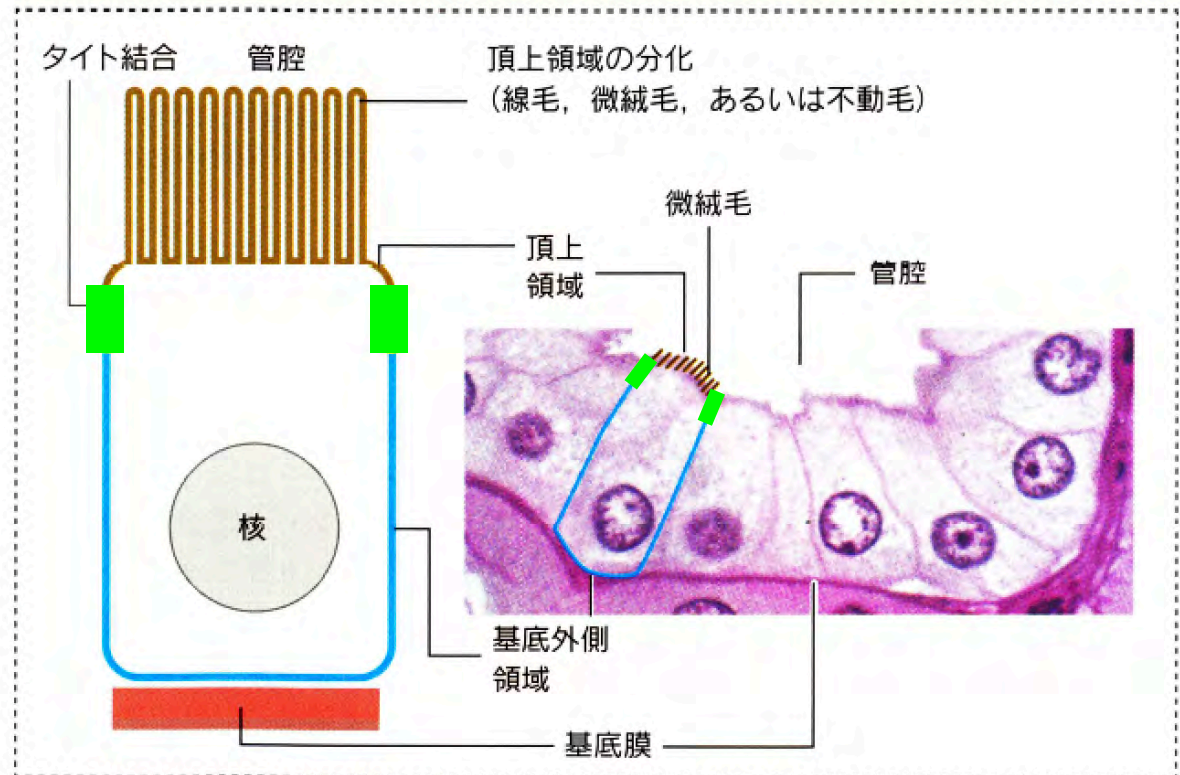
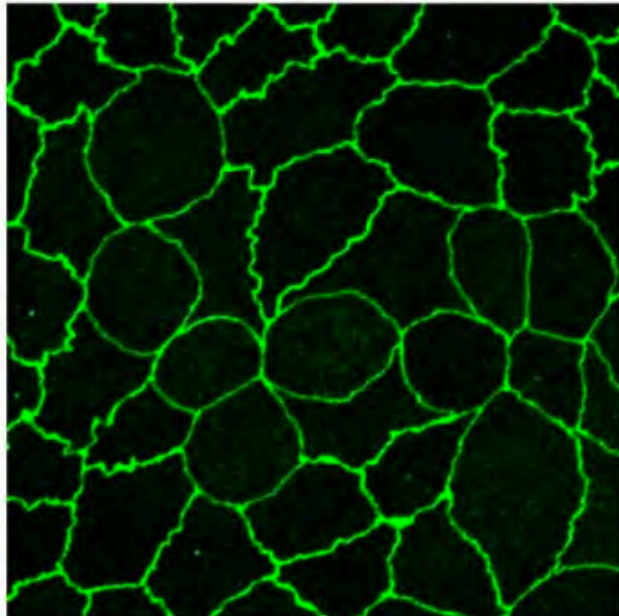
# Interdigitation of tight junction in MDCKII cells (Prof. Furuse, NIPS)





# Tight junction

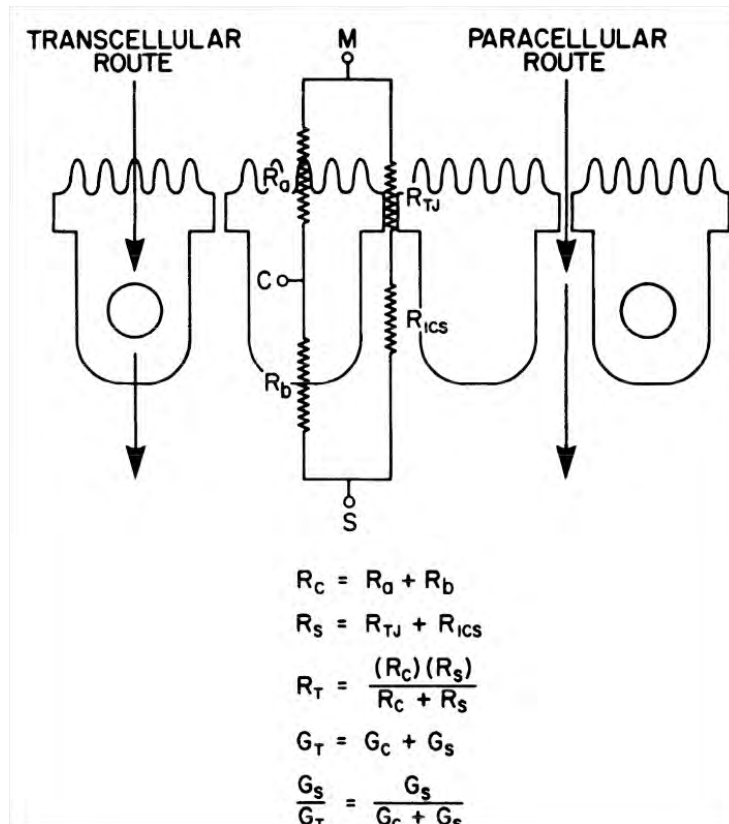
ZO-3



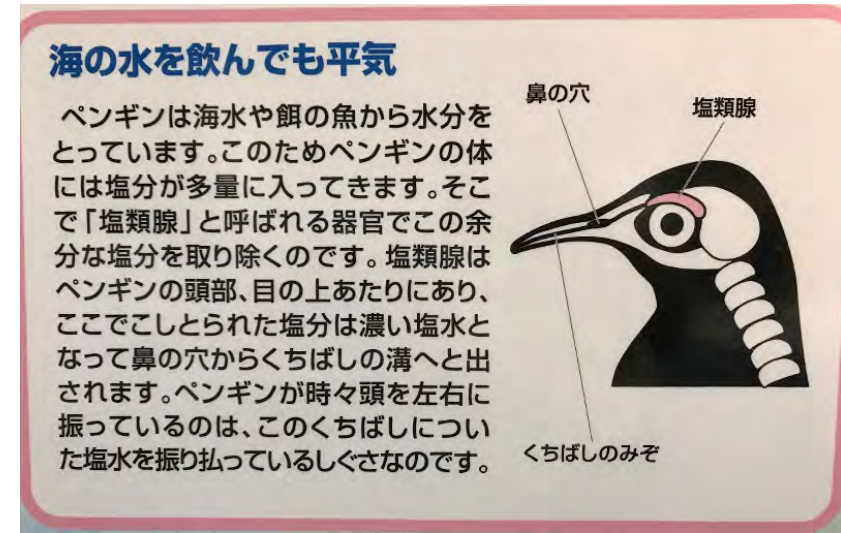
- Only tight junctions show interdigitation.



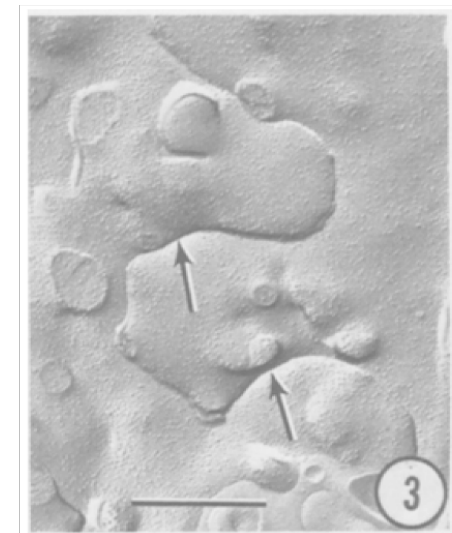
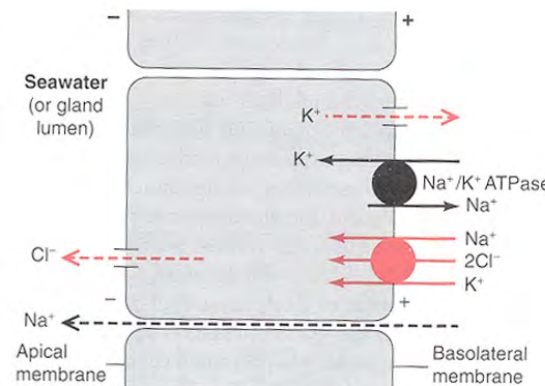
# Function: paracellular transport (Prof. Otani, NIPS > Tokyo metropolitan university)



Powell, D.W., *Am J Physiol*, 241: G275-88 (1981)

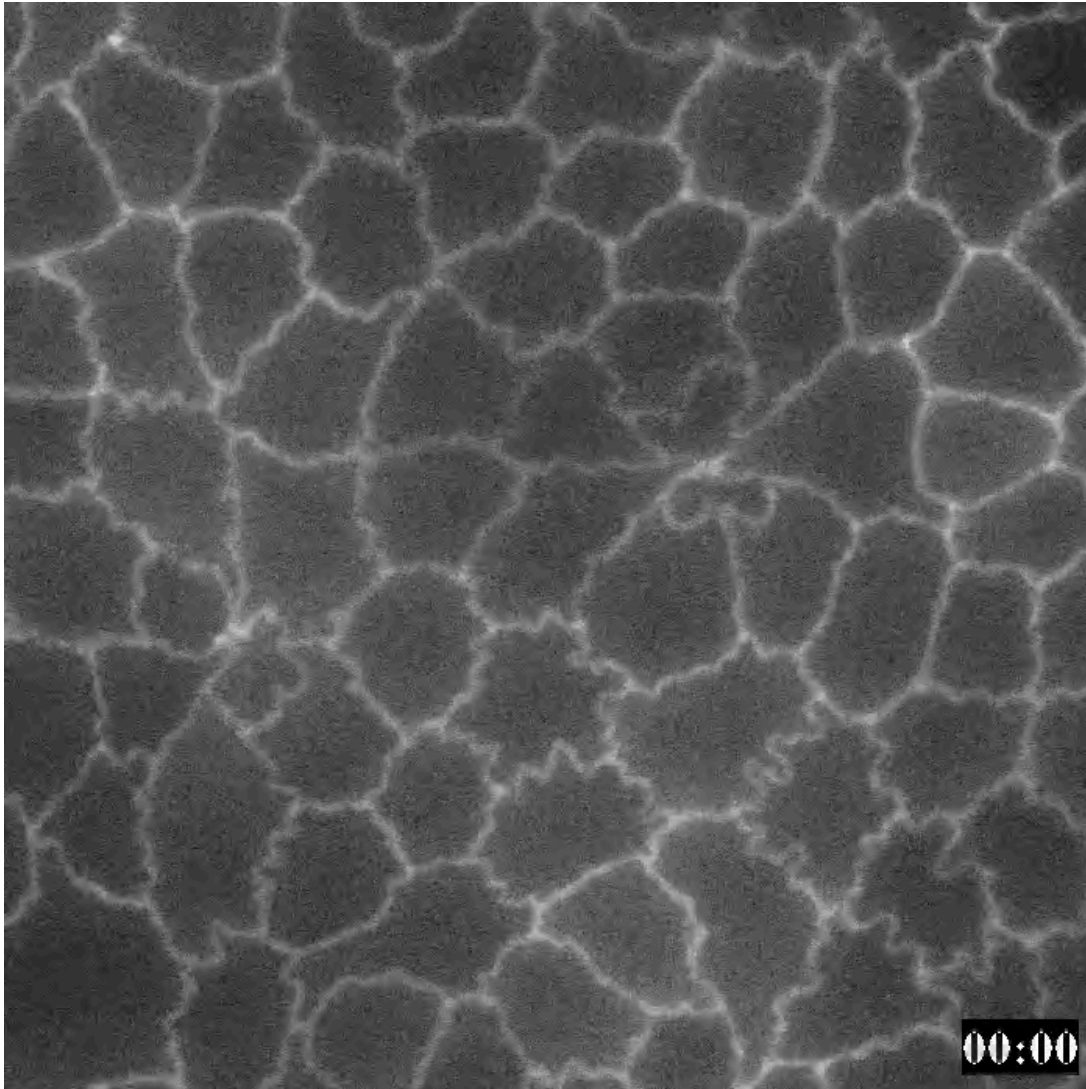


名古屋港水族館





# Time course of interdigititation formation in MDCKII cells



- Stochastic movement is involved
- No clear characteristic length
- 

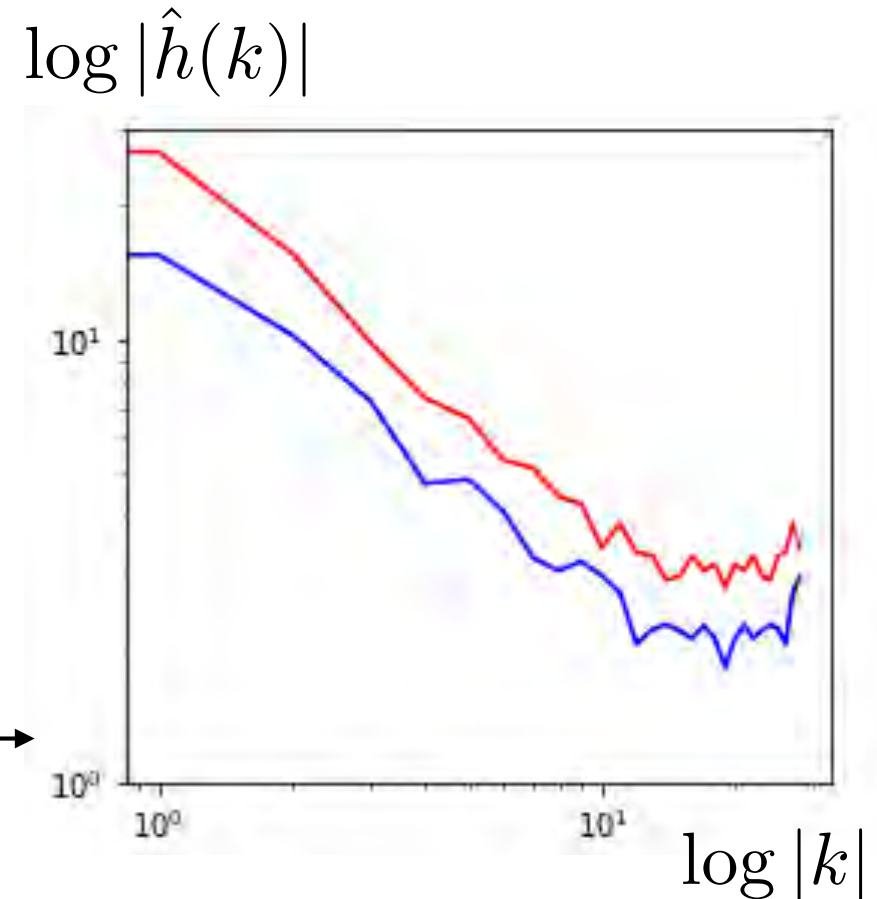
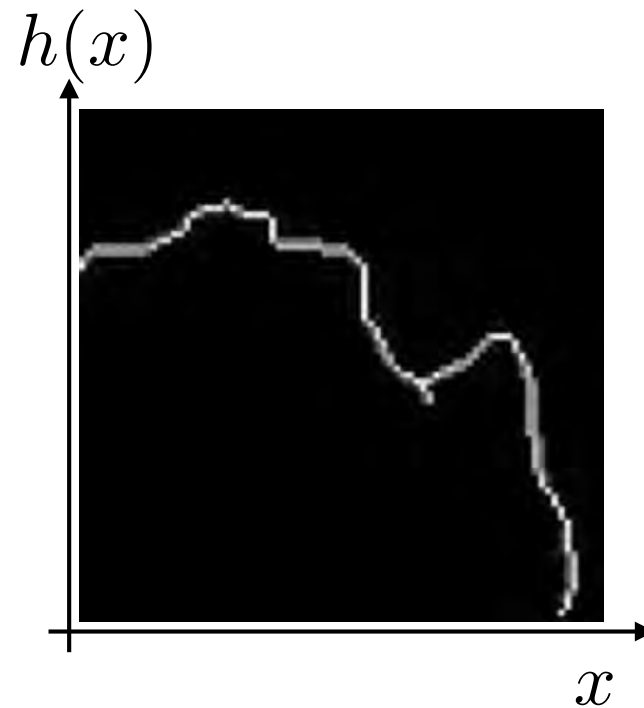
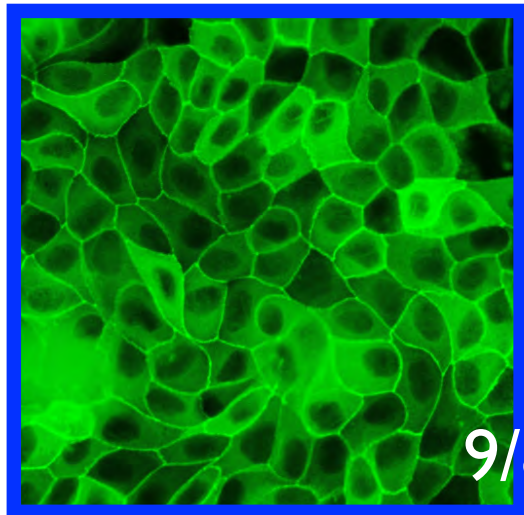
• [/10.1371/journal.pone.0104994](https://doi.org/10.1371/journal.pone.0104994)

Tokuda et al., 2014



Miyazaki-san

# Characteristics at frequency domain



- No peak wavenumber
- Show linearity at log-log plot



Naroda-san

# Edwards-Wilkinson equation (Edwards & Wilkinson 1982)

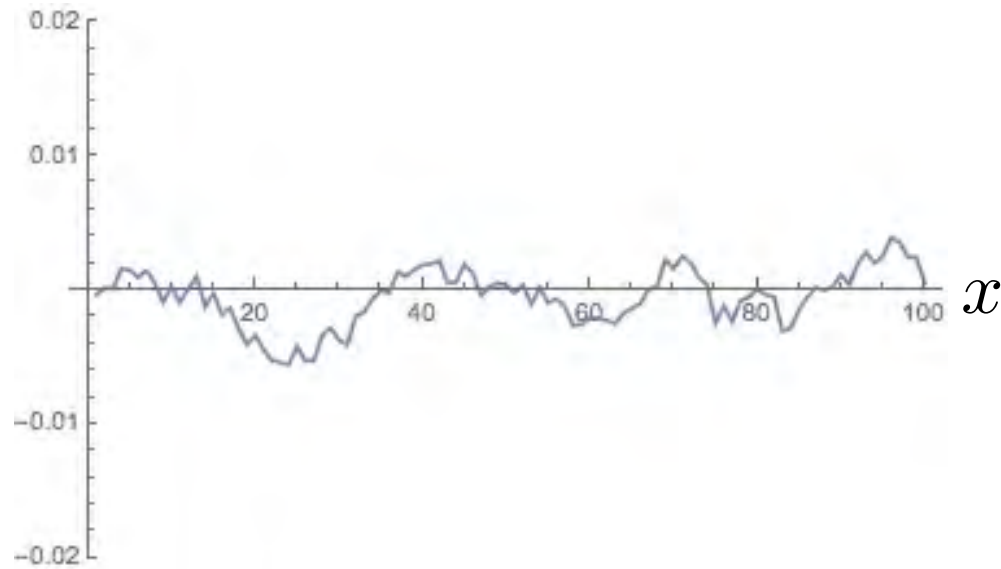
$$\frac{\partial h}{\partial t} = d_h \frac{\partial^2 h}{\partial x^2} + \eta(x, t)$$

Interface location

smoothing

noise

$h(x)$



- Linear system (exact solution available)
- Interface location is perturbed by noise  $\eta(x, t)$
- Diffusion term smoothen the interface



Reference: 本田勝也 「フラクタル」

Difficult to follow the brief description!

# Characteristics of the noise

- Sample mean is zero.

$$\langle \eta(x, t) \rangle = 0$$

- No spatial or temporal correlation.

$$\langle \eta(x, t) \eta(x', t') \rangle = 2D \delta(x - x') \delta(t - t')$$

$D$ : noise strength



# Governing equation in frequency domain

- $\hat{h}(k, t)$ : Fourier transform

$$h(x, t) = \sum \hat{h}(k, t) e^{ikx}$$

- $\frac{\partial h}{\partial t} = d_h \frac{\partial^2 h}{\partial x^2} + \eta(x, t)$  に代入

$$\frac{\partial \hat{h}(k, t)}{\partial t} = -k^2 \hat{h}(k, t) + \hat{\eta}(k, t)$$

# Characteristics of noise at frequency domain

- sample mean = 0

$$\langle \hat{\eta}(k, t) \rangle = 0$$

- Each frequency component is independent ( $L$ : system size,  $\delta$ : )

$$\langle \hat{\eta}(k, t) \hat{\eta}(k', t') \rangle = \frac{2D}{L} \delta(k - k') \delta(t - t')$$

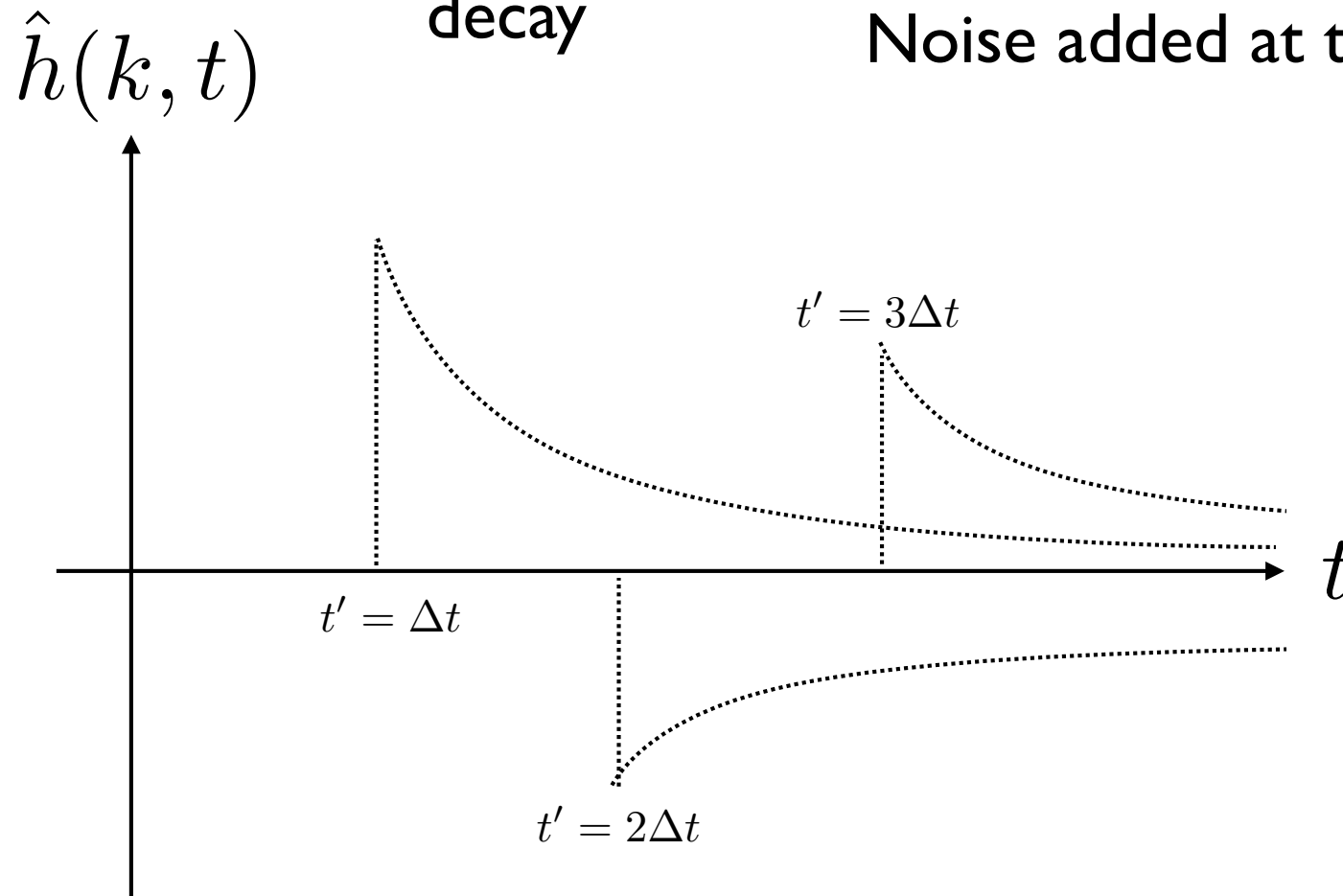
$D$  is constant for white noise.  $D(k)$  for colored noise.

# Solution of EW equation

$$\hat{h}(k, t) = \int_0^t e^{-k^2(t-t')} \hat{\eta}(k, t') dt'$$

decay

Noise added at time  $t'$





# Derivation of $\langle |\hat{h}(k, t)|^2 \rangle$

$$\langle \hat{h}(k, t)^2 \rangle = \left\langle \int_0^t \int_0^t e^{\hat{K}((t-t_1)+(t-t_2))} \eta(k, t_1) \eta(k, t_2) dt_1 dt_2 \right\rangle$$

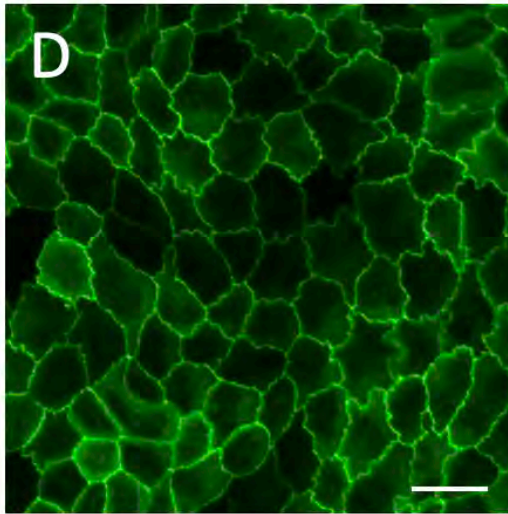
$$= \int_0^t e^{2\hat{K}(t-t_1)} \frac{2D}{L} dt_1 = \frac{2D}{L} e^{2\hat{K}t} \int_0^t e^{-2\hat{K}t_1} dt_1$$

$$= \frac{2D}{L} e^{2\hat{K}t} \left[ \frac{1}{-2\hat{K}} e^{-2\hat{K}t_1} \right]_0^t = \frac{D}{L} \hat{K}^{-1} (1 - e^{2\hat{K}t})$$

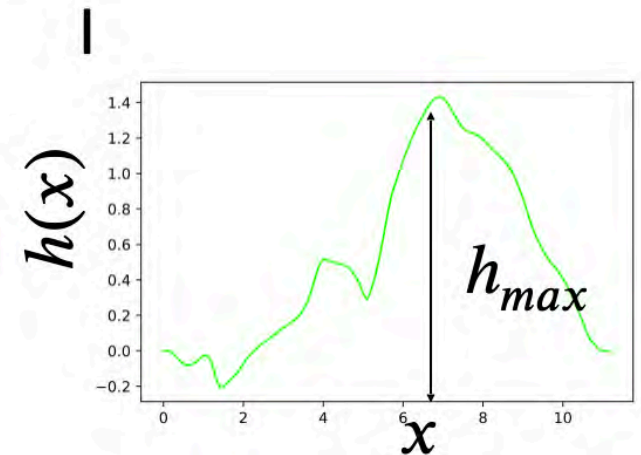
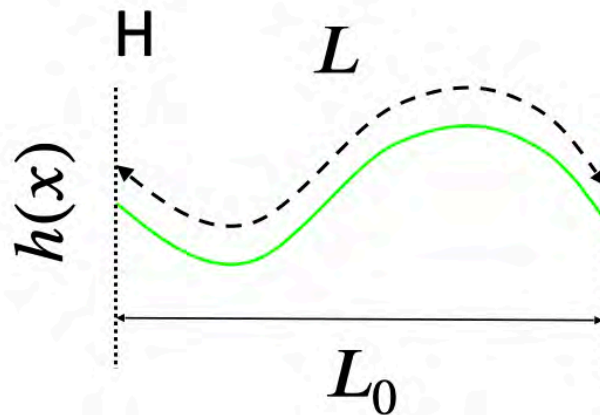
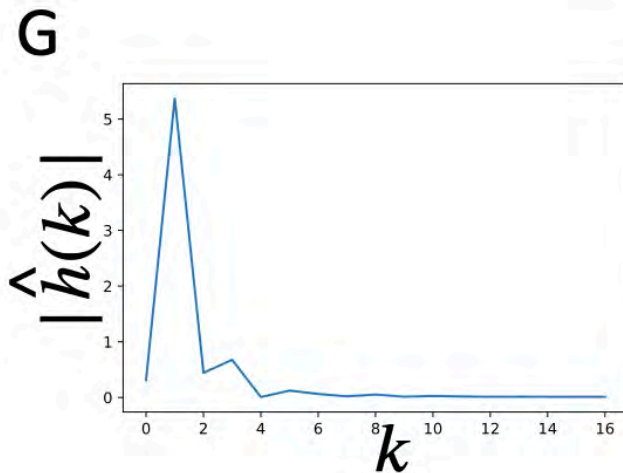
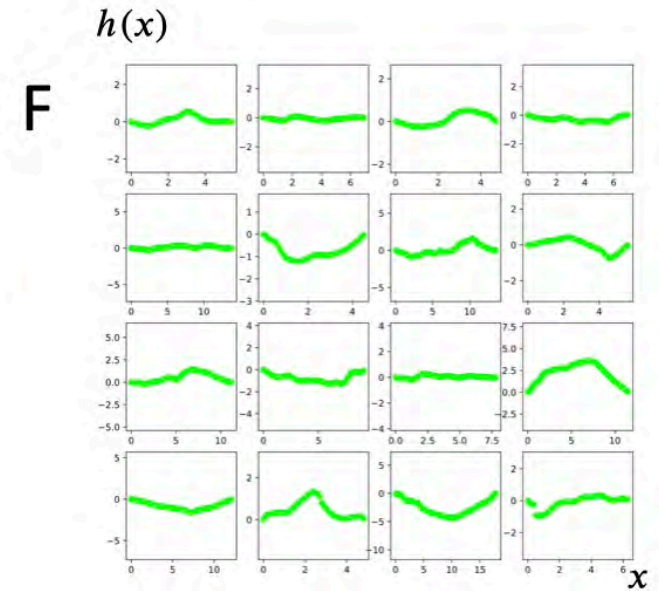
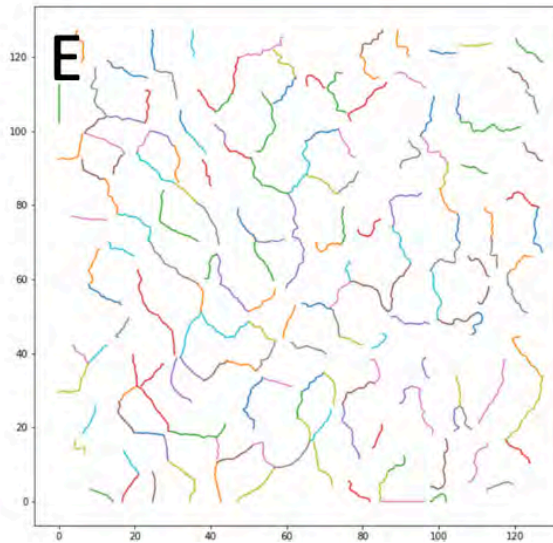
$$\langle \hat{h}(k, \infty)^2 \rangle = \frac{D}{L} \hat{K}^{-1} \quad \log(\langle \hat{h}(k, t)^2 \rangle) = -2 \log(k) + \log\left(\frac{2D}{L}\right)$$



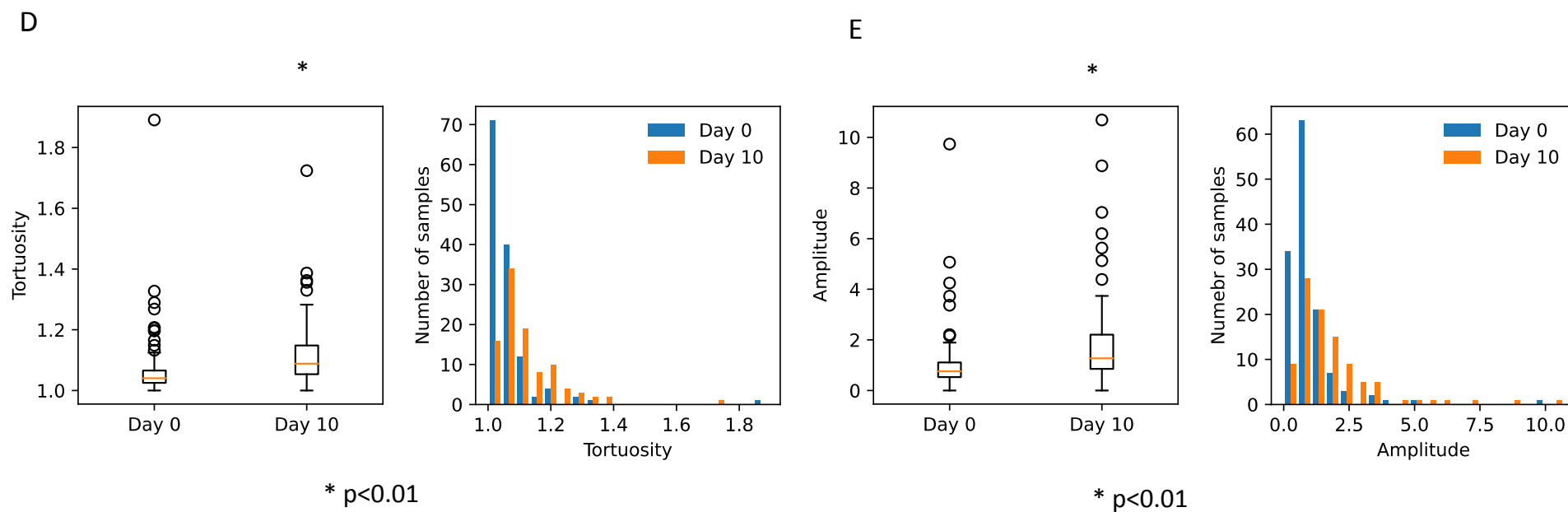
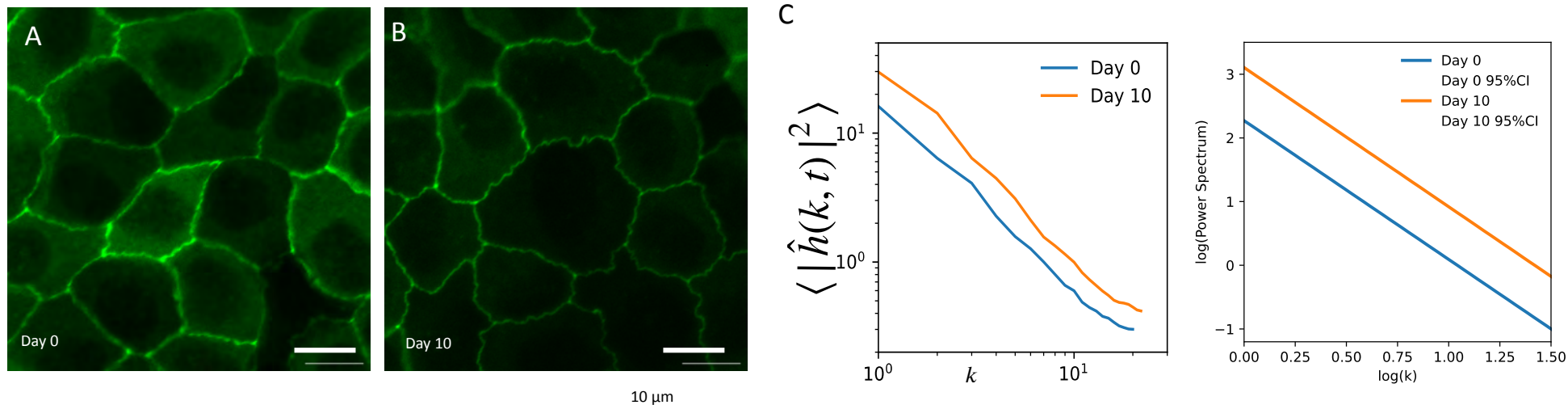
# Quantification of cell boundary shape by image processing



20  $\mu\text{m}$



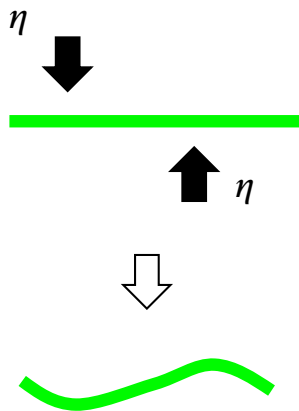
# Scaling



# Comparison of power spectrum generated by various models

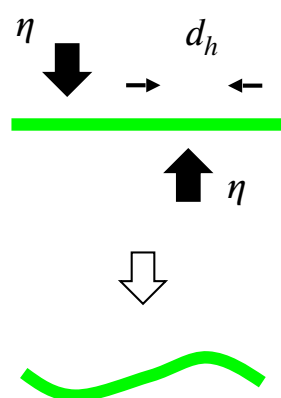
White noise

A



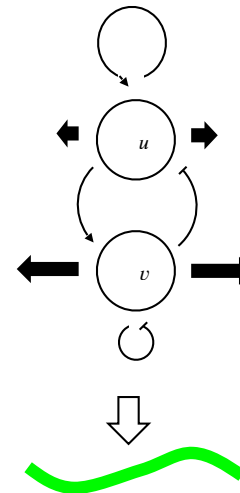
EW

B



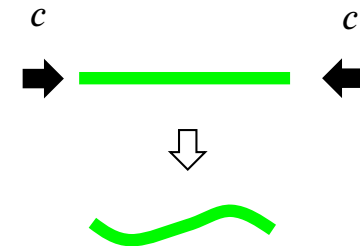
Turing

C



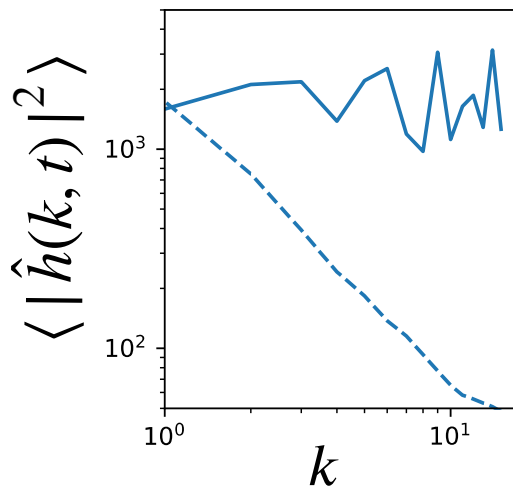
Buckling model

D



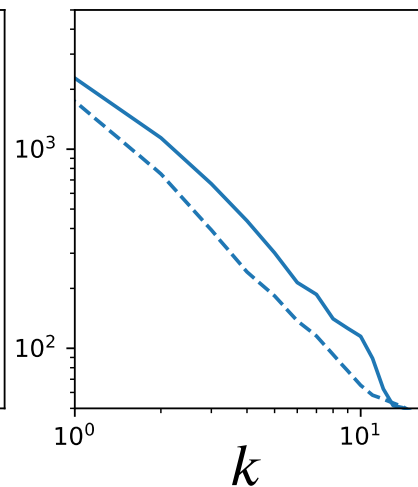
I

White noise



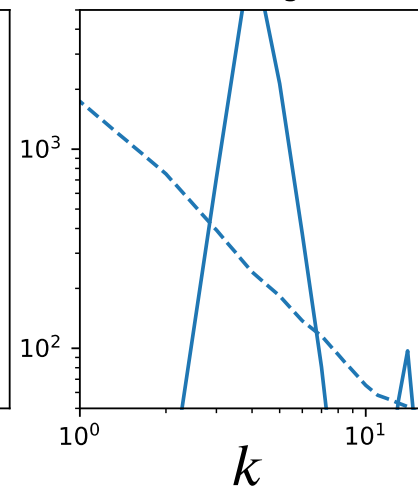
J

Edwards-Wilkinson



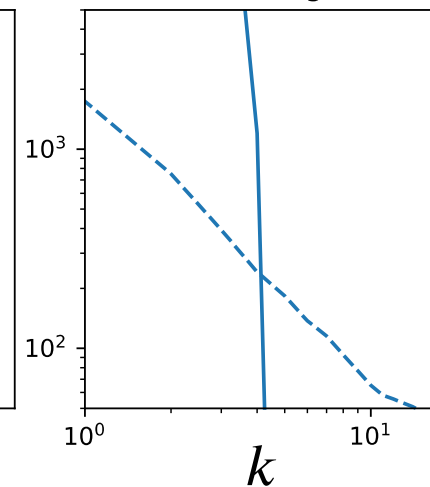
K

Turing

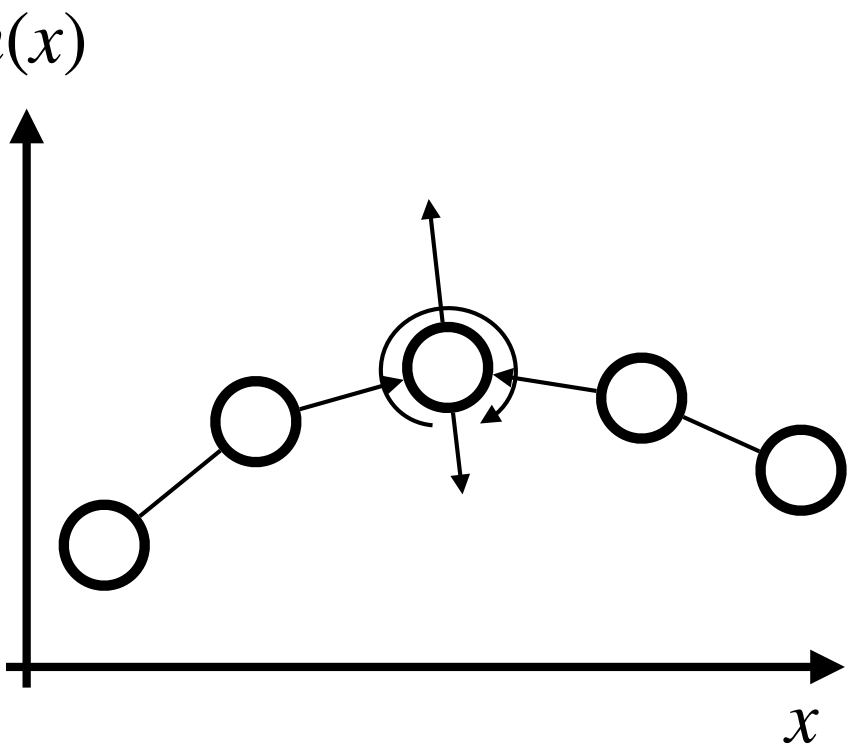


L

Buckling



# Buckling: Euler-Bernoulli model

$$0 = \underbrace{-\mu \frac{\partial h}{\partial t}}_{\text{Friction}} - \underbrace{P \frac{\partial^2 h}{\partial x^2}}_{\text{Load}} - \underbrace{EI \frac{\partial^4 h}{\partial x^4}}_{\text{Bending elasticity}}$$


The diagram illustrates a beam model in a coordinate system with a horizontal axis  $x$  and a vertical axis  $h(x)$ . The beam is represented by a series of four circles connected by straight lines, forming a curved shape. The central circle is highlighted with a double circle and has two arrows pointing vertically away from it, representing a load. A curved arrow around the central circle indicates bending elasticity. The beam starts at a low point on the left and ends at a low point on the right, with a peak in the middle.

- Force balance between friction, load and bending elasticity



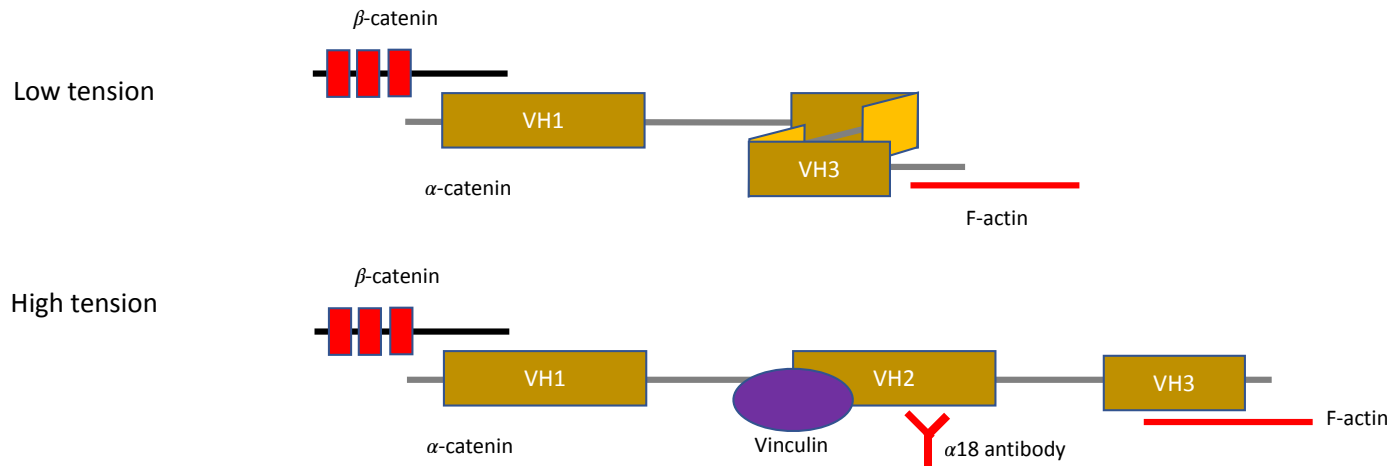
# Implementation of EW equation in MDCK cells

$$\frac{\partial h}{\partial t} = d_h \frac{\partial^2 h}{\partial x^2} + \eta(x, t)$$

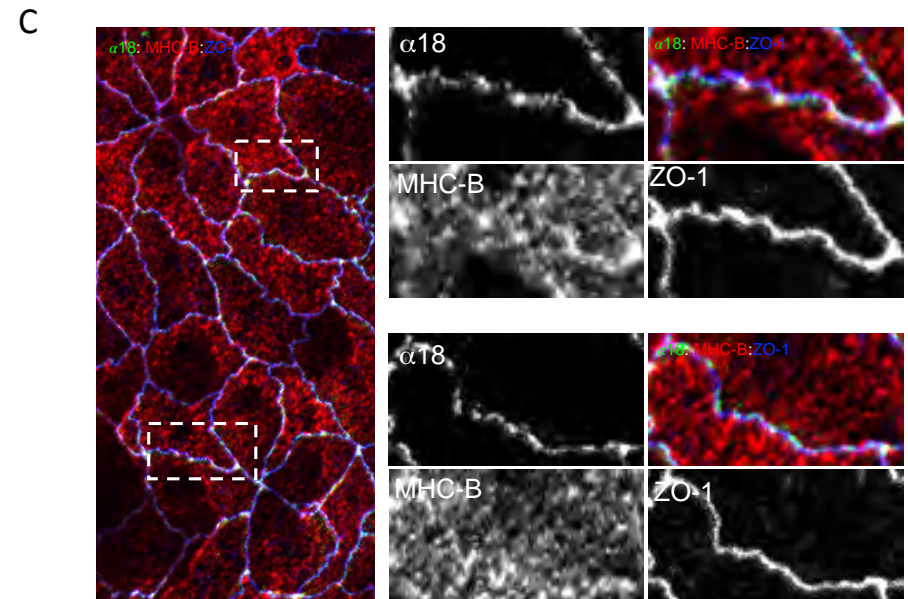
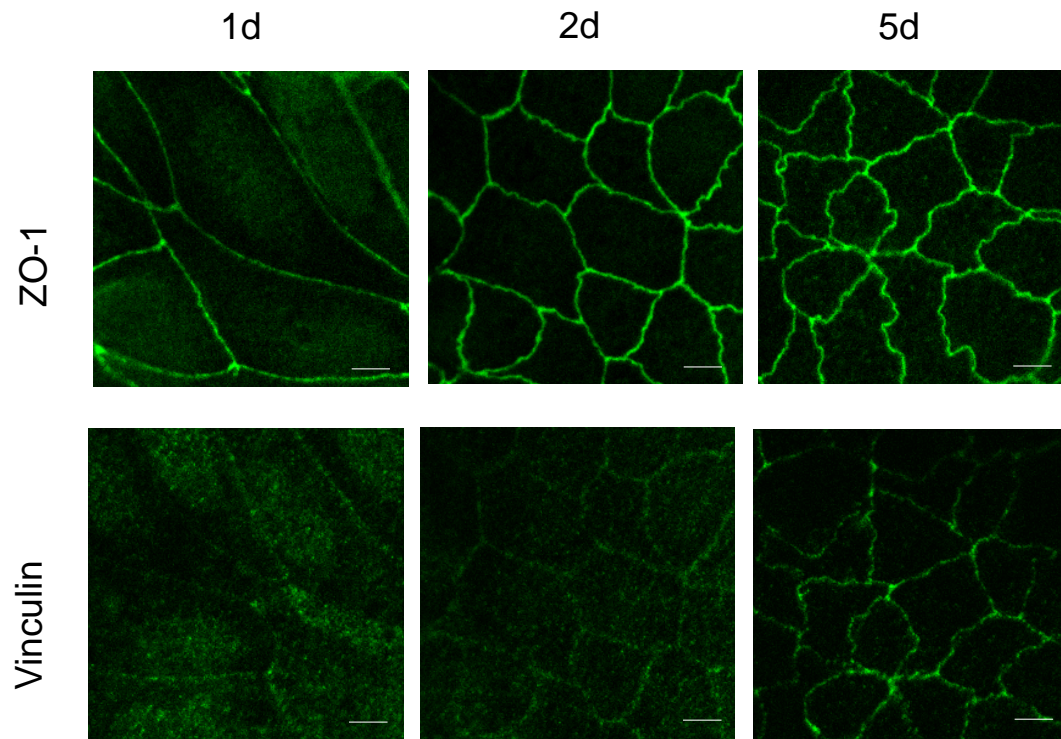
Interface location smoothing      noise

- Smoothing: minimization of tight junction length
- Noise: effect of myosin puncta?

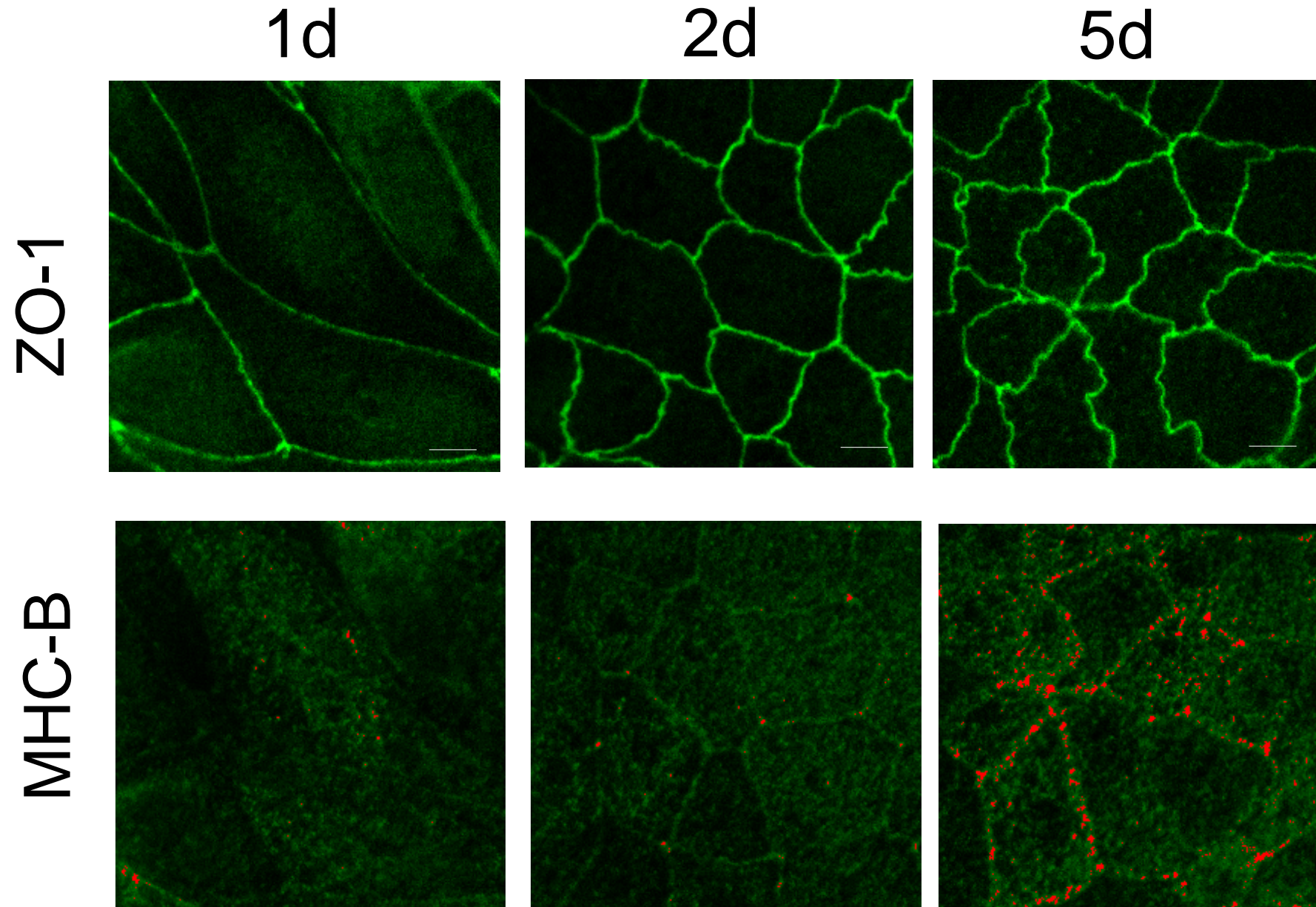
# Detection of external force at cell-cell junction



- $\alpha$ 18 antibody: detection of tensile force to tight junction



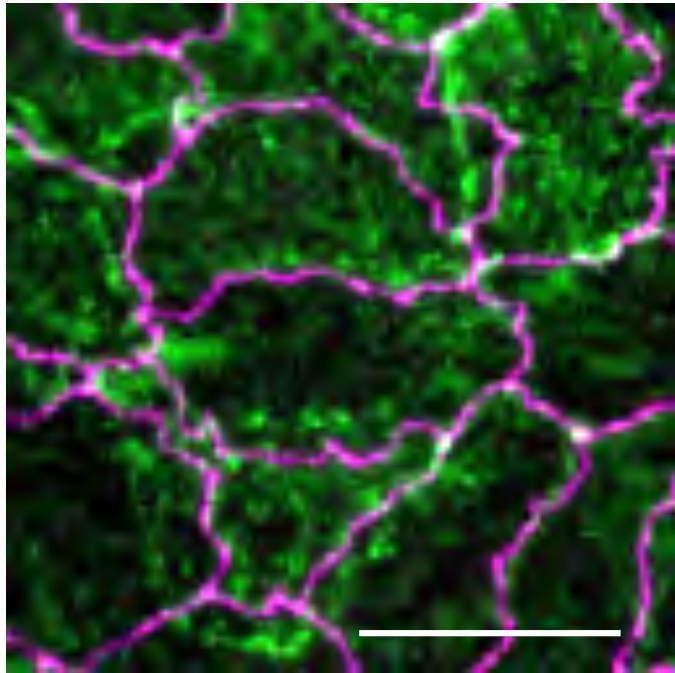
# Increased interdigitation and increased puncta number



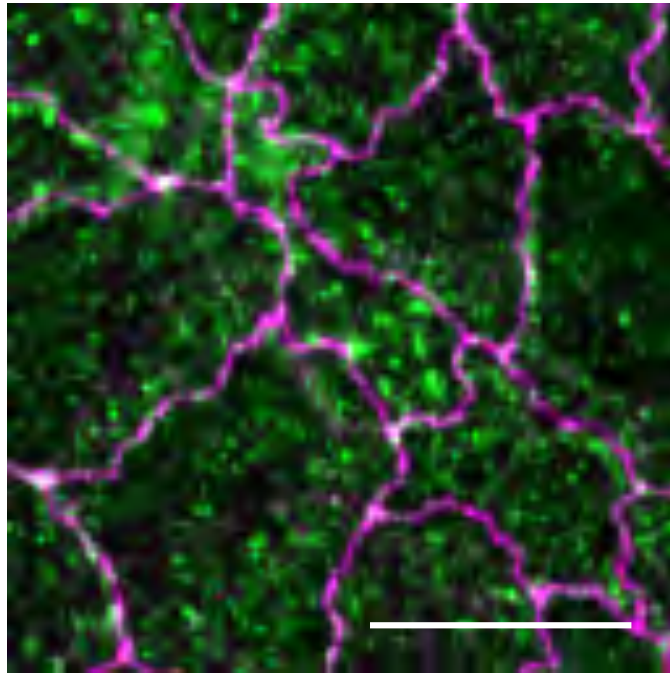


# Phosphorylation of myosin puncta

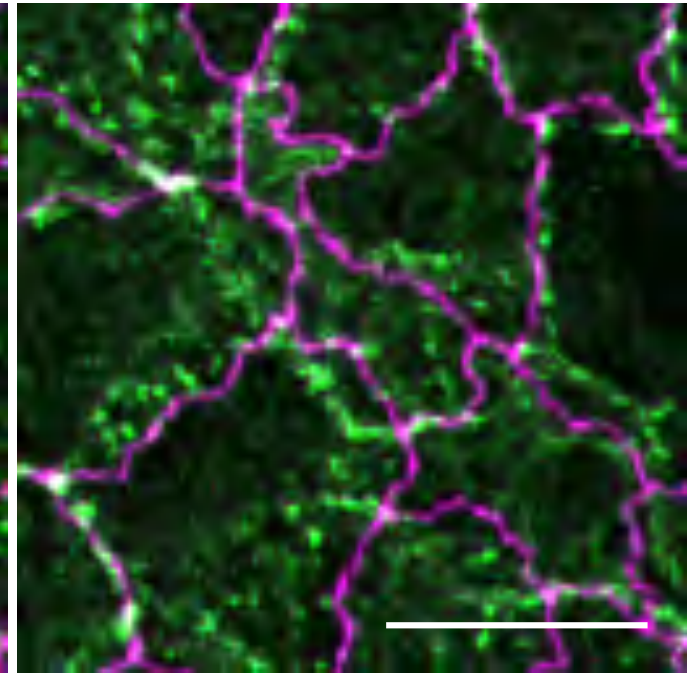
MHC-B:ZO-1



pS19-MLC:ZO-1

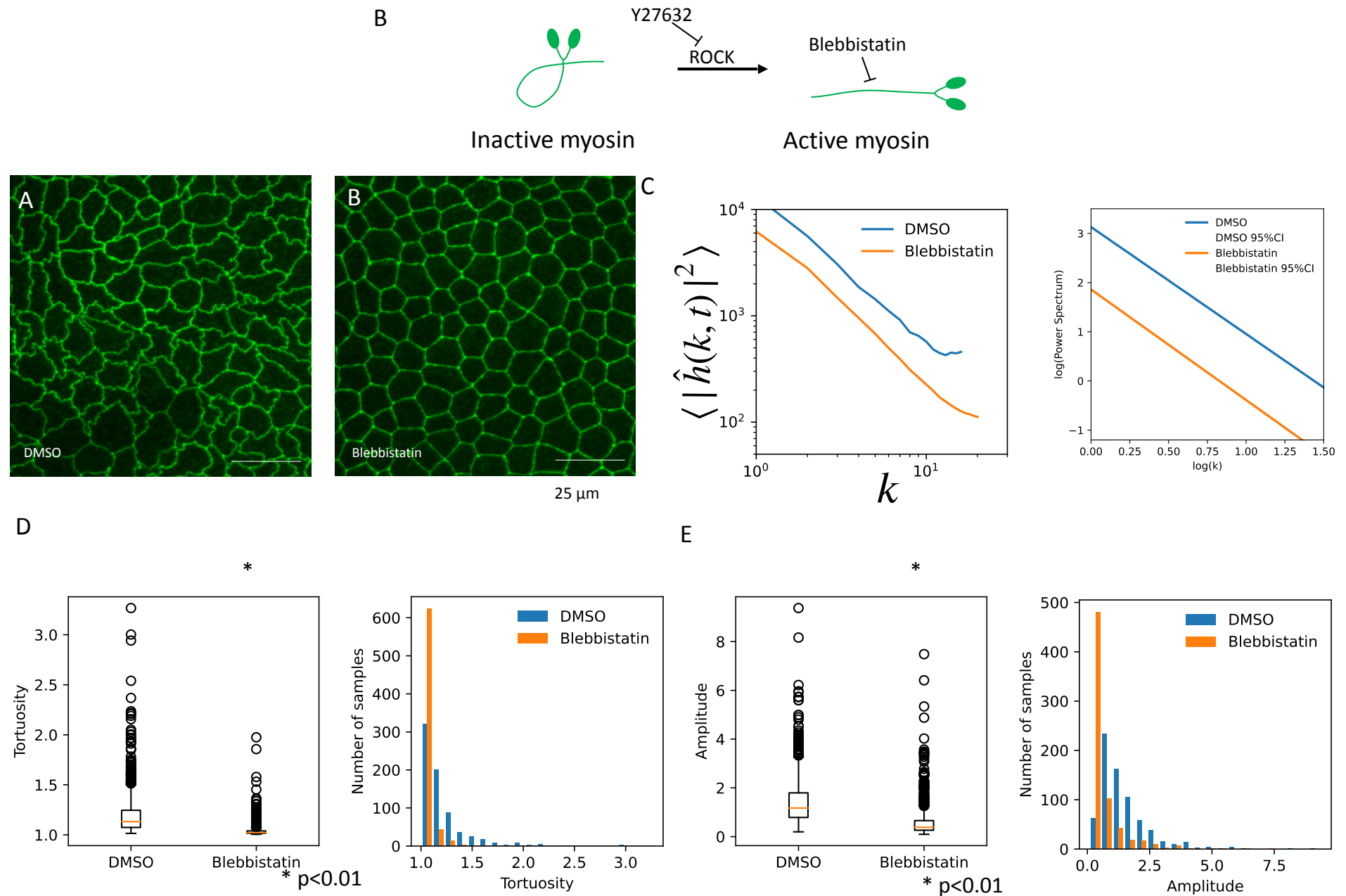


ppT18S19-MLC:ZO-1

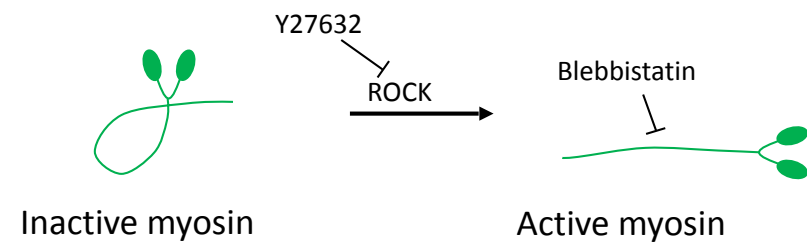
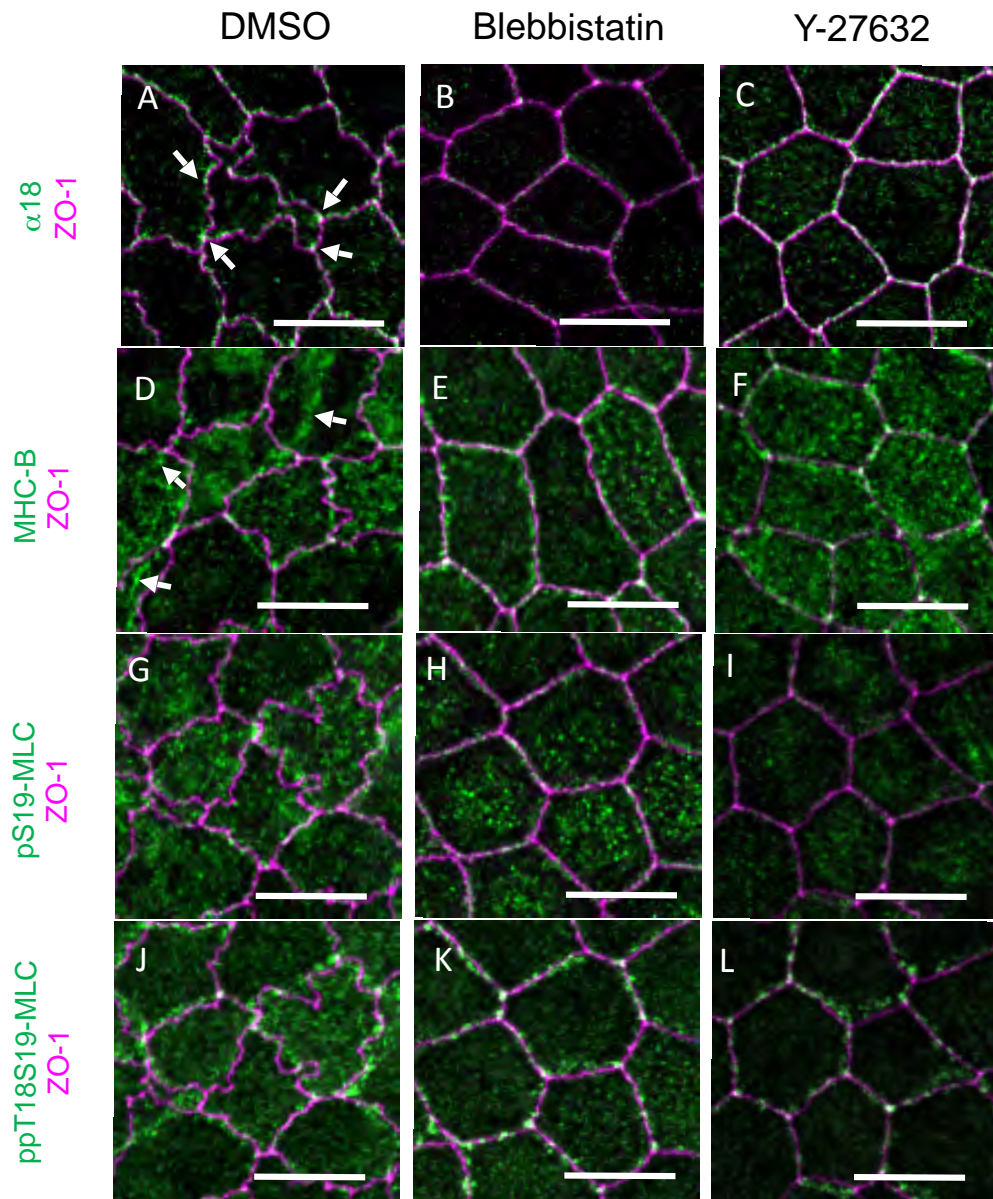




# Decrease of interdigitation by inhibition of myosin function



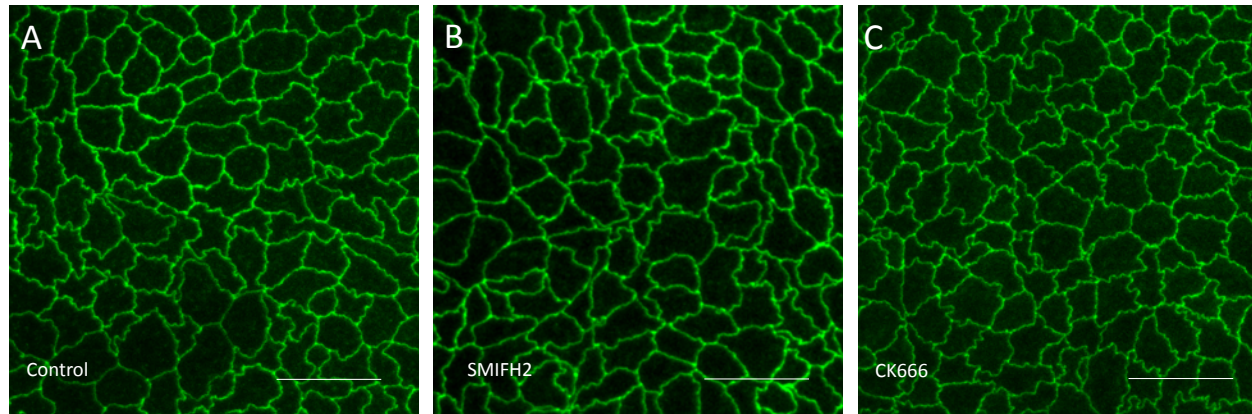
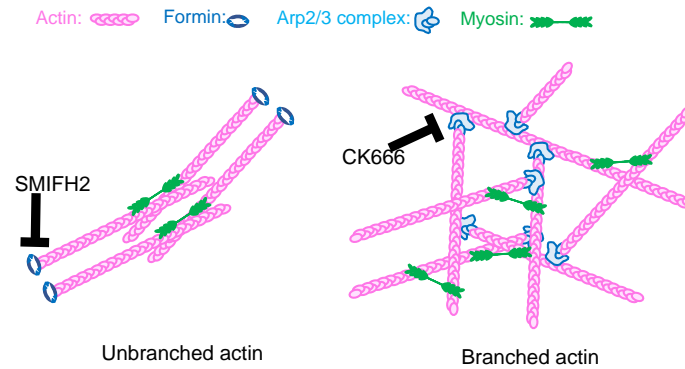
# Change of phosphorylation status by myosin inhibitors



- Consistent with the effect of Blebbistatin and Y-27632

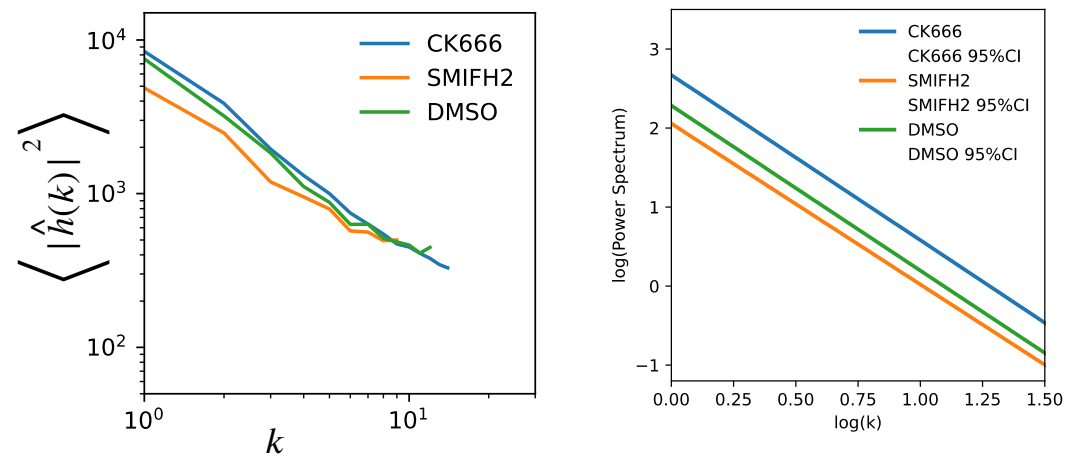
# Actin inhibitor does not affect scaling property

C

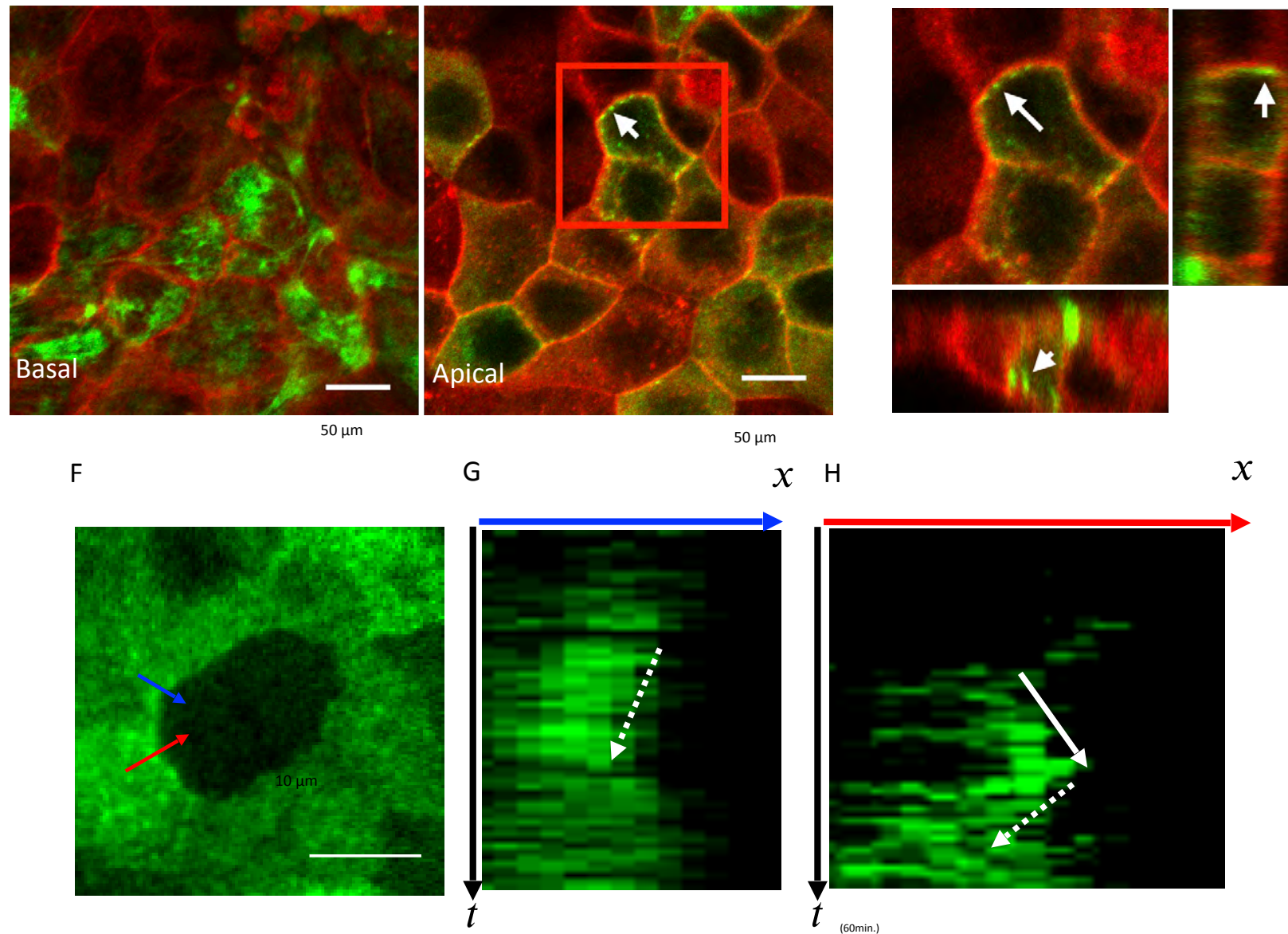


25  $\mu$ m

D



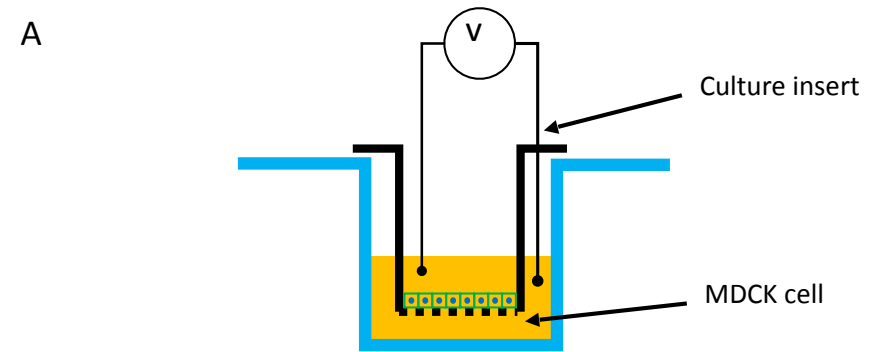
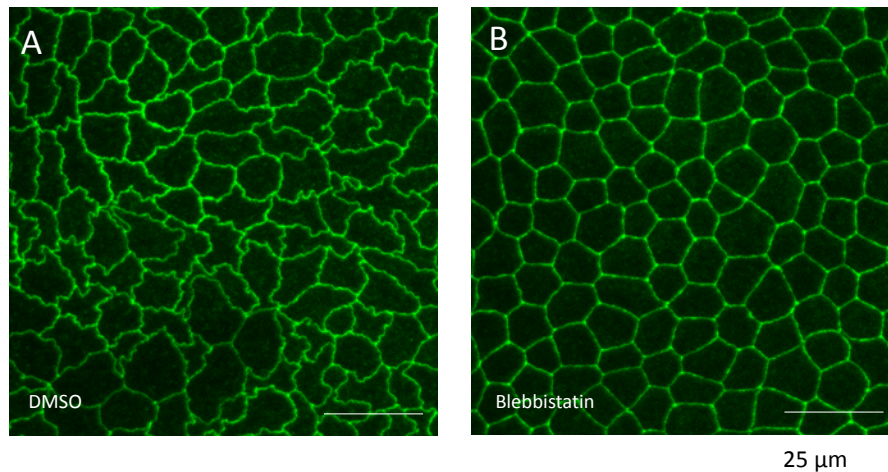
# Myosin puncta dynamics at tight junction



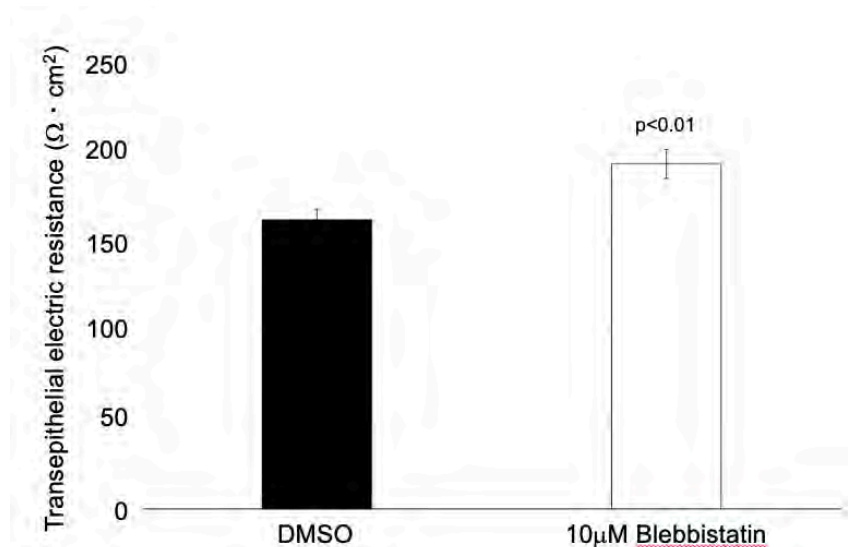
- Is myosin puncta pushing or pulling the tight junction?



# Effect of barrier function by changing interdigitation

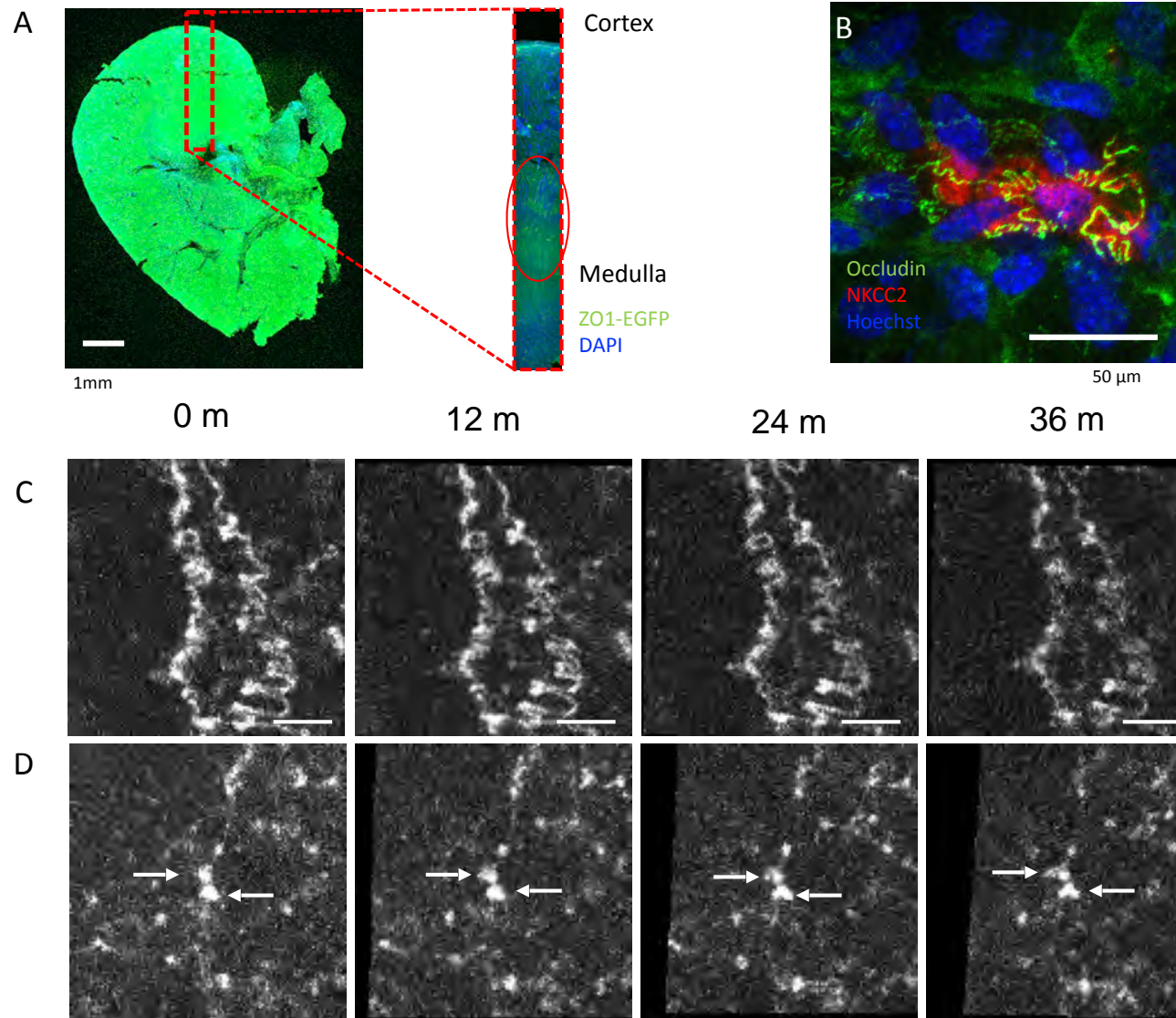


- Trans- Epithelial Resistance (TER)
- Decreased interdigitation > increased resistance





# Interdigititation formation in vivo



- Still unclear...

# Acknowledgement

- Kyushu University
  - Kei Sugihara
  - Yuto Naroda
  - Sintaro Miyazaki
- Hokkaido University
  - Shin-Ichiro Ei
  - Katsuhiko Sato
- NIPS
  - Mikio Furuse
  - Tetsuhisa Otani (now Tokyo Metropolitan University)
- NIBB
  - Toshihiko Fujimori



## Imperfect clocks that govern mammalian physiological functions –an overview from circadian to milliseconds scales

Aneta Stefanovska (Physics Department, Lancaster University, Lancaster, UK)

Oscillatory dynamics pervades the universe, appearing in systems on all scales. It can be studied within the frameworks of either autonomous or nonautonomous dynamics. Autonomous dynamical systems serve as mathematical models for the time-evolution of the states of isolated physical systems, whereas non-autonomous dynamics describes open systems subjected to external driving with time-varying parameters. While autonomous dynamics can be studied within the long-time asymptotic framework, including asymptotic stability, we will argue that this framework can be inadequate or unsuitable when investigating open systems and studying the parameter-dependence of their stability. We will provide a new framework for non-autonomous oscillatory dynamics, within which we can define intermittent phenomena such as intermittent phase synchronisation, evaluated as the stability of phase interactions.

We will briefly address the question of how to effectively analyse time series measured from open oscillatory systems operating on multiple timescales and with time-variable characteristic frequencies that enable explicit tracking of time-localised dynamical behaviour, as opposed to the traditional framework for dynamics analysis focused on time-independent dynamical systems and based on long-term statistics. Methods to extract modes, their coherences and couplings from measured data will be also presented.

We will then discuss imperfect biological clocks manifesting on scales of days, known as circadian or bi-circadian rhythms, metabolic oscillations acting on minutes' scales related to glucose and oxygen metabolism, to seconds' scales related to vascular motion, respiration, and heartbeat, to millisecond scales related to brain waves. Recent works on behavioural rhythms and rhythms related to cardiovascular and brain interactions in ageing will be reviewed.



# Imperfect clocks that govern mammalian physiological functions

An overview from circadian to milliseconds scales

Aneta Stefanovska

Physics Department, Lancaster University, Lancaster, UK

ICMMA 2024  
International conference on  
Self-organization in life and matter

Tokyo, 10 September 2024

## Recording simultaneous signals on multiple scales:

- Cardiovascular system (ECG, respiration) ●●●●●
- Brain (EEG, NIRS) ●●●●●
- Blood flow (LDF) ●●●●●
- Blood oxygenation (NIRS, ORS) ●●●●●
- Sympathetic nerve activity ■
- Cell metabolism (fluorescence) ●
- Cell membrane potential ●●
- Ion channels ●
- Oscillations on liquid helium ■

## Nonlinear and Biomedical Physics Group



Observation

Modelling

## Physical principles:

- Physical and mathematical models
- Non-autonomous dynamics
- Physics of ion channels
- Brain dynamics
- Glassy states in coupled oscillators
- Kuramoto model with time-varying parameters
- Chronotaxic systems ■

## Methods to cope with time-varying properties

- Time-frequency analysis
- Wavelet phase coherence
- Nonlinear mode decomposition
- Ridge extraction
- Bispectral analysis ■
- Mutual information ■
- Coupling functions ■
- Multiscale oscillatory dynamics analysis (MODA) toolbox

## Analysis

Collaborators

- LU Biology, UK
- LU Psychology, UK
- NHS, UK
- University of Pisa, Italy
- Josef Stefan Institute, Slovenia
- Oslo University Hospital, Norway
- University of Gothenburg, Sweden
- COSMOS, EU
- University of Ljubljana, Slovenia
- Czech Academy of Sciences
- Riken, Japan
- Virginia Commonwealth University, US
- University Clinical Centre, Slovenia
- Ss Cyril and Methodius University, Macedonia
- University Hospital Kano, Nigeria

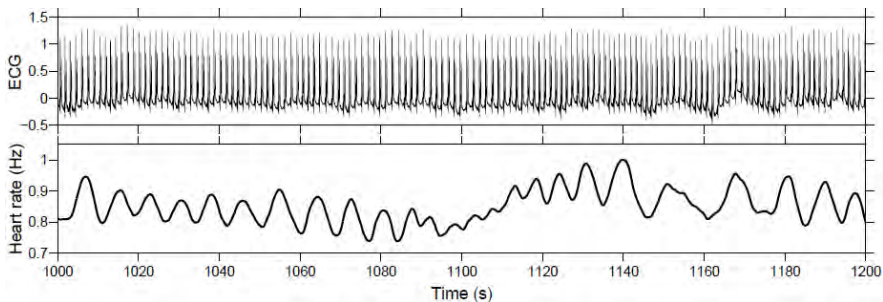
## Applications

- Anaesthesia ●●
- Autism ●
- Autonomic nervous system ■
- Cancer ●
- Dementia ●●
- Diabetes ■
- Heart failure ●
- Hypertension ●
- Hypoxia ●
- Intracranial pressure ●
- Malaria ■
- Secure communications ■

# Outline

- 1 Measurements on different timescales and size scales
  - Cardiovascular system
  - Brain dynamics
  - Cell metabolic oscillations
  - Circadian rhythms
- 2 A new framework for non-autonomous oscillatory dynamics
  - Oscillators and phase
  - Synchronisation and its quantification
  - Autonomous and non-autonomous systems
  - Non-autonomous dynamics: Chronotaxic systems
    - Time-varying frequency forcing
- 3 Time-series analysis methods
  - Time-dependent dynamics; interactions
  - The need for logarithmic frequency resolution
    - Multiscale oscillatory dynamics analysis – MODA
- 4 Applications
  - Ageing
    - Ageing of interactions
    - Coherence, ageing and treated hypertension
    - Ageing of the neurovascular unit
  - Methamphetamine
- 5 General summary

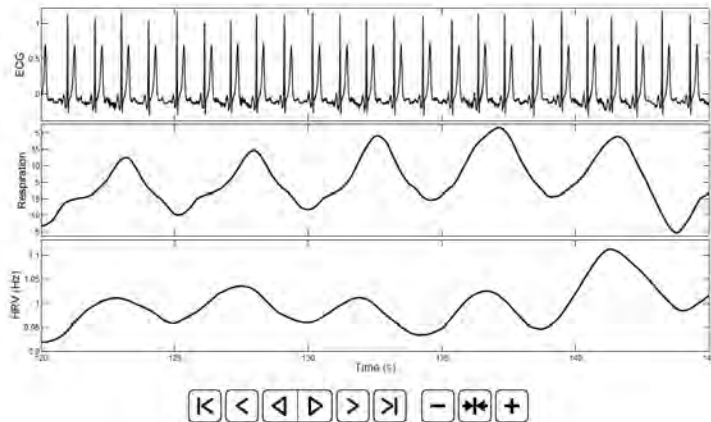
# Heart rate



- Cardiac frequency over time, mainly known as heart rate variability (HRV).
- Studied as a stochastic, a chaotic, or a discrete process.
- Can also be seen as the instantaneous frequency of the oscillatory cardiac pump, modulated by many other interacting oscillatory processes within the cardiovascular system.

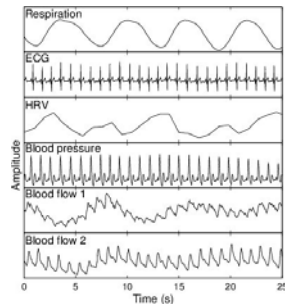
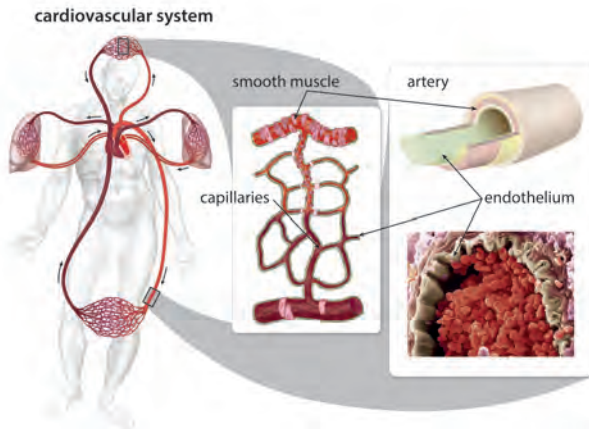


# Interactions with the respiration



The respiration modulates the cardiac frequency

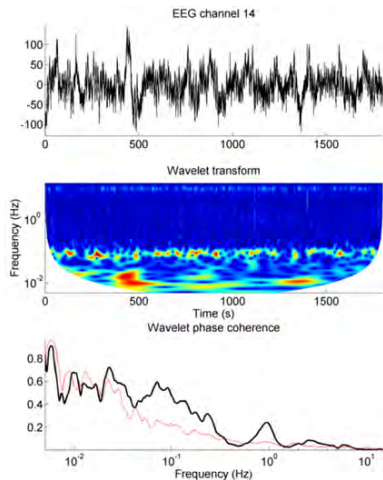
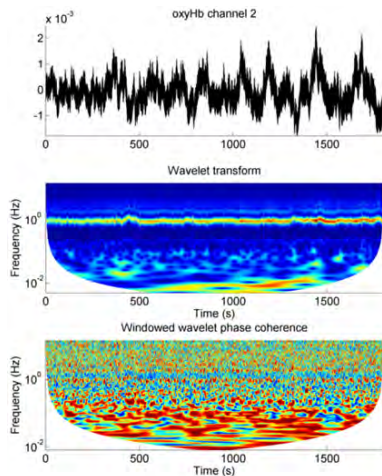
# Cardiovascular oscillations



Interval	Frequency (Hz)	Physiological origin
I	0.6-2.0	heartbeat
II	0.145-0.6	respiratory activity
III	0.052-0.145	intrinsic myogenic activity
IV	0.021-0.052	neurogenic (sympathetic) activity
V	0.0095-0.021	NO-dependent endothelial activity

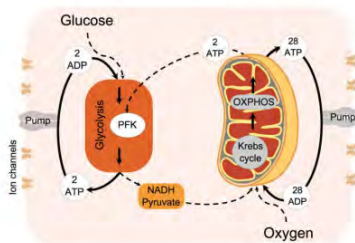
A Stefanovska, "Coupled oscillators: complex but not complicated cardiovascular and brain interactions", *IEEE Eng Med Biol Mag* **26**, 25-29, 2007.

# Oscillatory processes in the brain



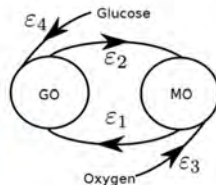
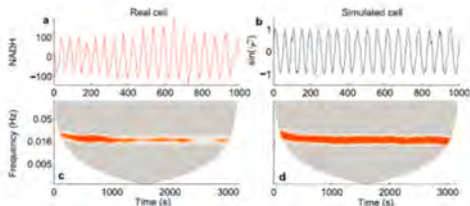
J Bjerkan, G Lancaster, B Megli, J Kobal, TJ Crawford, PVE McClintock, A Stefanovska, "Aging affects the phase coherence between spontaneous oscillations in **brain oxygenation and neural activity**", *Brain Res Bull* **201**: 110704, 2023.

# Cell metabolism



Lancaster, G., et al., *Scientific Reports* (2016)

- Cell metabolism is crucial to understand function and state
- ATP is a key molecule that powers many processes
- It's produced mainly by oxidative phosphorylation, with some glycolysis
- Cancer cells rely on glycolysis more than healthy cells



G Lancaster, Y F Suprunenko, K Jenkins, and A Stefanovska "Modelling chronotoxicity of cellular energy metabolism to facilitate the identification of altered metabolic states," *Scientific Reports* 6, 29584, 2016; J Rowland Adams, and A Stefanovska "Modeling cell energy metabolism as weighted networks of non-autonomous oscillators," *Frontiers in Physiology* 11, 613183, 2021.



# What happens when the circadian clock is removed?

Journal of Biological Rhythms

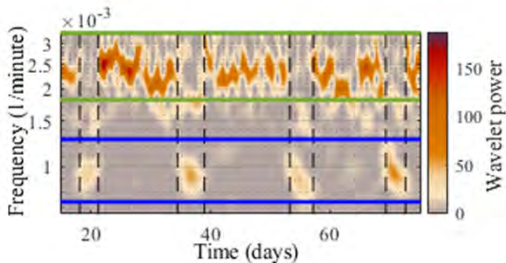
SAGE Publications

## Multiscale Time-resolved Analysis Reveals Remaining Behavioral Rhythms in Mice Without Canonical Circadian Clocks

Megan Morris, Shin Yamazaki, and Aneta

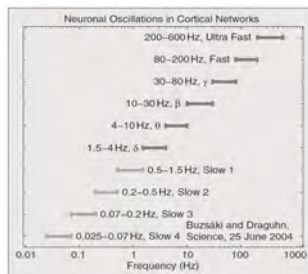
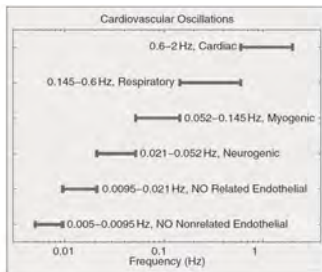
Stefanovska

- Inactivated circadian clock genes
- Kept in total darkness
- Constant access to food, water and a running wheel
- Recorded for 272 days



# What did we learn from the measurements?

- Oscillatory activity on many timescales: from circadian to fast brain oscillations
- Oscillatory processes interact – by mutually modulating their amplitudes and frequencies
- To better understand their interactions and couplings we need simultaneous measurements of relevant biological/physiological/neurophysiological processes
- Frequency intervals of cardiovascular oscillations and brain waves



# Oscillators and phase

Cyclic processes, a.k.a. **oscillators**, are ubiquitous across all scales: e.g. beating of heart, respiration, neuron impulses, planetary orbits.

Positions along cycle are calibrated by an angular variable  $\theta \in [0, 2\pi)$  called **phase**.

For oscillators with constant natural frequency  $f$ , phase  $\theta$  is calibrated so that

$$\text{instantaneous angular velocity } \dot{\theta}(t) = \text{angular frequency } 2\pi f$$

Oscillators can have **modulated** natural frequency  $f(t)$ , with slow dependence on  $t$ , in which case

$$\dot{\theta}(t) \approx 2\pi f(t)$$

# Synchronisation and its quantification

**Oscillator network:** a collection of oscillators that can influence each other.

**Synchronisation** in an oscillator network:

- the oscillators have **different natural frequencies**,
- and yet (due to their interactions with each other) they progress through their respective cycles at the **same rate**.

**Quantifying the level of synchronisation** among  $N$  oscillators:

$$\text{Kuramoto order parameter } r(t) := \frac{1}{N} \left| \sum_{j=1}^N e^{i\theta_j(t)} \right| \in [0, 1]$$

$r(t) \approx 1 \iff$  at time  $t$ , a large proportion of the oscillators' phases are closely aligned with each other



# Autonomous and non-autonomous systems

## Autonomous differential equations

$$\frac{dx(t)}{dt} = f(x(t))$$

describe **closed systems**: incorporate no influence from external forces that can vary over time.

More realistic framework for many situations: **non-autonomous differential equations** (Kloeden and Rasmussen, *Nonautonomous Dynamical Systems* (2011)).

$$\frac{dx(t)}{dt} = f_t(x(t))$$

If time is not taken explicitly into account, their behaviour is often misinterpreted as noise.

# Non-isolated systems usually treated as autonomous

The conventional mathematical modelling assumption that a system can be described by an autonomous differential equation represents the physical assumptions that

- The system can be treated either as entirely isolated from the rest of the universe, or
- At least as being unable to have any interaction with its environment apart from the dissipation of energy into its environment.

# Going outside the classical “( $t \rightarrow \infty$ )-behaviour of a dynamical system” framework

Most systems are significantly influenced by their time-evolving environment.

→ makes autonomous-dynamical-system model inappropriate.

All approaches based on behaviour of solutions as  $t \rightarrow \infty$  have the limitation that –

- for many systems, environmental influences cannot realistically be modelled as approximately following any given infinite-time deterministic or statistical behaviour!

This naturally motivates a theory of finite-time dynamical systems

- i.e. dynamical systems that have a start and an end.

This has been a recently growing area of study in dynamical systems theory.

P Kloeden, M Rasmussen, *Non-autonomous Dynamical Systems*, Springer, 2011.

J Newman, M Lucas, and A Stefanovska, Stabilization of cyclic processes by slowly varying forcing, *Chaos* **31**: 123129, 2021.

# Chronotaxic systems: Stability of non-autonomous interacting systems

A **new class** of non-autonomous oscillators:  
**chronotaxic systems** (from *chronos* – time and *taxis* – order).

Suprunenko, Clemson and Stefanovska, *PRL* (2013); *PRE* (2014)

Their definition is based on the following concepts –

- 1) Non-autonomous systems
- 2) Time-dependent point attractor (driven steady state)



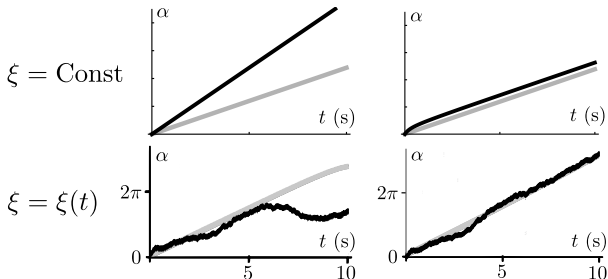
# Systems that can stabilise their rhythms

Conventional limit cycle oscillators:

- A phase shift does not decay and does not grow, it stays the same.
- A phase can be easily perturbed by any external perturbations.
- A frequency can be changed by the smallest continuous perturbation.

**Conventional:**  $\dot{\alpha} = \omega + \xi$

**New:**  $\dot{\alpha} = F(\alpha, t) + \xi$



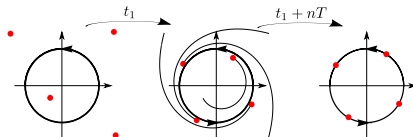
$\alpha$  is phase; gray – unperturbed ( $\xi = 0$ ); black – perturbed.

# Chronotaxic systems: Chronotaxic limit cycle

Conventional limit cycle oscillators, e.g. in polar coordinates  $(r, \alpha)$

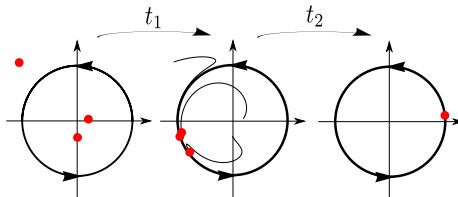
$$\begin{aligned}\dot{r} &= -\varepsilon r (r - r_0), \\ \dot{\alpha} &= \omega,\end{aligned}$$

are described by a phase  $\alpha$  with zero characteristic Lyapunov exponent.



In **chronotaxic systems** –

- By requiring that the **amplitude** is stable, all points must converge to a closed, isolated trajectory – a **limit cycle**.
- For the **frequency** to resist perturbations, once on the limit cycle the phase must be attracted to a **time-dependent point attractor**.
- Together these requirements for phase and amplitude create a **chronotaxic limit cycle**.



# Time-varying frequency forcing

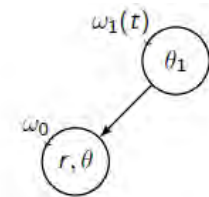
M Lucas, J Newman, and A Stefanovska, "Stabilisation of dynamics of oscillatory systems by non-autonomous perturbation", *Phys Rev E*, **97**: 042209, 2018.

Let us consider this model –

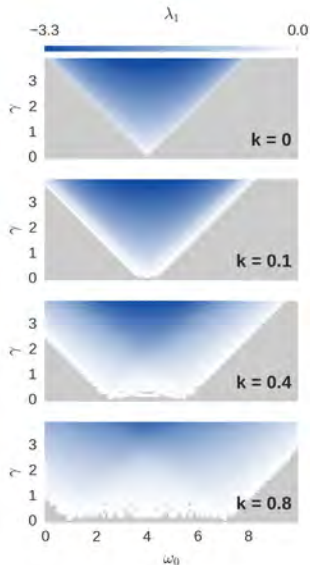
$$\begin{cases} \dot{r} = \epsilon(r_p - r)r \\ \dot{\theta} = \omega_0 + \gamma \sin(\theta - \theta_1(t)) \end{cases}$$

$$\dot{\theta}_1 = \omega_1(1 + kf(\omega_m t))$$

where  $f$  is an arbitrary function bounded in  $[-1,1]$  set to a sine for clarity and simplicity.  $k$  controls the **modulation amplitude**.



# The synchronisation region is widening



The synchronisation region (blue, *i.e.*  $\lambda_1 < 0$ ) increases as the amplitude of the modulation  $k$  is increased (top to bottom)<sup>a</sup>.

The system is more stable when the frequency is time-varying

The stronger the modulation, the more stable the system

---

<sup>a</sup> Synchronization occurs when the interaction is stable: then the phase difference is bounded, or the Lyapunov exponent is negative



# Is the effect present in networks?

Let us consider a generic driven network of  $N$  identical phase oscillators  $\theta_i$  with frequency  $\omega$ ,

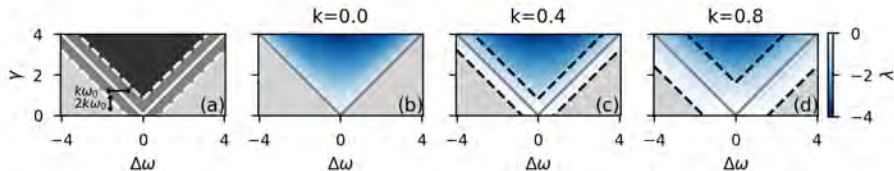
$$\dot{\theta}_i = \omega + D \sum_{j=1}^N A_{ij} \sin(\theta_i - \theta_j) + \gamma \sin(\theta_i - \theta_0(t)),$$

for  $i = 1, \dots, N$ , with coupling constant  $D$ . Each oscillator is driven with strength  $\gamma$  by the same external oscillator  $\theta_0(t)$  with time-varying frequency

$$\dot{\theta}_0 = \omega_0[1 + kf(\omega_m t)],$$

where  $\omega_0$  is the non-modulated frequency,  $f$  is a bounded function, and  $k$  and  $\omega_m$  are the amplitude and frequency of the frequency modulation.

Yes, stability region increases with amplitude of non-autonomicity  $k$

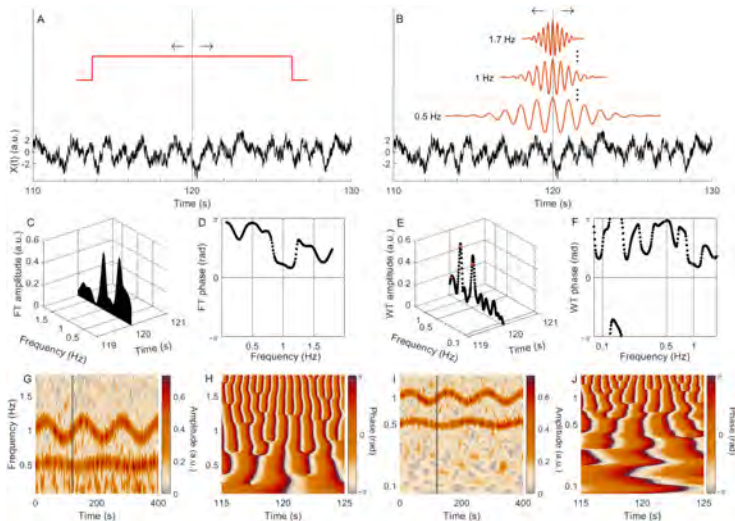


M Lucas, D Fanelli, and A Stefanovska, "Non-autonomous driving induces stability in network of identical oscillators", *Phys. Rev. E* **99**: 012309, 2019.

# So, how to analyse non-isolated systems and time-series recorded from them?

- Physical systems in the real world subject to ongoing external forcing will generally exhibit *bounded, non-static behaviour*
- *Cyclic or oscillatory* processes within the system
- Time-dependent dynamics appears to be highly complex and noise-like when analysed under the assumption of stationarity.
- Analysing time-series in sufficiently high dimensions, considering both the frequency and time domains, and with the possibility of time-variability in mind, is essential to identifying time-dependent components.
- Time-dependent dynamics is extremely common in natural systems. Much of what we consider to be noise might actually be understandable and informative non-autonomous determinism!
- An important role in the functioning of a system is played by **interactions** between oscillatory processes within the system (which may be of a time-dependent nature as well)

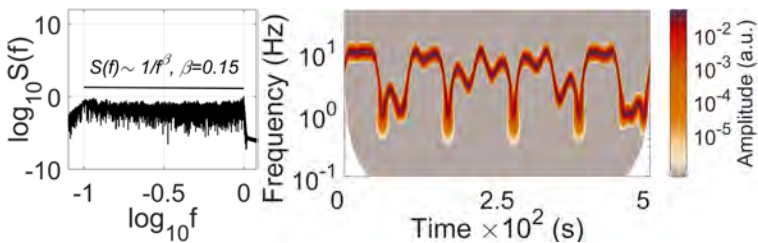
# The need for logarithmic frequency resolution



S J K Barnes, J Bjerkan, P T Clemson, J Newman, and A Stefanovska, Phase coherence – A time-localized approach to studying interactions, *Chaos* 34: 073155, 2024.



# Non-autonomous deterministic oscillations



The mean field of  $n = 10$  non-autonomous oscillators with a single natural frequency, aperiodically modulated. The oscillators evolve in time according to the equation

$$f(t) = 5.5 \text{ Hz} + 4.51 \text{ Hz} \sin(2\pi 10^{-2} t + \sin(10.8\pi 10^{-2} t)) .$$

Other methods, like complexity analysis or autocorrelation function, also fail to identify the time-localised nature of the dynamics.

# Mutiscale oscillatory dynamics analysis

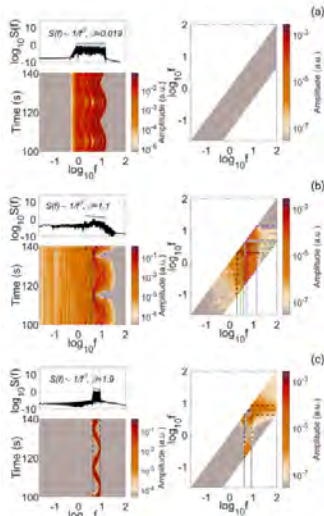
- For analysis of experimental time-series data arising from nonlinear, nonautonomous, multiscale systems, a finite-time methodology is needed to distinguish prominent, functionally important oscillatory components from noise.
- Algorithms available in MODA <https://github.com/luphysics/MODA>.



Described in

- A Bandrivskyy, A Bernjak, P V E McClintock, and A Stefanovska, "Wavelet phase coherence analysis: application to skin temperature and blood flow", *Cardiovasc Eng* **4**: 89, 2004.
- L W Sheppard, A Stefanovska, and P V E McClintock, "Detecting the harmonics of oscillations with time-variable frequencies", *Phys Rev E* **83**: 016206, 2011.
- D Iatsenko, PVE McClintock, A Stefanovska "Extraction of instantaneous frequencies from ridges in timefrequency representations of signals", *Signal Proc* **125**: 290–303, 2016.
- P Clemson, G Lancaster, and A Stefanovska, "Reconstructing time-dependent dynamics", *Proc IEEE* **104**: 223–241, 2016.
- T Stankovski, T Pereira, P V E McClintock and A Stefanovska "Coupling functions: Universal insights into dynamical interaction mechanisms", *Rev. Modern Phys.* **89**: 045001, 2017.
- G Lancaster, D Iatsenko, A Pidde, V Ticcinelli, and A Stefanovska, "Surrogate data for hypothesis testing of physical systems", *Phys Rep* **748**: 1, 2018.
- J Newman, A Pidde, A Stefanovska "Defining the wavelet bispectrum", *Appl Comput Harmon Anal* **51**: 171–224, 2021.

# Low-dimensional deterministic networks seem to yield noise



Coupling analysed using **wavelet bispectra**. The network coupling strengths  $A$  are (a) 0, (b) 5 and (c) 10.

Low-dimensional networks of deterministic nonautonomous oscillators can generate signals which, when treated within the stochastic dynamics approach, are commonly characterised as noise.

Eur. Phys. J. Spec. Top.  
<https://doi.org/10.1140/epj/s11734-022-00996-3>

THE EUROPEAN  
 PHYSICAL JOURNAL  
 SPECIAL TOPICS



Review

## Distinguishing between deterministic oscillations and noise

Joe Rowland Adams<sup>1</sup>, Julian Newman<sup>2</sup>, and Aneta Stefanovska<sup>1,2,\*</sup>

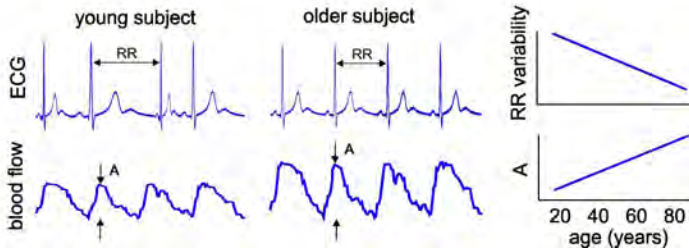
<sup>1</sup> Physics Department, Lancaster University, Lancaster, UK

<sup>2</sup> College of Engineering, Mathematics and Physical Sciences, University of Exeter, Exeter, UK

Received 3 March 2023 / Accepted 22 August 2023

© EDP Sciences, Springer-Verlag GmbH Germany, part of Springer Nature 2023

# Ageing at a system level



ECG and blood flow in capillary bed in a young and an older subject, and general trends as function of ageing

From: Cox, L. S., Mason, P. A., Bagley, M. C., Steinsaltz, D., Stefanovska, A., Bernjak, A., McClintock, P. V. E., Phillips, A. C., Upton, J., Latimer, J. E., and Davis, T. (2014). "Understanding ageing: biological and social perspectives". In *The New Science of Ageing*. Bristol, UK: Policy Press

► [Link](#)



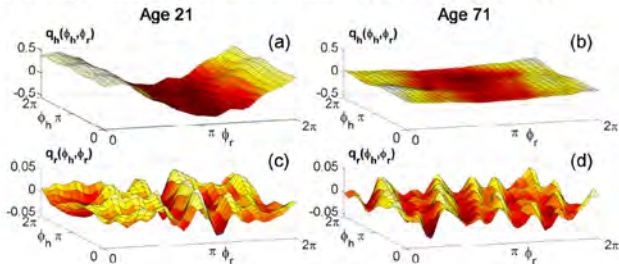
# Ageing of interactions



$$\dot{\phi}_h = \omega_h + q_h(\phi_h, \phi_r) + \xi_h$$

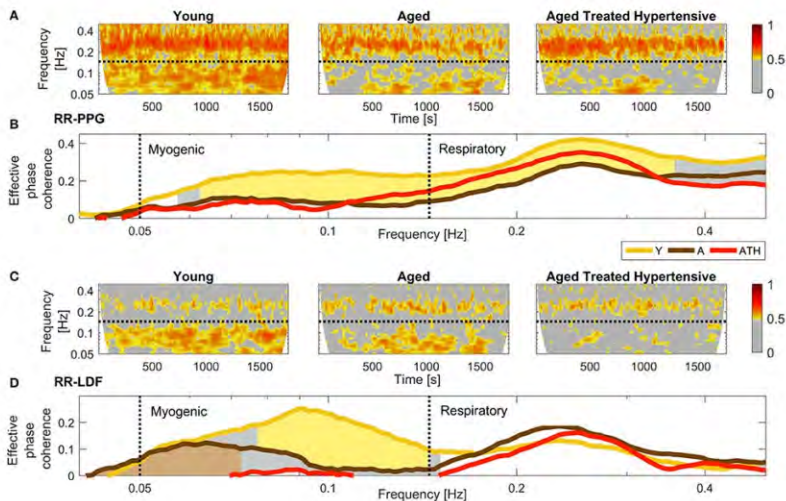
$$\dot{\phi}_r = \omega_r + q_r(\phi_h, \phi_r) + \xi_r$$

Time-averaged coupling function of heart ( $q_h$ ) and respiration ( $q_r$ )



The heart coupling function is dominated by RSA, which decreases with age, whereas the respiratory coupling function seems to be irregular and unaffected by age.

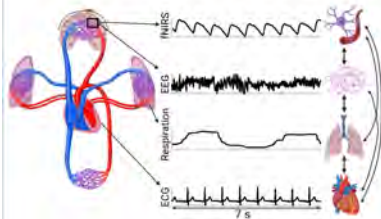
# Coherence, ageing and hypertension



# Ageing of the neurovascular unit

## Aging affects the phase coherence between spontaneous oscillations in brain oxygenation and neural activity

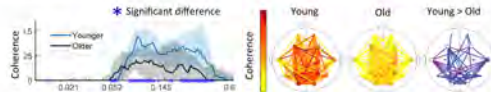
**Research question** How to noninvasively evaluate and quantify the function of the neurovascular unit and its changes with aging?



**Dataset** Young (N=21, age=31yrs), old (N=24, age=65yrs)

**Analysis methods** Time-frequency analysis and wavelet phase coherence

- Oxygenation— instantaneous heart rate coherence is reduced in older participants
- Oxygenation—neural coherence at around 0.1 Hz is reduced in older participants



### Results

- Younger group has higher coherence
- Older group has higher coherence



### Conclusion

Neurovascular phase coherence at  $\sim 0.1$  Hz is reduced with age, indicating impaired function of the neurovascular unit. The methods described can be used for non-invasive evaluation of neurovascular function in normal aging and in neurodegenerative disorders.

Bjerkan et al, *Brain Research Bulletin* 201, 110704 (2023)

# Effect of methamphetamine on behavioural rhythms

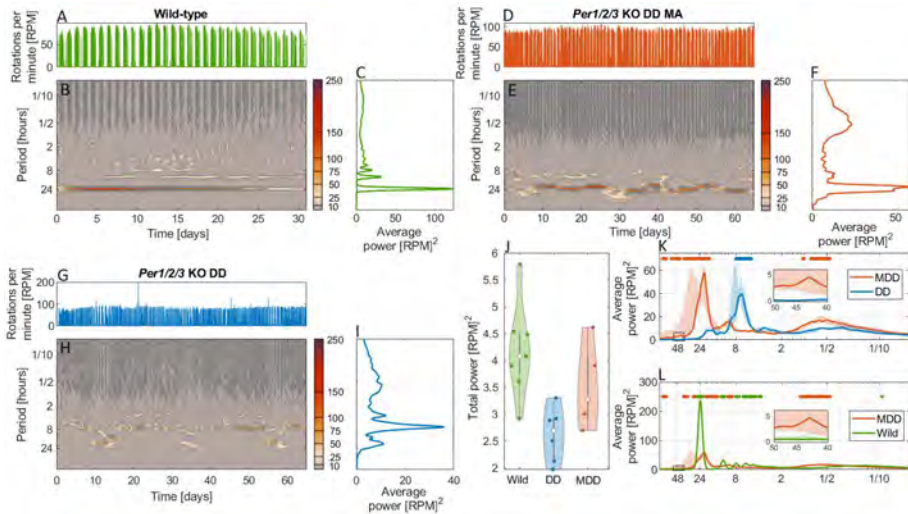
## Time-varying MASCO and multiscale activity alterations following methamphetamine exposure in *Per1/2/3* knockout mice

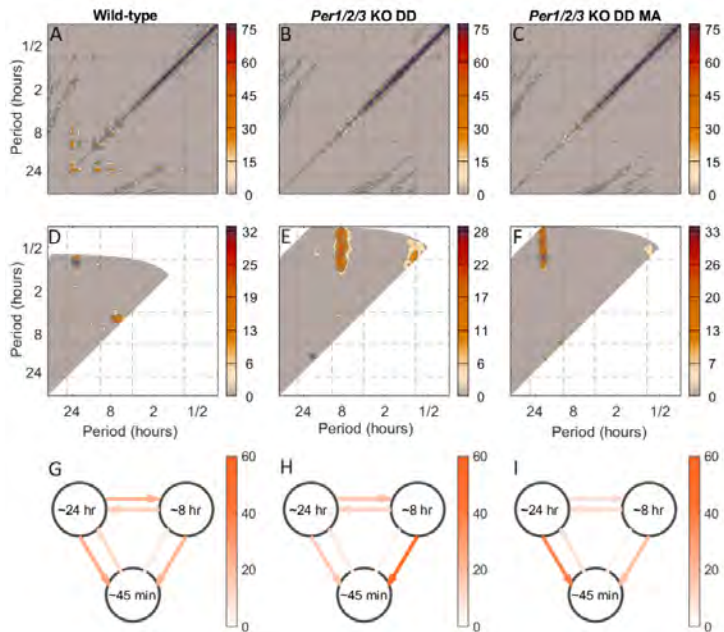
Samuel J.K. Barnes<sup>a</sup>, Mansour Alanazi<sup>a, b</sup>, Shin Yamazaki<sup>c</sup>, and Aneta Stefanovska<sup>a\*</sup>

This manuscript was compiled on September 5, 2024

- Disruptions to physiological cycles are associated with numerous pathologies.
- Attempts to analyse these biological oscillations often overlook key time-localised characteristics of the data.
- We apply time-resolved analysis to investigate changes in behavioural rhythms, focusing on circadian, ultradian, and circabidian oscillations in *Per1/2/3* knockout (KO) mice following methamphetamine administration.







# Implications

- Our novel cross-disciplinary approach, integrating physics-based methods with chronobiology has helped reveal the effect of methamphetamine on the circadian rhythm and its couplings to other rhythms.
- Multiscale, non-stationary dynamics analysis unveils previously hidden aspects of the circadian, circadian and ultradian rhythms.
- The approach enables precise time-localisation of multiscale oscillations, which is impossible to achieve using standard time-domain analysis methods such as actograms.
- We reveal changes to the couplings between behavioural modes following methamphetamine administration.

# General summary

- Imperfect clocks operating on circadian to milliseconds scales mutually interact and adjust their rhythms.
- A chronotaxic, nonautonomous framework is introduced to describe the cyclic oscillations with non-constant frequencies that appear in living systems on time scales spanning from days to milliseconds.
- Algorithms for time-localised, finite time analyses are available in the software toolbox MODA.
- Many applications are possible, two of which, on ageing at a systemic level and on studies of circadian rhythmicity, correspond to especially promising ways forward.



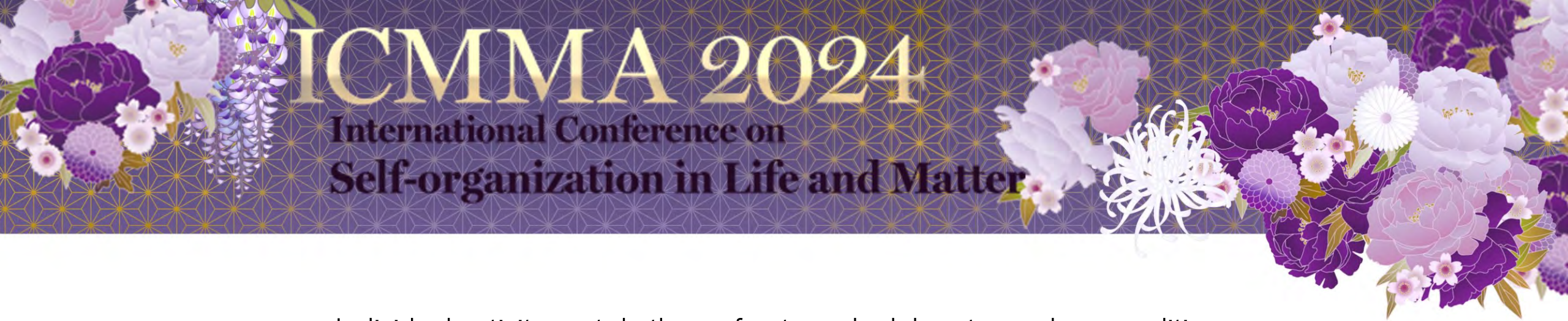
## Thanks

The work has been financially supported by the Engineering and Physical Sciences Research Council (UK) Grants No. EP/100999X1, EP/M006298/1 and EP/X004597/1, the EU projects BRACCIA [517133] and COSMOS [642563], the Action Medical Research (UK) project MASDA, the Slovene Research Agency (Program No. P20232) and the Sony Research Award Programme.

Thank you for your attention!

# References

- ➊ J M L Newman, M Lucas, A Stefanovska, Non-asymptotic-time dynamics. In *"Physics of Biological Oscillators"*, A Stefanovska, P V E McClintock (Eds), Springer, Cham, 111–129, 2021.
- ➋ J Newman, J P Scott, J Rowland Adams, A Stefanovska, Intermittent phase dynamics of non-autonomous oscillators through time-varying phase, *Physica D* **461**: 134108, 2024.
- ➌ J Rowland Adams, J Newman, A Stefanovska, Distinguishing between deterministic oscillations and noise, *Eur. Phys. J. Spec. Top.*, **232**: 3435–3457, 2023.
- ➍ D Iatsenko, PVE McClintock, A Stefanovska, Extraction of instantaneous frequencies from ridges in time-frequency representations of signals, *Sign. Process*, **125**: 290–303, 2016.
- ➎ S J K Barnes, J. Bjerkan, P T Clemson, J. Newman, and A. Stefanovska, Phase coherence – A time-localized approach to studying interactions, *Chaos* **34**, 073155, 2024 .
- ➏ T Stankovski, T Pereira, P V E McClintock, and A Stefanovska, Coupling functions: Universal insights into dynamical interaction mechanisms, *Rev. Mod. Phys.* **89**, 045001, 2017.
- ➐ M Morris, S Yamazaki, A Stefanovska, Multiscale Time-resolved Analysis Reveals Remaining Behavioral Rhythms in Mice Without Canonical Circadian Clocks, *J. Biol. Rhythms* **37**: 310–328, 2022.
- ➑ J Rowland Adams, A Stefanovska, Modeling Cell Energy Metabolism as Weighted Networks of Non-autonomous Oscillators, *Front. Physiol.* **11**: 613183, 2021.
- ➒ A Stefanovska, Coupled Oscillators: Complex But Not Complicated Cardiovascular and Brain Interactions, *IEEE Eng. Med. Biol. Magazine* **26**: 25-29, 2007.
- ➓ J Bjerkan, G Lancaster, B Meglič, J Kobal, TJ Crawford, PVE McClintock, A Stefanovska, Aging affects the phase coherence between spontaneous oscillations in brain oxygenation and neural activity, *Brain Res Bull* **201**: 110704, 2023.



## Individual activity-rest rhythms of ants under laboratory colony conditions

Haruna Fujioka (Okayama university)

Most organisms exhibit a periodic activity of about 24 hours. This circadian rhythm is considered to be an adaptation to the fluctuations of the environment. In ants, individual behaviors, including activity-rest rhythms, is influenced by social interactions within their colony [1]. However, monitoring individual activity-rest rhythms in an ant colony is challenging due to their large group size and small body size. To address this, we developed an image-based tracking system using 2D barcodes in a monomorphic ant (Fig 1a) and measured the locomotor activity of all colony members under laboratory conditions [2]. Activity-rest rhythms appeared only in isolated ants, not under colony conditions (Figure 1b). This suggests that a mixture of social interactions, not light and temperature, induces the loss of activity-rest rhythms. These findings contribute to our understanding of the diverse patterns of circadian activity rhythms in social insects.

### References

- [1]Fujioka, Haruna, et al. "Ant circadian activity associated with brood care type."Biology letters 13.2 (2017): 20160743.
- [2]Fujioka, Haruna, Masato S. Abe, and Yasukazu Okada. "Individual ants do not show activity-rest rhythms in nest conditions." Journal of biological rhythms 36.3(2021): 297-310.

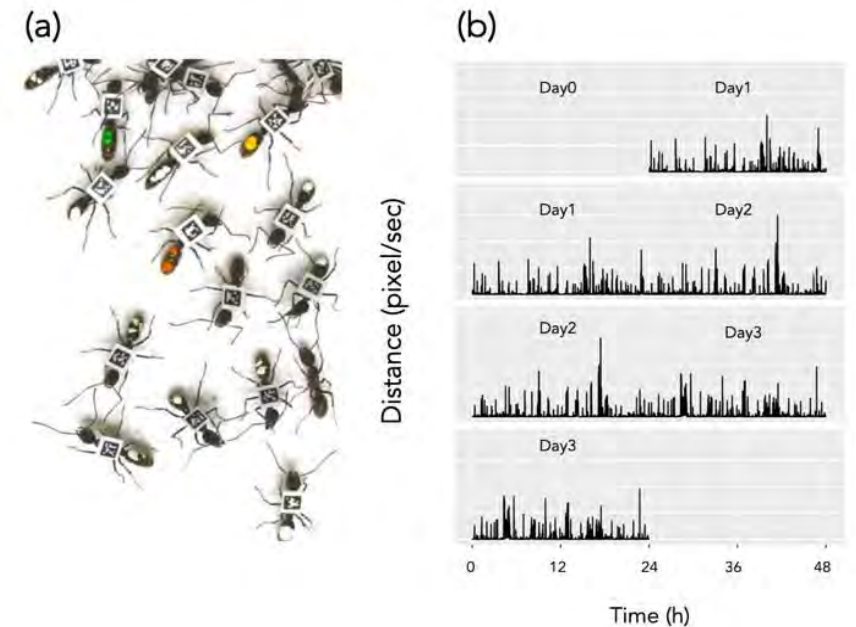


**Figure 1.** Tagged and untagged ants (a). The species is *Diacamma cf. indicum*. Different color on their gaster indicates different age. Actogram of worker for 3 days activity-rest rhythms (b).



ICMMA2024

# Individual activity-rest rhythms of ants under laboratory colony conditions

Haruna FUJIOKA (Okayama Univ.)

藤岡 春菜 (岡山大学、環境生命・農、助教)





# Circadian rhythms are ubiquitous



(Moore 1998)



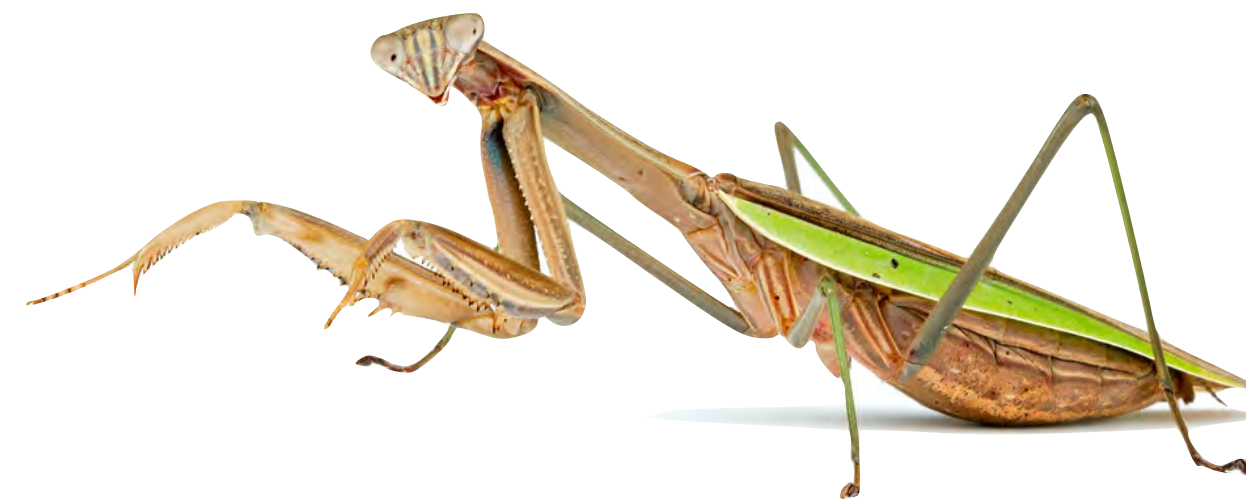
(Seyfarth 1980)



(Pittendrigh 1967)



(Floessner et al. 2019)



(Schirmer et al. 2014)



(Omkar et al. 2004)



(Viviani 1997)



(Harker 1956; Roberts 1960)

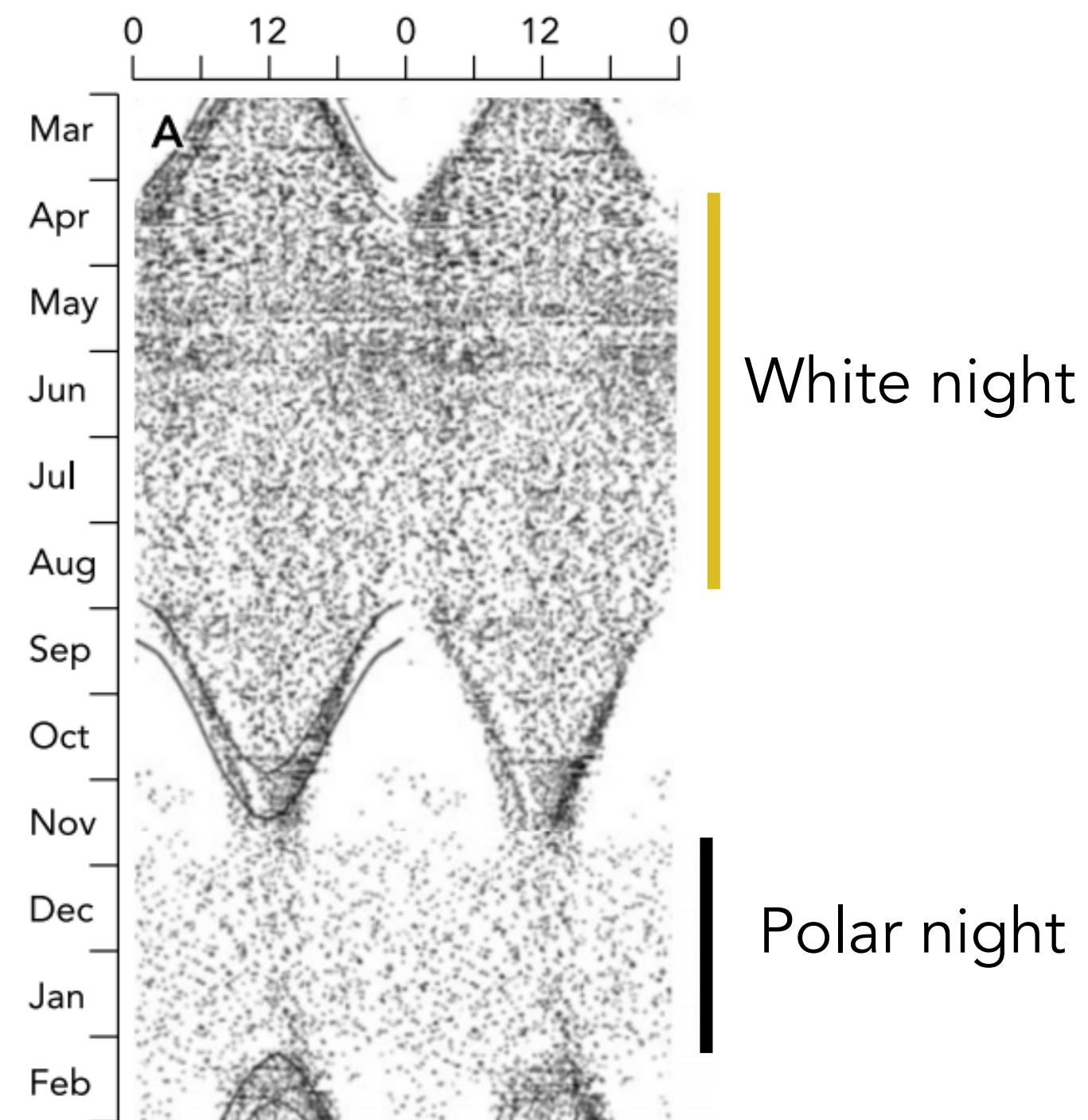


(Hoffman 1973;1974)

Ant room



# Animals in the wild



Constant light  
or darkness



Cave



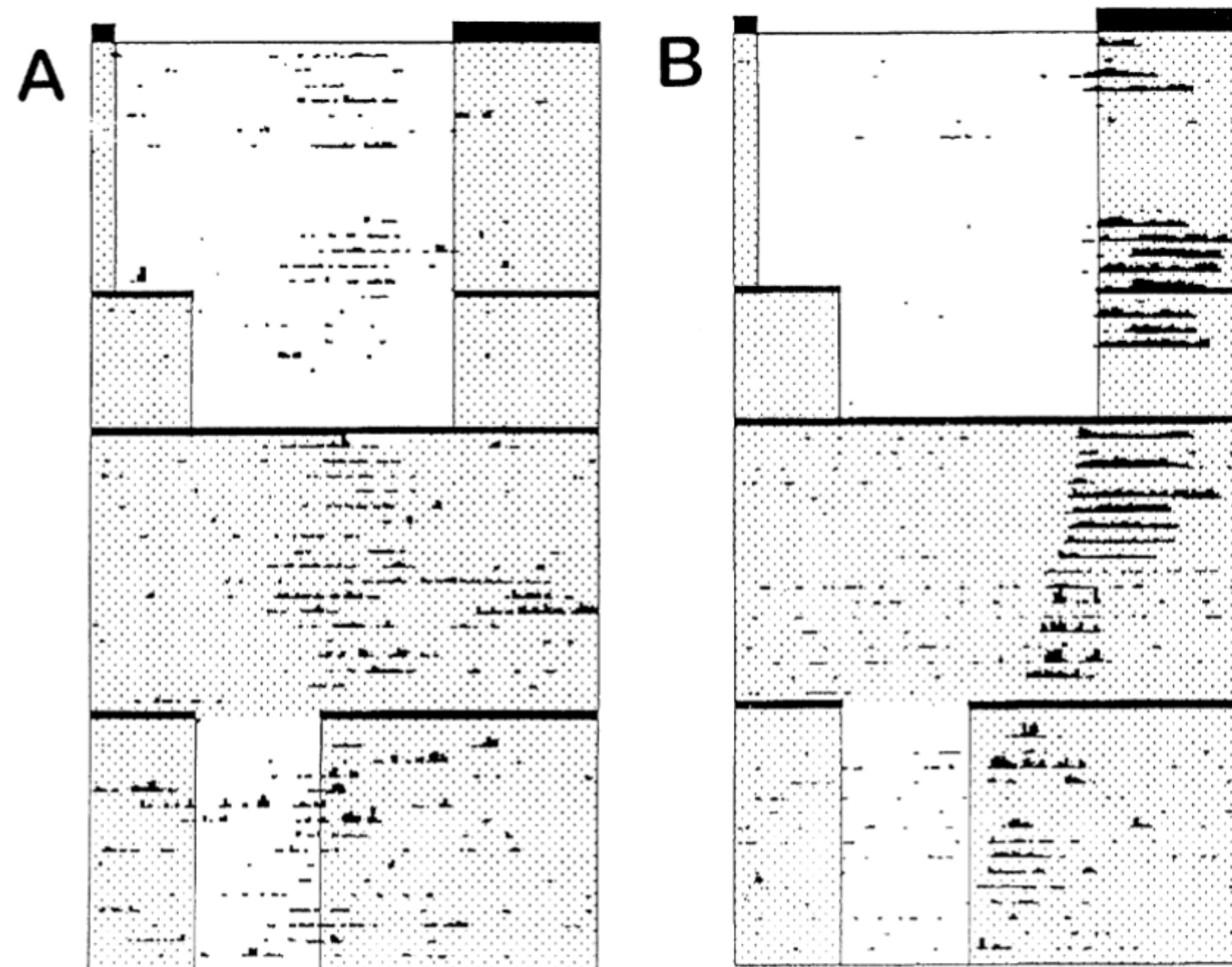
# Subterranean habitats

Light - within 10 cm of surface (Tester and Morris 1987)

Warming effect - only reaches 1 m (Geiger et al. 2003)

Despite the “arrhythmic” subterranean habitats,  
strong rhythms of activity are exhibited in all studied species of mole rats.

(Tobler et al. 1998; Riccio and Goldman 2000; Oosthuizen et al. 2003; Hart et al. 2004; Schöttner et al. 2006)



(Riccio and Goldman 2000)

**Sociality**

**Group-living**

# Regulation on circadian rhythms

Abiotic factors

Biotic factors

Temperature

Task / Work

Social interaction

Light

Meal time



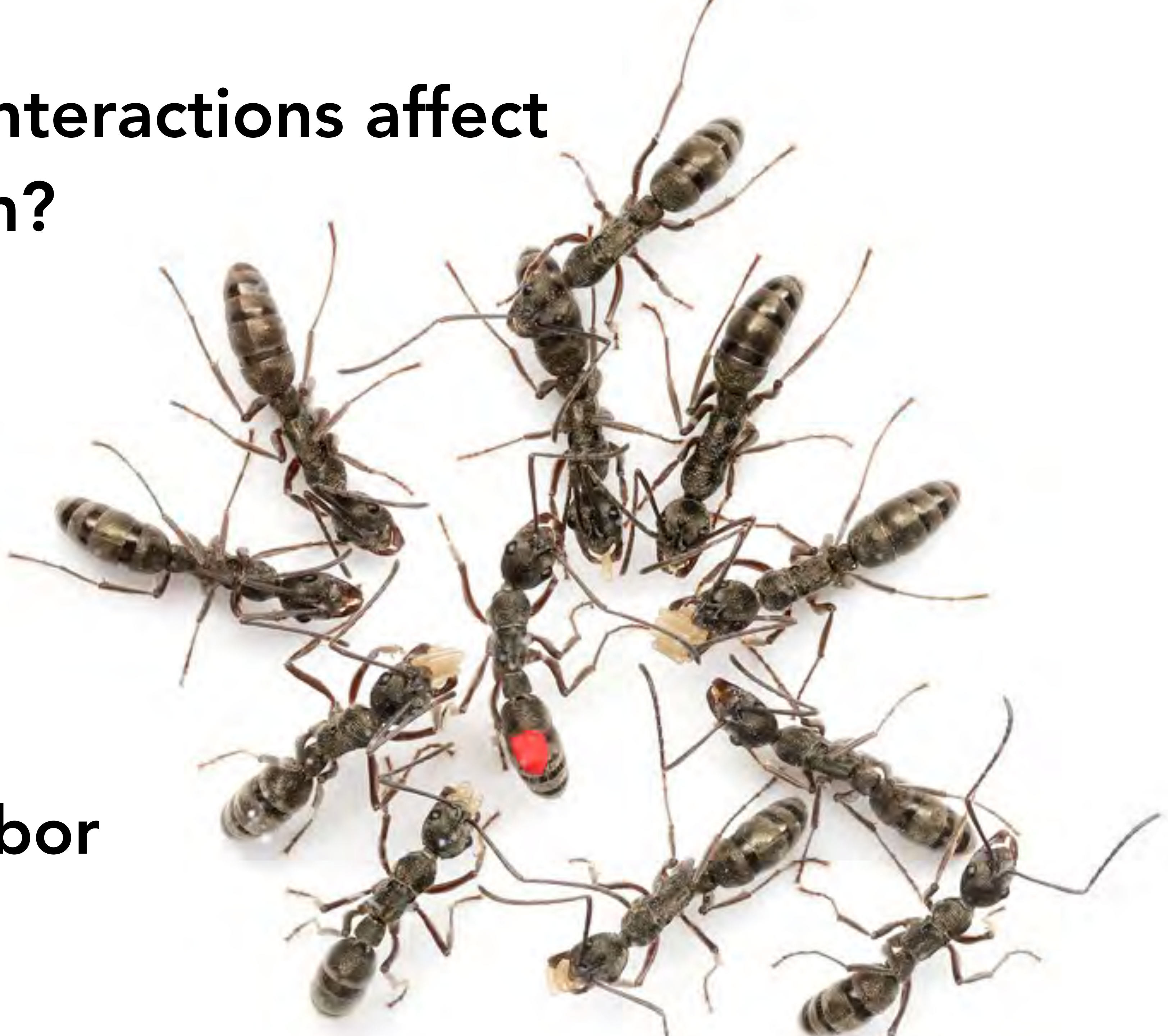


**How do social interactions affect  
the daily rhythm?**

**Ant**

**Social insect**

**Division of labor**





# Division of labor in ant

Individuals within a colony perform different tasks.

Reproductive



Queen

Sterile



Worker

Intranidal task



Nurse

Extranidal task



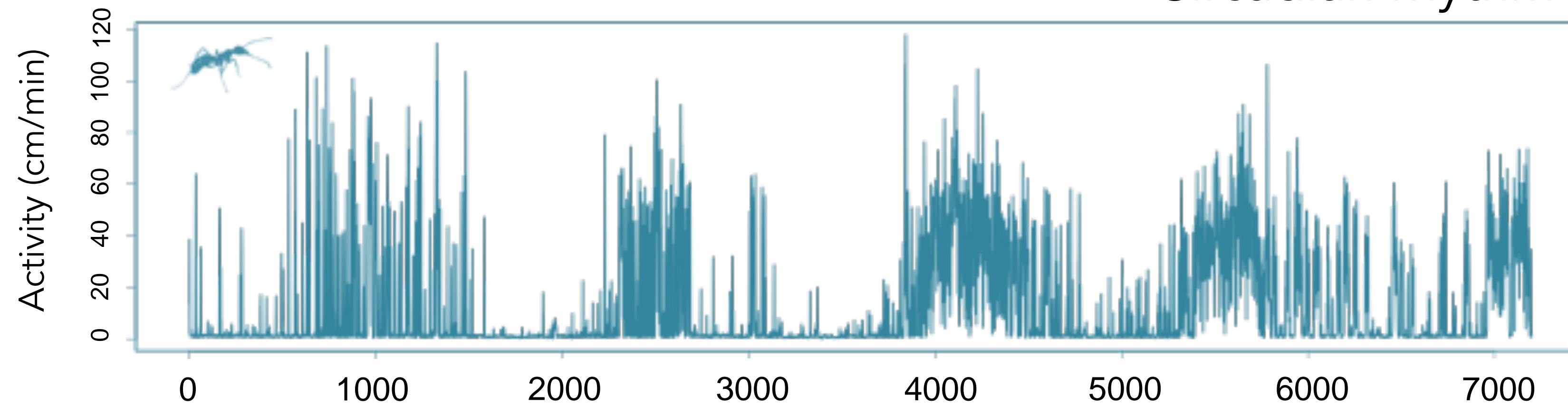
Forager

***Task allocation***

# Workers show circadian rhythm

Young worker (Nurse) - solitary

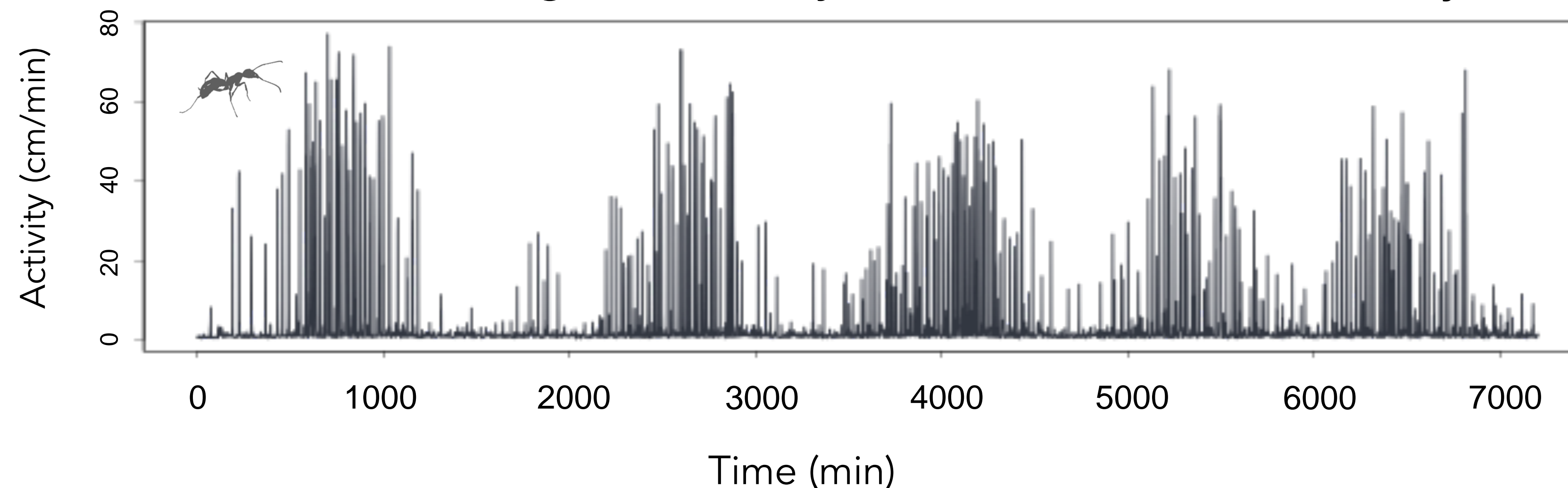
Circadian rhythm



- **Constant dark (DD)**
- **25°C**
- ***Diacamma***
- **Isolated from colony**

Old worker (Forager) - solitary

Circadian rhythm



*Diacamma* cf. *indicum*  
Okinawa, Japan



# Tasks and activity rhythms

Efficient active-rest patterns to accomplish the tasks may change according to their tasks.

## Reproductive



Bee: Eban-Rothschild et al. 2011

Ant: Sharma et al. 2004; Lone et al. 2012; Fuchikawa et al. 2014

## Foraging

Daily rhythms

Light Temperature  
Resource availability

Bee: Lindauer 1952; Spangler 1972; Kaiser & Steiner-Kaiser 1983; Moore et al. 1998; Toma et al. 2000; Moore et al. 2001; Bellusci & Marques 2001; Stelzer et al. 2010; Fuchikawa et al. 2007...

Ant: Sharma et al. 2004; Raimundo et al. 2009; Narendra et al., 2010; Piyankarie et al. 2011; Fuchikawa et al. 2014

## Brood-care



Bee: Bloch and Robinson 2001, *Nature*

Ant: Fujioka et al. 2017, *Biol. Lett.*



# Activity rhythm in nurses

Brood-care is required for all day long. (Bee: Bloch and Robinson 2001, Nature)

Egg



Grooming, feeding

**Intensive care**

Larva



Pupa



**No need intensive care**

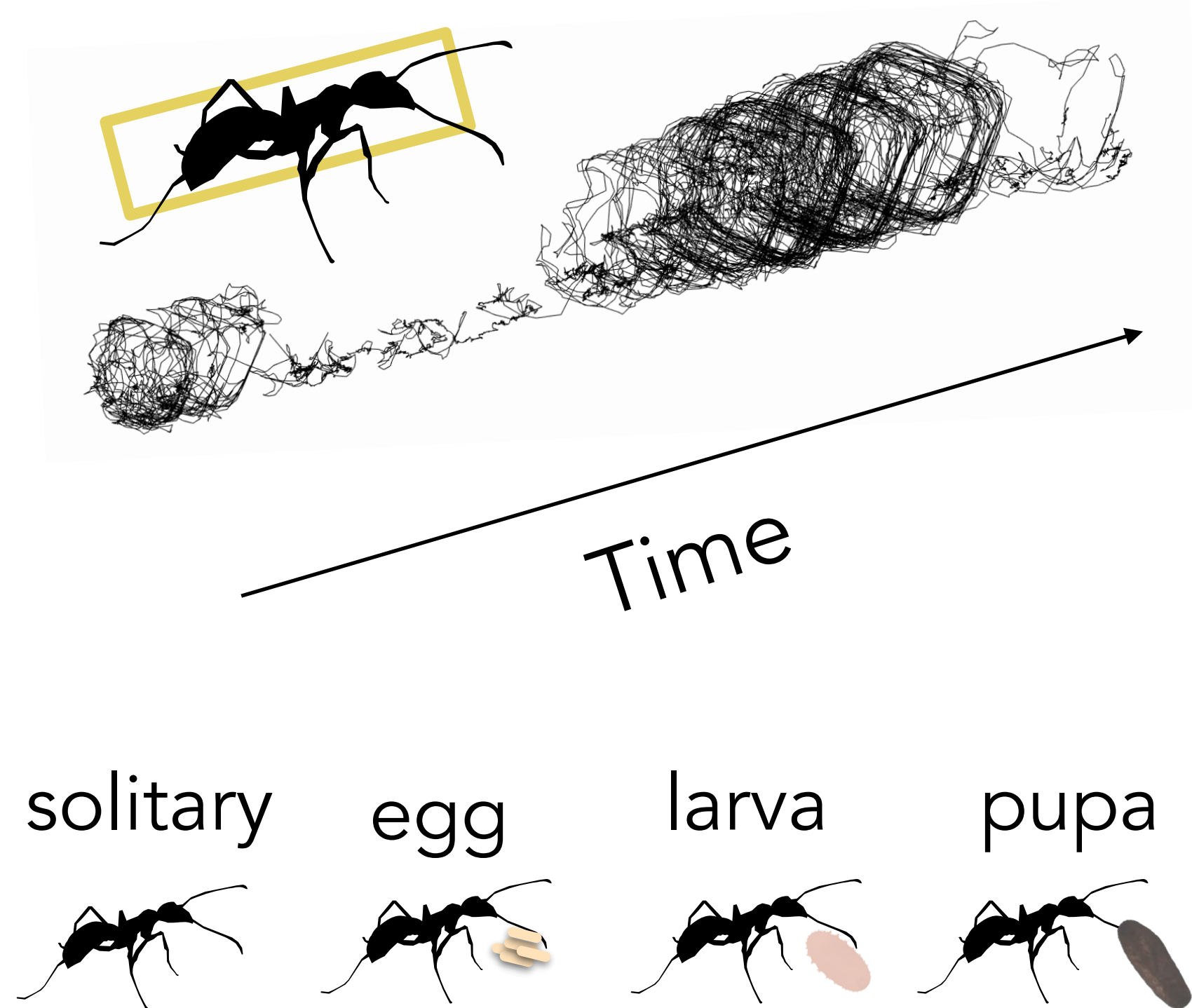
By pairing the nurses with different types of broods,  
I examined whether brood types differently affect nurse activities.

# Methods | Image-based tracking

Ant movement was automatically tracked from the recorded movie.  
I used a difference between background and target image for detection.

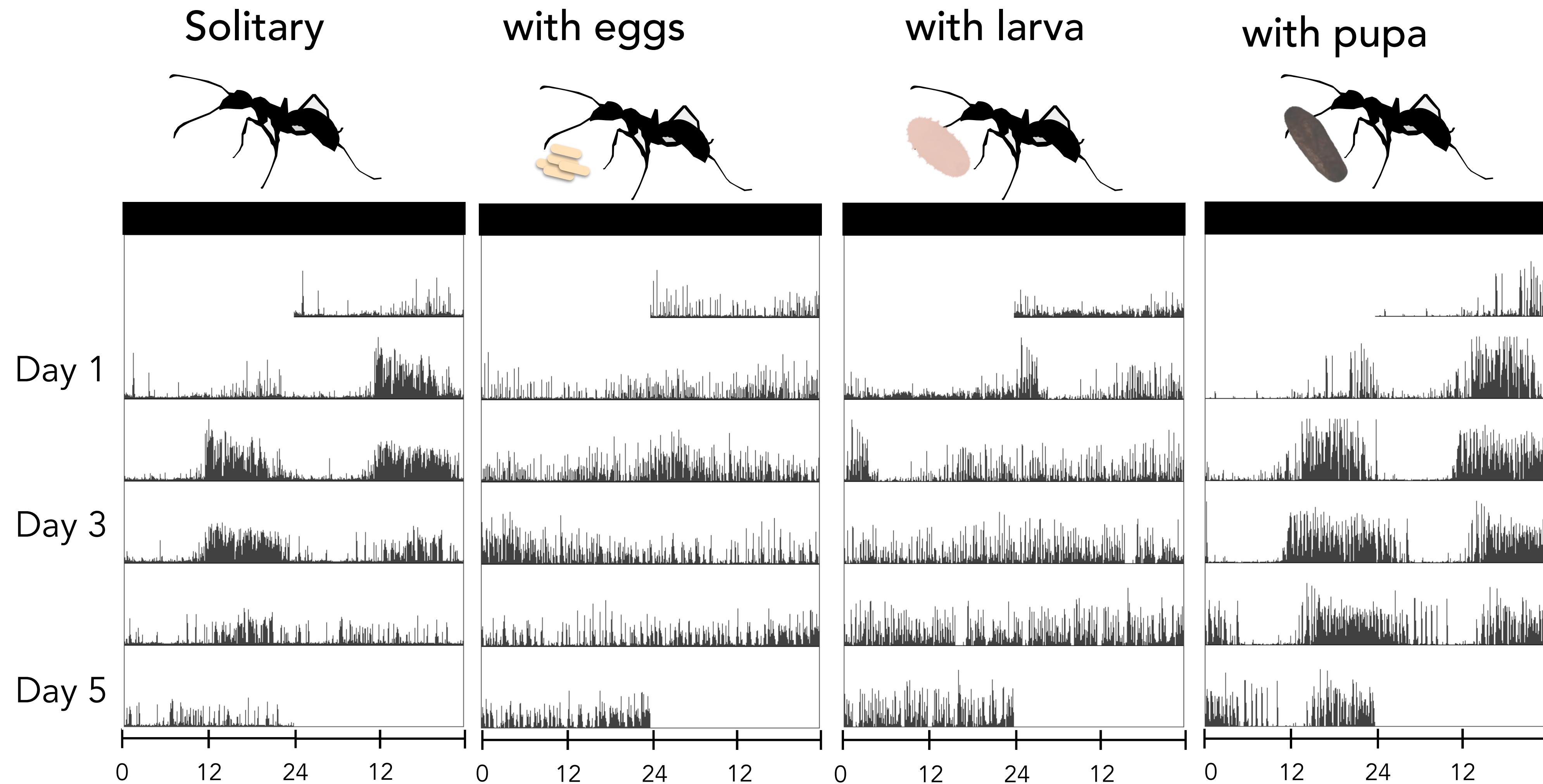


Under the dim-red light



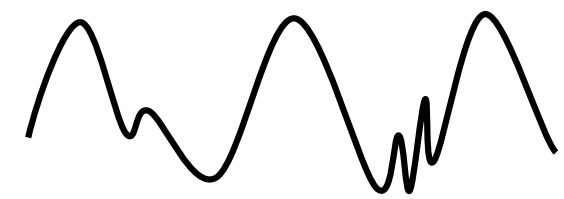
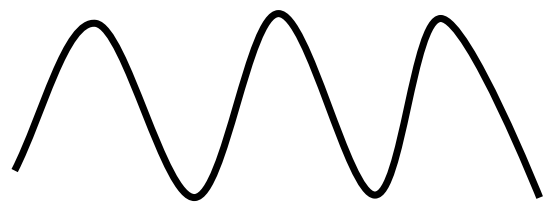
(Fujioka et al. 2017, Biol. lett.)

# Interaction with brood induce “arrhythmic”



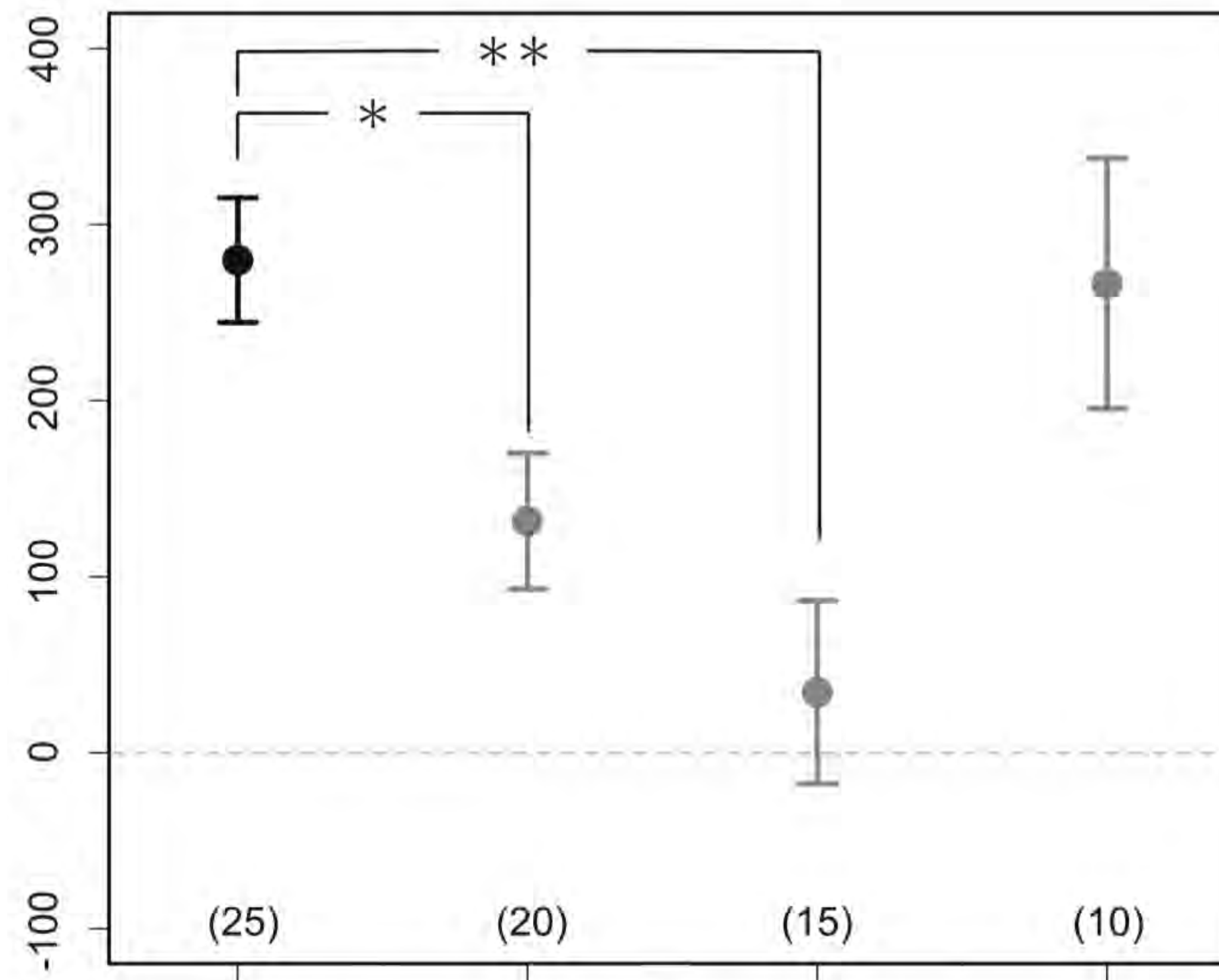
# Result | Brood-type dependent

Strong rhythm

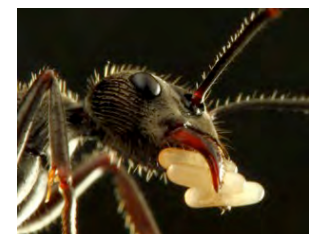


Weak rhythm

Mean of strength of circadian rhythm ( $\pm$ SE)



5 nurses



5 nurses  
+  
eggs



5 nurses  
+  
larvae



5 nurses  
+  
pupae

Nurses showed brood-type dependent change under the group condition.

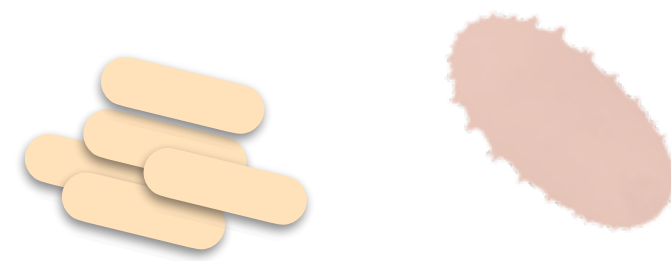
(Fujioka et al. 2019, *BES*)



# Discussion

The interaction with the brood was  
a strong trigger to induce nurses to weakly rhythmic or arrhythmic state.

**Egg Larva**



Grooming, feeding

**Intensive care**

**Pupa**



**No need intensive care**

The differences between caretaking demands

# Task allocation by age

## Young worker

Brood-care



## Old worker

Forage  
outside the nest



Reviewed in Hölldobler and Wilson 1990

*Pachycondyla* spp., *Myrmecia* spp., *Aphaenogaster albisetosus*, *Basiceros manni*,  
*Eurhopalpthrix heliscata*, *Messor* spp., *Myrmica* spp., *Oligomyrmex* spp., *Pheidole dentata*,  
*P. hortensis*, *P. spp.*, *Pogonomyrmex badius*, *Pristomyrmex punges*, *Procryptocerus*  
*scabriusculus*, *Solenopsis invicta*, *Aneuretus simoni*, *Tapinoma erraticum*, *Camponotus*  
*herculeanus*, *C. ligniperda*, *Cataglyphis bicolor*, *Formica sanguinea*, *F. yessensis*, *F. spp.*  
*Lasius niger*, *L. spp.*, *Oecophylla longinoda*

*Diacamma*: Nakata 1995

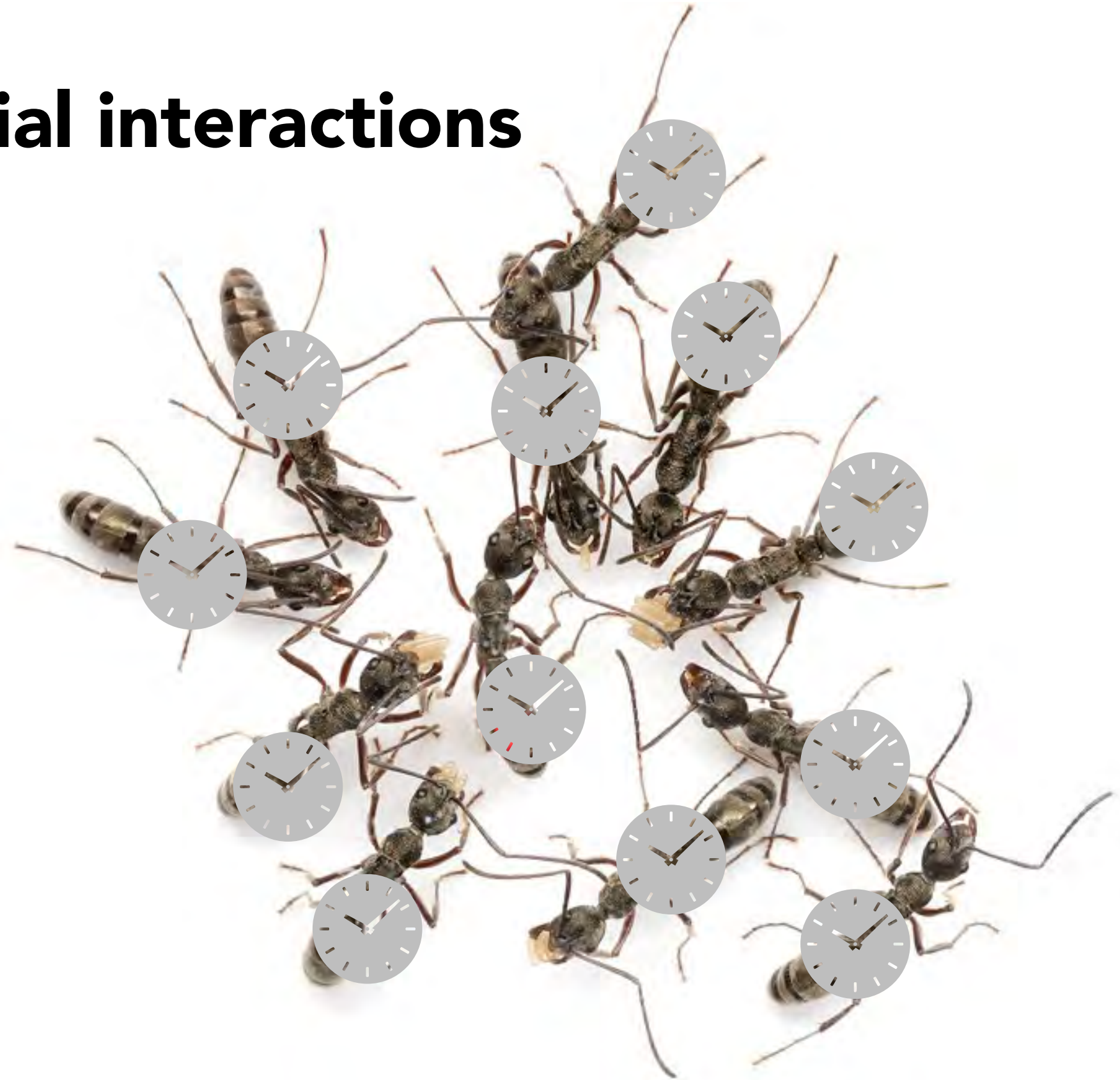
*Rhytidoponera metallica*: Thomas and Elgar 2003;

*Pheidole dentata*: Seid and Traniello 2006; *Platythyrea punctata*: Bernadou et al. 2015;

*Acromyrmex subterraneus brunneus*: Camargo et al. 2007

# Worker-worker interaction

## Social interactions



Interaction with Brood



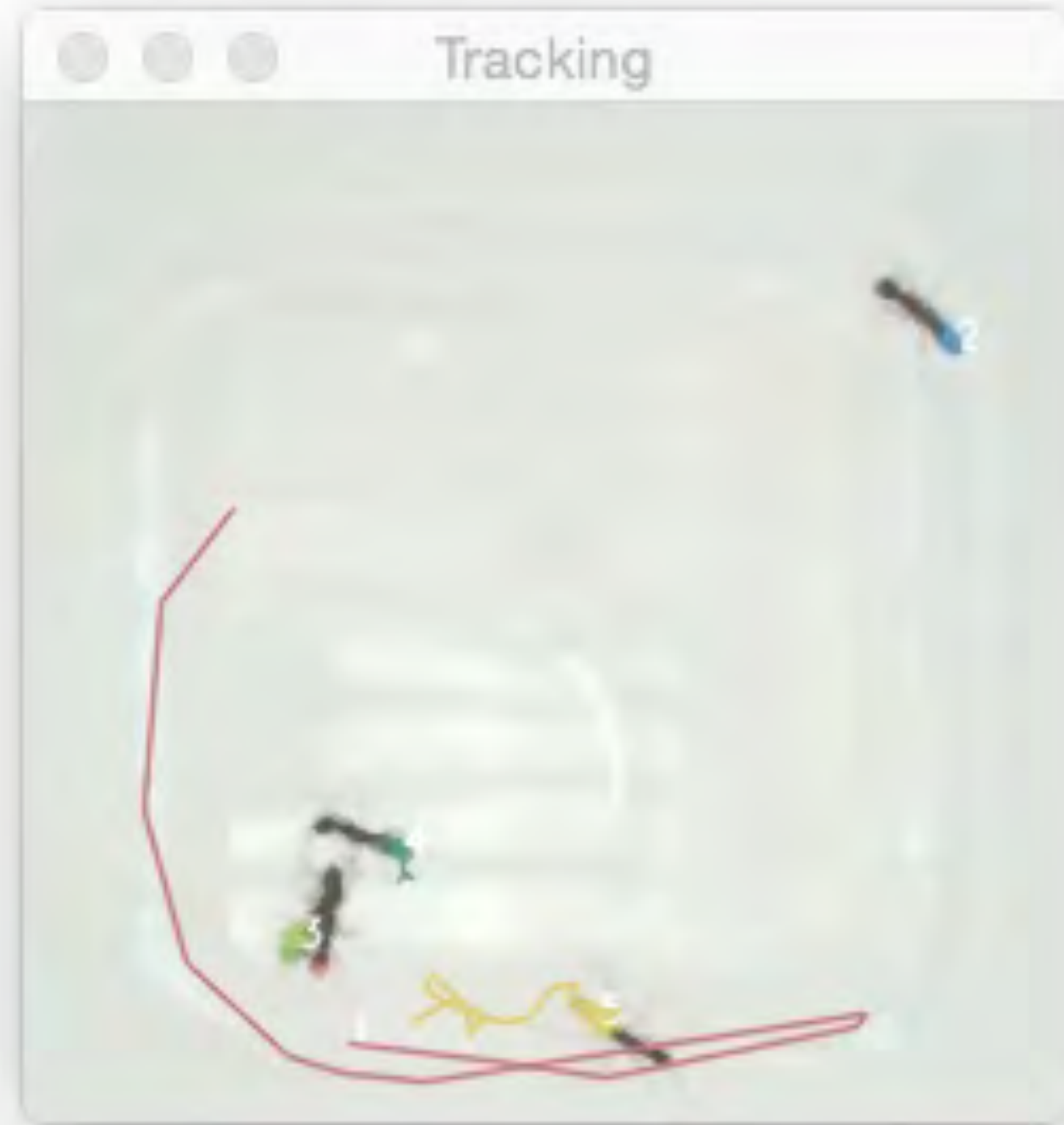
Worker - Worker

How do intra-worker interactions alter individual worker behavior?

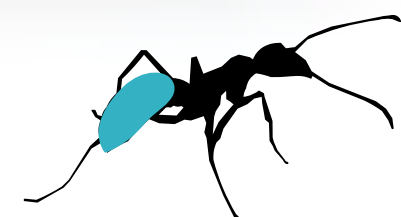


# Method | color tracking

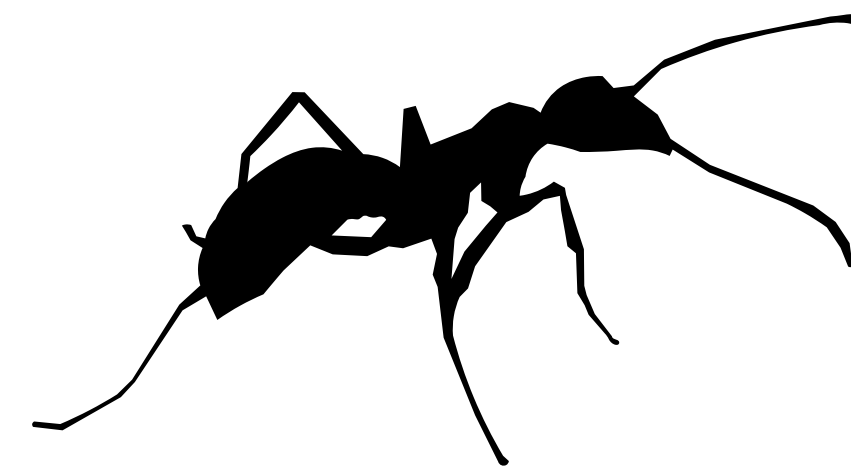
Measured active-rest rhythms using a color-tag tracking system



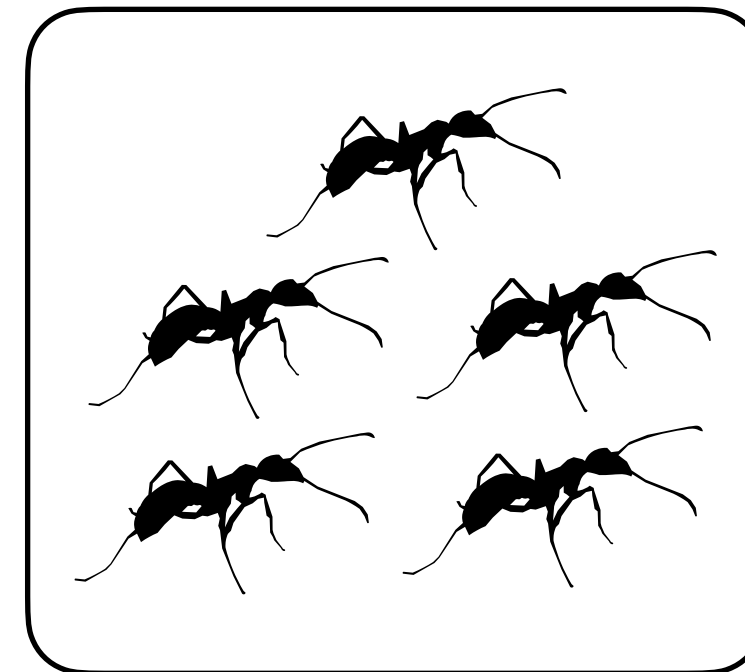
The gaster of ant was marked by the enamel paints.



Young worker



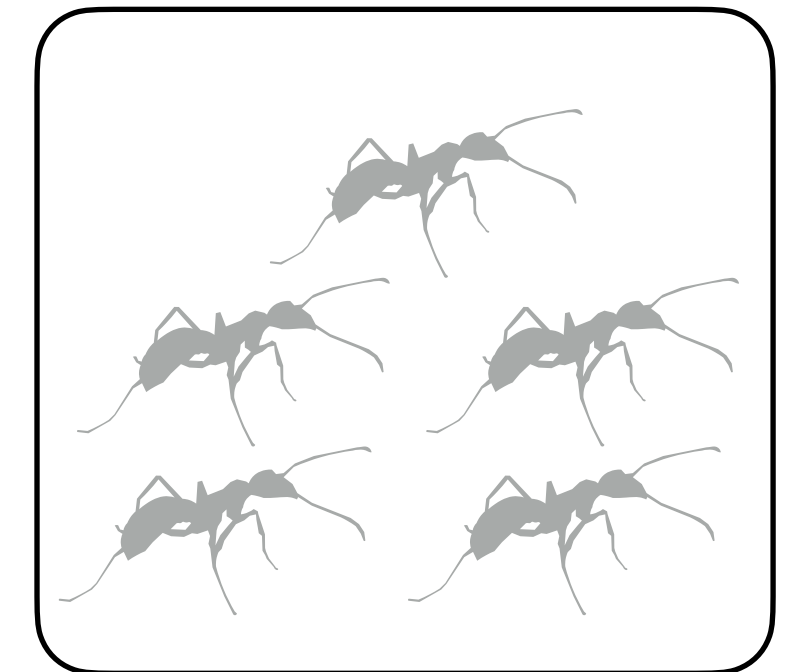
> 30 days



Old worker



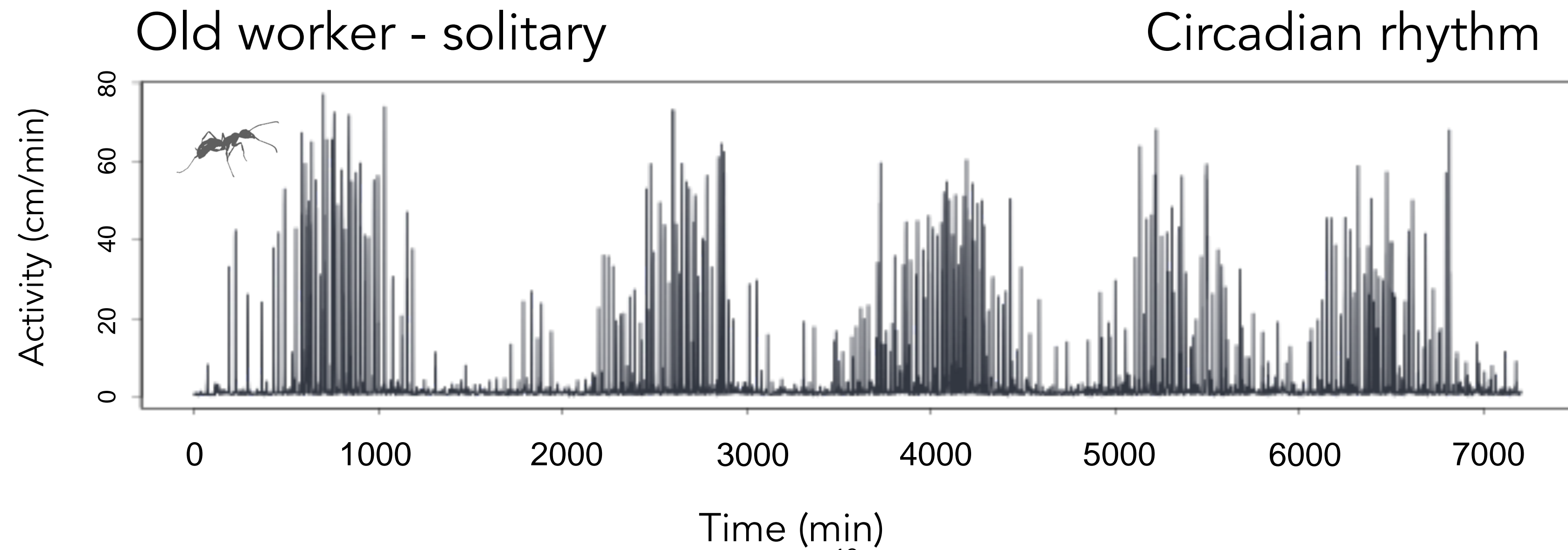
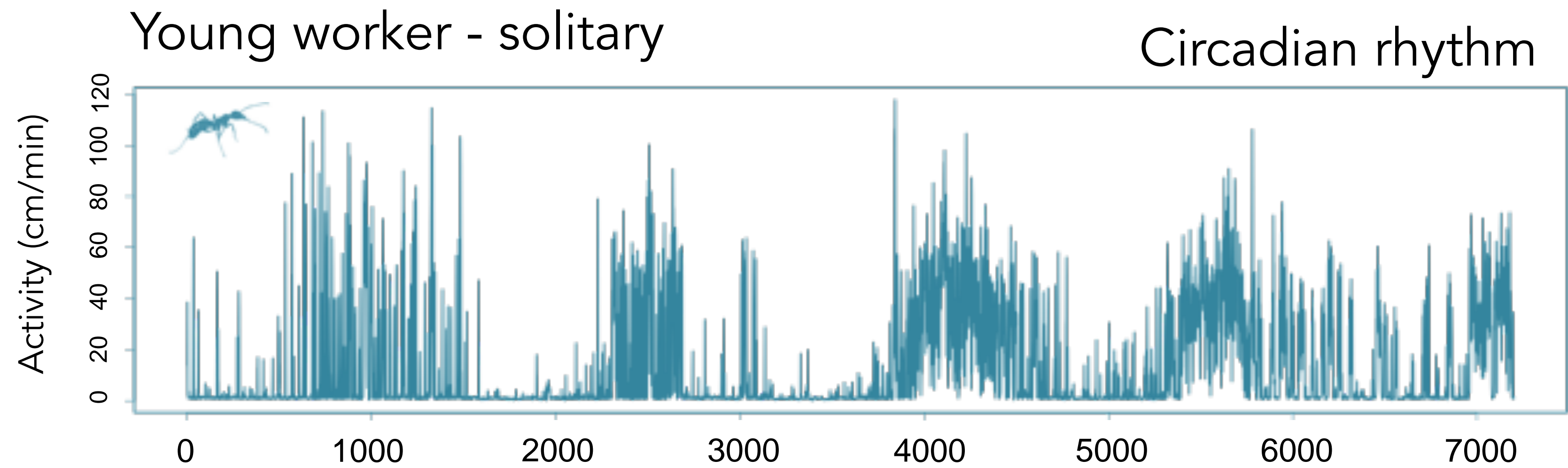
0-30 days



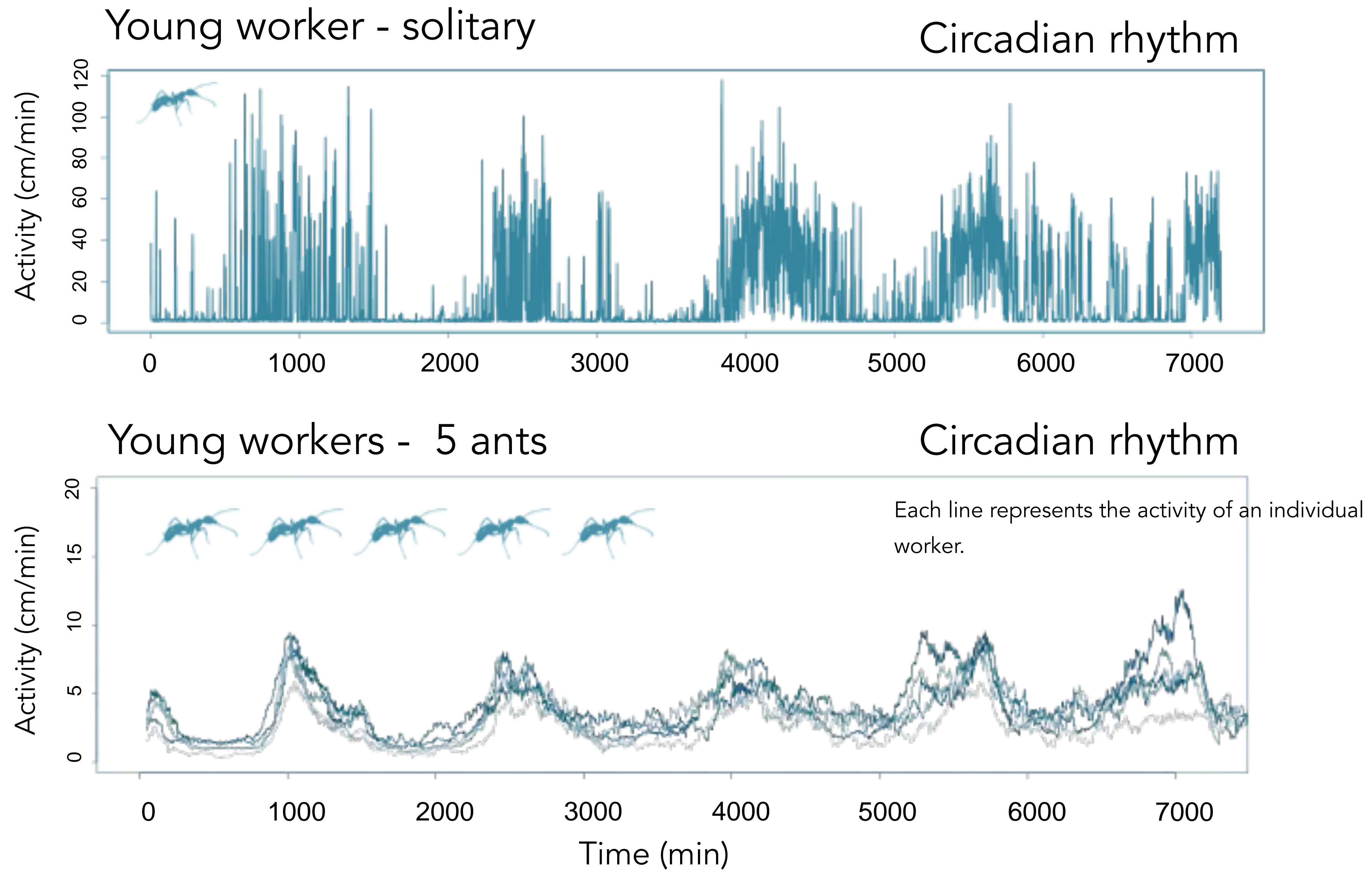
- **Under constant light-on condition**



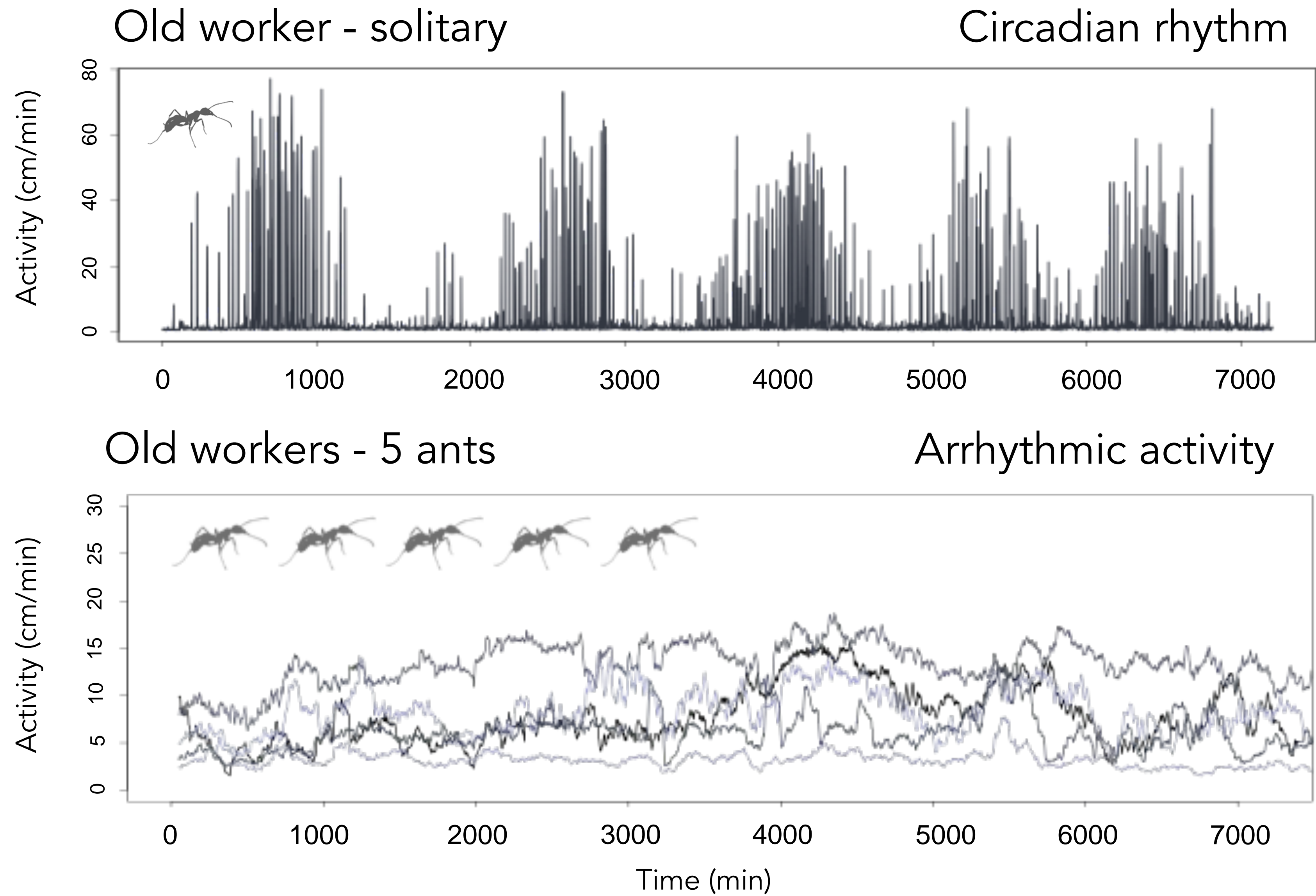
# Result | solitary



# Result | young worker



# Result | old worker



# Question

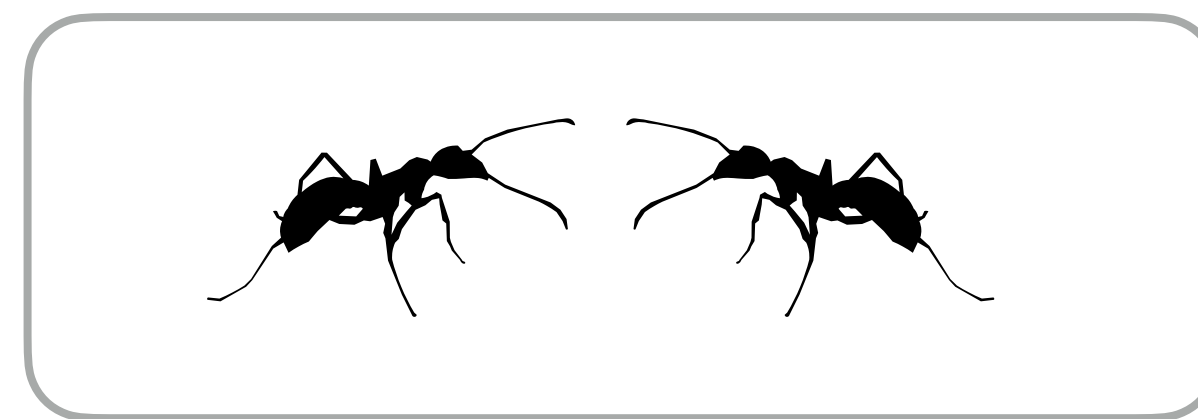
## Previous studies



Arrhythmic activity



(Fujioka et al. 2017, *Biol. Lett.*)

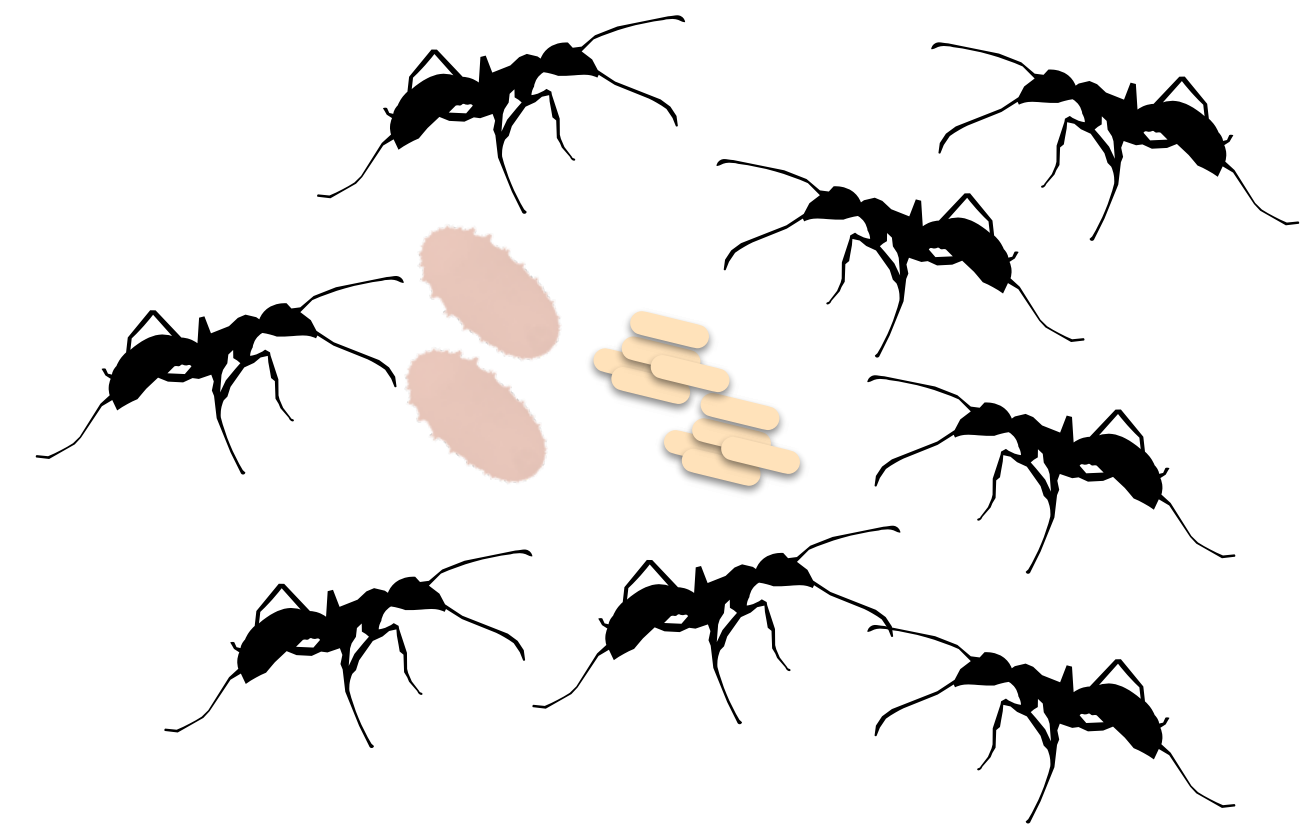


Arrhythmic activity



(Fujioka et al. 2019, *BES*)

In the colony?





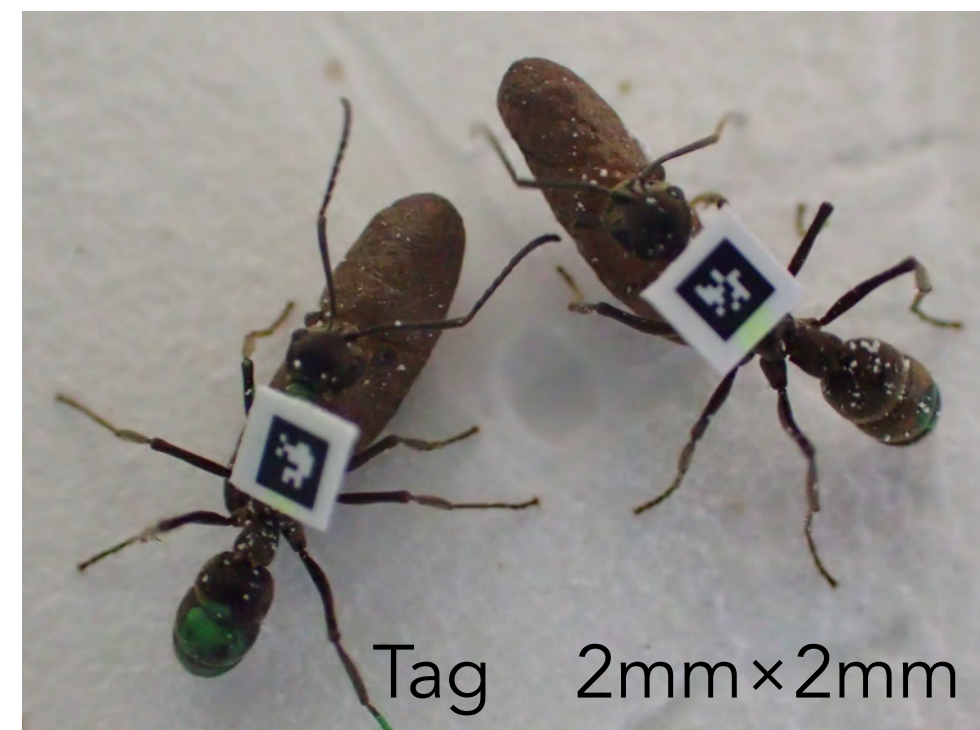
# Introduction

Previous colony-level studies focused on

- Foraging activity (e.g., Stelzer et al. 2010)
- Oxygen consumption, Temperature (Moritz and Kryger 1994)

Few studies have addressed individuals' activities.

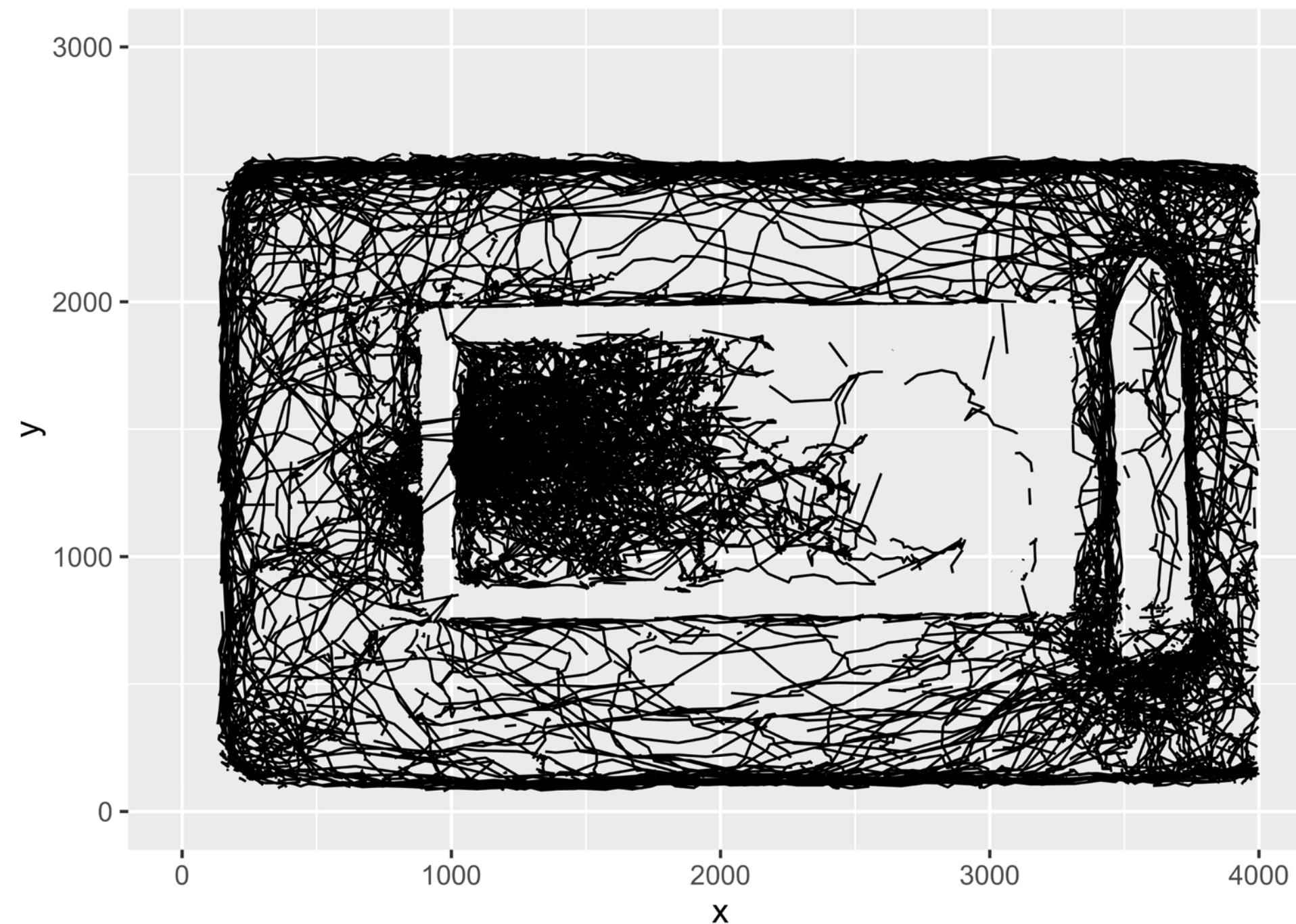
**Technical issues** difficult to monitor individuals' activities under the colony condition



I developed the tracking system  
using 2D barcodes in *Diacamma* ant

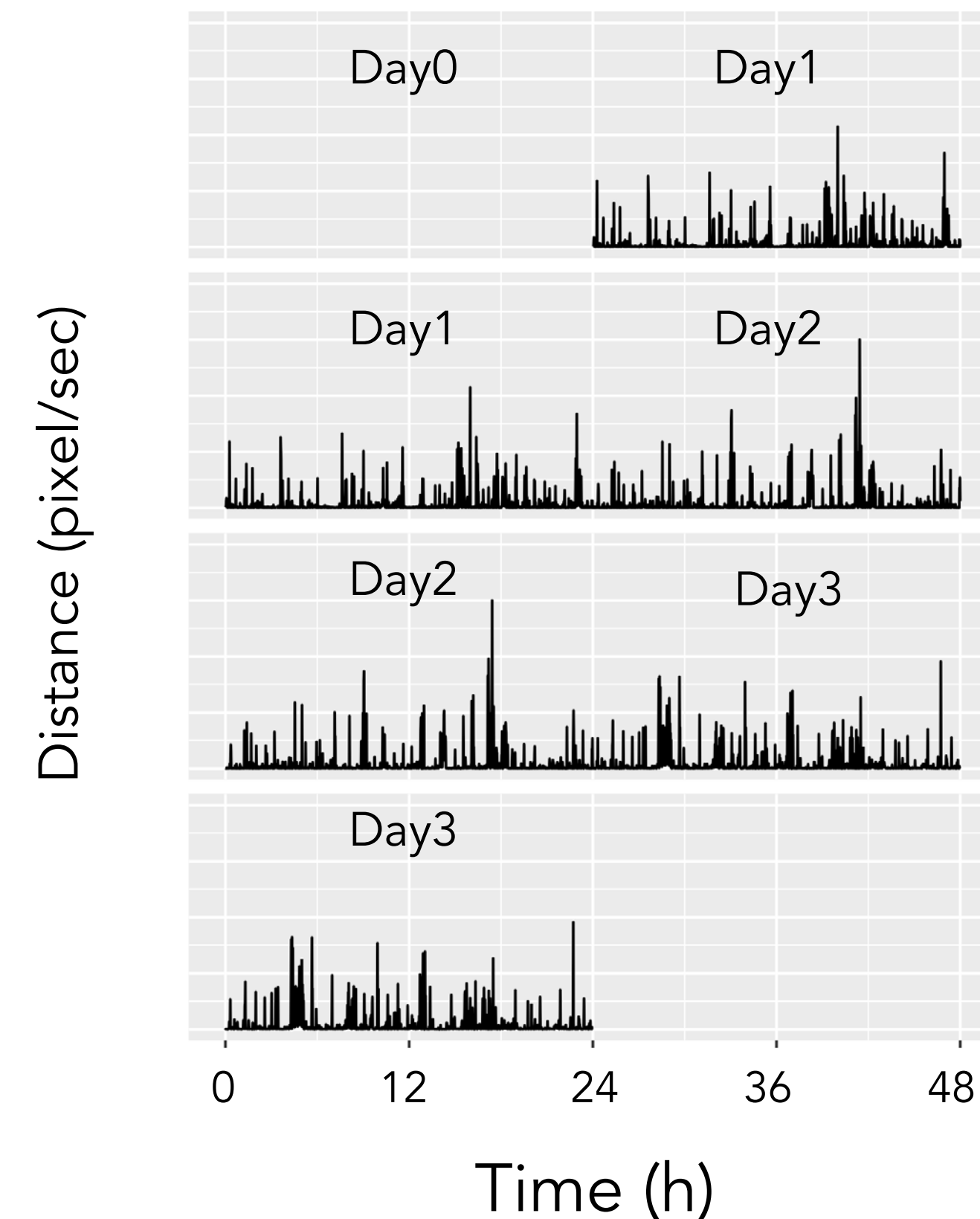
# Method | 2D barcode tag tracking

Trajectory of an ant



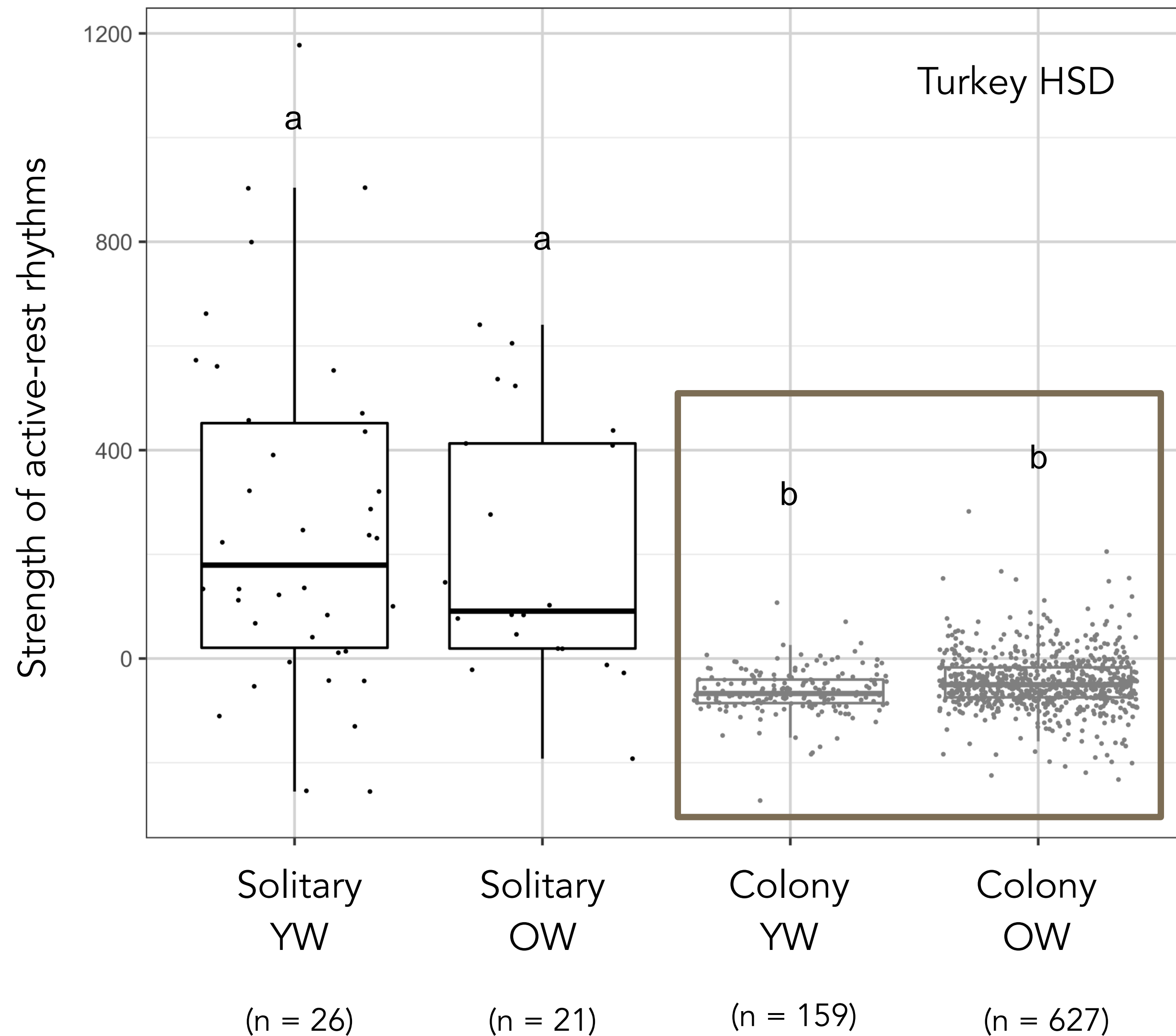
$60\text{sec} * 60\text{min} * 24\text{h} * 3\text{d}$

3 days 259200 data points



- Omitted the detachment of tags or deaths
- Omitted data with High missing detection time (>50 %)
- Traveled distance/sec was larger than 40.0 mm → NA

# Results | Solitary - Colony



Individuals in colonies (with brood) almost totally lost active-rest rhythms.

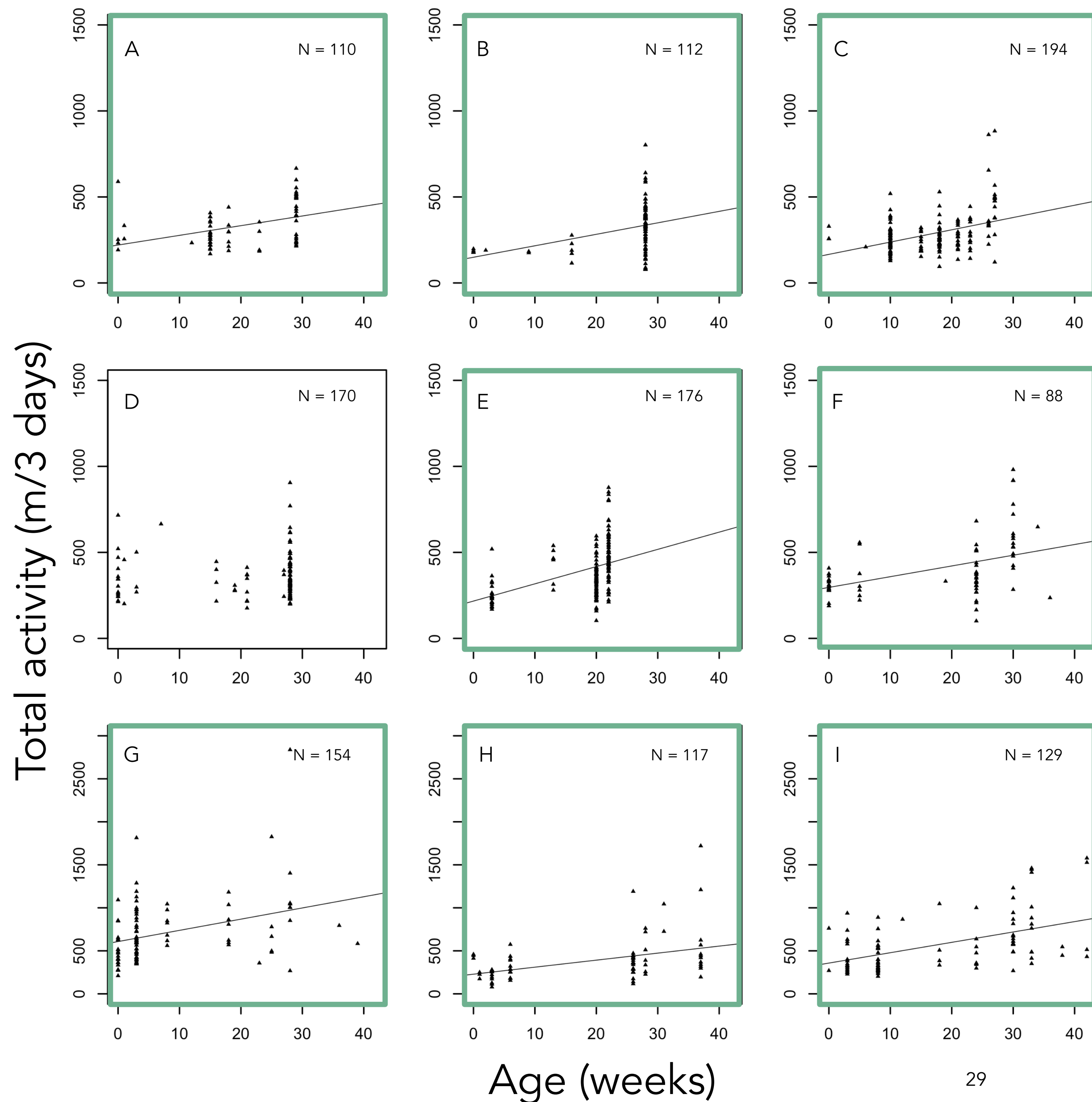
YW: 0-30 days  
OW: 30- days

Under constant DD condition



# Activity

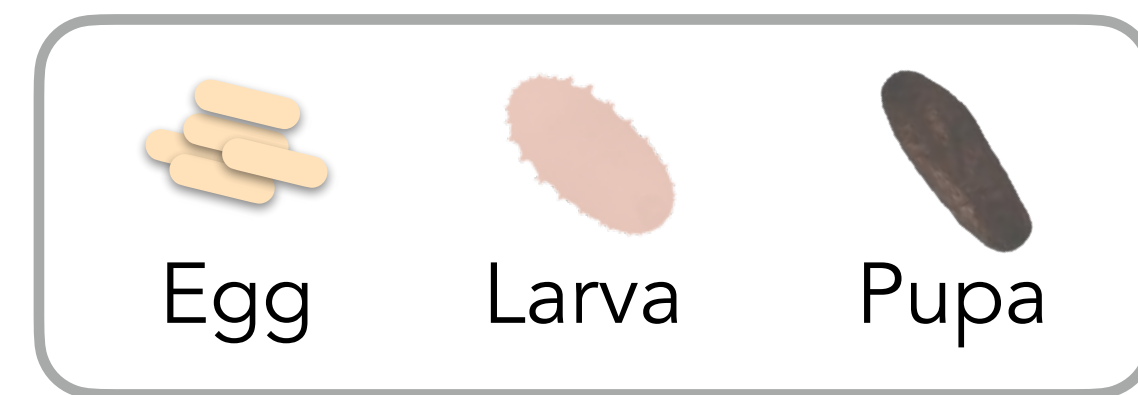
There were positive relationships between total activity and age in all colonies except colony D.





# Brood removal

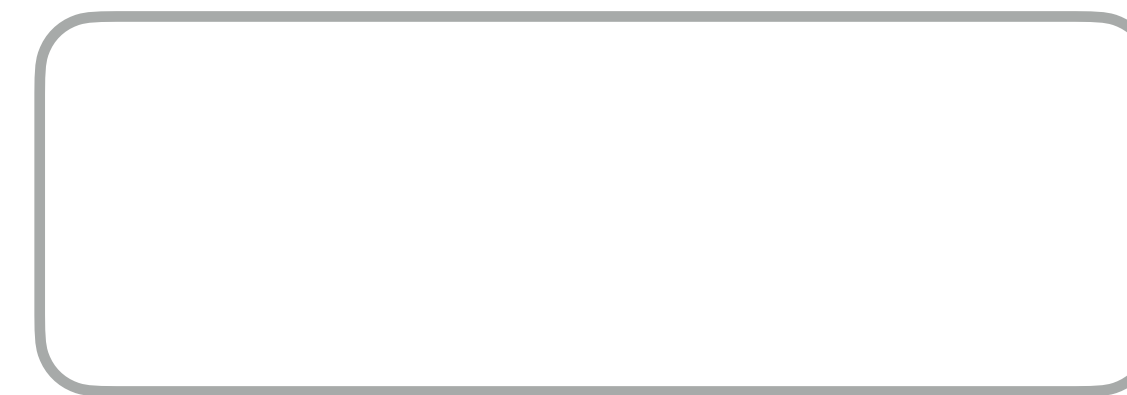
To further investigate the effect of brood in more naturalistic colony condition, I experimentally removed all brood in two colonies (A and B).



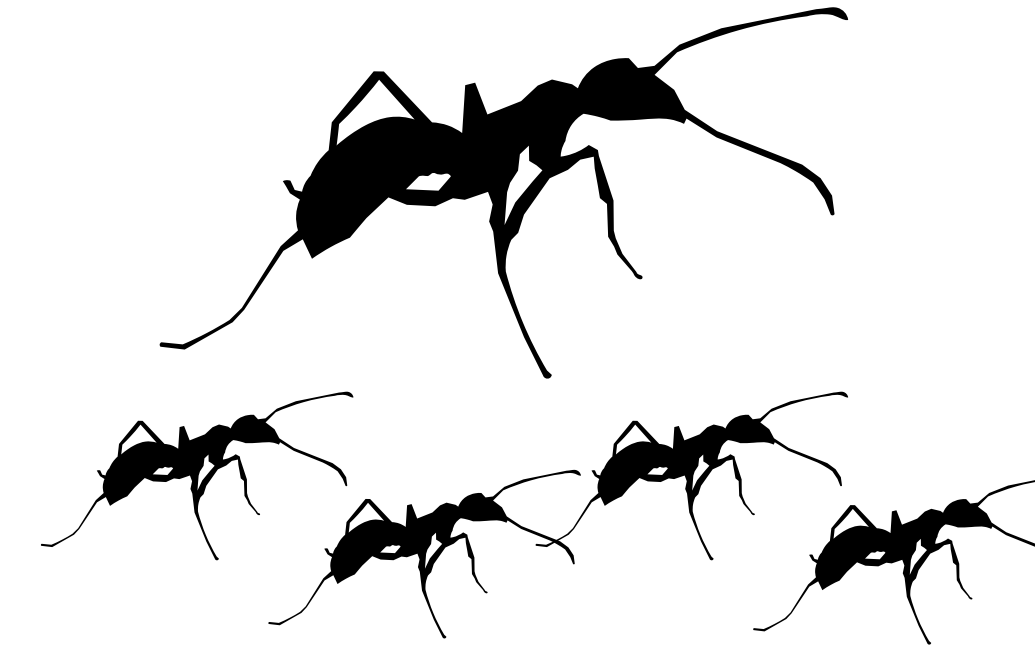
Arrhythmic activity



Colony condition



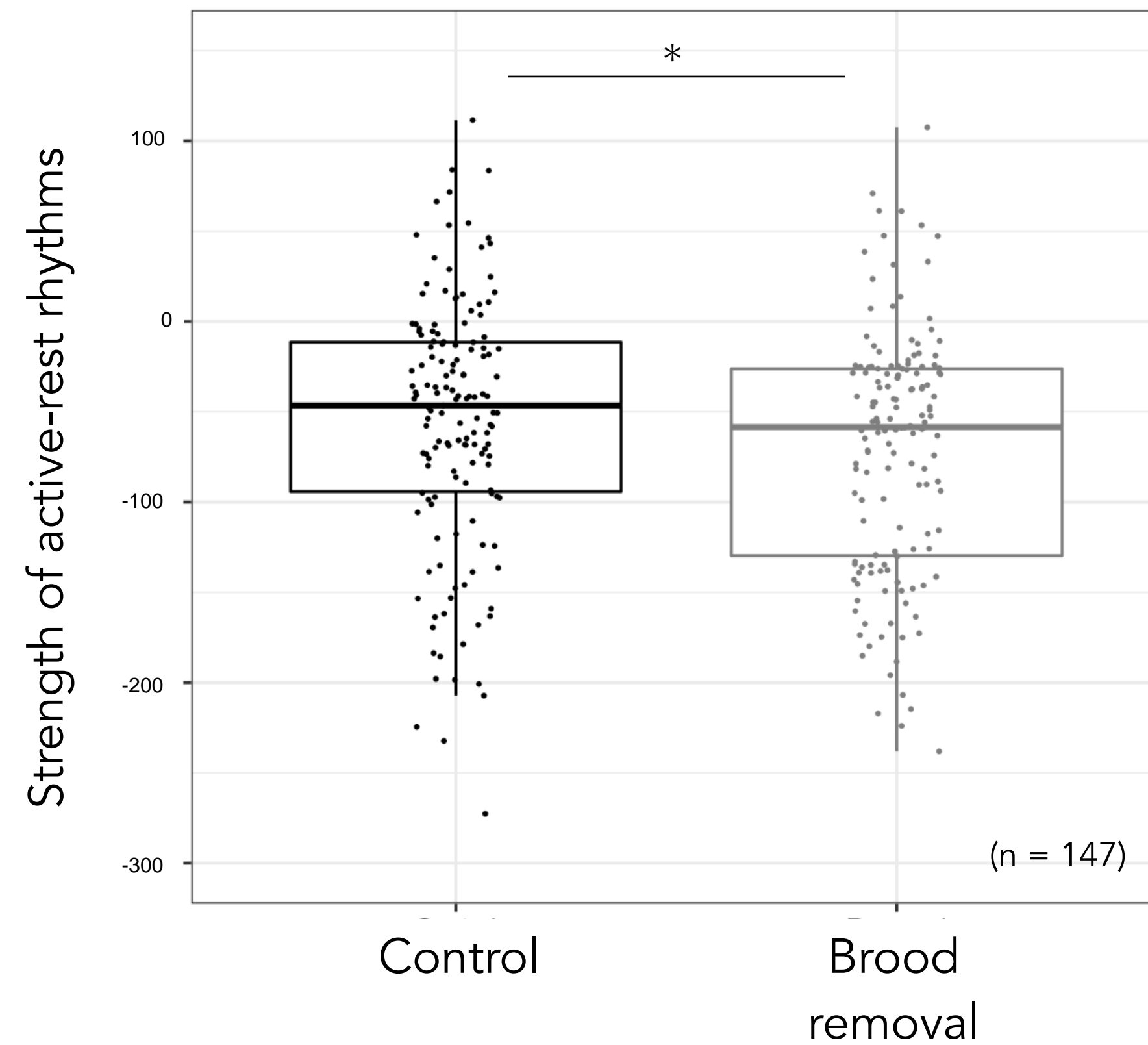
Rhythmic activity



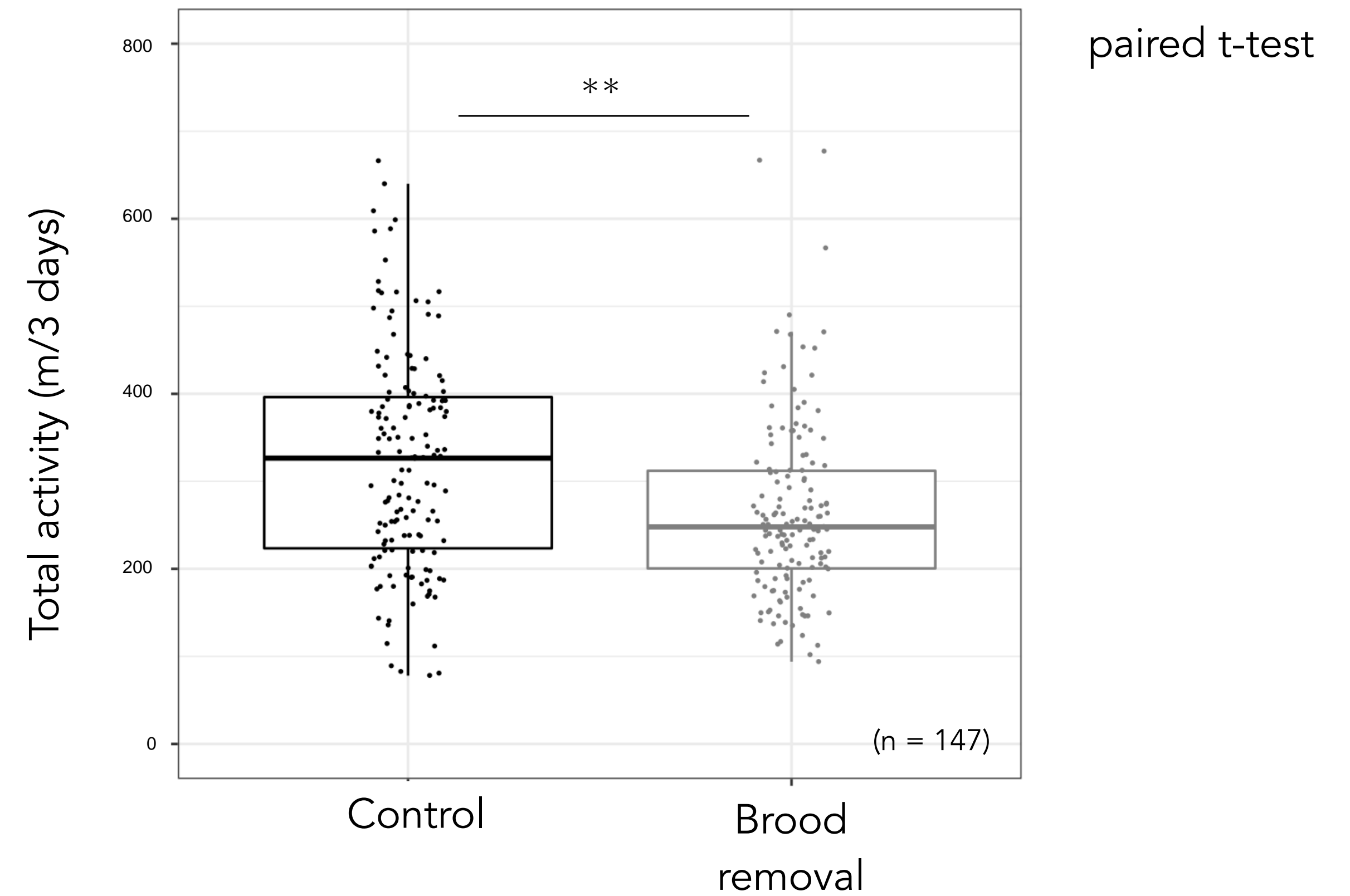
Colony condition

# Brood removal

## Rhythmicity



## Activity



Both rhythmicity and total activity were significantly lower than control.

# Discussion | colony condition

Both colony and solitary conditions

- Constant temperature
- Constant dim-red light

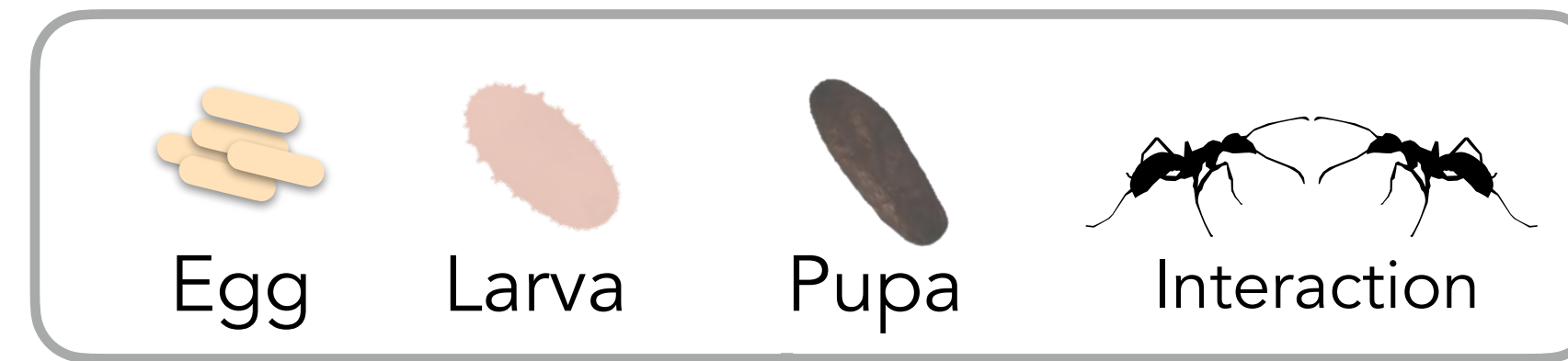
Solitary ants



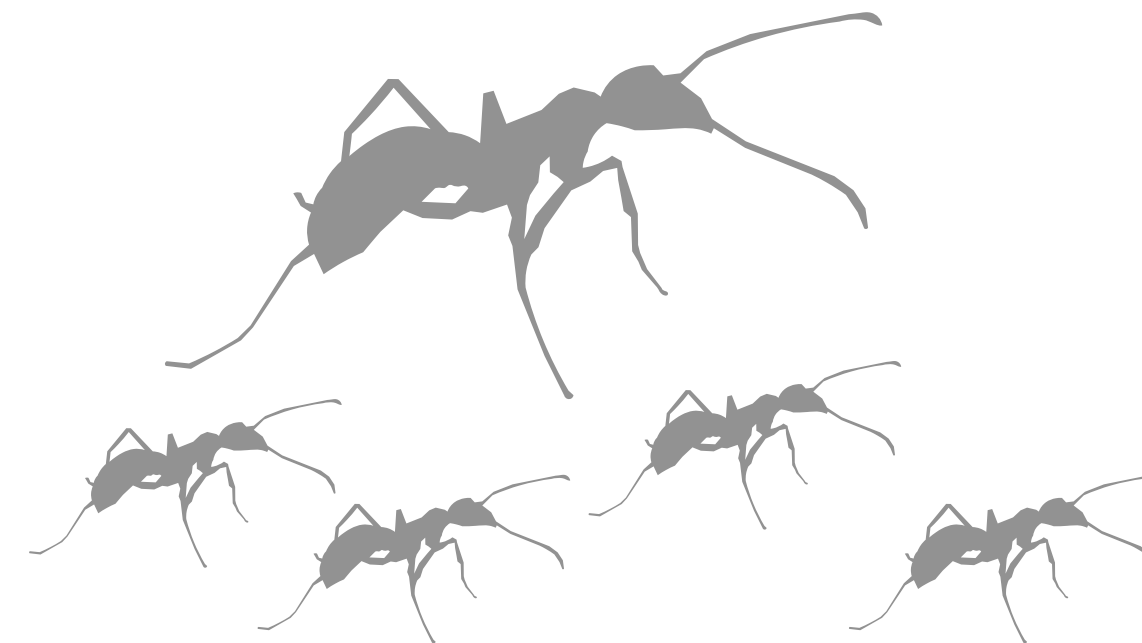
Active-rest rhythms

If rhythmicity is affected by light or temperature, solitary ants also show arrhythmic activities.

Mixture of social interaction



Colony condition

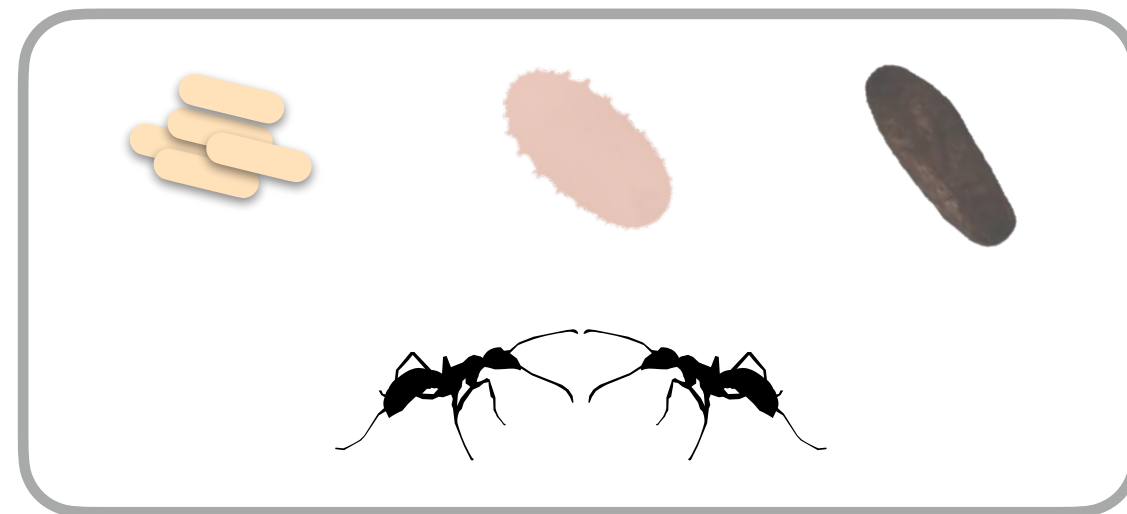


**Arrhythmic activity**

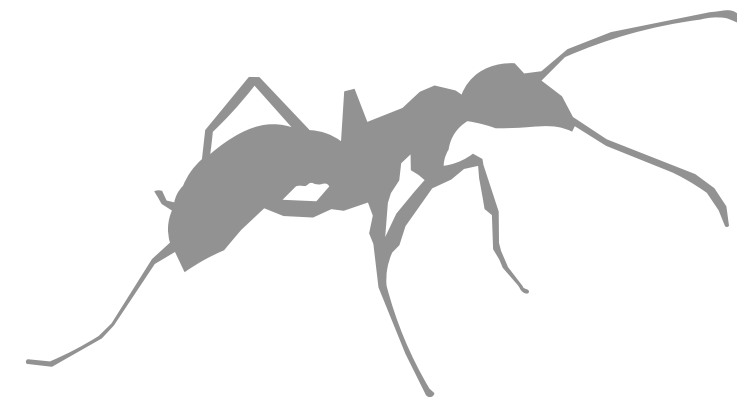
The mixture of social interactions reduced active-rest rhythms.

# Brood removal

Mixture of social interaction



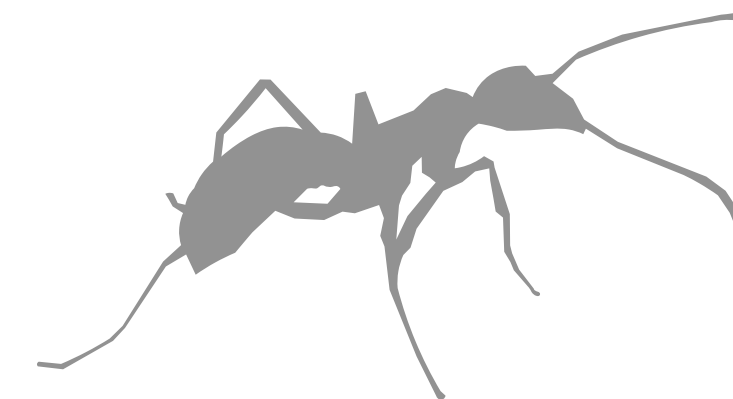
Arrhythmic activity



Brood removal



Arrhythmic rhythms  
Low activity level



Brood removal  
||  
Decrease of the  
amount of work ?

- Workers retained arrhythmic activity by worker-worker interactions.
- Workers might react to the amount of work and become an inactive state.



# Discussion | Foraging habitats

In social insects, it is considered that foragers have clear daily rhythms.

(*Apis*: Moore 1998; Crailsheim et al. 1996; Bloch and Robinson 2003; *Bombus*: Stelzer et al. 2010; *Pseudomyrmex termitarius*, *Solenopsis saevissima*, and *Camponotus*: Orivel and Dejean 2002; Mildner and Roces 2017; *Dinoponera quadriceps*: Medeiros, et al. 2014; *Atta colombica*: Bochynek, et al. 2017; *Odontomachus chelifer*: Raimundo, et al. 2009; *Ectatomma ruidum*: Passera, et al. 1994; *Pheidole pallidula* and *Tetramorium semilaeve*: Retana, et al. 1992; *Eciton*, *Nomamyrmex* and *Neivamyrmex*: Hoenle et al. 2019; *Solenopsis invicta*: Lei et al. 2019)



**Bees**



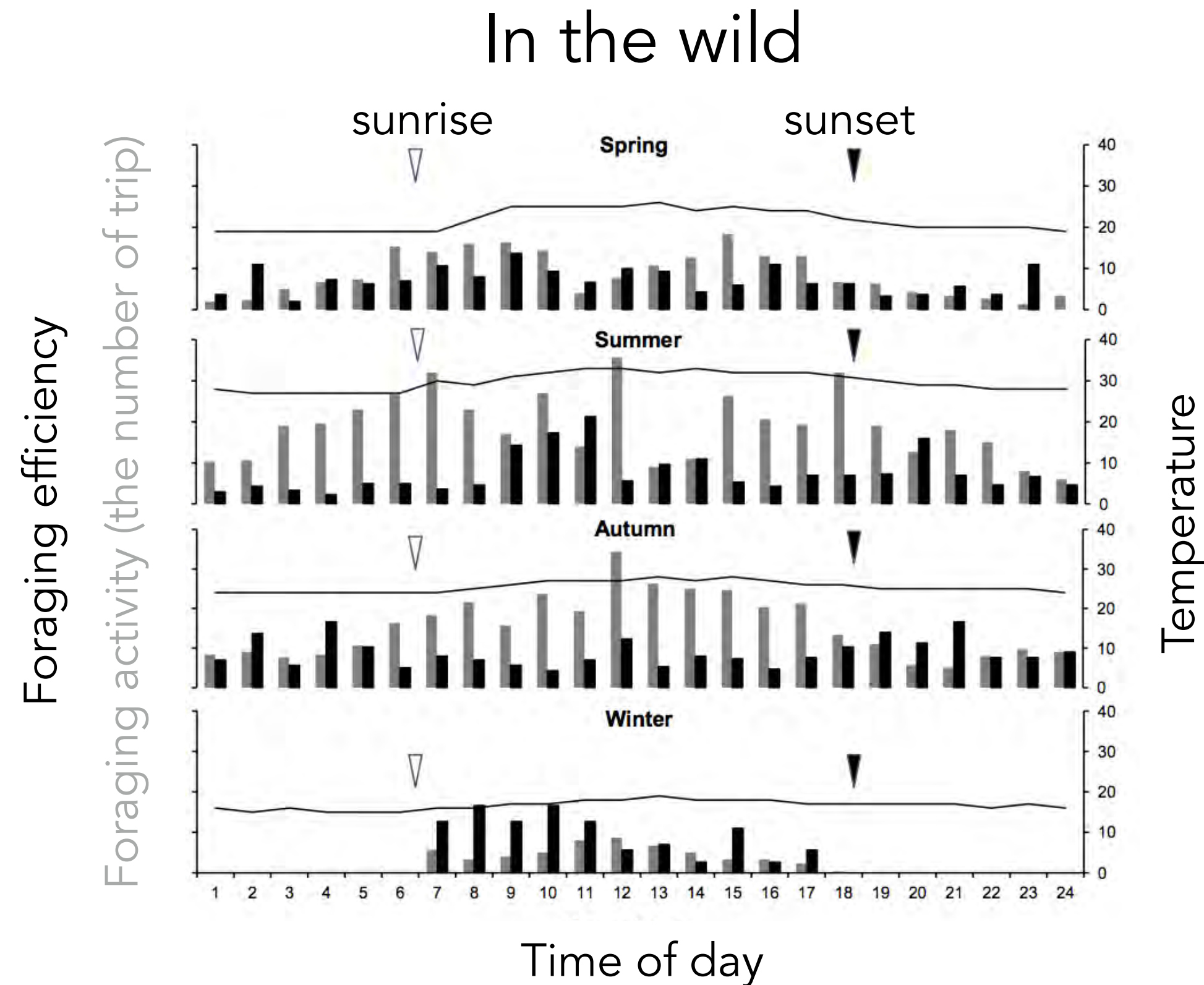
Floral nectars and pollens



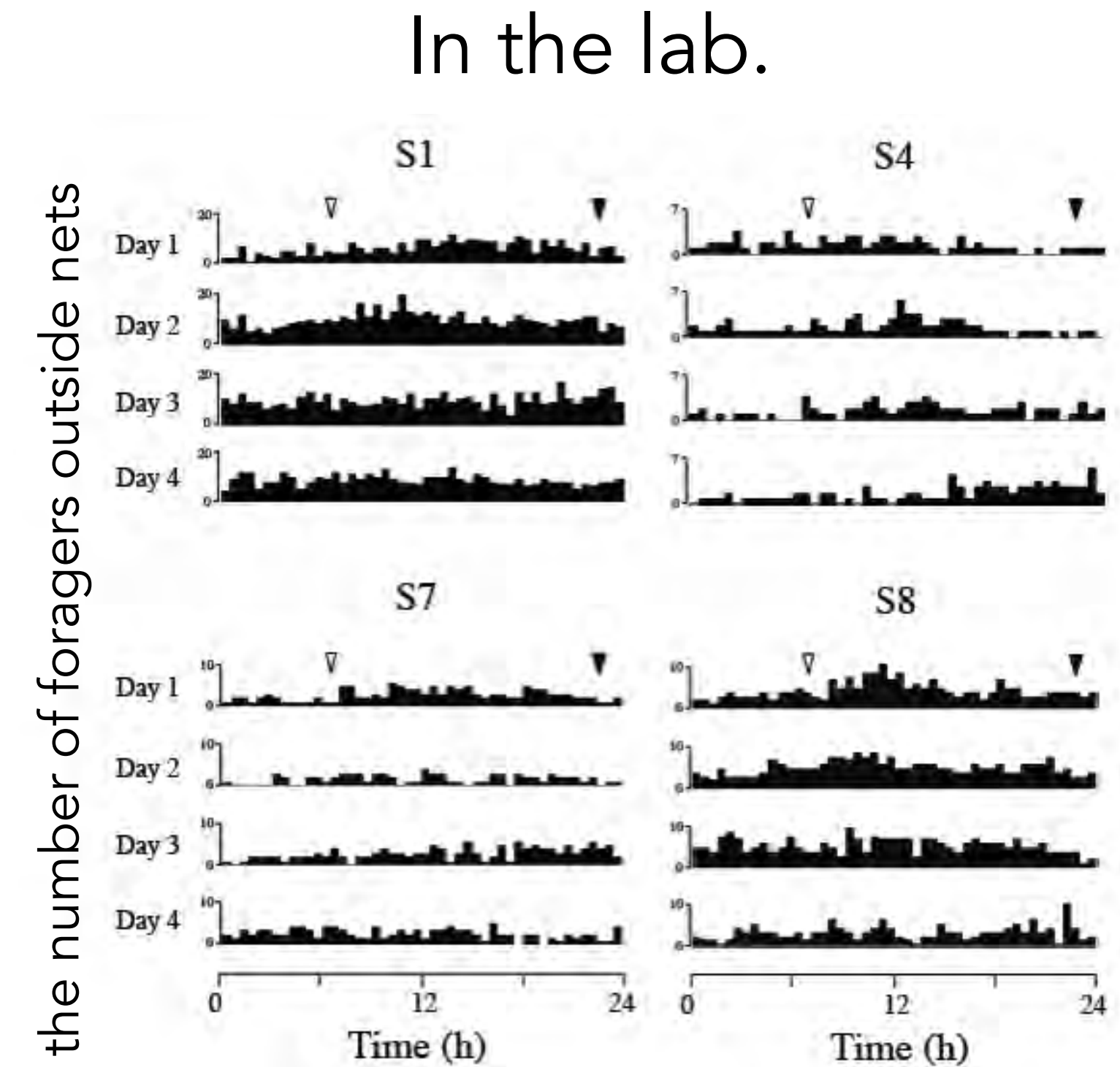
**Ants**

Diversity of food types  
such as arthropods

# Foraging activity in *Diacamma*



(Win et al. 2018)

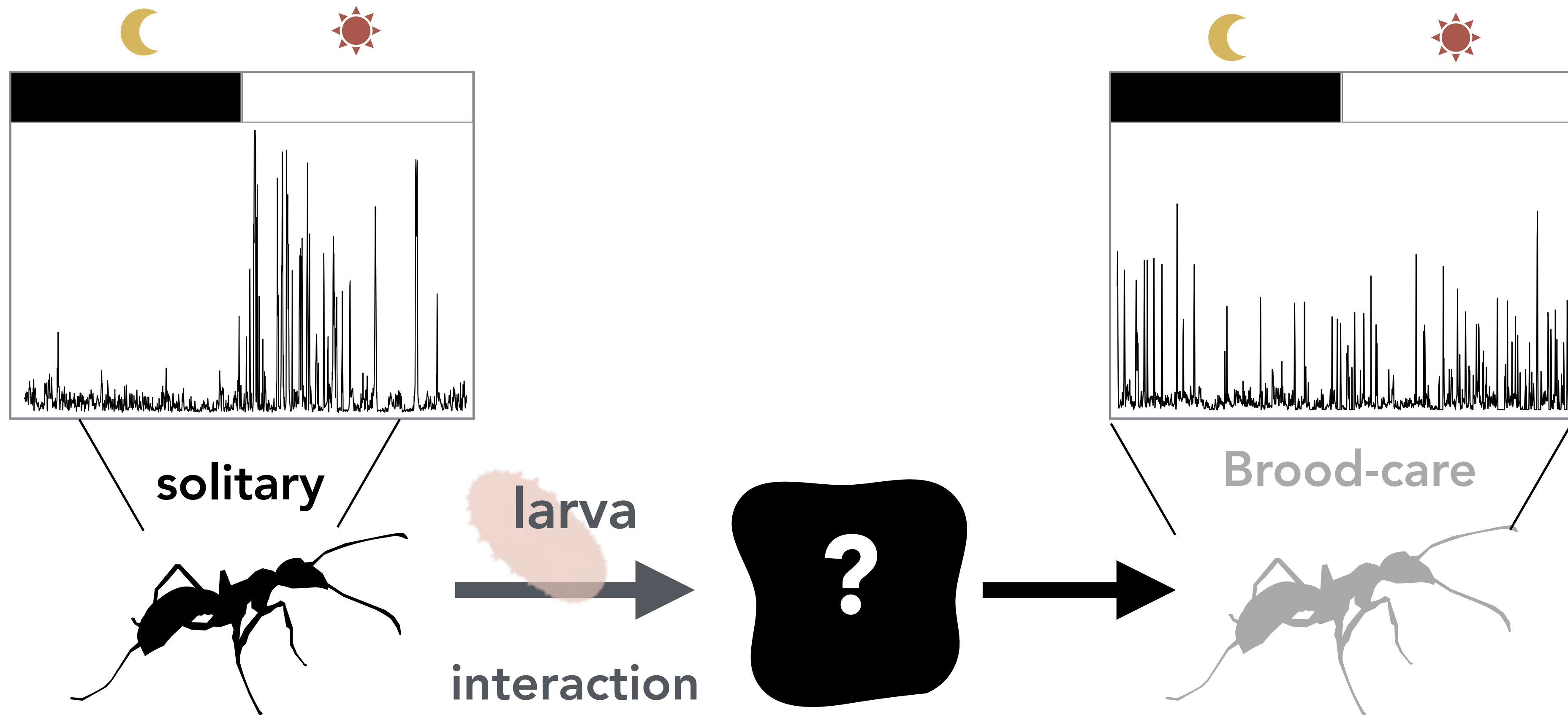


(Fuchikawa et al. 2014)

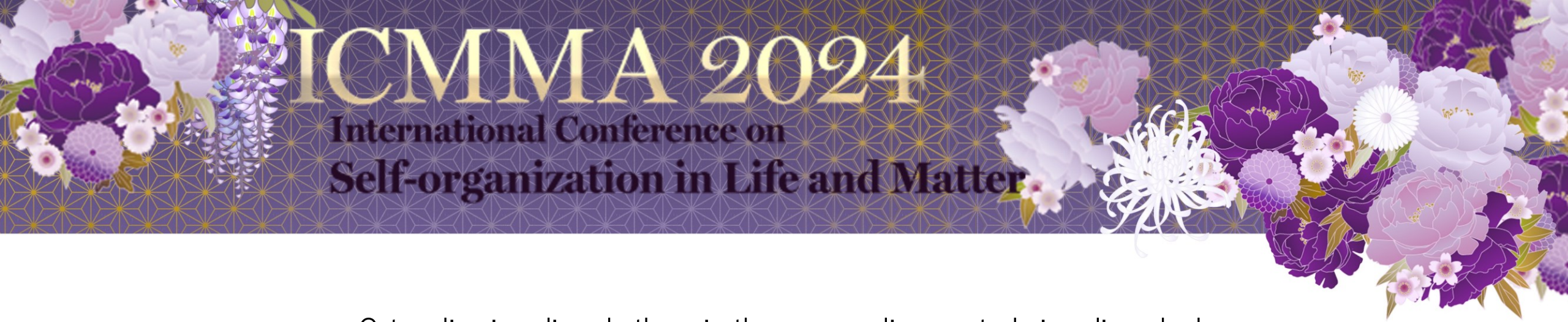
Colony-level foraging activities = Individual-level activity?

My results suggested that foragers showed all-day-long activities.

# Future prospect







## Cytosolic circadian rhythms in the mammalian central circadian clock

Daisuke Ono (Nagoya University, Japan)

In mammals, the suprachiasmatic nucleus (SCN) plays a crucial role in the timing of physiology and behavior, such as sleep/wakefulness. In the SCN, several neurotransmitters are involved in the neuronal network. The receptors for these neurotransmitters are coupled with G-proteins and second messenger signaling pathways, including cAMP and  $\text{Ca}^{2+}$ . Pharmacological studies suggest that in the SCN, intracellular cAMP and  $\text{Ca}^{2+}$  are involved in the input and/or output of the molecular circadian clock and/or in the circadian oscillations within the SCN. However, the functional roles and dynamics of cAMP and  $\text{Ca}^{2+}$  within the SCN neuronal network remain largely unclear.

To investigate the functional roles of cAMP, we first visualized the spatiotemporal pattern of circadian rhythms of cAMP in the SCN using bioluminescent cAMP probes (Okiluc-aCT) that we recently developed (Ono et al., 2023, Science Advances). For comparison, we also visualized the rhythm patterns of  $\text{Ca}^{2+}$  using the fluorescent  $\text{Ca}^{2+}$  probe (GCaMP6s). Blocking the function of the neural network in the SCN slice resulted in the loss of circadian rhythms of cAMP, whereas circadian rhythms of  $\text{Ca}^{2+}$  persisted but decreased in amplitude. These results suggest that in the SCN, circadian rhythms of cAMP are regulated by the neural network, while circadian rhythms of  $\text{Ca}^{2+}$  are regulated by both intracellular mechanisms and neural networks.

To further understand these cytosolic events and their relation to the circadian clock, we used *Bmal1*-deficient mice that show arrhythmic behavior under constant conditions. We confirmed the presence of circadian rhythms of PER2::LUC in the SCN of *Bmal1*-deficient mice, as previously reported (Ko et al., 2010, PLoS Biology). These rhythms exhibited the three key aspects of the circadian clock: autonomous oscillation, temperature compensation, and entrainment. Additionally, we observed cAMP and  $\text{Ca}^{2+}$  rhythms in the SCN of these animals. These results suggest that *Bmal1* is not essential for circadian rhythms in the SCN.



# Cytosolic circadian rhythms in the mammalian central circadian clock

○Daisuke Ono<sup>1,2</sup>, Takashi Sugiyama<sup>3</sup>, and Naohiro Kon<sup>4</sup>

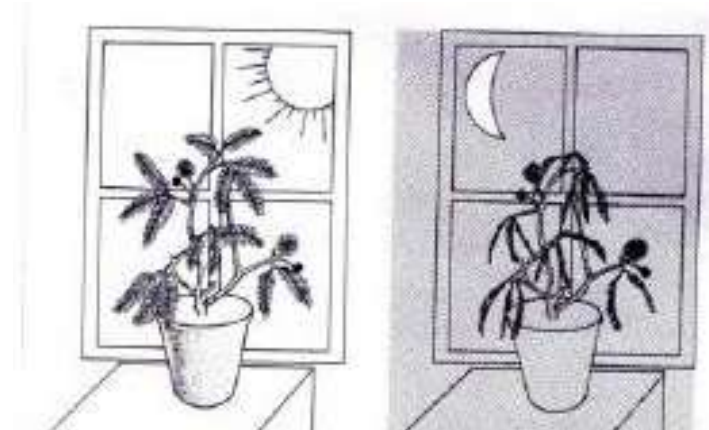


1. Stress Recognition and Response, Research Institute of Environmental Medicine, Nagoya University, Furo-cho, Chikusa-ku, Nagoya, Japan
2. Department of Neural Regulation, Nagoya University Graduate School of Medicine, Nagoya, Japan
3. Advanced Technology, Evident Corporation, Tokyo, Japan
4. Institute of Transformative Bio-Molecules (WPI-ITbM), Nagoya University, Furo-cho, Chikusa-ku, Nagoya, Japan

## The beginning of circadian rhythm research



*Mimosa pudica*

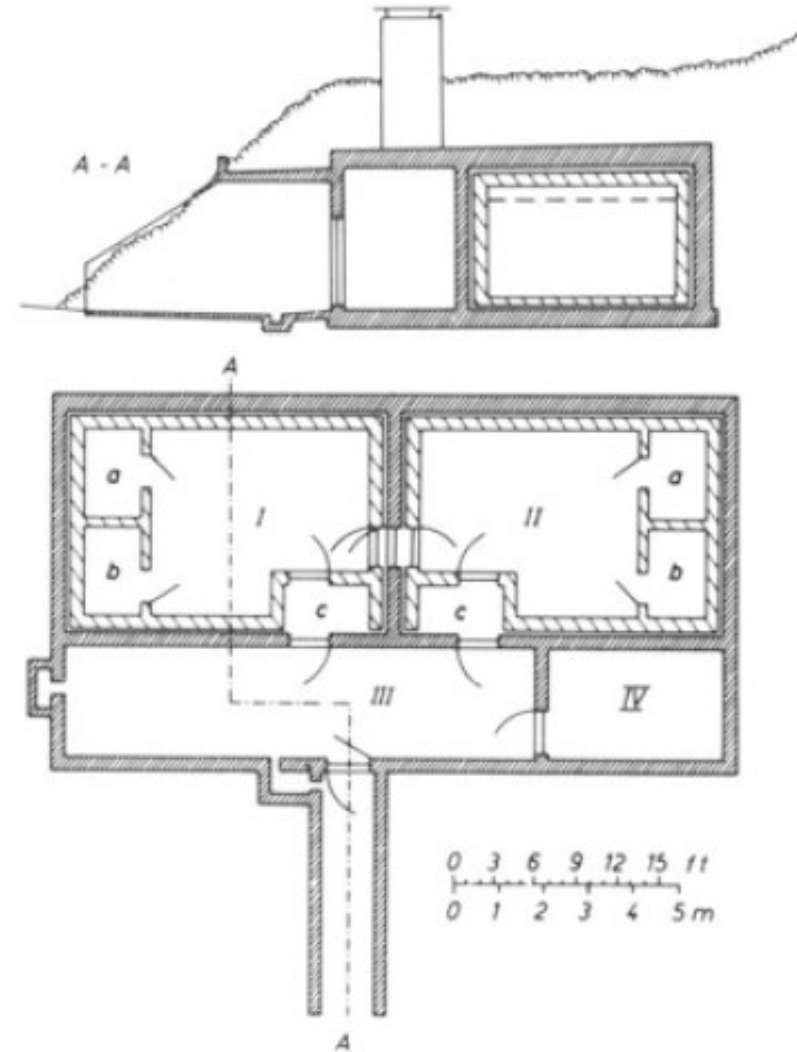


Jean-Jacques d'Ortous de Mairan (1678–1771).

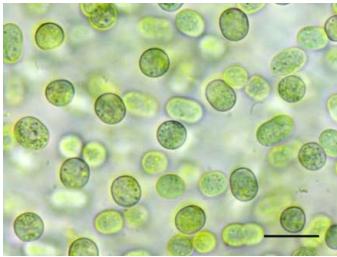
## Measurement of human circadian rhythms



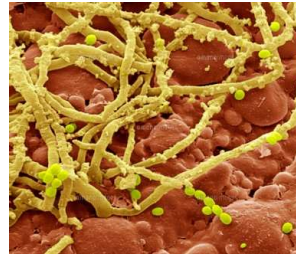
Jürgen Aschoff (1913-1998)



Circadian rhythm in many lives on the earth



Bacteria



Fungi



lies

# Clock gene



Plants



Mice



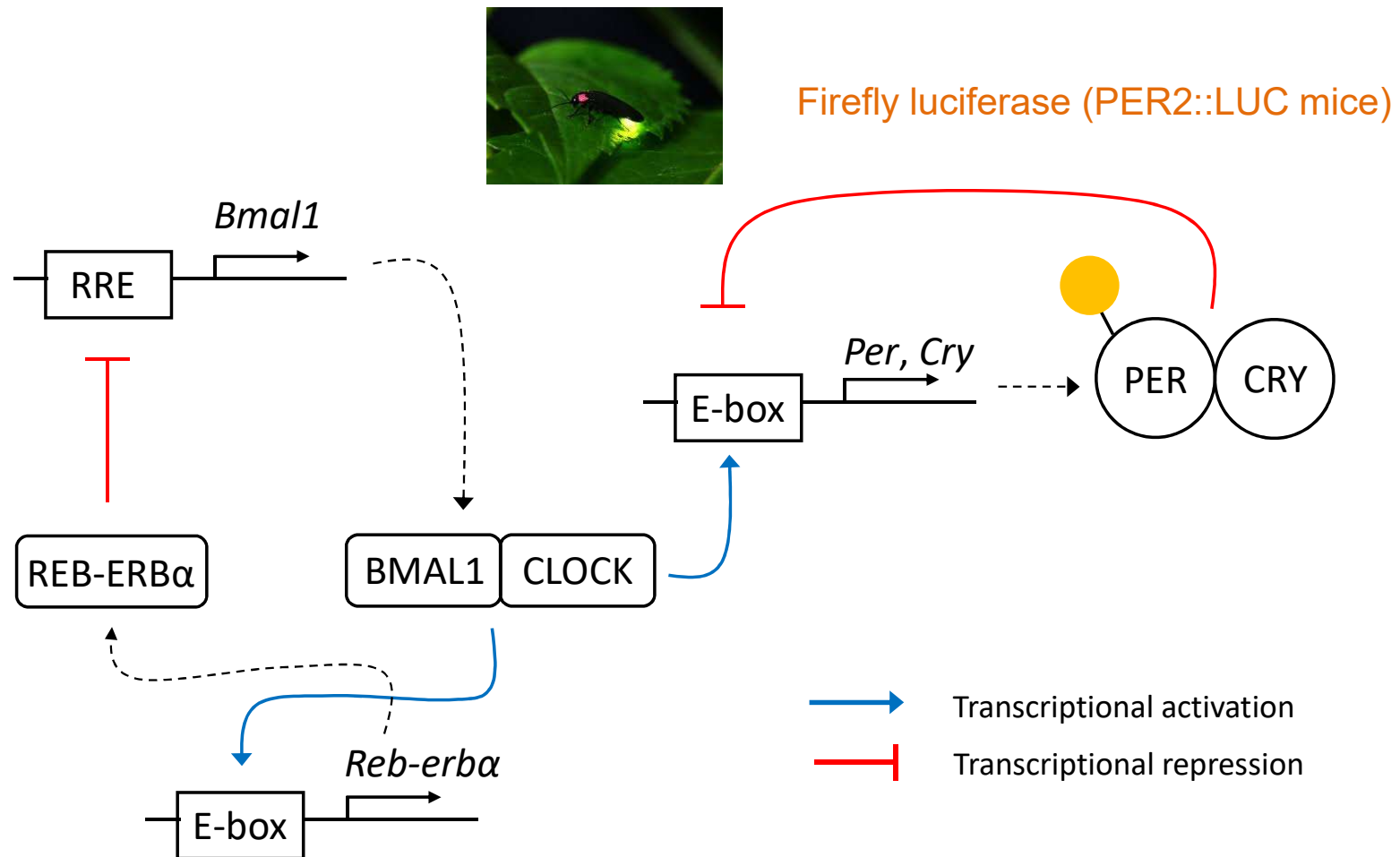
Birds



Fishes

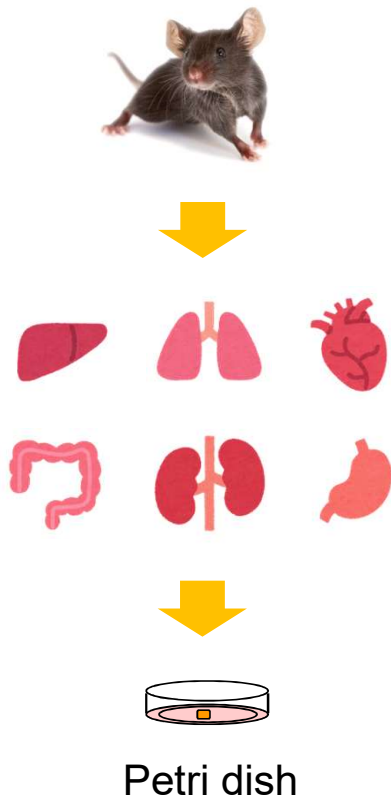


## Inter-locked negative feedback loop

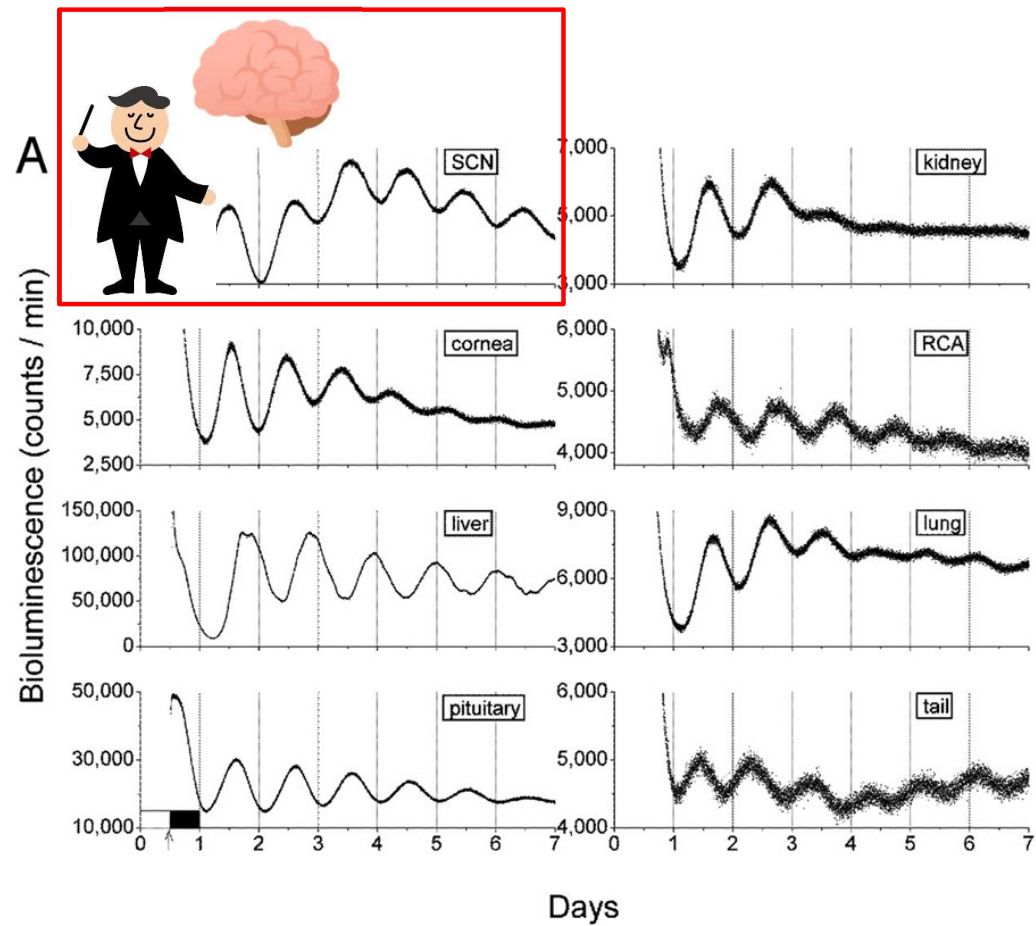


The mammalian circadian clock mechanism are distributed throughout the body

PER2::LUC mice

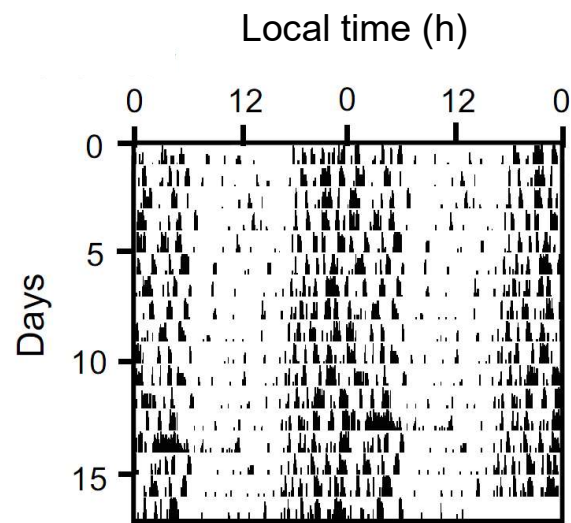
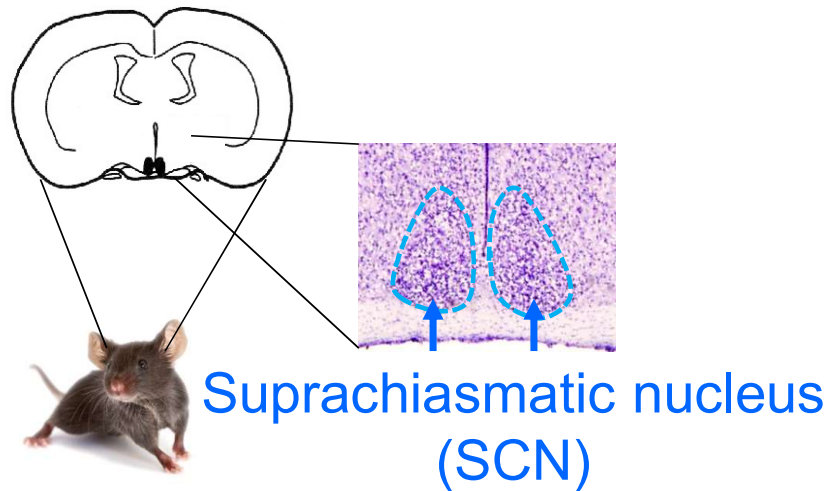


Suprachiasmatic nucleus (SCN)

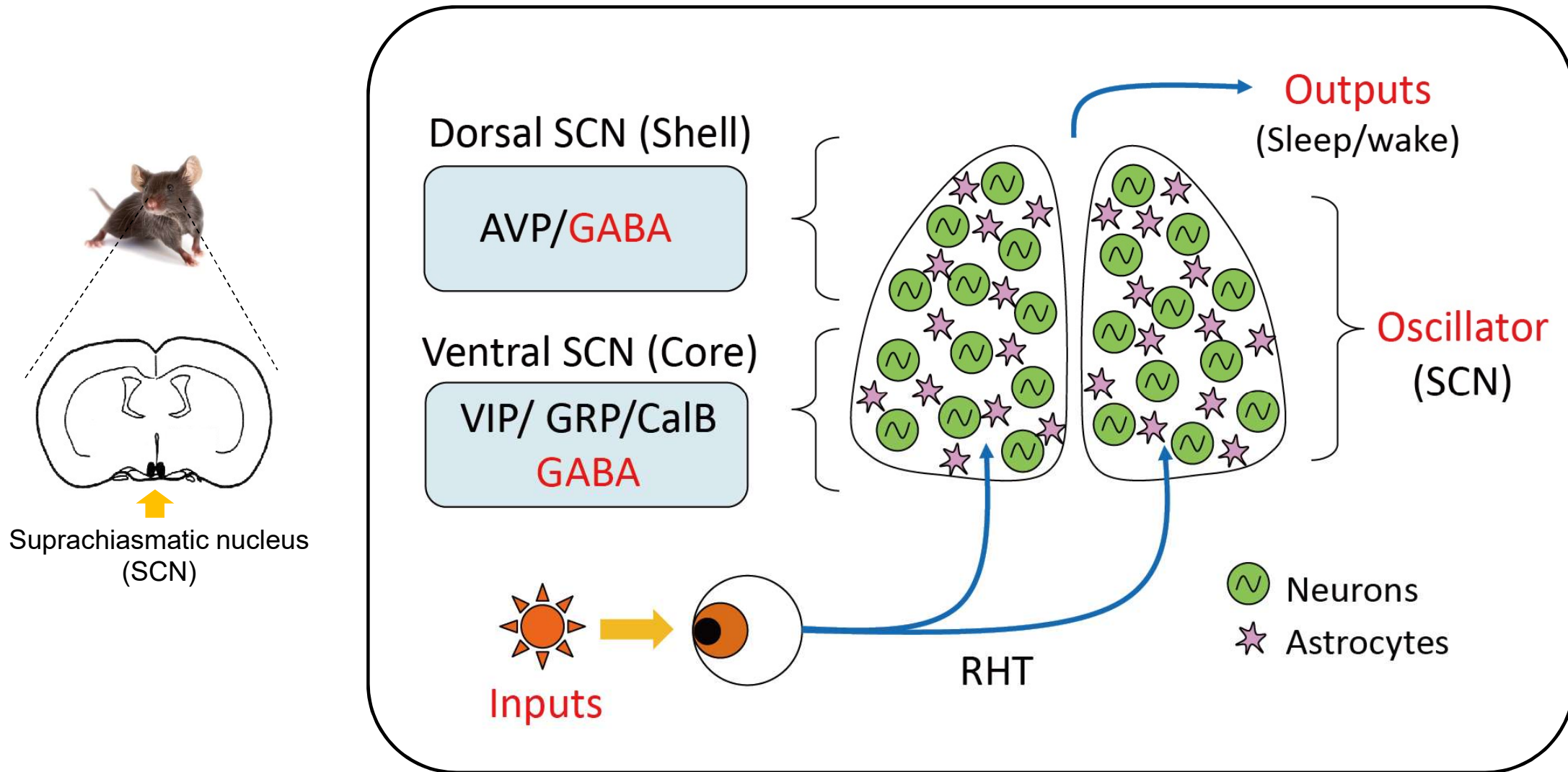


Yoo et al., 2004 PNAS

## The central circadian clock located in the suprachiasmatic nucleus (SCN)

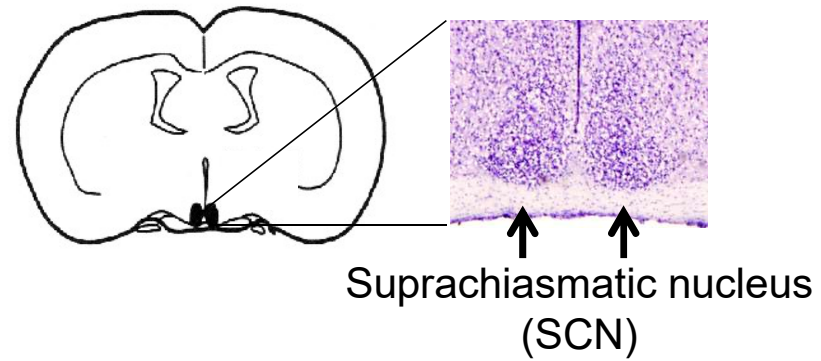


## The central circadian clock located in the suprachiasmatic nucleus (SCN)

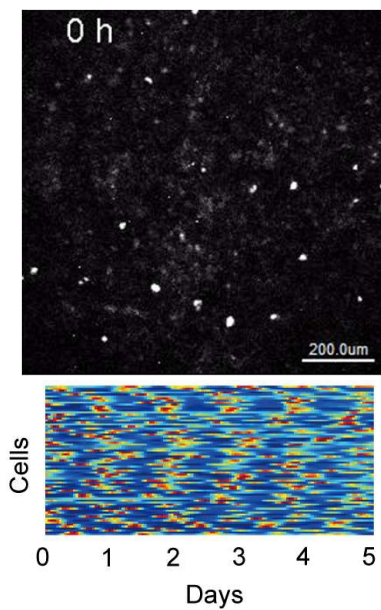




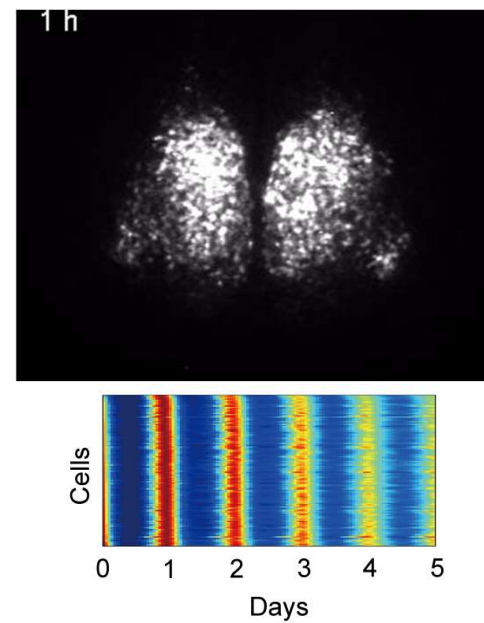
## The central circadian clock located in the suprachiasmatic nucleus (SCN)



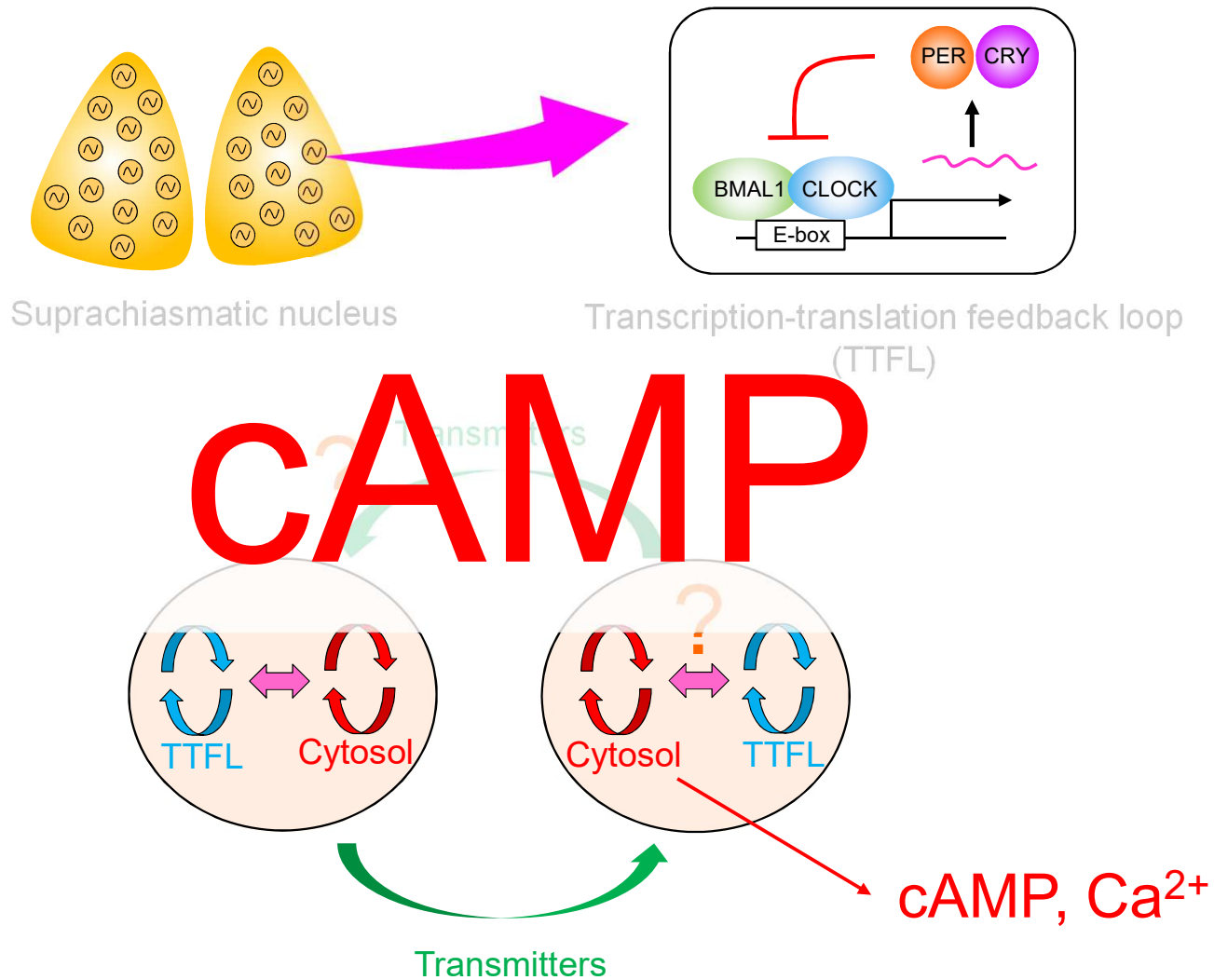
Dispersed SCN cells



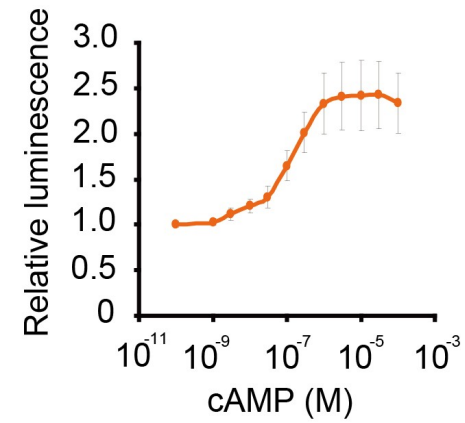
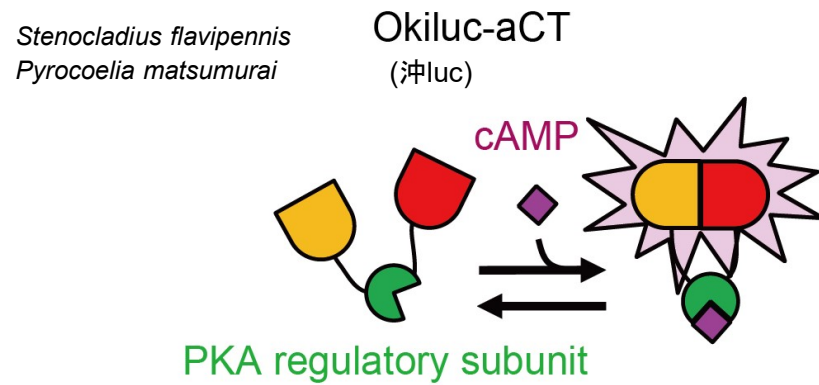
SCN slice



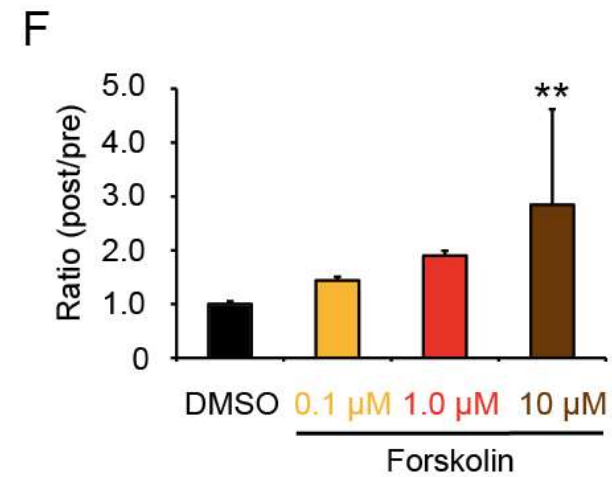
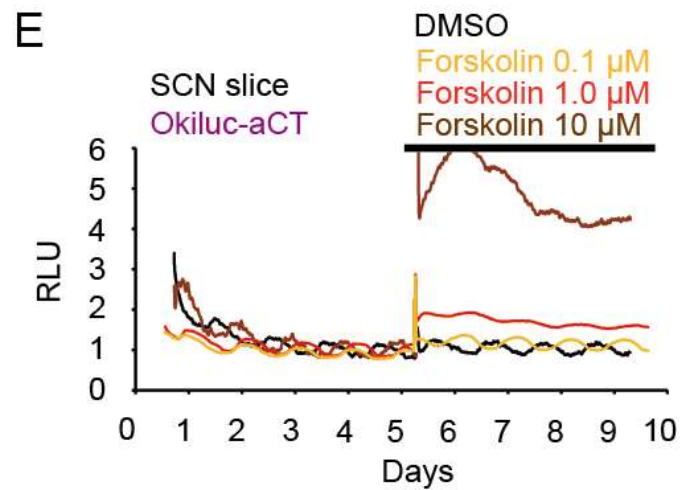
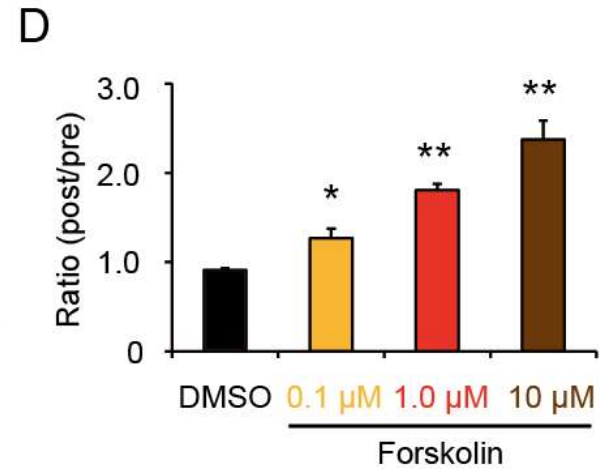
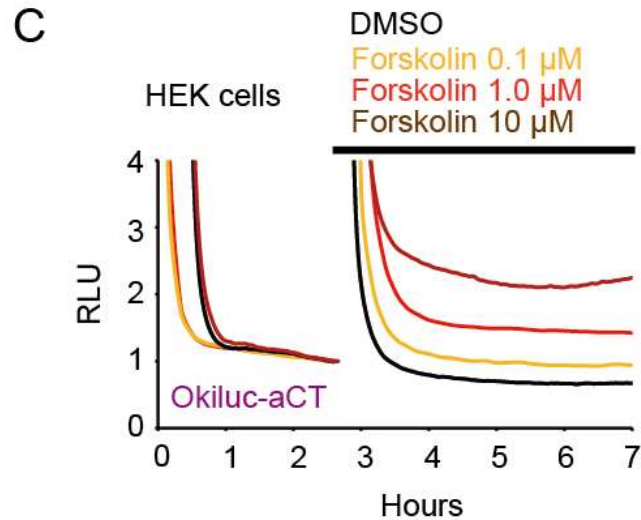
## Synchronization of cellular circadian rhythms in the SCN



## Development of new cAMP bioluminescent probe (Okiluc-aCT)



## Characteristics of Okiluc-aCT in the HEK cells and SCN neurons

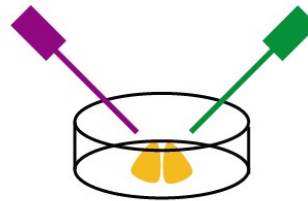




## Recording of cAMP and $\text{Ca}^{2+}$ in the SCN slice

AAV-hSyn-Okiluc-aCT

AAV-hSyn-GCaMP6s



SCN slice

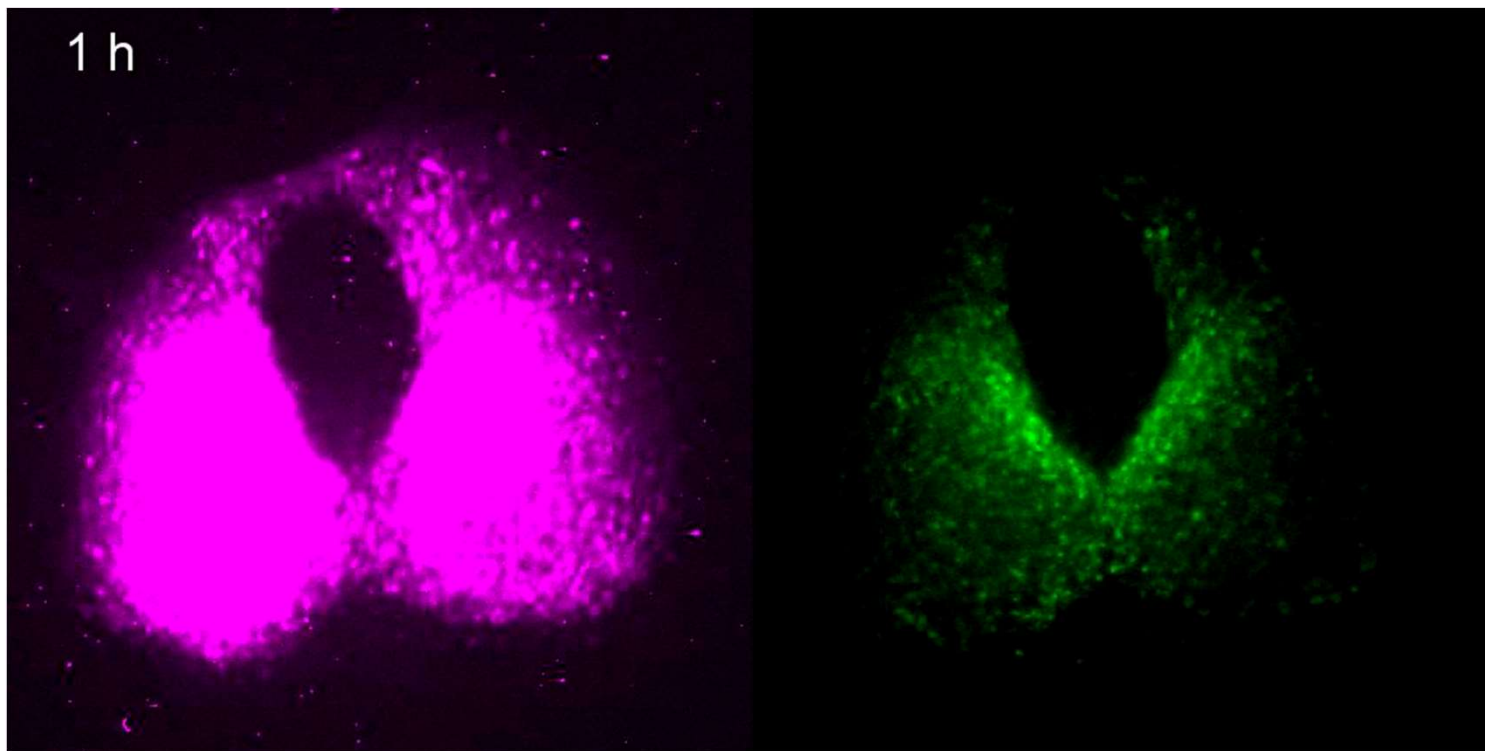


Time-laps imaging

## Development of new cAMP bioluminescent probe (Okiluc-aCT)

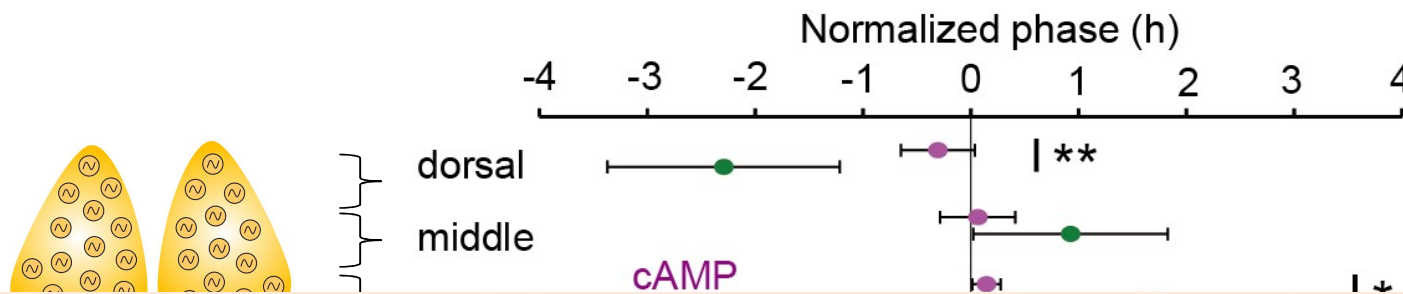
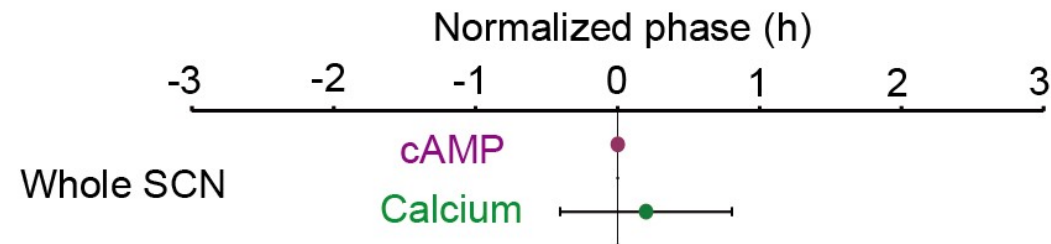
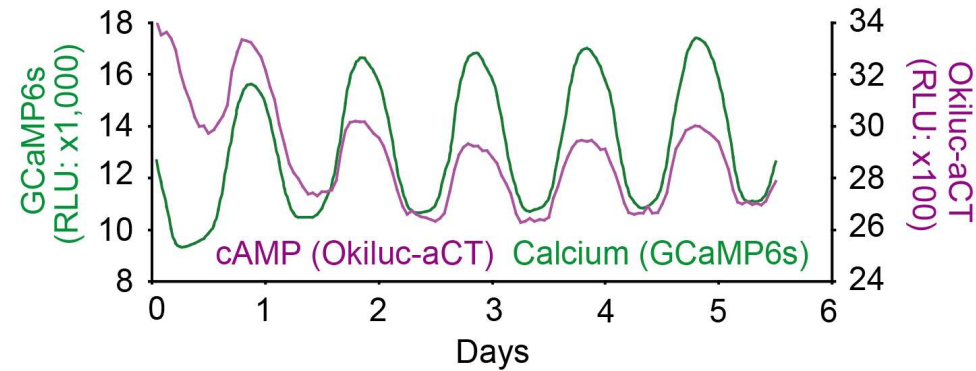
Okiluc-aCT (cAMP)

GCaMP6s ( $\text{Ca}^{2+}$ )



59min (Okiluc-aCT) → 3sec (GCaMP6s), every 1hour

## Circadian cAMP and Ca<sup>2+</sup> rhythms in the SCN



cAMP and Ca<sup>2+</sup> might have different functions for the circadian rhythms in the SCN

## Circadian cAMP and Ca<sup>2+</sup> rhythms in the SCN under TTX application

TTX (sodium channel blocker) → shutting down of neuronal networks in the SCN

Circadian rhythms are observed → It is regulated by intracellular mechanisms

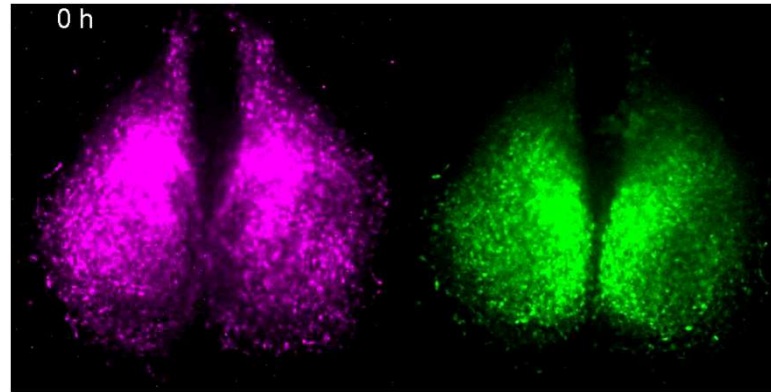
Circadian rhythms are NOT observed → It is regulated by neuronal networks



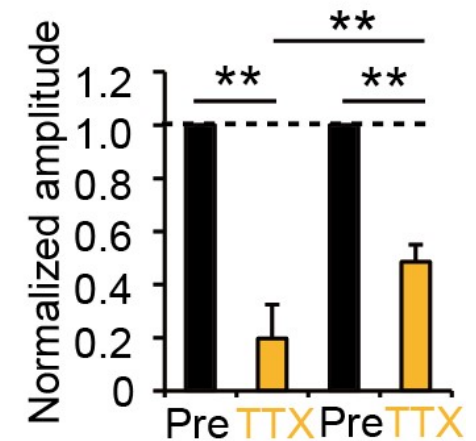
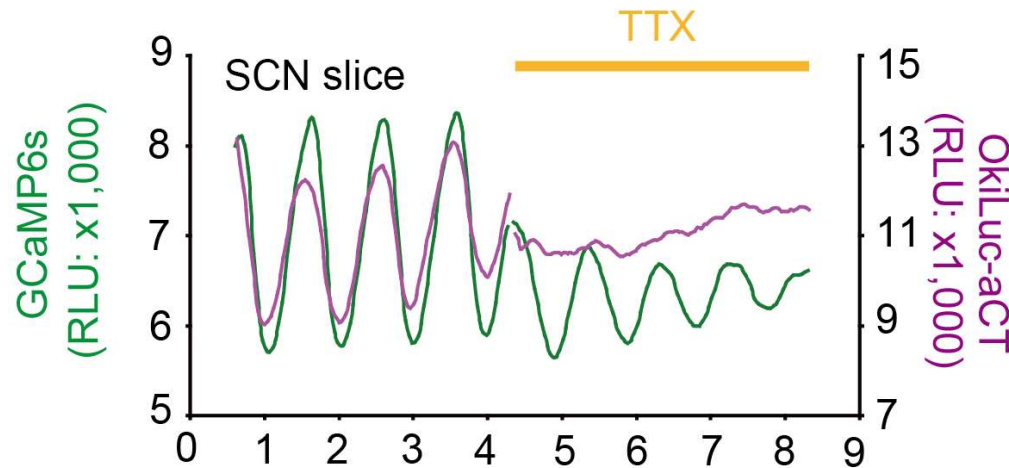
## Circadian cAMP and $\text{Ca}^{2+}$ rhythms in the SCN under TTX application

TTX (sodium channel blocker) → shutting down of neuronal networks in the SCN

Okiluc-aCT (cAMP)

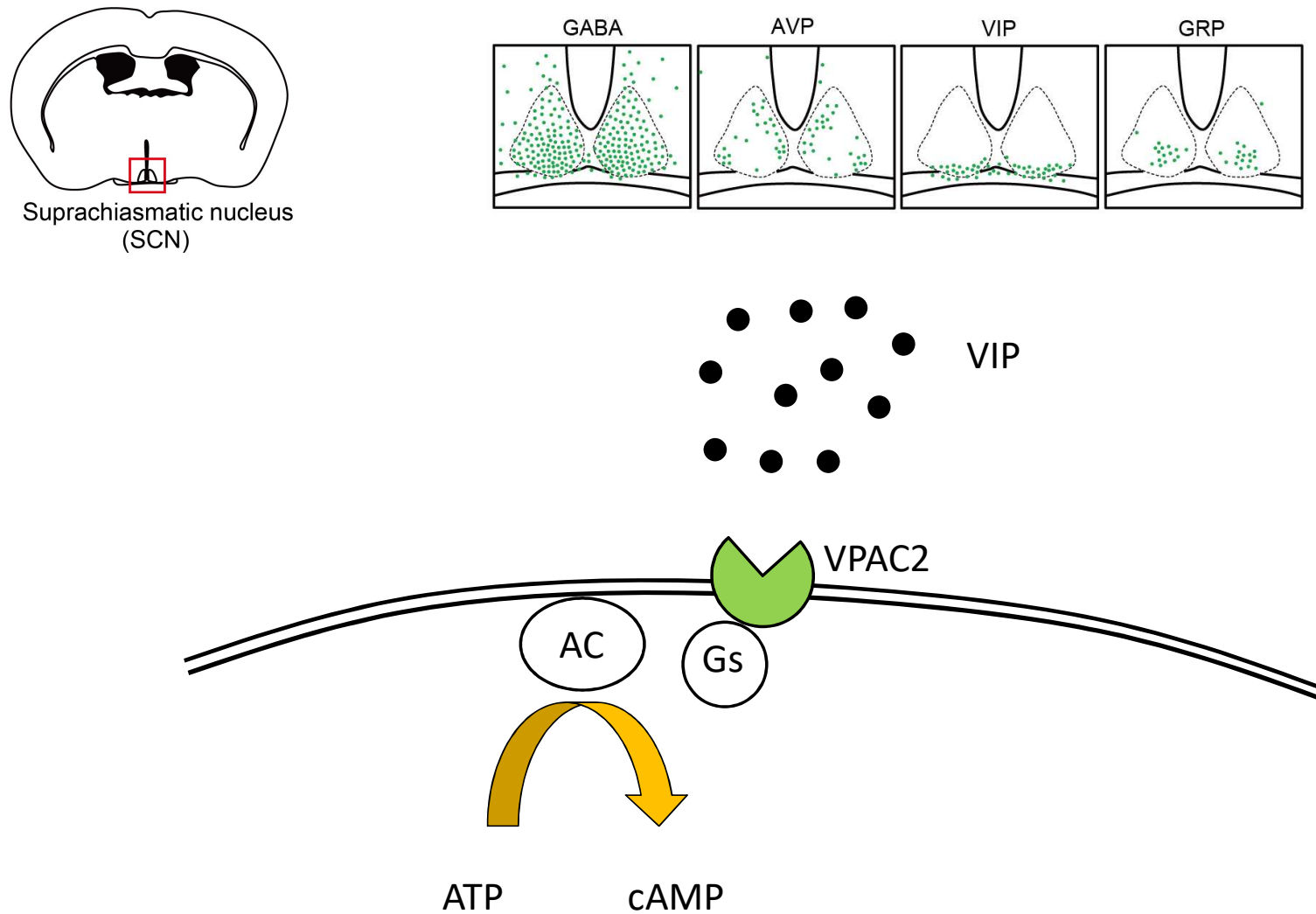


GCaMP6s ( $\text{Ca}^{2+}$ )



Circadian cAMP rhythms in the SCN are driven by action potential dependent mechanisms

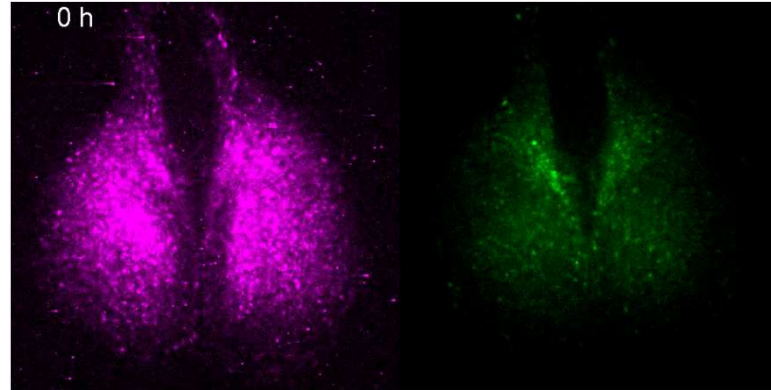
## Neuropeptidergic signaling in the SCN



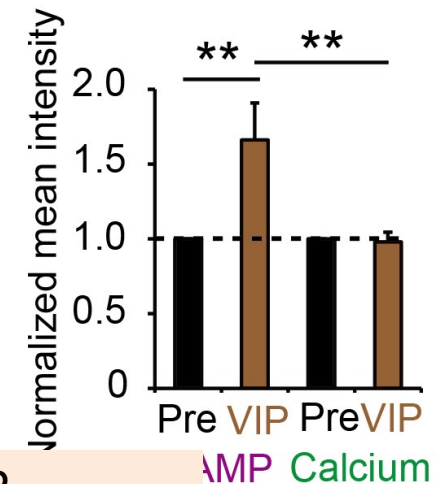
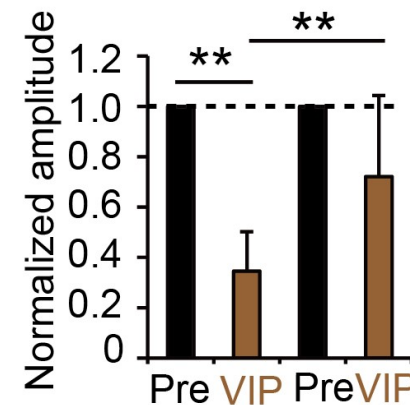
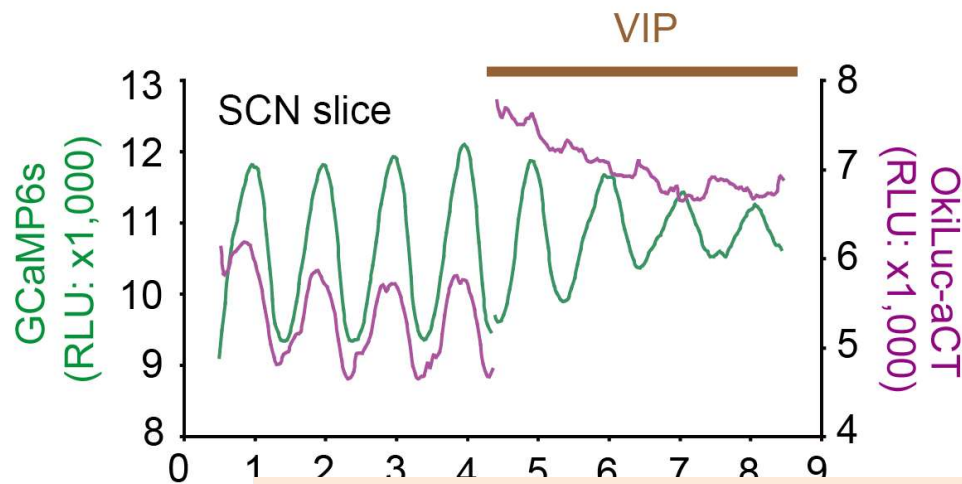
## Circadian cAMP and Ca<sup>2+</sup> rhythms in the SCN under VIP application

Excessive amount of VIP application (1  $\mu$ M)

Okiluc-aCT (cAMP)



GCaMP6s (Ca<sup>2+</sup>)

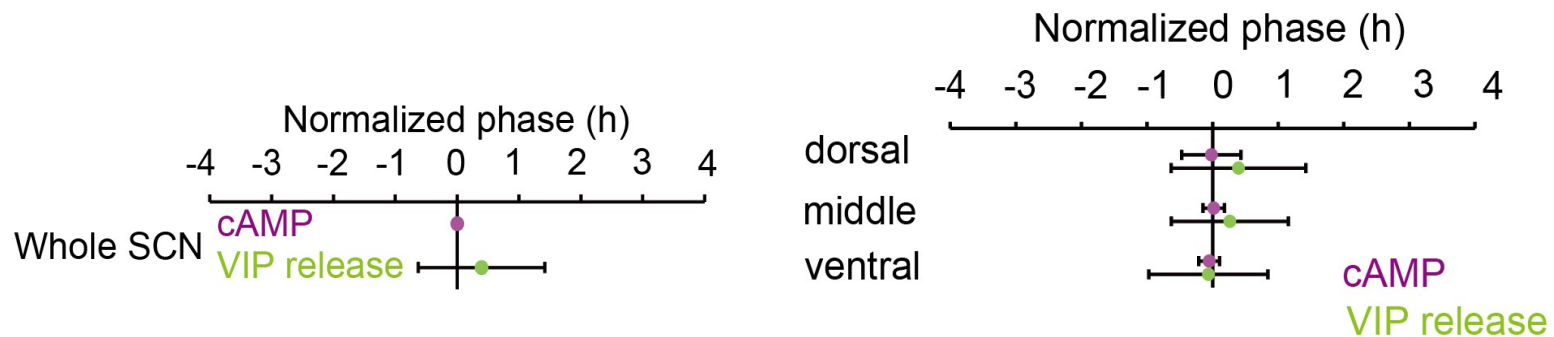
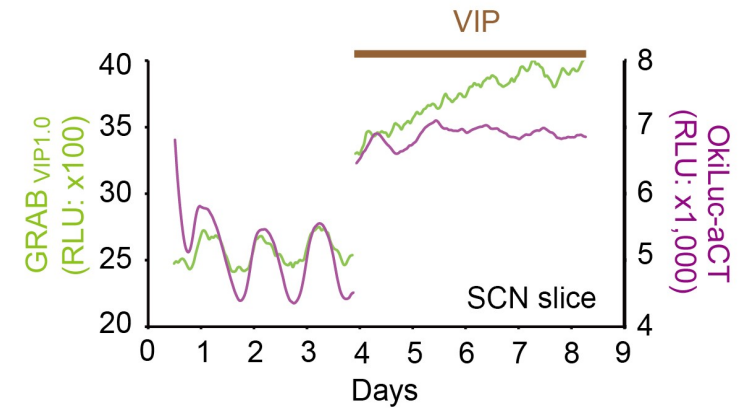
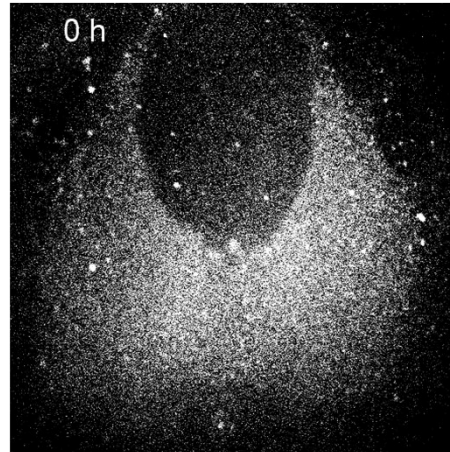
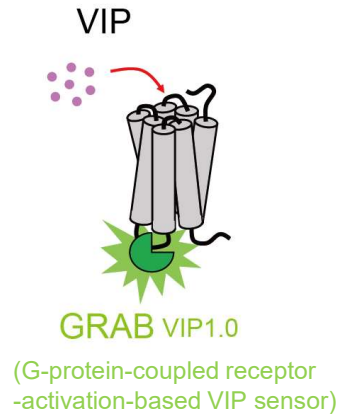


Circadian cAMP rhythms in the SCN are driven by VIP

# Optical recording of the VIP release in the SCN

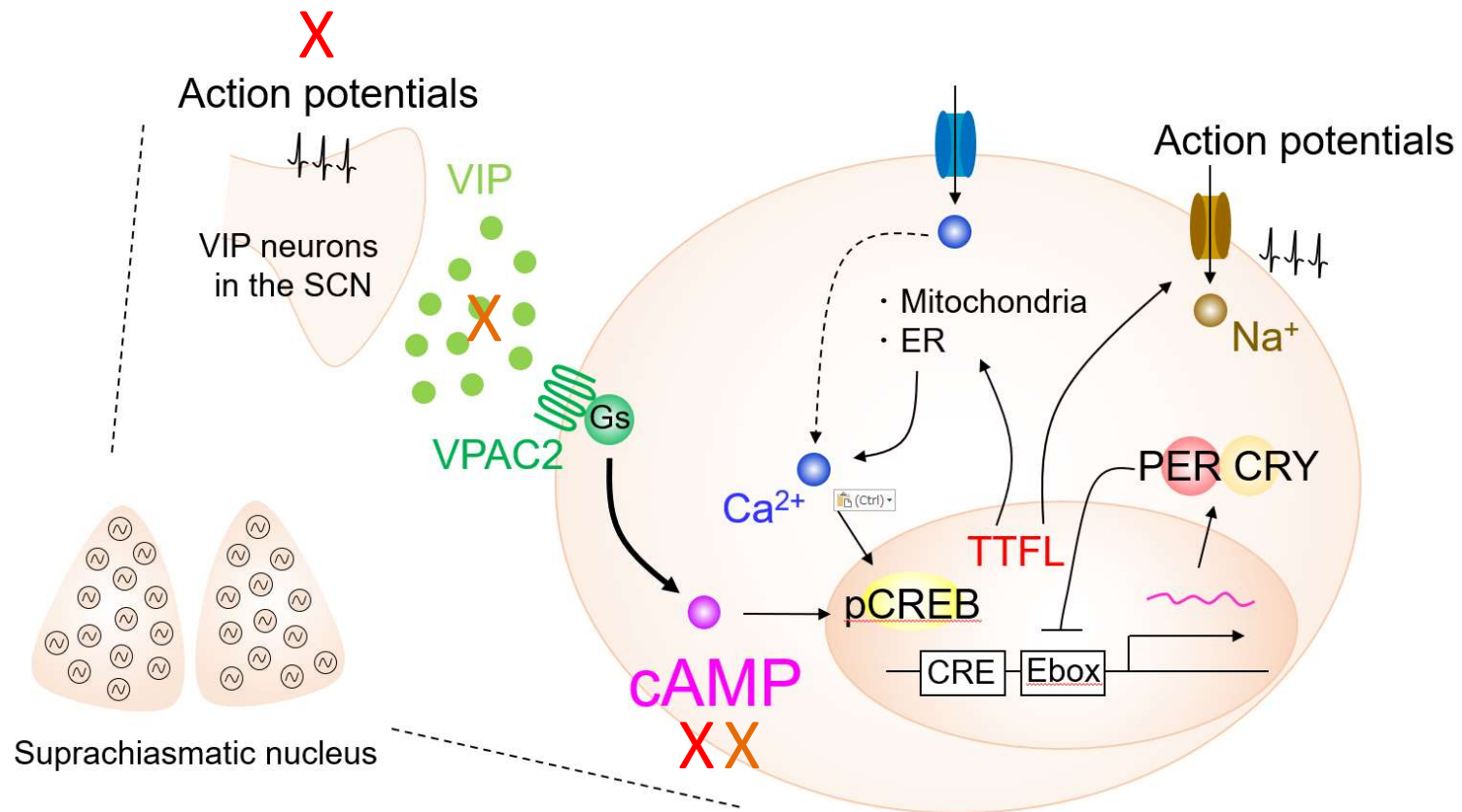


Dr. Yulong Li



VIP release in the SCN shows circadian rhythms

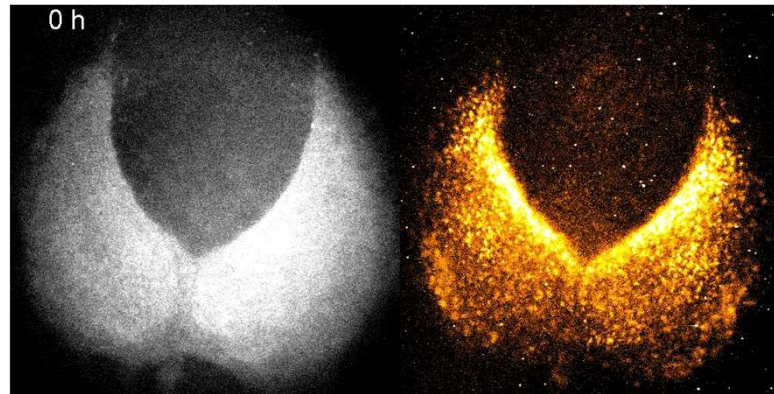




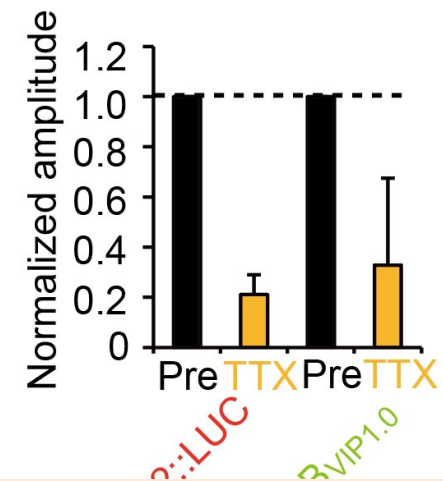
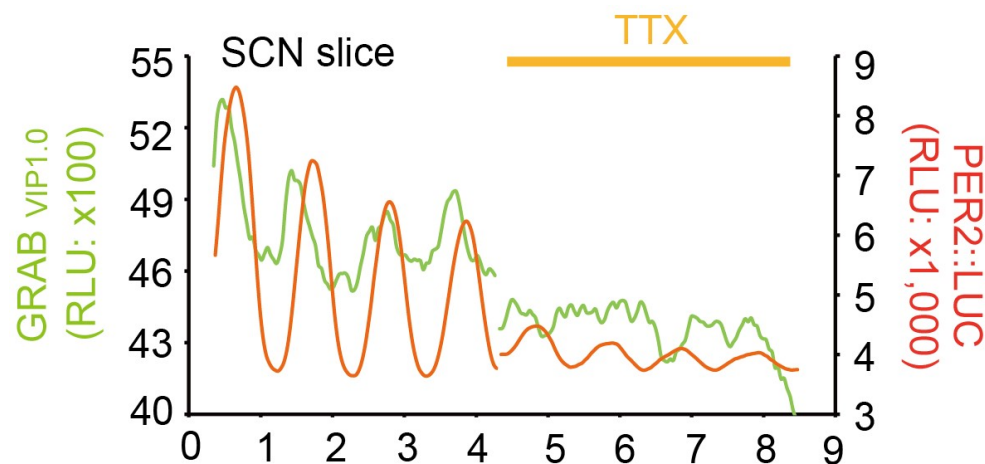
## Circadian VIP release and PER2::LUC rhythms in the SCN under TTX application

TTX (sodium channel blocker) → shutting down of neuronal networks in the SCN

GRAB<sub>VIP1.0</sub>  
(VIP release)



PER2::LUC  
(TTFL)



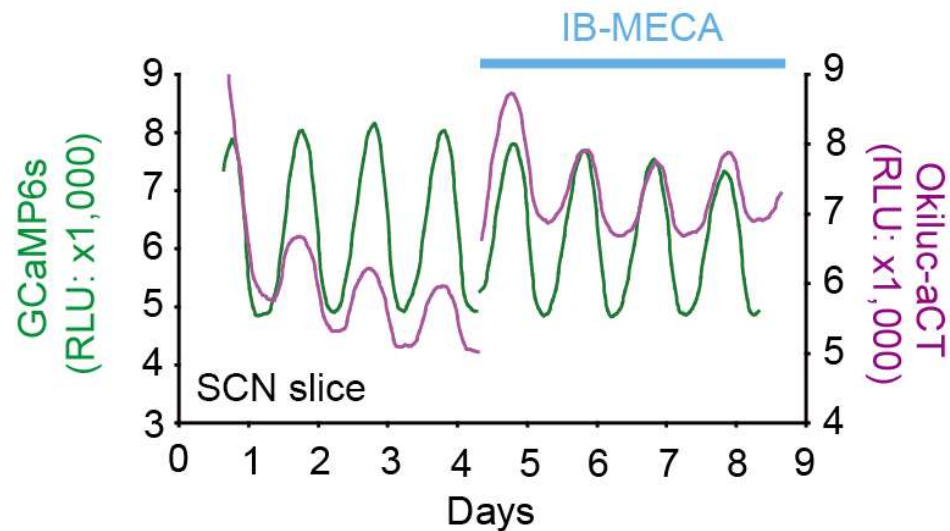
Neuronal activity is critical for the circadian rhythms of VIP release in the SCN

## Circadian cAMP and Ca<sup>2+</sup> rhythms in the SCN under adenosine receptor agonist

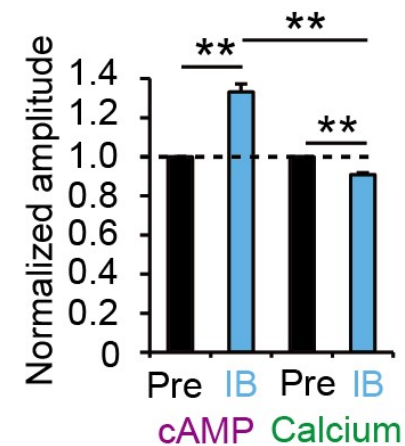


A2A

Jagannath et al., 2021



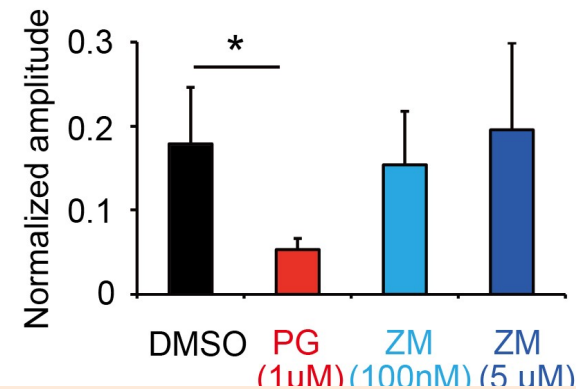
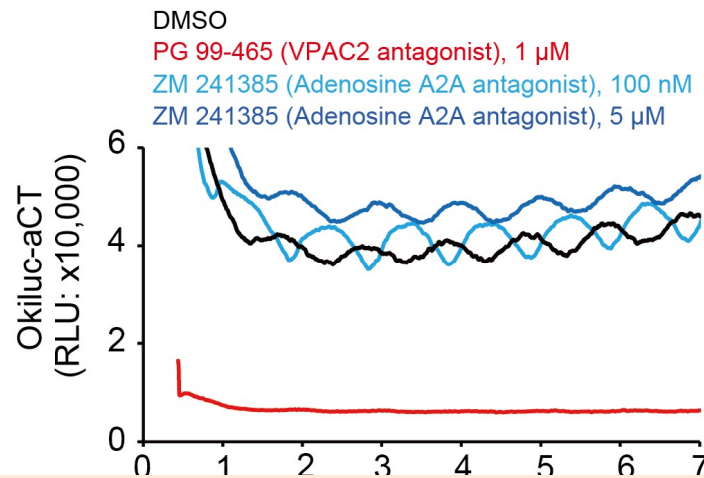
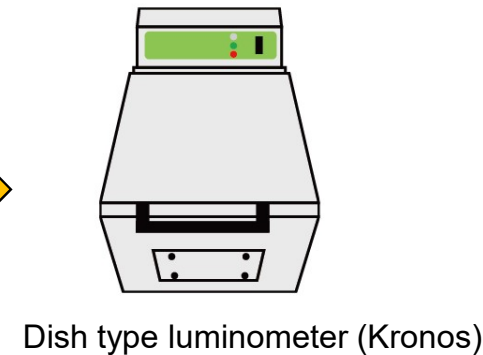
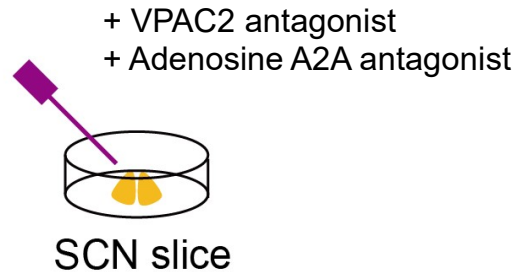
IB-MECA: Adenosine receptor agonist



Circadian cAMP dynamics in the SCN are modulated by VIP and adenosine

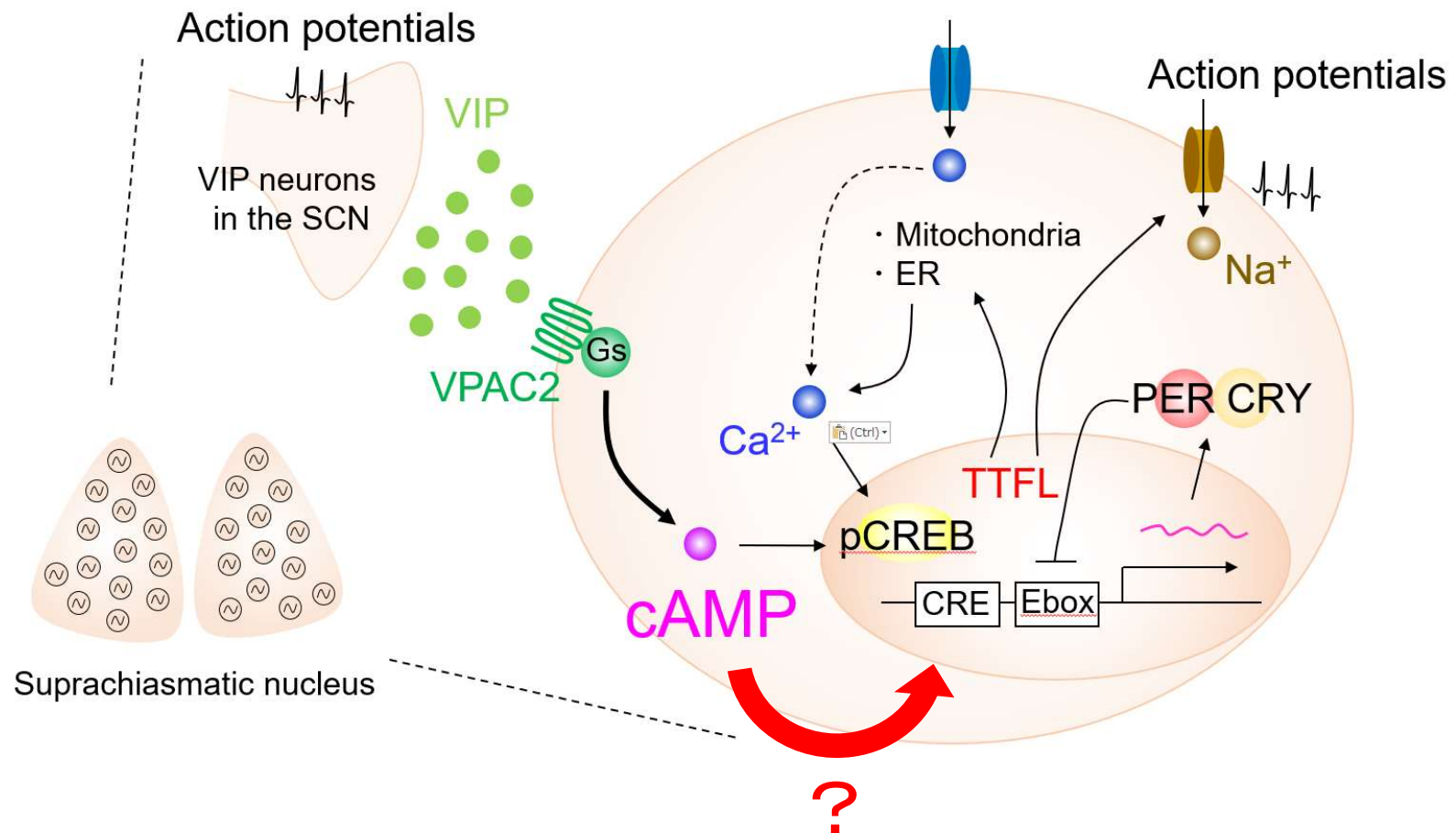
## Circadian cAMP rhythms in the SCN slice under VIP or adenosine receptor antagonists

AAV-hSyn-Okiluc-aCT

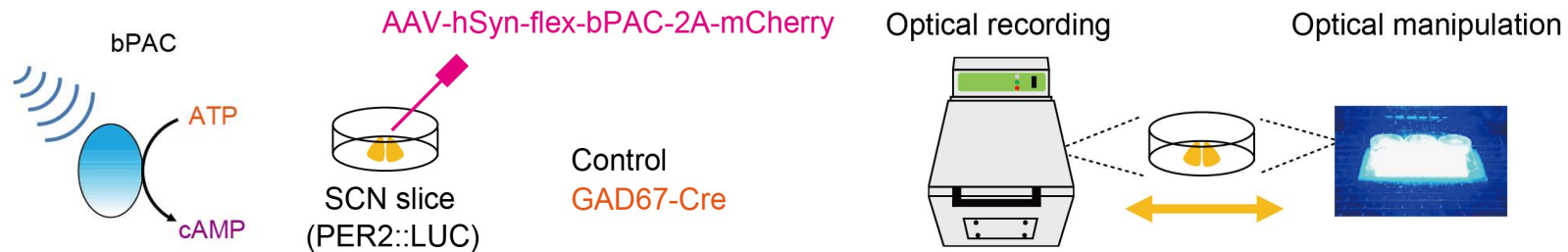


Circadian cAMP rhythms in the SCN are regulated by the rhythmic release of VIP, not adenosine



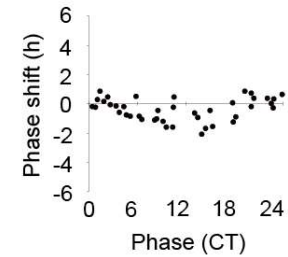
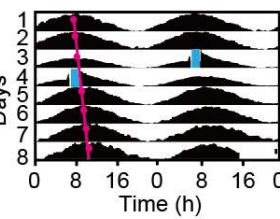
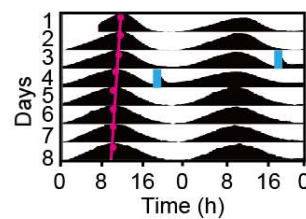
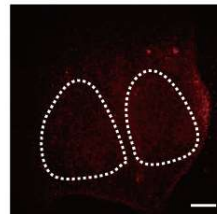


# Optical manipulation of intracellular cAMP in the SCN slice

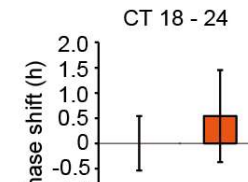
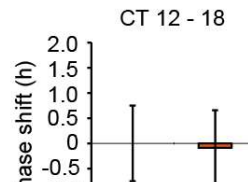
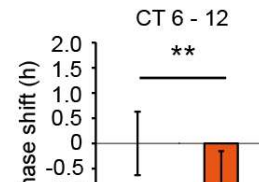
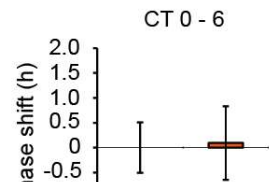
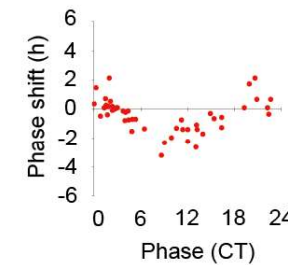
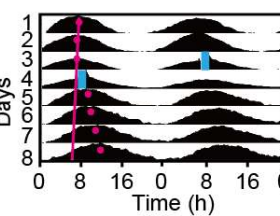
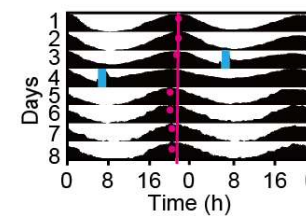
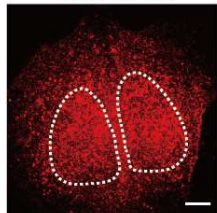


bPAC: photoactivatable adenylyl cyclase

Control

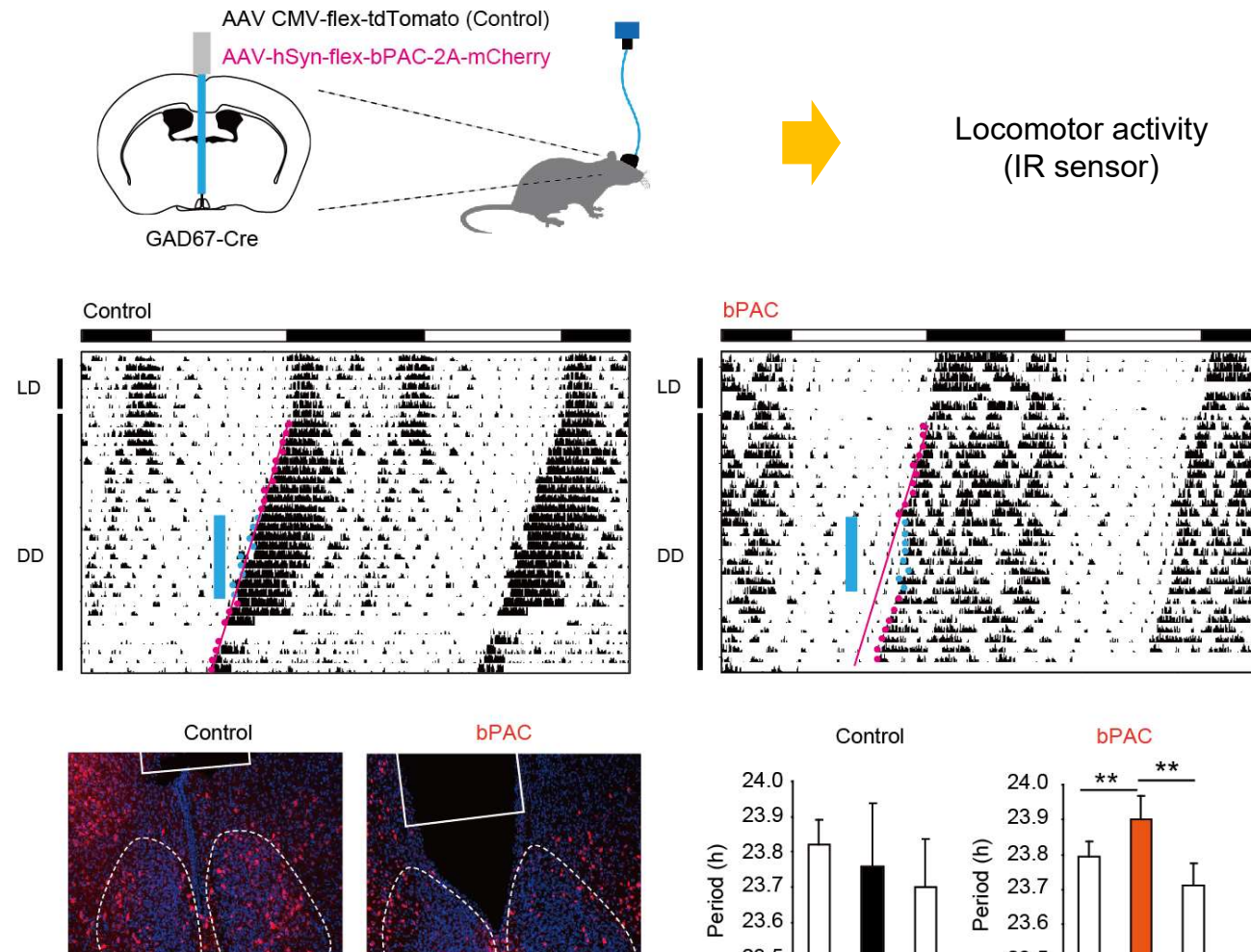


GAD67-Cre



Circadian phase-dependent manipulation of cAMP shifts circadian rhythms in the SCN slice

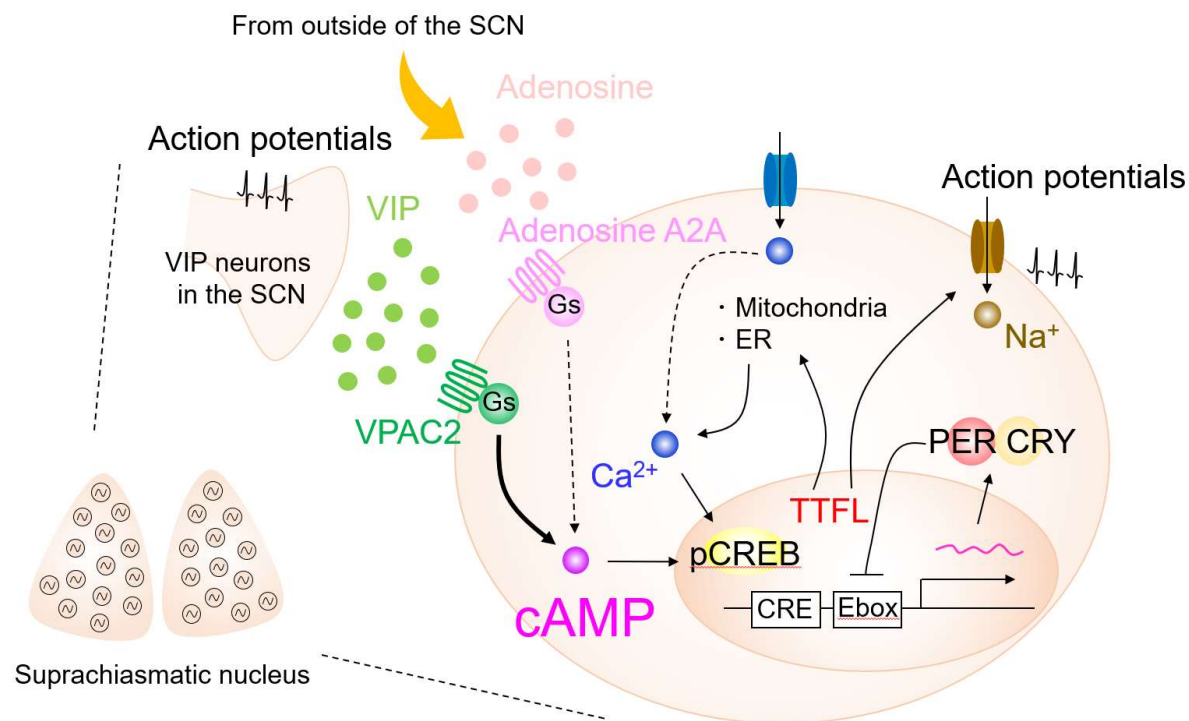
## Optical manipulation of intracellular cAMP in the SCN in vivo



Optical manipulation of intracellular cAMP shifts circadian behavioral rhythms

## Summary 1

- Intracellular cAMP rhythm in the SCN is regulated by VIP-dependent neuronal networks.
- The network-driven cAMP rhythm coordinates circadian molecular rhythms in the SCN and behavioral rhythms.



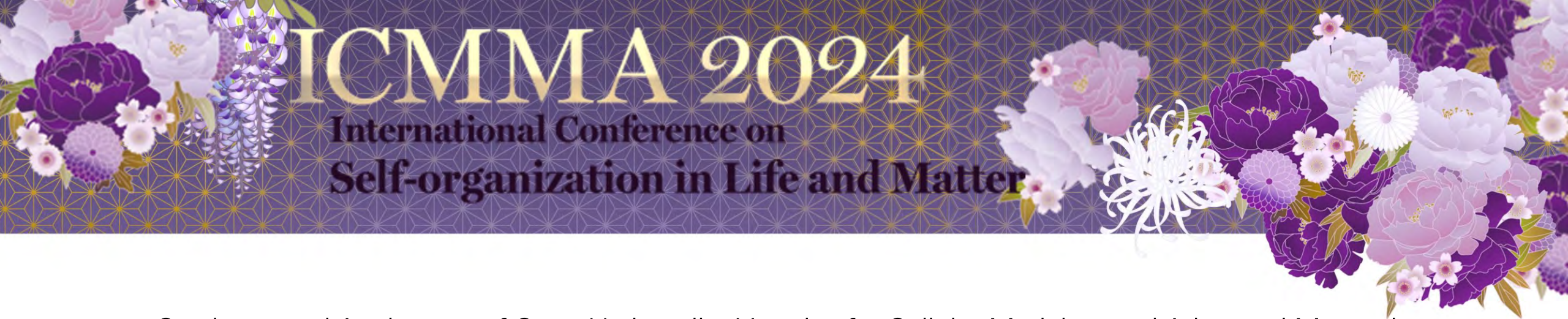


## Acknowledgements

Nagoya University,  
Research Institute of Environmental Medicine  
Ono Lab



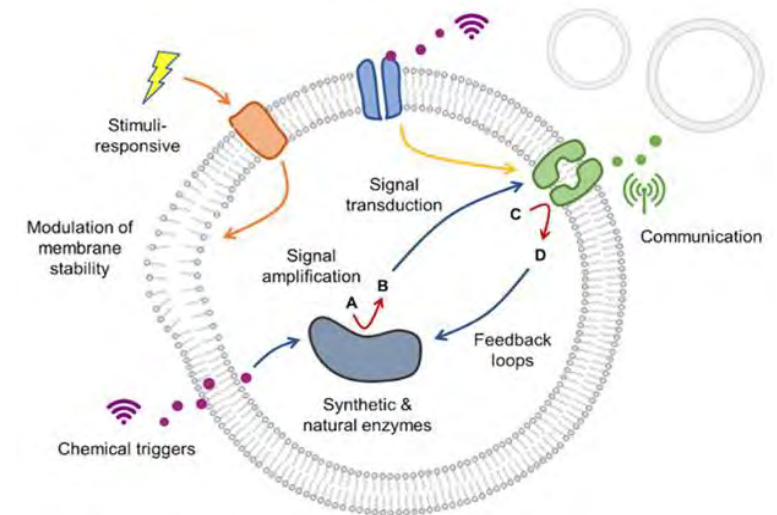
Naohiro Kon (Nagoya U.)  
Hsin-tzu Wang (Nagoya U.)  
Yulong Li (Peking U.)  
Huan Wang (Peking U.)  
Shigeru Kuroda (Aomori U.)  
Yujiro Yamanaka (Hokkaido U.)  
Takashi Sugiyama (Evident)  
Matthew Butler (OHSU)  
Sato Honma (Hokkaido U.)  
Ken-ichi Honma (Hokkaido U.)  
Shigeki Shimba (Nihon U.)  
J.S. Takahashi (UT Southwestern Medical Center)



## Synthesis and Application of Giant Unilamellar Vesicles for Cellular Modeling and Advanced Materials

Federico Rossi (Department of Physical Sciences, Earth and Environment, University of Siena, Italy)

We present the synthesis and multifaceted applications of Giant Unilamellar Vesicles (GUVs) in cellular modeling and the development of advanced materials. GUVs, known for their capacity to mimic cell membranes, are synthesized through a phase transfer method using self-assembling amphiphilic molecules that form bilayers, creating isolated environments ideal for both biological and material science experiments. In the realm of cellular modeling, GUVs are utilized to replicate complex cellular behaviors, such as enzymatic reaction networks, signal transduction, and self-division, offering a simplified yet dynamic model to explore fundamental biological processes and the mechanisms underlying cellular communication. The reconstitution of photoswitchable amphiphilic molecules within GUV membranes, also enable the modulation of membrane properties in response to external stimuli like light. This development is pivotal for creating stimulus-responsive biomimetic systems that have potential applications in smart drug delivery and biocompatible devices. Concurrently, these vesicles can serve as microreactors for the controlled synthesis of novel materials, including Metal-Organic Frameworks (MOFs) like Zeolitic Imidazolate Frameworks 8 (ZIF-8). The unique environment provided by GUVs may allow for precise control over the nucleation and growth of these crystalline structures, leading to materials with potential applications in catalysis, drug delivery, and gas storage.





ICMMA2024

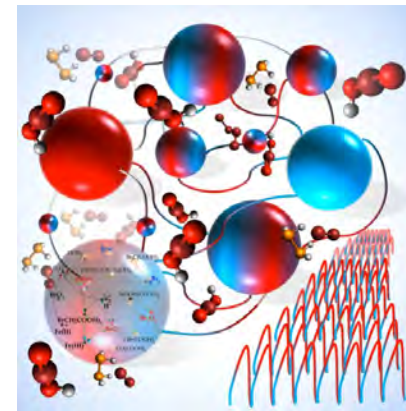
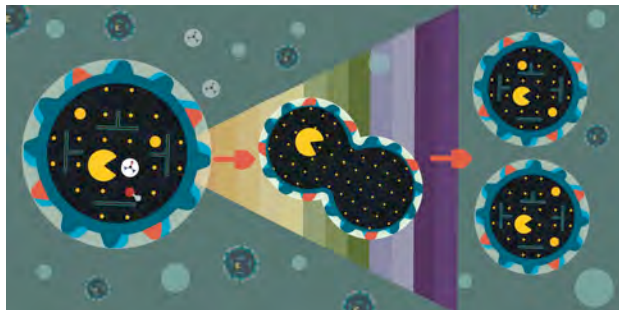
*International Conference on “Self-organization in Life and Matter”*

# Synthesis and Application of Giant Unilamellar Vesicles for Cellular Modeling and Advanced Materials

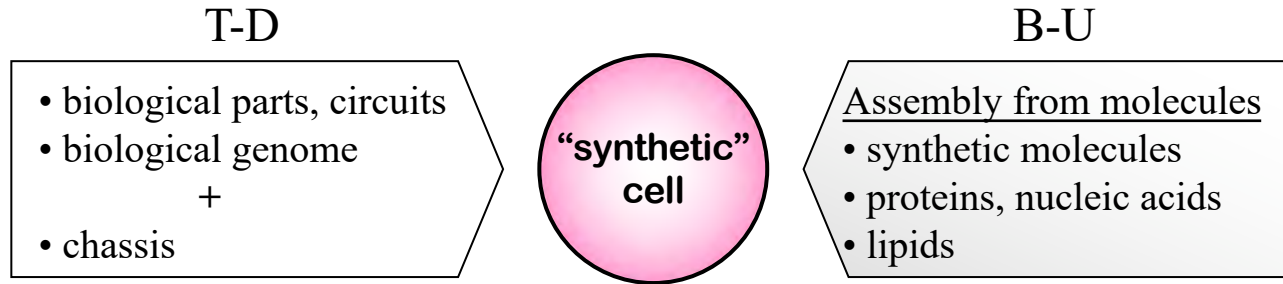
**Federico Rossi**

Department of Physical Sciences, Earth and Environment  
University of Siena

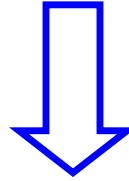
*[federico.rossi2@unisi.it](mailto:federico.rossi2@unisi.it)*



# “Bottom-up” assembly of synthetic cells



## Synthetic Minimal Cells

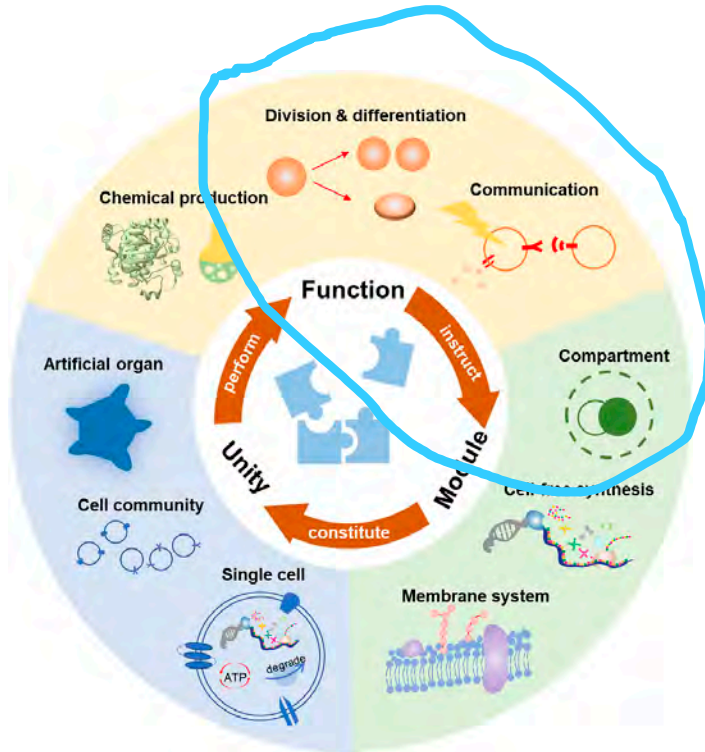


*À la carte* design and construction  
of “synthetic cells”  
-- not necessarily alive --  
for biotechnological applications  
(example: intelligent drug delivery systems)

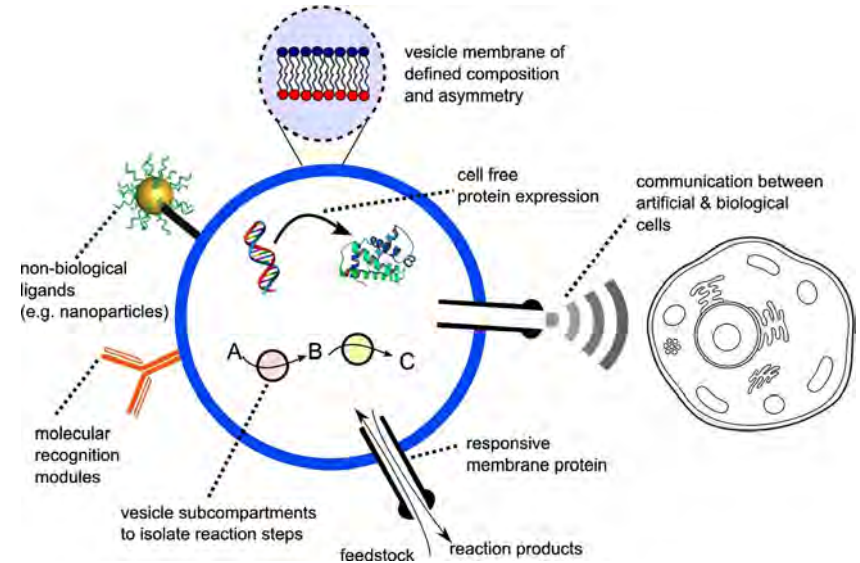
- Stanó, P. Minimal Cellular Models for Origins-of-Life Studies and Biotechnology. in *The Biophysics of Cell Membranes* 177–219 (2017).
- Caspi, Y. & Dekker, C. Divided we stand: splitting synthetic cells for their proliferation. *Syst Synth Biol* 8, 249–269 (2014).



# “Bottom-up” assembly of synthetic cells



Wang, C., et al. *Frontiers in Molecular Biosciences* 8, 781986 (2021).

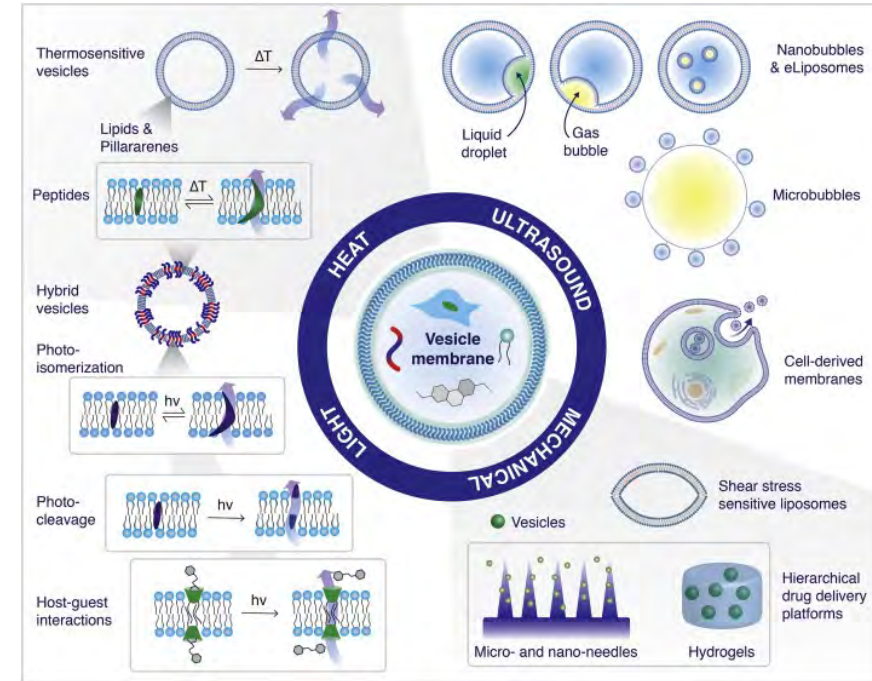
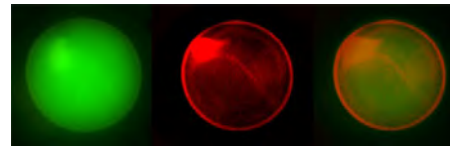
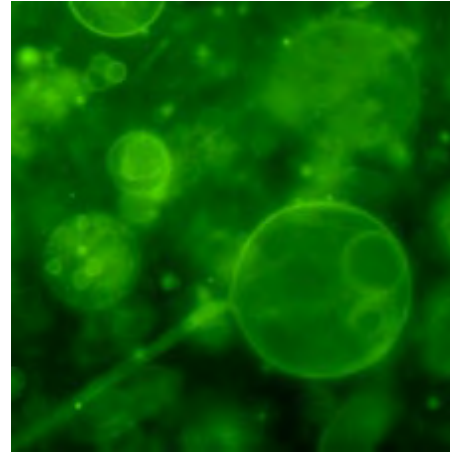
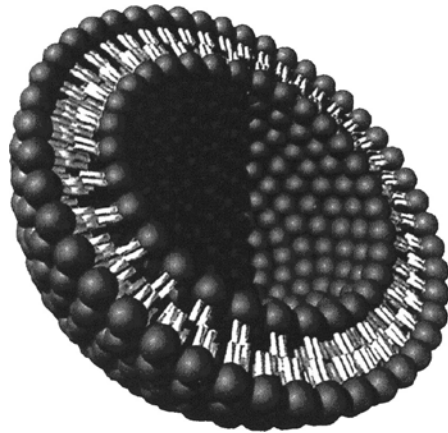


1. Elani, Y. *Biochemical Society Transactions* 44, 723–730 (2016).

- Stano, P. Minimal Cellular Models for Origins-of-Life Studies and Biotechnology. in *The Biophysics of Cell Membranes* 177–219 (2017).
- F.R.: et al. Current Directions in Synthetic Cell Research. in *Advances in Bionanomaterials* 141–154 (2018).

# Giant Unilamellar vesicles (5-100 $\mu\text{m}$ )

- Water in Water compartments
- Host reactors for chemical and biochemical processes
- Tunable permeability
- Lipids, fatty acids, polymers, etc.

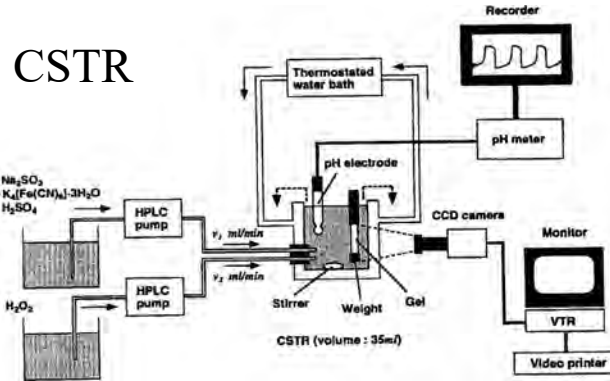


KEEP THE SYSTEM FAR FROM EQUILIBRIUM

STIMULI-RESPONSIVE MEMBRANES

# Self-organizing chemical processes

- “Chemically fueled”
- “Autonomous systems”
- “Active matter”
- “Self-organization”



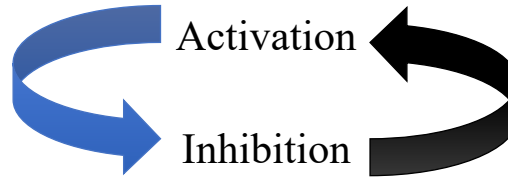
Semi-batch

Selective permeability  
of membranes

Oscillations



Nonlinear kinetics  
(e.g. autocatalysis)



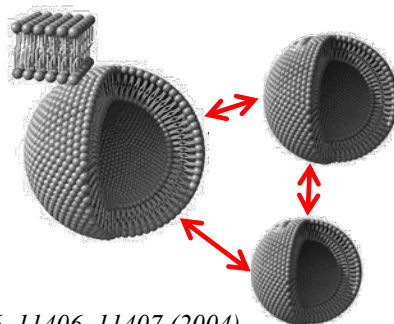
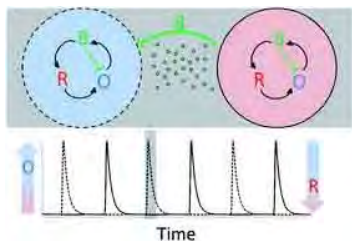
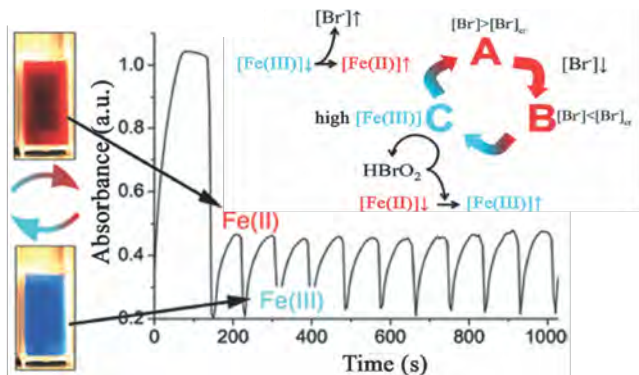
Pattern formation



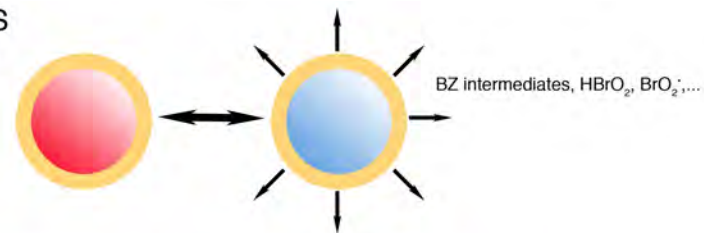
# Communication in populations of homogeneous GUVs: Microfluidic techniques and periodic signalling

- Belousov-Zhabotinsky Reaction
- Compartmentalization and Communication

- Study and control the dynamics of networks of oscillators
- Models for biological communication



HOMOGENEOUS  
OSCILLATIONS



WAVES



The messenger molecule determines the coupling nature:

- Inhibitory coupling: anti-phase oscillations and Turing regimes
- Activatory coupling: in-phase oscillations and signal amplification



# Encapsulation: Flow-focusing technique

Ali Abou-Hassan



UPMC  
SORBONNE UNIVERSITÉS

Sandra Ristori

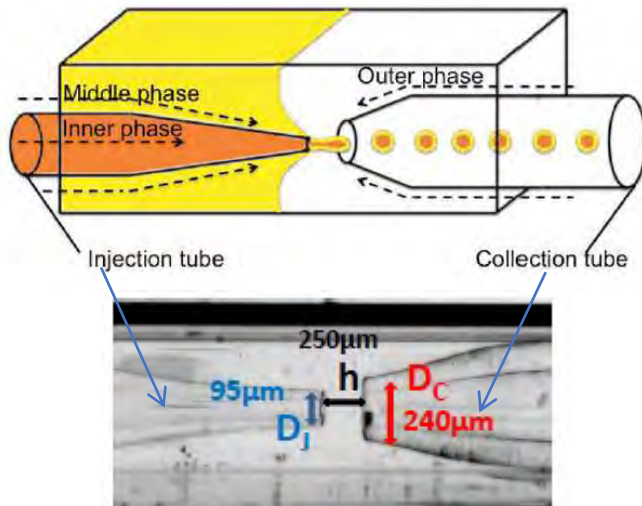


University of Firenze

Marcello Budroni

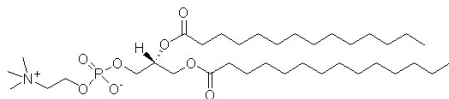


University of Sassari



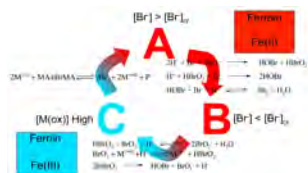
Rayleigh – Plateau Instability

- Middle Phase:  
Chloroform:cyclohexane  
DMPC

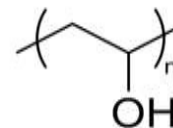


- Utada et Al. *Science*, 2005  
- Seth et al. *Adv. Mat.* 2012

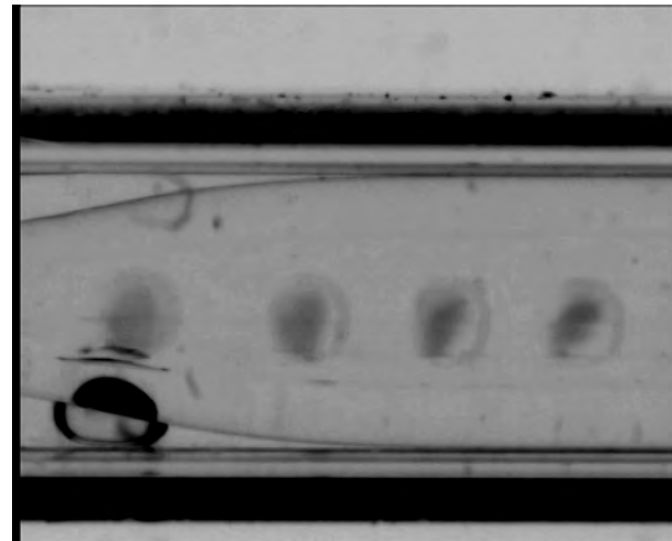
- Inner Phase:  
BZ mixture



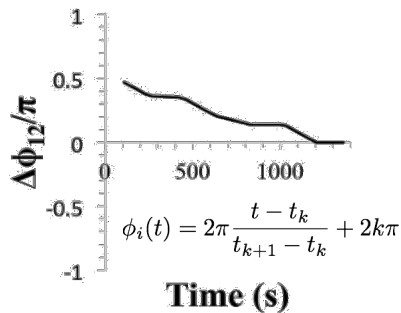
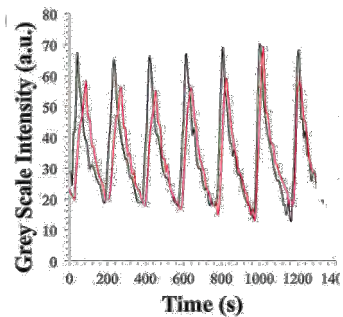
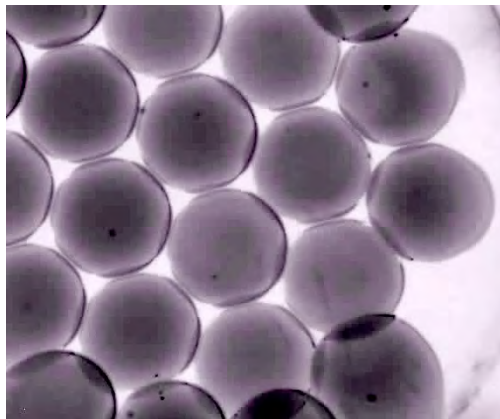
- Outer Phase:  
Polyvinyl alcohol (PVA)



FR et al. *Chem. Sci.* 5, 1854–1859 (2014).

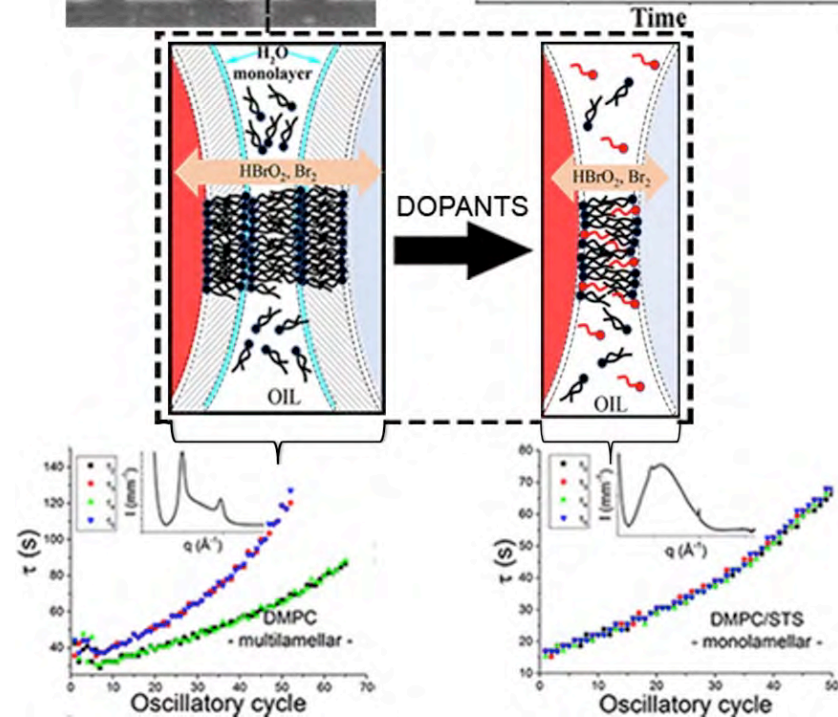
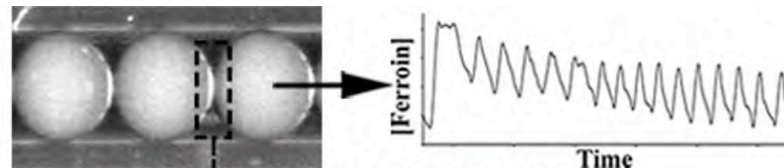


# Communication and global network dynamics



- FR et Al. *Chem. Sci.* **5**, 1854–1859 (2014)
- FR et Al. *J. Phys. Chem. Lett.* **11**, 2014–2020 (2020)
- FR et Al. *Chemcomm* **56** 11771–11774 (2020)
- FR et al. *Int. J. Unconven. Comp.* (2015).

# Membrane properties (nano-scale) impact on the global behavior (macro-scale)

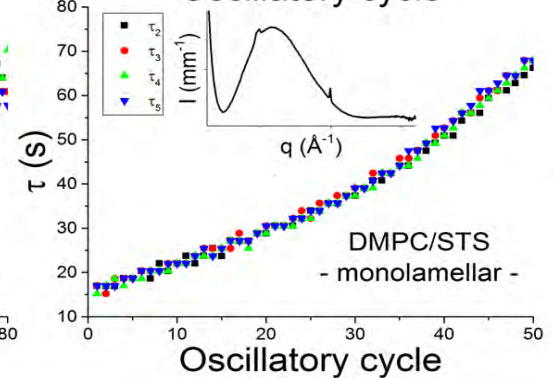
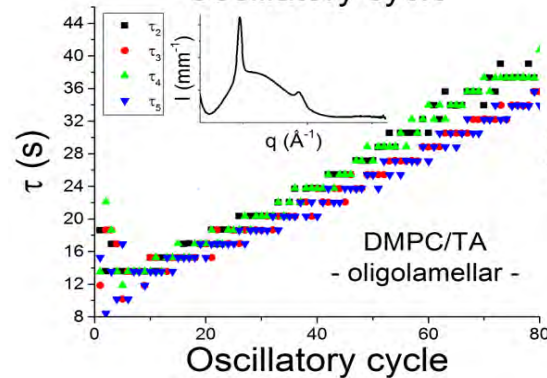
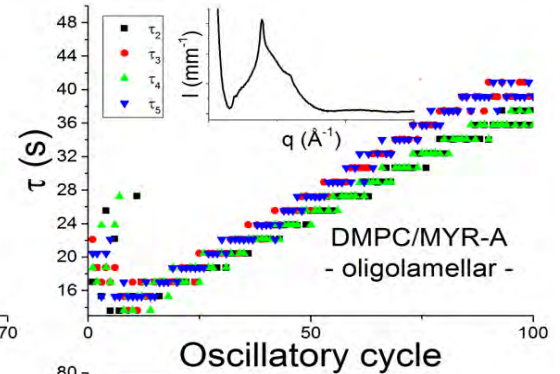
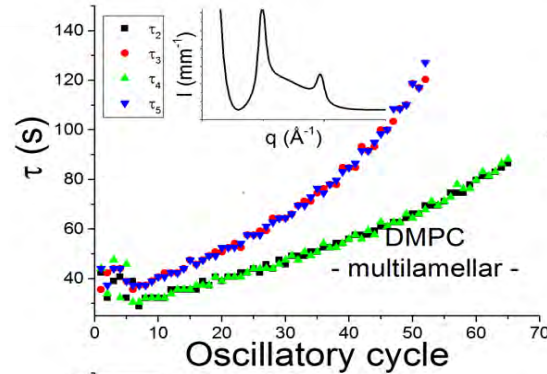
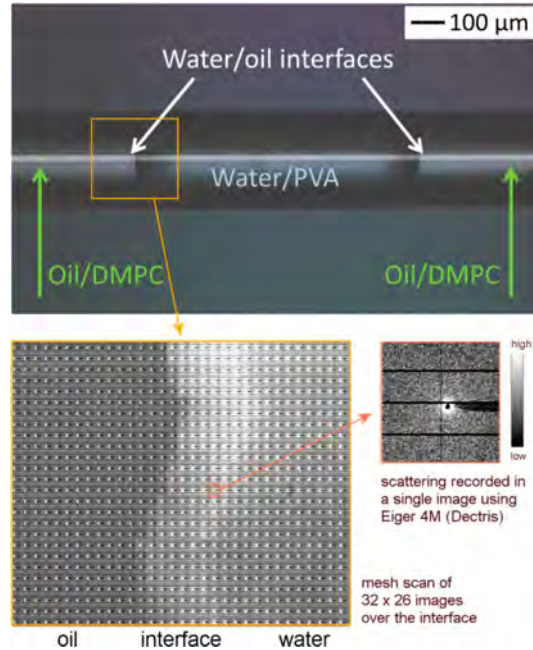


# Global Network Behavior

Weak Inhibition:  
2-periods clustering  $1:2:1:2$  resonance

Weak Inhibition:  
2-periods clustering  $1:1.2:1:1.2$

## SAXS Analyses



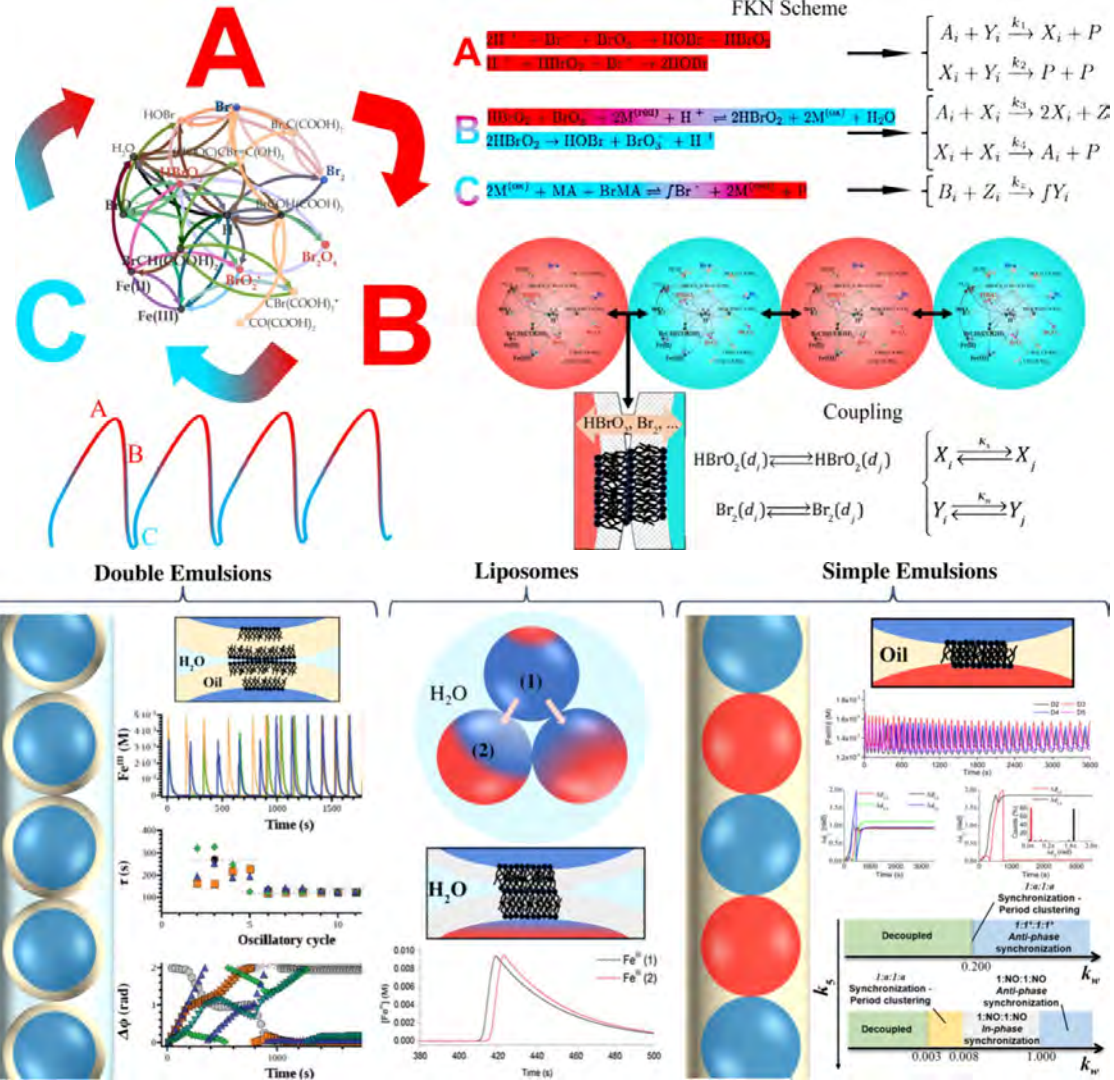
- FR et Al. RSC Adv. 9, 33429 (2019)  
- FR et Al. Langmuir 33 9100 (2017)

Weak Inhibition:  
2-periods clustering  $1:1.2:1:1.2$

Strong Inhibition:  
Anti-phase  $1:1*:1:1*$



# Simulations

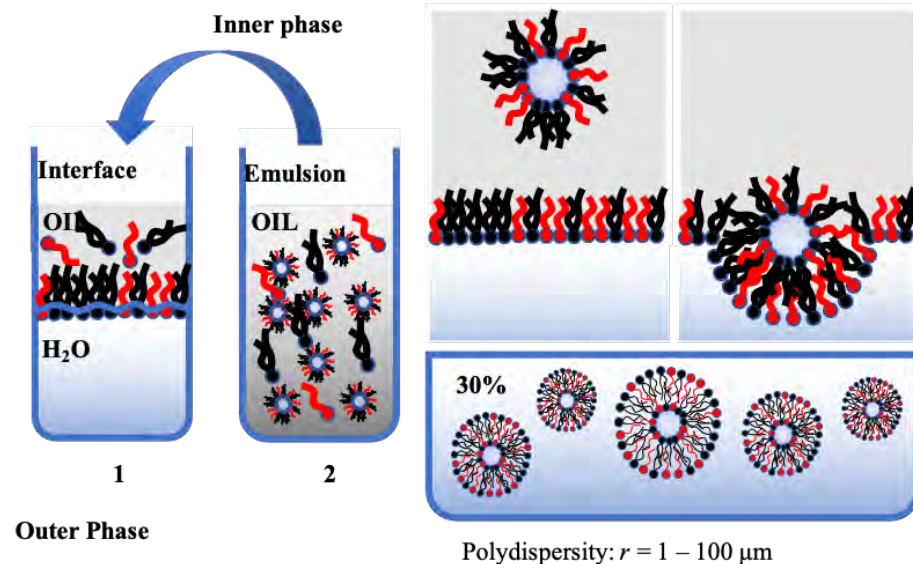




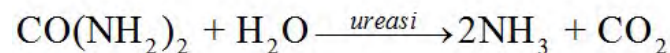


# Communication in populations of heterogeneous GUVs: bulk methods and clock reaction

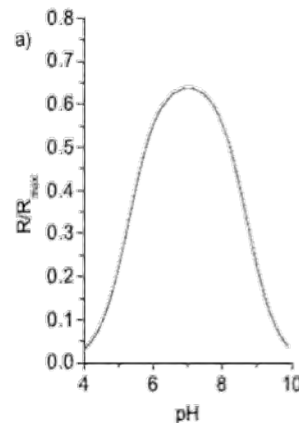
## Preparation: Phase transfer method



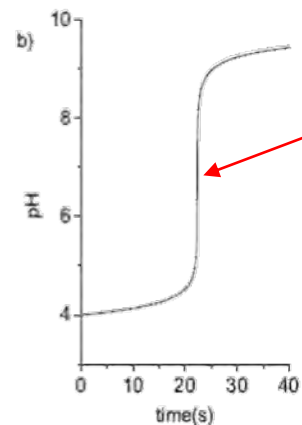
## Urea-urease reaction



### Nonlinear Rate pH-dependence



### pH autocatalytic profile



Clock time

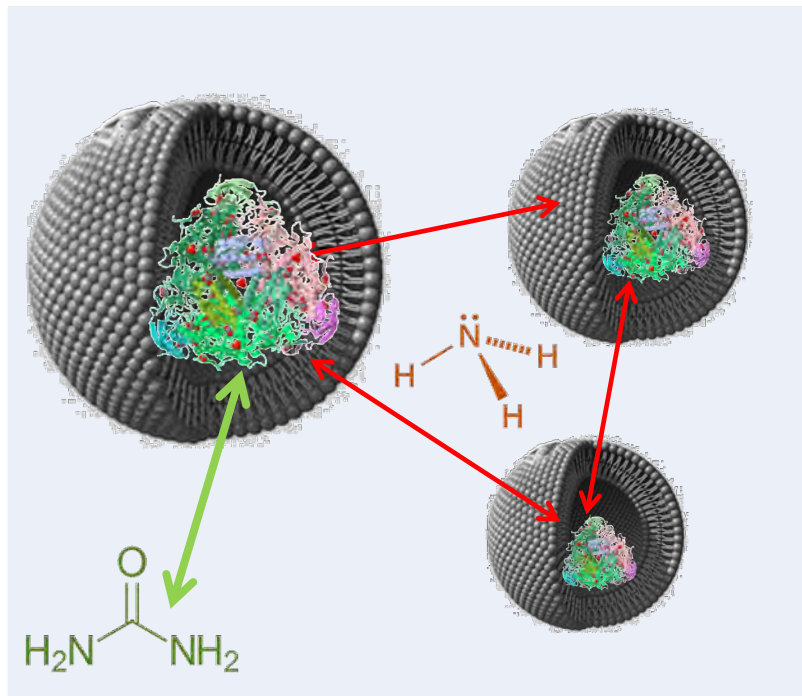
$[\text{urea}]_0 = 6 \times 10^{-3} \text{ M}$   
 $[\text{H}_2\text{SO}_4] = 1 \times 10^{-4} \text{ M}$   
 $[\text{urease}] = 10 \text{ U/mL}$

- FR et al. *Advances in Bionanomaterials* 63–74 (2018)
- FR et al. *Advances in Artificial Life, Evolutionary Computation and Systems Chemistry* 197–208 (2016)s

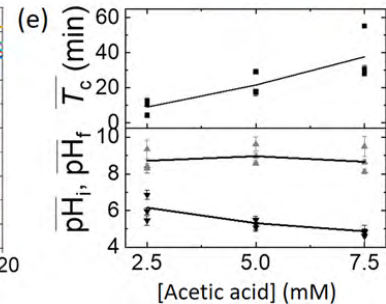
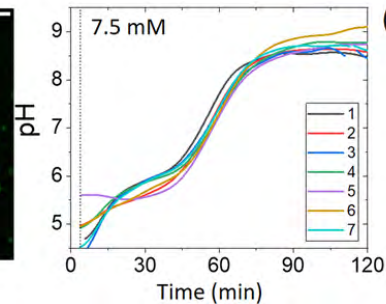
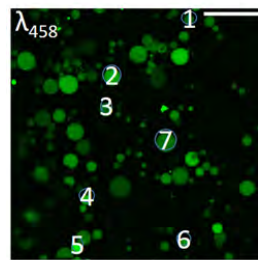
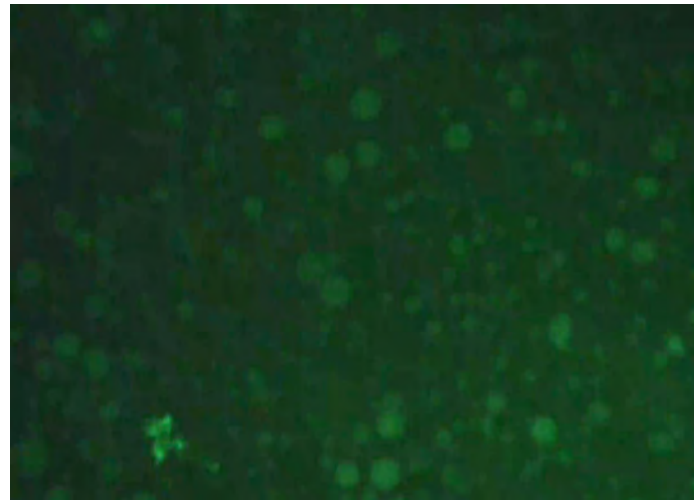
- **Nonlinear clock behaviour**
- *Fairly known in terms of kinetics*
- *Works in mild pH ranges*

- Hu, G. et al. 2010. *J. Phys. Chem. B* **114**, 14059–14063.
- Krajewska, B., and Ciurli, S., 2005. *Plant Physiol. Biochem.* **43**, 651–658

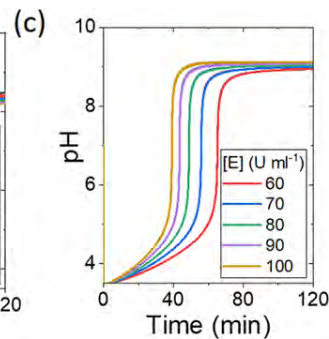
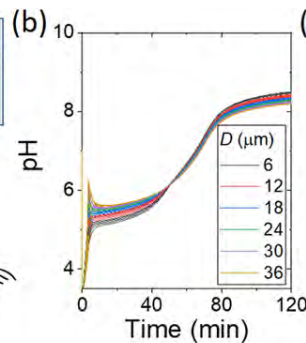
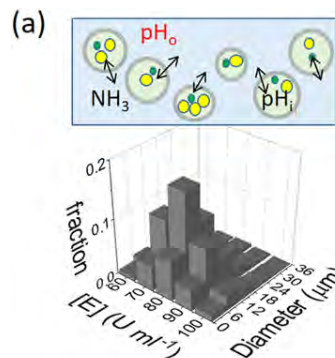
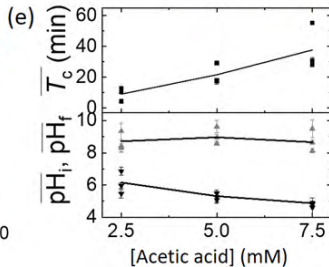
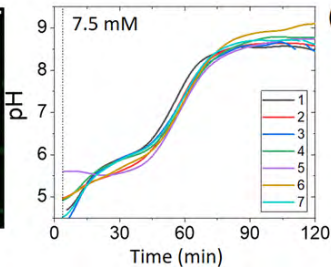
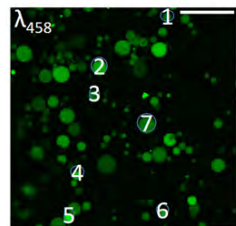
# Temporal synchronization of a populations of heterogeneous GUVs through ammonia transport



- *Semi-Batch reactor: Passive diffusion through lipid membranes*
- *Fluorescent probe (pyranine) to monitor pH*
- *Free ammonia fluxes*

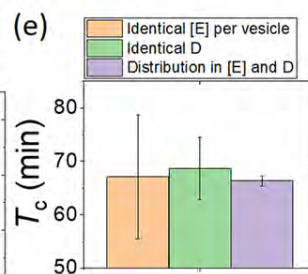
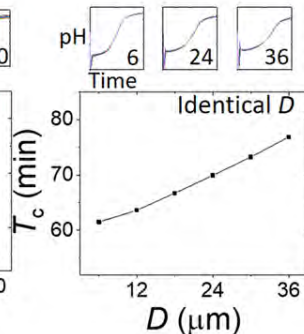
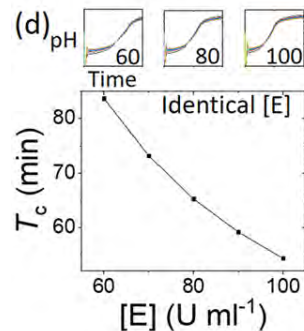


# Temporal synchronization of a populations of heterogeneous GUVs through ammonia transport



$$\frac{dA_i}{dt} = f(A_i) + \frac{3P_i}{r}(A_o - A_i)$$

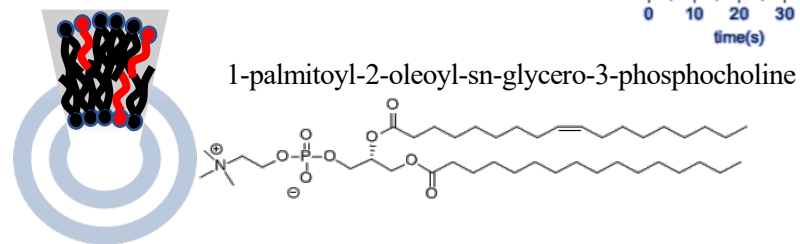
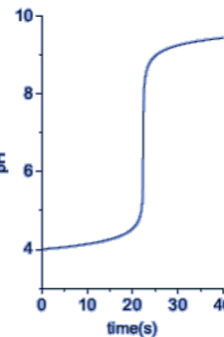
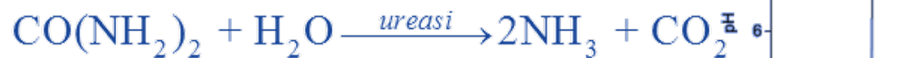
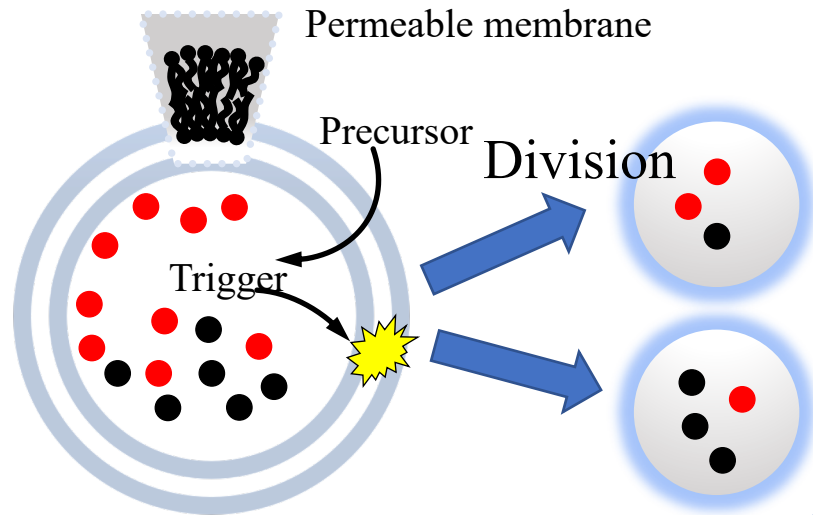
$$\frac{dA_o}{dt} = g(A_o) + \phi \frac{3P_i}{r}(A_i - A_o)$$



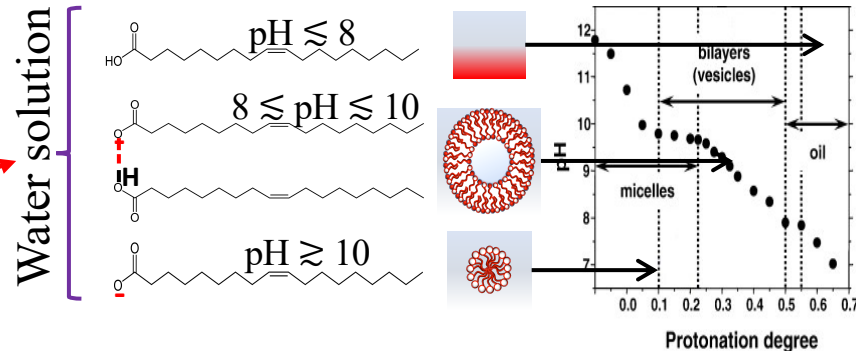


# Division through simple chemical triggers

Obtaining self-division of GUVs through a simple internal chemical stimulus (pH change)

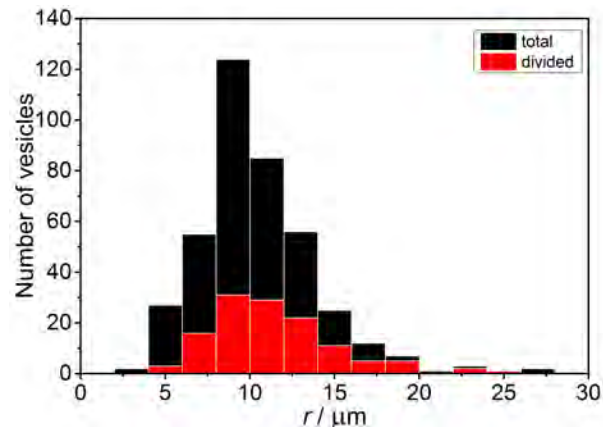


- Nonlinear mechanism
- Stimuli-responsive membrane
- Far from equilibrium through passive transport

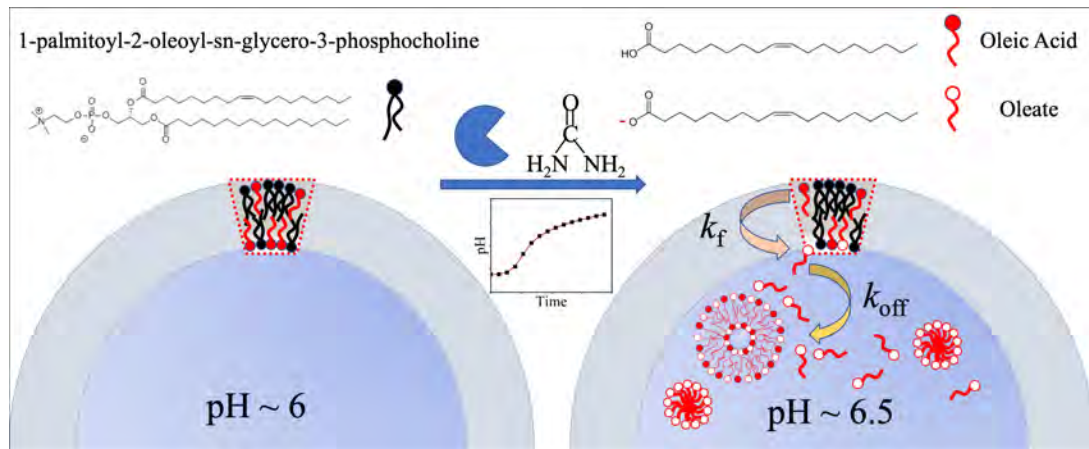




# Division Dynamics



~ 25% success  
irrespective of  
the size



- Solubilization of oleate molecules
- Diffusion of oleic acid from the outer to the inner leaflet

# ADE theory (Area Difference Elasticity)

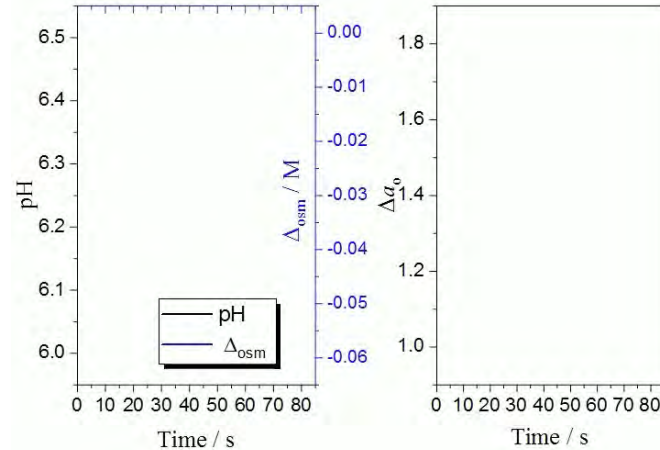
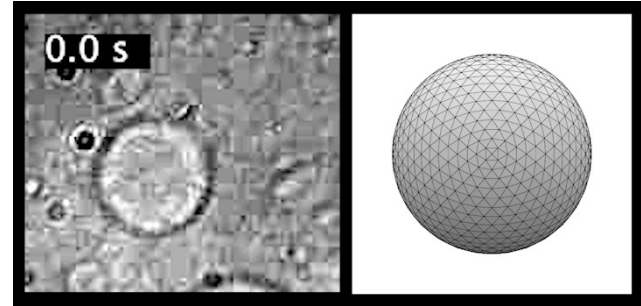
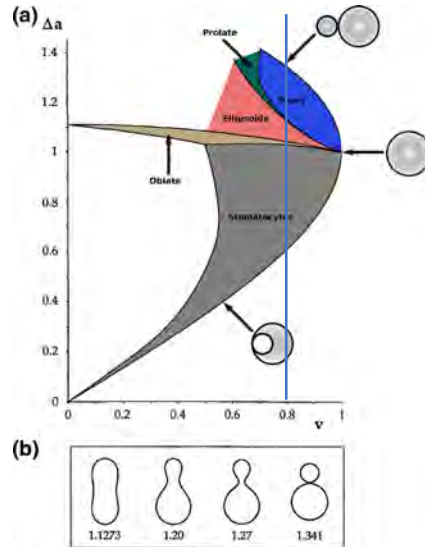
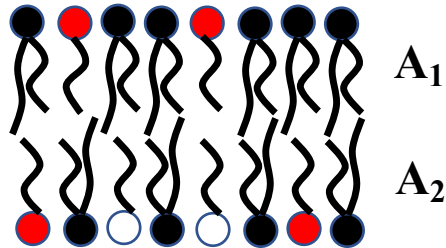
In general, the **equilibrium shape** of a vesicle can be described by **two parameters**:

$$\Delta a_0 \equiv \frac{\Delta A_0}{8\pi hR}$$

Area difference between  
membrane leaflets  
(pH change)

$$v \equiv \frac{3V}{4\pi R^3}$$

Vesicle volume  
(Osmosis)

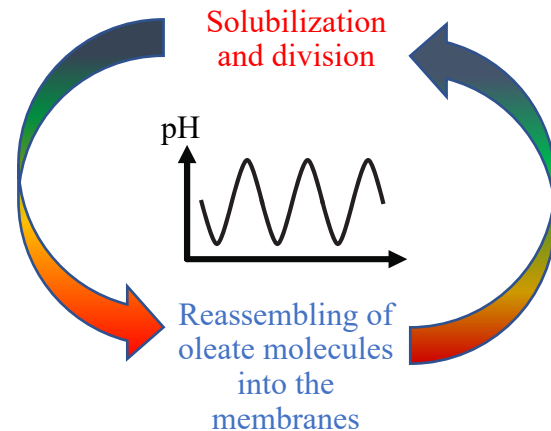
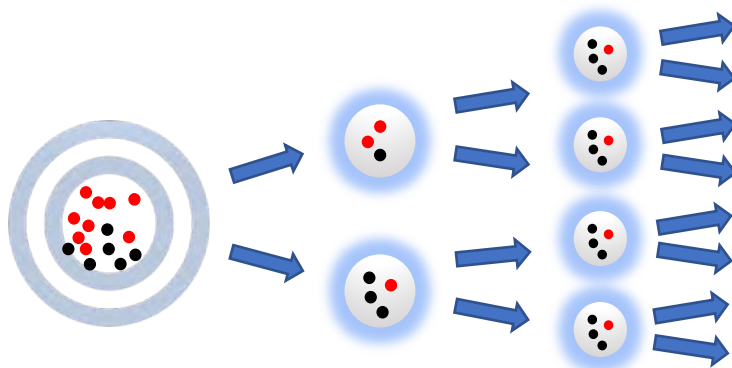


- Seifert, U., Berndl, K. & Lipowsky, R. Phys. Rev. A 44, 1182–1202 (1991).  
- Svetina, S. ChemPhysChem 10, 2769–2776 (2009).

- F.R. et Al. Phys. Chem. Chem. Phys. 23, 4262–4270 (2021).



Masaki Itatani



## Enzymatic Reaction Networks

CHEMICAL  
REVIEWS

pubs.acs.org/CR

Open Access  
This article is licensed under [CC-BY 4.0](#)  
Review

### Exploring Emergent Properties in Enzymatic Reaction Networks: Design and Control of Dynamic Functional Systems

Souvik Ghosh, Mathieu G. Baltussen, Nikita M. Ivanov, Rianne Haije, Miglė Jakštaitė, Tao Zhou, and Wilhelm T. S. Huck\*

Cite This: <https://doi.org/10.1021/acs.chemrev.3c00681>

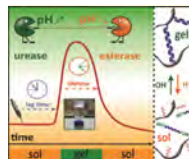
Read Online

NANO LETTERS

Letter  
pubs.acs.org/NanoLett

### Antagonistic Enzymes in a Biocatalytic pH Feedback System Program Autonomous DNA Hydrogel Life Cycles

Laura Heinen,<sup>†,‡,§,¶</sup> Thomas Heuser,<sup>||,¶</sup> Alexander Steinschulte,<sup>⊥</sup> and Andreas Walther<sup>\*,†,‡,§</sup>



MSDE

PAPER

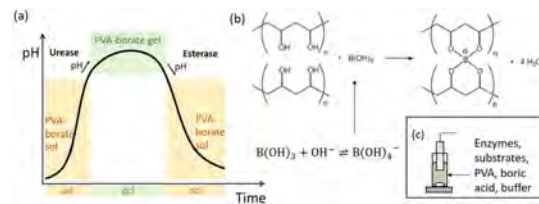
ROYAL SOCIETY  
OF CHEMISTRY

View Article Online  
View Journal

Check for updates  
Cite this: DOI: 10.1039/d3me00138e

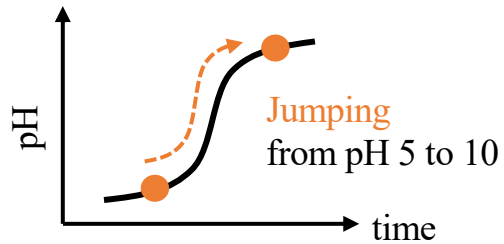
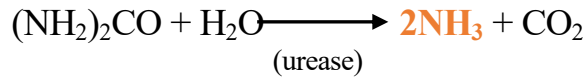
On the use of modelling antagonistic enzymes to  
aid in temporal programming of pH and PVA-  
borate gelation†

Nadeem Bashir,<sup>‡§</sup> Anna S. Leathard,<sup>§</sup> Madeline McHugh,<sup>‡</sup> Imogen Hoffman,<sup>‡</sup>  
Fatima Shaon,<sup>†</sup> Jorge A. Belgodere,<sup>§</sup>  
Annette F. Taylor,<sup>‡§</sup> and John A. Pojman Sr.<sup>\*,§</sup>

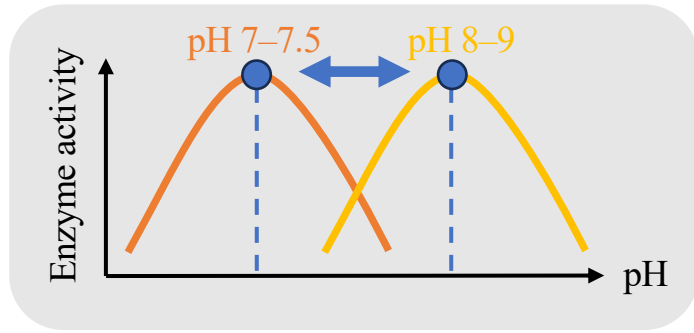
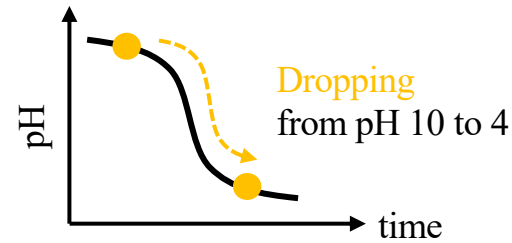
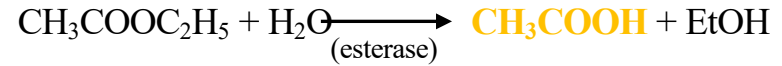


# Antagonistic enzymatic reactions

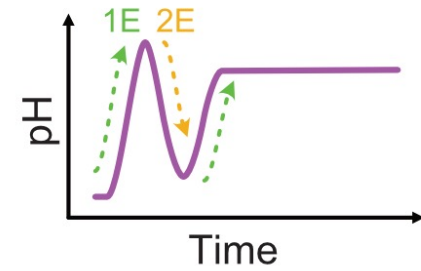
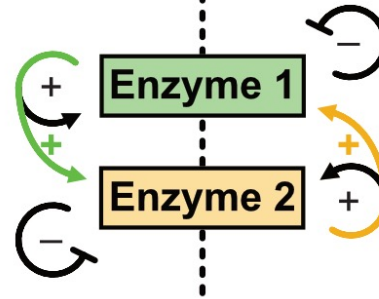
## ■ Urea-urease reaction



## ■ Ethyl acetate (EtOAc)-esterase reaction



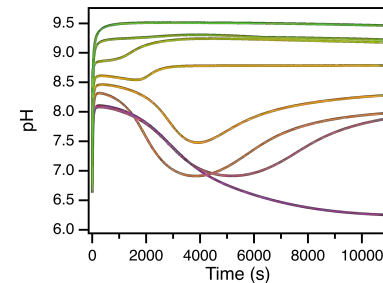
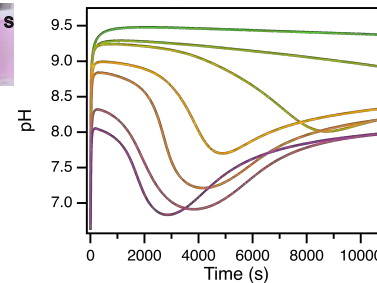
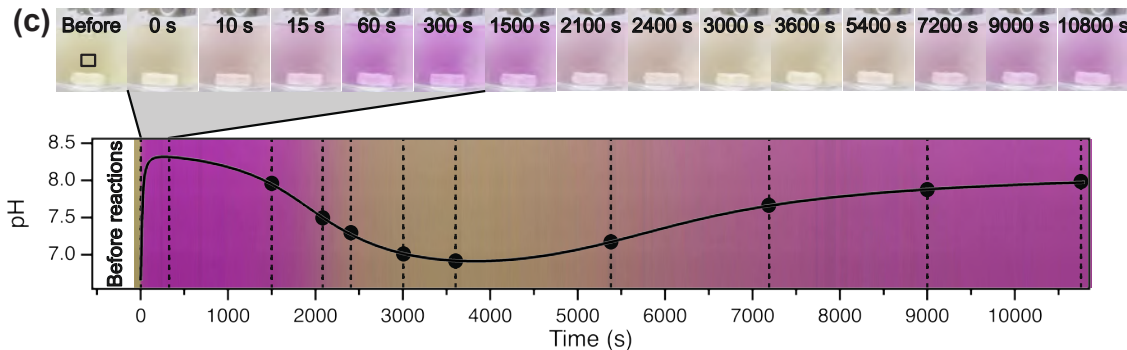
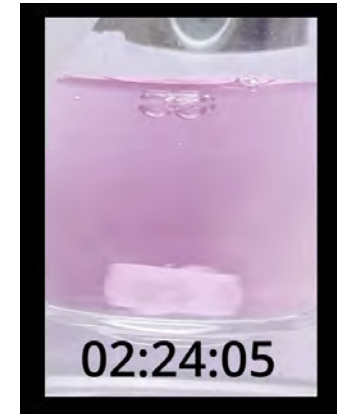
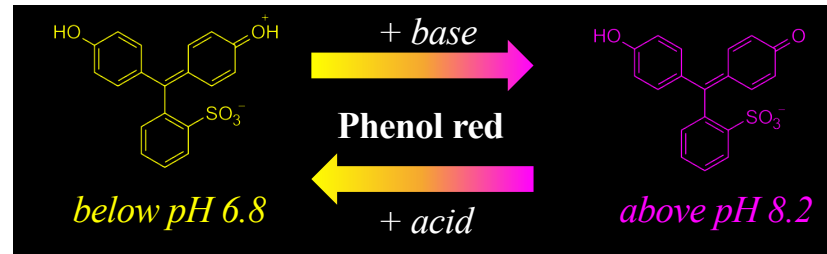
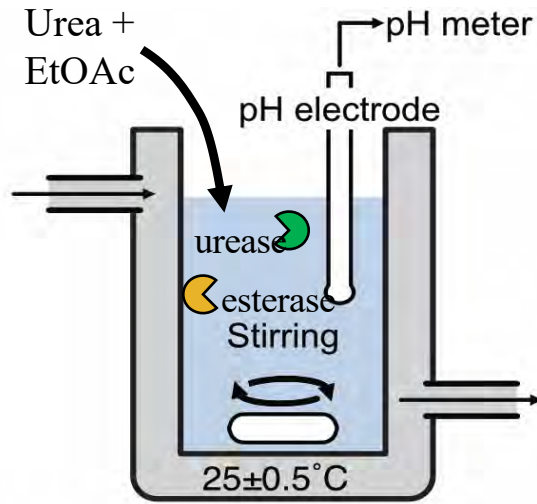
Acidic  $\longleftrightarrow$  Optimum  $\longleftrightarrow$  Basic



Complementary activation by each product ( $\text{H}^+$ ,  $\text{OH}^-$ ) recurses enzymatic reactions.



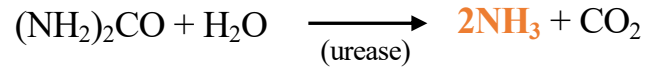
# Experiments: pH measurement in a batch system



The amplitude of pH change: from ~6.8 to 8.3

# Encapsulating antagonistic enzymatic reactions in GUVs

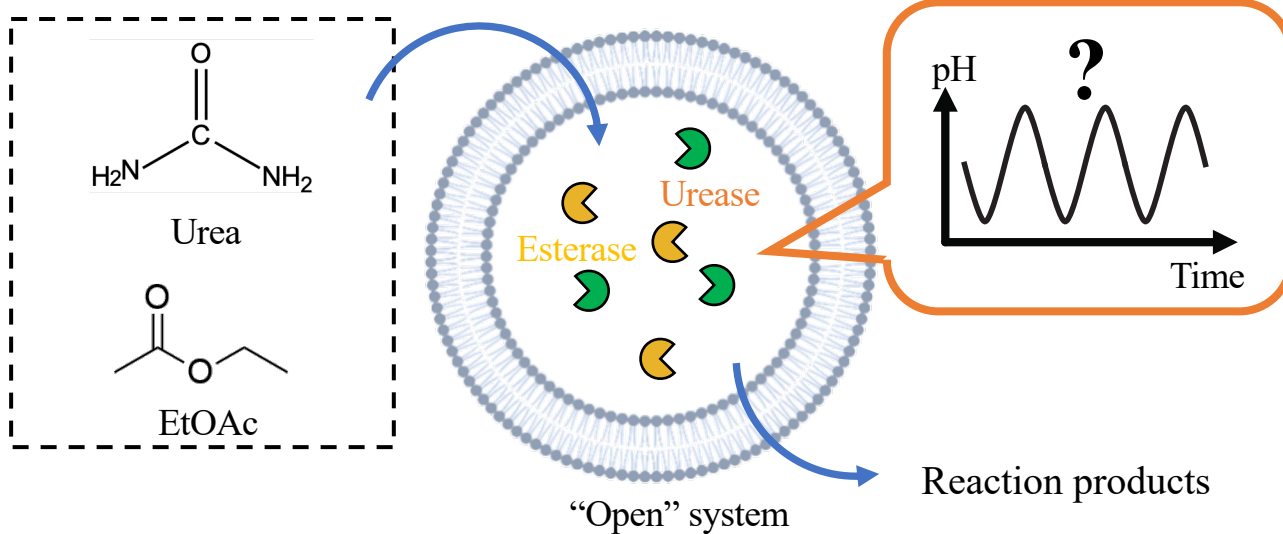
## ■ Urea–urease reaction



## ■ Ethyl acetate (EtOAc)–esterase reaction

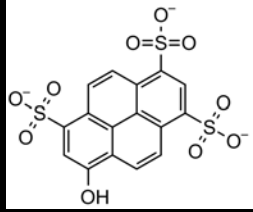


### Cross-membrane transport



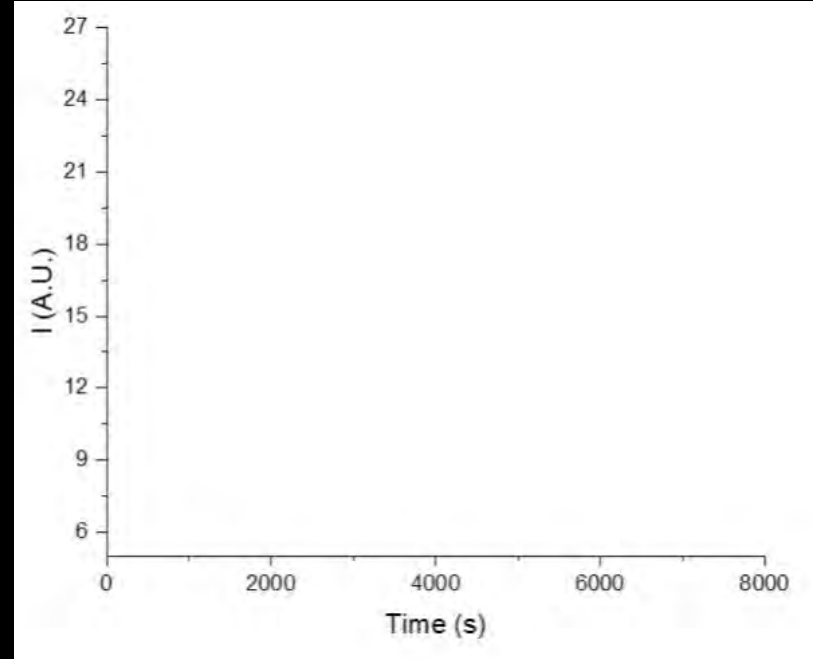
What's happened if the antagonistic enzymatic reactions are confined in GUVs?

# Time-course of pH in GUVs



pH sensitive dye: pyranine

20  $\mu\text{m}$



Transient pH changes

# Some Insights into the mechanism (bulk)

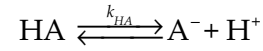
## Urease

$$v = \frac{k_u [E]_0 [S]}{\left( K_M + [S] \left( 1 + \frac{[S]}{K_S} \right) \left( 1 + \frac{[P]}{K_P} \right) \left( 1 + \frac{K_{es2}}{[H^+]} + \frac{[H^+]}{K_{es1}} \right) \right)}$$

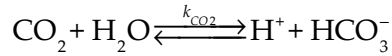
## Esterase

$$v = \frac{V_{mH} [S]^2 + V_{mL} K_{MH} [S]}{\left( [S]^2 + 2K_{MH} [S] + K_{ML} K_{MH} \right) \left( 1 + \frac{[H^+]}{K_{bes}} + \frac{K_{aes}}{[H^+]} \right) \left( 1 + \frac{[P]}{K_P} \right)}$$

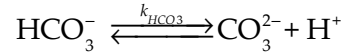
## pH equilibria



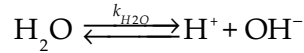
$$\text{rate} = k_{HA} [HA] - k_{HA-r} [A^-] [H^+]$$



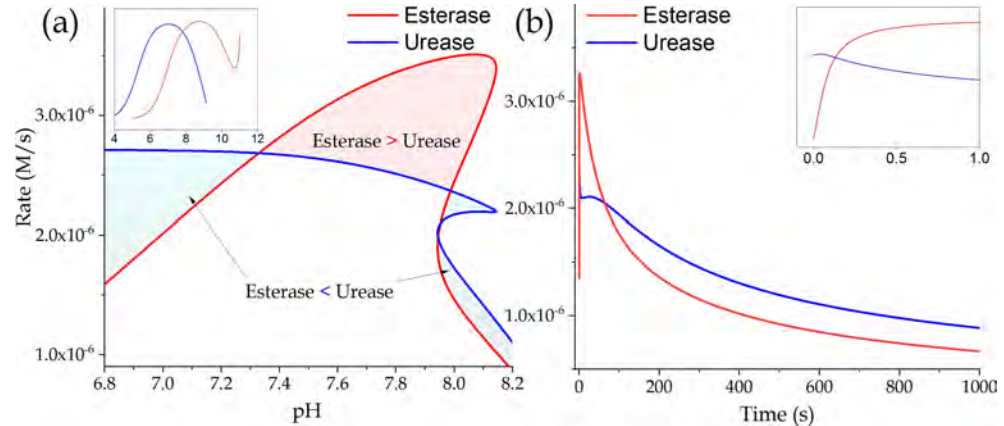
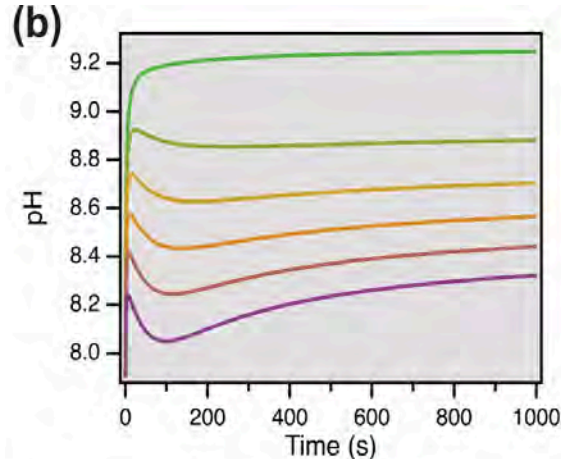
$$\text{rate} = k_{CO2} [CO_2] - k_{CO2-r} [HCO_3^-] [H^+]$$



$$\text{rate} = k_{HCO3} [HCO_3^-] - k_{HCO3-r} [CO_3^{2-}] [H^+]$$



$$\text{rate} = k_{H2O} - k_{H2O-r} [OH^-] [H^+]$$





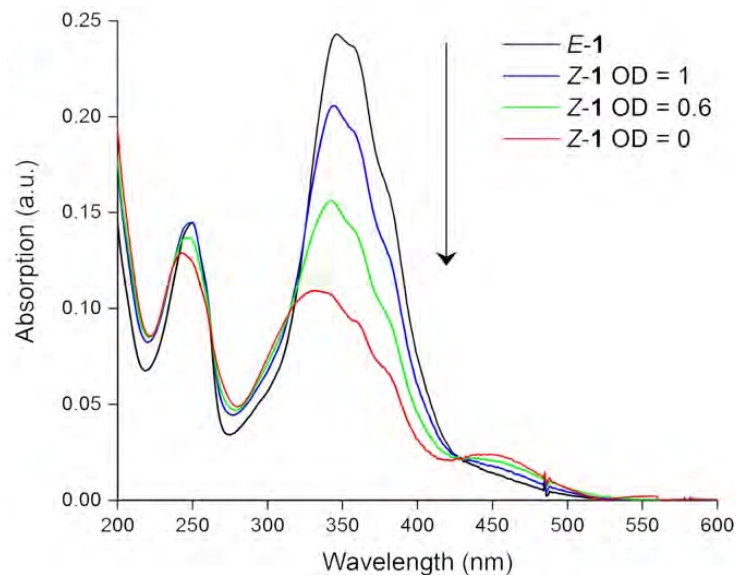
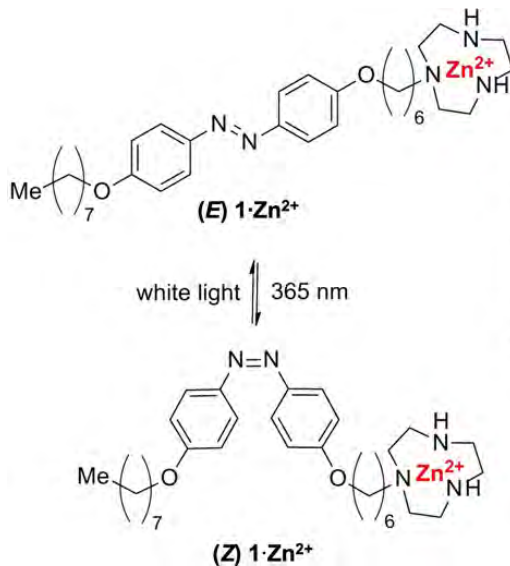
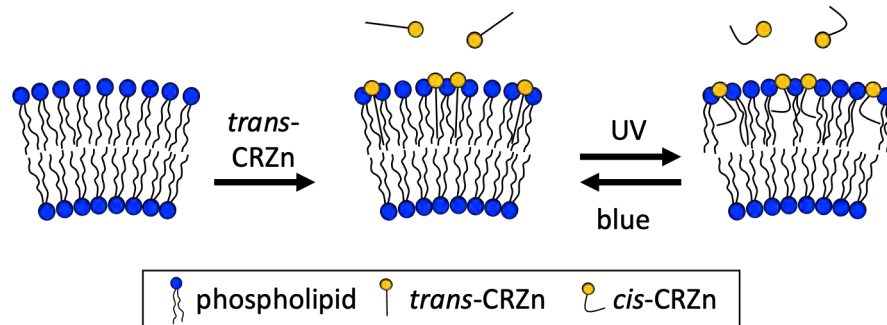
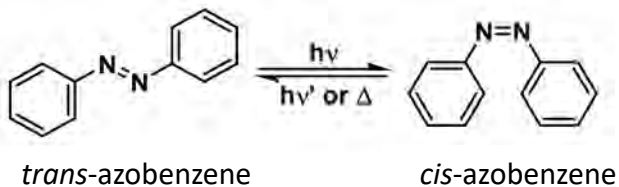
# Light control of Artificial Cells: Photo-switchable Membrane Properties



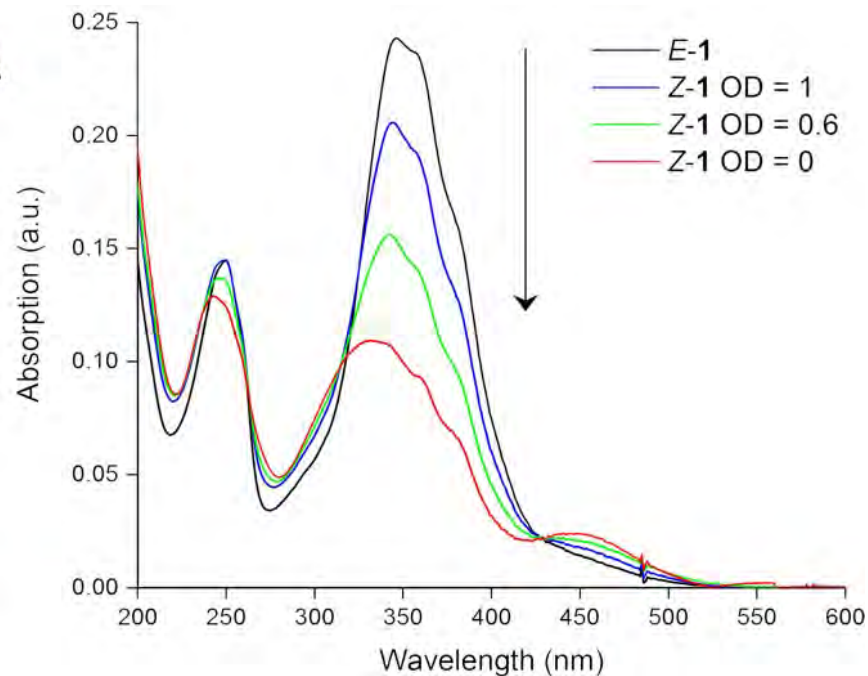
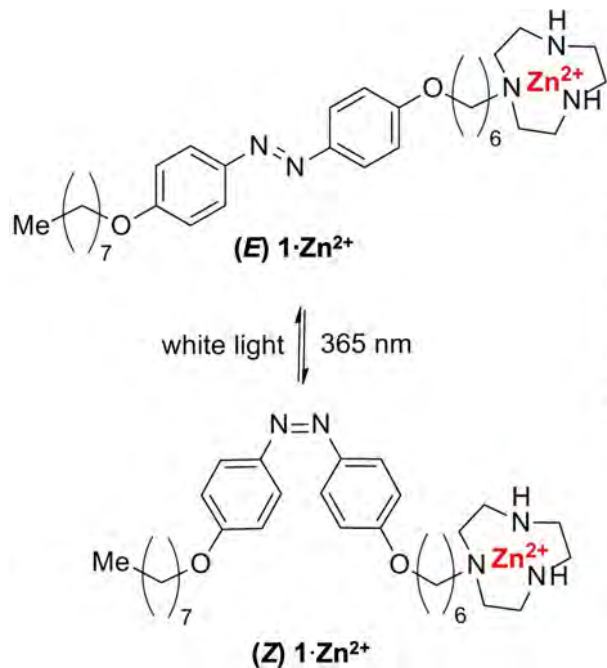
Prof. Jack Chen  
UNISI



Dr. Paola Albanese  
UNISI

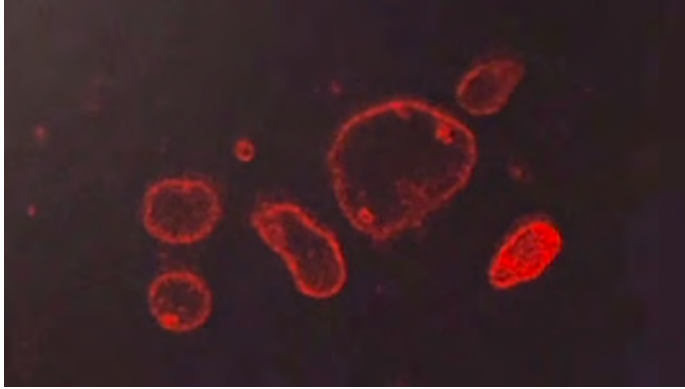


# Photoinduced *E-Z* Isomerization $1 \cdot \text{Zn}^{2+}$

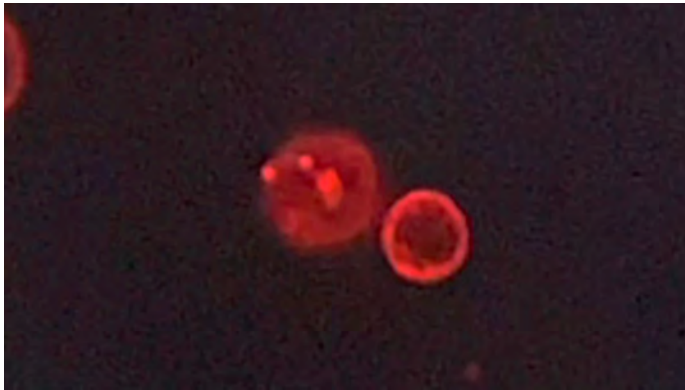
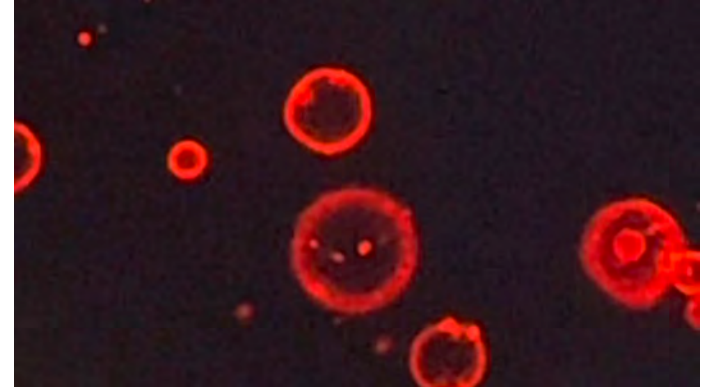


# UV-triggered shape deformations in preformed spherical GUVs

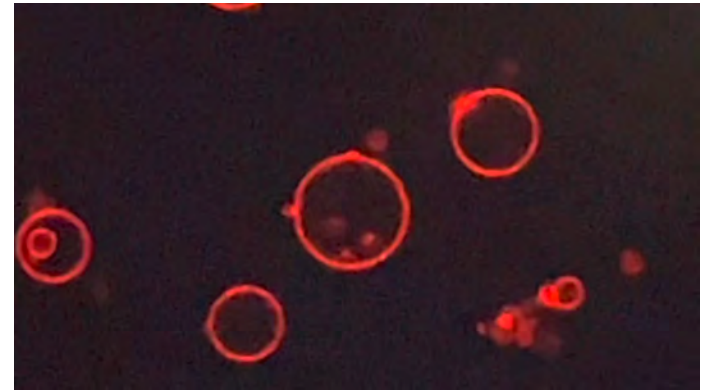
Prolate



Pearling



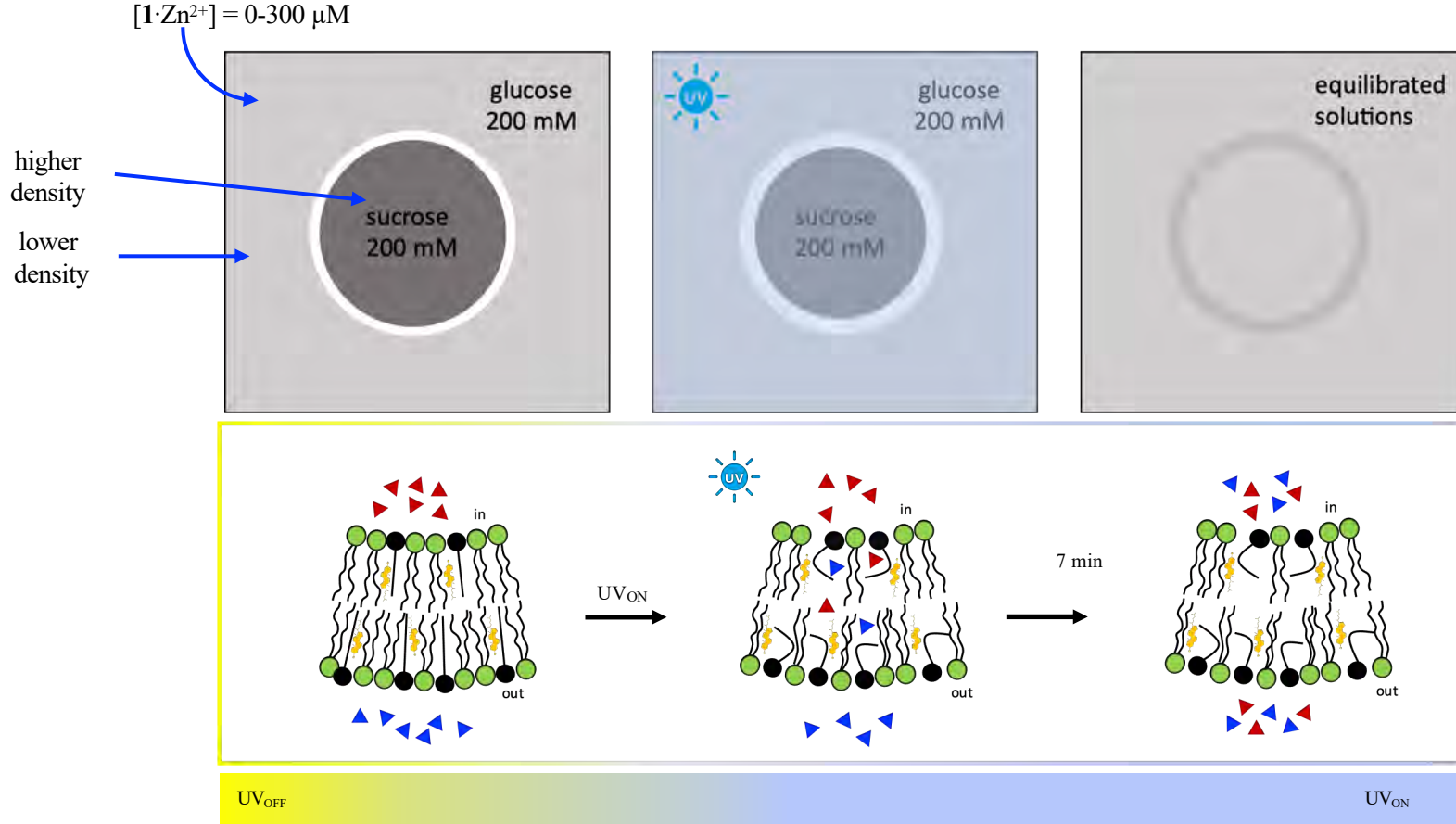
Budding



Invagination

$1 \cdot \text{Zn}^{2+} : \text{POPC} : \text{chol} \ 1:2:0.8$  - NR staining  
 $E\text{-Z-}1 \cdot \text{Zn}^{2+}$  photoisomerization induced with 405 nm-UV laser line

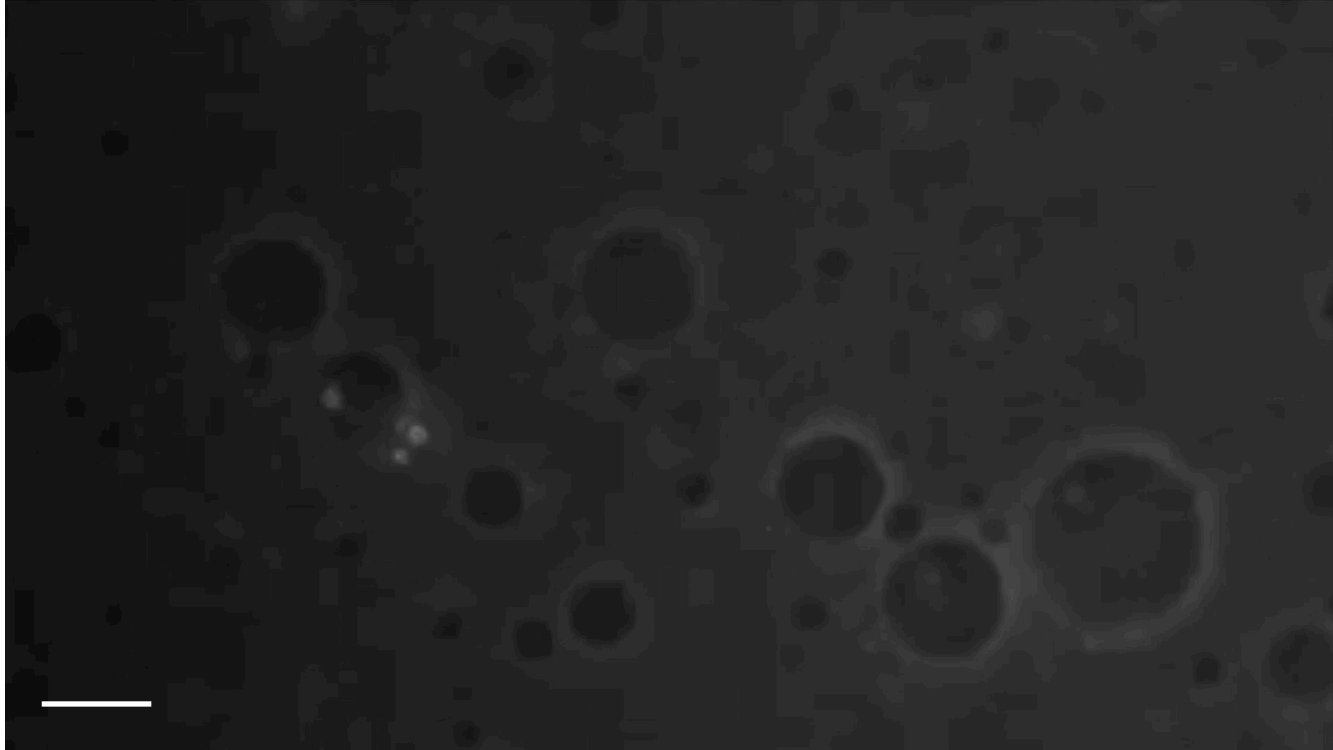
# Cargo release from GUVs in phase contrast





# Cargo release from GUVs in phase contrast

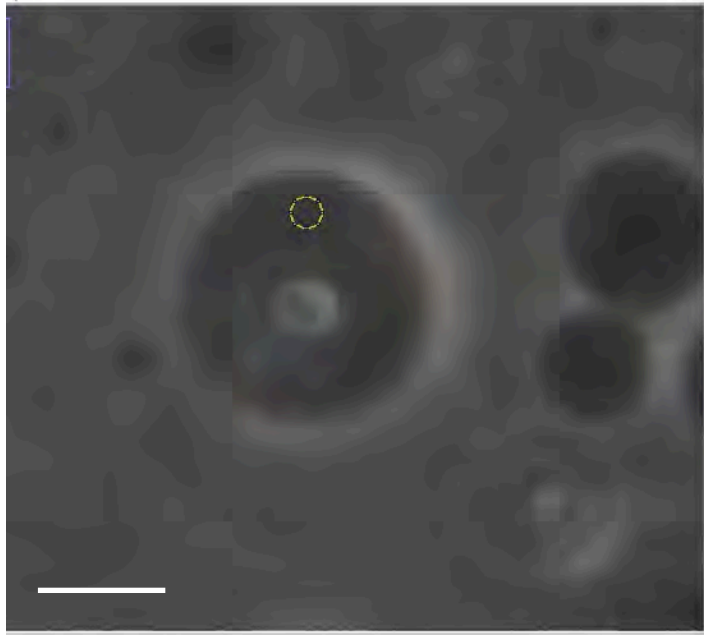
1·Zn<sup>2+</sup>:POPC:Chol 1:2:0.8



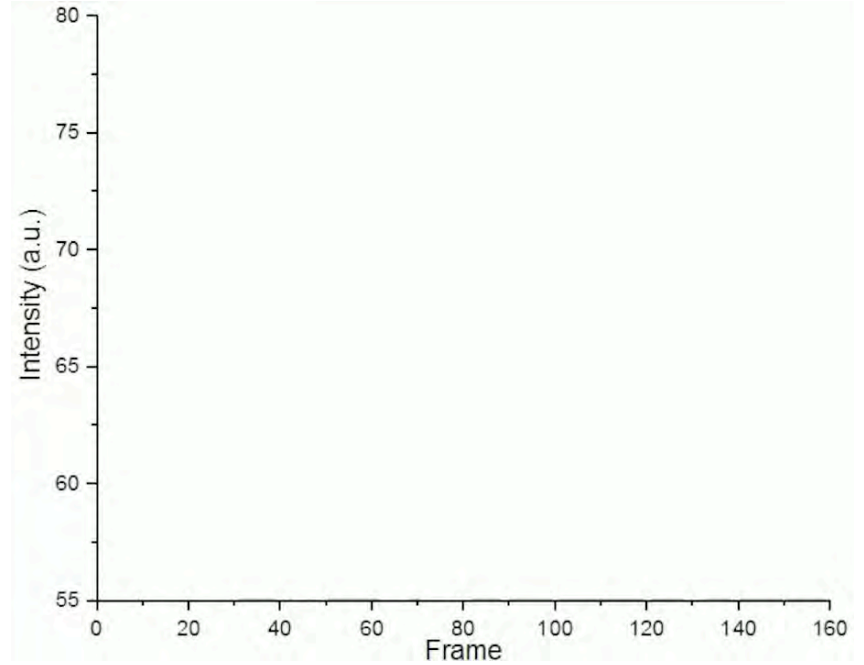
size bar 20  $\mu\text{m}$

# Content release from GUVs in phase contrast

Release kinetic



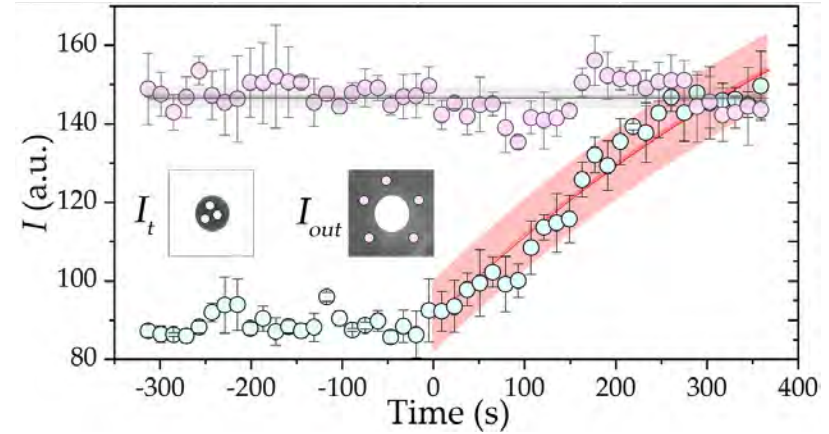
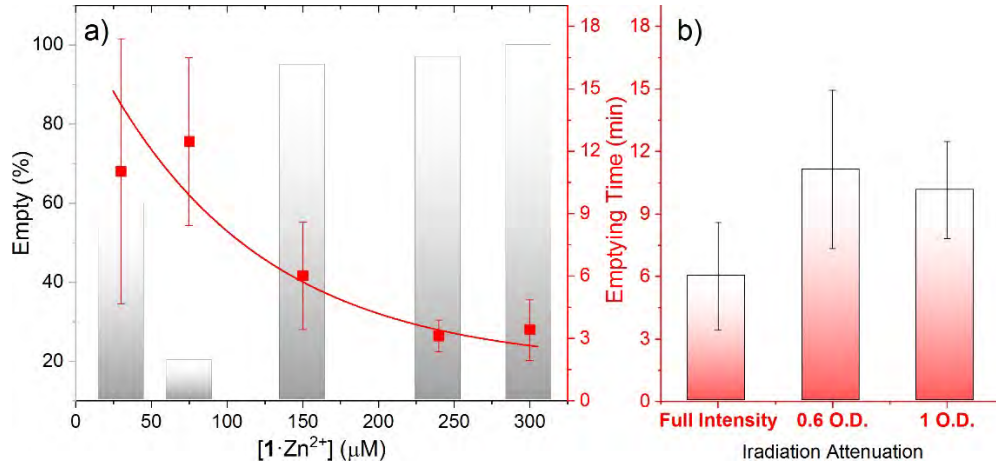
size bar 10  $\mu\text{m}$



# Tuning the membrane permeability for cargo release

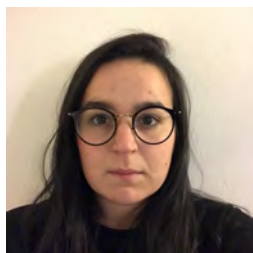
$$\frac{dC_{in}}{dt} = -\frac{aP(C_{in} - C_{out})}{V_{in}}$$

$$I_t = I_{out} \left( 1 + \frac{I_0}{I_{out}} - e^{-\frac{3P}{r}t} \right)$$



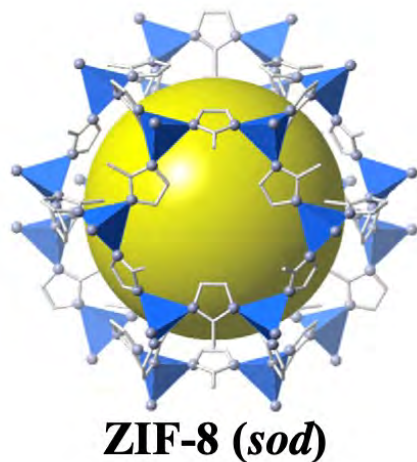
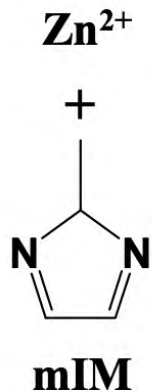
sucrose permeability at  $[1 \cdot \text{Zn}^{2+}] = 0 \mu\text{M}$   
 $\sim 10^{-6} - 10^{-5} \mu\text{m/s}$

sucrose permeability at  $[1 \cdot \text{Zn}^{2+}] = 150 \mu\text{M}$   
 $2.06 \pm 0.02 \times 10^{-3} \mu\text{m/s}$



Nadia Valletti  
UNISI

# ZIF-8: zeolite imidazole framework-8 synthesis



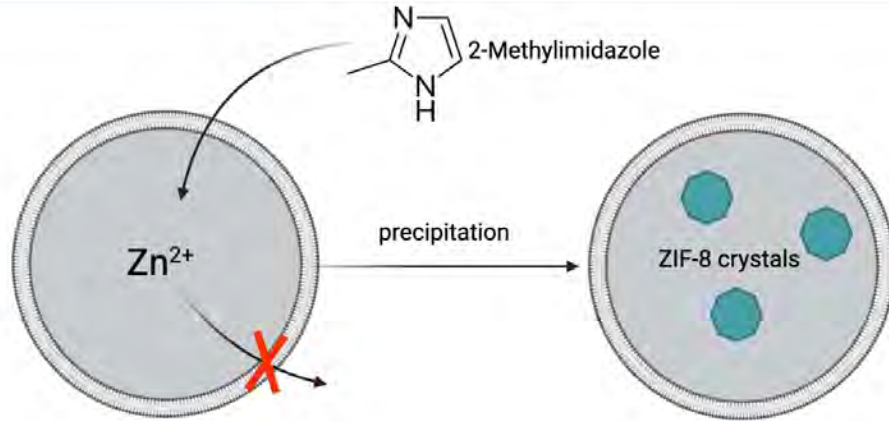
Microwave-assisted ([bmim]BF <sub>4</sub> )	Microwave-assisted (H <sub>2</sub> O)	Microwave-assisted (P123)	Microwave-assisted (F127)	Microwave-assisted (methanol)
Solvothermal (H <sub>2</sub> O)	Solvothermal (methanol)	Sonochemical (DMF+Triethylamine)	Sonochemical (DMF)	Mechanochemical (without zinc acetate)
Mechanochemical (zinc acetate)	Dry-gel conversion (H <sub>2</sub> O)	Dry-gel conversion (methanol)	Dry-gel conversion (DMF)	Dry-gel conversion (n-heptane)
Microfluidic (MeOH)	Microfluidic (MeOH/NH <sub>3</sub> )	Microfluidic (decane/water)	Microfluidic (ODE/water)	Microfluidic (silicone oil/water)

SEM images of ZIF-8 synthesized by various methods



# The role of the membrane and the experimental setup

## Our idea...



### GUVs COMPOSITION:

#### Inner solution:

- Sucrose
- $\text{ZnCl}_2$

#### Outer solution:

- Glucose
- HMIM

#### Organic phase:

- POPC

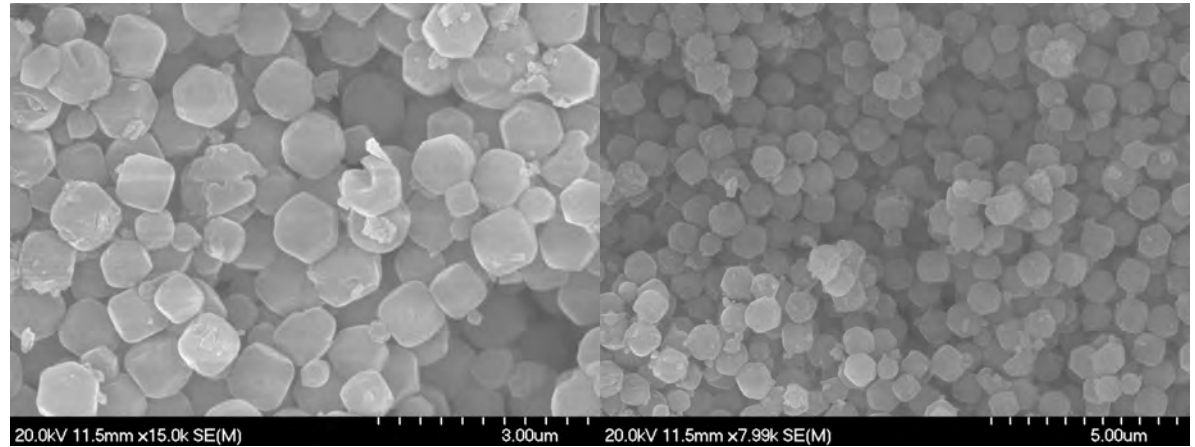
Compartmentalization  
Semi-permeability



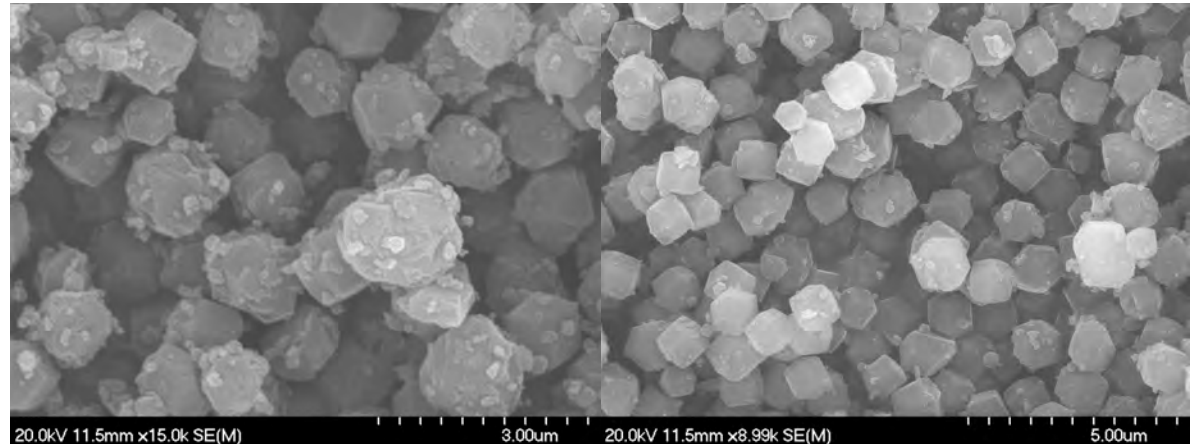
Far from equilibrium

## SEM Measurements

Experimental conditions in bulk:  
 $\text{ZnCl}_2:\text{HMIIm}=1:20$



Experimental conditions in bulk:  
 $\text{ZnCl}_2:\text{HMIIm}=1:20$ , sugars, POPC



# Zinc ions encapsulation

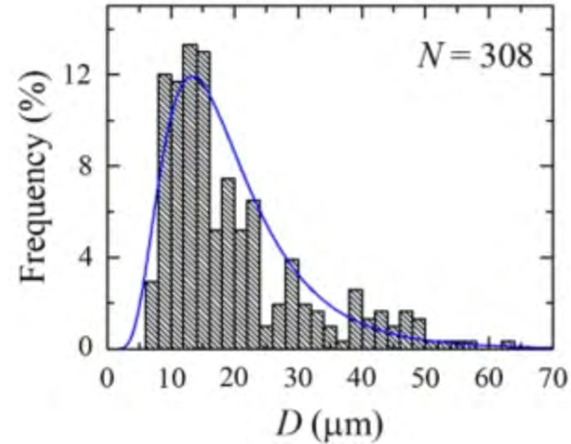
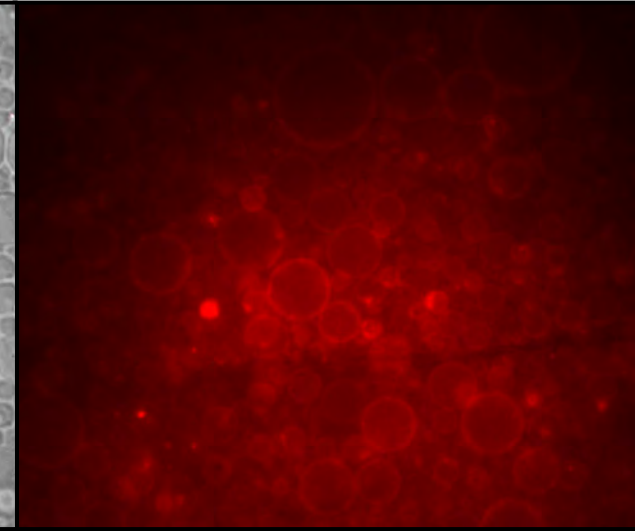
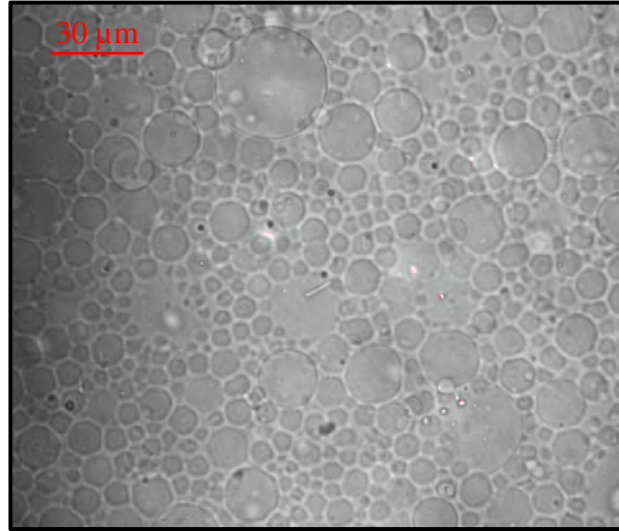
## Experimental conditions:

### Inner solution:

- water
- sucrose 500 mM
- $\text{ZnCl}_2$  0-30 mM

### Outer solution:

- water
- glucose 500 mM

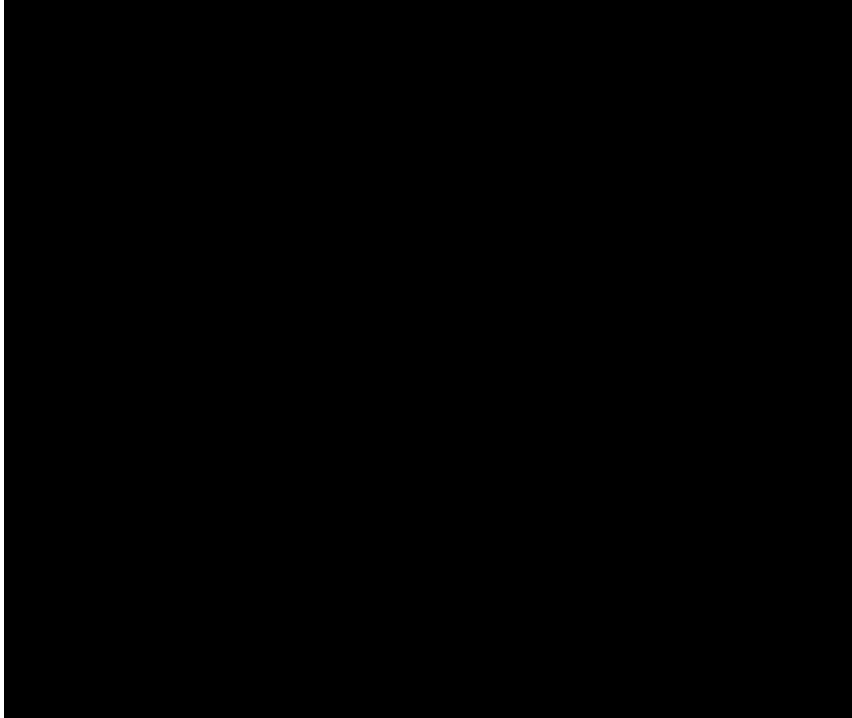


# GUVs experiments

GUVs experiment (1h)

ZnCl<sub>2</sub> 20 mM

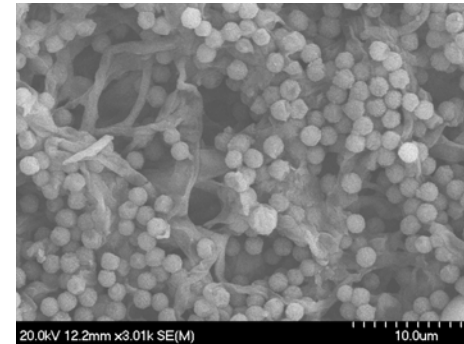
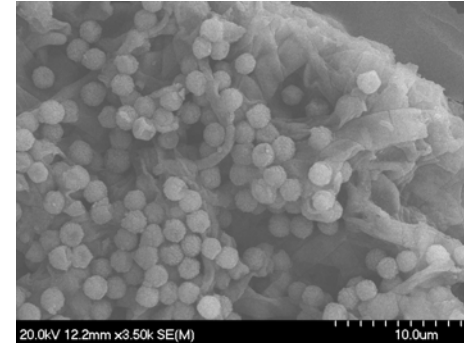
HMIM 400 mM



GUVs experiment (1day)

Zn 20 mM

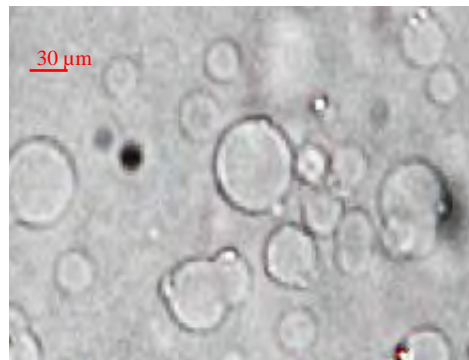
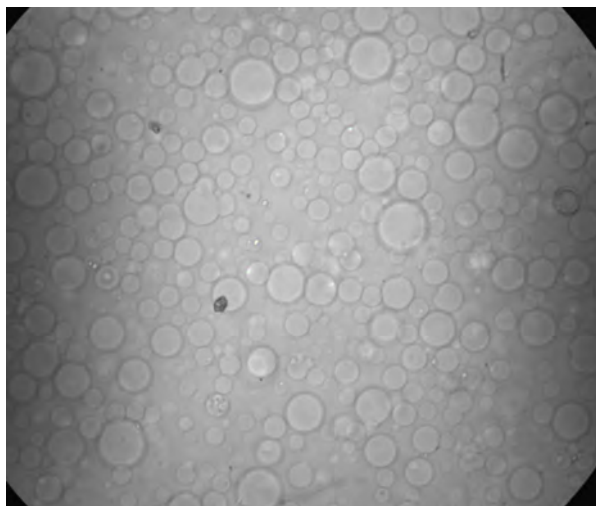
HMIM 400 mM





# Preliminary results: ZIF-8 synthesis

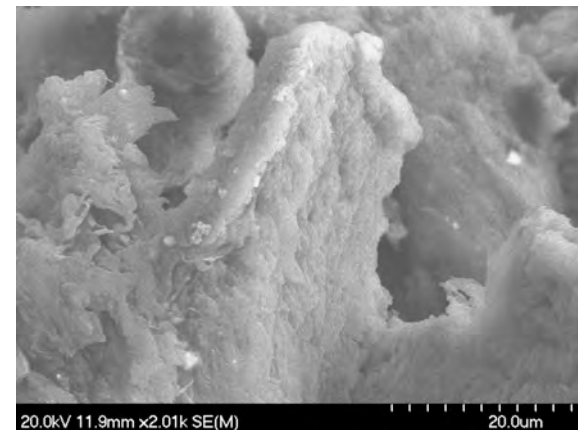
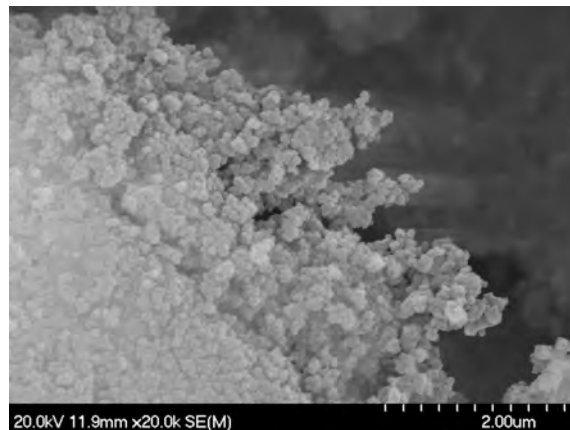
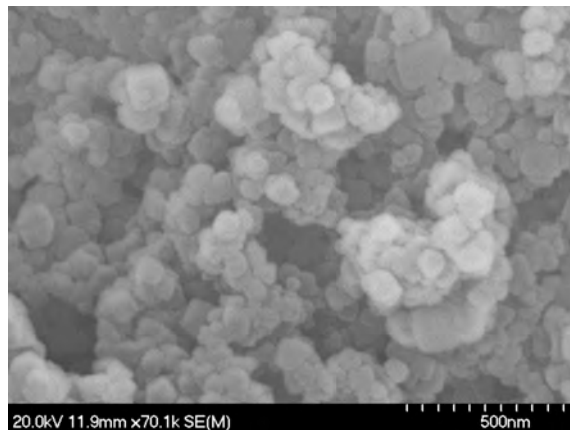
ZnCl<sub>2</sub> 10mM  
HMIM 200mM



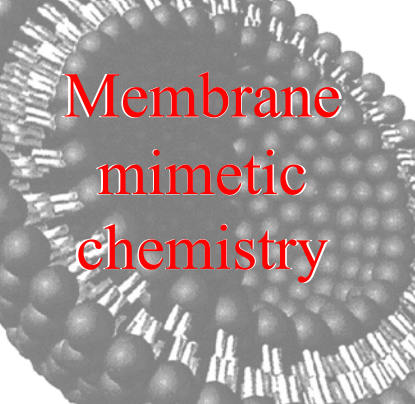
t = 0 min



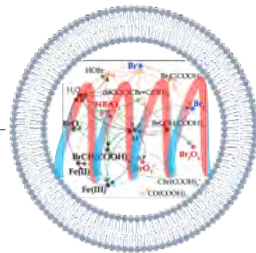
t = 60 min



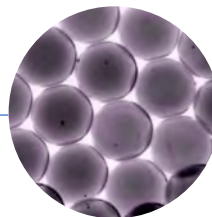
## Conclusions



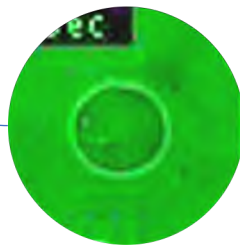
Membrane  
mimetic  
chemistry



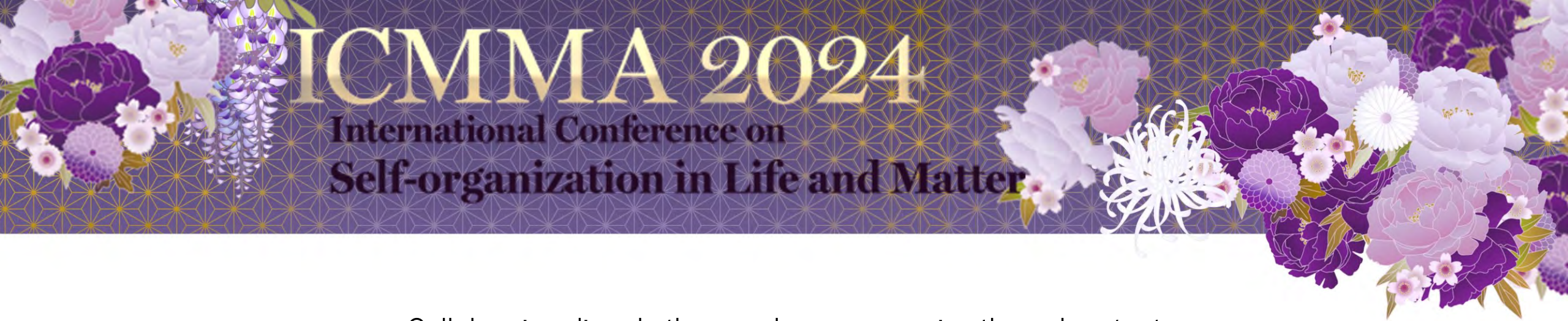
## Tunable and programmable system



Network signaling and communication can be controlled through compartment manipulation



## Effective division triggered by an internal stimulus



## Cellular circadian rhythm can be more precise through output

Hiroshi Ito (Faculty of Design, Kyushu University)

Circadian rhythms are biological phenomena that repeat with a 24-hour cycle. Even individual cells can exhibit a self-sustained rhythmicity. In this talk, I will focus on the accuracy of cellular circadian rhythms. Circadian rhythms exhibit smaller fluctuations when cells are coupled as a group, e.g. organs. However, at the single-cell level, circadian rhythms are less robust. For instance, mammalian cultured cells have a period variation of about 1 hour. In contrast, prokaryotic cyanobacteria show a fluctuation of 0.1 hours, indicating a more accurate circadian clock. Why do these differences arise? One possibility we theoretically proposed is the control of fluctuations in the output system. We considered a simple circadian clock model coupled with its output system. We found that the output system's fluctuations could be smaller than those of the circadian clock itself. Furthermore, this is not dependent on the expression level of the promoter but rather on the degradation rate of the output protein or the functional system that determines its transmission. We also discovered that the sinusoidal regulation effectively reduces fluctuations. Compared to the rhythms of neuronal firing or cell cycles, the rhythm of the circadian clock tends to be sinusoidal. This might be the result of optimization aimed at reducing circadian rhythm fluctuations. Furthermore, our recent analysis revealed that feedback loops output waveforms very close to sine function. The fact that the circadian clock is generated by feedback might be linked to these fluctuations. So far, chronobiologists have devoted huge effort to examine the central circadian oscillator. Yet, there would be unresolved issues on the clock's output.

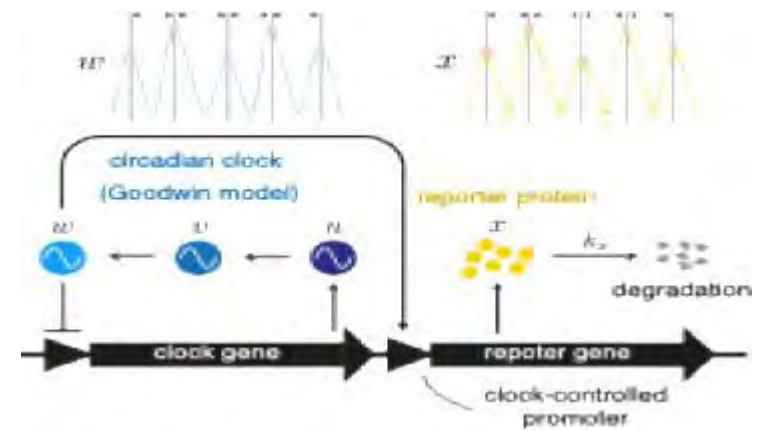


**Figure 1.** Fluctuation in period of circadian clock and its output.



Our projects:

Observe fascinating rhythms, understand theoretically them.

# Cellular circadian rhythm can be more precise through output

Faculty of Design, Kyushu University, Japan

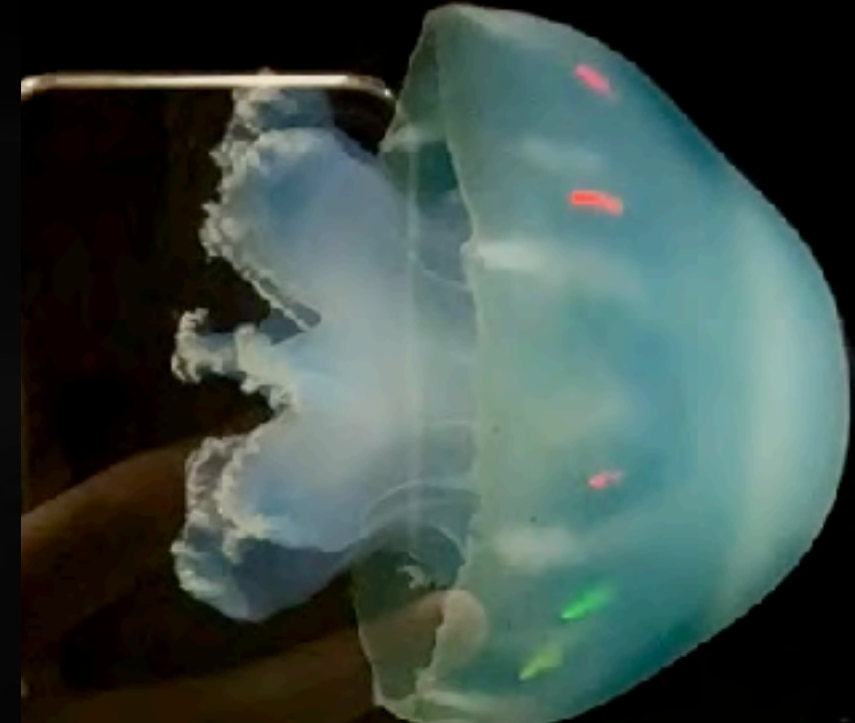
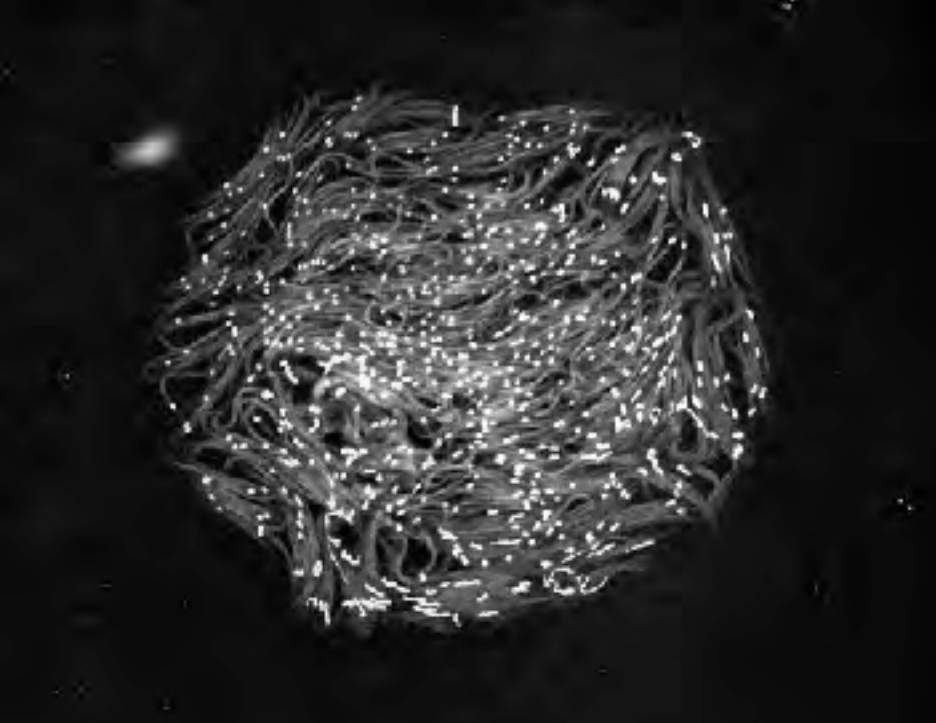
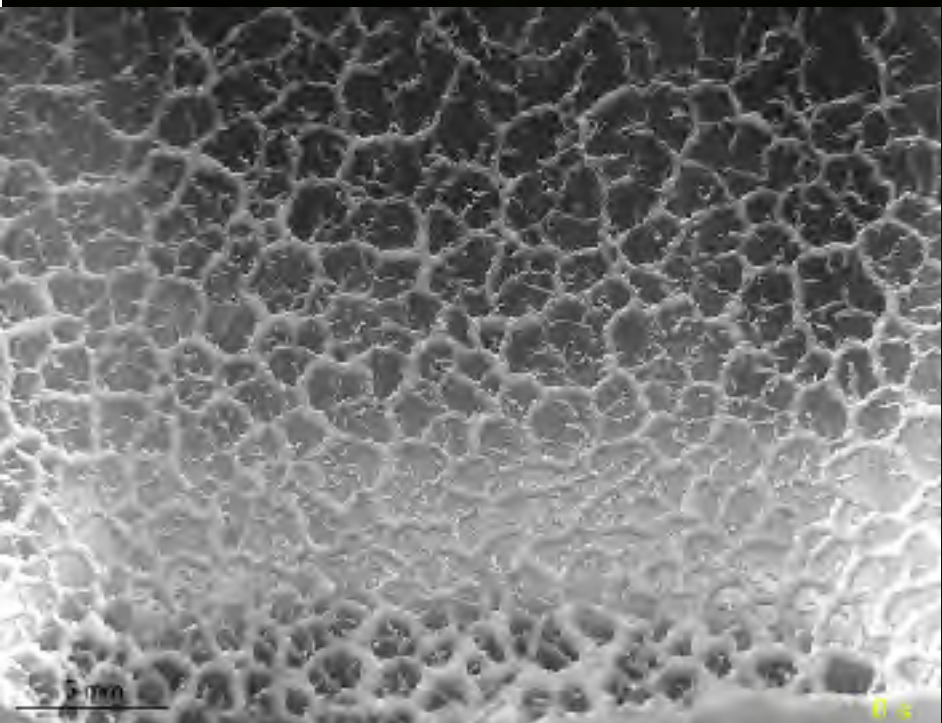
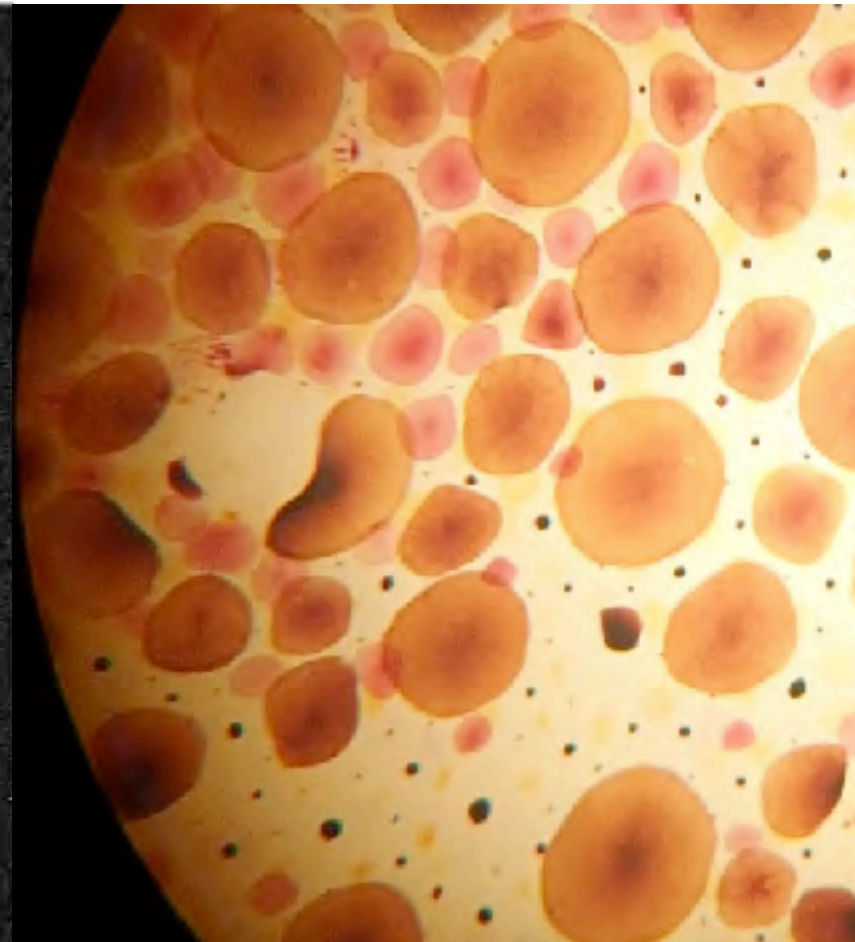
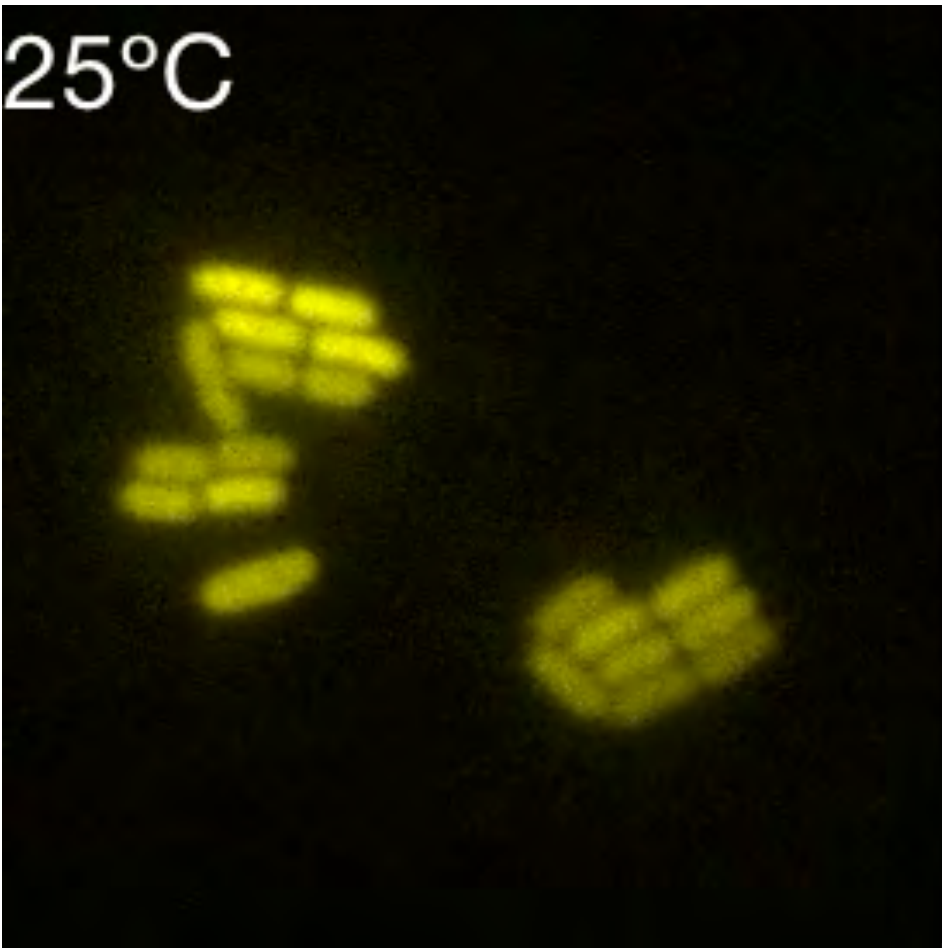
Hiroshi Ito (伊藤浩史)

9:00-10:00 ICMMA2024 11 Sep 2024



# Our projects:

observe fascinating rhythms, understand theoretically them



# Today's topics, theory-related researches

1. Controlling reconstituted circadian clock by temperature
2. Cellular circadian rhythm can be more precise through output
3. What time flowers flower?



# Phylogenetic tree of my academic career

Post-doc

Student



W Hastings



T Kondo



Me

Common denominator :  
**Circadian rhythm  
in microorganisms**

Student

Inspired

Student

Post-doc



CS Pittendrigh



A Winfree



Y Kuramoto



H Kori

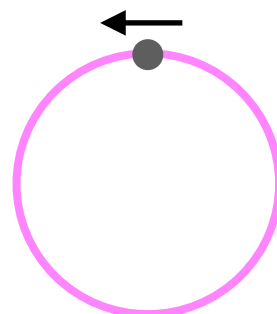


Me

Common denominator : **Think with phase** cf. Nakao's talk



$$\dot{\theta} = \omega$$



Synchronization (Pittendrigh)

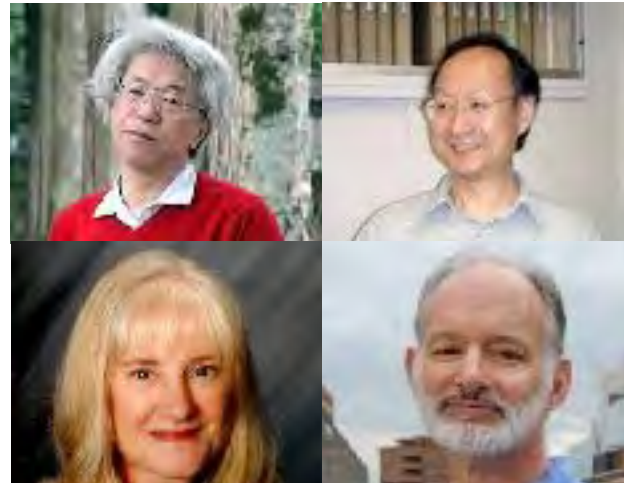
Singularity (Winfree)

Collective synchronization (Kuramoto)

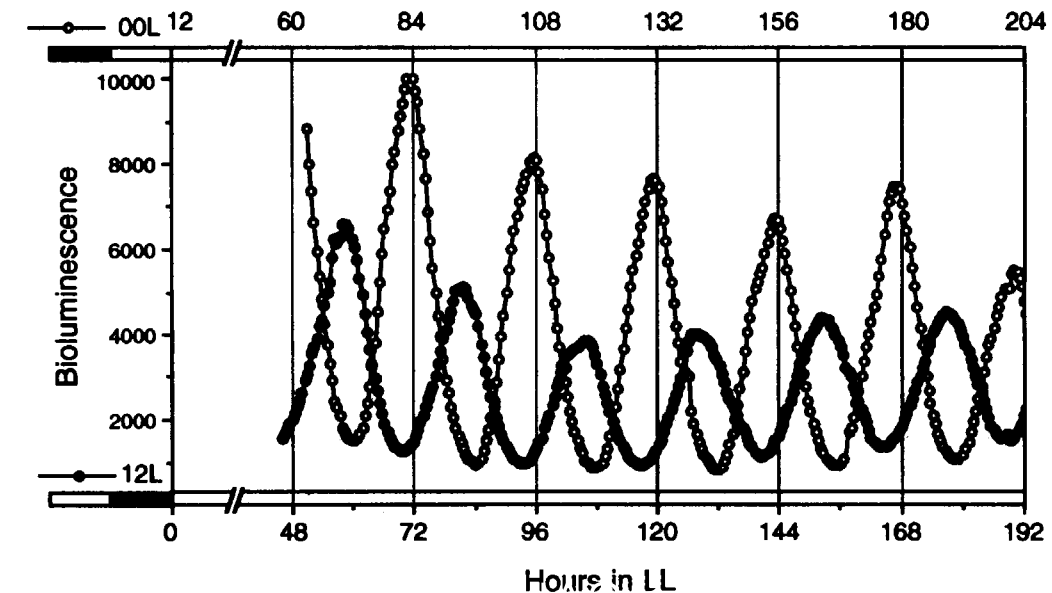
# Bacteria have “body” clock (circadian rhythm)



**Cyanobacteria**

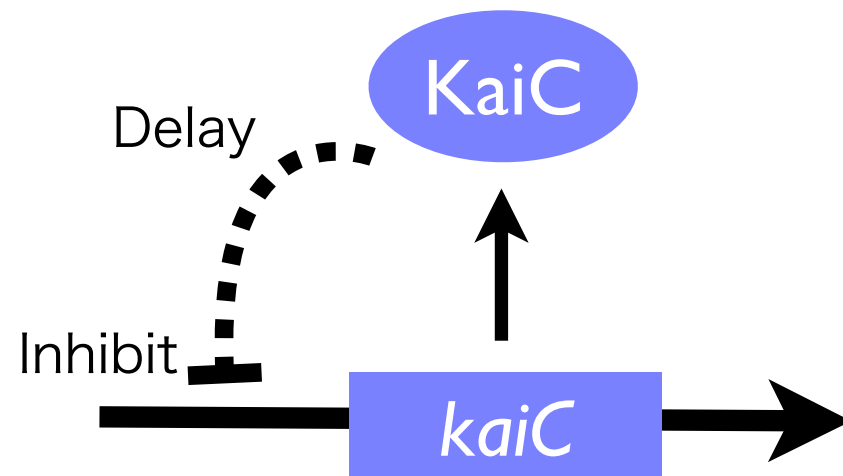


**Kondo Ishiura  
Golden Johnson**



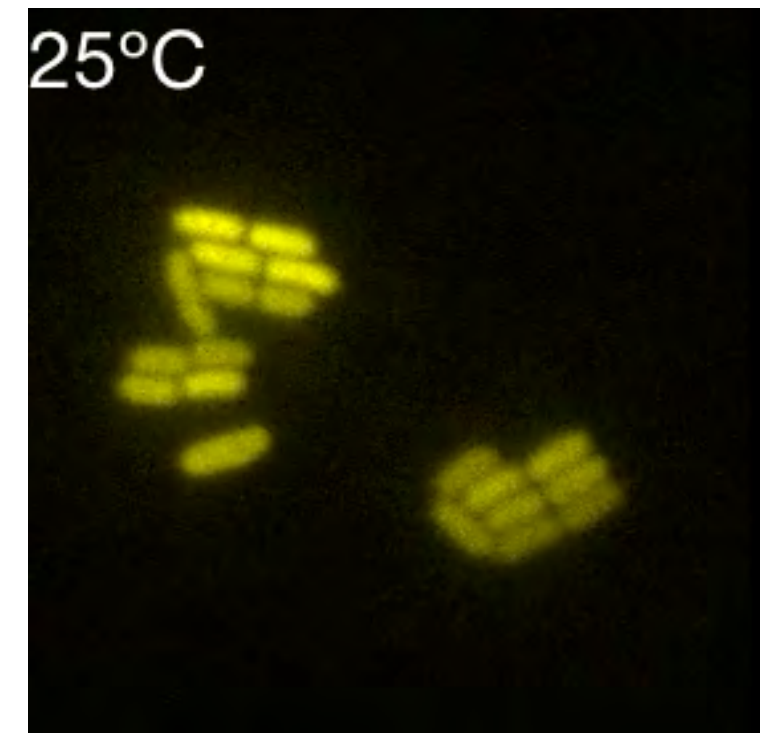
**Bioluminescence rhythms**  
(Kondo et al. PNAS 1992)

- obtained many (~100!) clock mutants (Kondo et al. Nature 1994)
- cloned three clock genes; *kaiA*, *kaiB*, *kaiC* (Ishiura et al. Science 1998)
- found negative feedback of *kaiC* (Ishiura et al. Science 1998)



cf. Nobel prize 2017

- reconstitution of circadian clock (Nakajima et al. Science 2005) ...



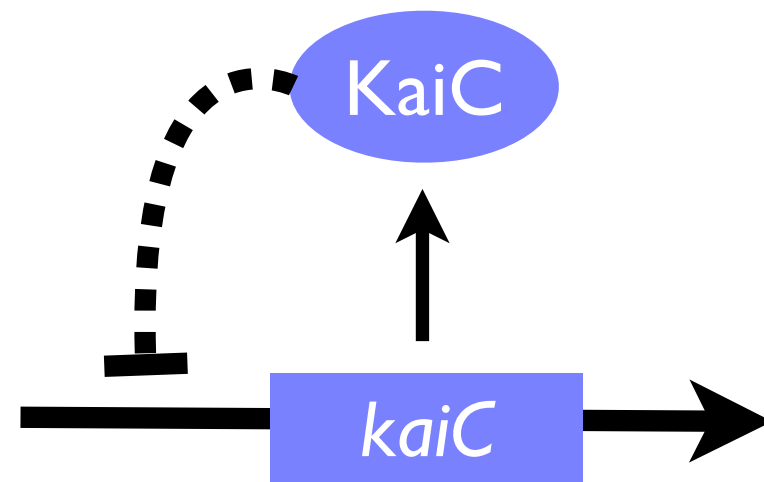
**Fluorescent rhythms**



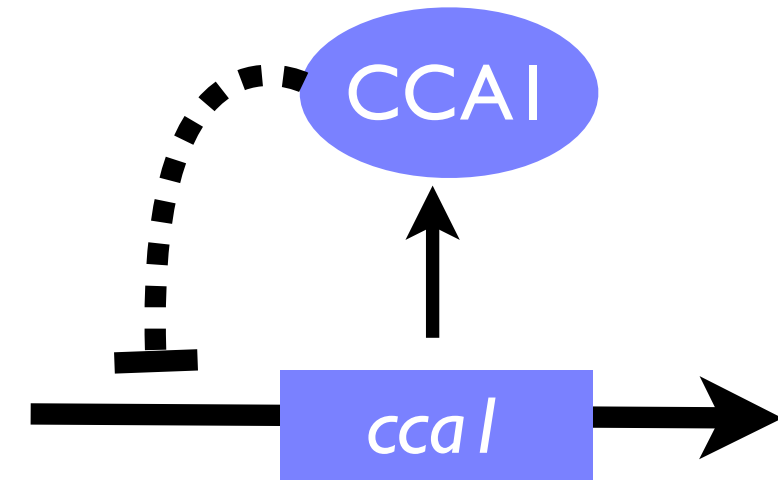
# Feedback loop is shared in circadian systems



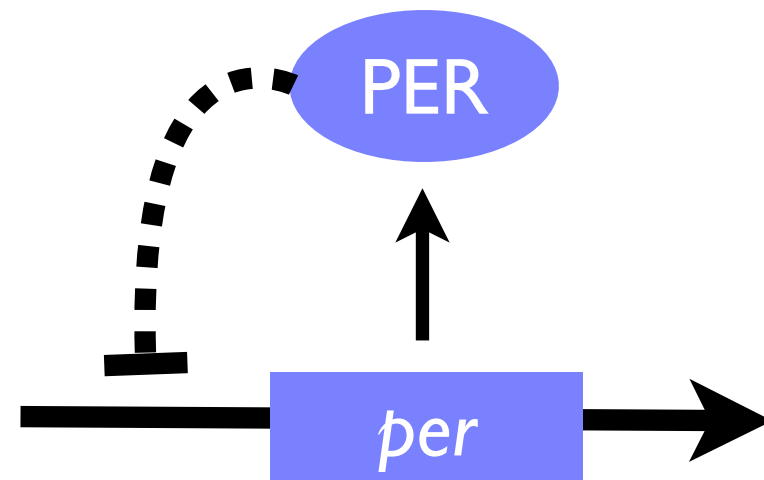
**Cyanobacteria**  
(1998)



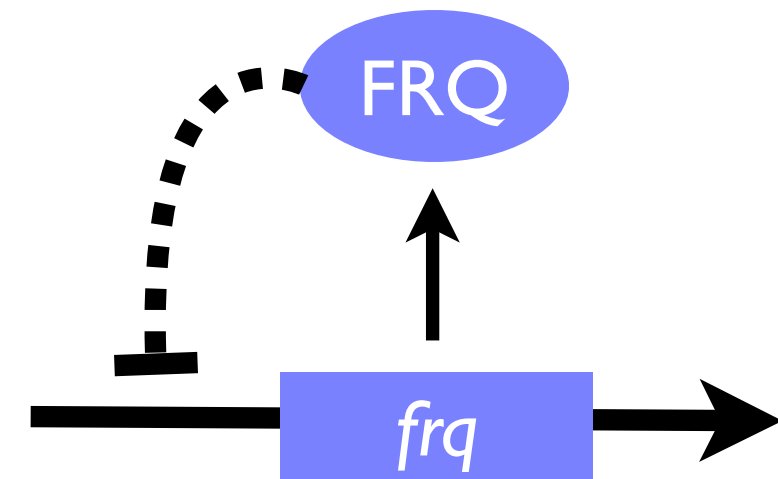
**Plant**  
(1998)



**Drosophila** (1990)  
**Mammals** (1998)  
**Zebrafish** (1998)



**Fungus**  
(1998)

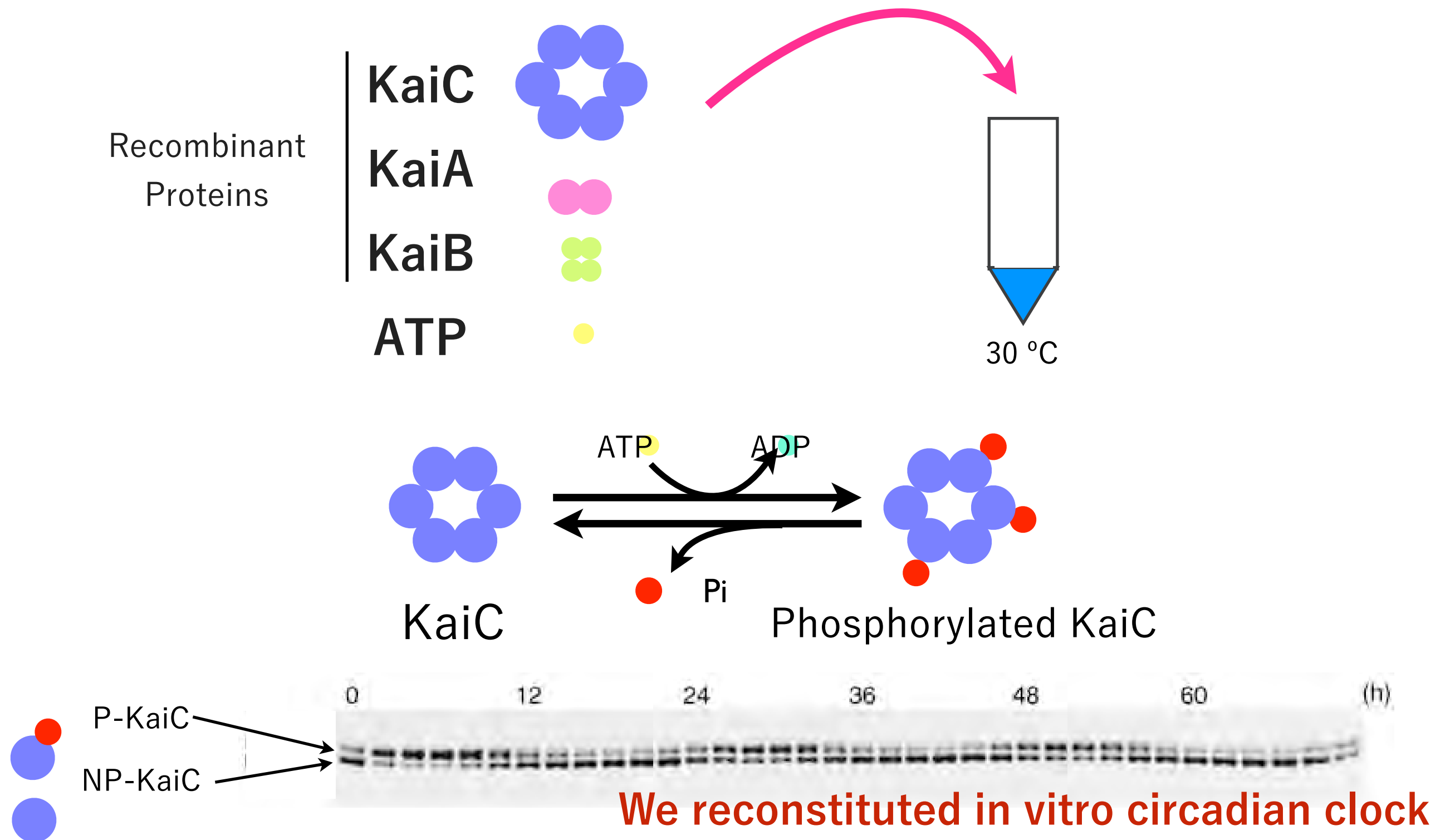


Nobel prize laureates in 2017



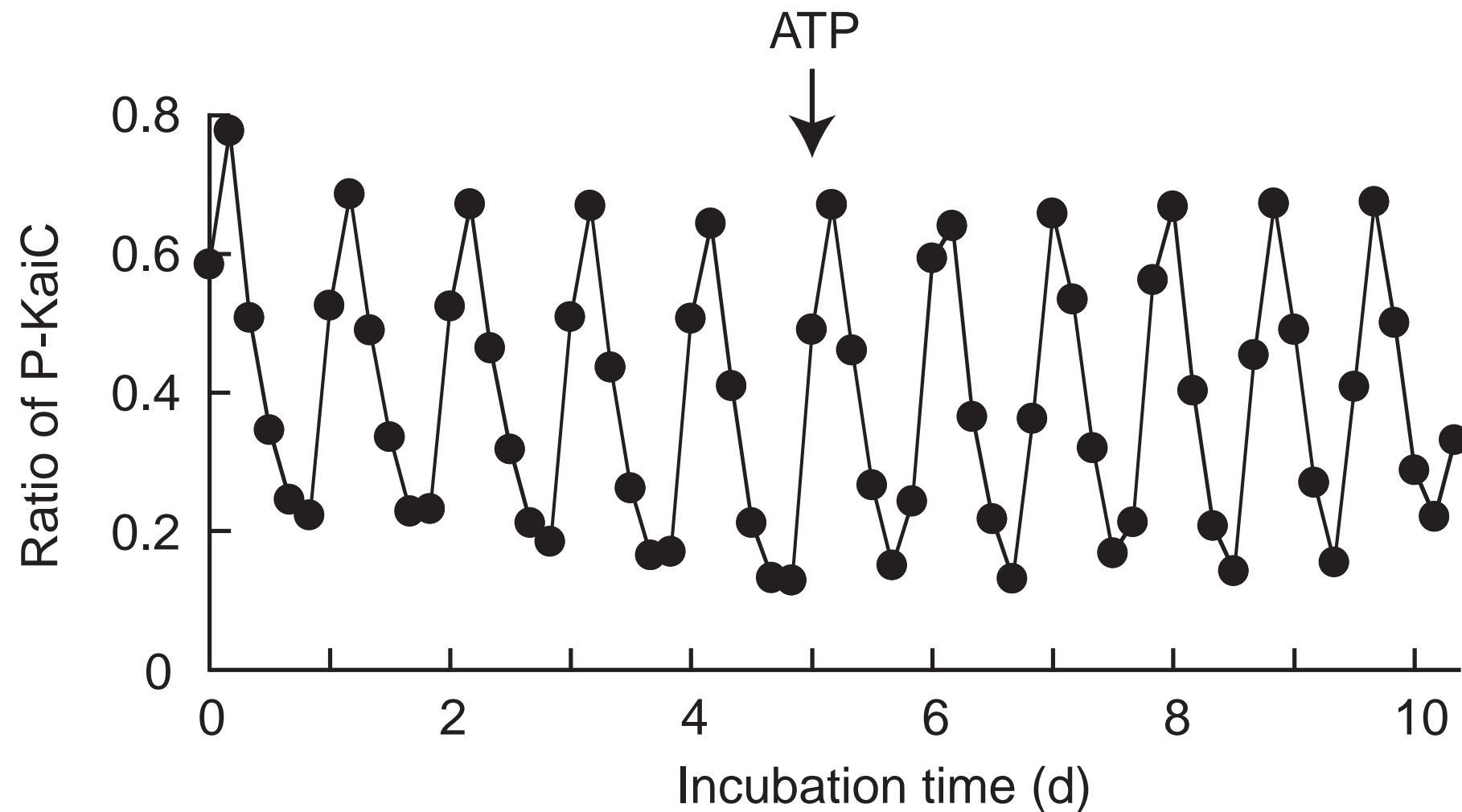
Hall Rosbash Young

# Circadian clock in a test tube



Nakajima, Imai, **HL**, Nishiwaki, Murayama Iwasaki Oyama & Kondo  
*Science* **308**, 414-415 (2005)

# Circadian clock in a test tube

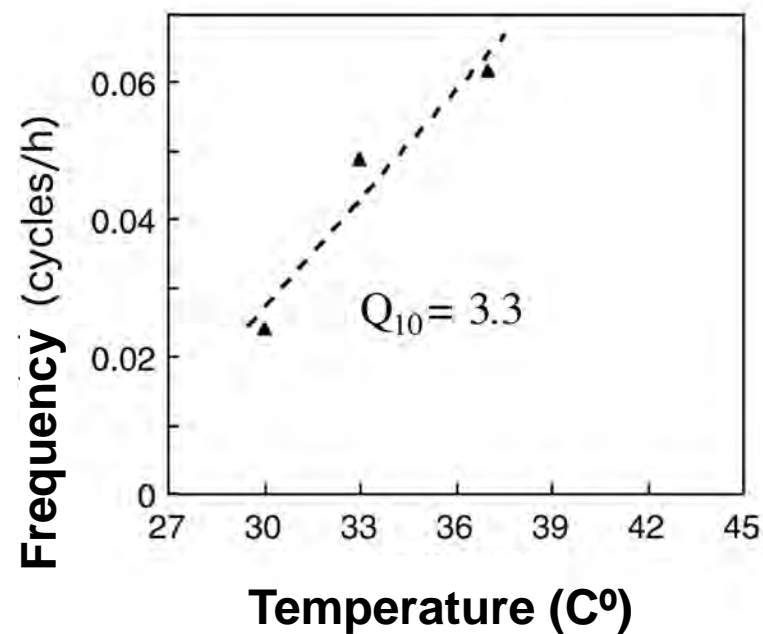
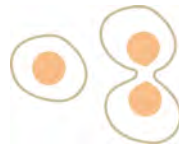


Hi et al. Nature Struct. Mol. Biol. 2008

The KaiC phosphorylation rhythms persists for 10 days without damping in the presence of sufficient ATP.

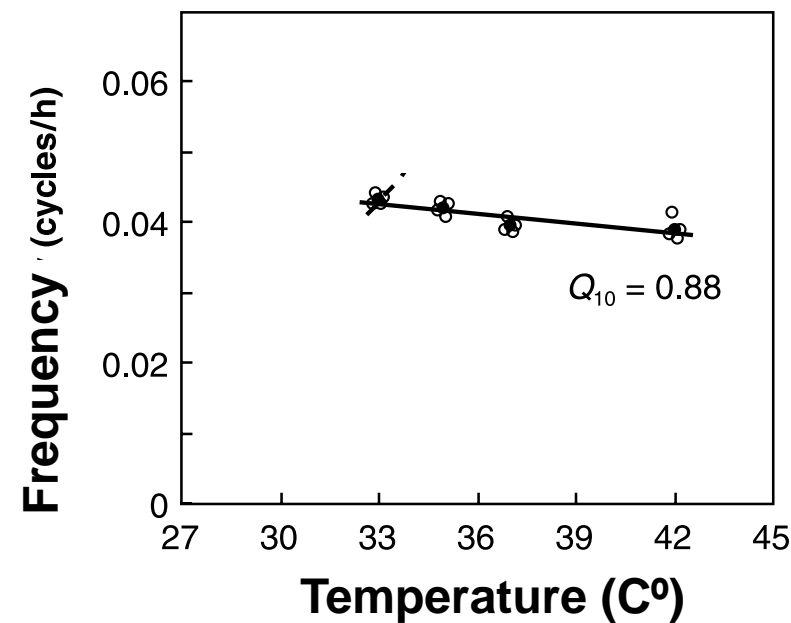
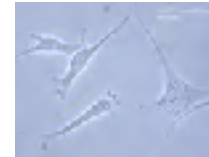
# Insensitivity of temperature on the period

Cell divisions



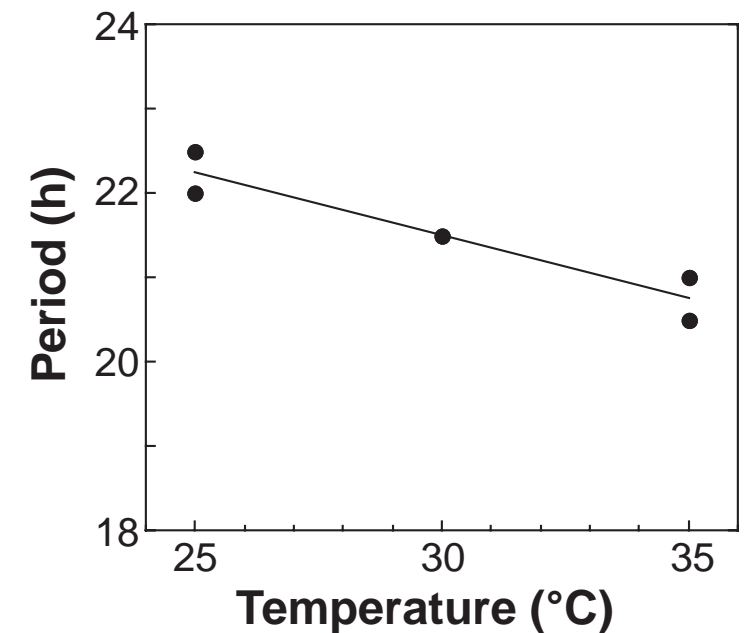
temperature sensitive

circadian rhythm of mammalian cells



temperature compensated

In vitro clock



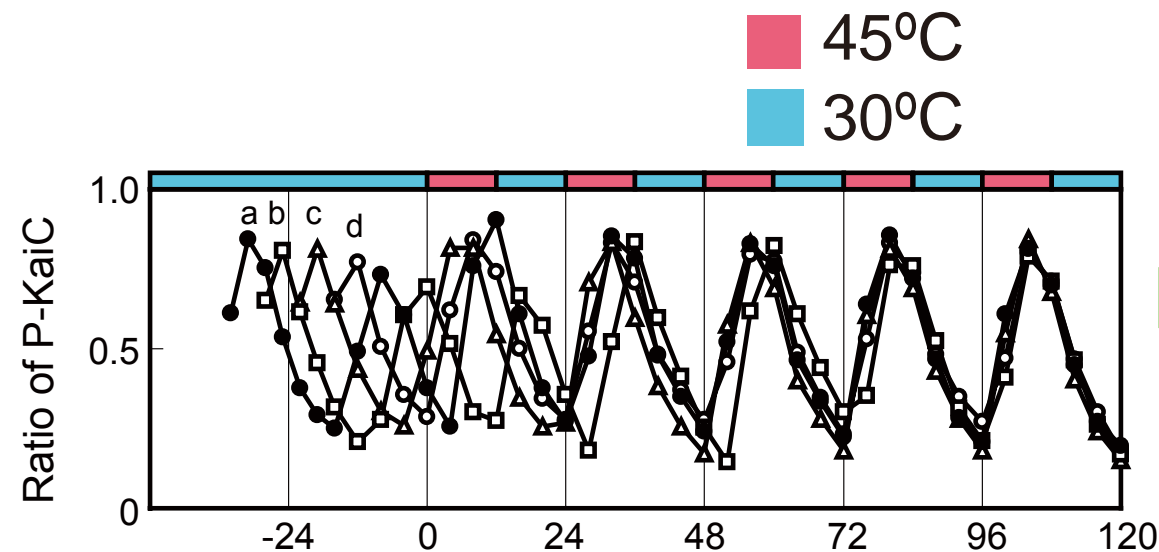
temperature compensated

Nakajima et al. Science 2005



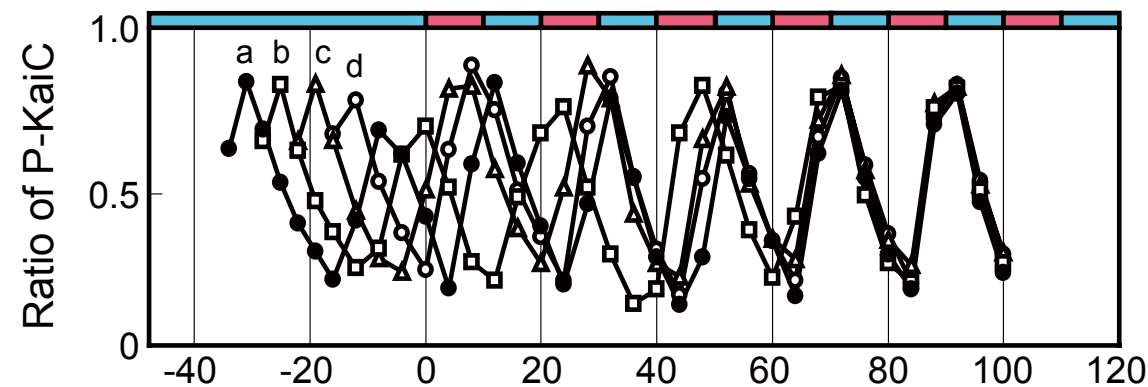
# Synchronization to temperature cycles

**45°C 12h**  
**30°C 12h**



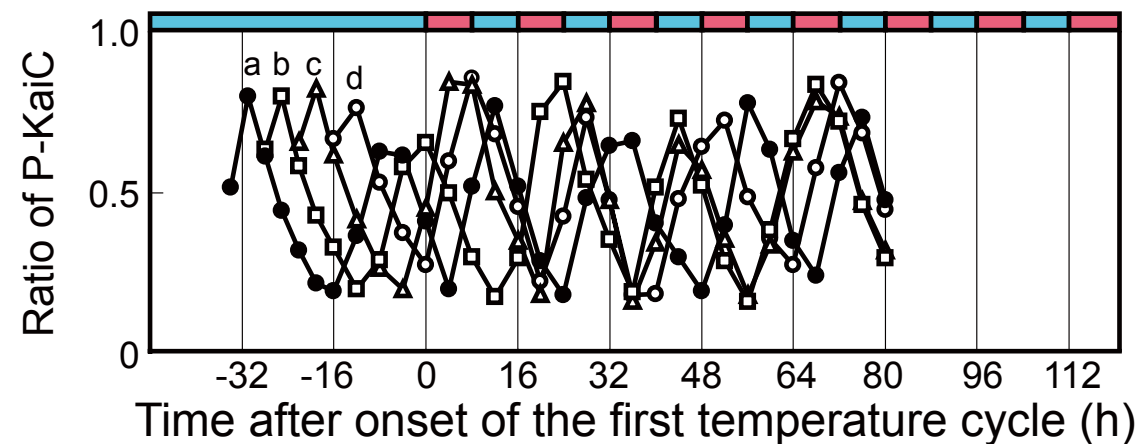
**Entrained**  
**23.0h → 23.9h**

**45°C 10h**  
**30°C 10h**



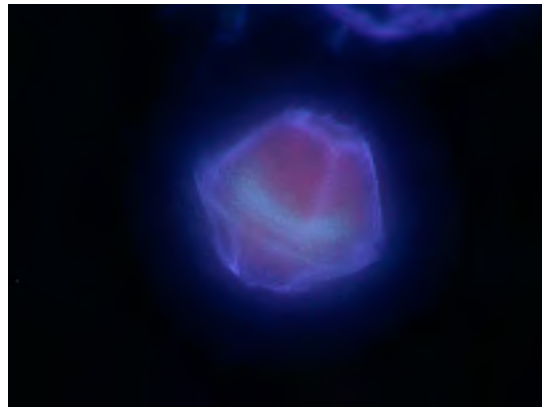
**Entrained**  
**23.0h → 19.9h**

**45°C 8h**  
**30°C 8h**



**Not entrained**

# Low temperature abolishes circadian rhythms



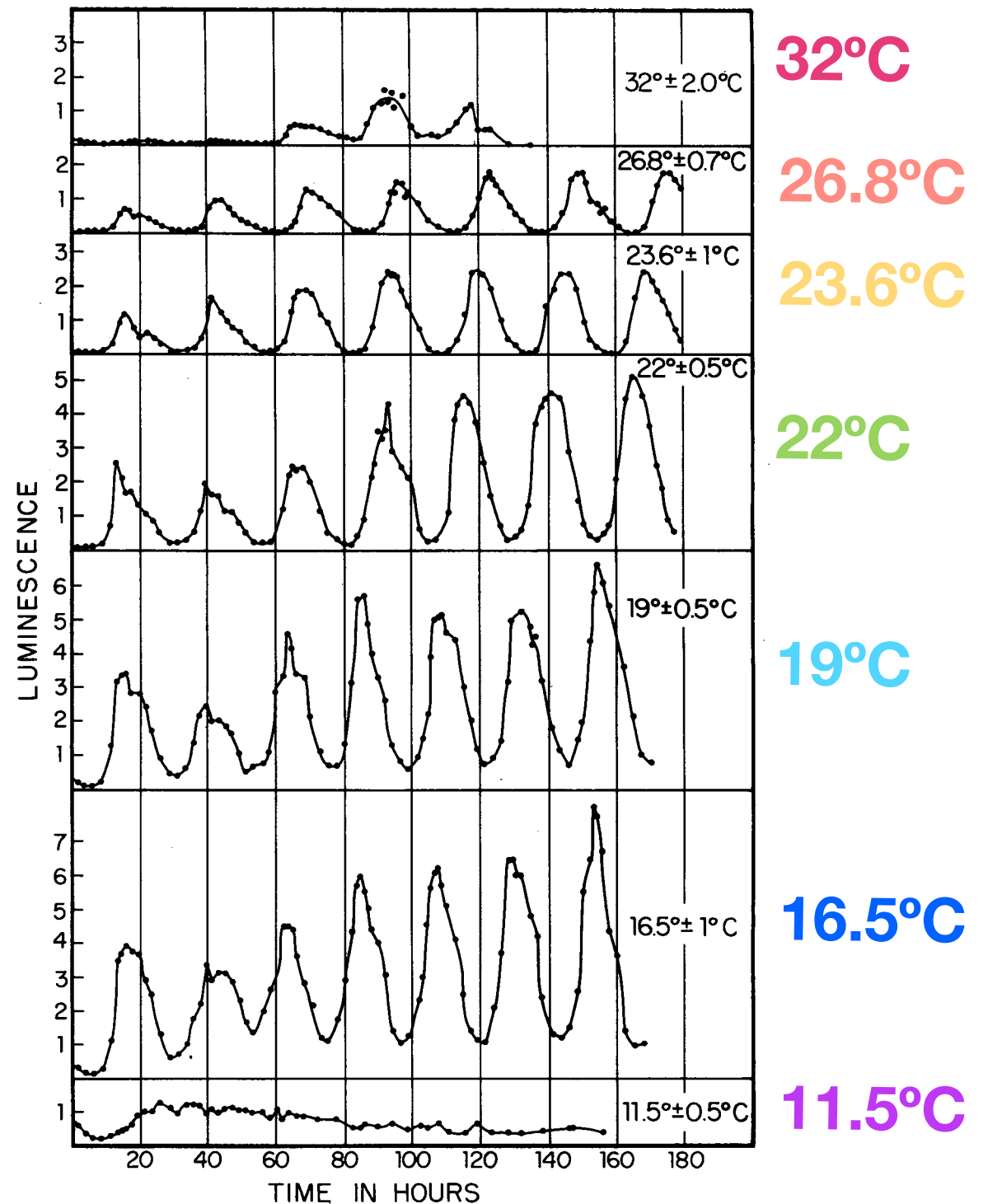
Dinoflagellates

(*Gonyaulax*)

Hastings & Sweeney

PNAS (1957)

- \* Period of the rhythm is not significantly changed when the ambient temperature is lowered.
- \* The rhythm is nullified when the ambient temperature is lowered more.



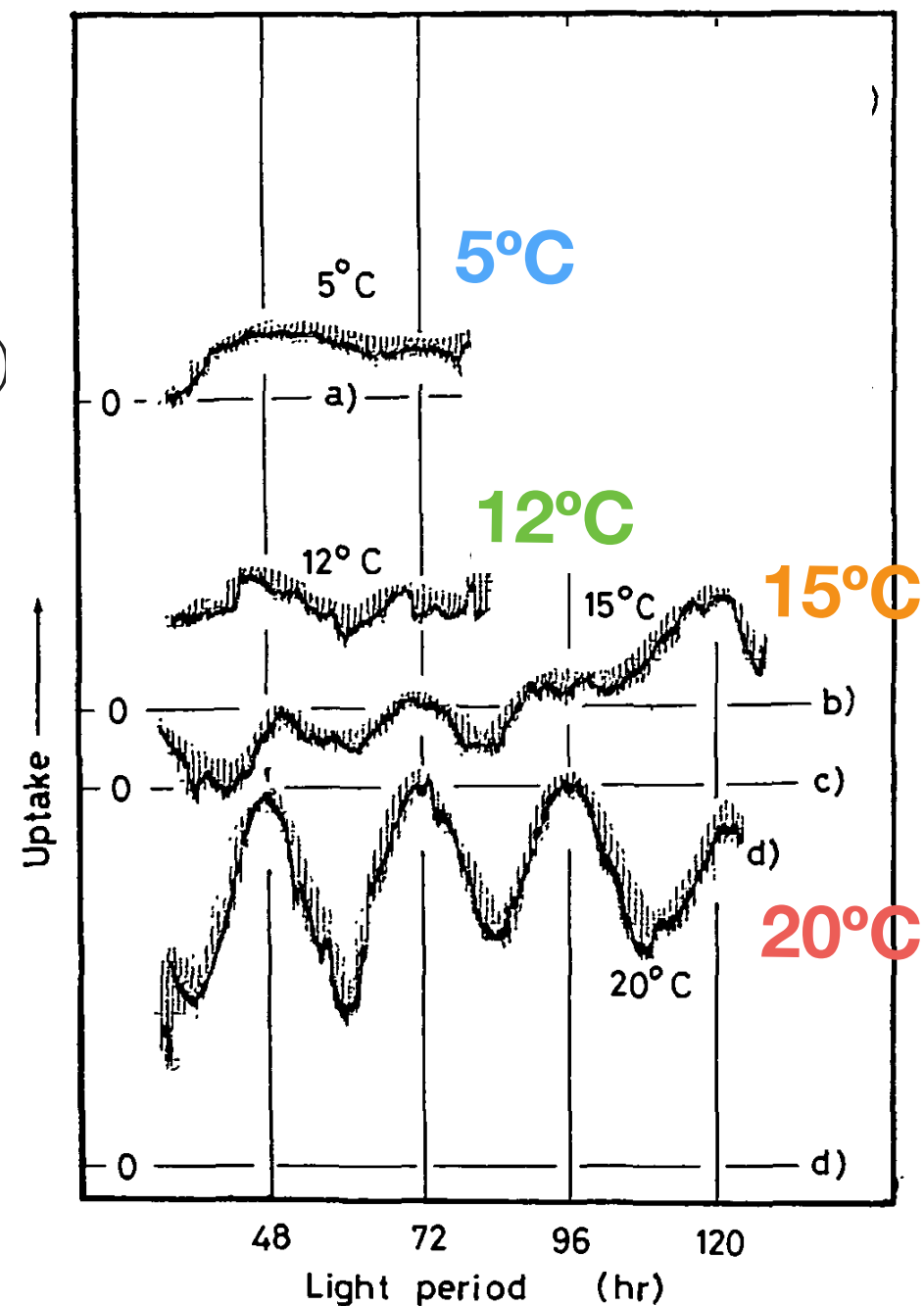
# Low temperature abolishes circadian rhythms



## Duckweed (*Lemna Gippa*)

Kondo & Tsudzuki  
Plant Cell Physiol. (1980)

- \* Period of the rhythm is not significantly changed when the ambient temperature is lowered.
- \* The rhythm is nullified when the ambient temperature is lowered more.



# Bifurcation theory: scenarios for arrhythmicity

Stuart-Landau oscillator

$$\dot{z} = (\mu + ia + |z|^2)z + ie$$

**Hopf  
Bifurcation**

Damping  
oscillations

Amplitude down, Period constant

**Saddle-node  
Bifurcation**

Amplitude constant, Period up



# Bifurcation theory: scenarios for arrhythmicity

Stuart-Landau oscillator

$$\dot{z} = (\mu + ia + |z|^2)z + ie$$

**Hopf  
Bifurcation**

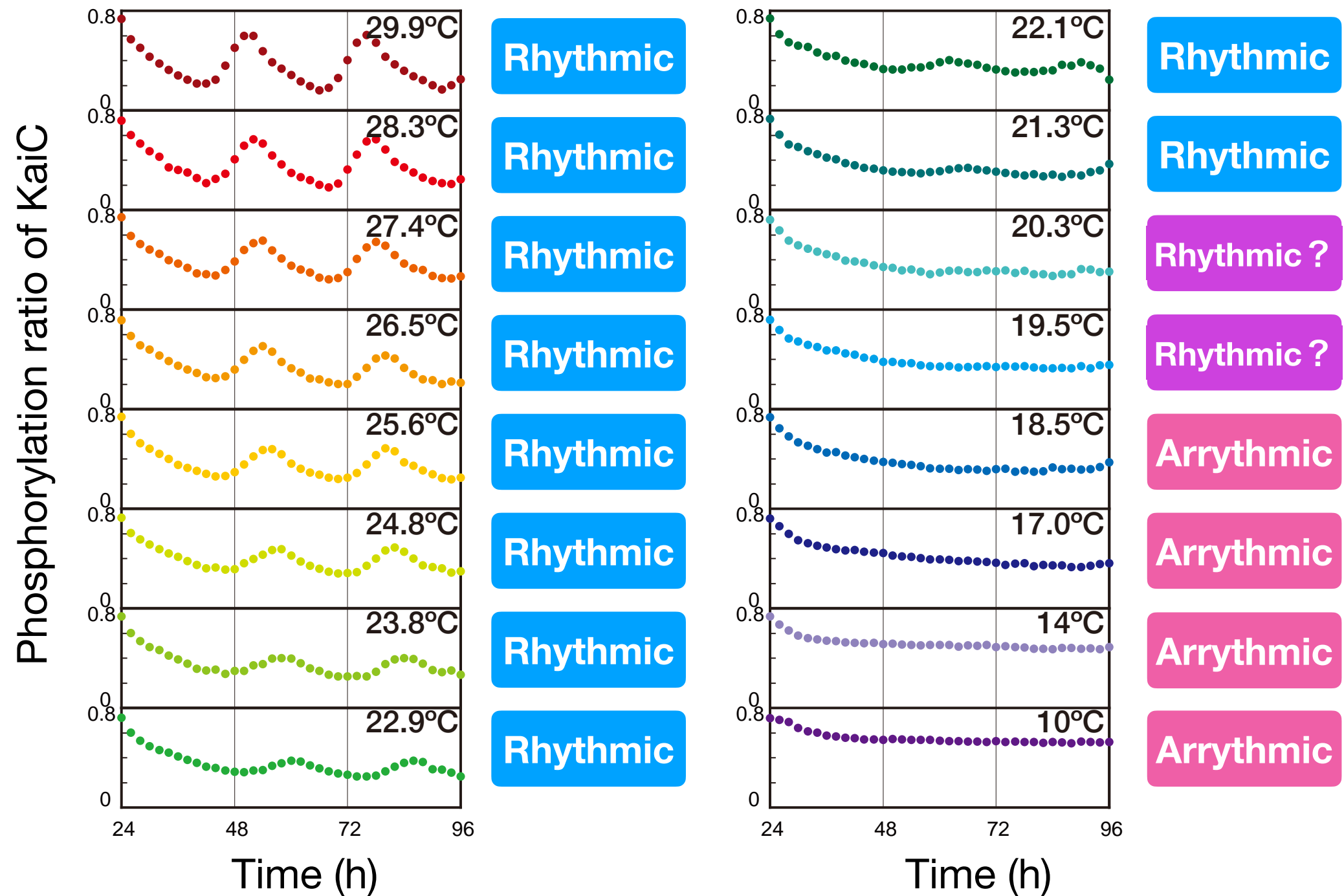
**Damping  
oscillations**

Amplitude down. Period constant.

**Saddle-node  
Bifurcation**

Amplitude constant. Period up.

# In vitro clock stops under low temperature



Murayama et al. PNAS 2017

# Change of amplitude $\rightarrow$ Hopf bifurcation

Stuart-Landau oscillator  $\dot{z} = (\mu + ia + |z|^2)z + ie$

**Hopf  
Bifurcation**



Amplitude down, Period constant

Damped  
oscillations

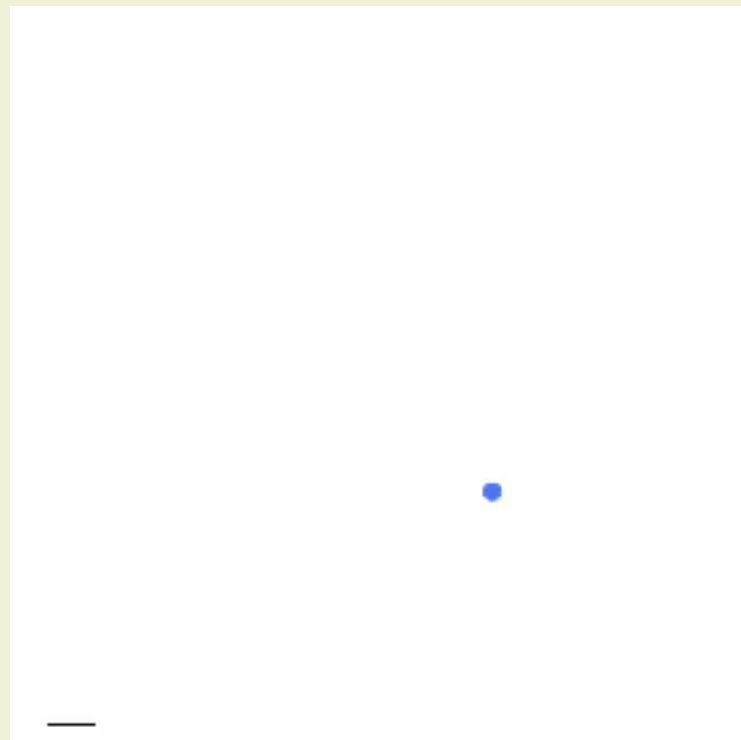
**Saddle-node  
Bifurcation**

Amplitude constant, Period up

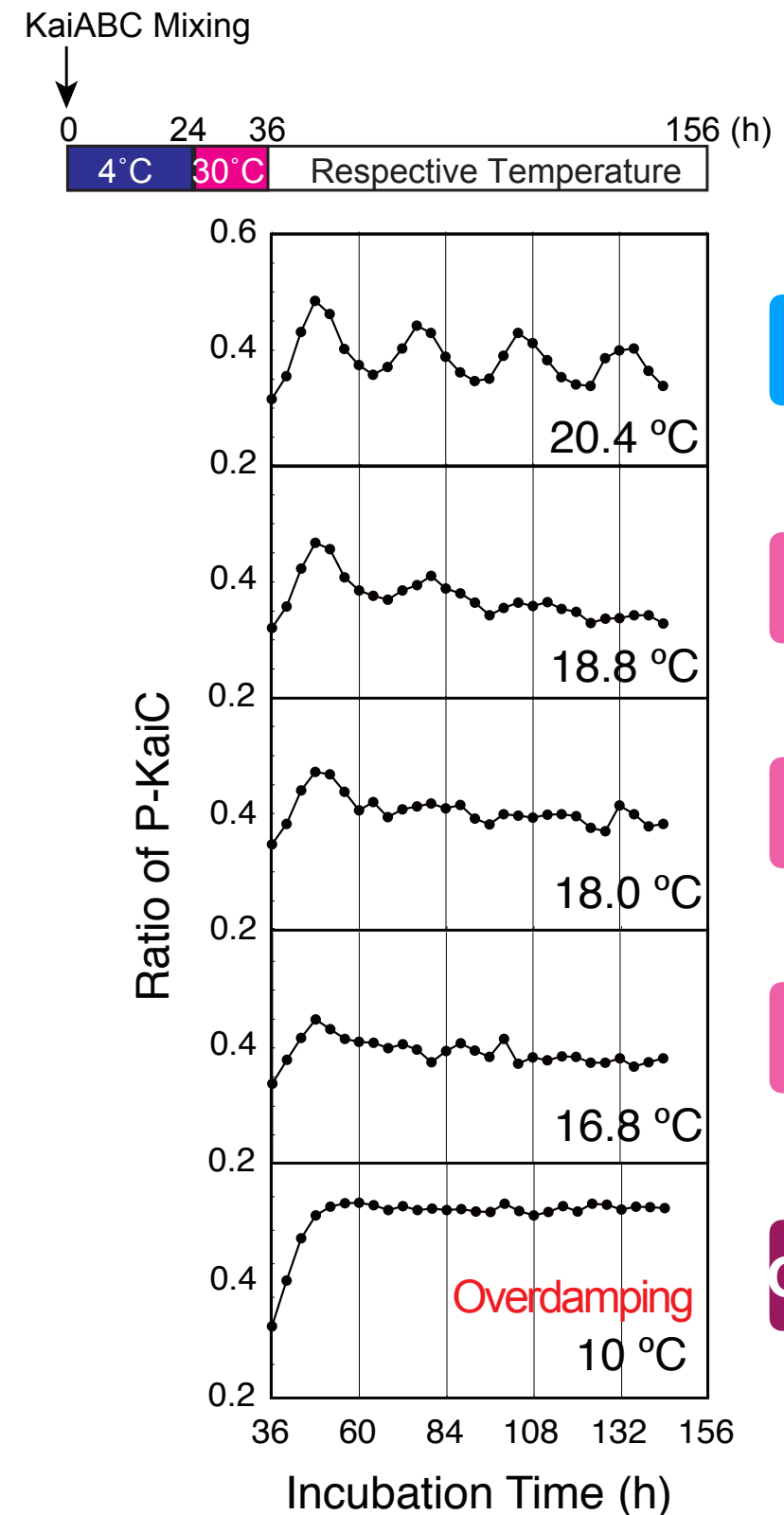
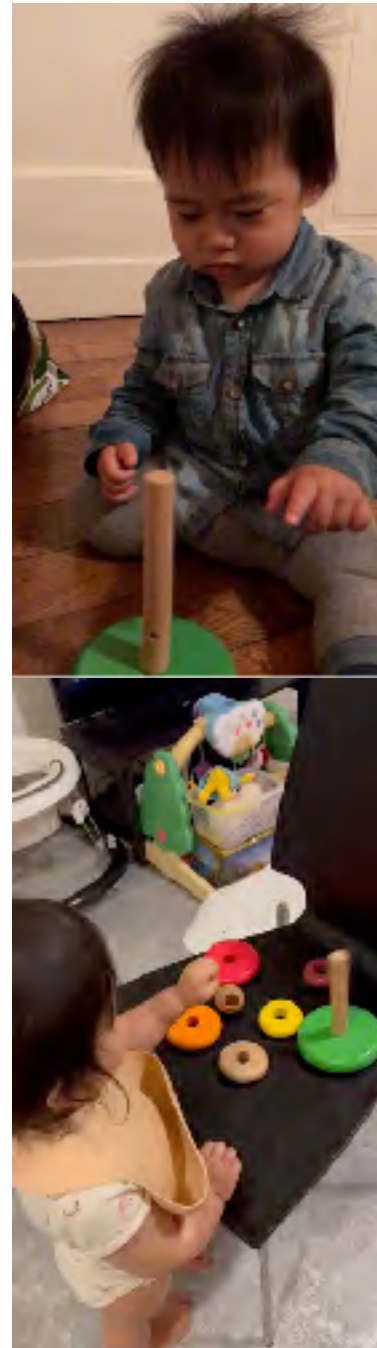
Excited  
system

**FAQ by biologists: So what?**

# Self sustained $\rightarrow$ damped oscillations via Hopf

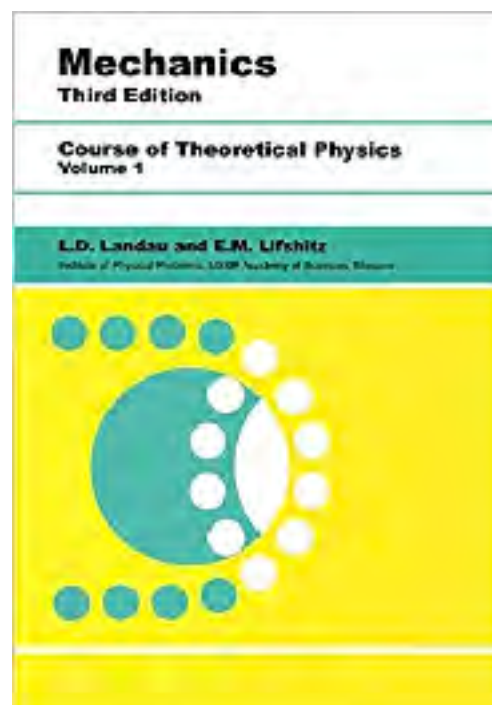


Stuart-Landau oscillator  
at below critical point

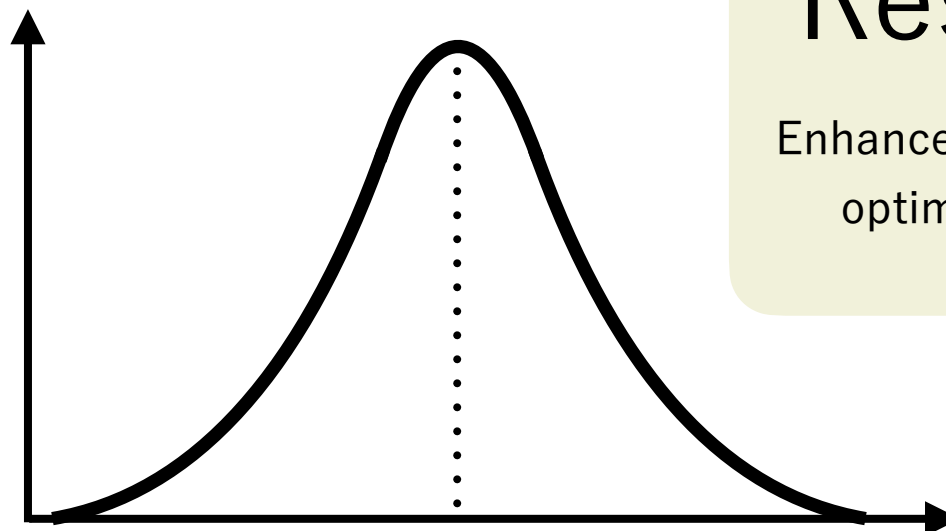




# Self sustained $\rightarrow$ damped oscillations via Hopf



Amplitude



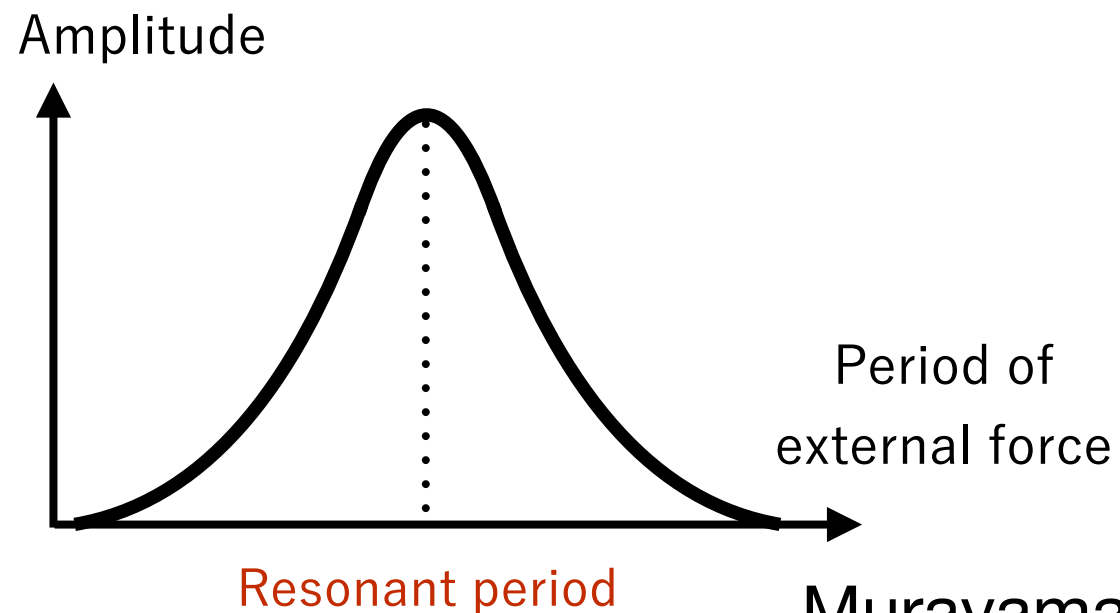
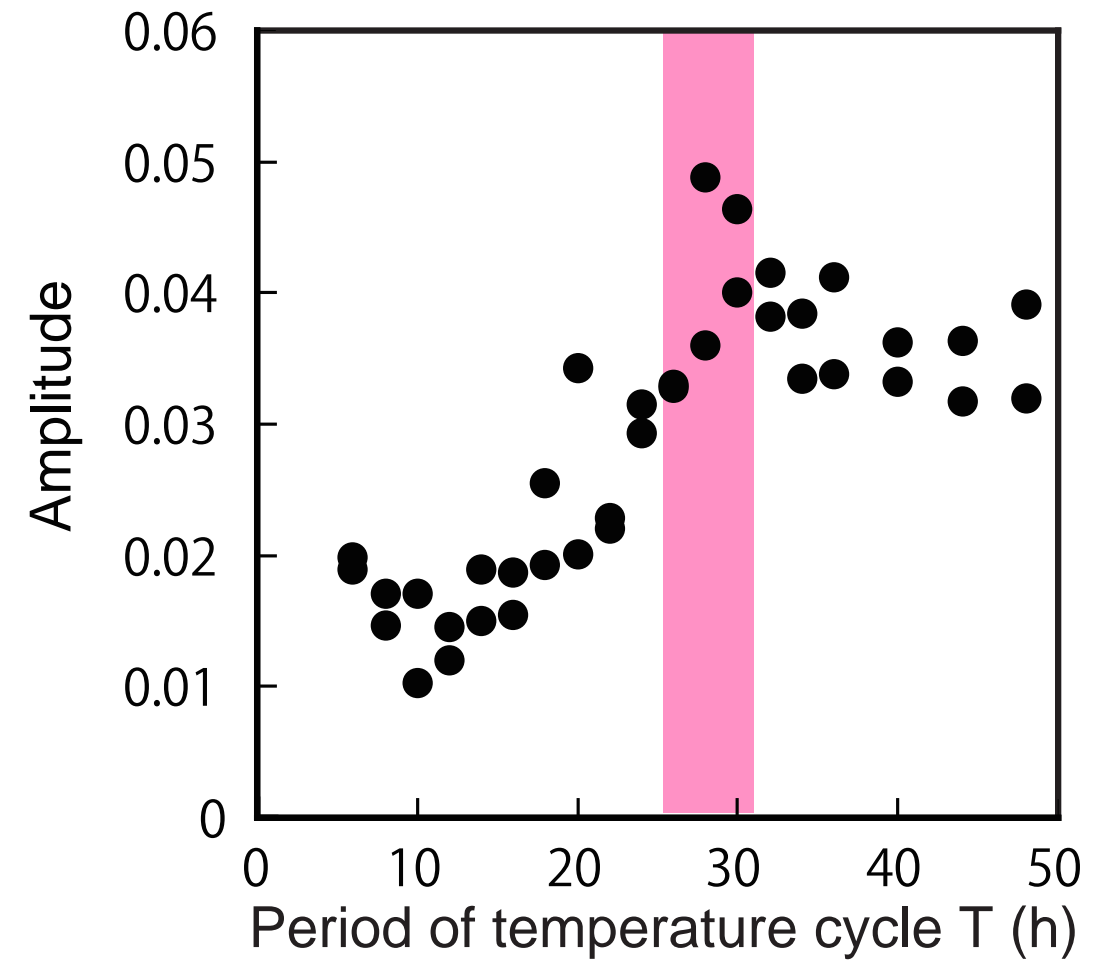
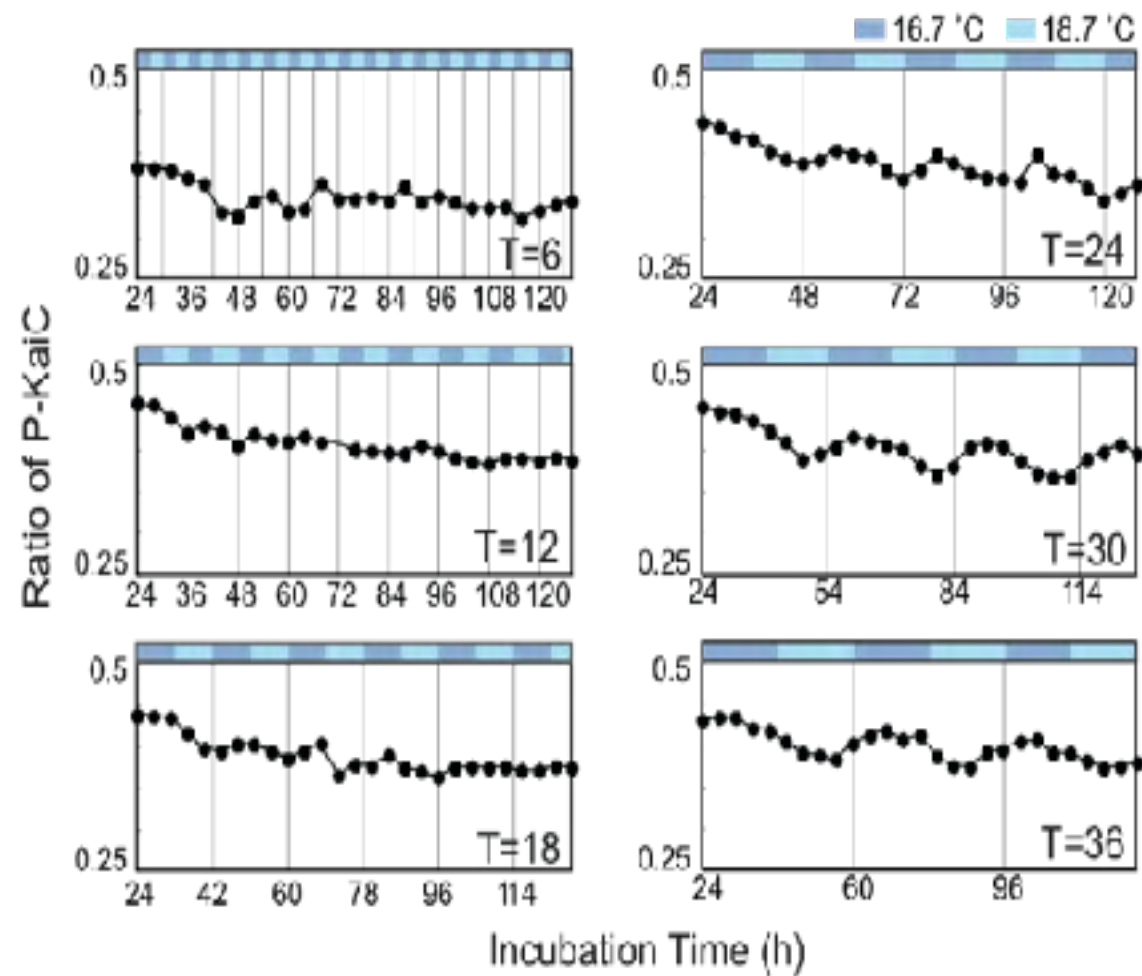
Resonating period

## Resonance

Enhancement of amplitude by optimal periodical force

Period of  
External force

# Resonance of in vitro clocks



Murayama et al. PNAS 2017



# Hopf bifurcation in plants

Arabidopsis



CCA1:Luc

8 °C

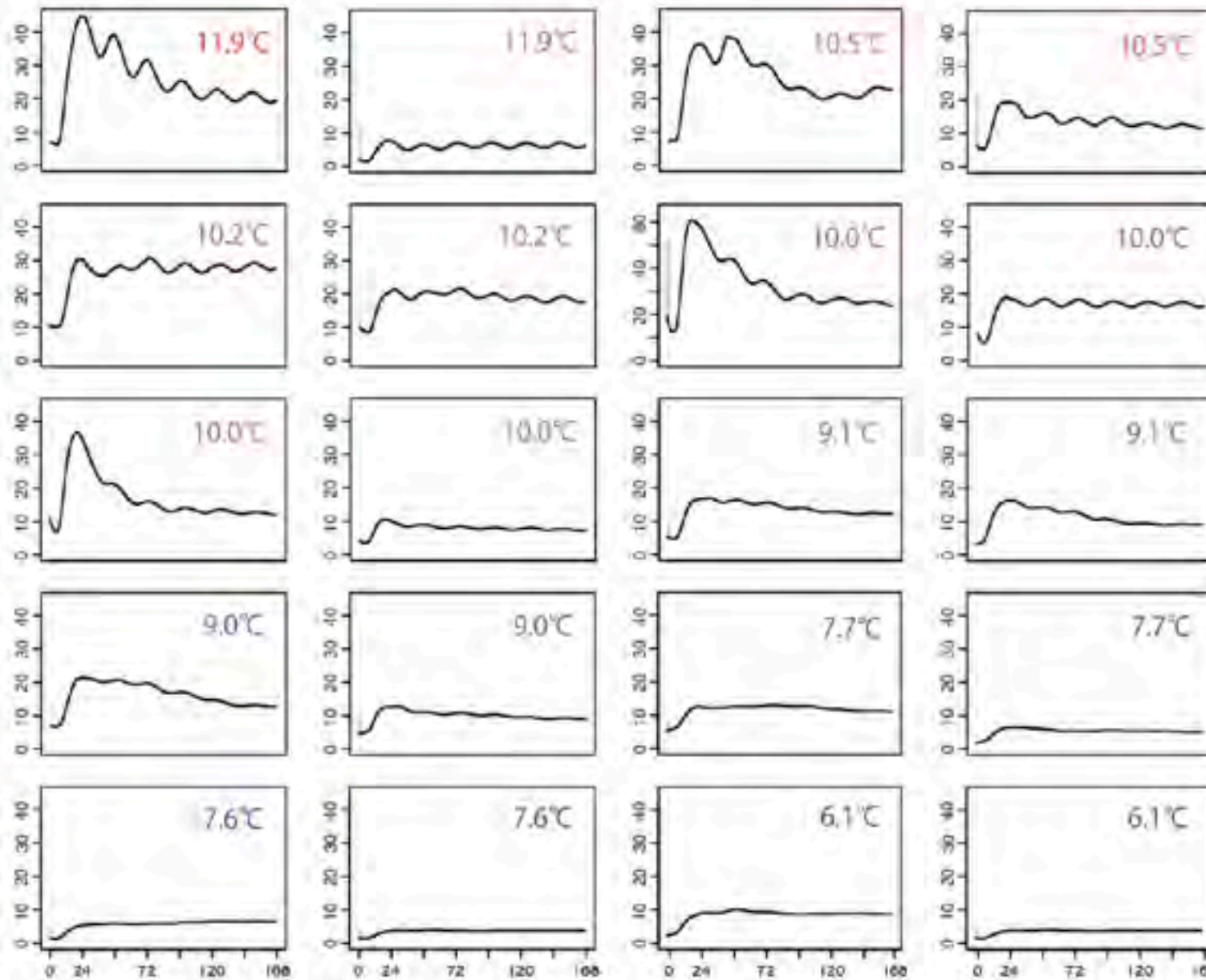
Critical temperature

High

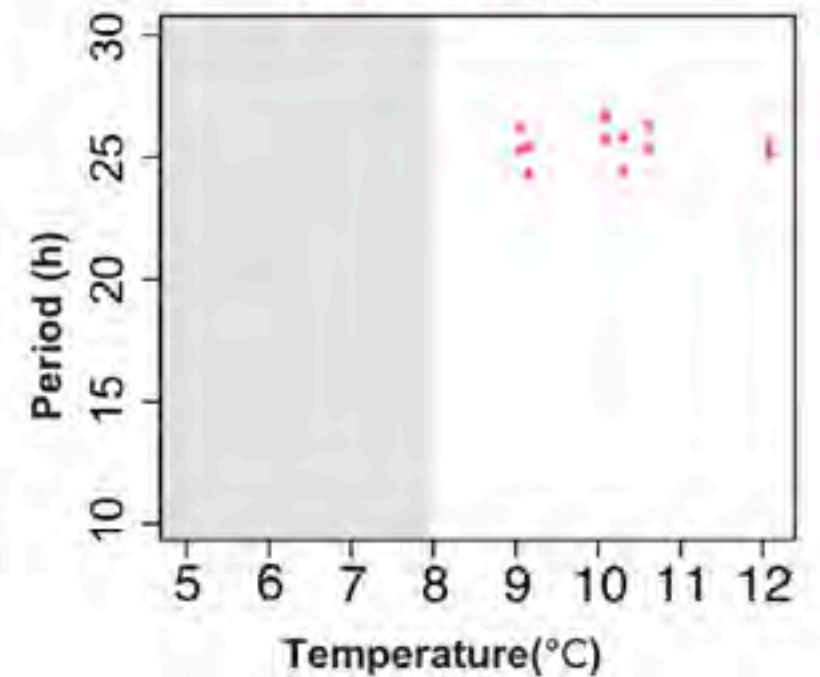
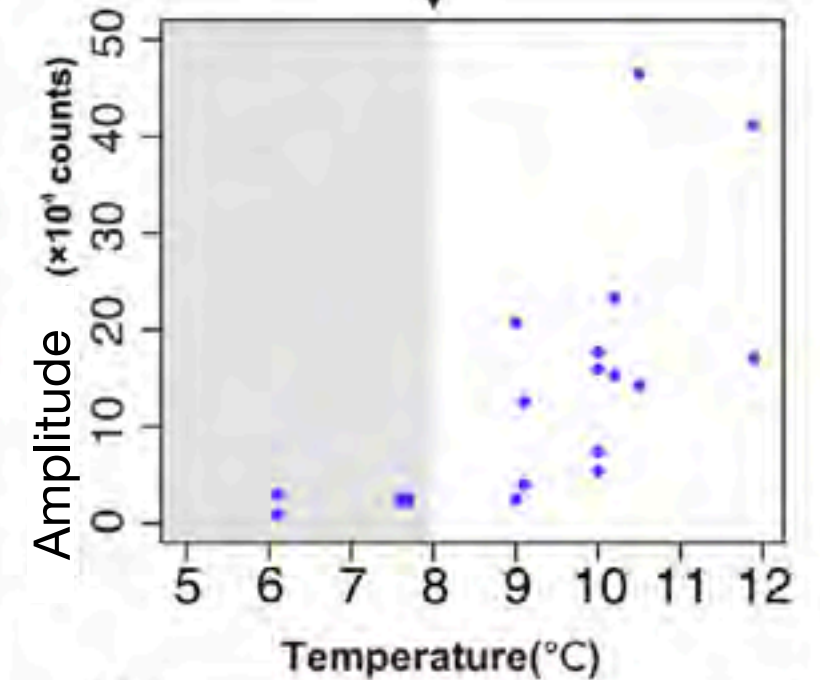


Low

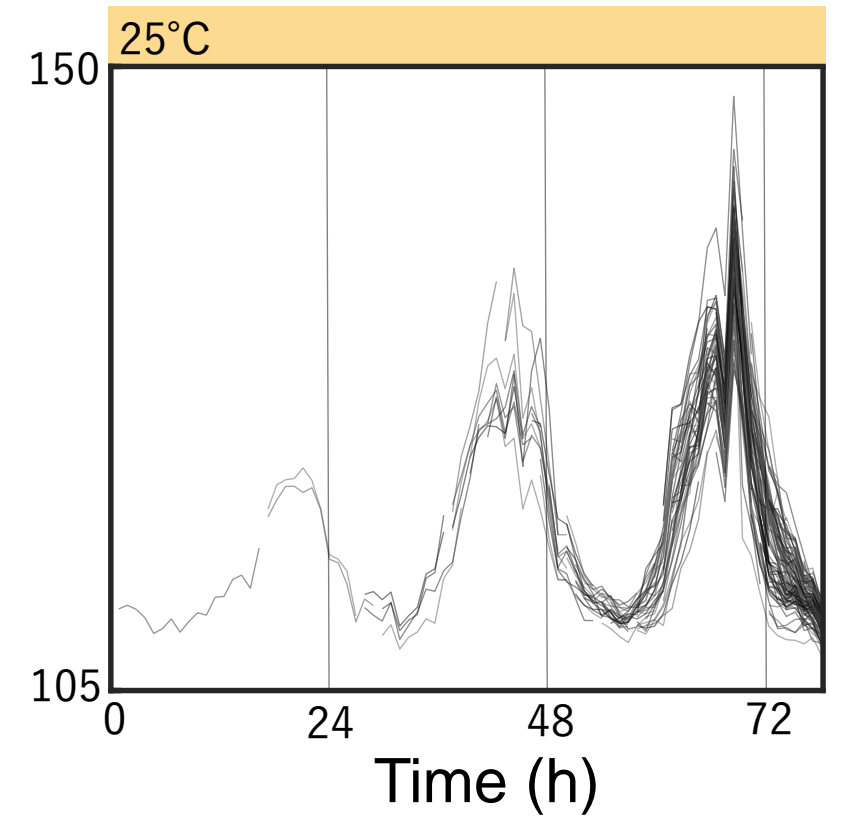
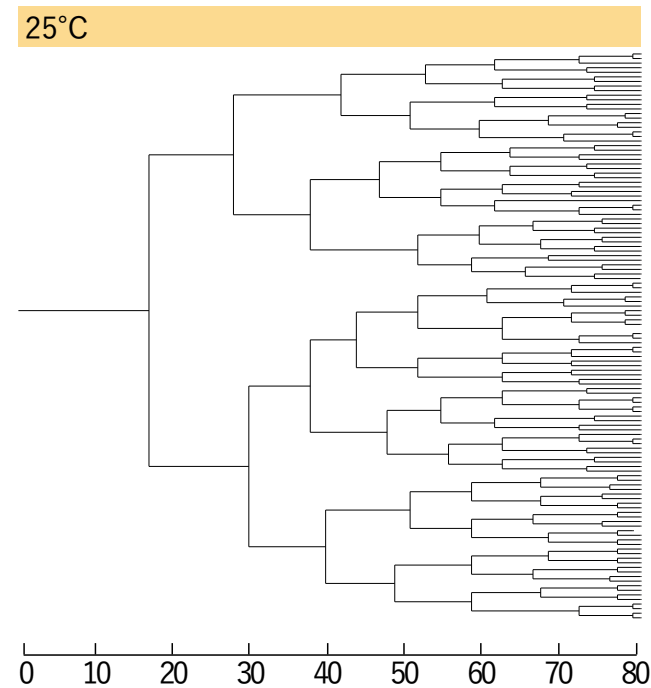
Bioluminescence ( $\times 10^5$  counts)



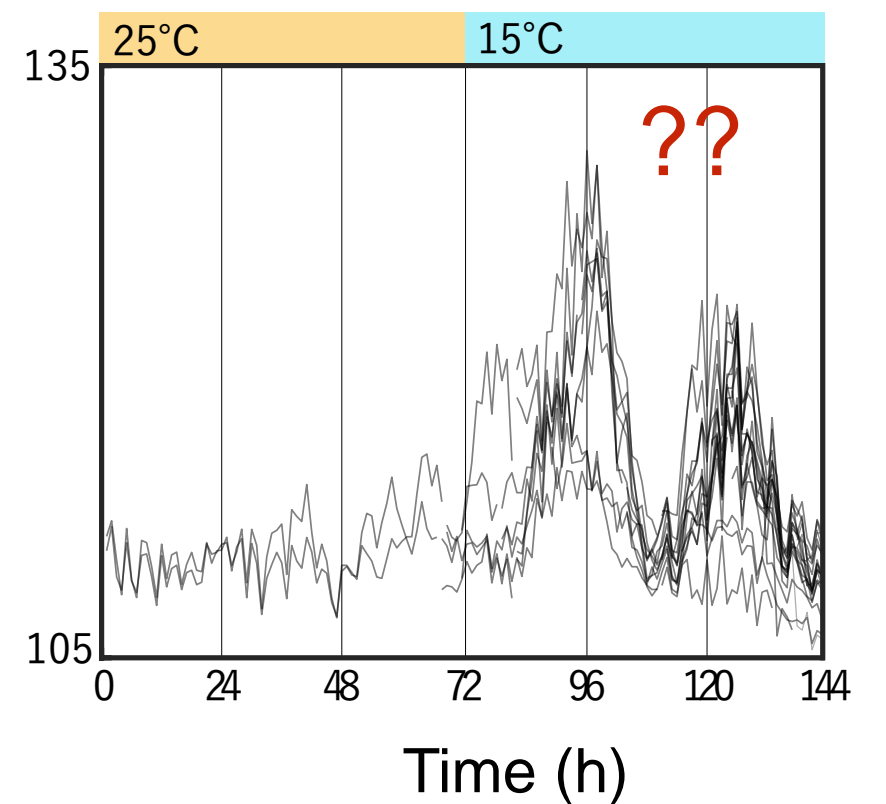
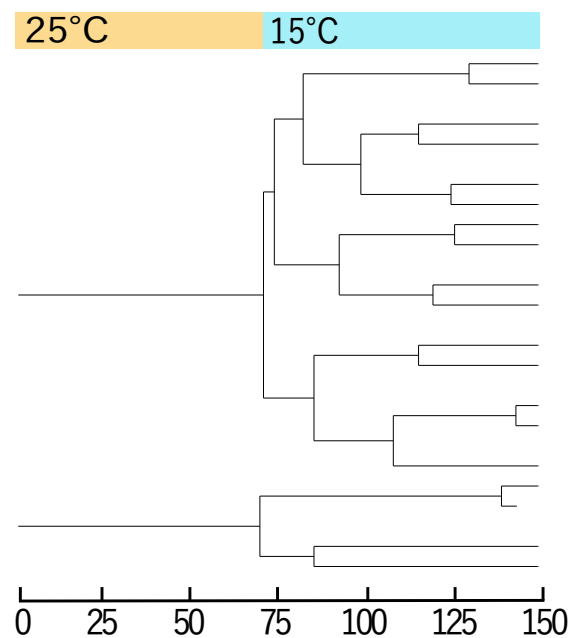
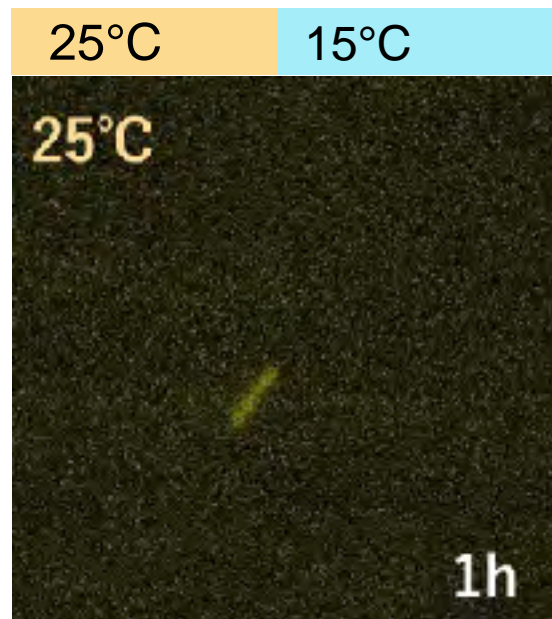
Hours in DD



# On going: critical temperature mutant?



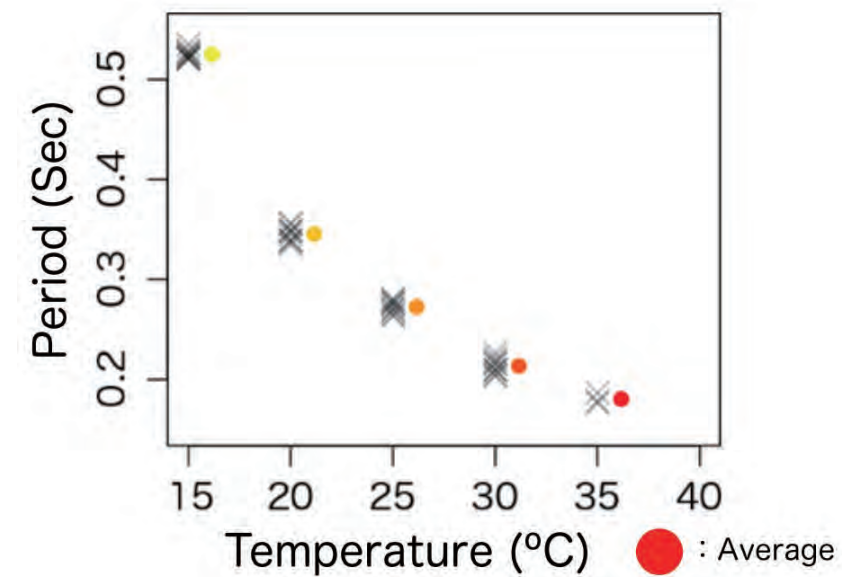
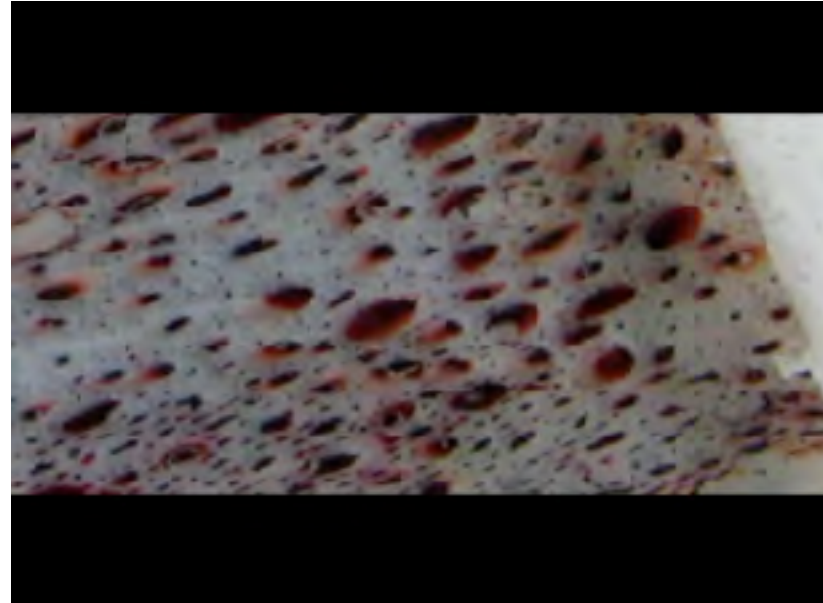
♀ **Acclimation?**





# Digression: cold response to other rhythms

## Squid pigment cells



## BZ reaction

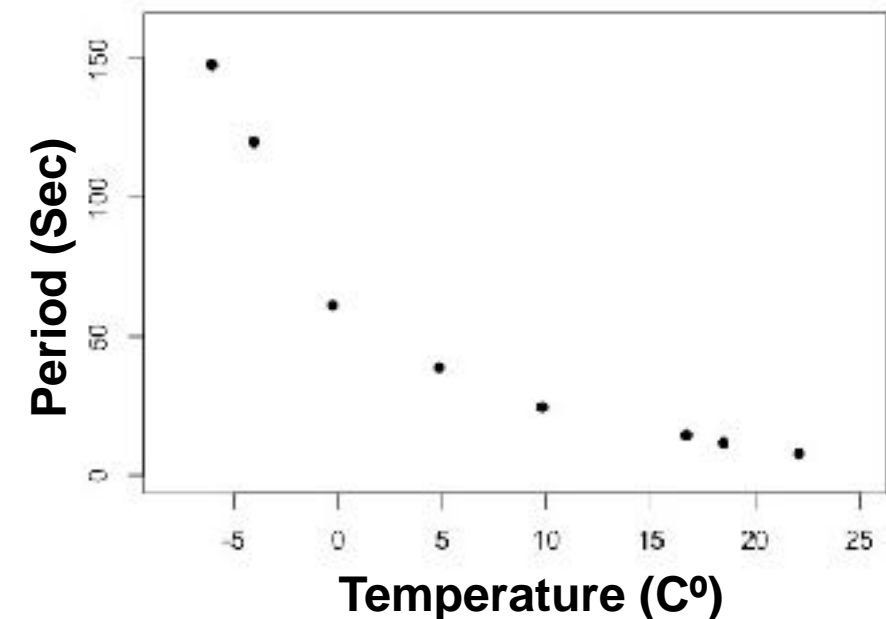
-10°C

-5°C

0°C

5°C

10°C



Period extension → ~~x~~Hopf Saddle-node bifurcation



# Pulsatile swimming of Cannonball Jellyfish

Kamo aquarium

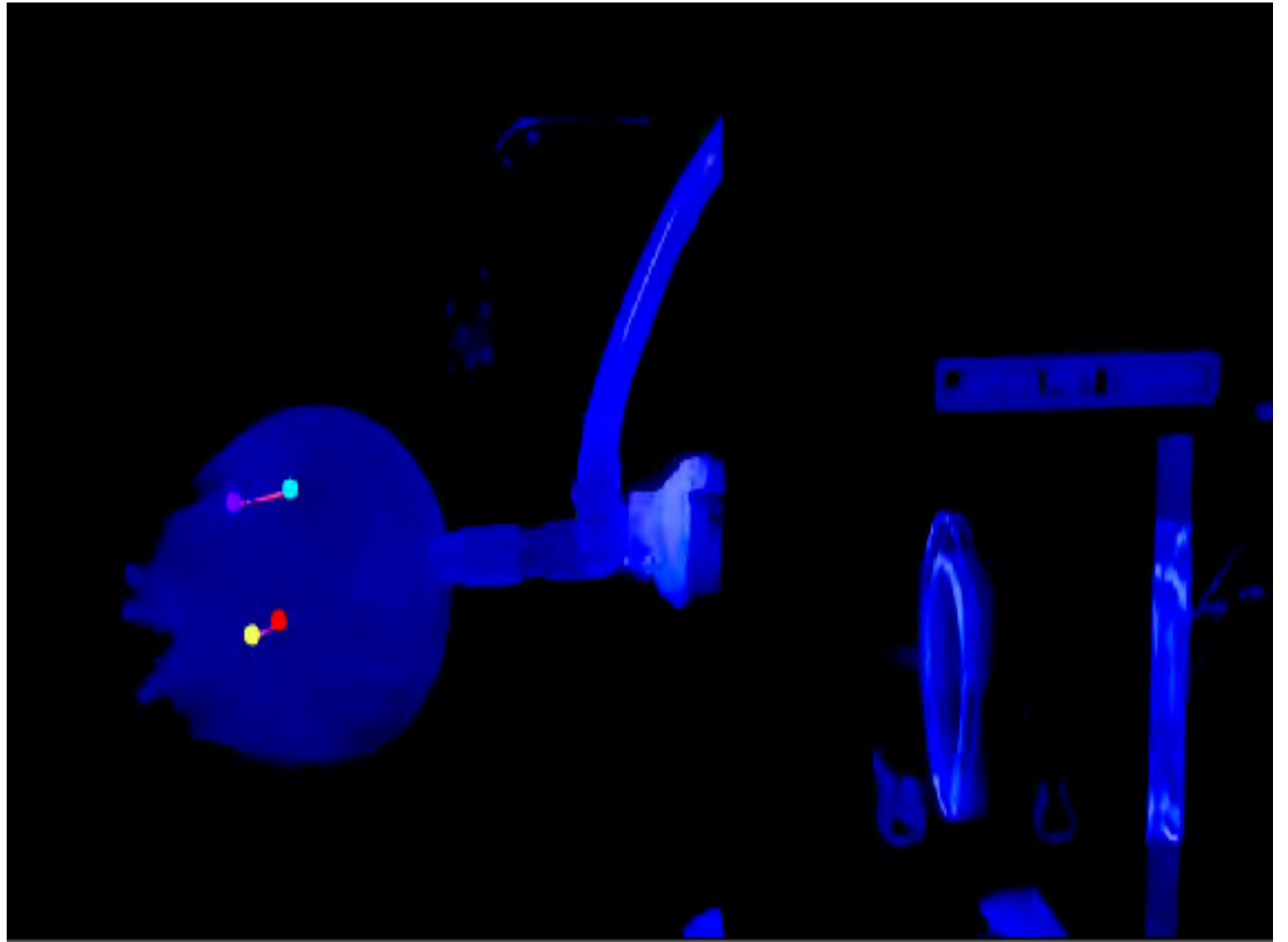


# Pulsatile swimming of Cannonball Jellyfish

Injection of dye

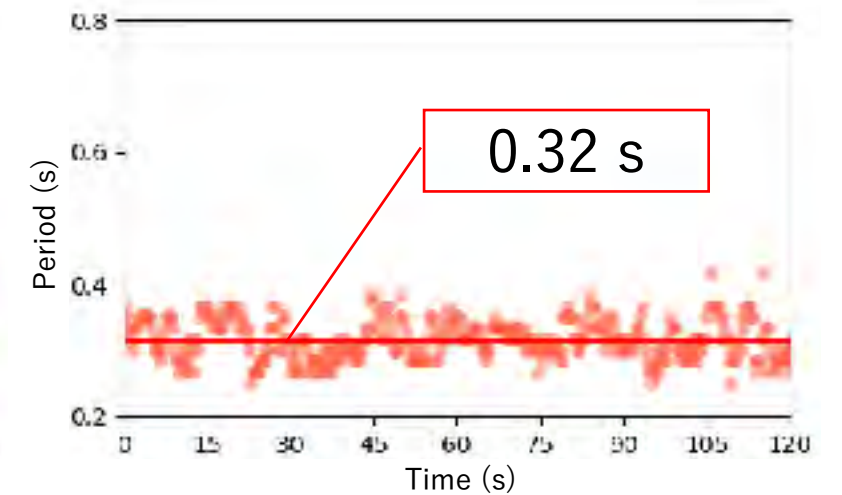
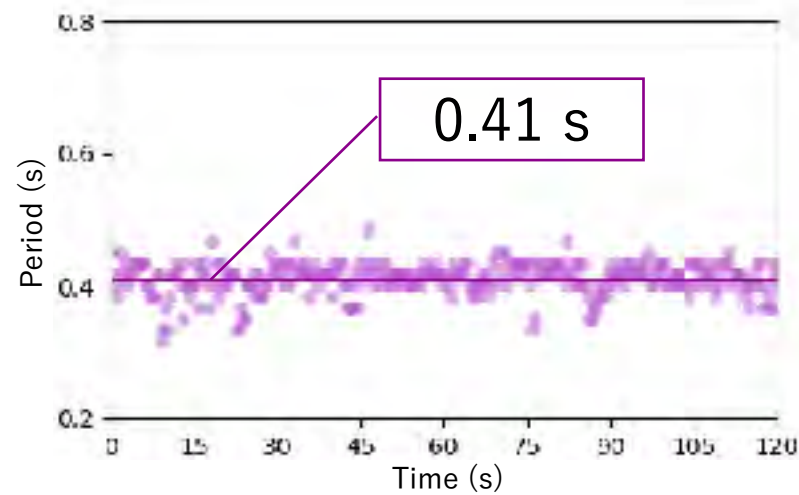
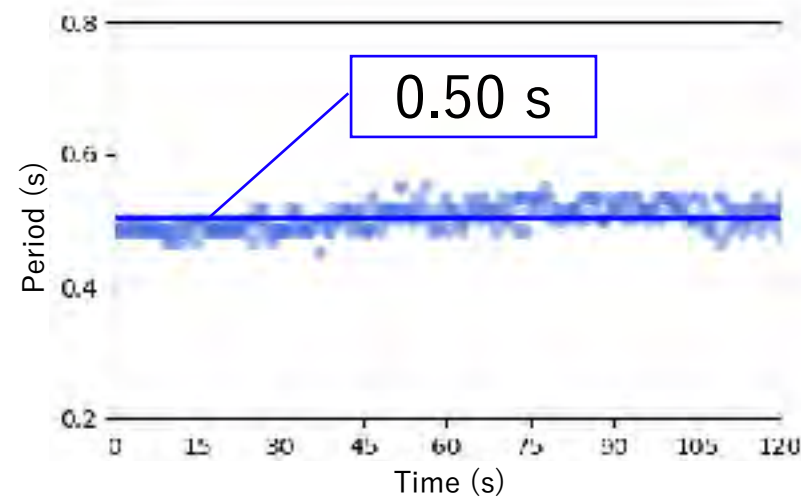
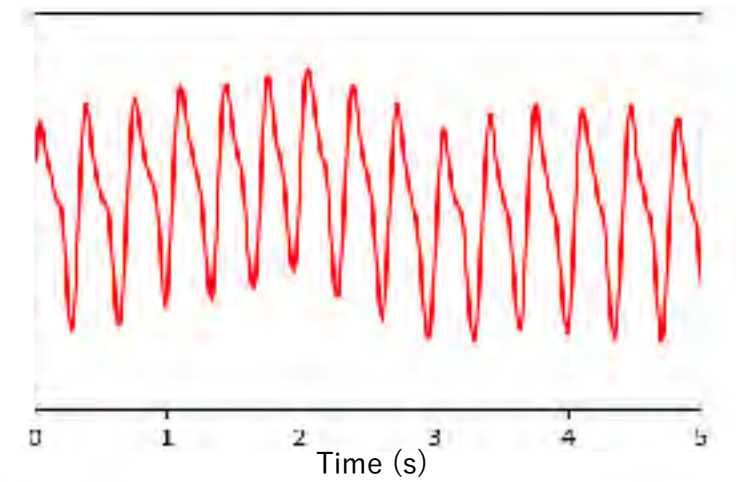
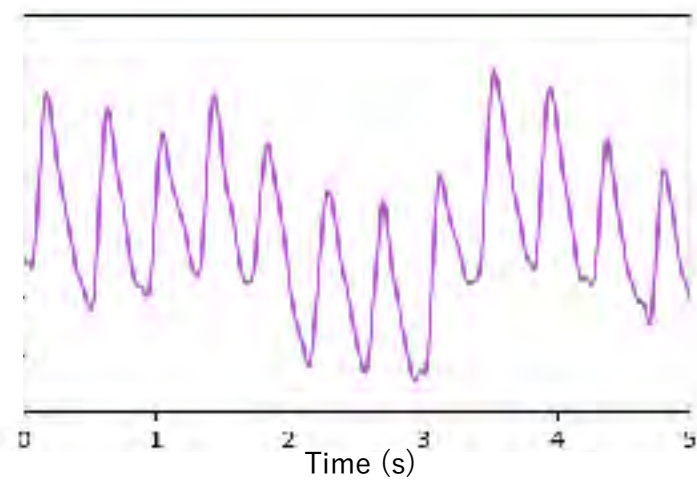
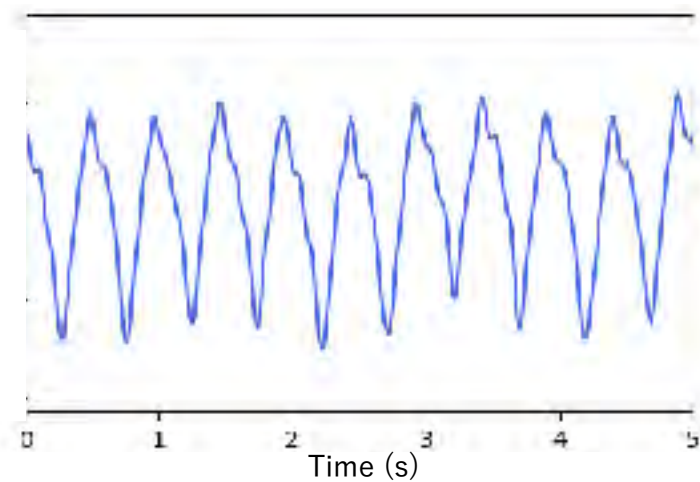
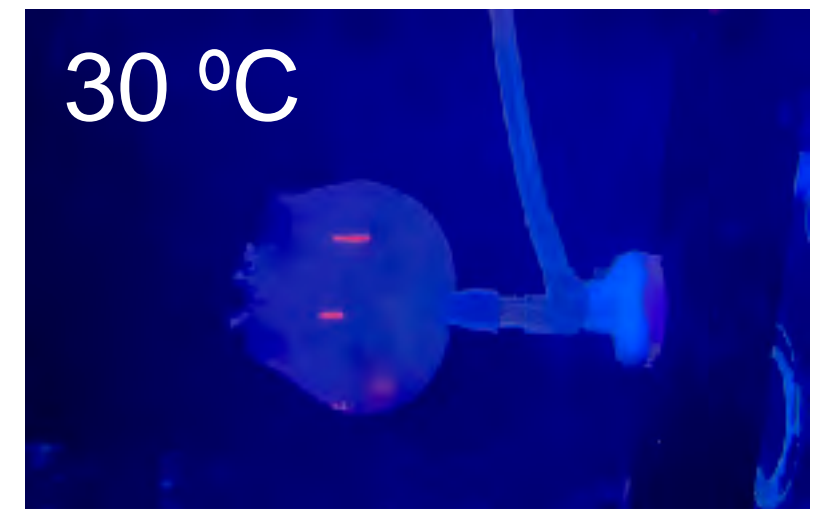
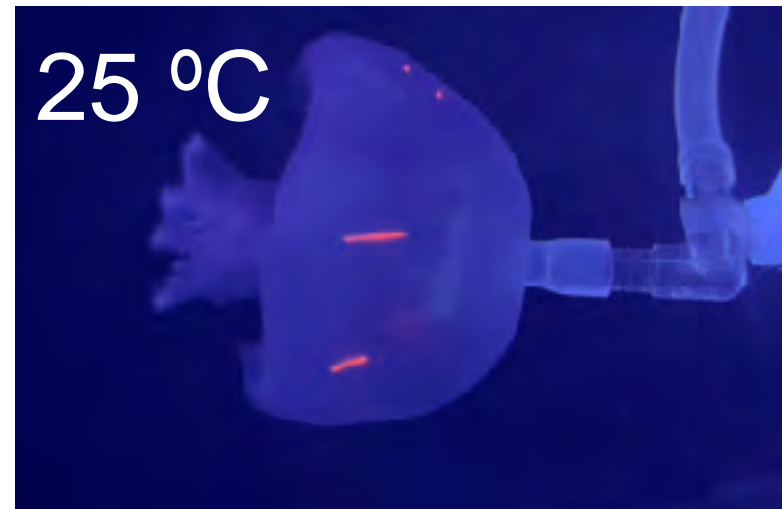
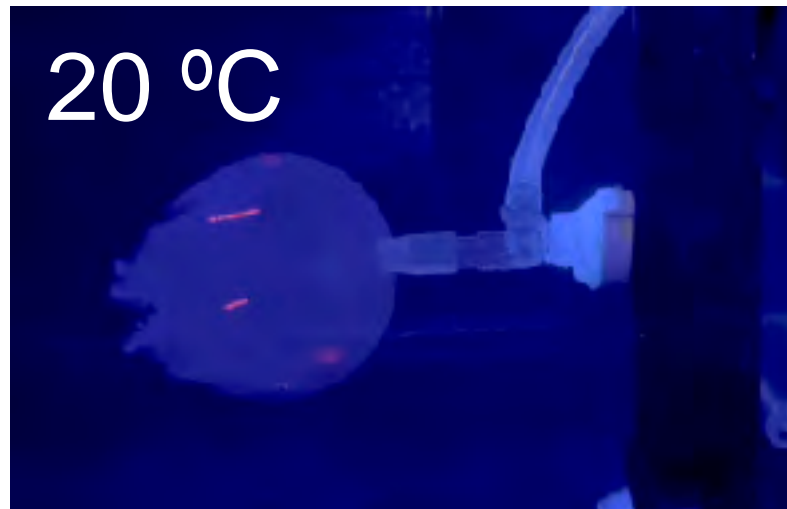


Tracking a swimming rhythm



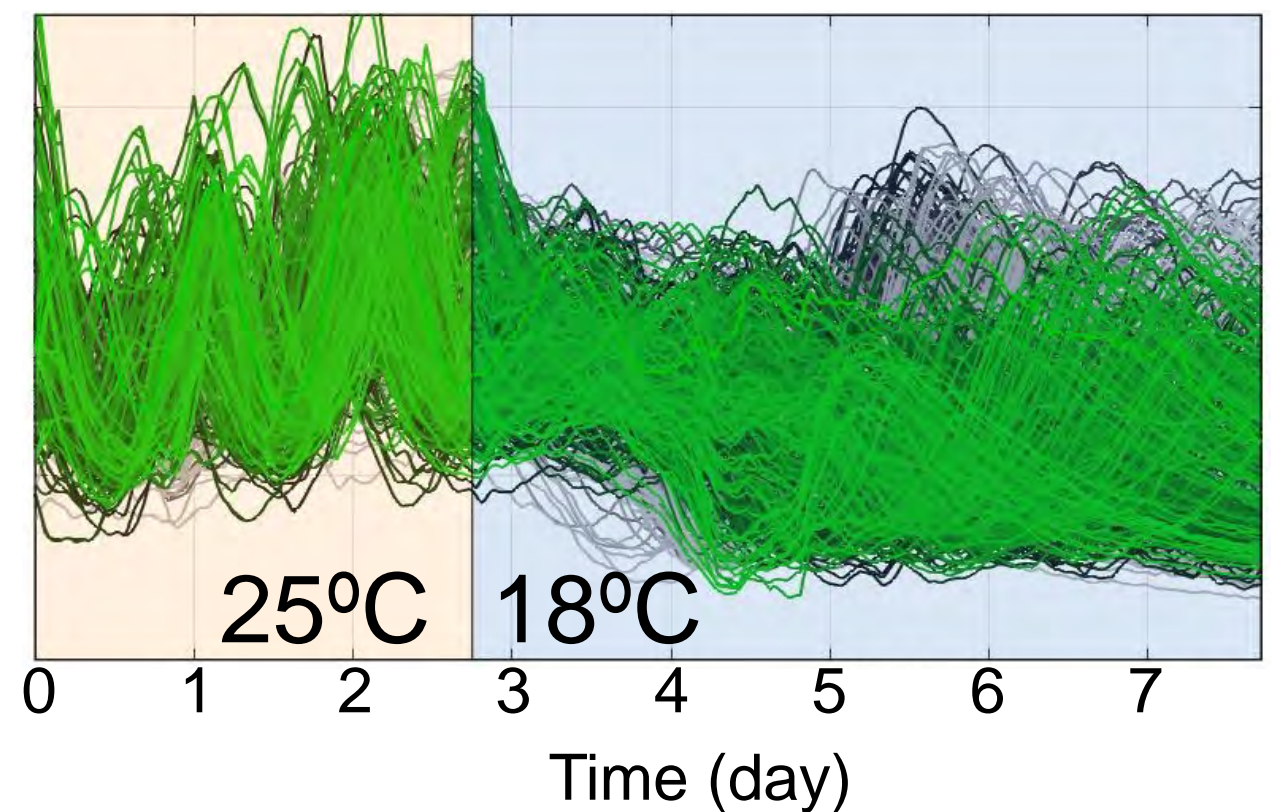
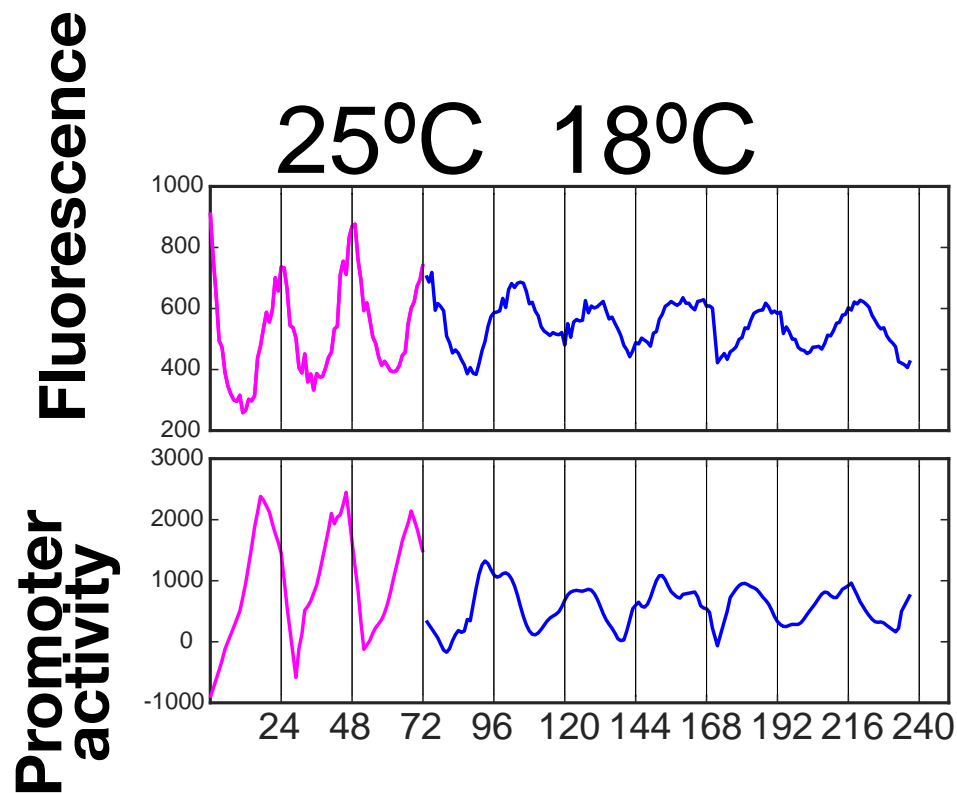
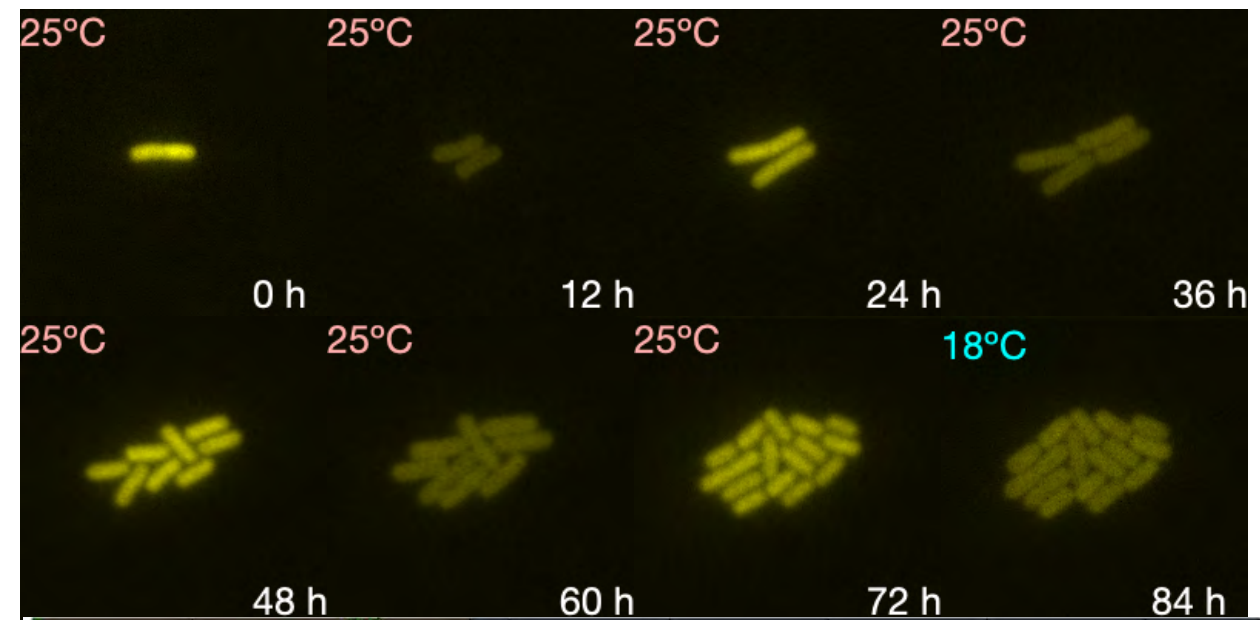
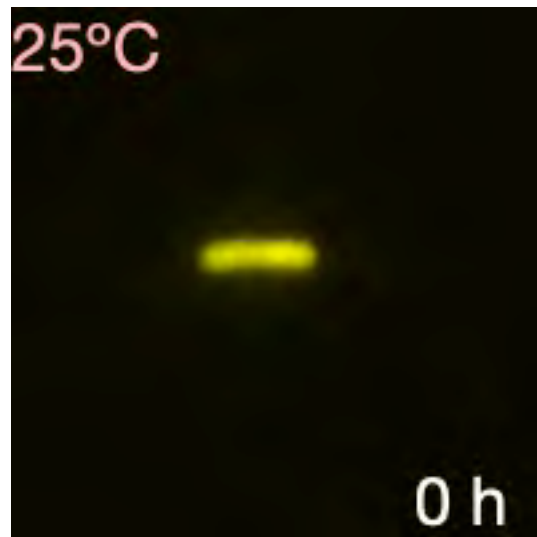


# Pulsatile swimming of Cannonball Jellyfish





# Fluctuation in cyanobacteria circadian rhythm



# Fluctuation in human circadian rhythm

**Circadian Rhythms in Man: A self-sustained oscillator with an inherent frequency underlies human 24-hour periodicity**

Jürgen Aschoff

*Science* **148**, 1427-32 1965

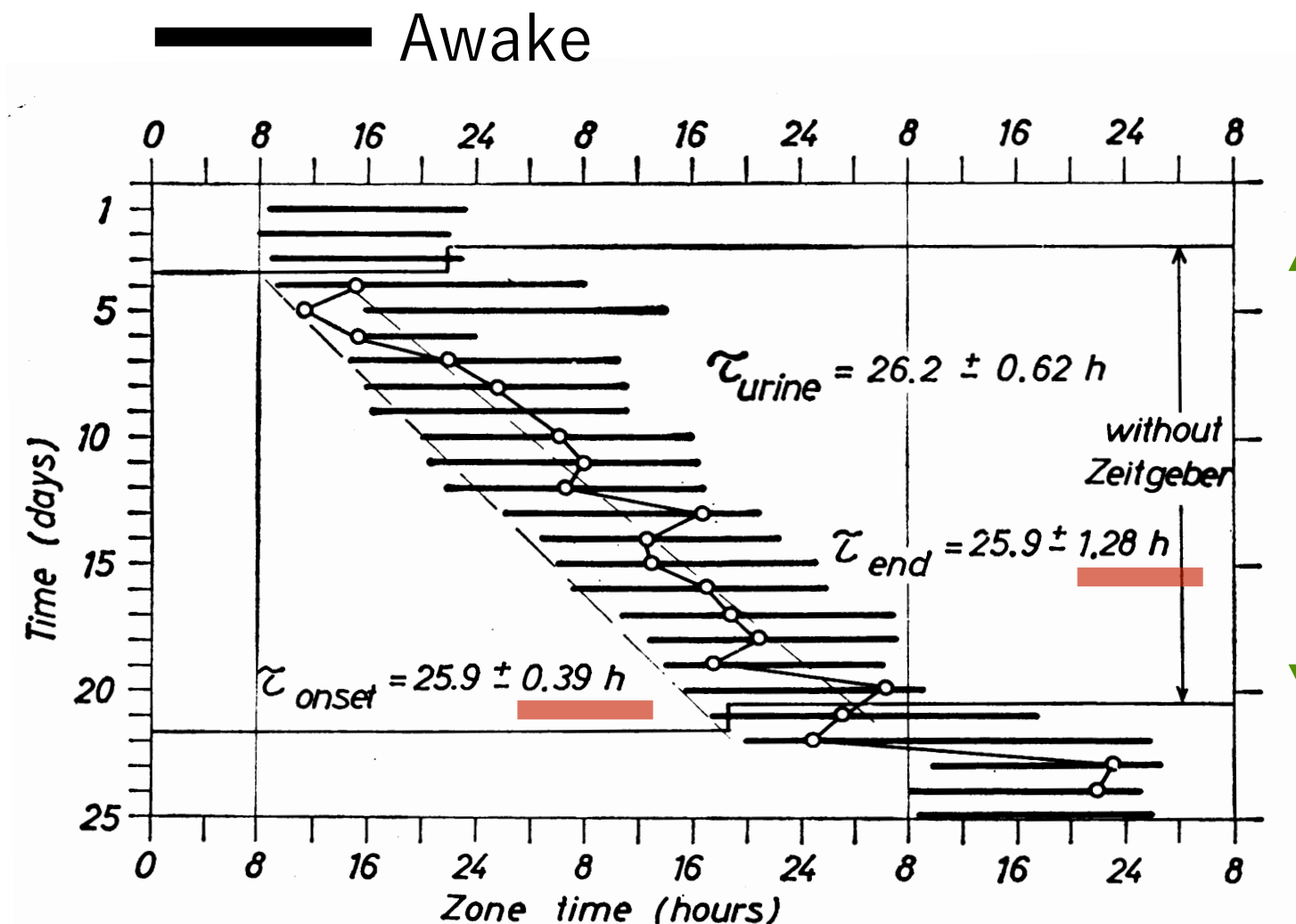
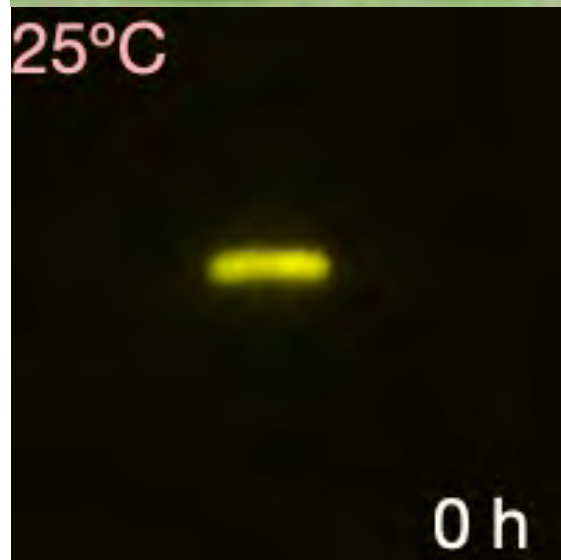
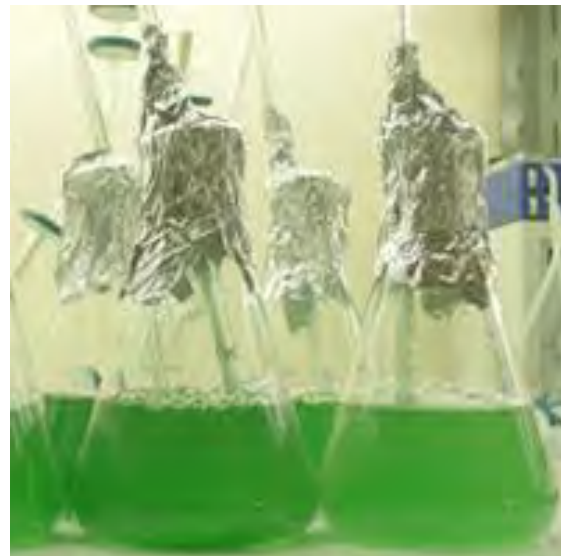


Fig. 4. Circadian rhythm of activity and urine excretion in a human subject kept for 3 days under normal conditions, then for 18 days in isolation, and finally again under normal conditions. Black bars, times of being awake; circles, maxima of urine excretion;  $\tau$ , mean values of period for onset and end of activity and for urine maxima.

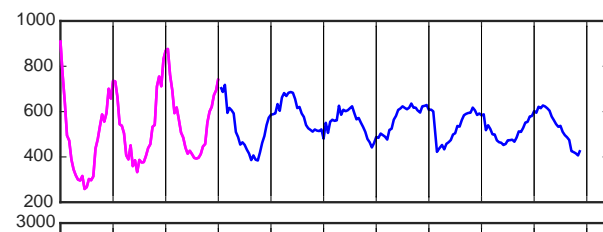
**SD in period =  
Fluctuation of clock**

# Individuality in cellular rhythms

## Cyanobacteria

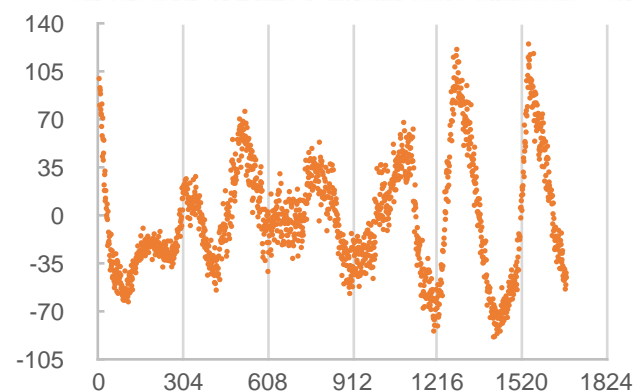


Fluorescence



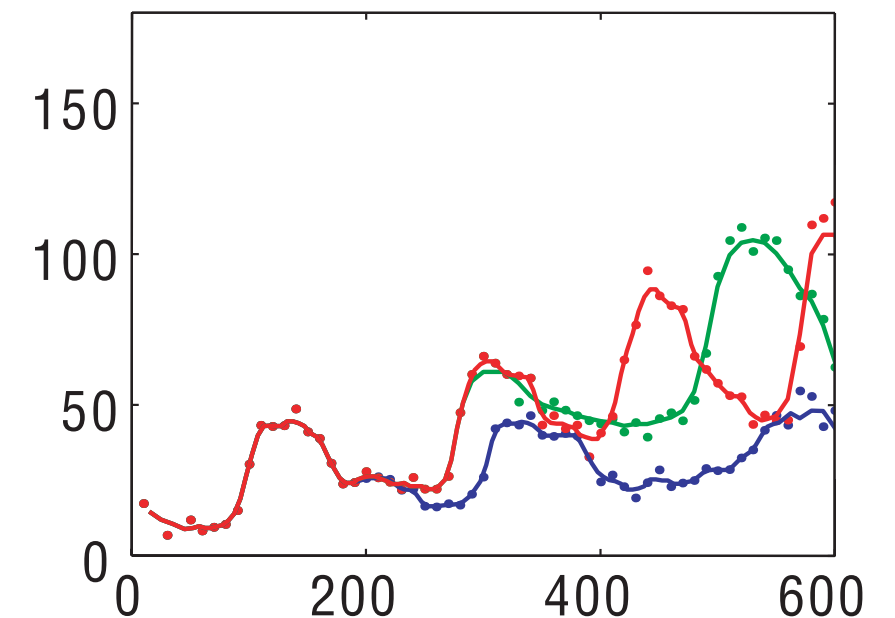
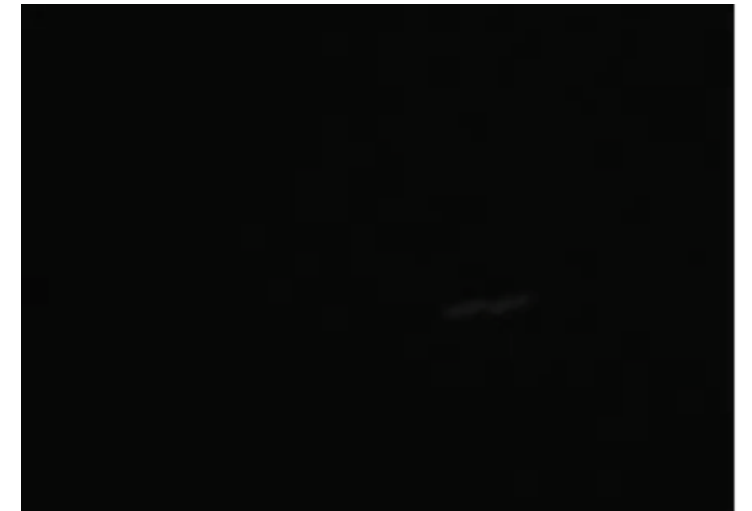
submitted

## Morning glory



unpublished

## E. coli, repressilator



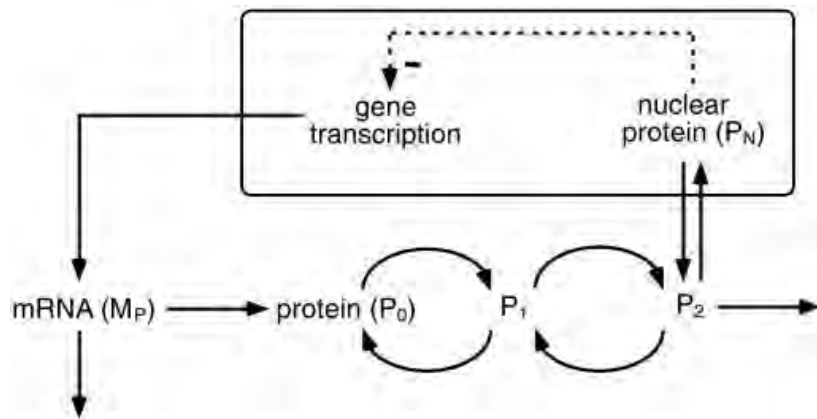
Elowitz & Leibler 2000 Nature



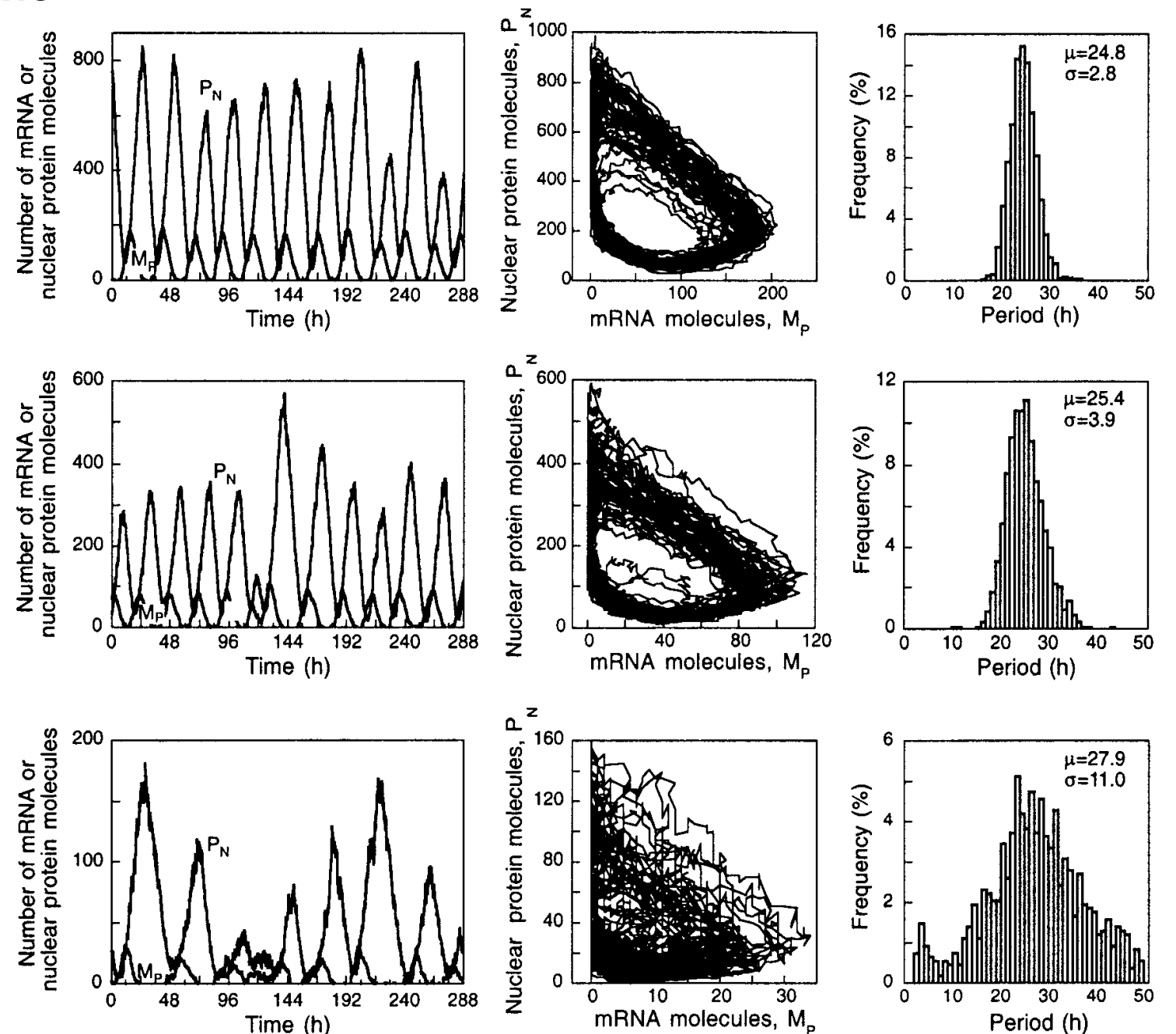
# Theoretical background: noisy circadian rhythm

Cell volume

Genetic feedback +  
stochastic expression



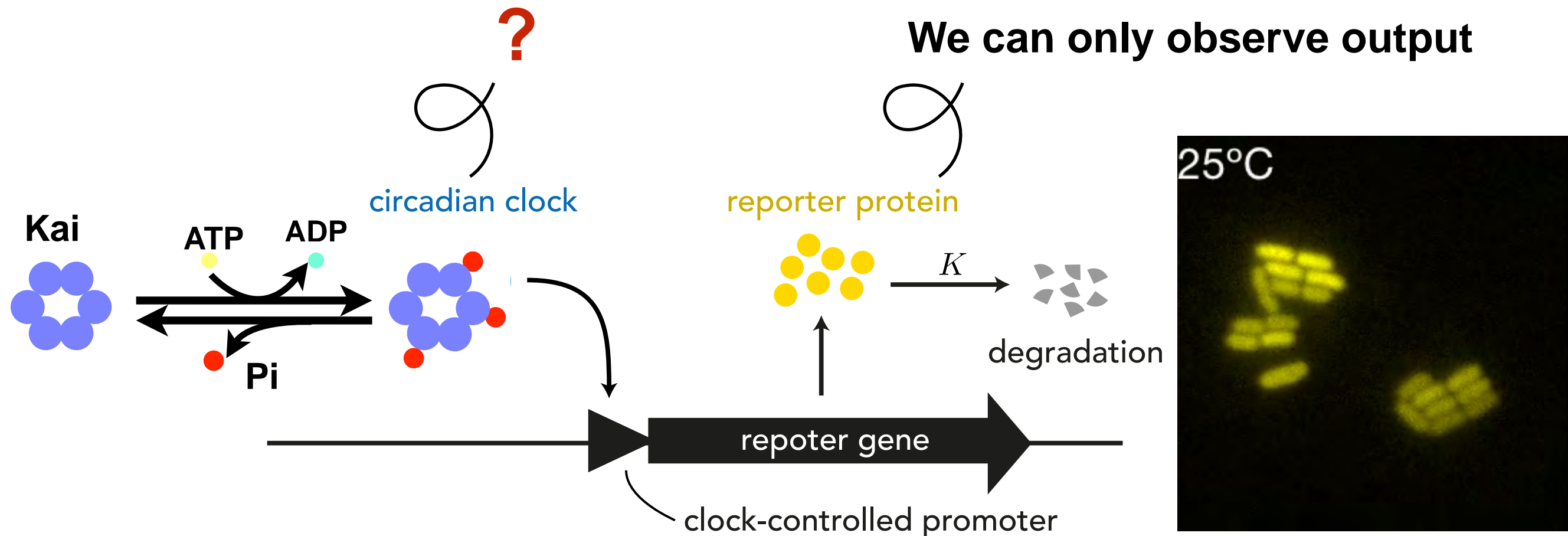
Gonze et al. PNAS 2002



Smaller cell → Smaller # of clock protein → Break of law of mass reaction  
→ Stochastic reactions → Noisy orbits → Variations in periods



# Yet, we don't know the stochastic dynamics of clock



Question of this talk:

- \* **Clock** is more precise than **output**?
- \* **Clock** is as precise as **output**?
- \* **Clock** is less precise than **output**?

Answer

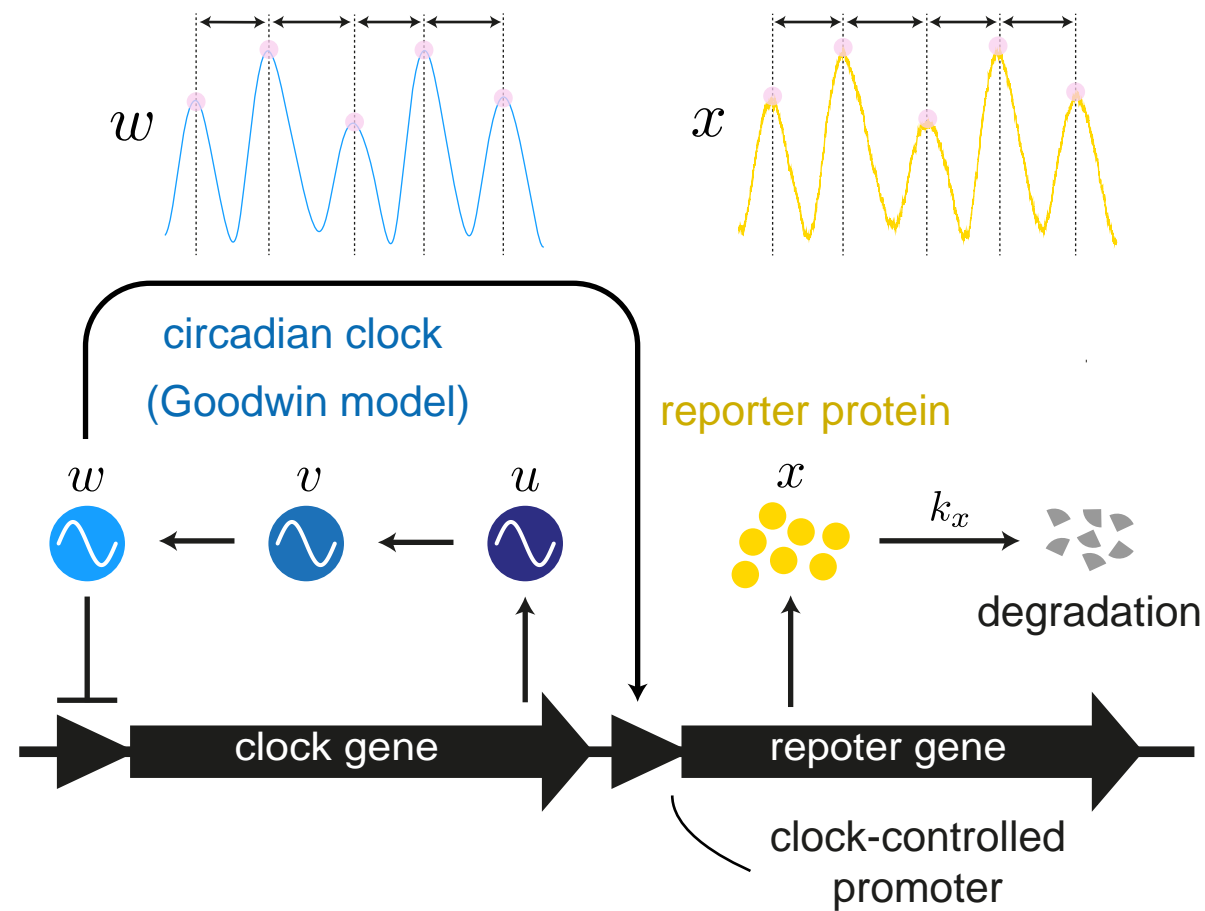
✓Yes

✓Yes

✓Yes

# Goodwin model + noise

Kaji, Mori, Ito J Theor Biol (2023)



## Goodwin model

$$\frac{1}{T}\dot{u} = \frac{1}{1 + w^m} - k_u u + \underbrace{\epsilon\sqrt{D_u}\xi_u(t)}_{\text{Noise}}$$

$$\frac{1}{T}\dot{v} = u - k_v v$$

$$\frac{1}{T}\dot{w} = v - k_w w$$

## Output system

$$\dot{x} = a + bw - k_x x + \underbrace{\epsilon\sqrt{D_x}\xi_x(t)}_{\text{Noise}}$$

circadian clock

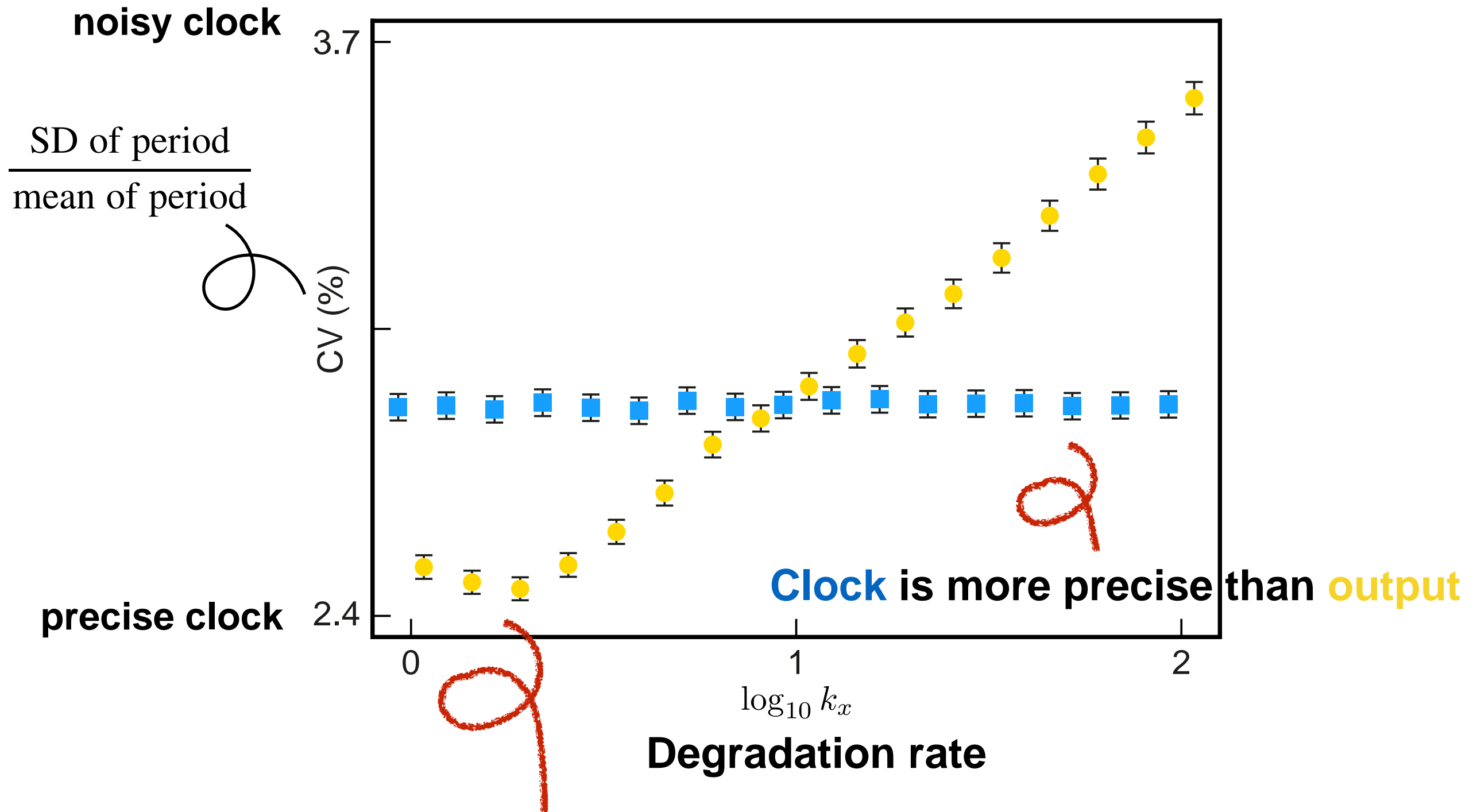


reporter protein



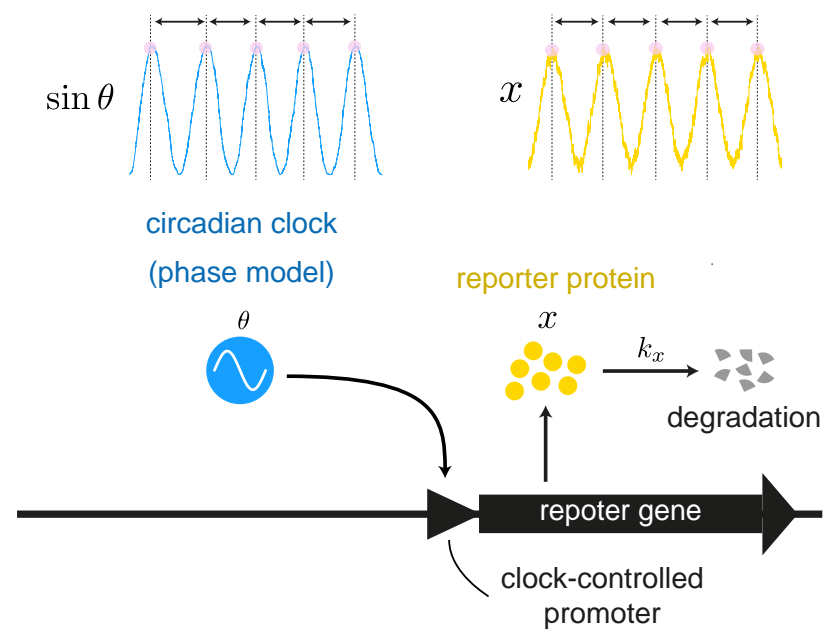
# Output can be more precise

■ clock (numerical)    ● output (numerical)



**Output** is more precise than **clock**

# Checked universality: phase model



## Phase model

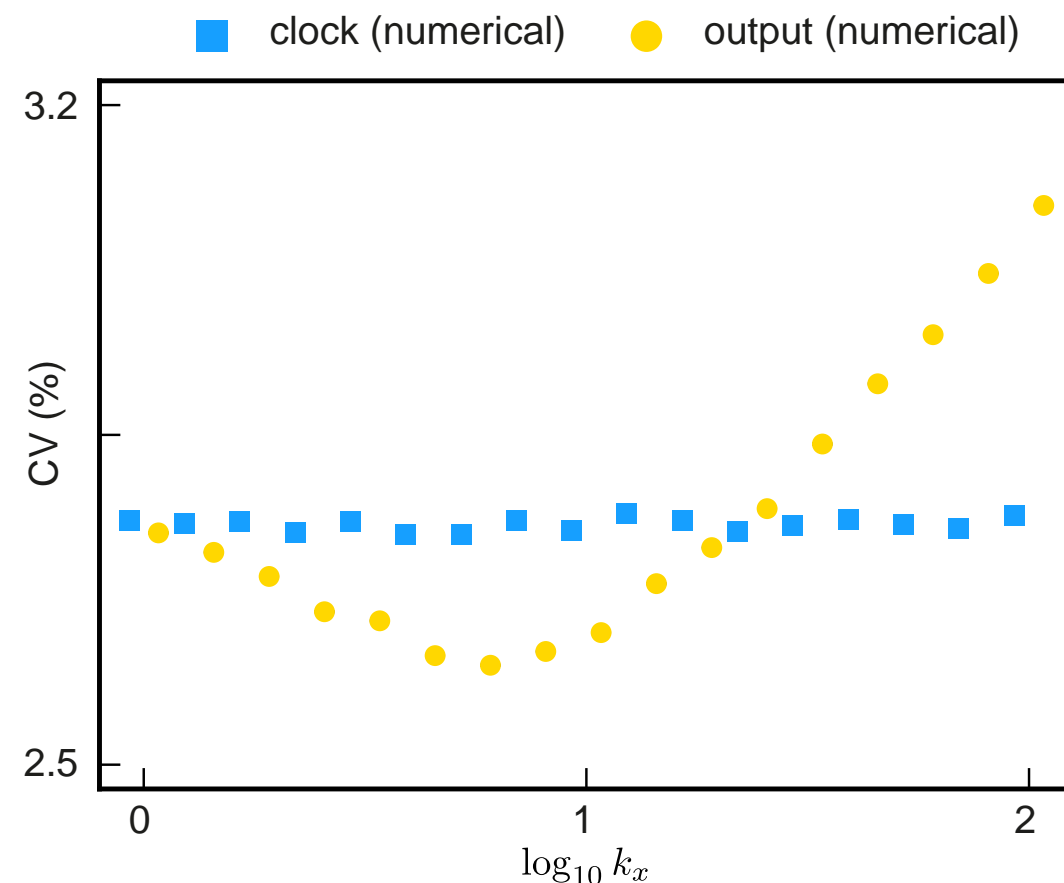
$$\dot{\theta} = \omega + \sqrt{D} \xi_{\theta}(t)$$

Noise

## Output system

$$\dot{x} = a + b \sin \theta - k_x x + \epsilon \sqrt{D_x} \xi_x(t)$$

Noise



Qualitatively equivalent as Goodwin.



# Note: theoretical works for period variations

## 1. Decrease of fluctuation in coupled phase oscillators

Kori Kawamura Masuda JTB 2012

$$\dot{\phi}_i(t) = \omega_i + \kappa \sum_{j=1}^N A_{ij} f(\phi_j - \phi_i) + \sqrt{D} \xi_i(t),$$

## 2. Fluctuations in coupled phase oscillators Mori Kori PRE 2013

$$\dot{\theta}_1 = \omega + \kappa J(\theta_1, \theta_2) + Z(\theta_1) \sqrt{D} \xi_1(t),$$

$$\dot{\theta}_2 = \omega + \kappa J(\theta_2, \theta_1) + Z(\theta_2) \sqrt{D} \xi_2(t),$$

## 3. Fluctuations in general limit cycle Mori Mikhailov PRE 2016

$$\frac{dx}{dt} = f[x(t)] + \epsilon G[x(t)] \xi(t) \quad \text{Floquet theory} \quad \text{We adopted this method.}$$

## 4. Inference of coupling based on fluctuations Mori Kori PNAS 2022

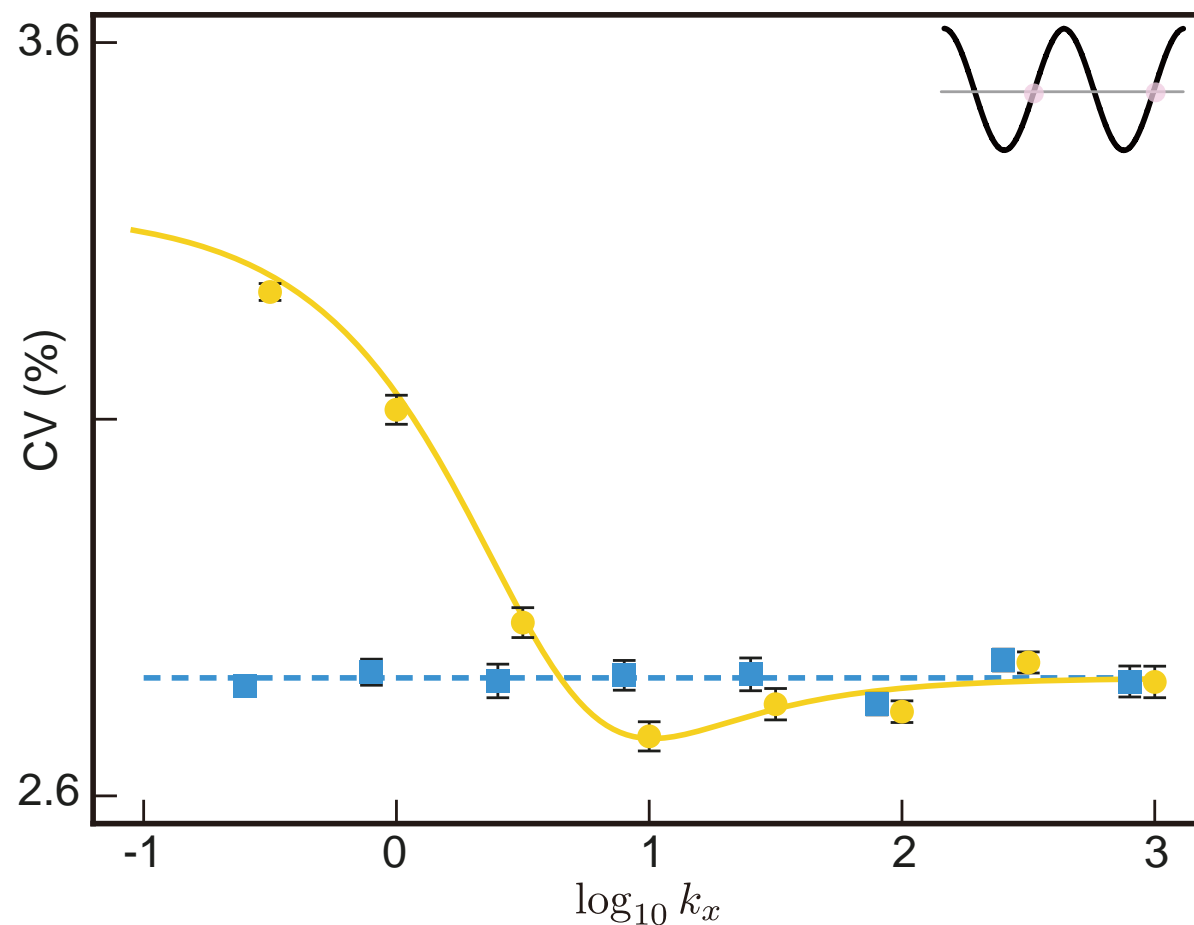
$$\dot{\theta}_1 = \omega + \kappa J(\theta_1, \theta_2) + Z(\theta_1) \sqrt{D} \xi_1(t),$$

$$\dot{\theta}_2 = \omega + \kappa J(\theta_2, \theta_1) + Z(\theta_2) \sqrt{D} \xi_2(t),$$

# Analytical calculations tells only degradation contribute to the noise in downstream.

$$CV_{\text{output}} = \epsilon \left\{ \underbrace{\frac{D_\theta}{2\pi\omega} \left[ 1 + \frac{1 - e^\kappa}{\kappa(\kappa^2 + 4\pi^2)} (-\kappa^2 - 2\pi\kappa \tan \Phi_{\text{cp}} + 2\pi^2 + 2\pi^2 \tan^2 \Phi_{\text{cp}}) \right]}_{\text{from clock noise}} + \underbrace{\frac{D_x}{2\pi\omega} \cdot \frac{(1 - e^{-\kappa})\omega^2}{4\pi^2 b^2 \kappa} (\kappa^2 + 4\pi^2) (1 + \tan^2 \Phi_{\text{cp}})}_{\text{from output noise}} \right\}^{\frac{1}{2}}.$$

■ clock (numerical)    --- clock (analytic)  
● output (numerical)    --- output (analytic)



**Phase model**

$$\dot{\theta} = \omega + \sqrt{D} \underbrace{\xi_\theta(t)}_{\text{Noise}}$$

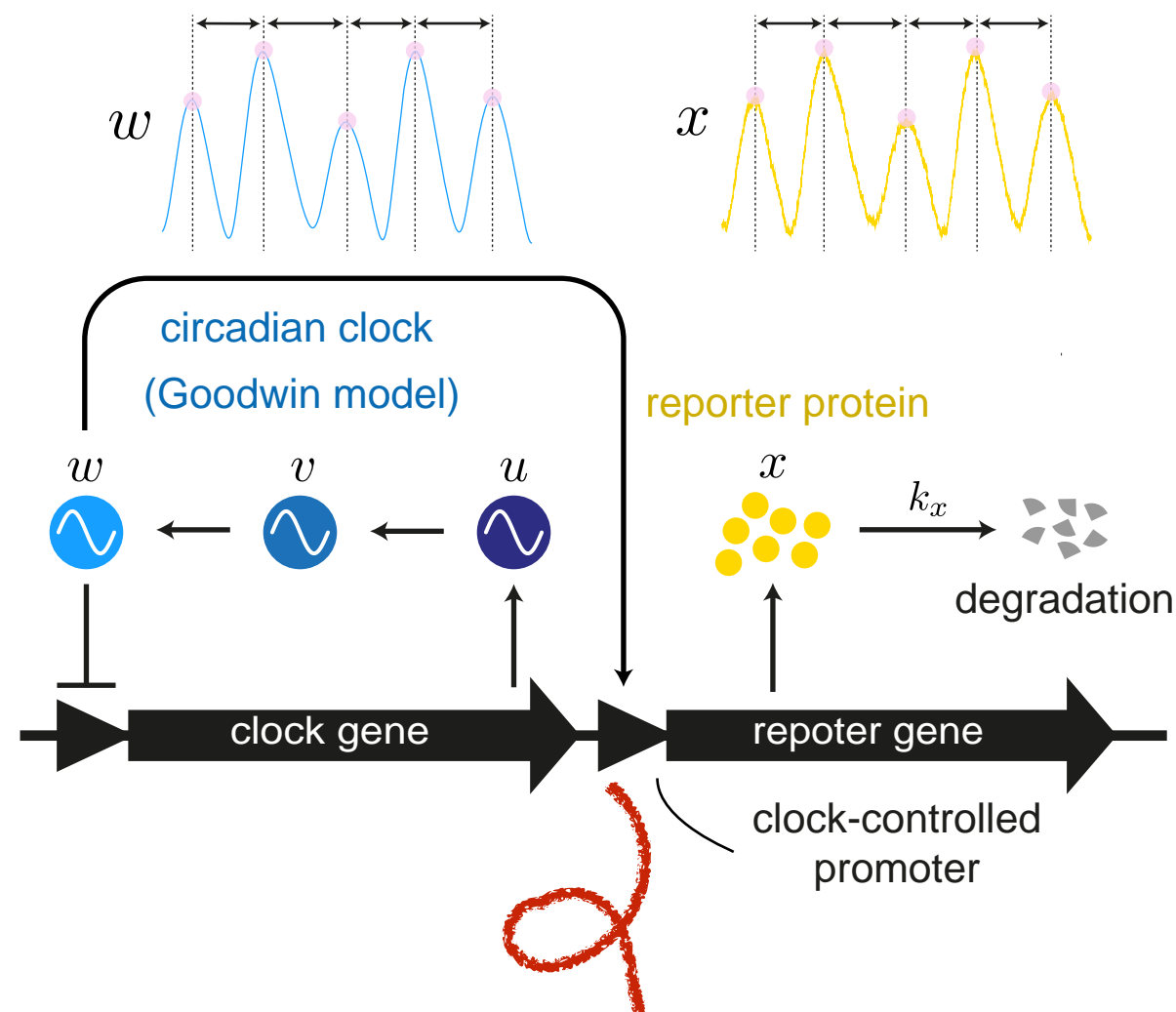
**Output system**

$$\dot{x} = a + b \sin \theta - k_x x + \epsilon \sqrt{D_x} \underbrace{\xi_x(t)}_{\text{Noise}}$$

- \* Analytic and numerical results are consistent.
- \* Clock noise and output noise independently contribute to the CV of output.
- \* CV is dependent on  $k, \omega, D_\theta, D_x$
- \* CV is not dependent on  $a, b$

# What if the function of regulation?

Kaji, Mori, Ito in prep.



## Goodwin model

$$\frac{1}{T}\dot{u} = \frac{1}{1+w^m} - k_u u + \epsilon\sqrt{D_u}\xi_u(t)$$

$$\frac{1}{T}\dot{v} = u - k_v v$$

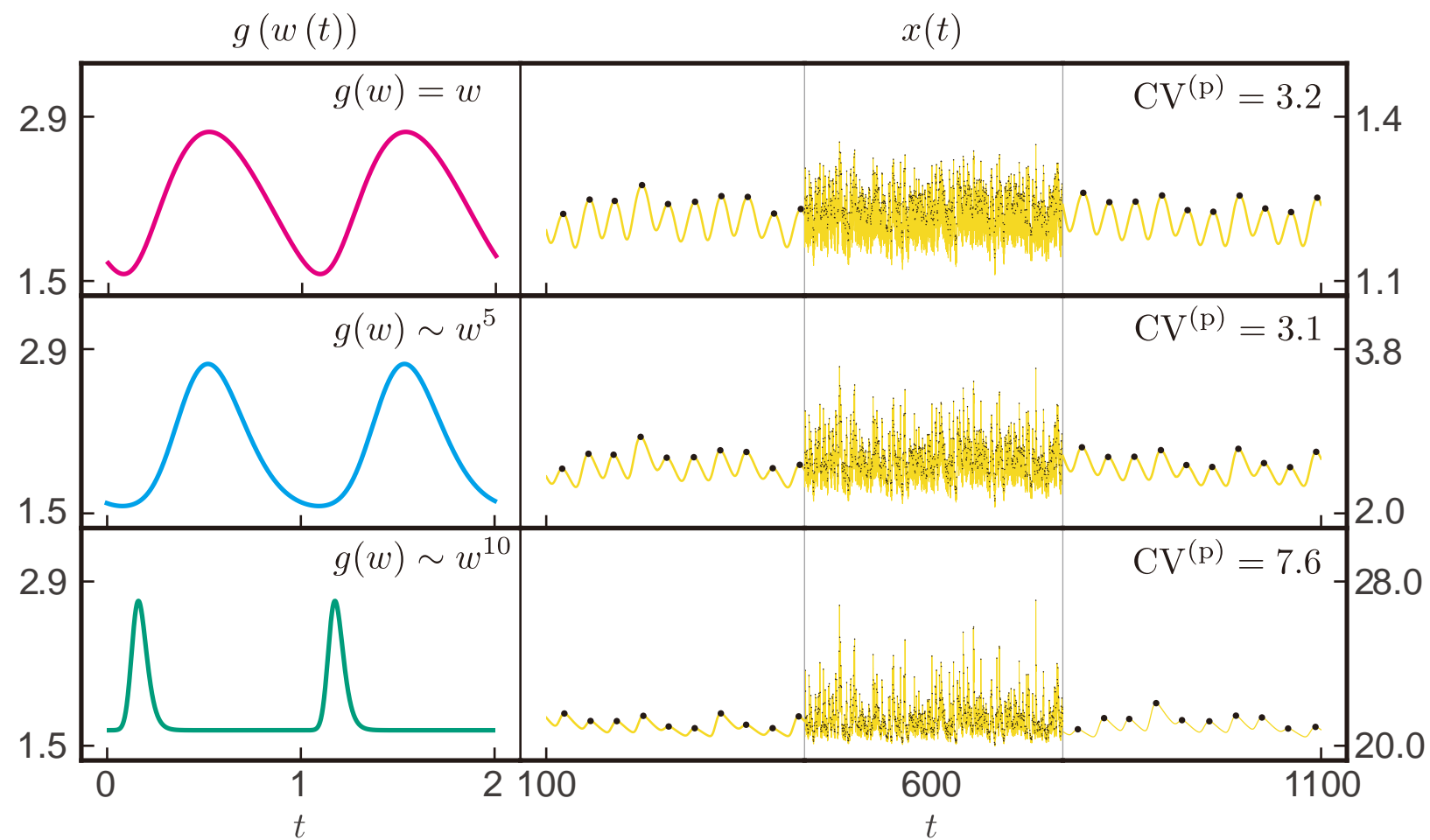
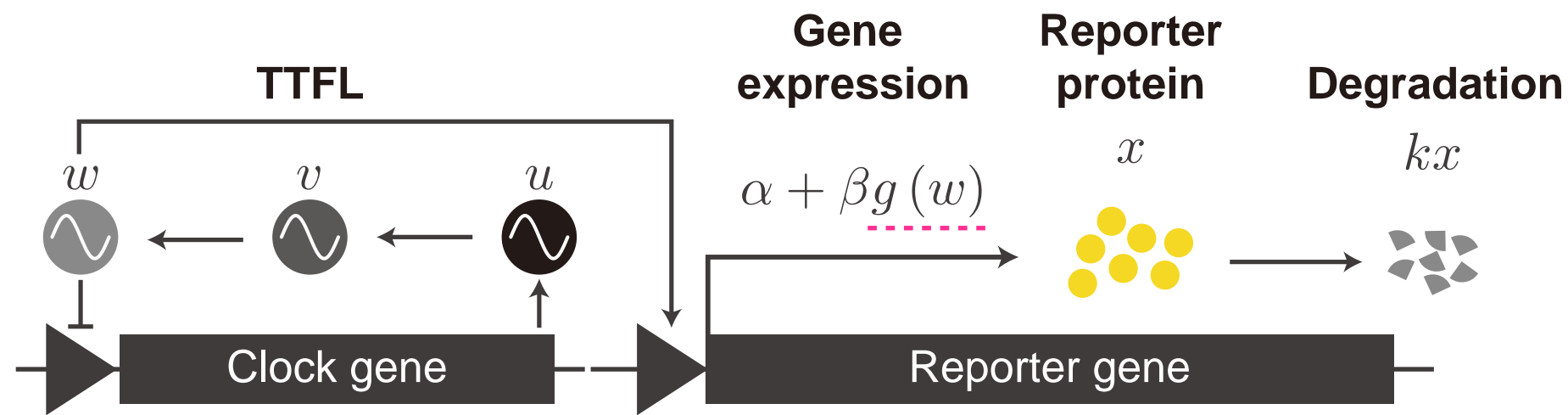
$$\frac{1}{T}\dot{w} = v - k_w w$$

## Output system

$$\dot{x} = a + b g(w) - k_x x$$

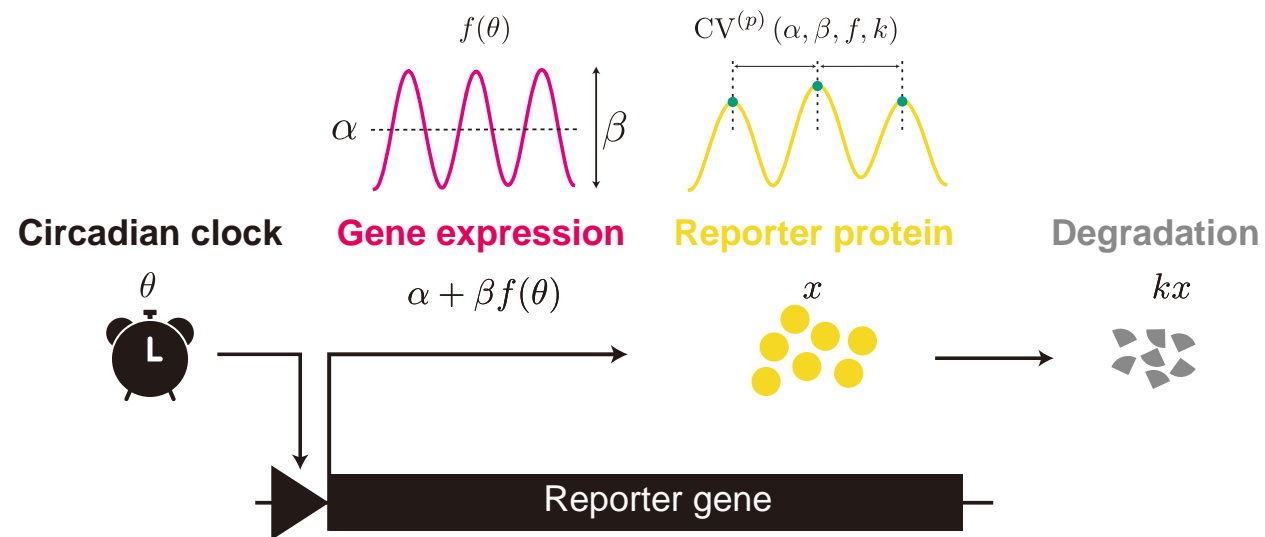
Choice of clock-controlled promoter affects fluctuation? ✓Yes

# CV is dependent on the manner of clock-regulation





# Again, phase model

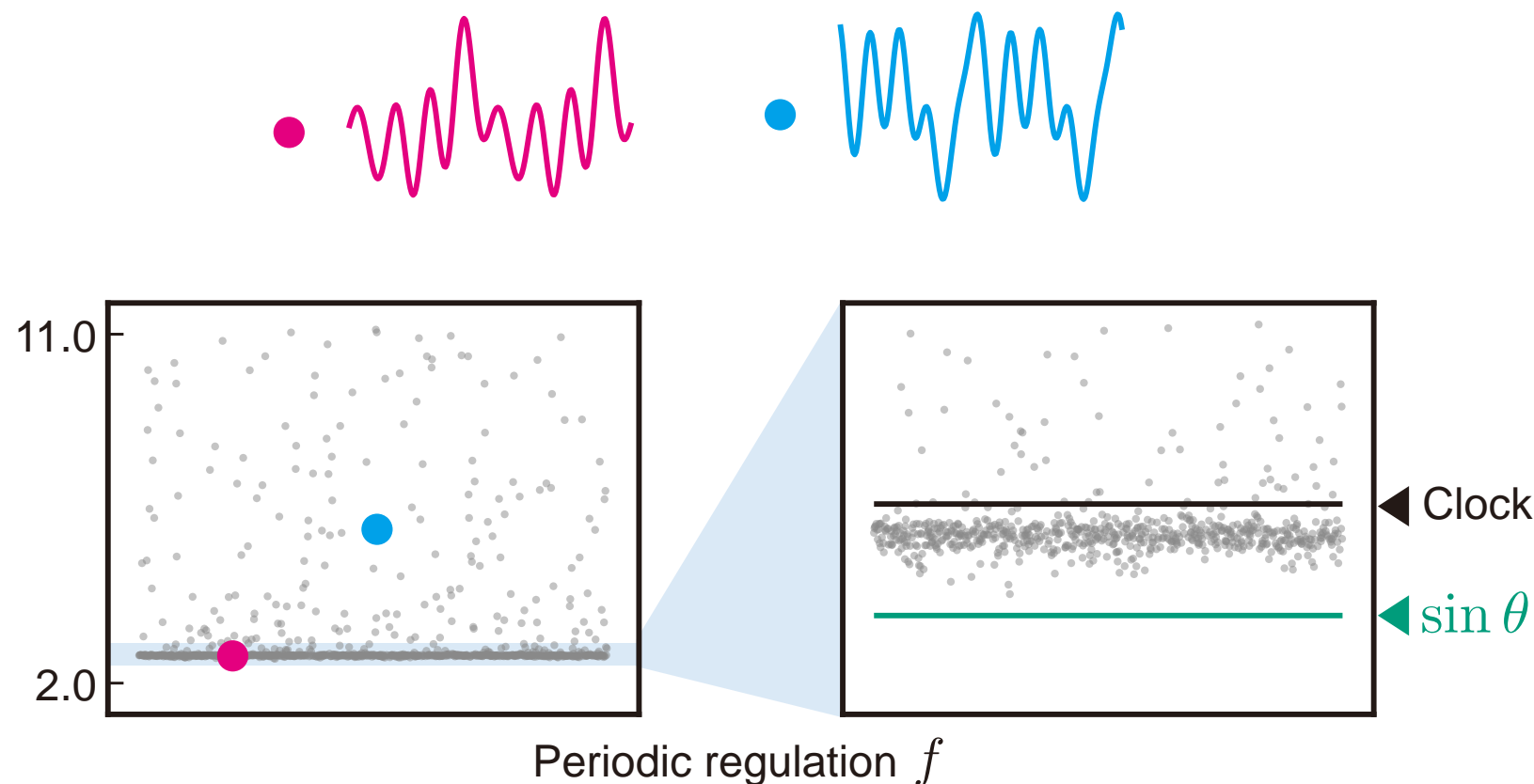


## Phaes model

$$\dot{\theta} = \omega + \sqrt{D}\xi(t)$$

## Output system

$$\dot{x} = a + bf(\theta) - kx$$



sin is best?

✓ almost yes

# Sampling confirmed near-sinusoidal functions tend to give precise output

## \* We got analytical CV

$$CV = \frac{\epsilon}{\tau} \sqrt{R_{\Theta\Theta} + R_{hh} + 2R_{\Theta h}}$$

$$R_{\Theta\Theta}^{(\theta)} = \frac{\tau^2}{2\pi\omega},$$

$$R_{hh}^{(\theta)} = \frac{D(1 - e^{-k_x\tau})}{\left(\sum_{n=1}^N n\omega \sqrt{\frac{A_n^2 + B_n^2}{k_x^2 + (n\omega)^2}} \cos \Phi_n(t_{cp})\right)^2} \sum_{n=1}^N \sum_{m=1}^N nm \sqrt{\frac{(A_n^2 + B_n^2)(A_m^2 + B_m^2)}{(k_x^2 + (n\omega)^2)(k_x^2 + (m\omega)^2)}} \\ \times \left\{ \frac{1}{4k_x^2 + (n-m)^2\omega^2} [(n-m)\omega \sin(\Phi_n(t_{cp}) - \Phi_m(t_{cp})) + 2k_x \cos(\Phi_n(t_{cp}) - \Phi_m(t_{cp}))] \right. \\ \left. + \frac{1}{4k_x^2 + (n+m)^2\omega^2} [(n+m)\omega \sin(\Phi_n(t_{cp}) + \Phi_m(t_{cp})) + 2k_x \cos(\Phi_n(t_{cp}) + \Phi_m(t_{cp}))] \right\},$$

$$R_{\Theta h}^{(\theta)} = \frac{-D(1 - e^{-k_x\tau})}{\omega \left(\sum_{n=1}^N n\omega \sqrt{\frac{A_n^2 + B_n^2}{k_x^2 + (n\omega)^2}} \cos \Phi_n(t_{cp})\right)} \sum_{n=1}^N n \sqrt{\frac{A_n^2 + B_n^2}{k_x^2 + (n\omega)^2}} \\ \times \frac{1}{k_x^2 + (n\omega)^2} [n\omega \sin \Phi_n(t_{cp}) + k_x \cos \Phi_n(t_{cp})].$$

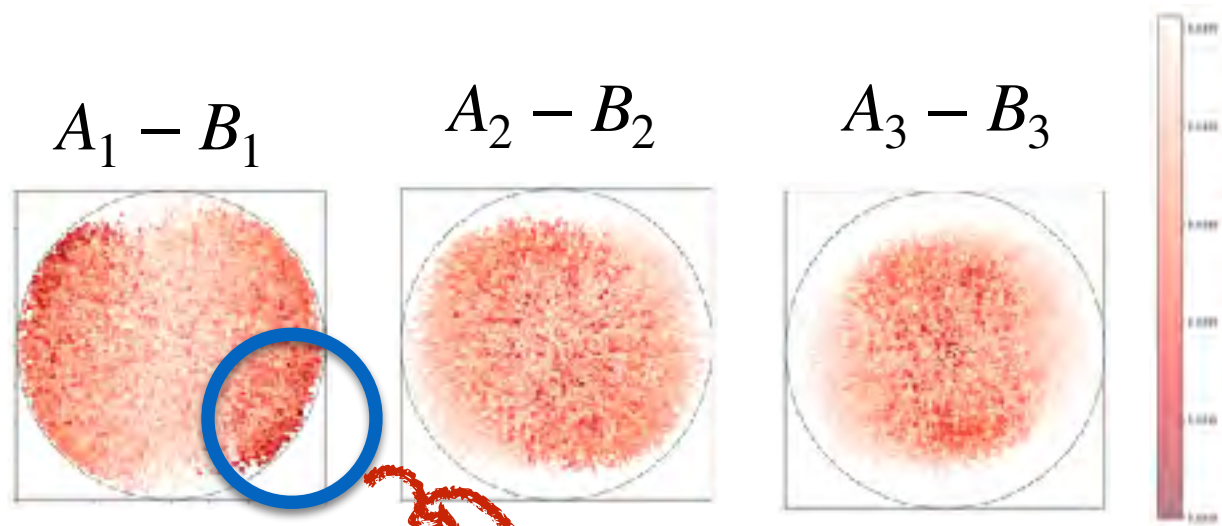
- \* Analytic and numerical results are consistent.
- \* Clock noise and output noise independently contribute to the CV of output.
- \* CV is not dependent on  $a, b$
- \* CV is dependent on  $k, \omega, D, \underline{A_n}, \underline{B_n}$



Fourier coefficients of  $f$

$$f = A_1 \sin \theta + B_1 \cos \theta + A_2 \sin 2\theta + B_2 \cos 2\theta \dots$$

## \* Gibbs Sampling

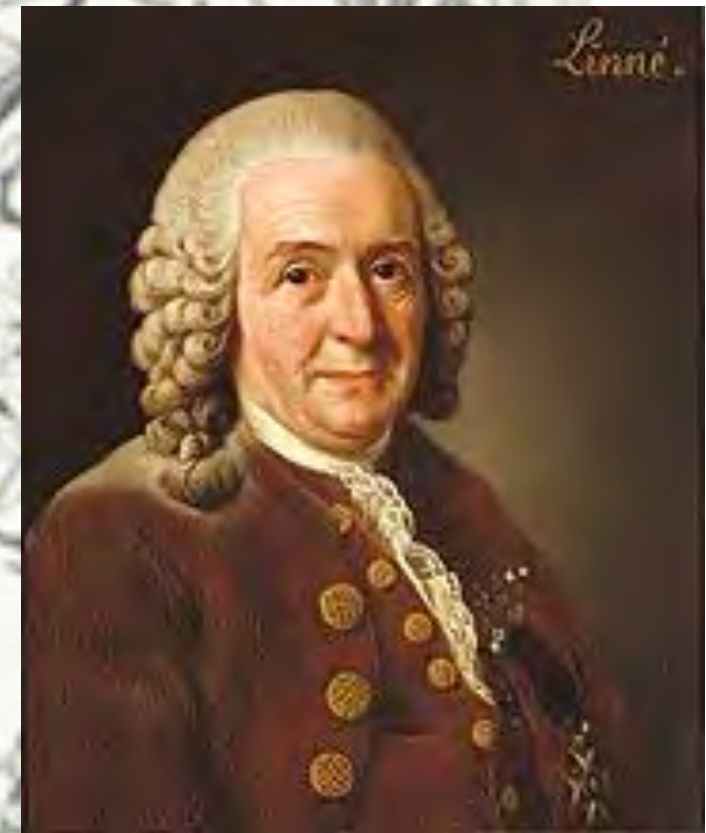


The clock regulation  $f$  determines the noise in the downstream

$\sin \theta$  denoise effectively!



# Linné's flower clock



Carl von Linné,  
*Horologium Florae* (1751)



# Linnaeus's flower clock (wikipedia)

Dandelion



5 am — 9 am

Sow thistle



5 am — 12 am

Hawkweed



6 am — 5 pm

Garden Lettuce



7 am — 10 am

White Waterlily



7 am — 5 pm

Ice-plant



9 am — 3 pm



# Beautiful example: daylily vs nightlily

Daylily

(*Heimerocallis fulva*)



Nightlily

(*Heimerocallis citrina*)



Yahara  
(Kyushu)

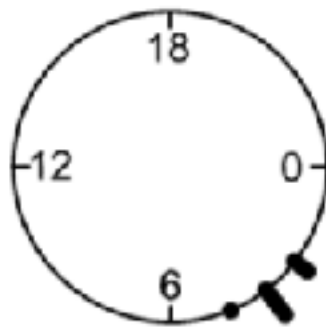


Nitta  
(Azabu)

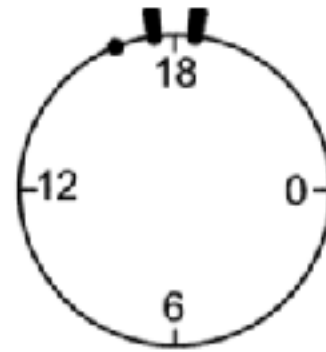
F1

F2

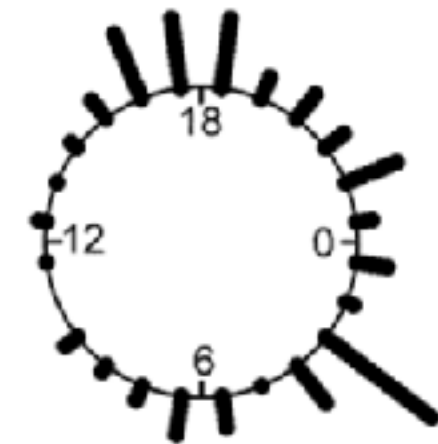
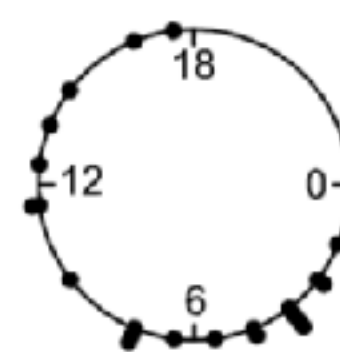
Flower  
opening  
time



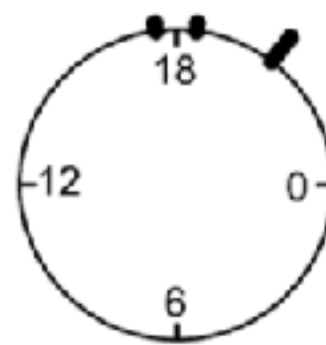
morning



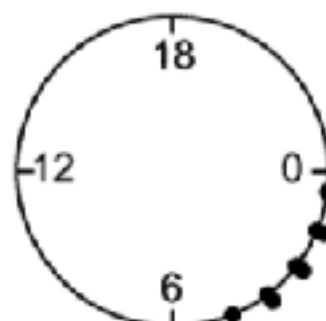
night



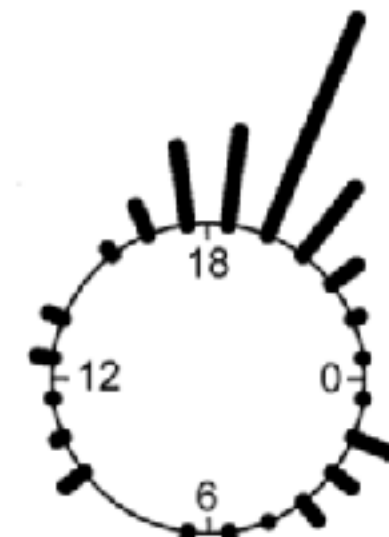
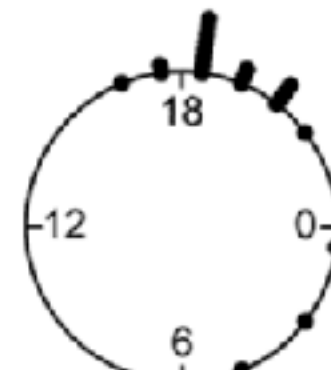
Flower  
closing  
time



night

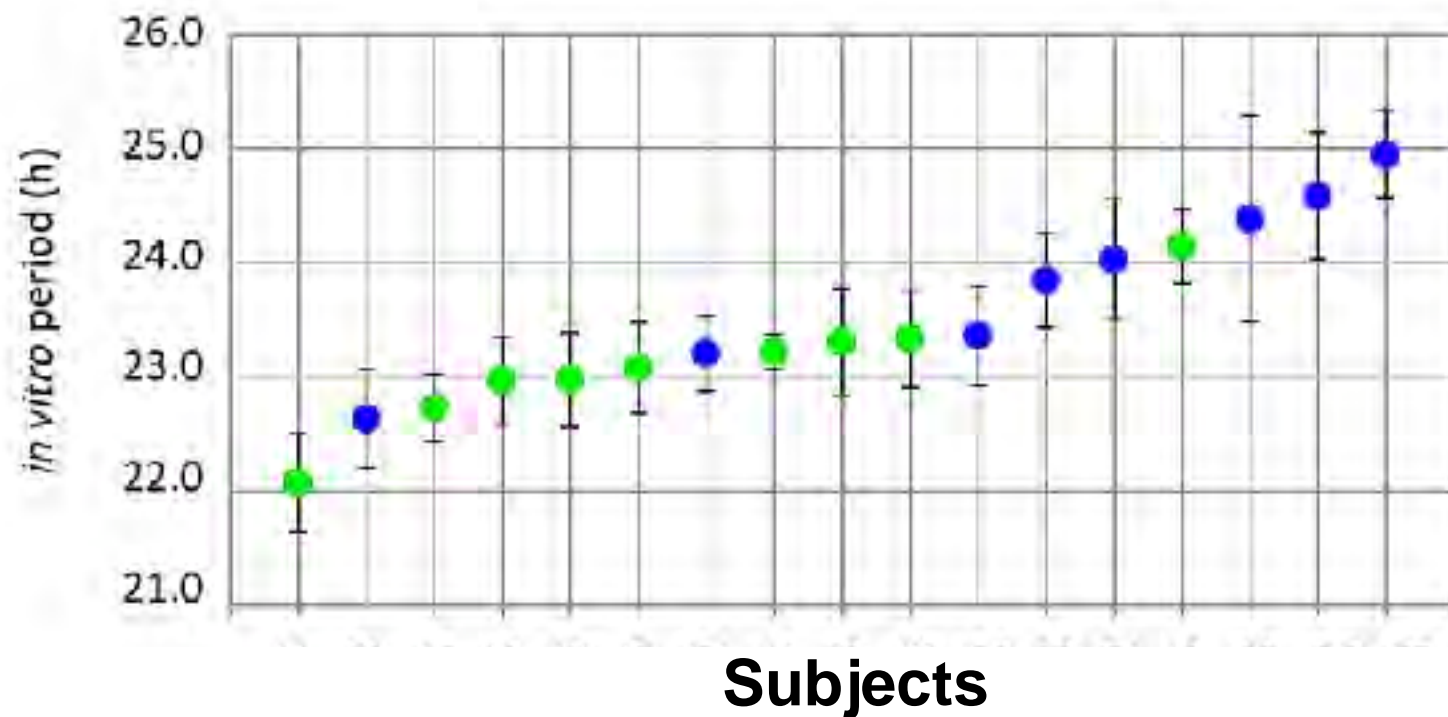


midnight



## ① Free-run period

A black and white portrait of an elderly man with white hair and glasses. He is resting his chin on his right hand, looking thoughtfully towards the camera. He is wearing a dark jacket over a light-colored shirt. The background is slightly blurred, showing what appears to be a bookshelf.



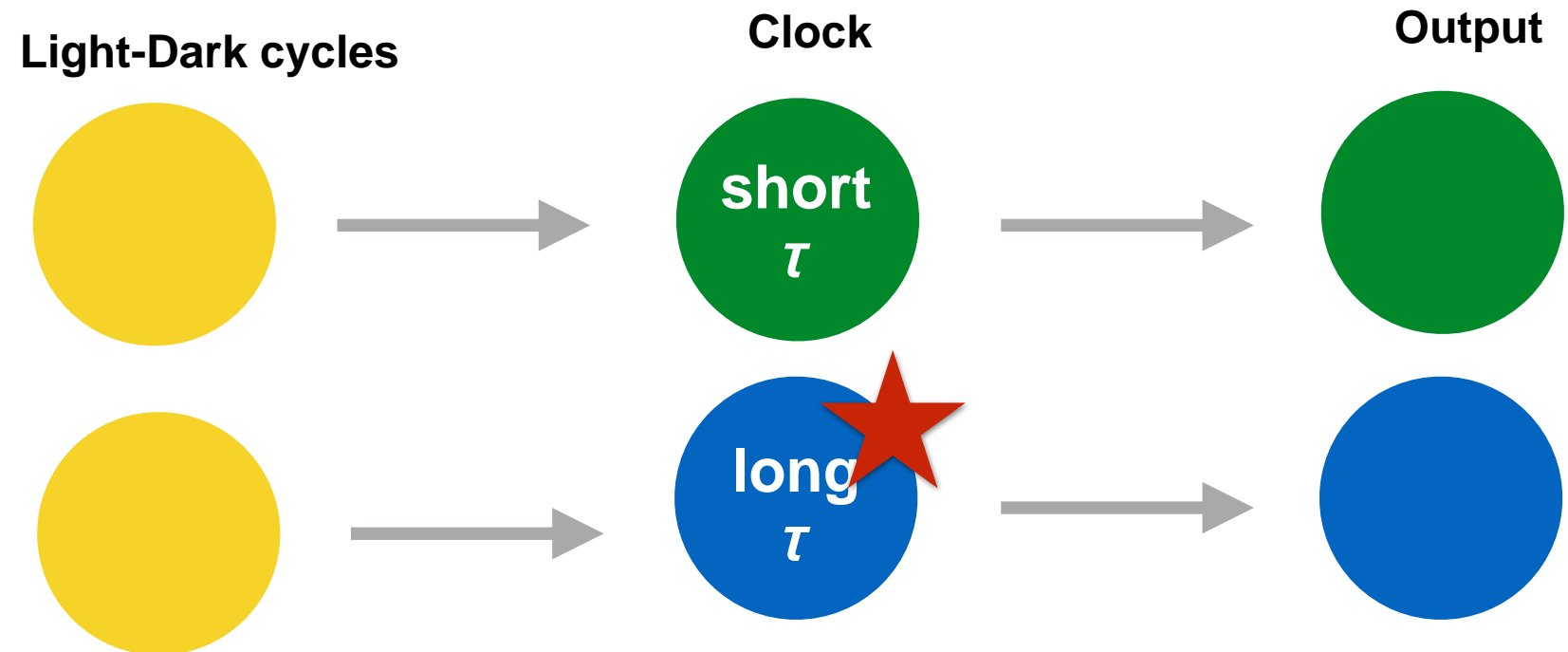
## Free-run period in human determines chrono-type

Hida et al. Sci Rep(2012)

# How can plants change the flowering time?

## ① Free-run period

Cf. Pittendrigh & Daan



**Light**  $\dot{\Theta} = \Omega$

**Clock**  $\dot{\theta} = \omega + A \sin(\Theta - \theta)$

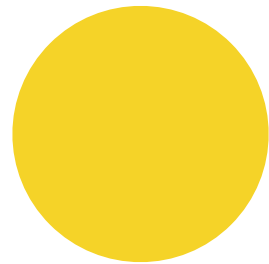
**Output**  $\dot{x} = a \cos \theta - dx$



# Question: which scenario gives variation in flowering time

## ① Free-run period

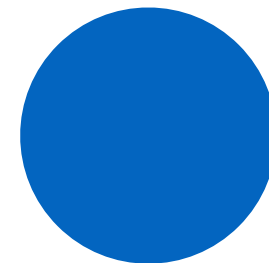
Light-Dark cycles



Clock

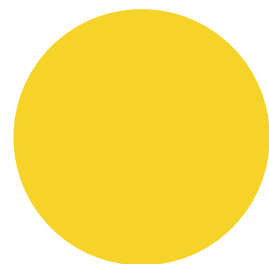


Output

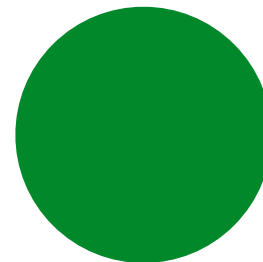


## ② Variation in output pathway

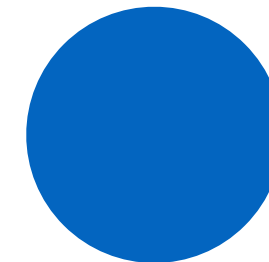
Light-Dark cycles



Clock



Output



But, molecular methodology is hard for these lilies...



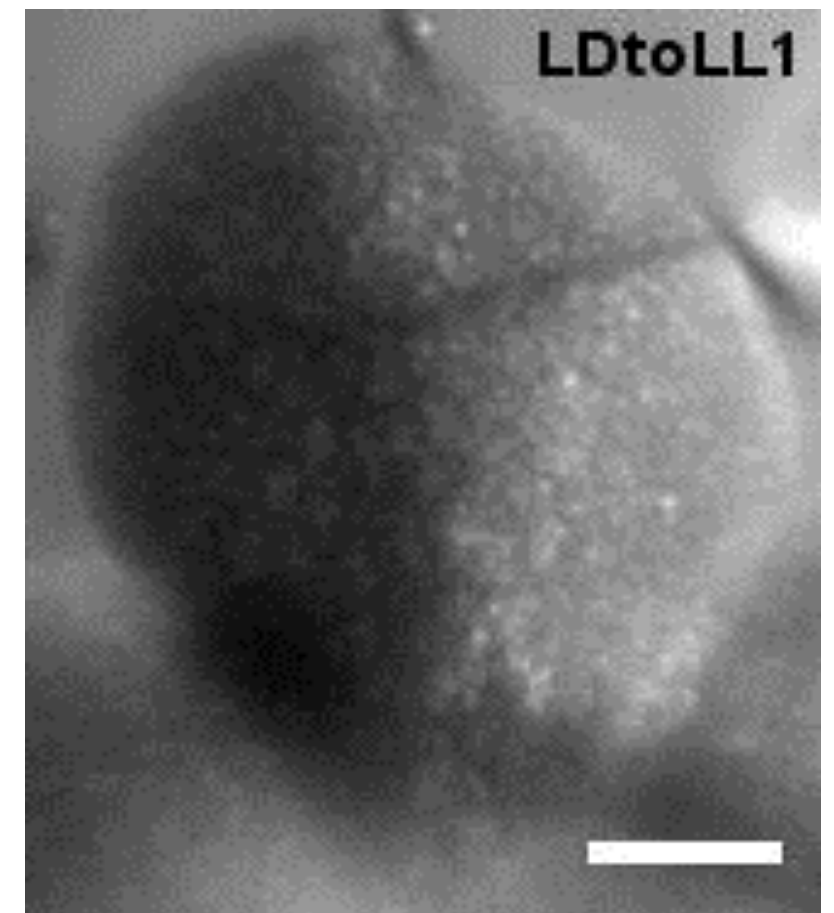
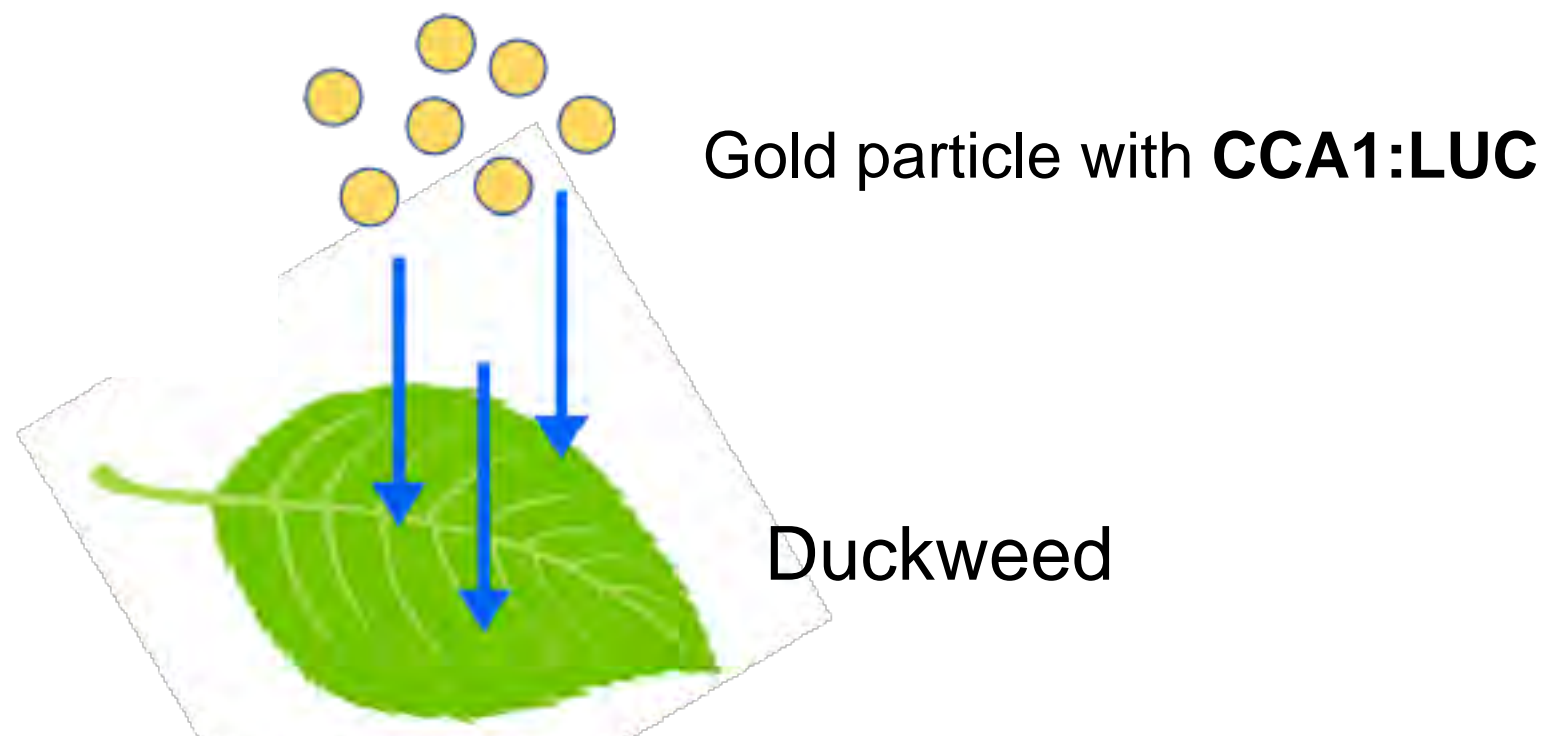
# Circadian rhythms of non-model organisms of by gene gun



Oyama (Kyoto)

## Gene gun (particle bombardment method)

- \* Gold particles of about 1  $\mu\text{m}$  diameter are coated with plasmids CCA1:LUC.
- \* He gas pressure gun injects the gold particles the sample plants.
- \* Clock-driven expression of luciferase gives rhythmic light emission.







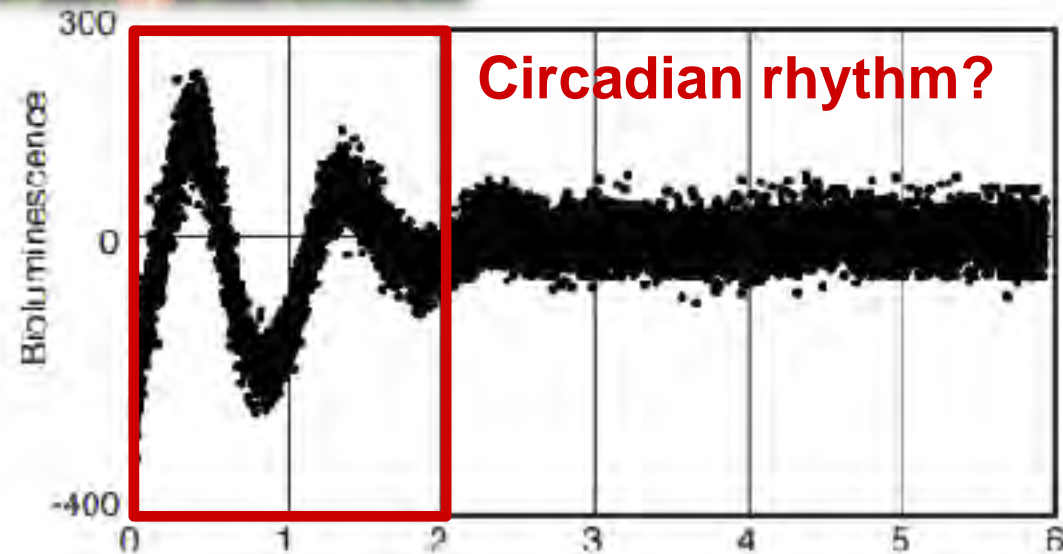
Yahara



# Gene gun didn't work well fo daylily and nightlily



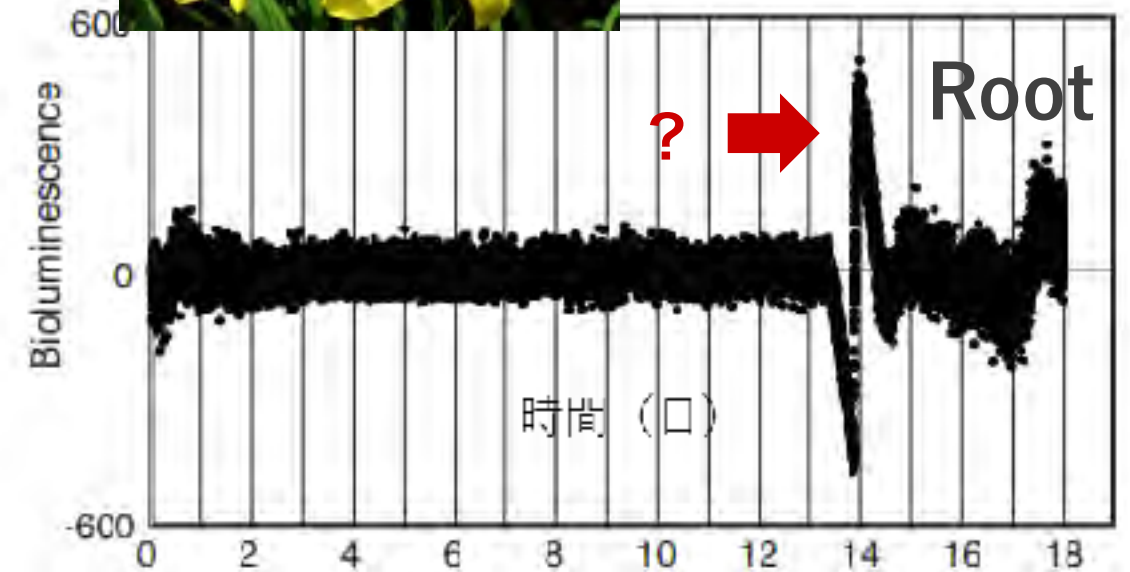
Daylily



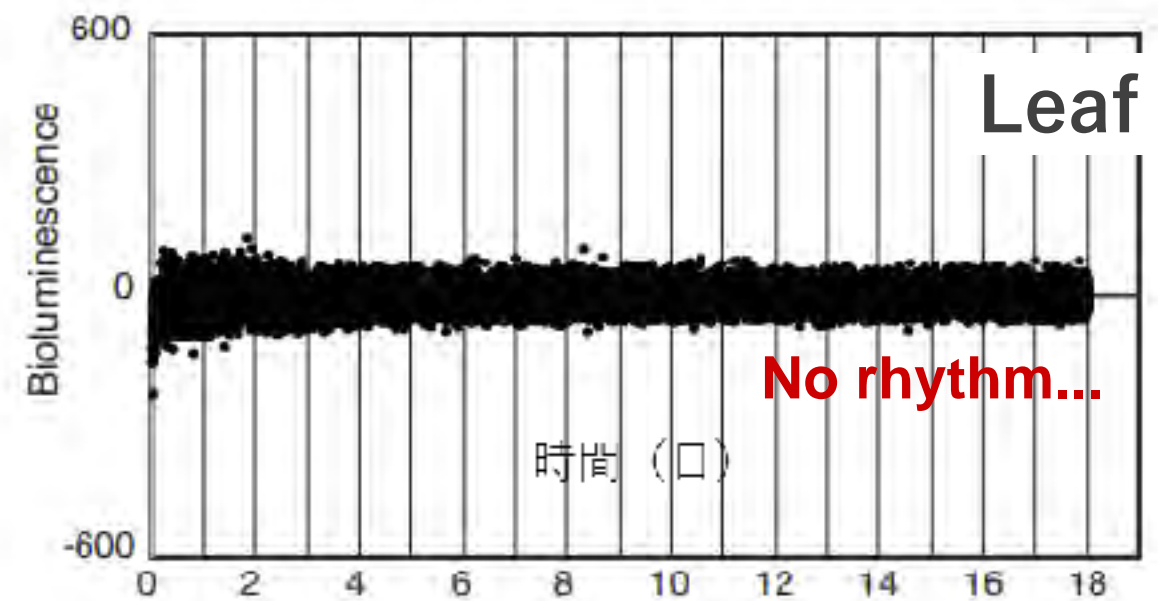
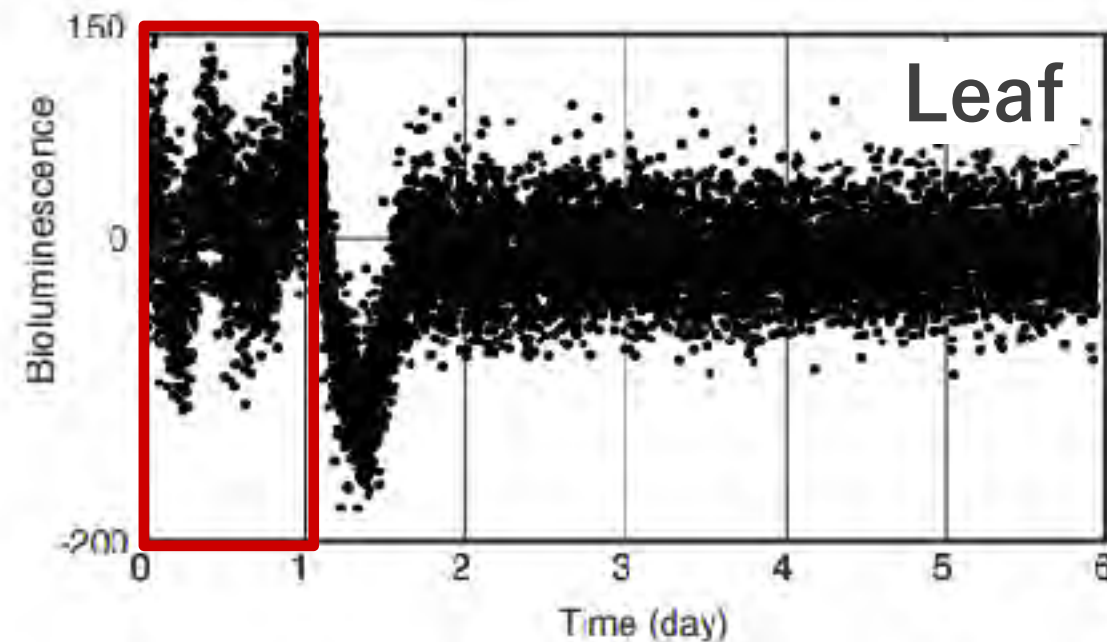
Root



Nightlily



Circadian rhythm?



Leaf





Nitasaka's greenhouse





Nitasaka's greenhouse



Lots of Morning glory!!

All 6-years-old kids take care morning glory in Japan.



July 2023



# Nitasaka collected a morning glory strains that flowers in the evening!



Nitasaka (Kyushu)

I have a mutant strain for flowering time.

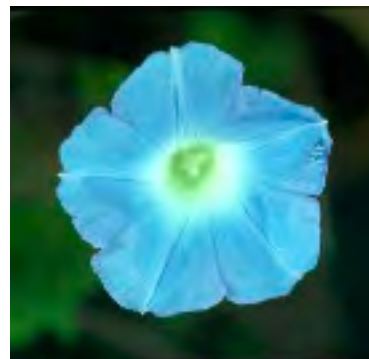
**Murasaki**

(Standard strain)

Flowering in the morning

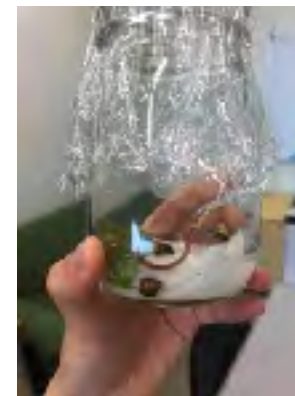


**Mexican strain (QX909)**  
Flowering in the evening

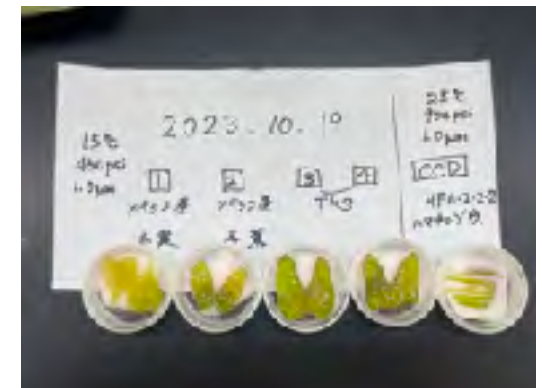


Oyama (Kyoto)

Gene gun doesn't work well for the plant in the field...



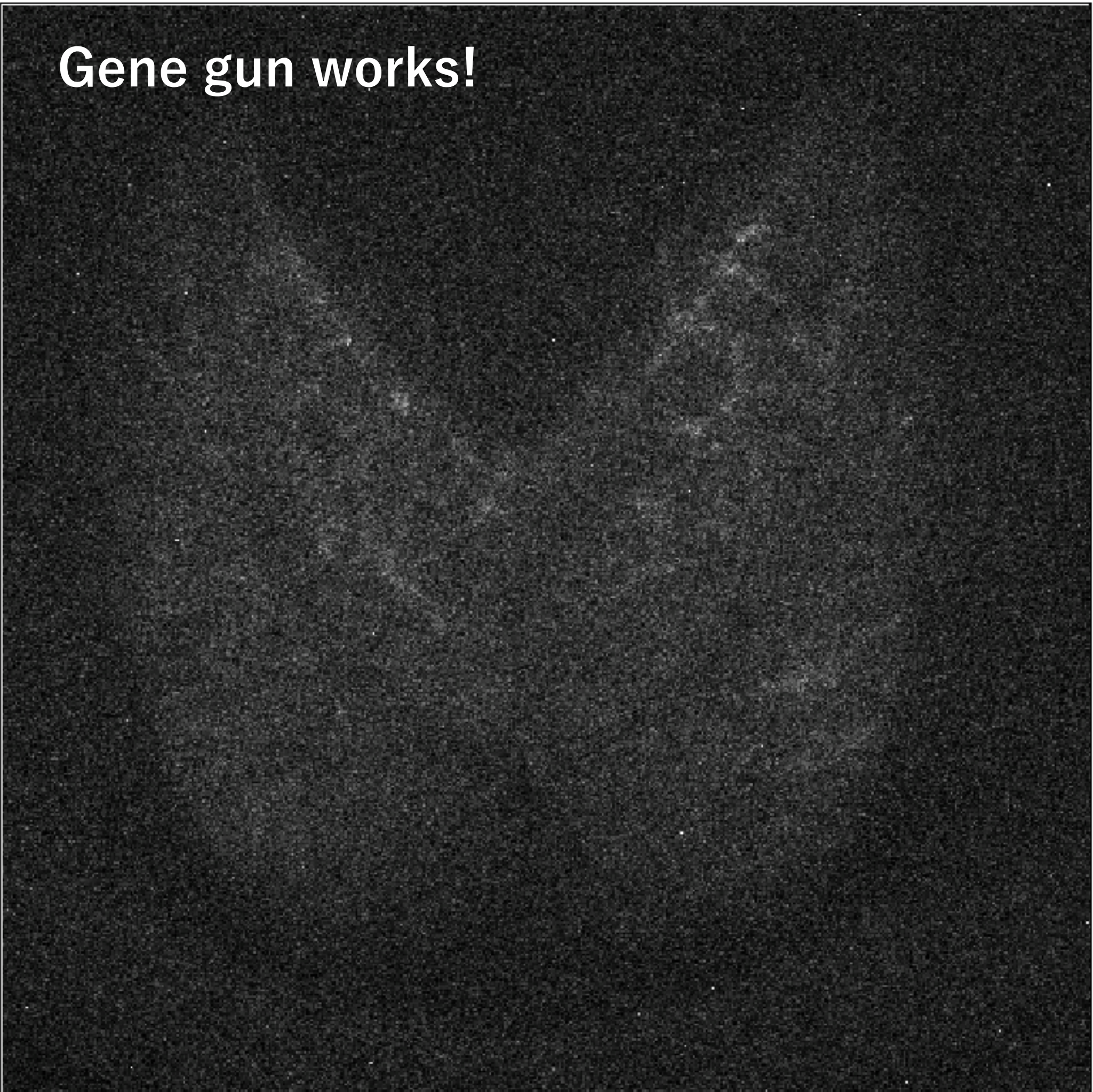
Germination in a bottle



Cultivated cotyledons



Gene gun works!





# Free-run rhythm of morning glory

Murasaki  
(Standard strain)

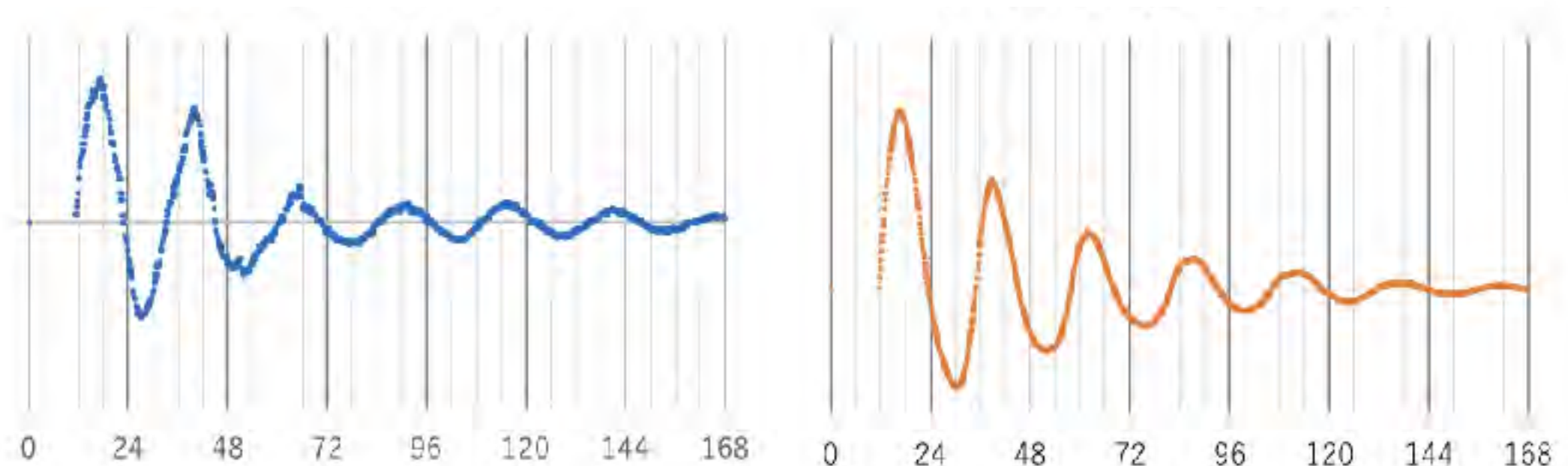
Flowering in the morning



Mexican strain (QX909)  
Flowering in the evening



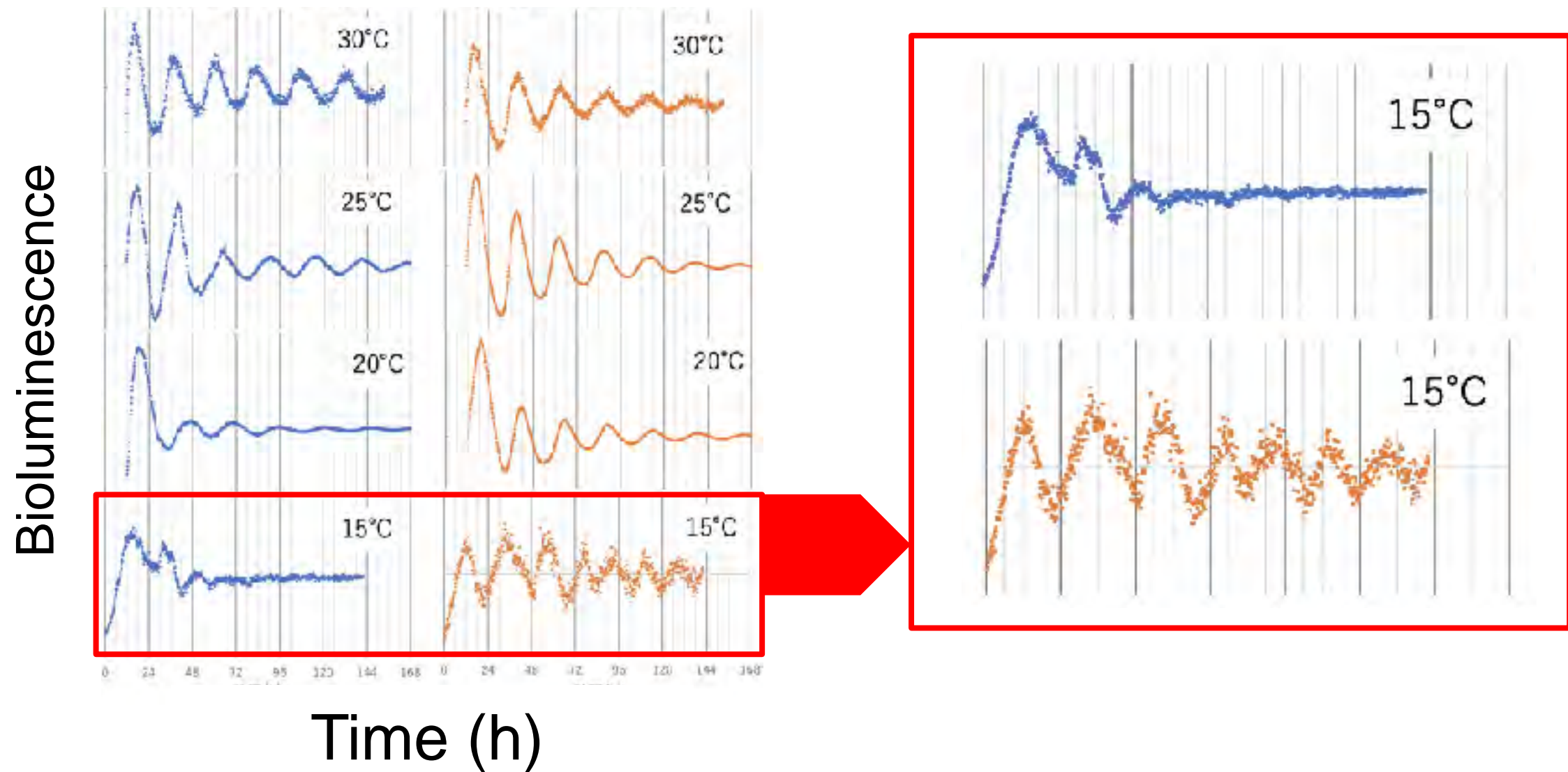
Bioluminescence



No difference in free-run period and phase



# Temperature dependency

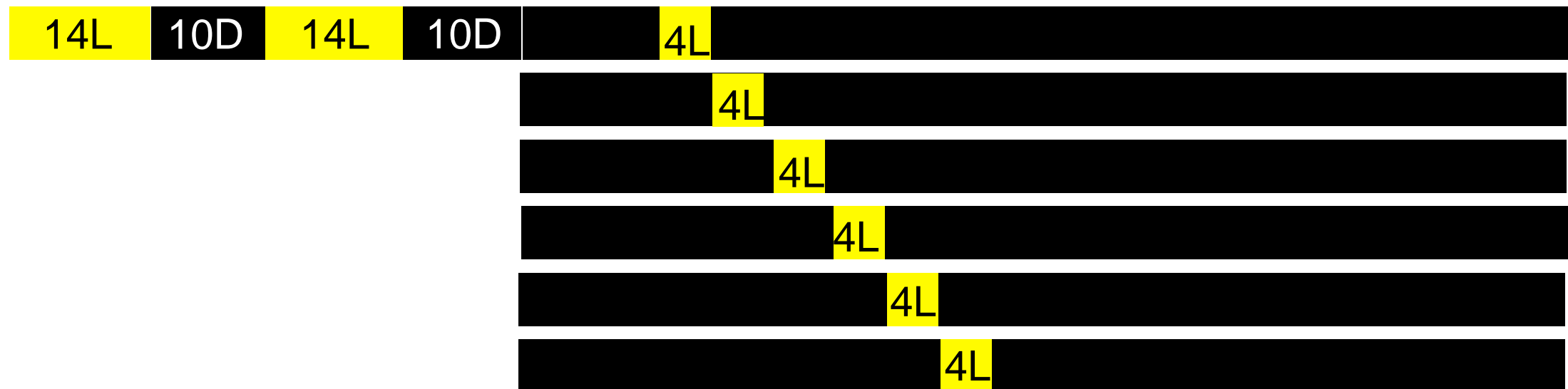


Periods are temperature-compensated

Critical temperature are different

# Phase response curve

Constant dark



Murasaki

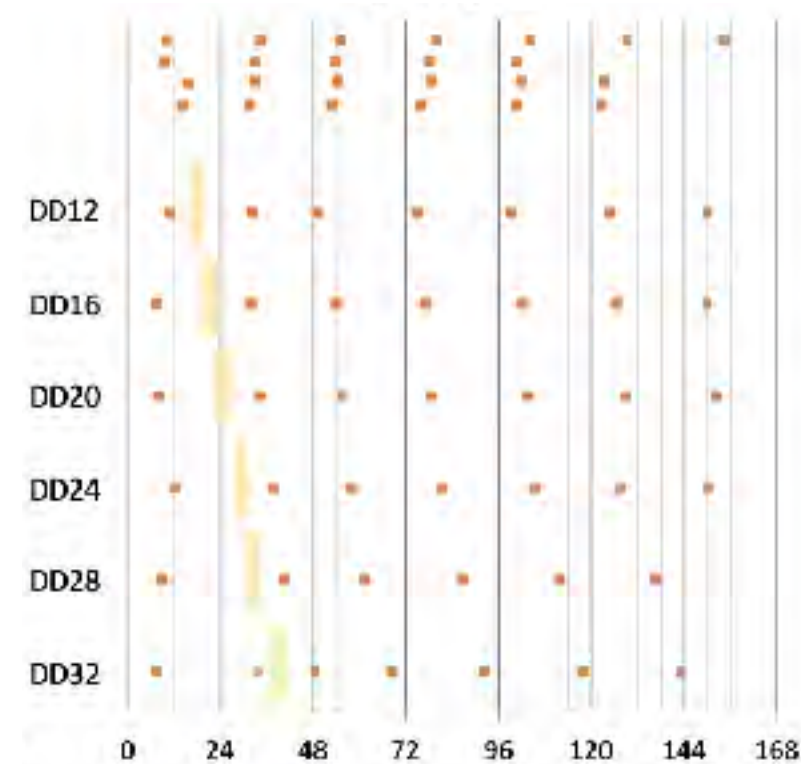
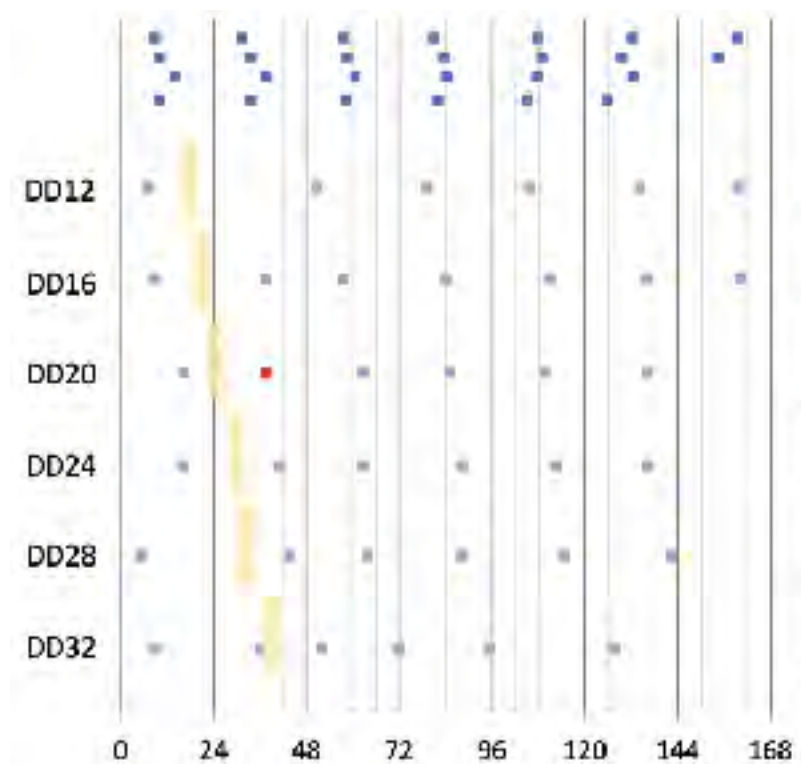
(Standard strain)

Flowering in the morning

Mexican strain (QX909)

Flowering in the evening

Peak times

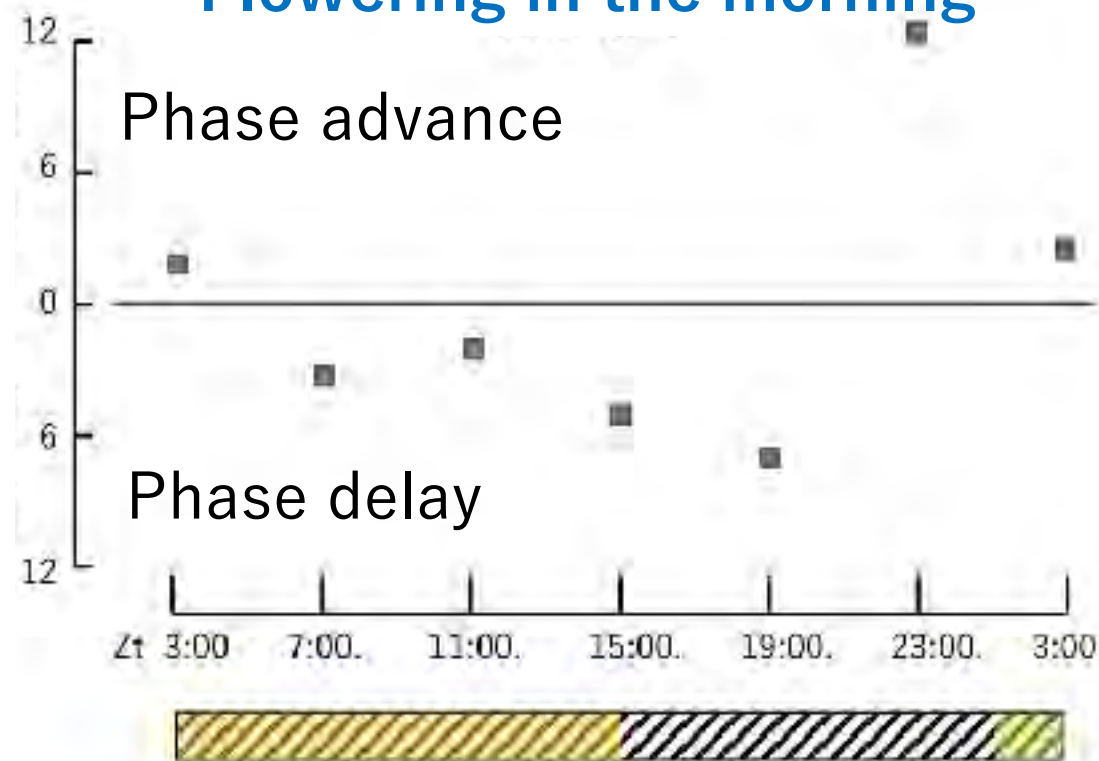


# Phase response curve

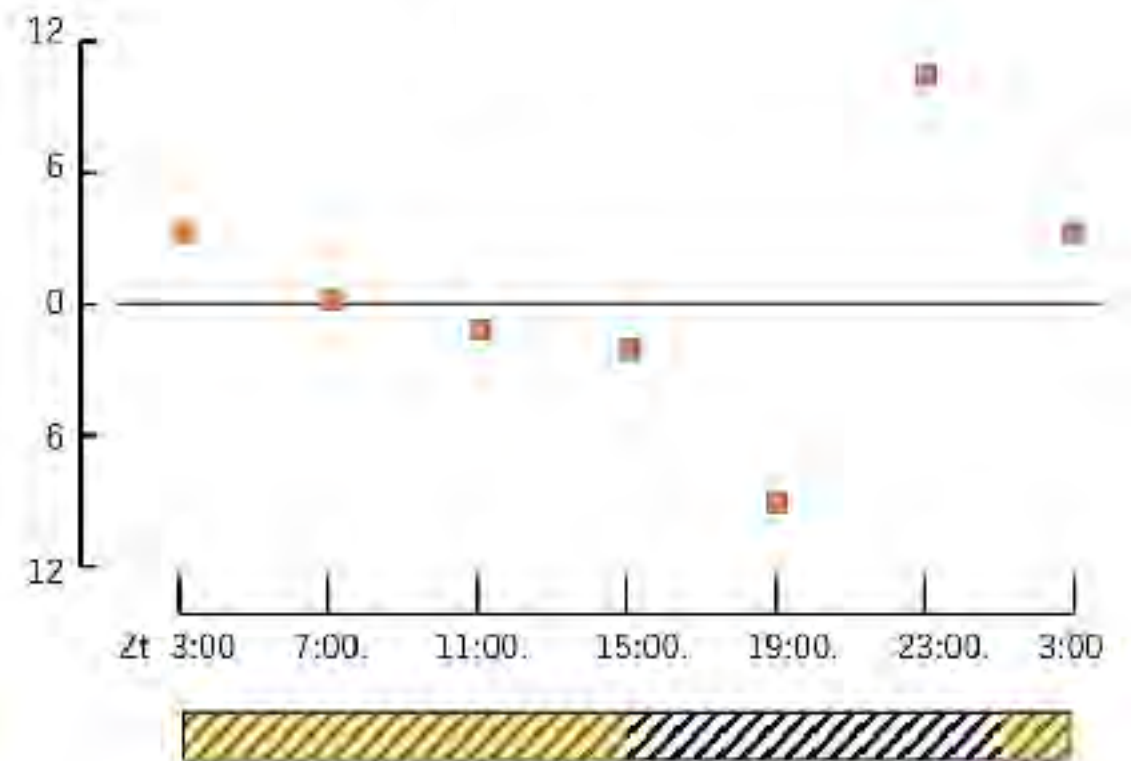
**Murasaki**  
(Standard strain)

**Flowering in the morning**

Phase shift (h)



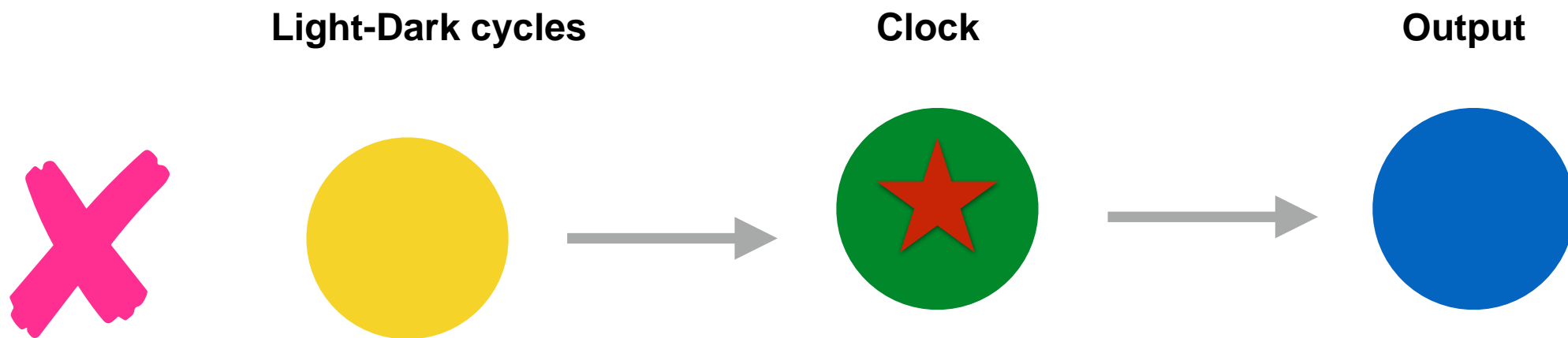
**Mexican strain (QX909)**  
**Flowering in the evening**



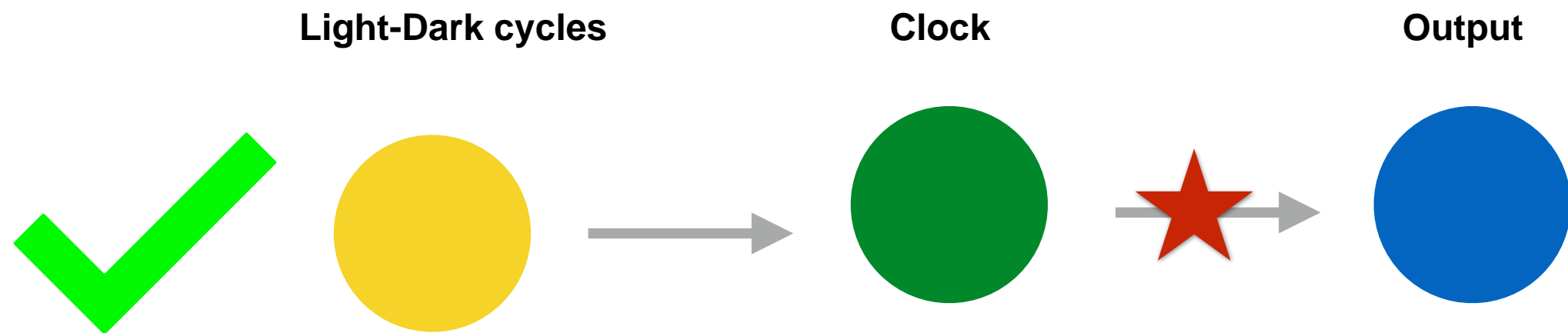
Both strains similarly responded to light

# Summary

## ① Free-run period



## ② Variation in output pathway





# Summary & acknowledgements

- The synthesized clock can be controlled by temperature
- Output can be more precise than clock
- There is unknown mechanism controlling flowering time

## Cyanobacteria

**Yoriko Murayama, Hideo Iwasaki** (Waseda)  
**Irina Mihalcescu** (Université Grenoble Alpes)  
**Hotaka Kaji, Akari Ishihara** (Kyushu)  
**Late Takao Kondo** (Nagoya)

## Morning glowly

**Eiji Nitasaka** (Kyushu)  
**Tokitaka Oyanma** (Kyoto)

## Jellyfish

**Nozomi Yamada** (Kyushu)  
**Masahiro Shimizu** (Nagahama)  
**Shuhei Ikeda, Kazuya Okuizumi** (Kamo Aqualium)

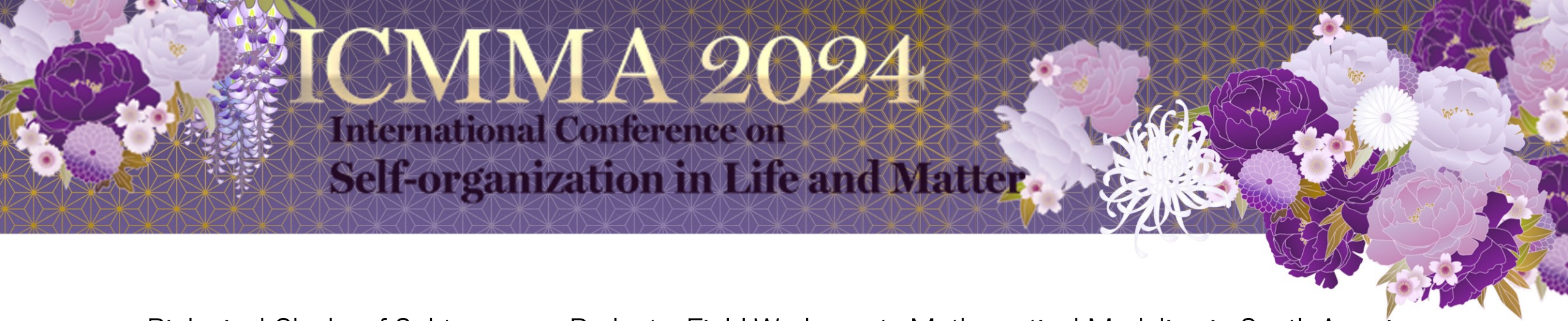
## Theory for fluctuations

**Kaiji Hotaka, Fumito Mori** (Kyushu)  
**Hiroshi Kori** (Tokyo)

Nakamura-san







## Biological Clocks of Subterranean Rodents: Field Work meets Mathematical Modeling in South America

Gisele A. Oda, Veronica S. Valentinuzzi

(Laboratório Binacional Argentina-Brasil de Cronobiologia, CRILAR Argentina, University of São Paulo, Brazil)

Photic synchronization mechanisms of biological clocks have long been investigated in model species, under manipulation of light/dark cycle parameters in the laboratory. In particular, it has been shown that even daily minute light pulses are able to synchronize circadian oscillators, being this a link between biological clock studies and periodically pulsed oscillator theories. Parallel lines of investigation, have considered how wild organisms are daily exposed to the light/dark cycle in nature, questioning the artificially imposed light/dark conditions in the lab and associated models. Wild organisms that inhabit the extreme photic environment of the subterranean provide an opportunity to verify persistence and minimal photic input for daily and seasonal synchronization. Here we present our joint field, laboratory and modeling work investigating the chronobiology of subterranean rodents known as “tuco-tucos” (*Ctenomys coludo*), which are widespread in South America. Using miniature bio-loggers, we obtained automated, continuous and individual recordings of daily light exposure and activity rhythms of these desert subterranean animals (La Rioja, Argentina, 32°S Latitude), which revealed how they expose to light throughout the 24h and the drastic changes of these patterns throughout the seasons. The joint analysis of seasonal variation of daily light exposure and the associated changes in daily activity rhythms enabled testing the two-oscillator model of the biological clock, whose seasonal changes in phase relationship accounts for decoding of daylength in mammals. By using minimal light inputs in computer simulations, we developed a mathematical model of a clock that works for all seasons, even in the subterranean. Support: (FAPESP, CONICET, CAPES, CNPq).

# Biological Clocks of Subterranean Rodents: Field Work meets Mathematical Modeling in South America

Gisele Oda & Veronica Valentinuzzi  
Laboratorio Binacional de Cronobiologia  
Argentina - Brasil

USP/CRILAR

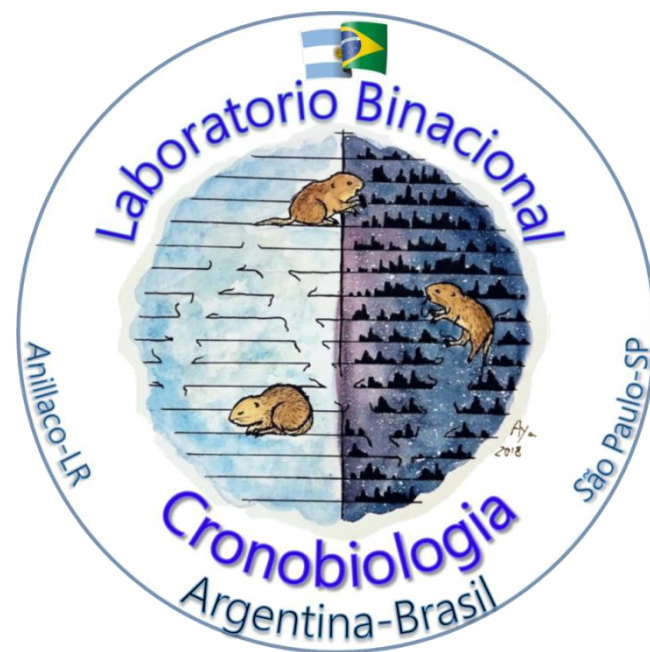






**Dr. Veronica Valentinuzzi - CRILAR, La Rioja, Argentina**





CONICET





## Extreme Photic Environments:

- Subterranean
- Caves
- Deep Sea
- Arctic...

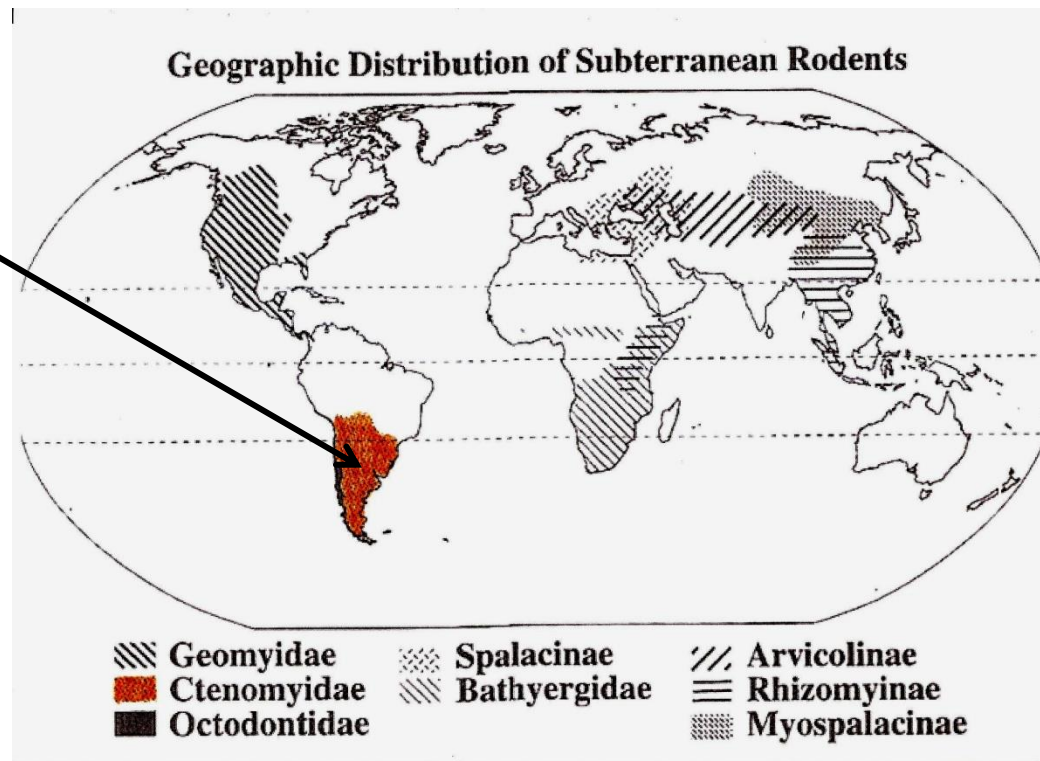
Night and Day?  
Seasons?





## TUCO-TUCO

*Ctenomys coludo*



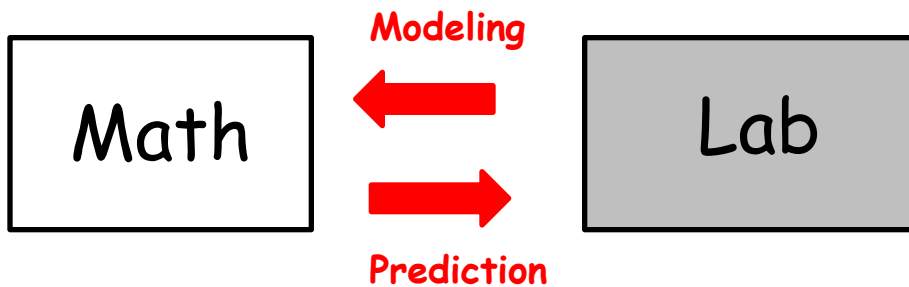
(Stein, 2000)





**TUCO-TUCO**

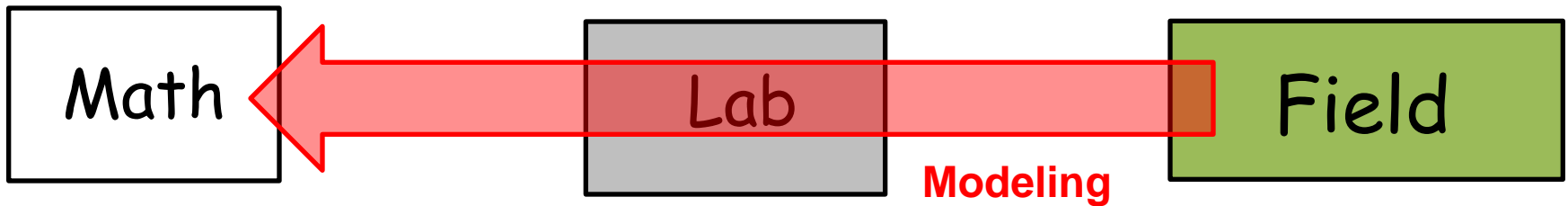
*Ctenomys aff. knighti*





## TUCO-TUCO

*Ctenomys aff. knighti*



**Prediction**

# **LAB studies**



0

12h

24h

Days

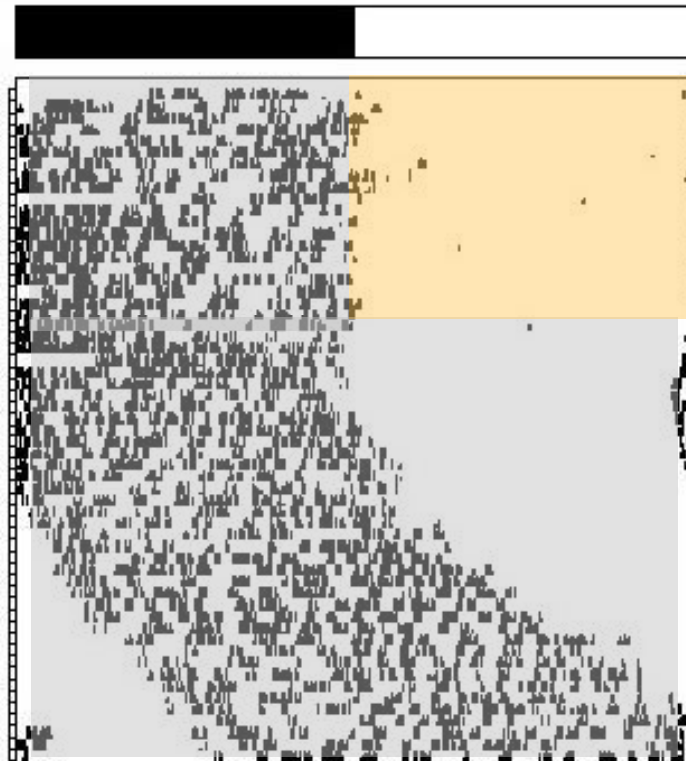


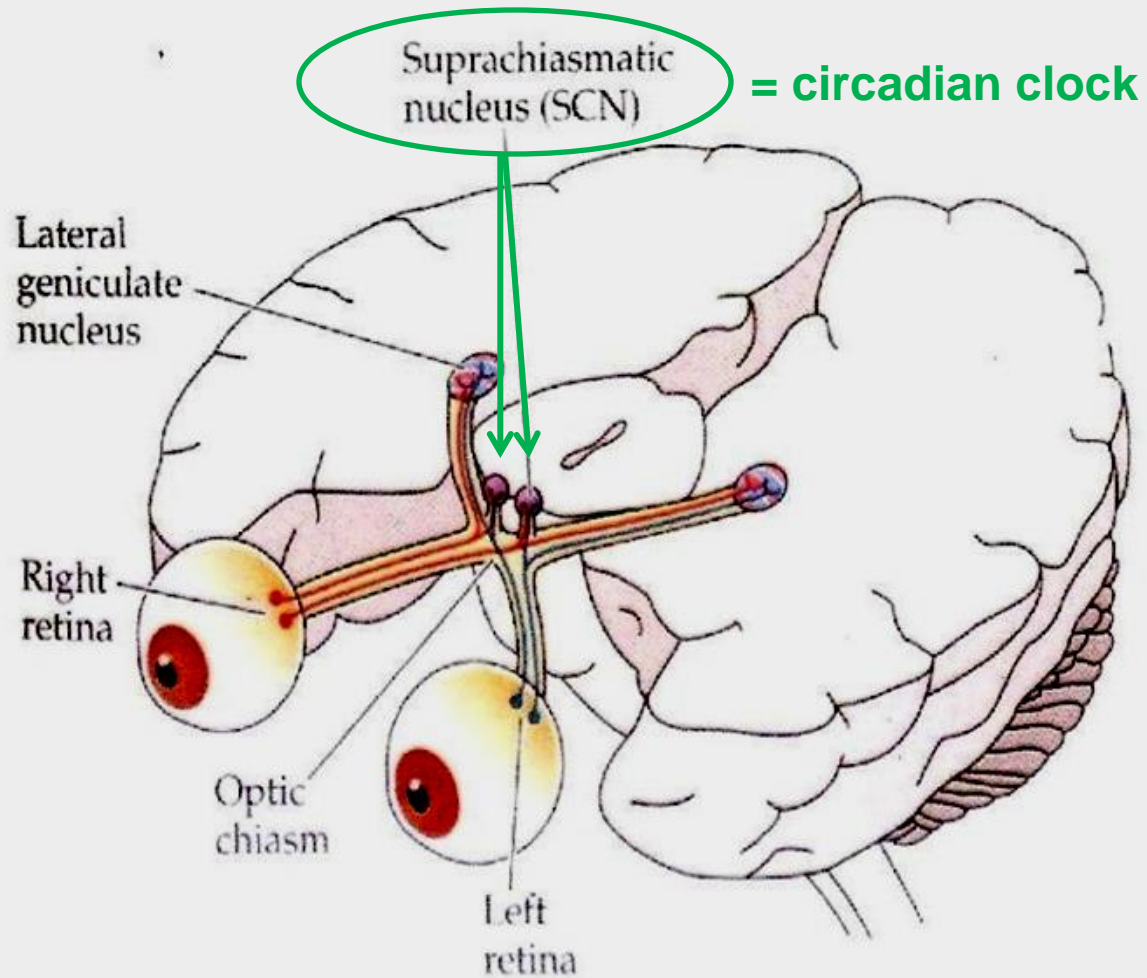


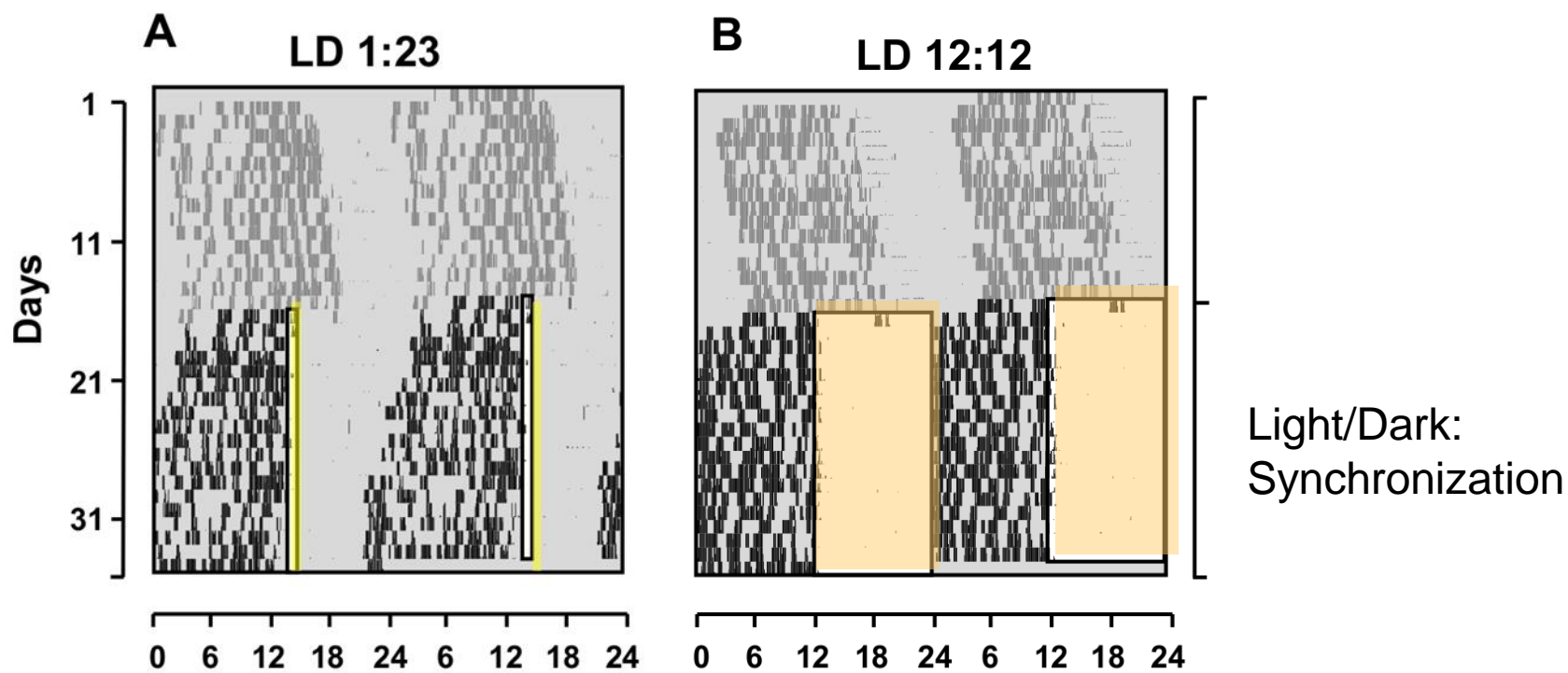


synchronized

Free-running

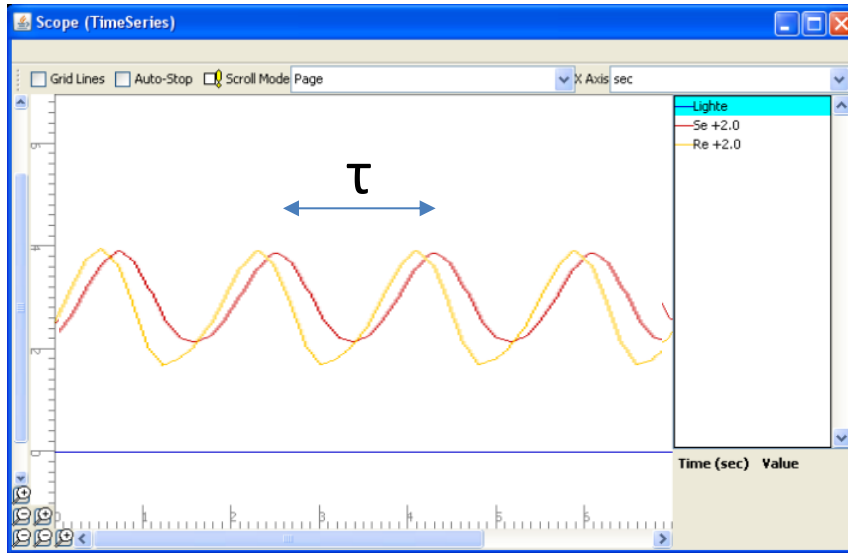






(Flôres et al., PlosOne 2013)

# Mathematical Model of Photic Synchronization

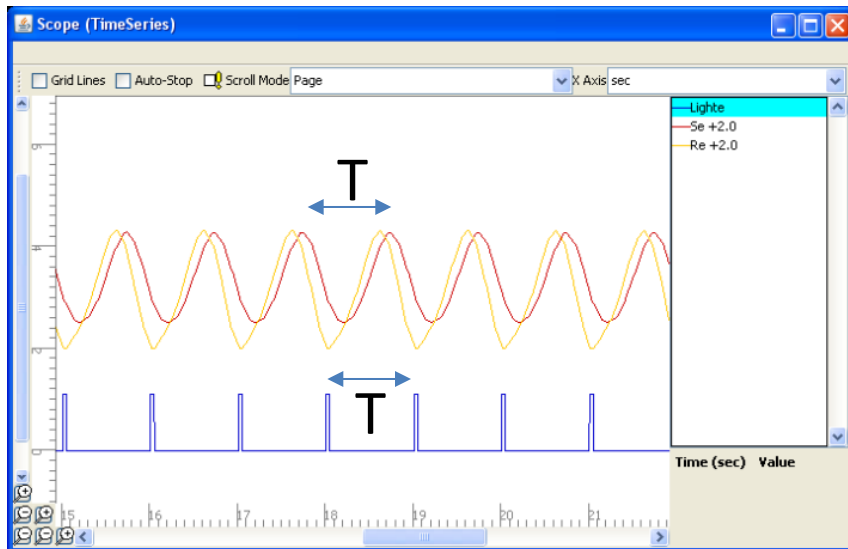


Free Limit-Cycle Oscillator

$$\begin{aligned} dR/dt &= R - cS - bS^2 + d + K \\ dS/dt &= R - aS \end{aligned}$$

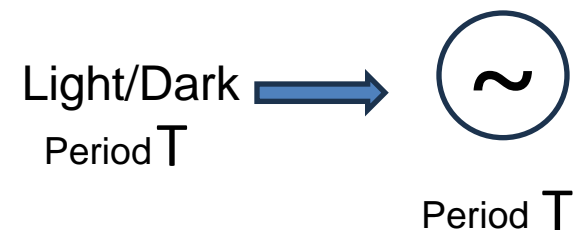


Period  $\tau$



Periodically Forced  
Limit-Cycle Oscillator

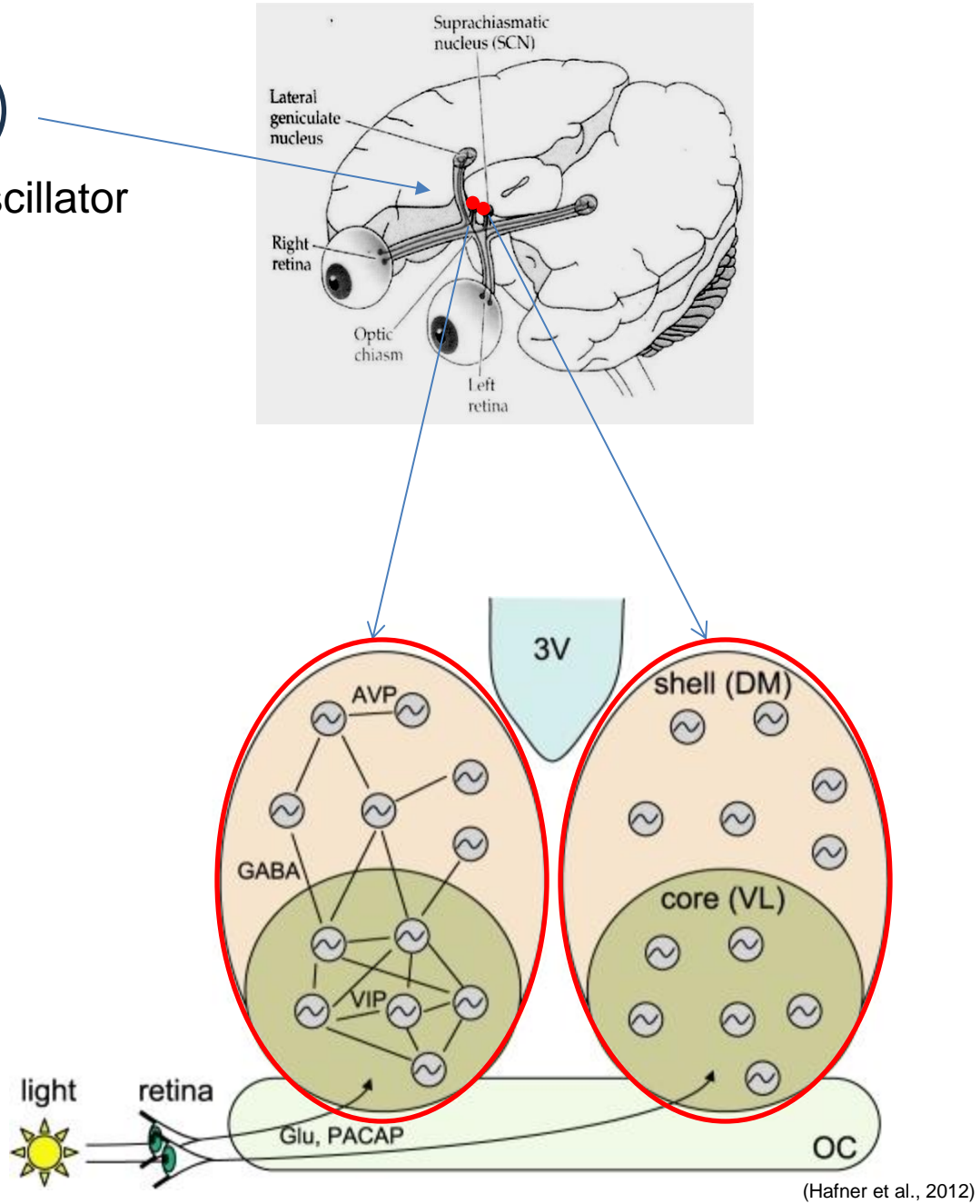
$$\begin{aligned} dR/dt &= R - cS - bS^2 + (d - L) + K \\ dS/dt &= R - aS \end{aligned}$$



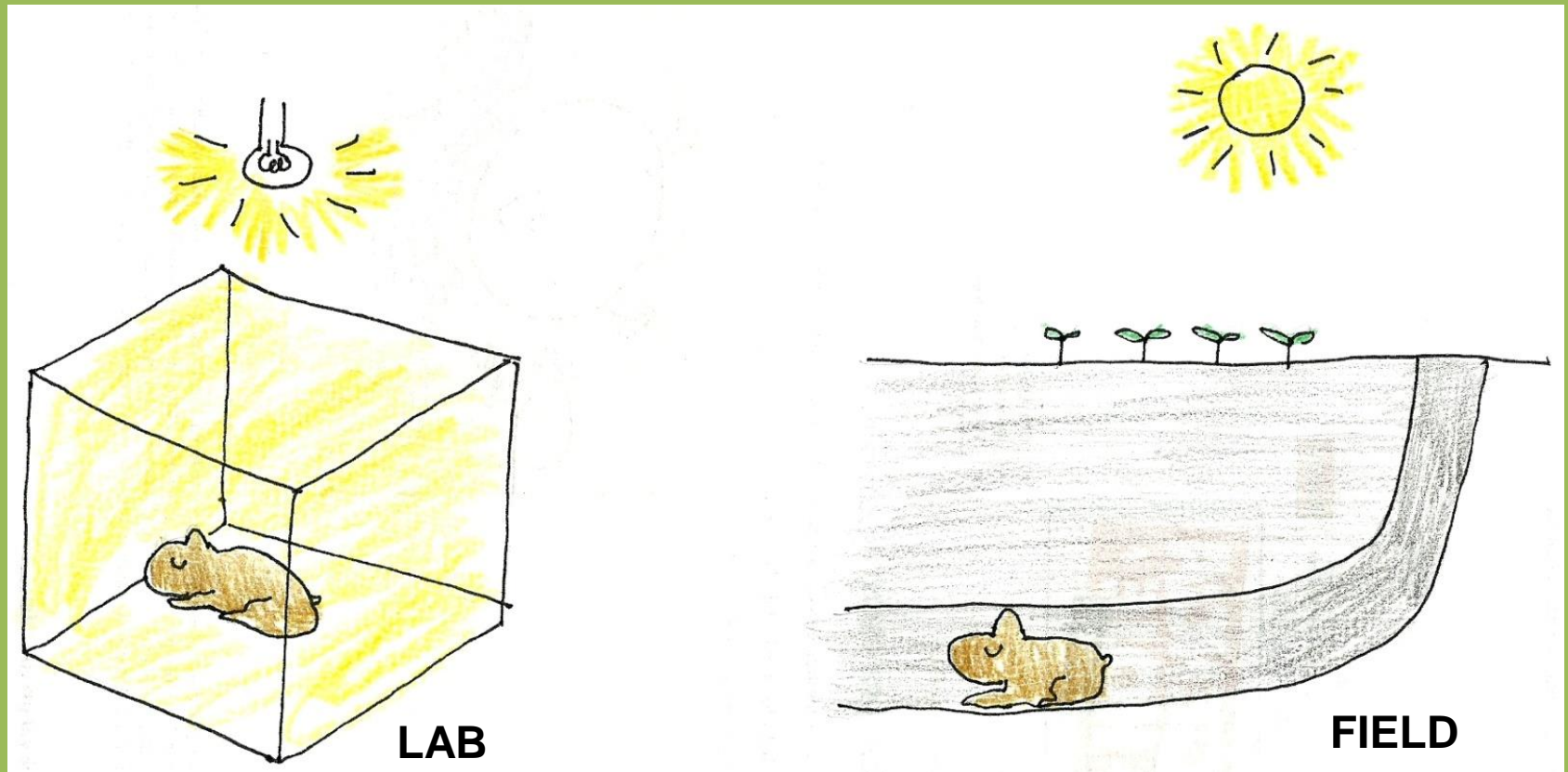




Circadian oscillator



But... When do the tuco-tucos **expose to light** in the "real world"?



How is synchronizaton achieved in the field?...





In the Field...



## TUCO-TUCO

*Ctenomys aff. knighti*

Math

Lab

"Semi"  
Field!

Field

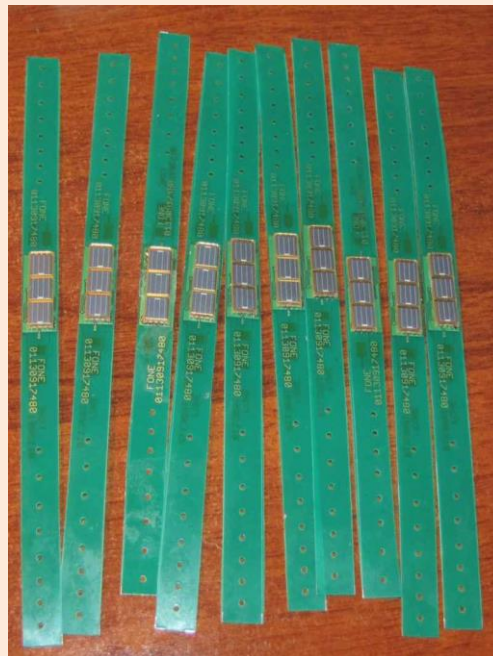
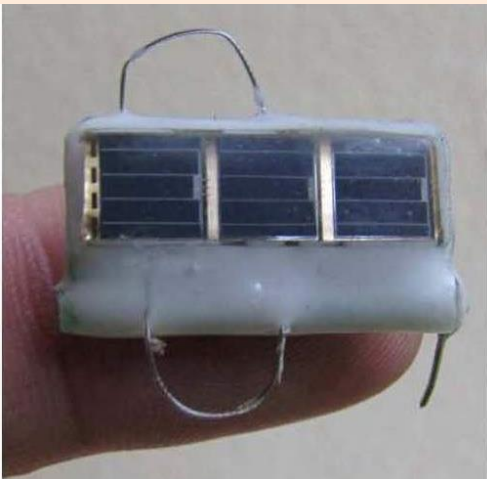
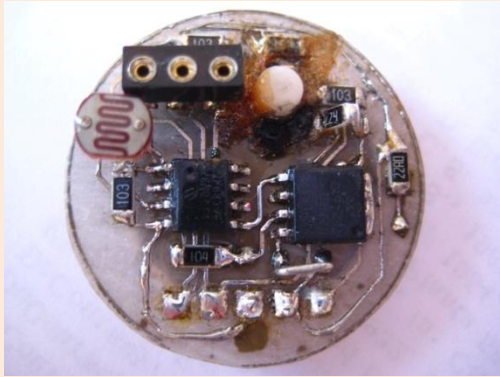


## "Semi-Field"

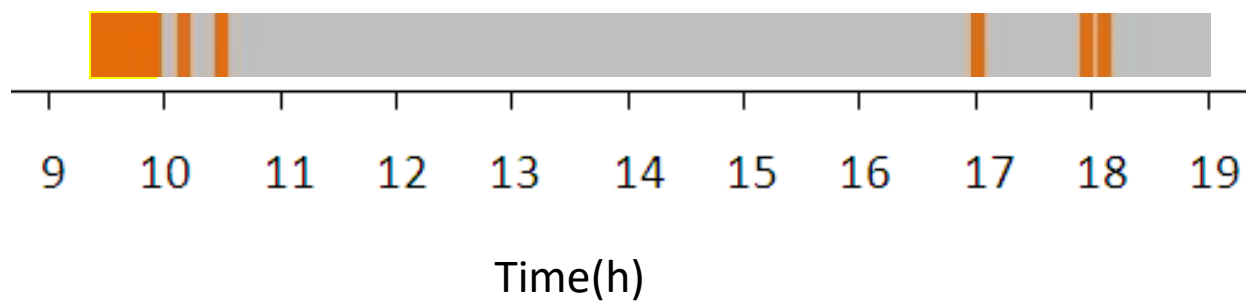
2008



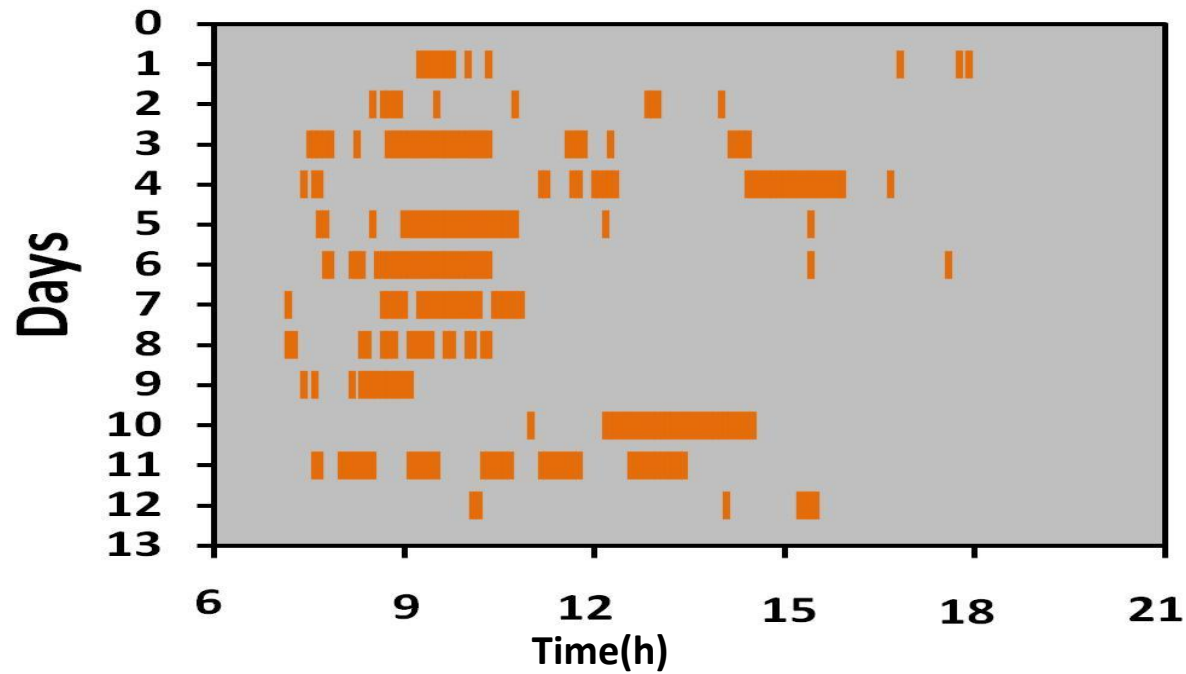
# Evolution of our light- registration method: 2008-2013







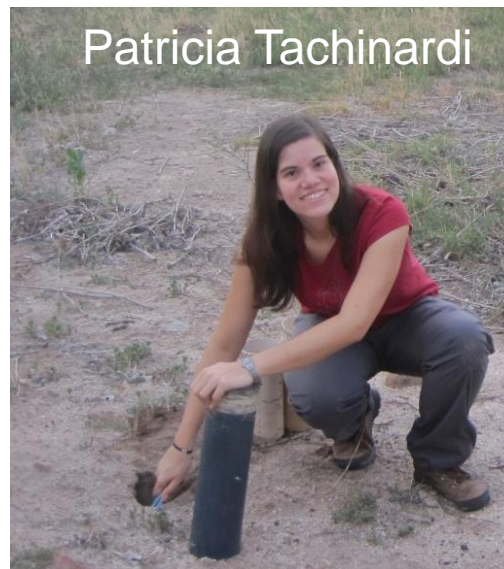
# Light-exposure - summer 2010



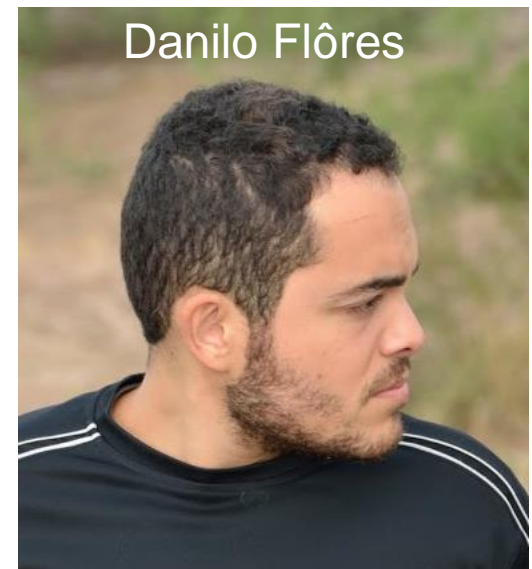
(Tomotani et al. 2012,  
PlosOne)



Barbara Tomotani



Patricia Tachinardi

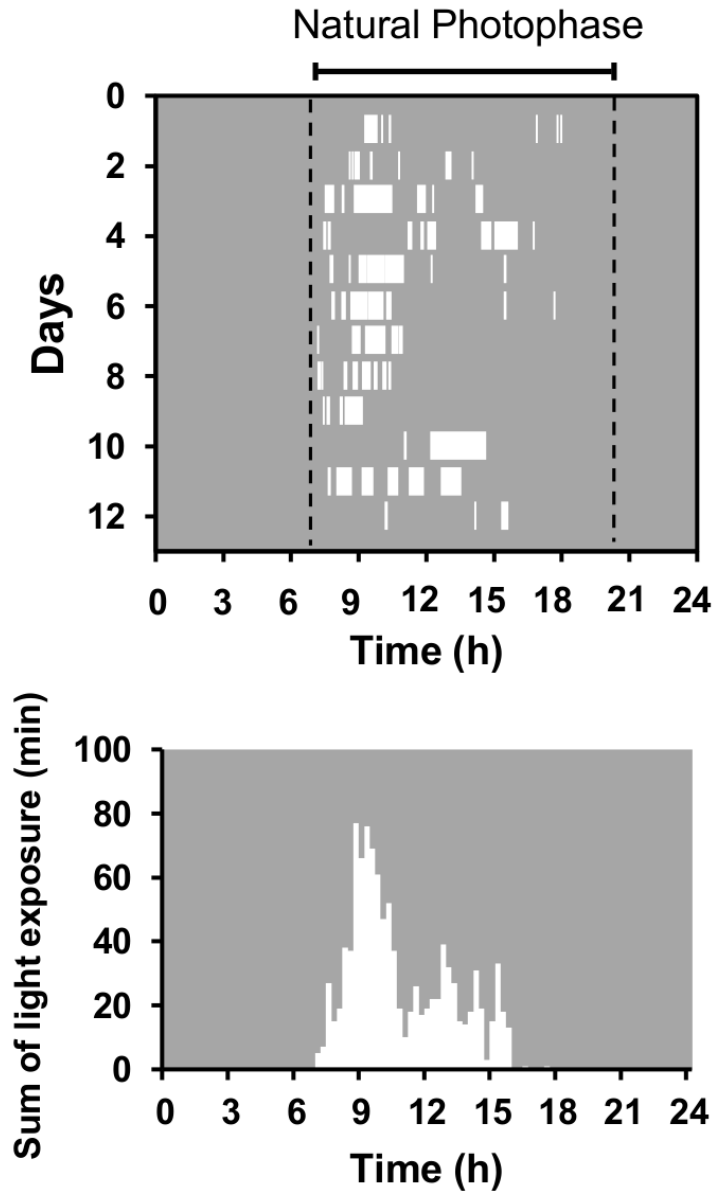


Danilo Flôres



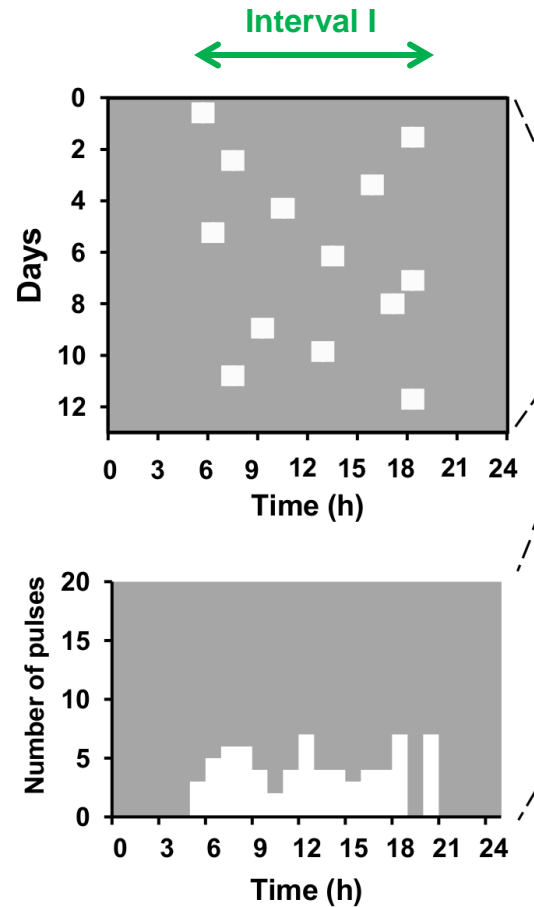
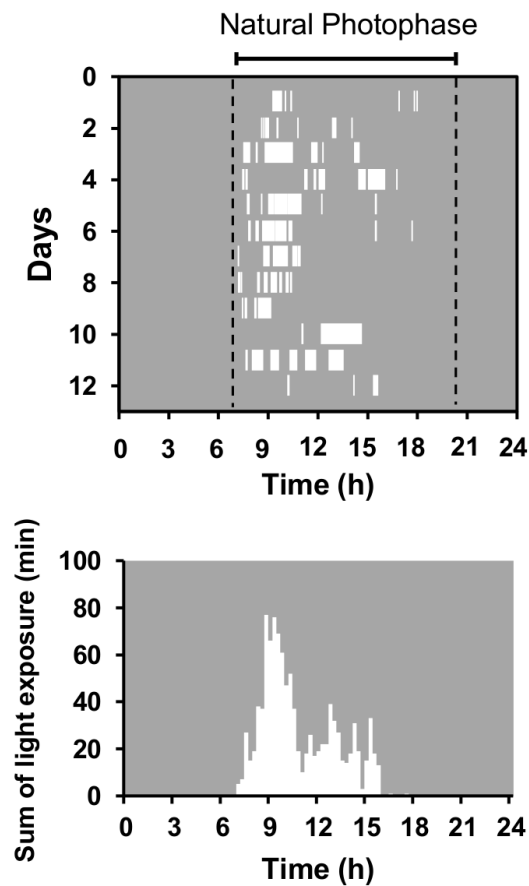


## Natural Light Exposure



**Is a random daily exposure to light  
sufficient for photic synchronization?**

# Modeling



## Simplest model:

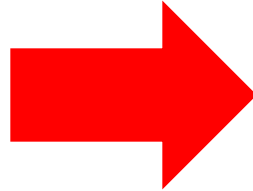
- 1 pulse per day
- Uniform light intensity
- Uniform probability for occurring any time in na **interval I**

(Flôres et al., PlosOne 2013)

Day light

Model

1 random light pulse at any time  
in a **interval I**



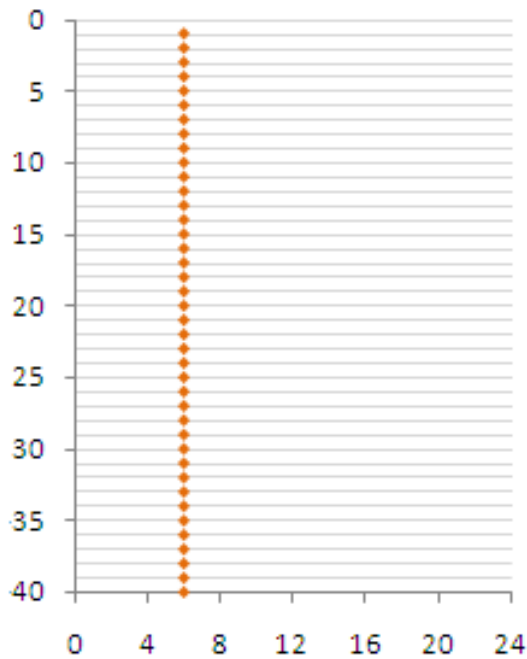
Circadian oscillator of the tuco-tuco

Limit-cycle oscillator

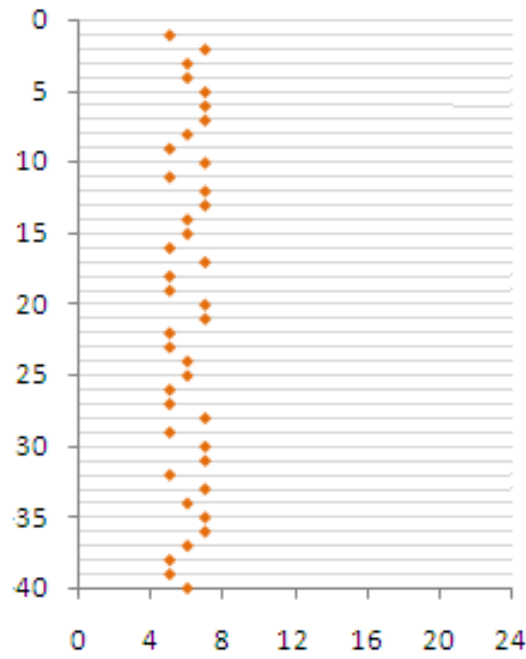


Limits of the  
day-length ( $l$ ) that allows synchronization of  
limit-cycles by random pulses.

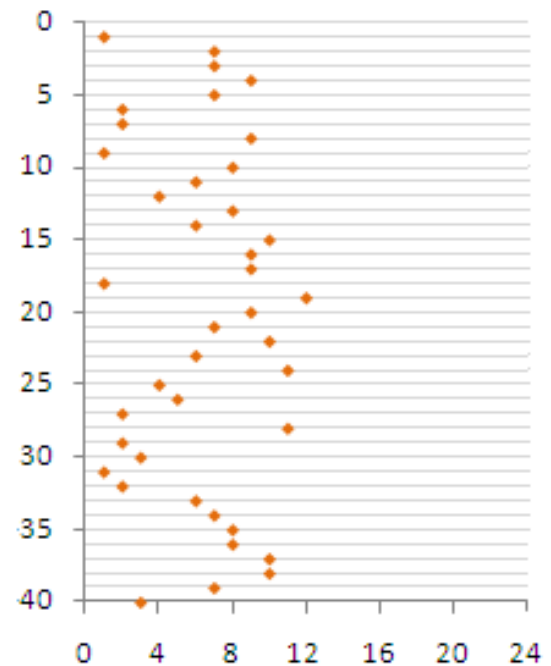
$l=0$

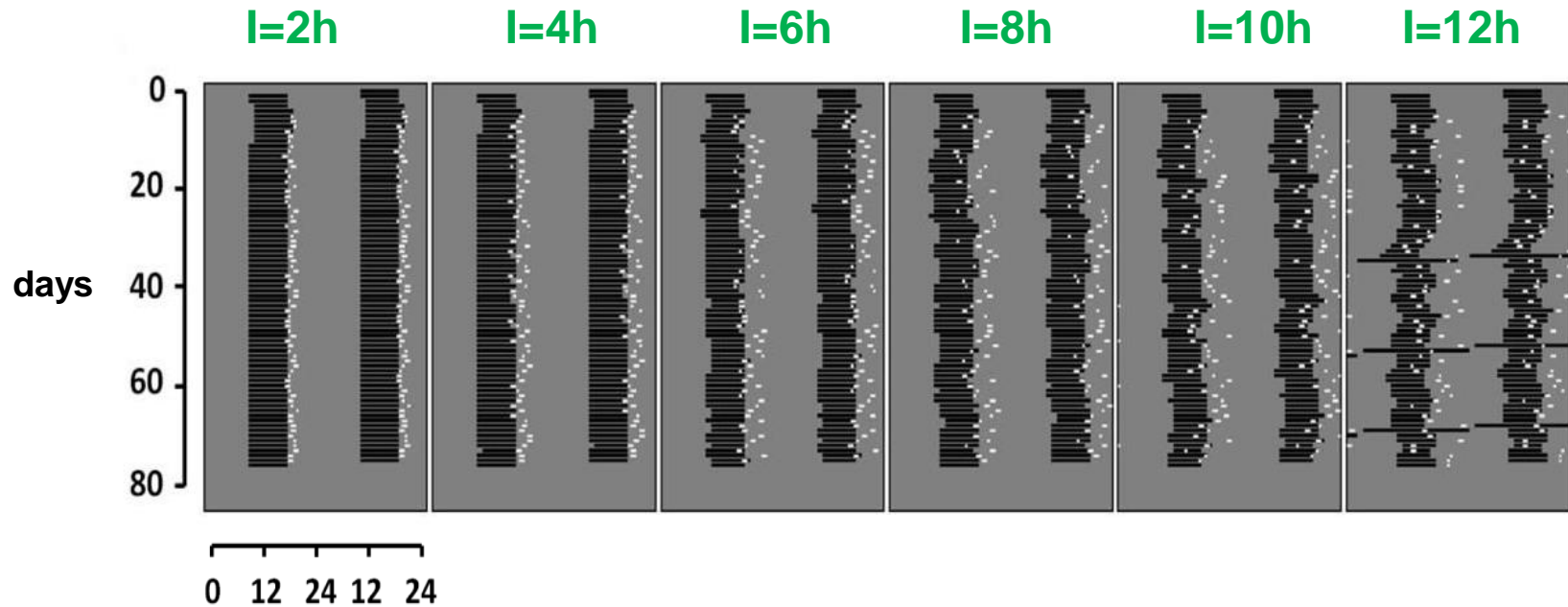


$l=4h$

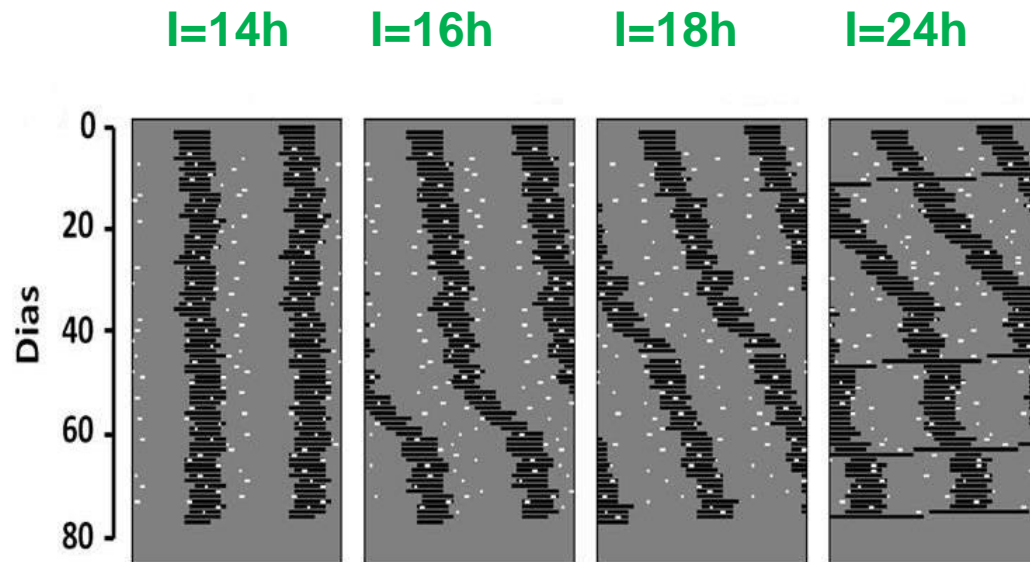


$l=12h$

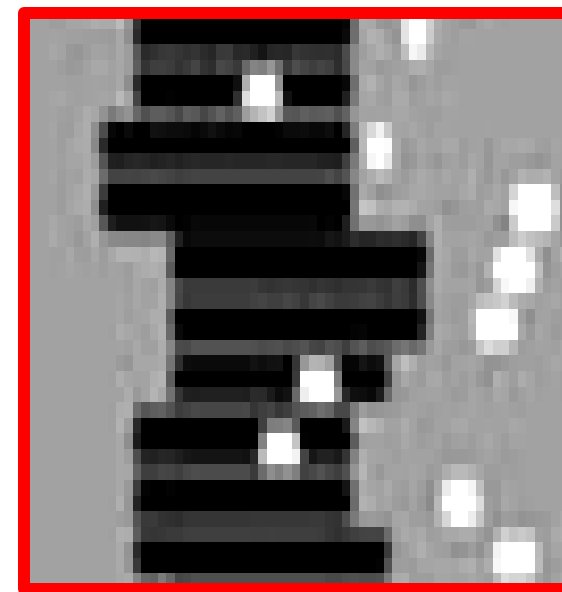
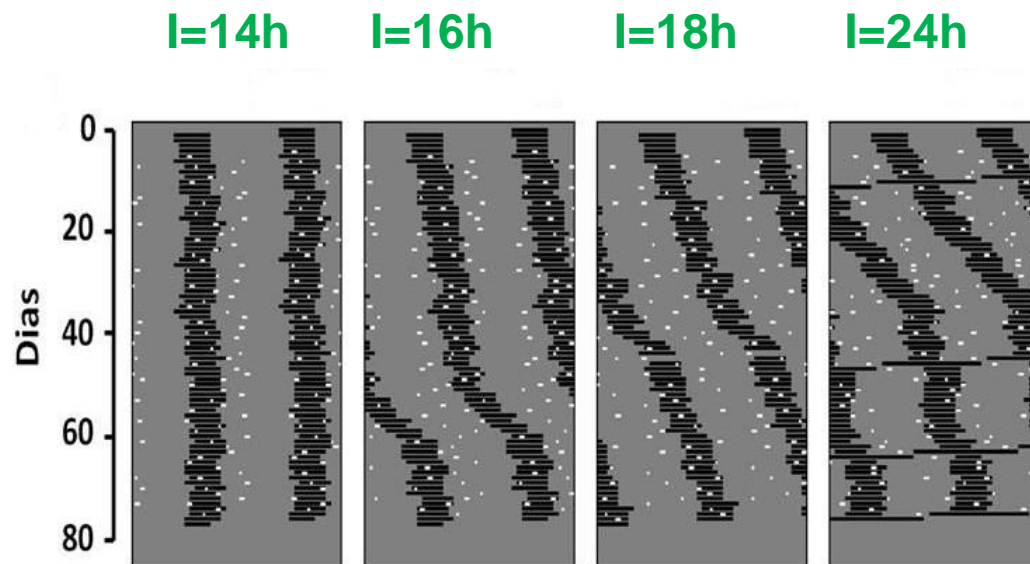
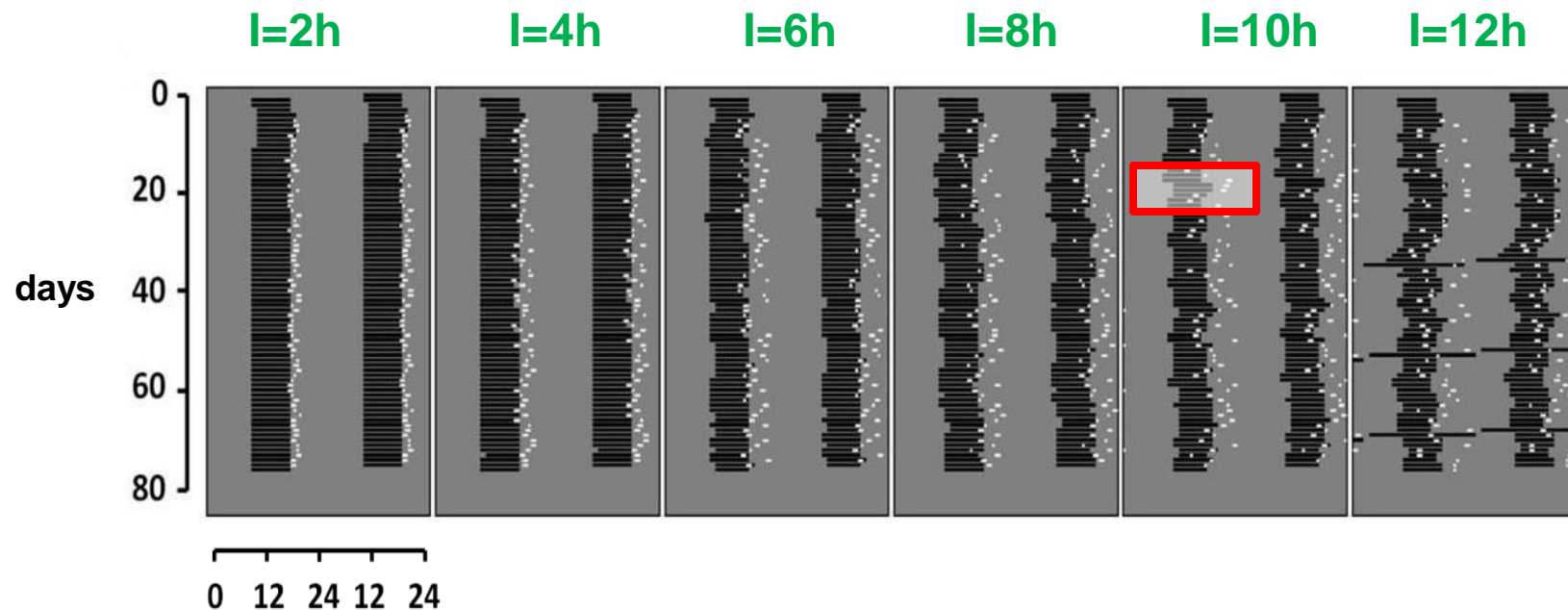




Computer simulations

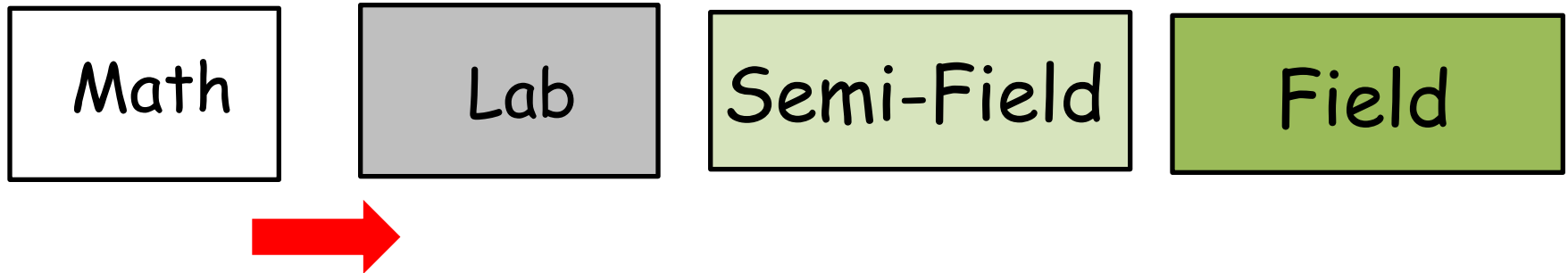


(Flôres et al., PlosOne2013)



## Unexpected Prediction from the Model:

Prediction!



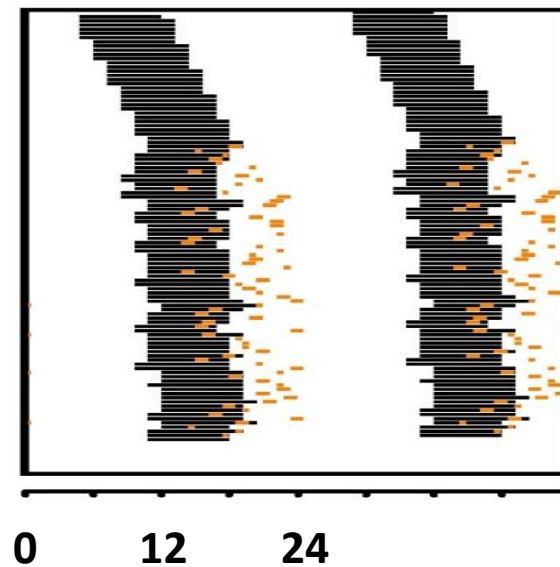
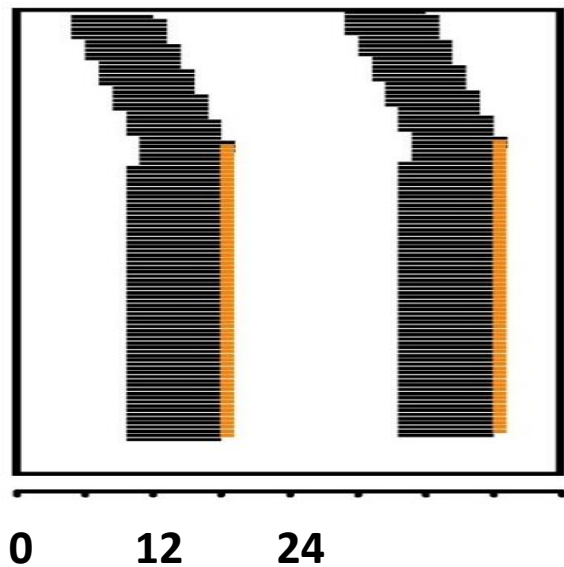
Even a single pulse at a random time  
spread in a 10h interval, per day,  
is sufficient to synchronize the  
circadian oscillator to 24h period!



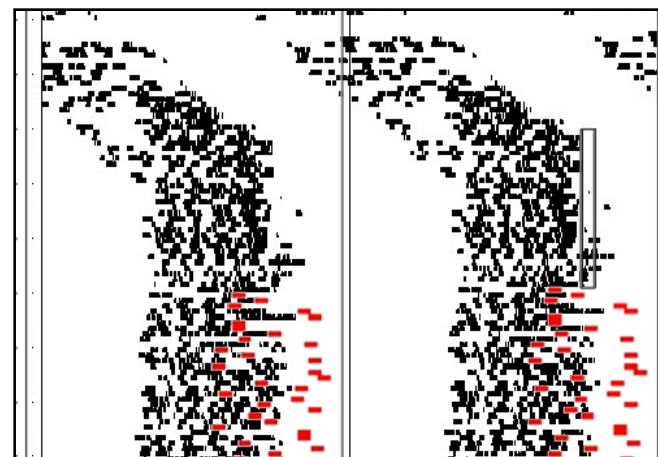
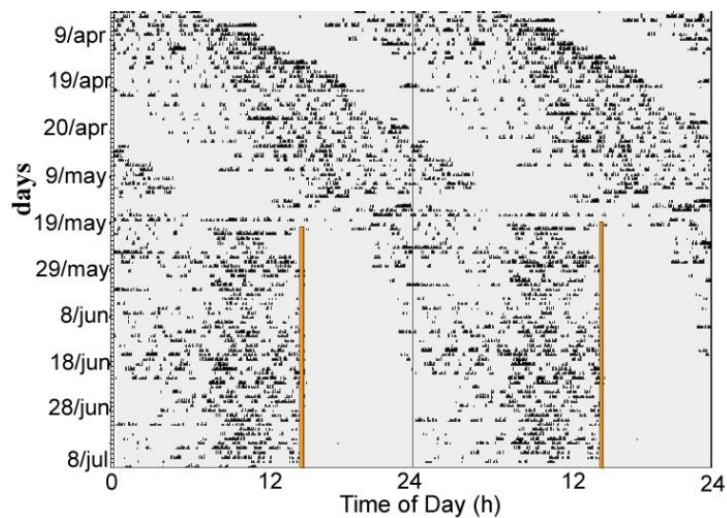
Test the theoretical prediction using one more oscillator:



The circadian clock of the tuco-tuco!



model



experiment

(Flôres et al., Scientific Reports 2016)



Danilo Flôres



Barbara Tomotani



Patricia Tachinardi





<http://www.polarfield.com/blog/tag/loren-buck/>

Dr. Loren Buck, University of Alaska



## Evolution of light sensor method: 2014



Photo: Milene Jannetti

0.42g, 1 min interval,  
11 month battery, 30 month memory  
(Migrate Company, UK)



**New “Semi-Natural” enclosures**



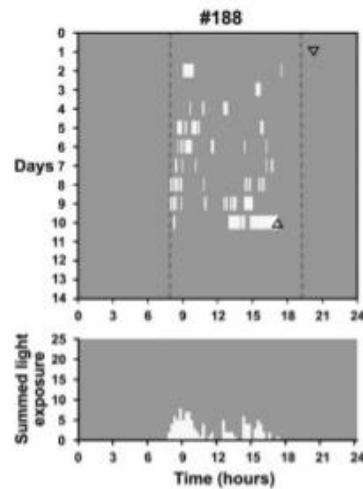
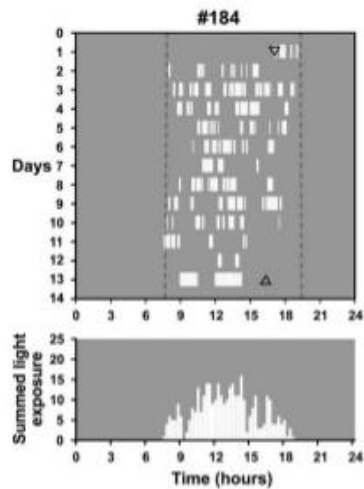
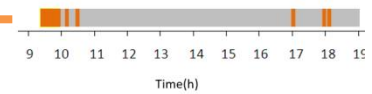
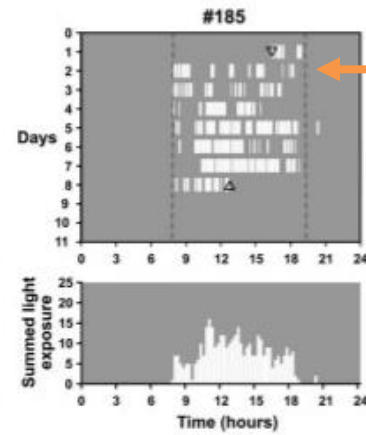
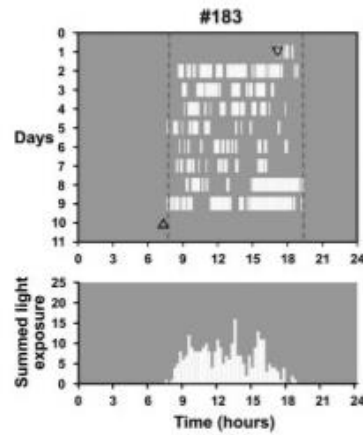
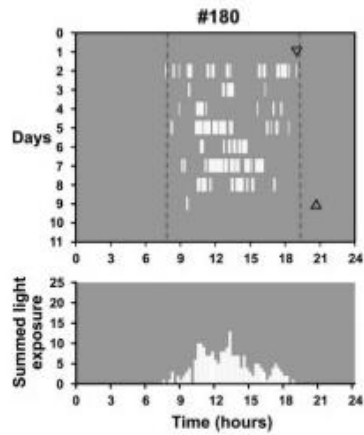
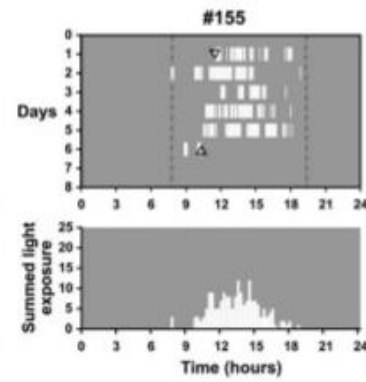
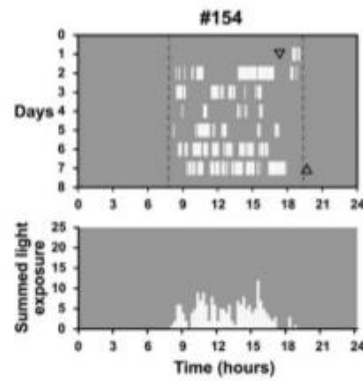
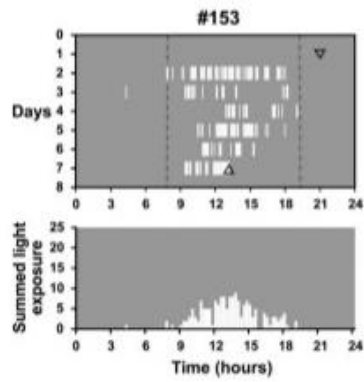


Foto: Milene Jannetti









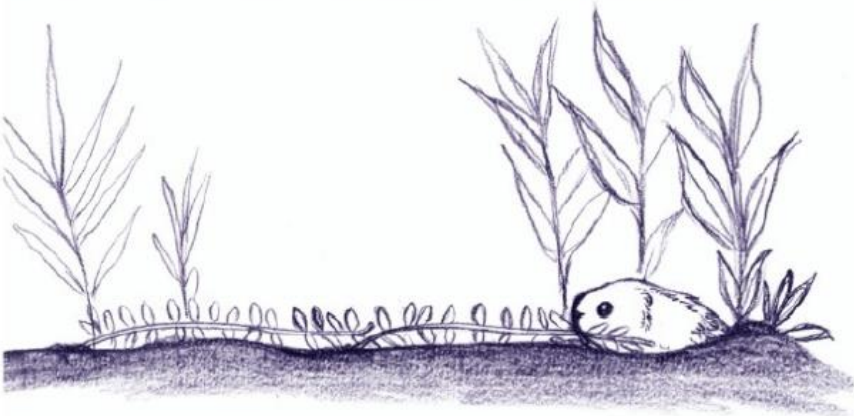
(Flôres et al. 2016, Scientific Reports)

# What they do on surface?...

**foraging**



**soil removal**

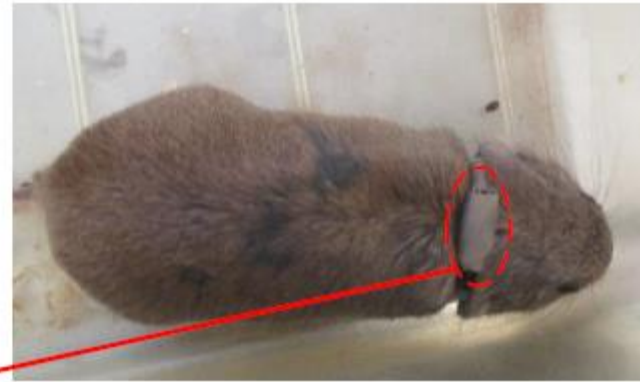


**"nothing"**

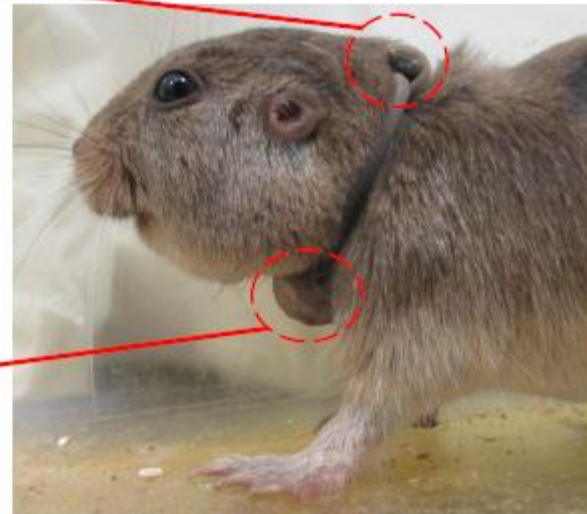


(Photo and illustration:  
Barbara Tomotani)

# Miniature "Biologgers" since 2017: light + activity



Light-logger

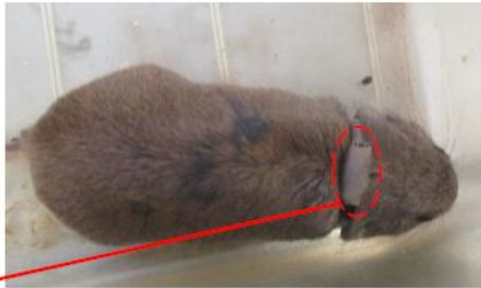


**Accelerometer**

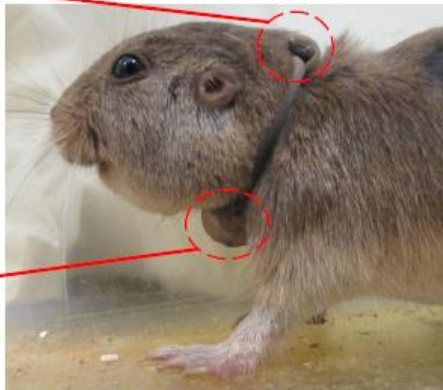
2g, 10 Hz, 40 day memory  
(Axy-4, Technosmart, IT)

(Figure: Milene Jannetti)

**lightlogger**

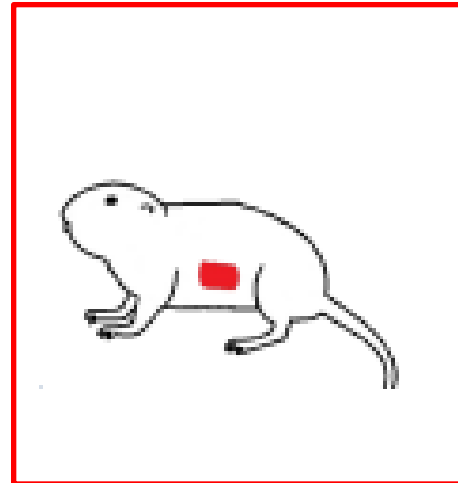


**accelerometer**



**+**

**2019: + temperature logger**





24h



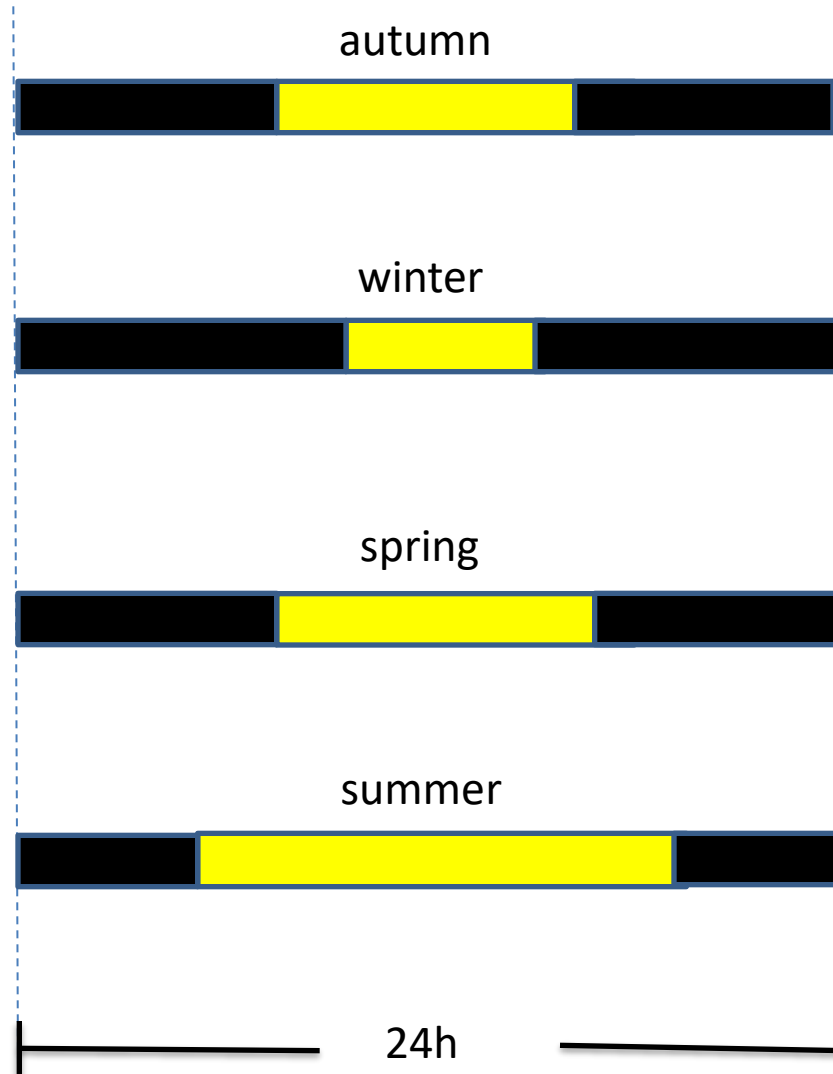
365 days

Photoperiodism?...

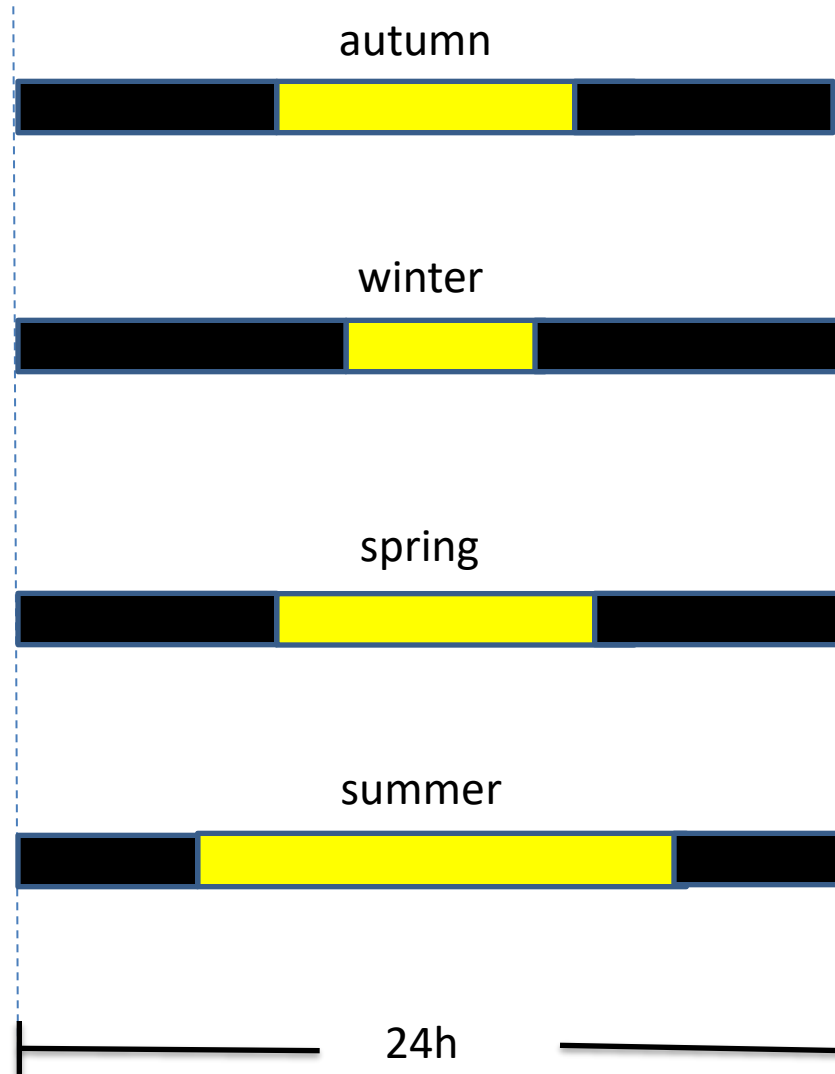




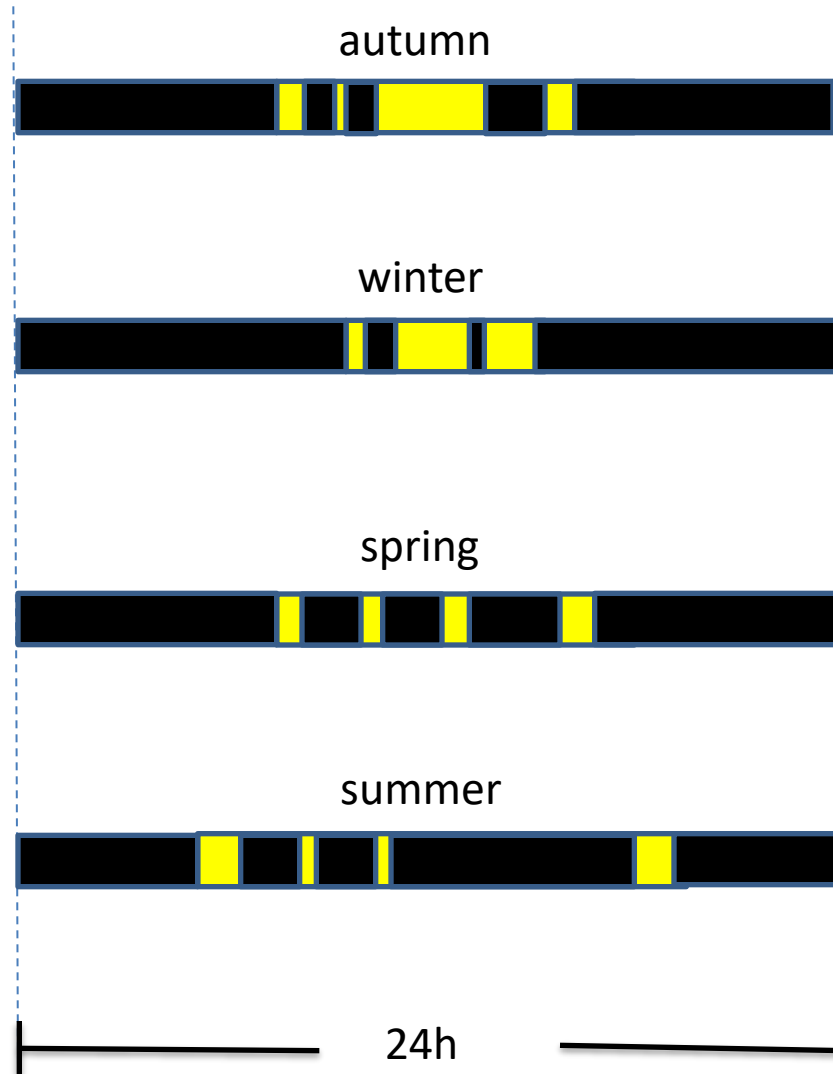
Annual variation of **Photoperiod** (ratio daylength/nightlength)



# How do organisms measure photoperiod?!



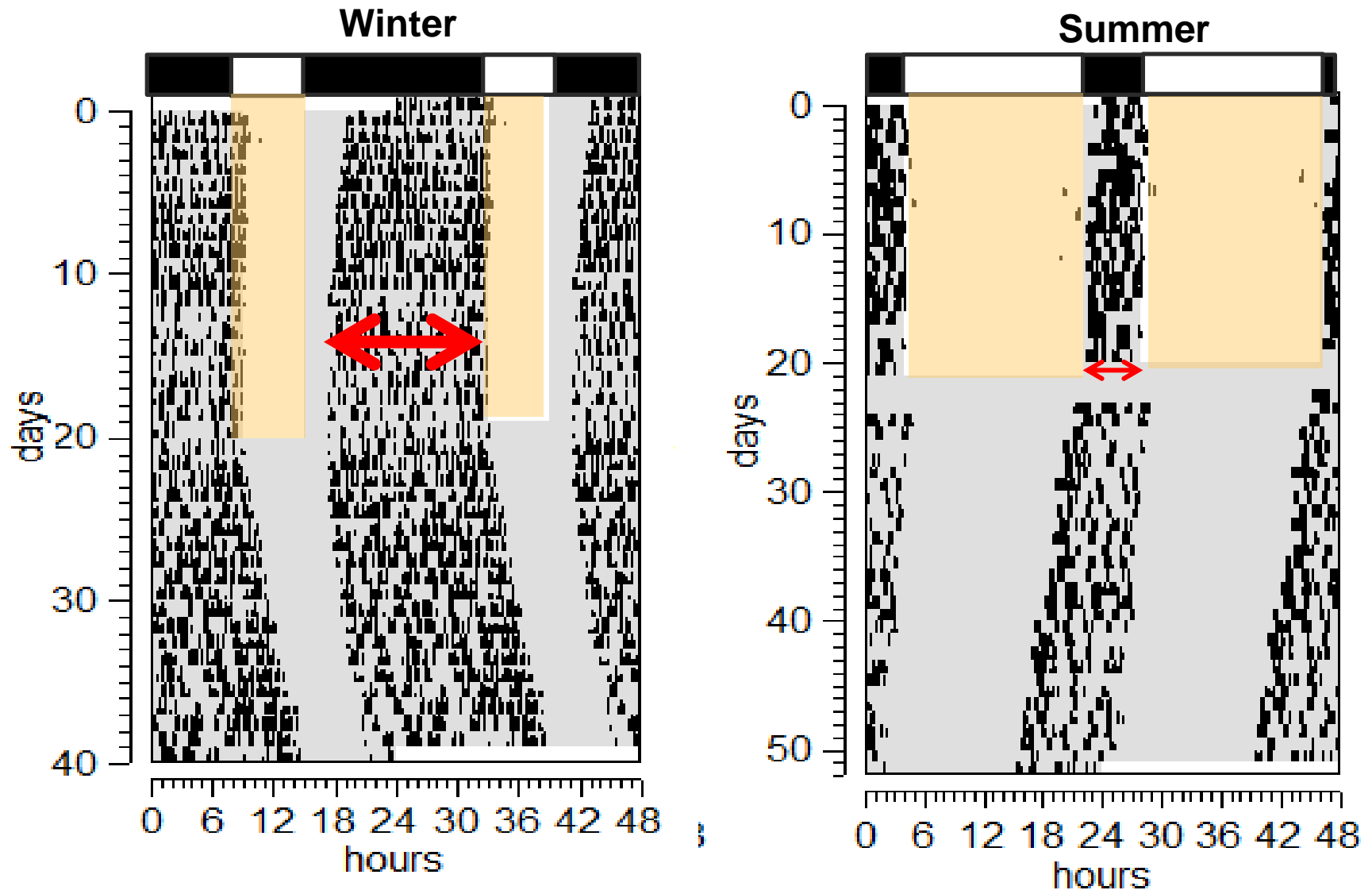
# How does the tuco-tuco measure photoperiod?!





# Artificial Photoperiods in the LAB

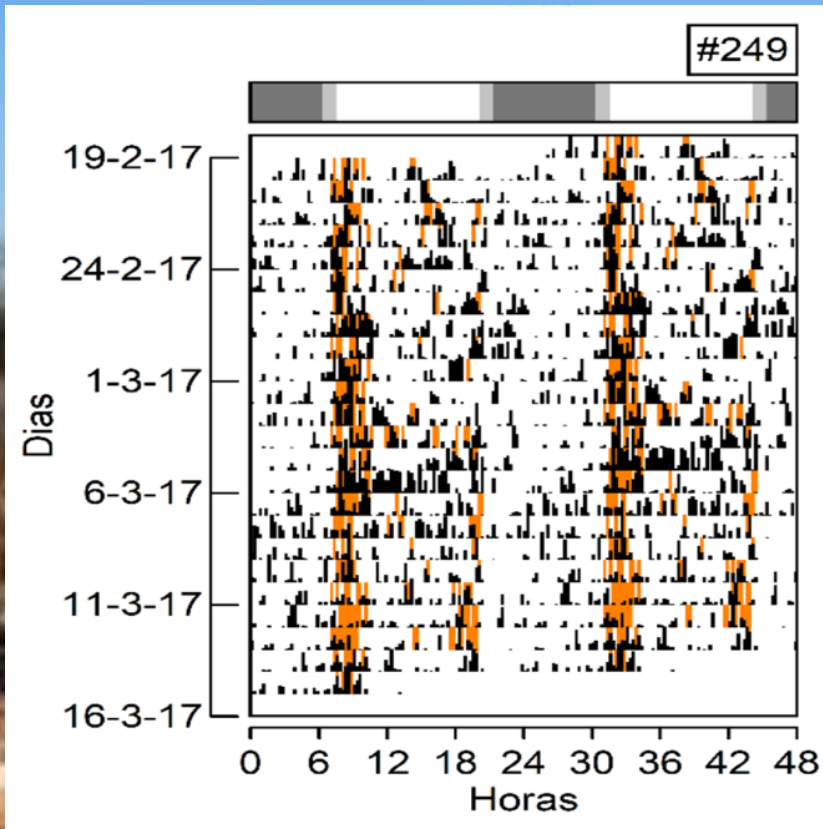
Activity duration changes



(Improta et al., J Biol Rhythms 2022)

## In the Field

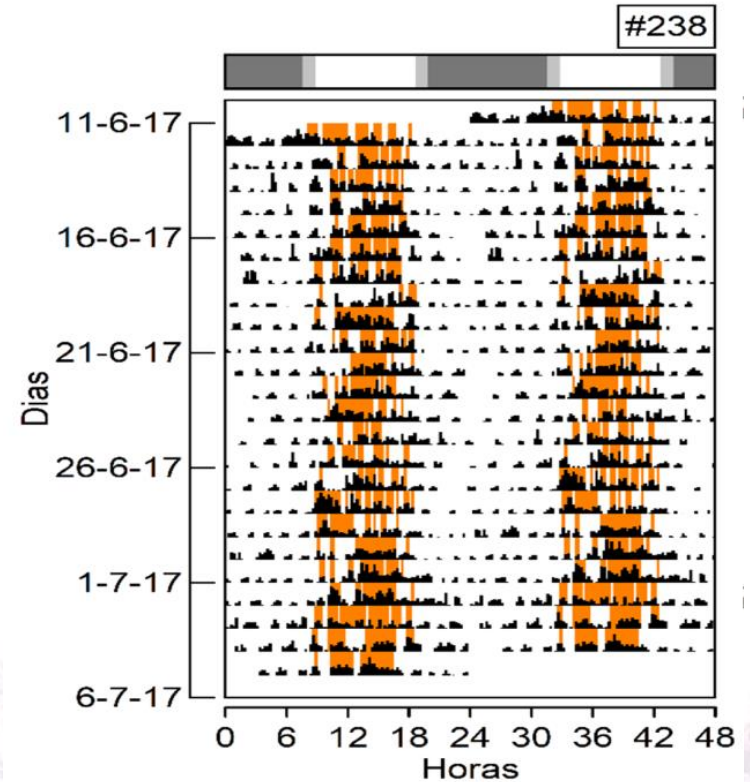
Summer



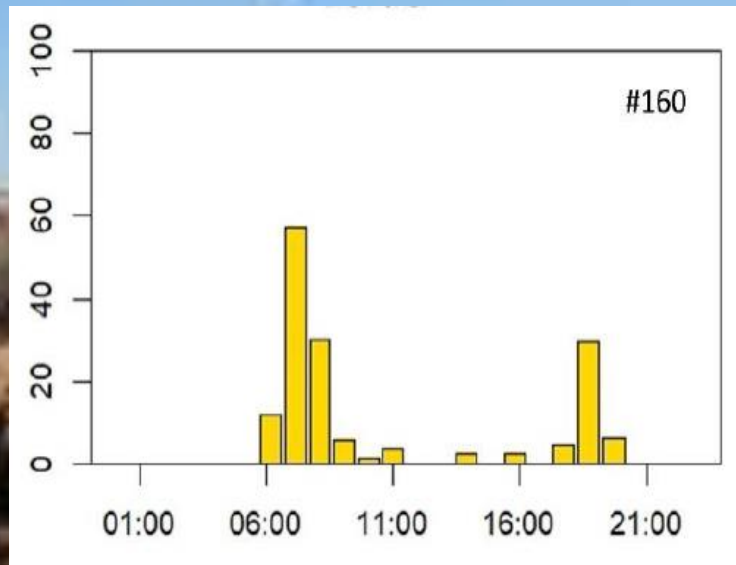
light exposure

activity

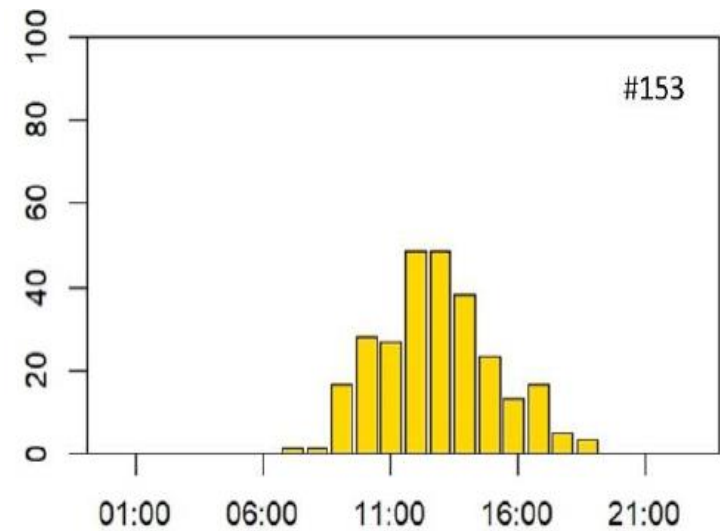
Winter



## Summer

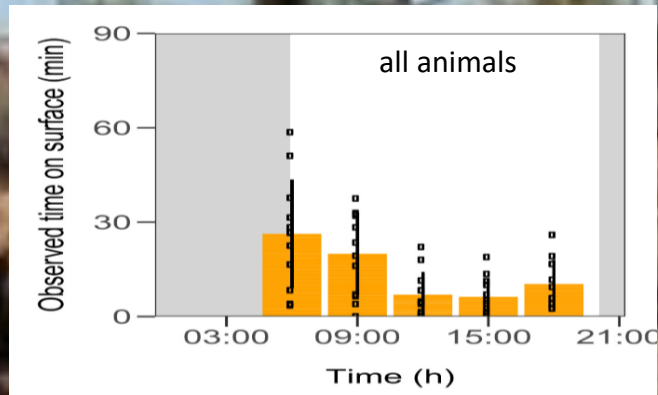


## Winter

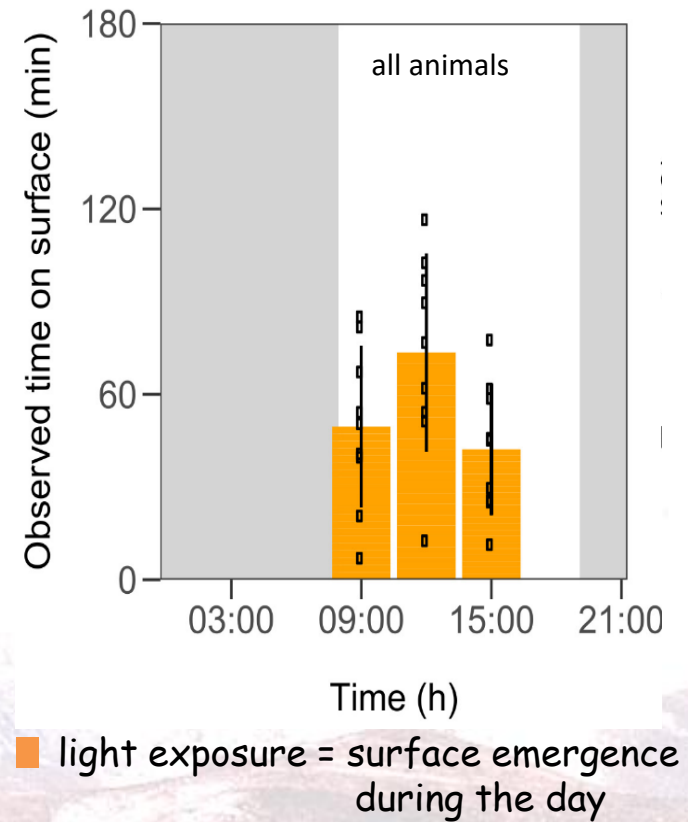


■ light exposure = surface emergence during the day

## Summer

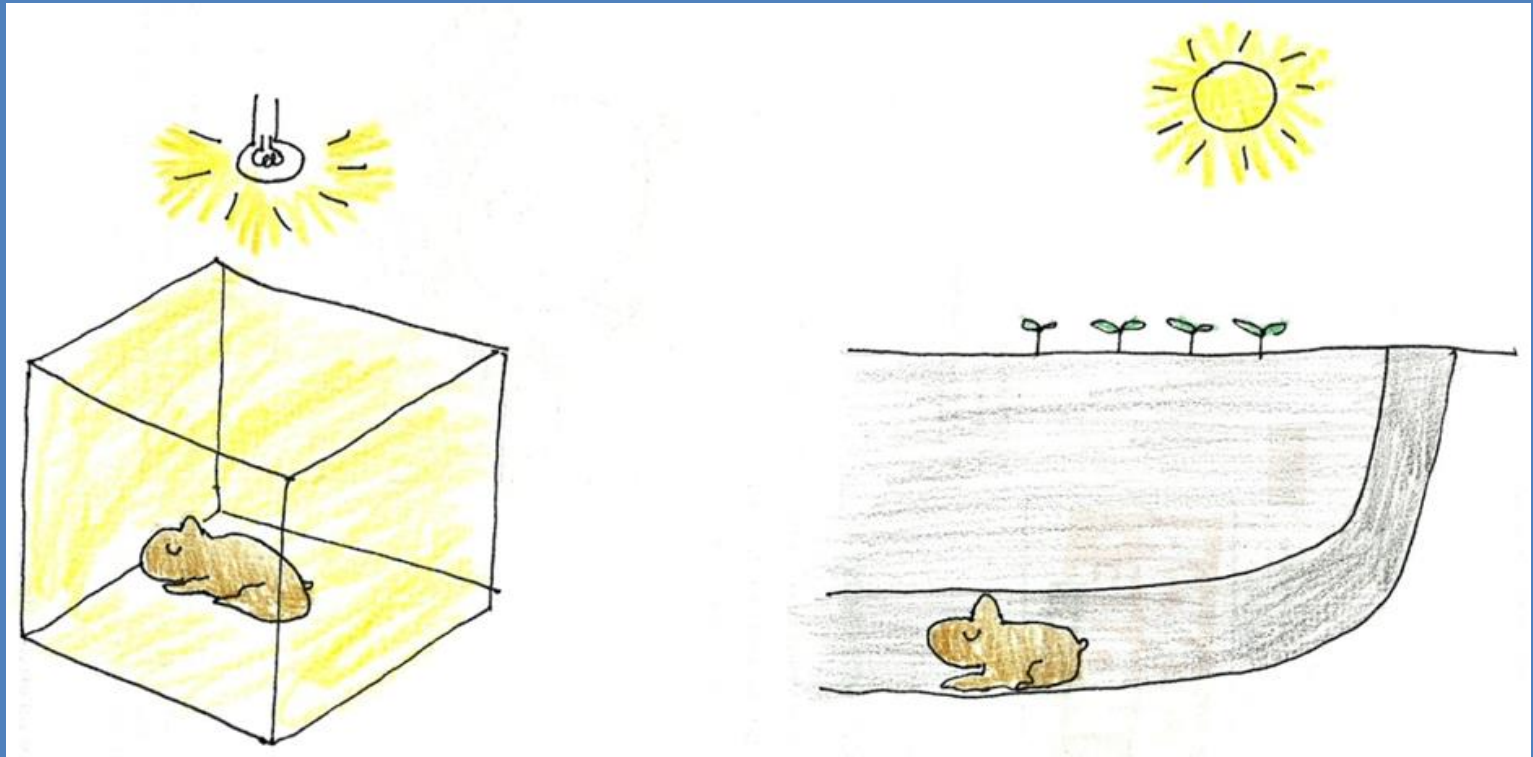


## Winter





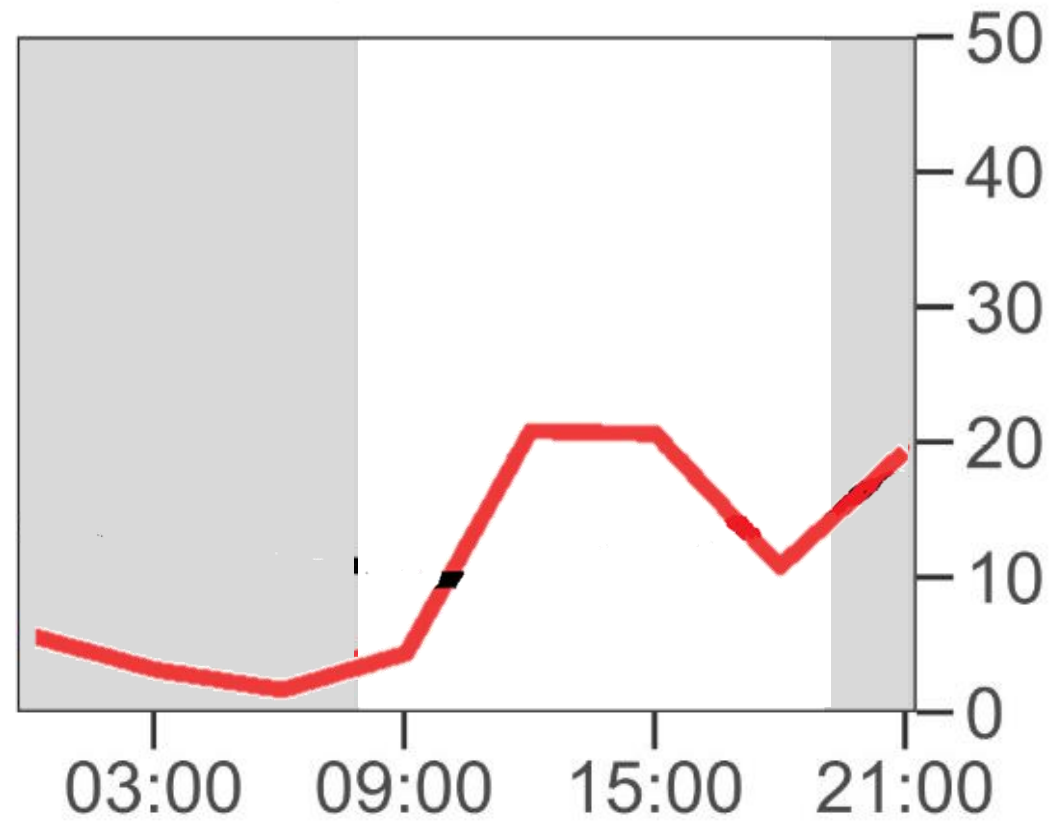
Light exposure is the  
result of their own  
behavior



Which factors make tuco-tucos  
expose to light in different times  
in different seasons?

## Winter

Air Temperature



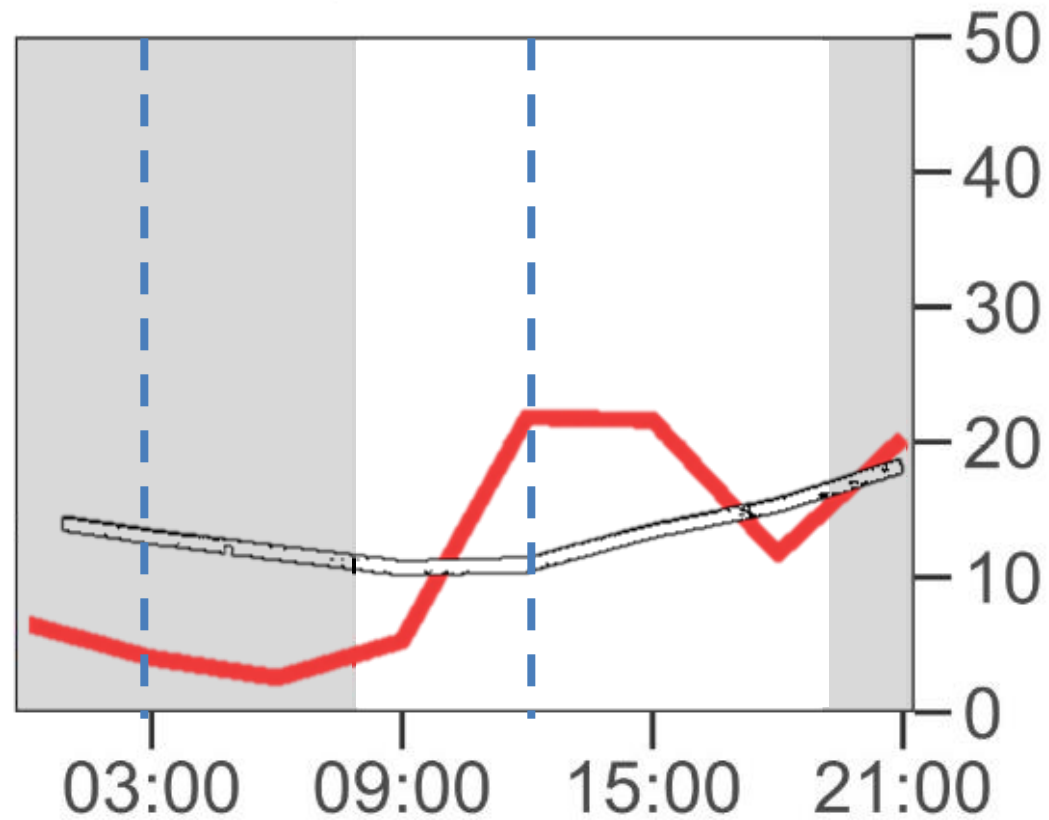
Milene Jannetti

## Winter

Air Temperature

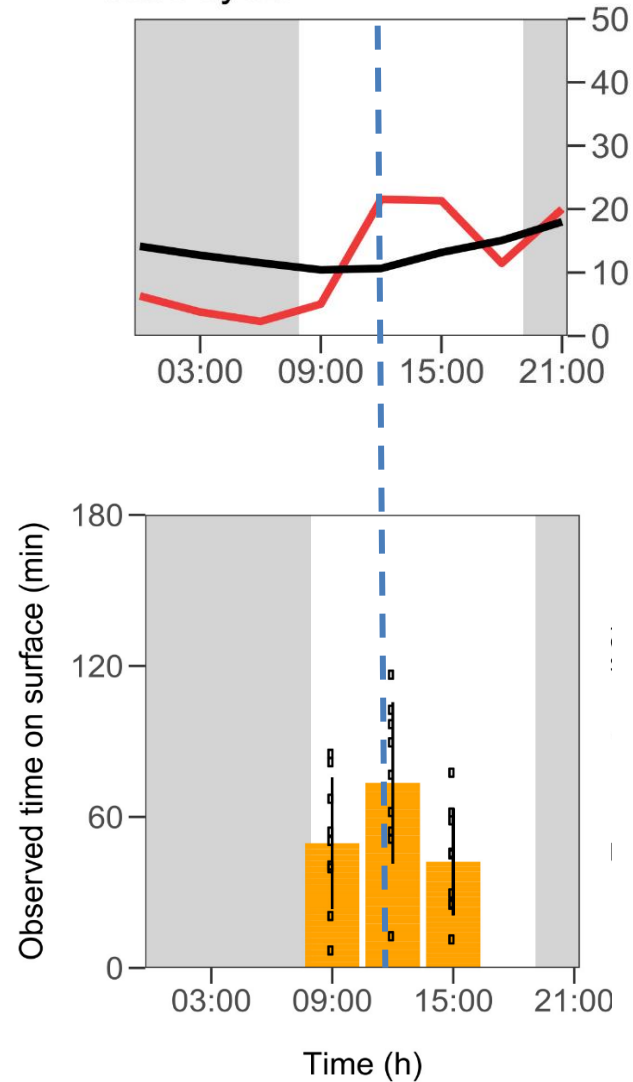
+

Soil Temperature



# Winter

## Ambient Temperature



Observed time on surface

(Jannetti et al., 2019  
Conservation Physiology)



# What they do on surface?...

foraging



soil removal

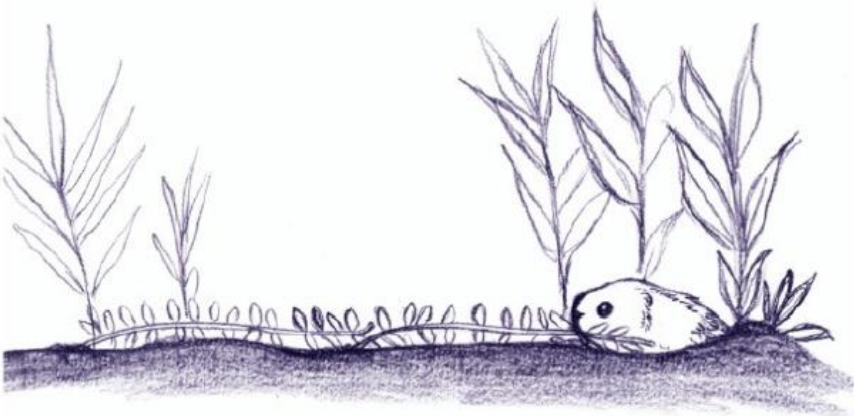
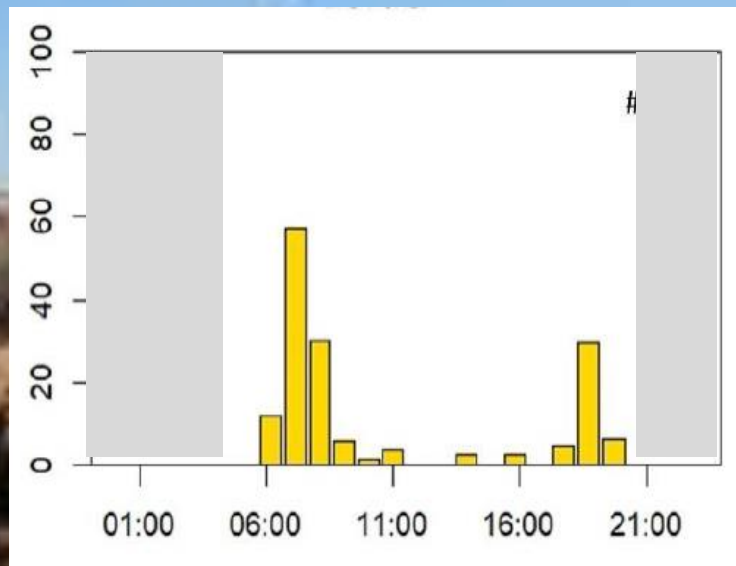


(Photo and illustration:  
Barbara Tomotani)

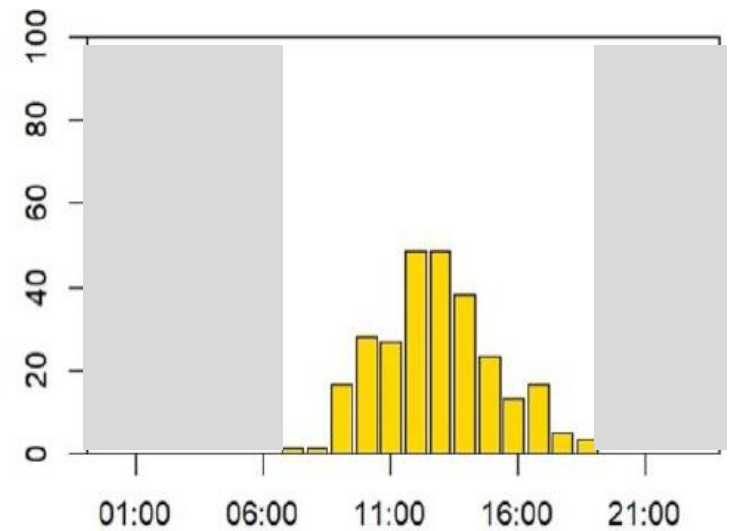
"nothing" → "basking"?



## Summer

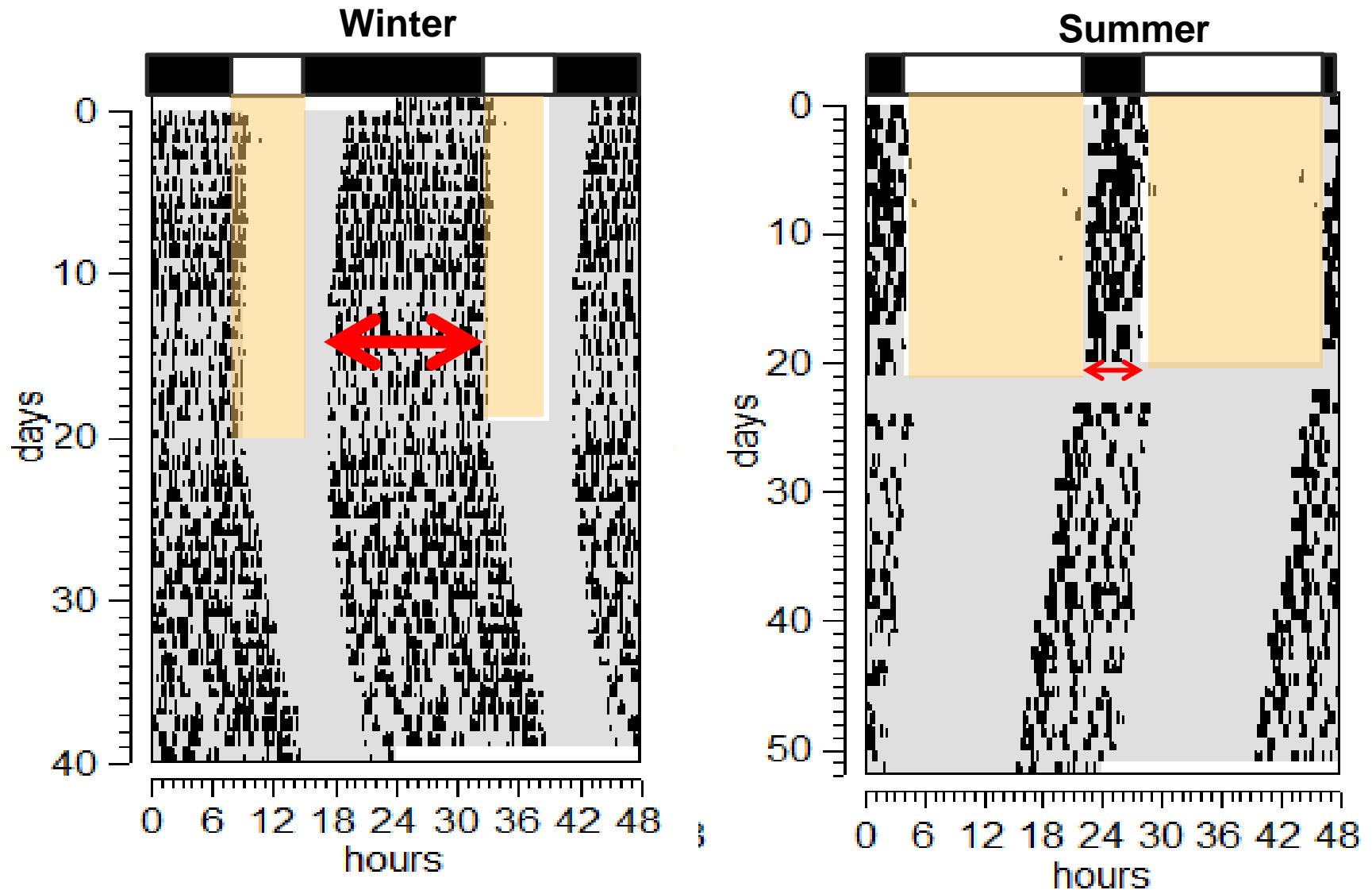


## Winter



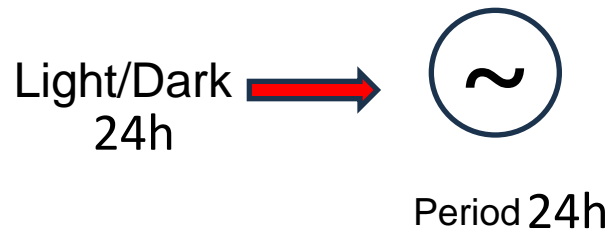
■ light exposure = surface emergence during the day

Artificial Photoperiods in the  
LAB, **constant temperature**

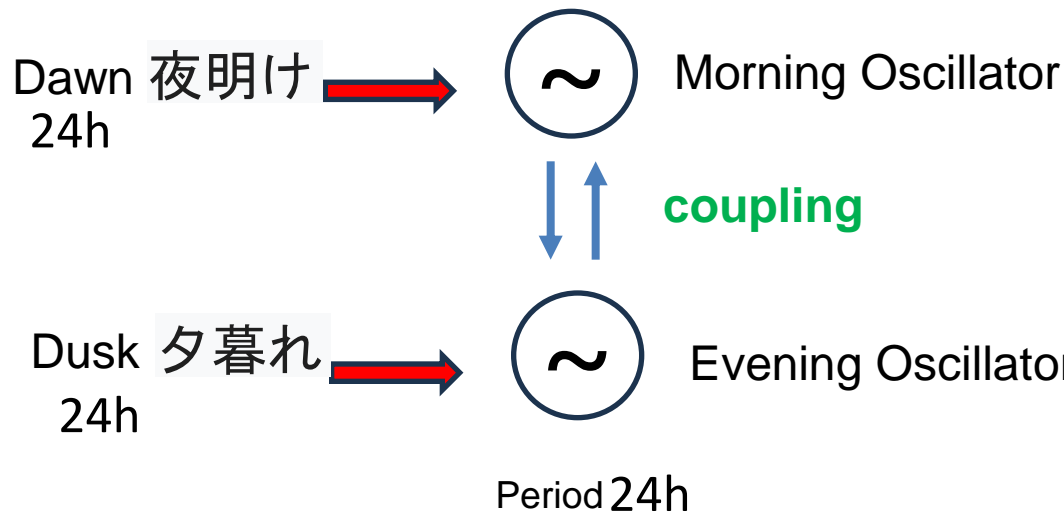


(Improta et al., J Biol Rhythms 2022)

# Two-Oscillator/Two Forcing Cycle Model of Photoperiodic Time Measurement (Pittendrigh and Daan 1976)



$$\begin{aligned} dR/dt &= R - cS - bS^2 + (d - L) + K \\ dS/dt &= R - aS \end{aligned}$$



Evening oscillator (E):

$$dR_E / dt = R_E - c_E S_E - b_E S_E^2 + (d_E - L) + K$$

$$dS_E / dt = R_E - a_E S_E + C_{ME} S_M$$

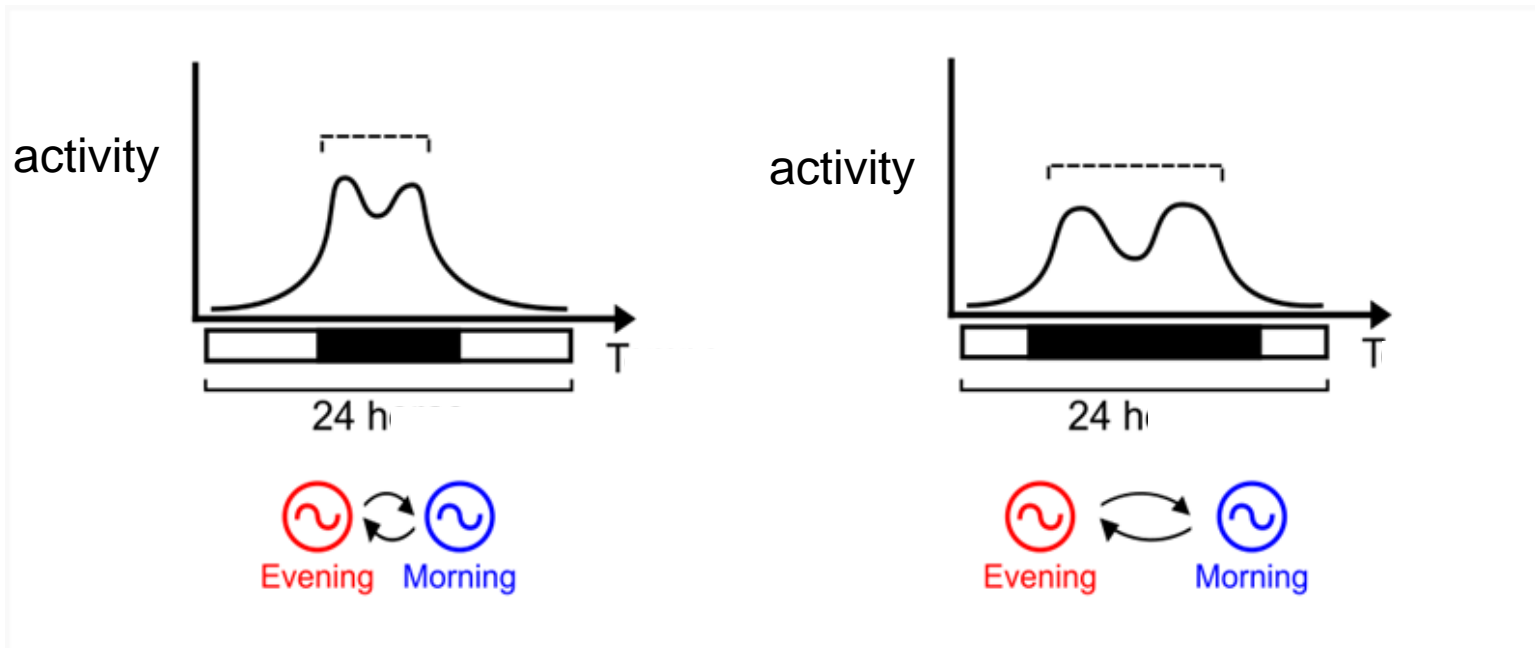
Morning oscillator (M):

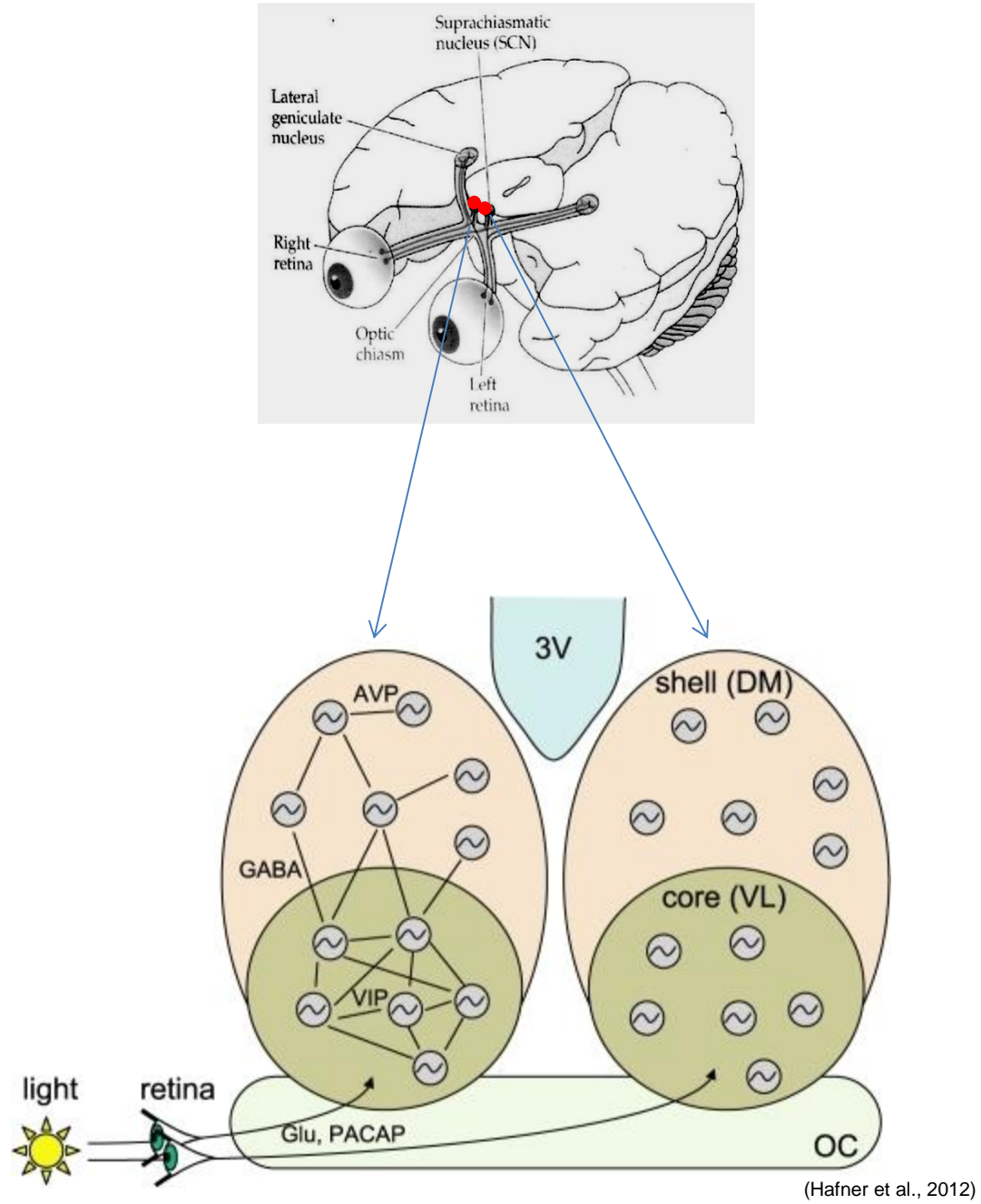
$$dR_M / dt = R_M - c_M S_M - b_M S_M^2 + (d_M - L) + K$$

$$dS_M / dt = R_M - a_M S_M + C_{EM} S_E$$

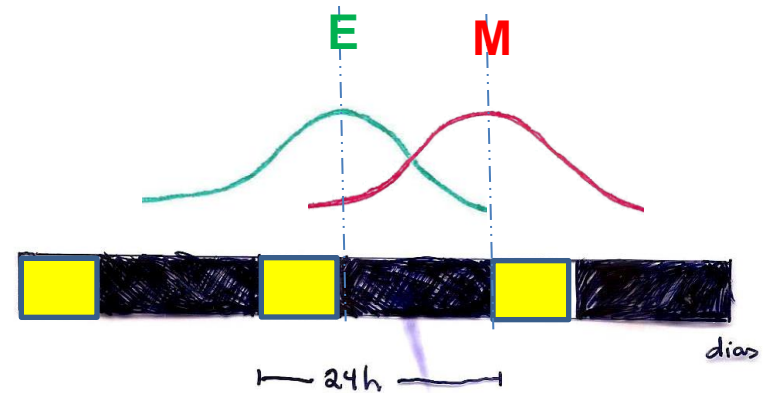
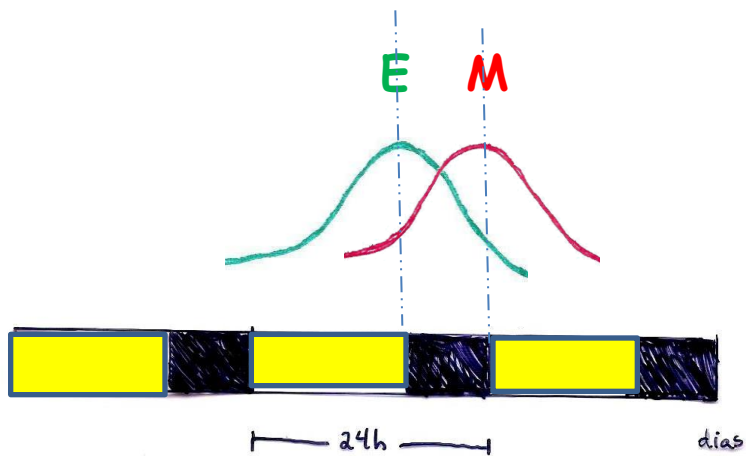


# Two-Oscillator Model of Photoperiodic Time Measurement

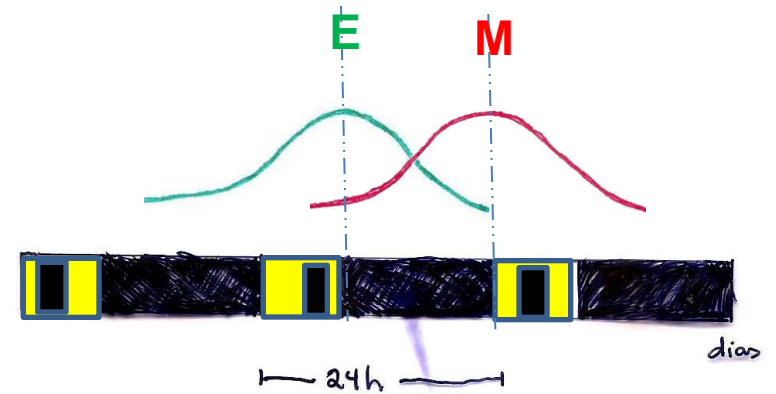
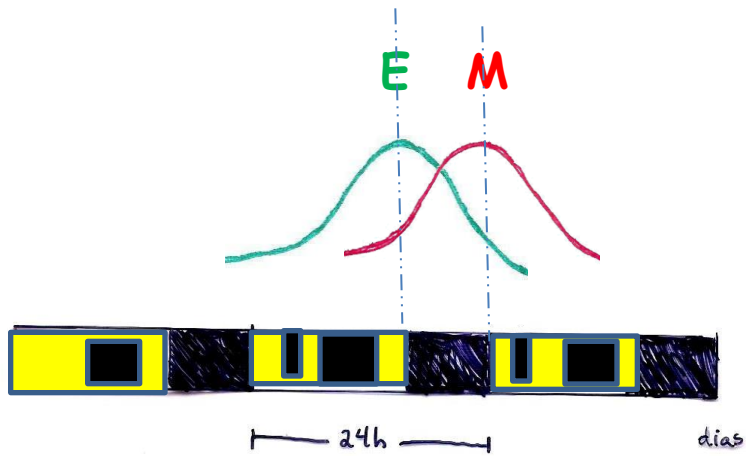




## "Internal Coincidence" Model of Photoperiod Measurement



In Tuco-tucos?...



How does it work?...

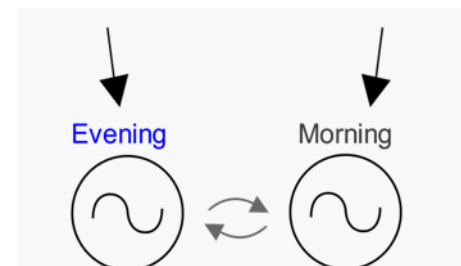
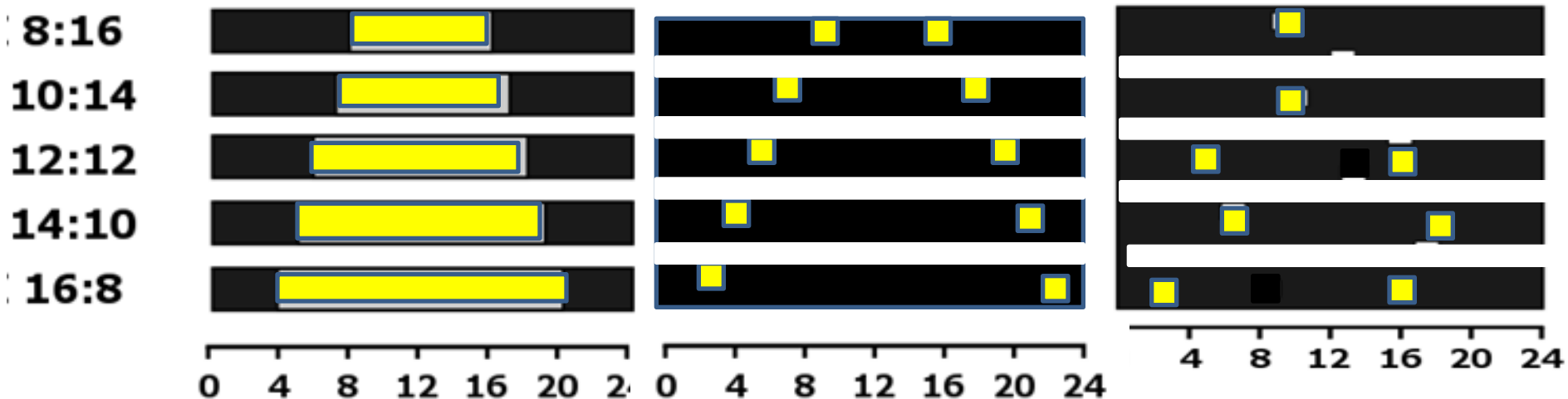


?

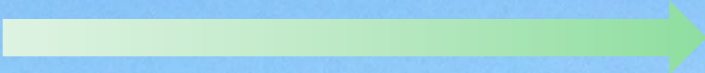


LAB photoperiod

Skeleton photoperiod



(Flôres et al., Frontiers in Physiol 2021)



Math

Lab

"Semi"  
Field

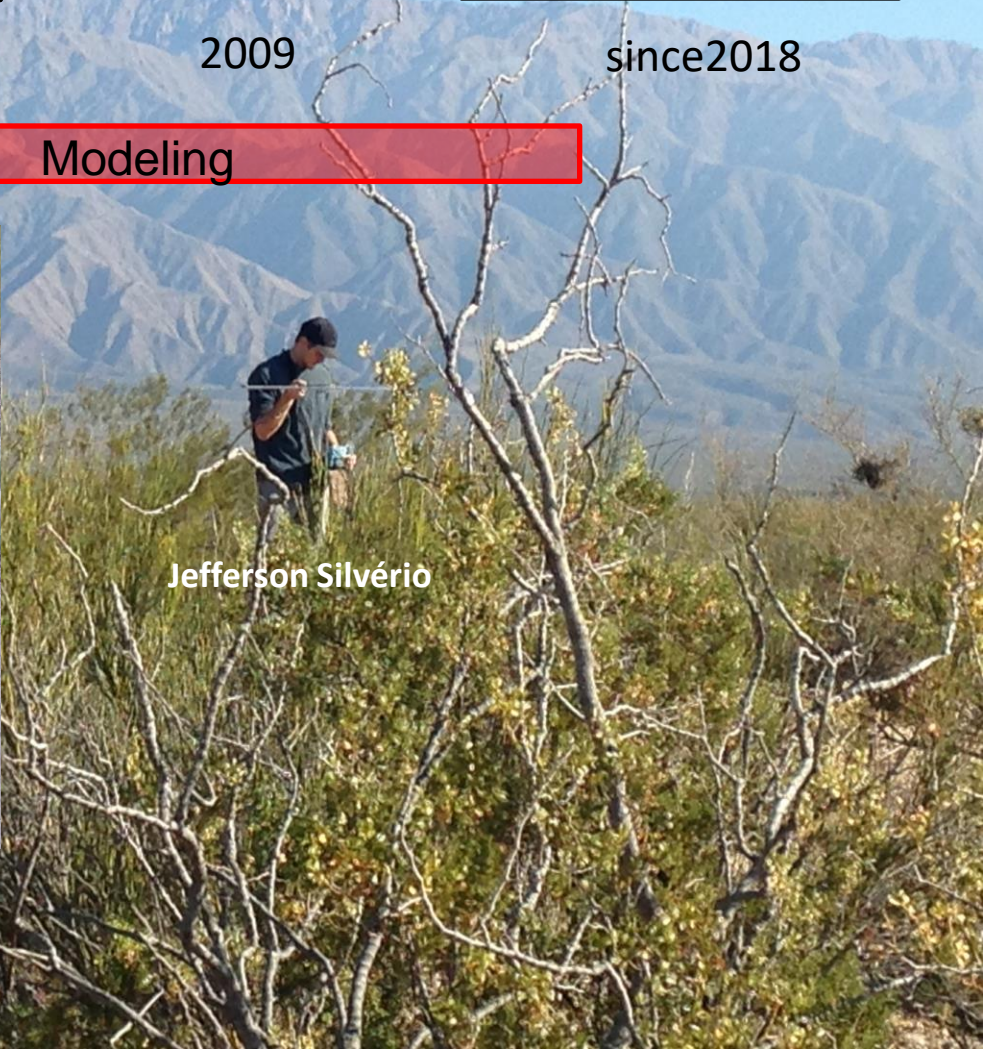
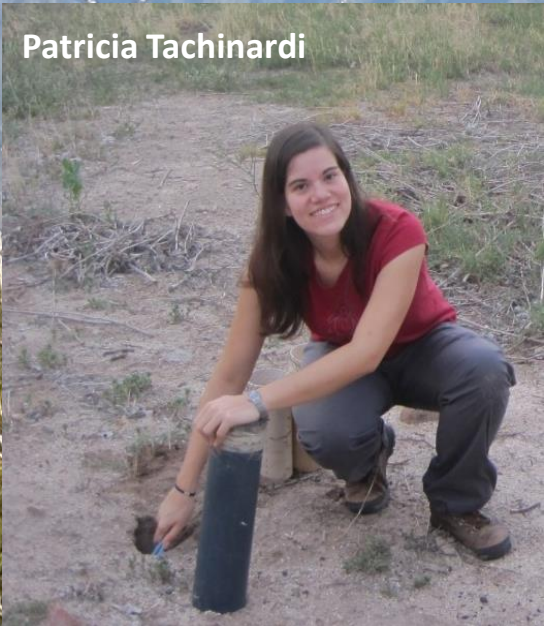
Field

2008

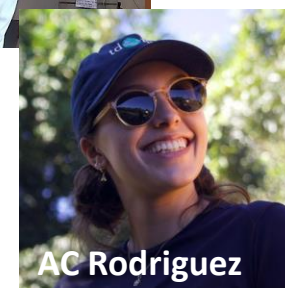
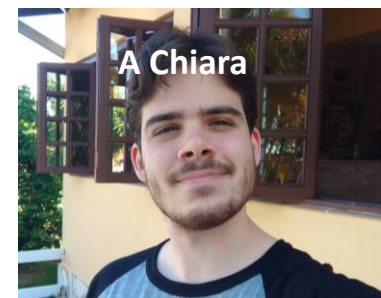
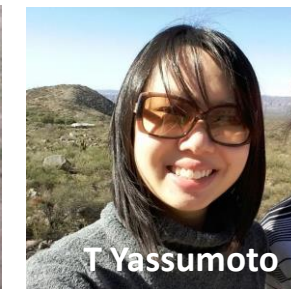
2009

since 2018

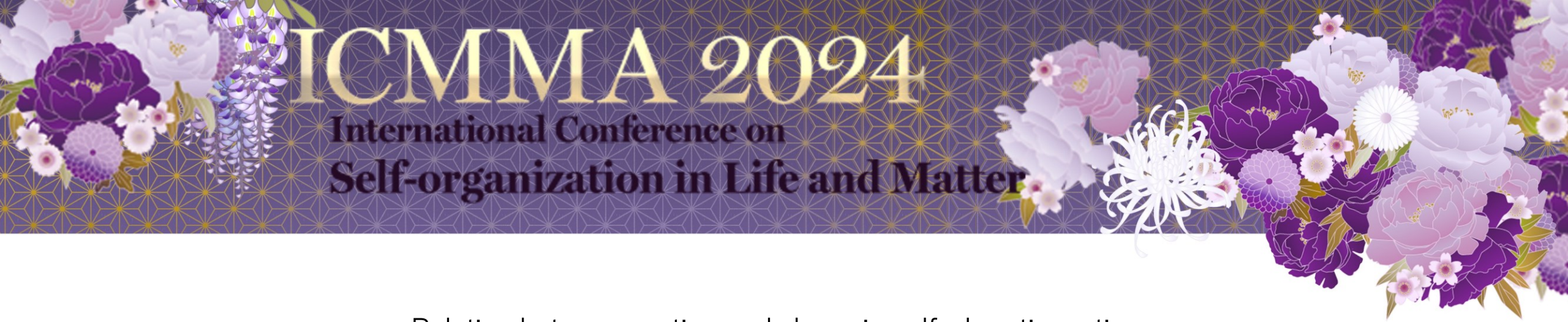
Modeling











## Relation between motion and shape in self-phoretic motions

Hiroyuki Kitahata (Department of Physics, Chiba University)

When a particle or droplet of surface-active chemicals like camphor is floated on the water surface, surface-active molecules are released from it to the water surface. Due to the spatial difference in concentration, a surface tension gradient is generated and can drive the particle or droplet. When its shape is circular, the concentration field should be isotropic with respect to the center, and the forces originating from the surface tension acting on it should be balanced. However, such an isotropic balanced state can become unstable due to fluctuations. Consequently, the particle or droplet starts to move in a direction determined by the fluctuations. This can be called "self-phoretic motion" since the concentration field is generated by itself. This self-phoretic motion can be adopted in some other cases. For example, if a living cell emits a harmful chemical for itself and it escapes from the region with a higher concentration, then the cell motion should exhibit qualitatively the same characteristics.

If the shape of a particle or droplet has anisotropy, its shape should affect motion. We constructed the mathematical model describing such motions of a particle or droplet, including the effect of its shape, and performed the numerical simulation and theoretical analyses. For example, the mathematical analysis suggests that an elliptic particle moves in its minor-axis direction, and we confirmed it by experiments [1]. Using an alcohol droplet floating at the surface of an almost saturated solution of the alcohol, we can realize a spontaneous motion with deformation [2]. We experimentally observed the relationship between motion and deformation and analyzed the generic features of the coupling between motion and deformation. We also discussed the large deformation of an oil droplet with camphor moving and deforming on a water surface [3].

### References

- [1] H. Kitahata, K. Iida, M. Nagayama, Phys. Rev. E 84, 015101 (2013).
- [2] K. Nagai, Y. Sumino, H. Kitahata, and K. Yoshikawa, Phys. Rev. E 71, 065301 (2005).
- [3] S. Otani, et al. arXiv.2402.01161 (2024).

September 9-11, 2024  
ICMMA2024  
International Conference on  
“Self-organization in Life and Matter”  
Meiji University

# Relation Between Motion and Shape in Self-Phoretic Motions

Hiroyuki KITAHATA  
Department of Physics, Graduate School of Science, Chiba Univ  
kitahata@chiba-u.jp

# My research interest

- Mechanism of self-organization in nonequilibrium systems (so-called "Dissipative structure")

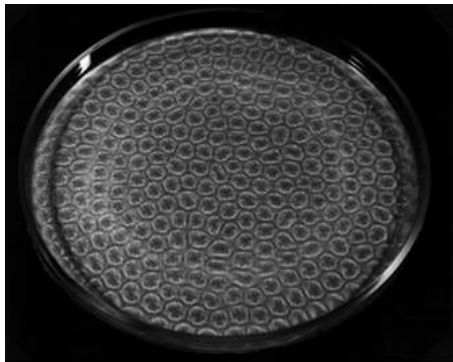
➡ Nonlinear oscillator, Coupled oscillators

➡ Pattern formation

➡ Self-propelled particles, Active matter

Correspondence between experiments and modelling.  
Is there any universality ?

Benard convection



BZ (Belousov-Zhabotinsky)  
reaction



(x4 real speed)

3 mm

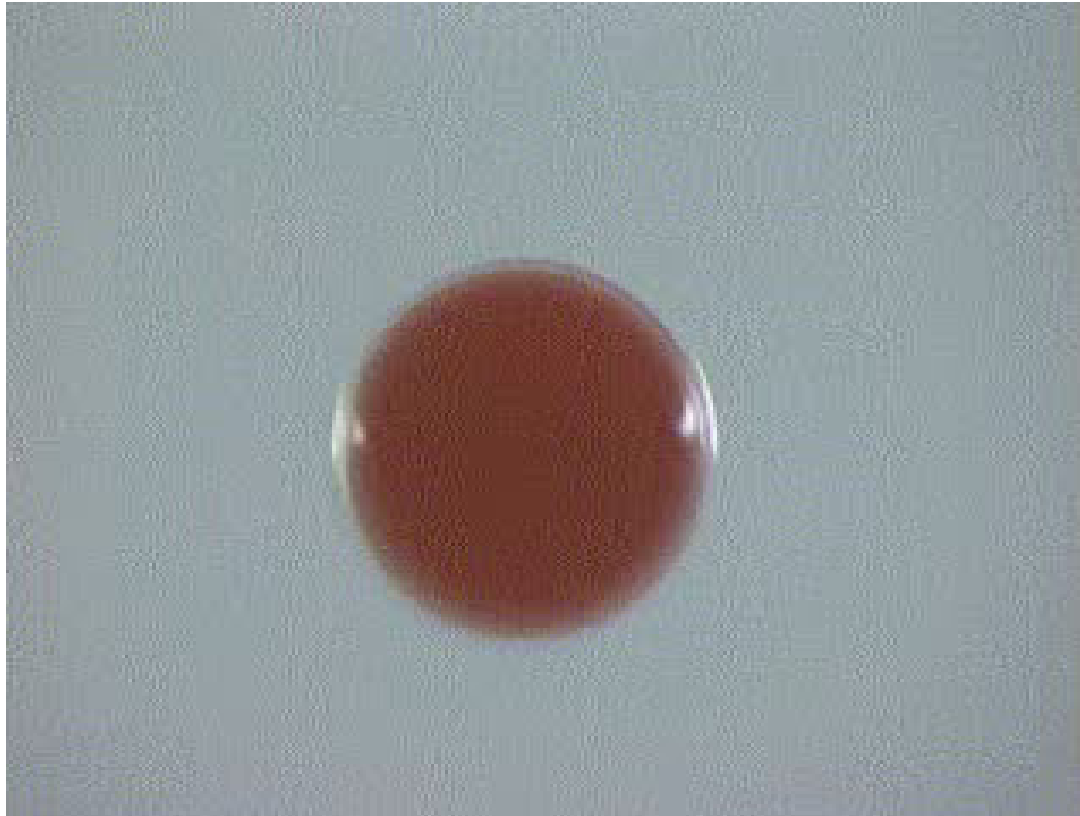


Ilya Prigogine

<http://in-flux.seesaa.net/article/4535601.html>

# Previous research

## Motion of a Belousov-Zhabotinsky droplet



(real speed)



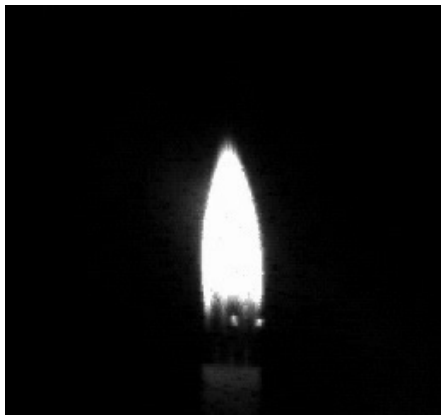
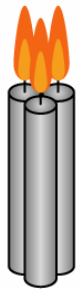
1 mm

HK, Aihara, Magome, Yoshikawa, *JCP*, (2002).

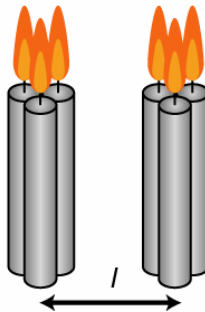
HK, Yoshinaga, Sumino, Nagai, *PRE*, (2011).



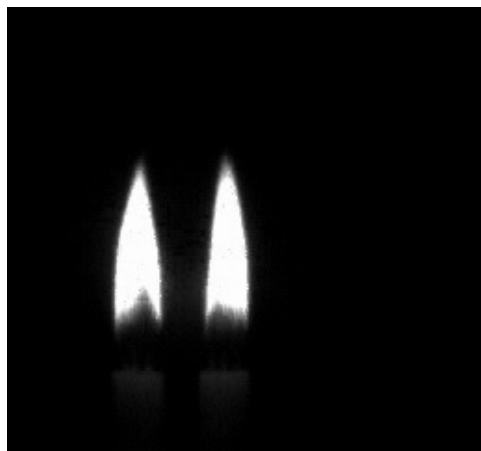
## Oscillation of candle flames



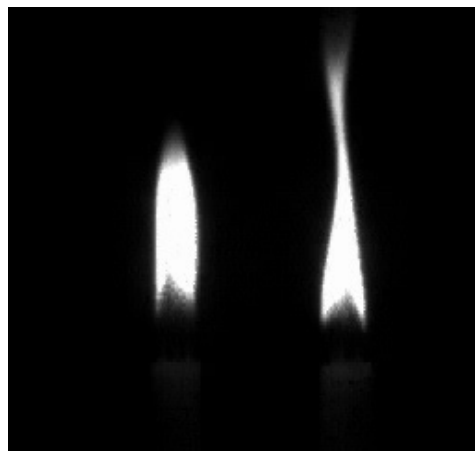
$l = 2.0 \text{ mm}$



$l = 4.0 \text{ mm}$



HK, et al. *JPCA* (2009).  
Araya, Ito, HK, *PRE* (2022).



x0.15 real speed

## Oscillations of precipitation at solution surface

Camphor methanol solution on a plate



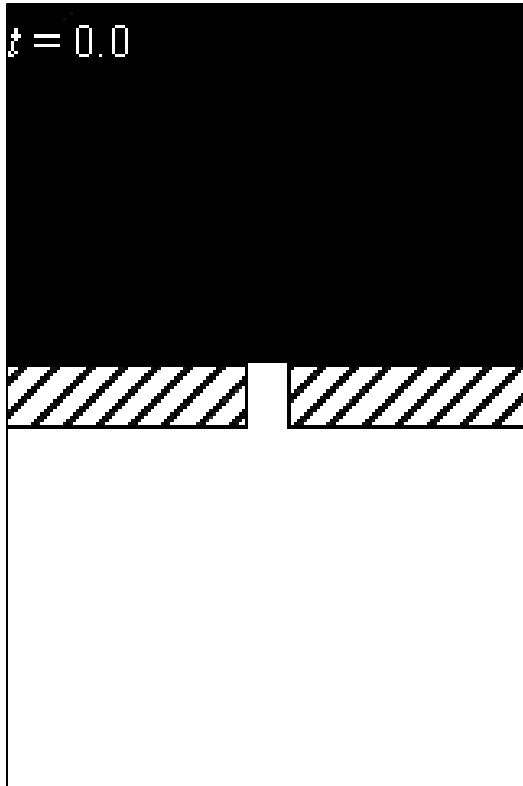
Real speed

1 mm

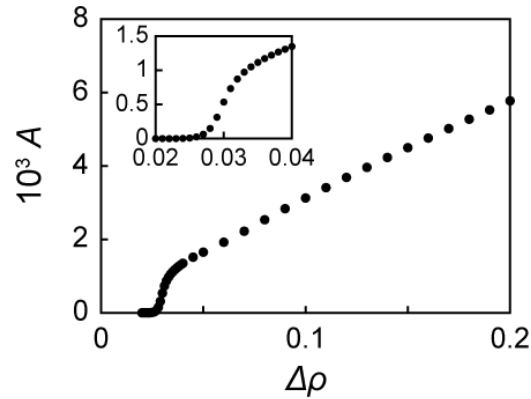
Sasaki, Suematsu, Sakurai, HK, *JPCB* (2015).  
Onishi, HK, Suematsu, *PRE* (2024).

# Density oscillators

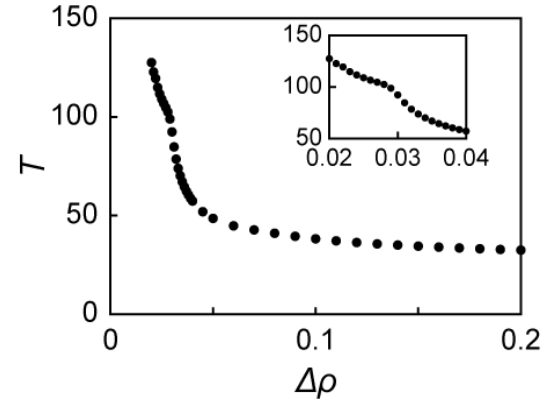
(Hydrodynamic simulation)



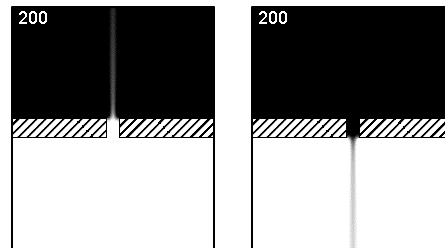
Amplitude



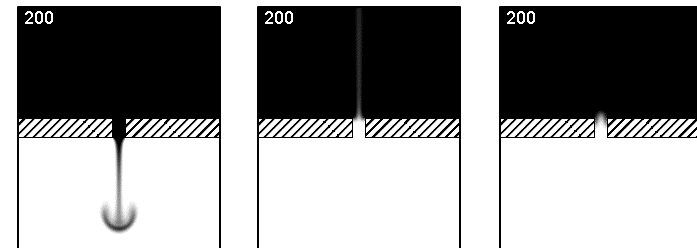
Period



Hopf bifurcation



2 coupled oscillators



3 coupled oscillators

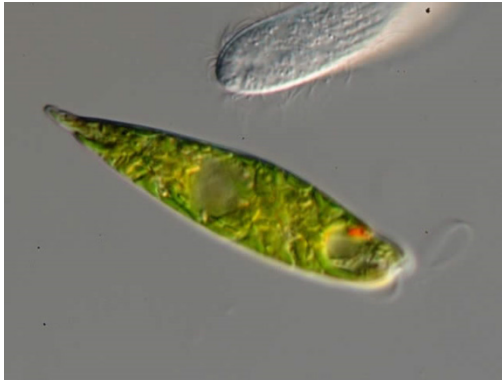
Ito, Itasaka, Takeda, HK, *EPL* (2020).

Takeda, Kurata, Ito, Kitahata, *PRE* (2020).

Takeda, Ito, Kitahata, *PRE* (2023).

# Introduction: Self-propelled objects

Motion of a single element



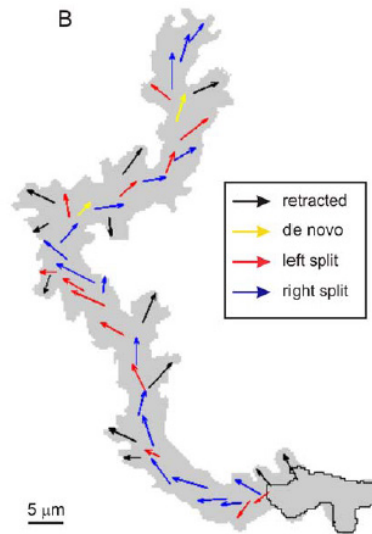
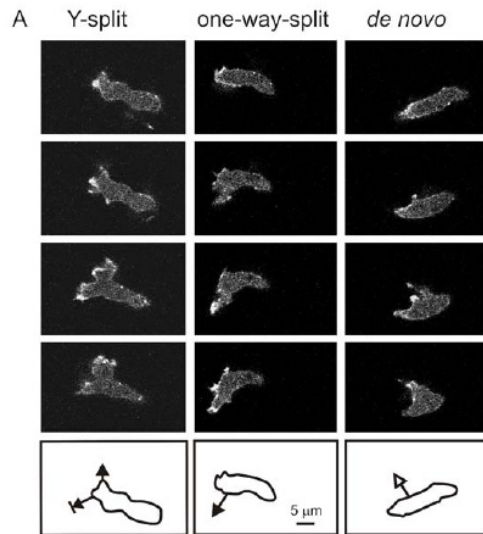
Collective motion



Motion of living organisms are interesting, but very complex.

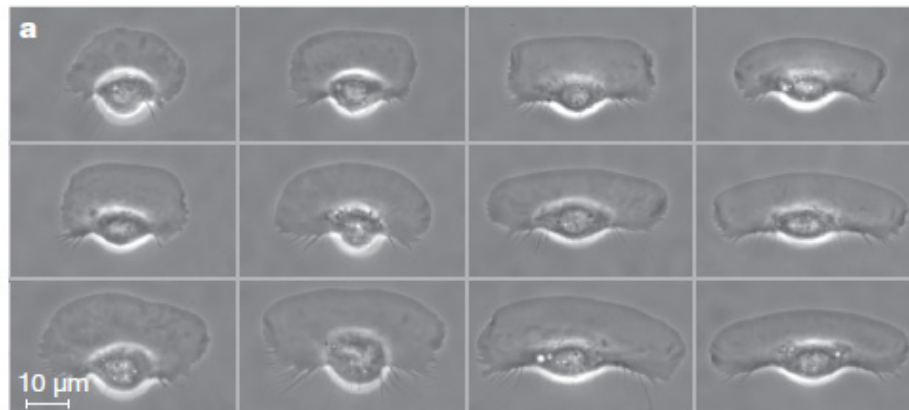
Physico-chemical systems can mimic the motion of the living organisms. Using such systems, we want to understand the mechanism from viewpoint of physics.

# Motion and deformation observed in cell motion



*Dictyostelium*

Bosgraaf *et al.*, *PLoS ONE*, **4**, e5253 (2009)



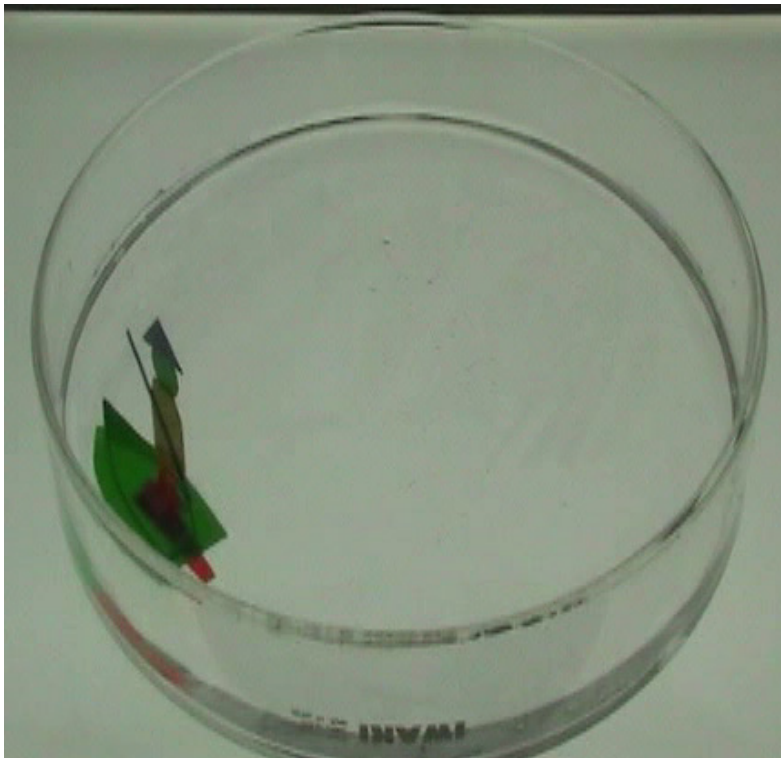
Keratocyte  
Originating  
from fish skin

Keren *et al.*, *Nature*, **453**, 475 (2008).

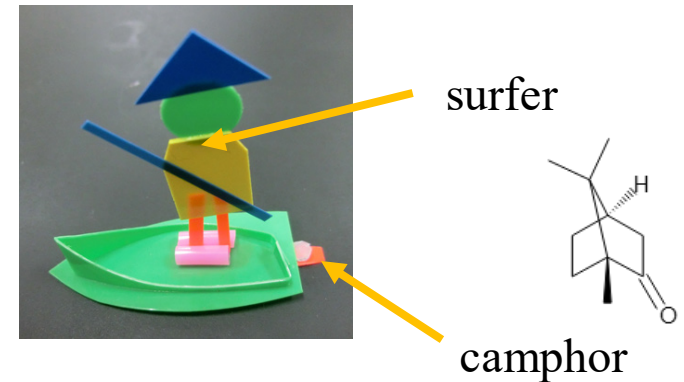


# Marangoni surfer: Motion at a liquid surface due to surface tension gradient

Japanese old toy "Camphor boat"



5 cm

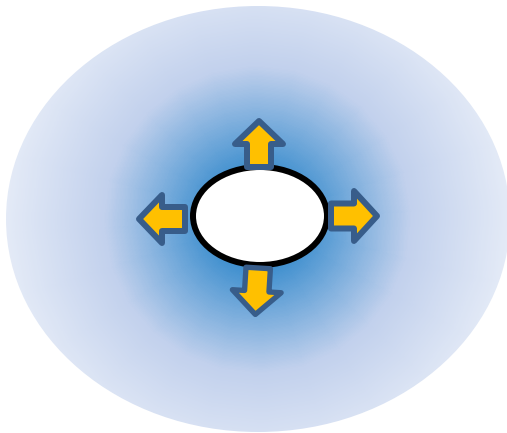


- The localized source of camphor produces spatial distribution of camphor molecule concentration.
- Camphor molecules decrease surface tension.
- Surface tension gradient can drive the object.

# "Self-phoretic motion"

Self-phoresis (self-difusiophoresis)

The object emits chemicals to the surroundings and the object moves depending on the concentration gradient.

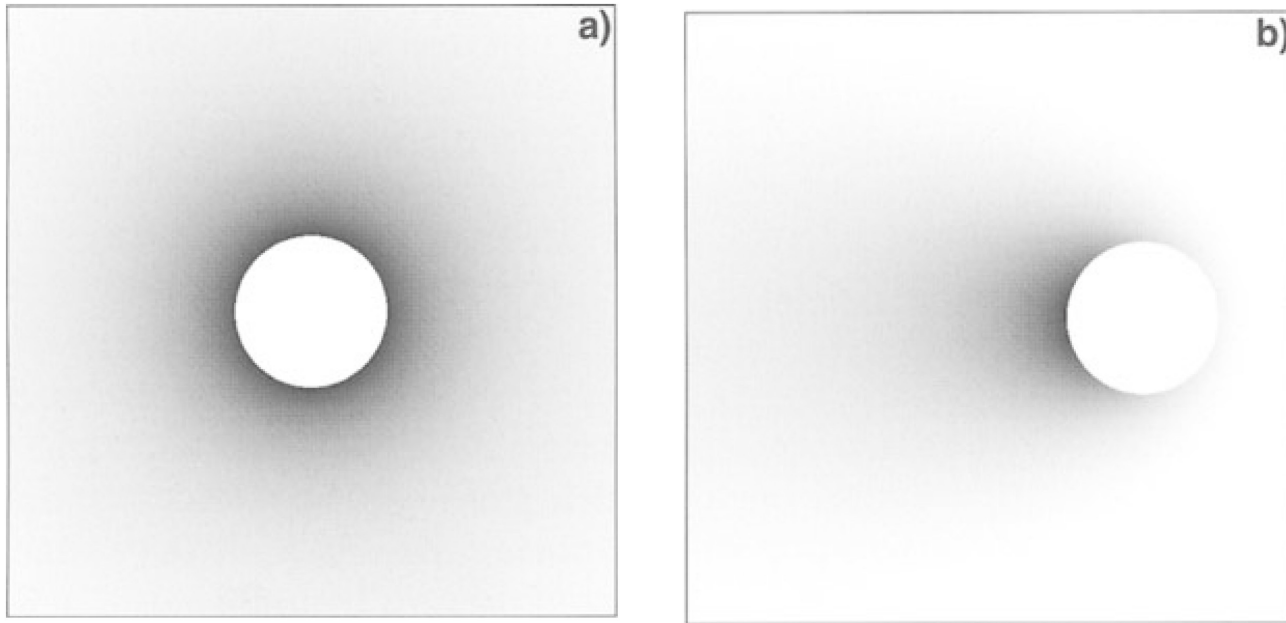


If asymmetry in shape or external condition exists, the object can move.

Even if the system is symmetric, the object can move through "spontaneous symmetry breaking."

The 2020 motile active matter roadmap To cite this article  
Gompper *J. Phys.: Condens. Matter* 32 193001 (2020).

## Active motion



$$\dot{c} = -\gamma c + D\nabla^2 c + J\delta(\mathbf{r} - \mathbf{R}(t))$$

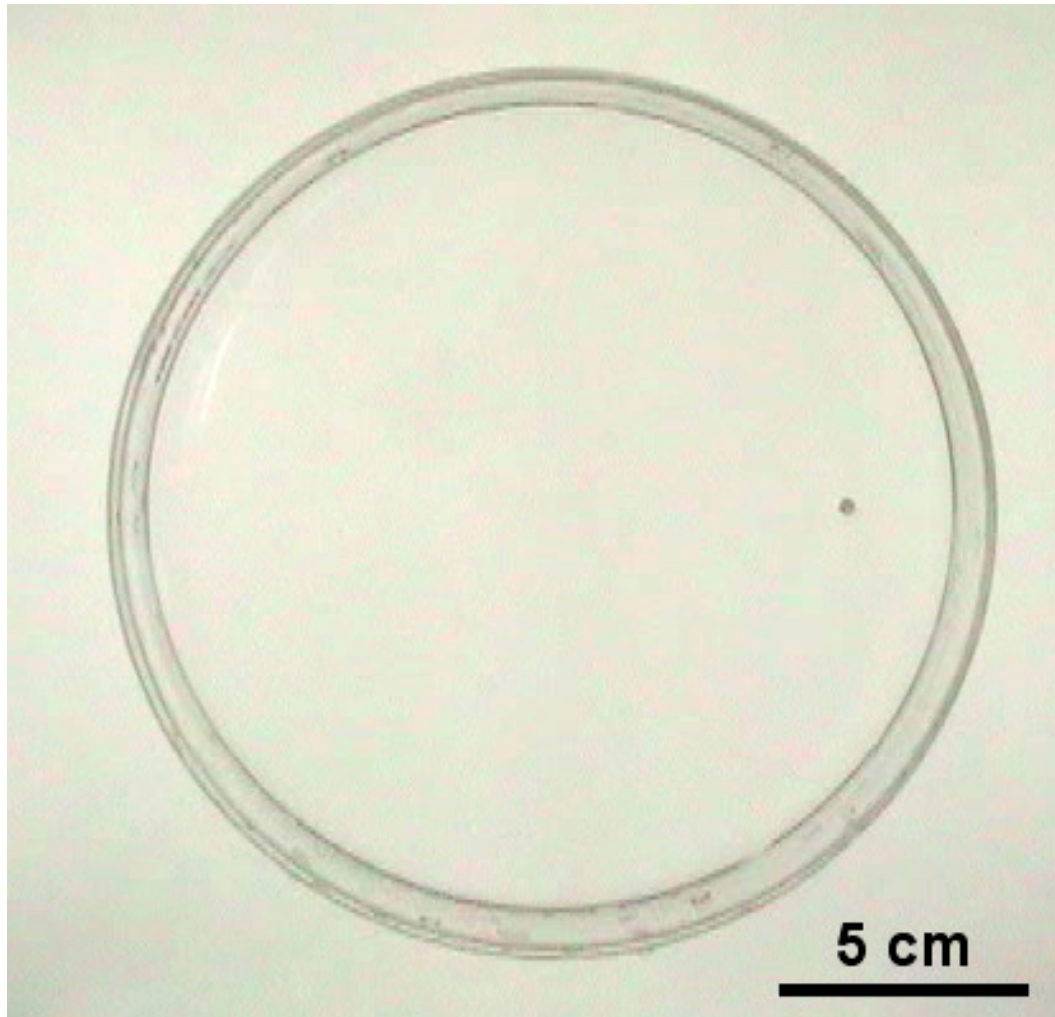
$$\Gamma = \Gamma_0 - \mu c$$

$$\mathbf{F}_c = \int \Gamma \mathbf{n} dl$$

Mikhailov and Calenbuhr, "From cells to Societies" (2001).

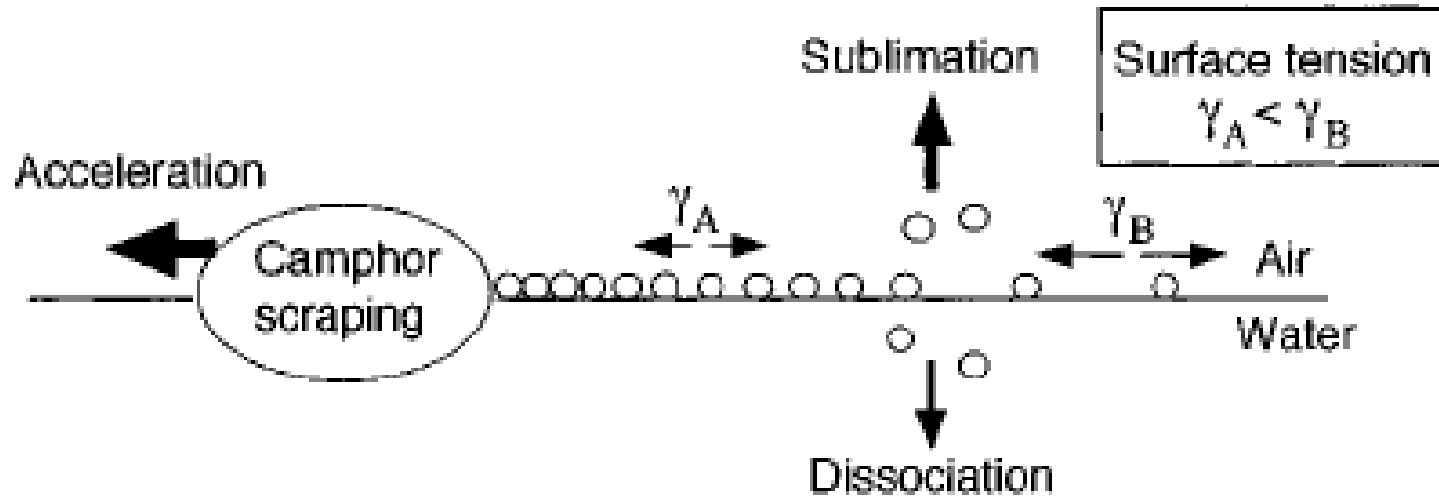
# Motion of a circular camphor disk

A circular camphor disk can move by spontaneously breaking symmetry.





# Spontaneous motion of a camphor particle



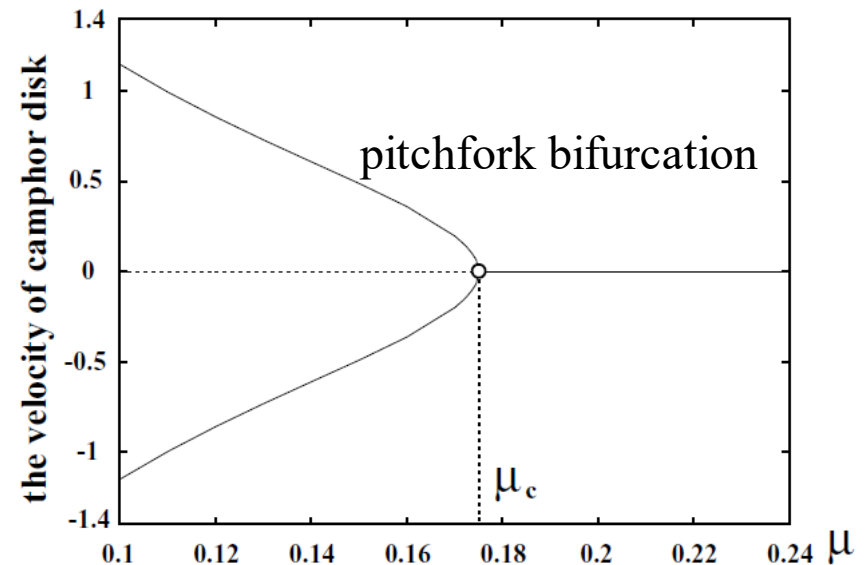
## Mathematical model

$$\rho S \ddot{x}_c(t) = S \nabla \gamma(u(x_c(t), t)) - \mu_s \dot{x}_c(t),$$

$$\frac{\partial u}{\partial t} = D \Delta u - k_0 u + F(x_c(t); r_0),$$

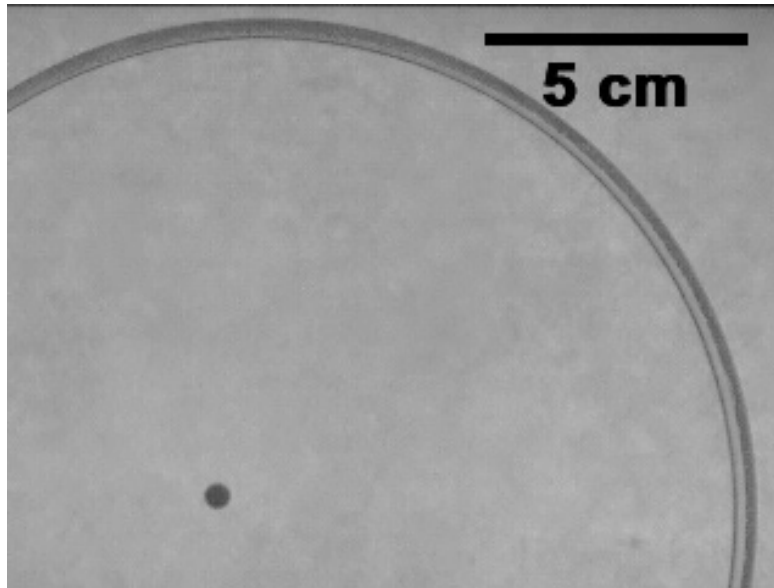
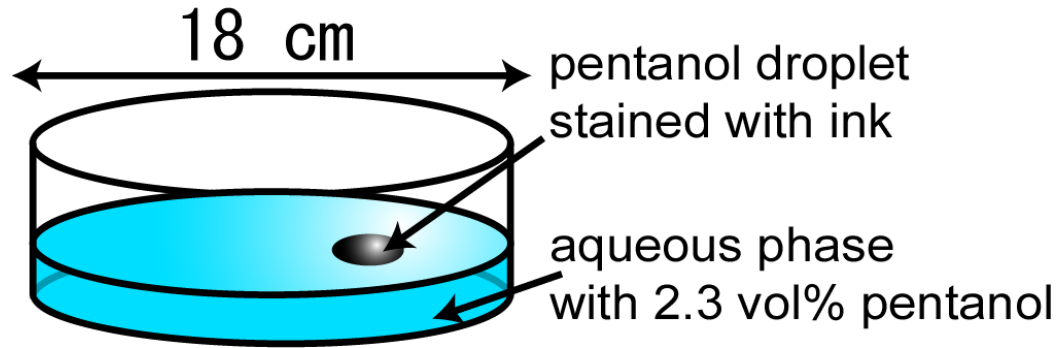
$$\gamma(u(x_c, t)) = \frac{\gamma_0}{a_0 u(x_c, t) + 1},$$

Nakata et al. *Langmuir*, 1997.

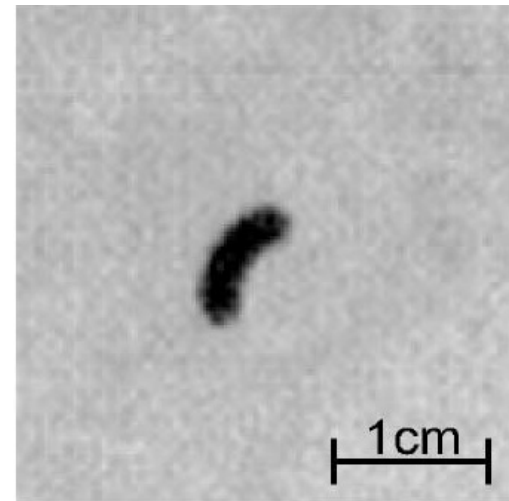


Nagayama et al. *Physica D*, 2004.<sup>13</sup>

# Motion and deformation of a pentanol droplet



(real speed)



Nagai, Sumino, HK, Yoshikawa, *Phys. Rev. E*, (2005).

# Motivation

In the system with self-propelled objects driven by surface tension gradient (negative chemotactic objects interacting through the concentration field), is there any universality in the relation between the motion and shape?

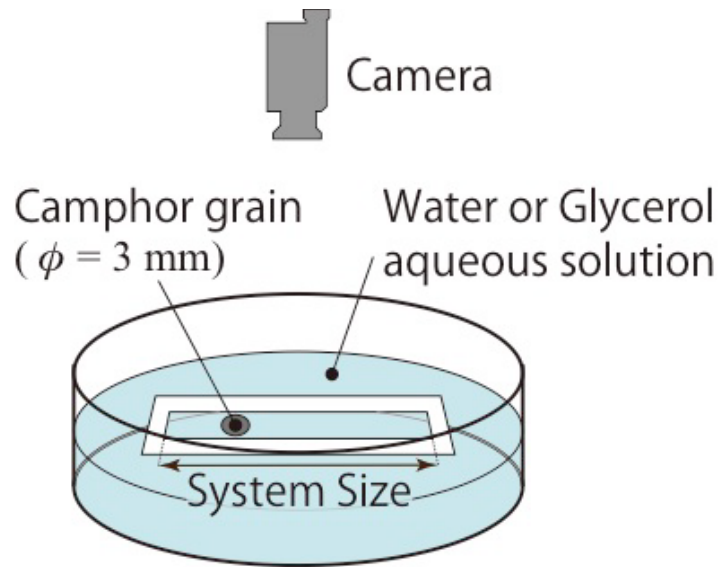
- 1) Experimental and theoretical approach for Marangoni surfer (camphor disk)
- 2) Effect of the shape on the motion of a camphor particle
- 3) Interaction between the motion and deformation of an alcohol droplet
- 4) Large deformation coupled with motion of an oil droplet with oil red O.

# Contents

- 1) Experimental and theoretical approach for Maranogni surfer (camphor disk)
- 2) Effect of the shape on the motion of a camphor particle
- 3) Interaction between the motion and deformation of an alcohol droplet
- 4) Large deformation coupled with motion of an oil droplet with oil red O



# Reciprocal motion in a 1D system



Experimental setup

3.5 M Glycerol aq. (**Higher** viscosity),  
 $R = 35$  mm



Water (**Lower** viscosity),  $R = 35$  mm



## Mathematical model

$$\frac{\partial c}{\partial t} = D \frac{\partial^2 c}{\partial x^2} - ac + \delta(x - x_c)$$

$$m \frac{d^2 x_c}{dt^2} = -\eta \frac{dx_c}{dt} - \Gamma \left( \left. \frac{\partial c}{\partial x} \right|_{x=x_c+0} - \left. \frac{\partial c}{\partial x} \right|_{x=x_c-0} \right)$$

$$\left. \frac{\partial c}{\partial x} \right|_{x=0} = \left. \frac{\partial c}{\partial x} \right|_{x=R} = 0$$

$$\frac{\partial c}{\partial t} = D \frac{\partial^2 c}{\partial x^2} - ac + \delta(x - x_c) \delta(t) \quad \text{(Green function)}$$

$$\Rightarrow c(x, t) = \int_{-\infty}^t G(x - x', t - t') x_c(t') dt'$$

cf) In an infinite system  $G(x, t) = \frac{1}{\sqrt{4\pi Dt}} \exp\left(-\frac{x^2}{2Dt} - at\right)$

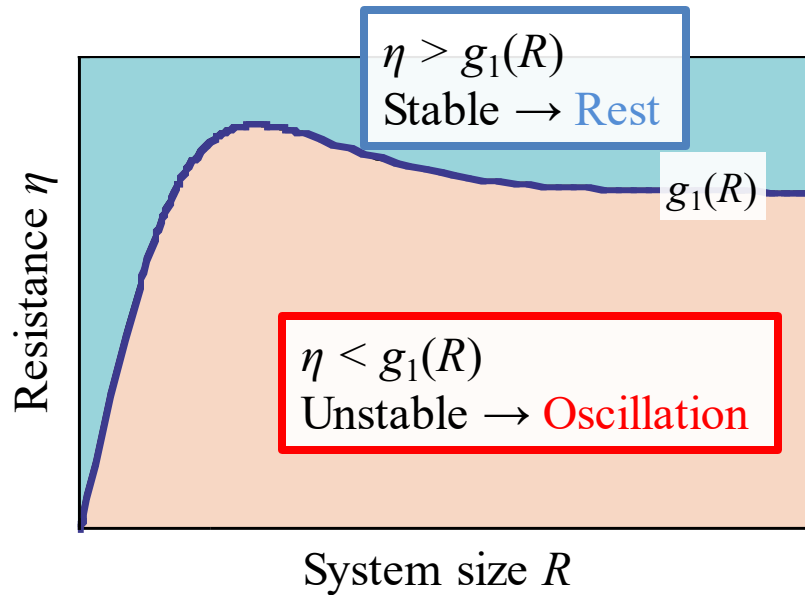
By expanding  $c(x, t)$  with respect to  $x_c = R/2$  (system center)

$$m \frac{d^2 x_c}{dt^2} = -\eta \frac{dx_c}{dt} - \Gamma \left( \left. \frac{\partial c}{\partial x} \right|_{x=x_c+0} - \left. \frac{\partial c}{\partial x} \right|_{x=x_c-0} \right)$$



$$\begin{aligned} & g_1 \left( x_c - \frac{R}{2} \right) + f_1 \frac{dx_c}{dt} + g_2 \left( \frac{dx_c}{dt} \right)^2 \left( x_c - \frac{R}{2} \right) + g_3 \left( x_c - \frac{R}{2} \right)^3 \\ & + f_2 \left( x_c - \frac{R}{2} \right)^2 \frac{dx_c}{dt} + f_3 \left( \frac{dx_c}{dt} \right)^3 - h_1 \frac{d^2 x_c}{dt^2} \end{aligned}$$

# Theoretical Analysis Results



$$m \frac{d^2 x_c}{dt^2} = -\eta \frac{dx_c}{dt} - \Gamma \left( \left. \frac{\partial c}{\partial x} \right|_{x=x_c+0} - \left. \frac{\partial c}{\partial x} \right|_{x=x_c-0} \right)$$

$$g_1 \left( x_c - \frac{R}{2} \right) + f_1 \frac{dx_c}{dt} + g_2 \left( \frac{dx_c}{dt} \right)^2 \left( x_c - \frac{R}{2} \right) + g_3 \left( x_c - \frac{R}{2} \right)^3$$

$$+ f_2 \left( x_c - \frac{R}{2} \right)^2 \frac{dx_c}{dt} + f_3 \left( \frac{dx_c}{dt} \right)^3 - h_1 \frac{d^2 x_c}{dt^2}$$

Hopf bifurcation occurs

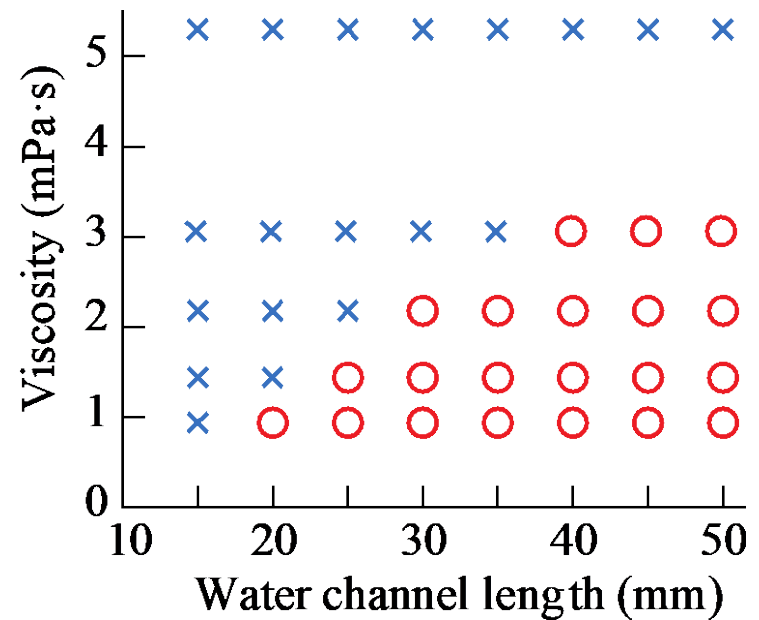
Koyano, Sakurai, HK *PRE*, 2016.

For the case with an infinite system size

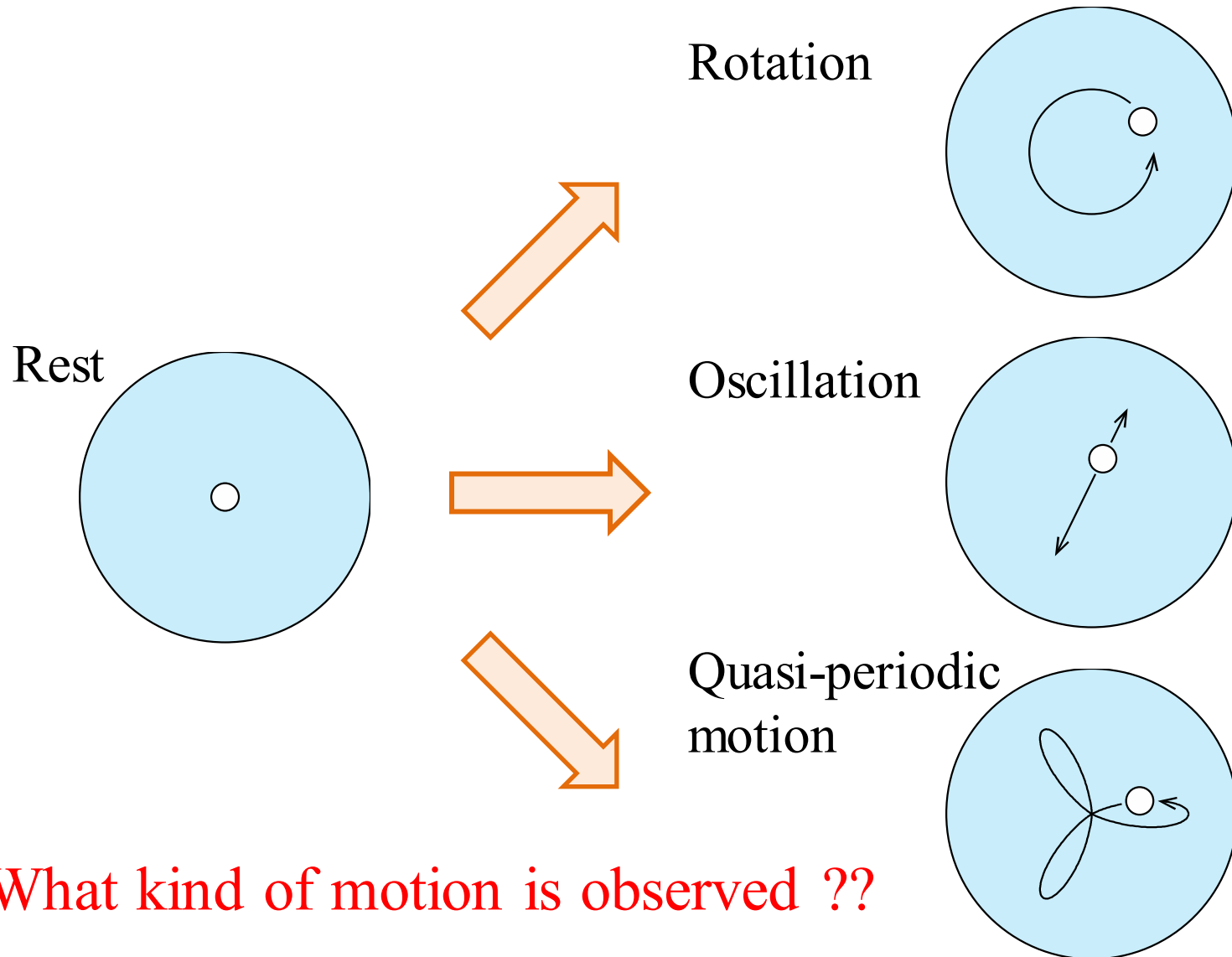
$$m \frac{d^2 x_c}{dt^2} = (f_1 - \eta) \frac{dx_c}{dt} - f_3 \left( \frac{dx_c}{dt} \right)^3$$

pitchfork bifurcation occurs

# Experimental Results



# Motion of a camphor disk in a 2D circular region

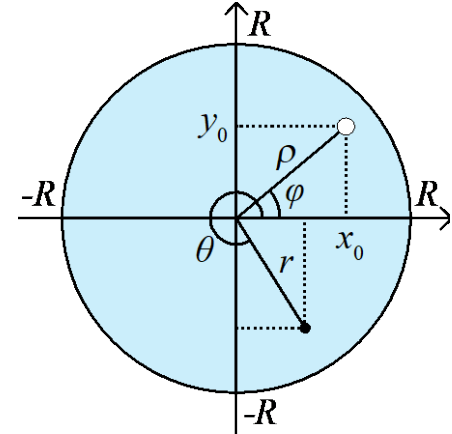


What kind of motion is observed ??



$$\frac{\partial c}{\partial t} = \left( \frac{\partial^2}{\partial r^2} + \frac{1}{r} \frac{\partial}{\partial r} + \frac{1}{r^2} \frac{\partial^2}{\partial \theta^2} \right) c - c + f(\mathbf{r}; \boldsymbol{\rho})$$

$$f = \delta(\mathbf{r} - \boldsymbol{\rho}) = \begin{cases} \frac{1}{r} \delta(r - \rho) \delta(\theta - \phi) & (\rho > 0) \\ \frac{1}{\pi r} \delta(r - \rho) & (\rho = 0) \end{cases}$$



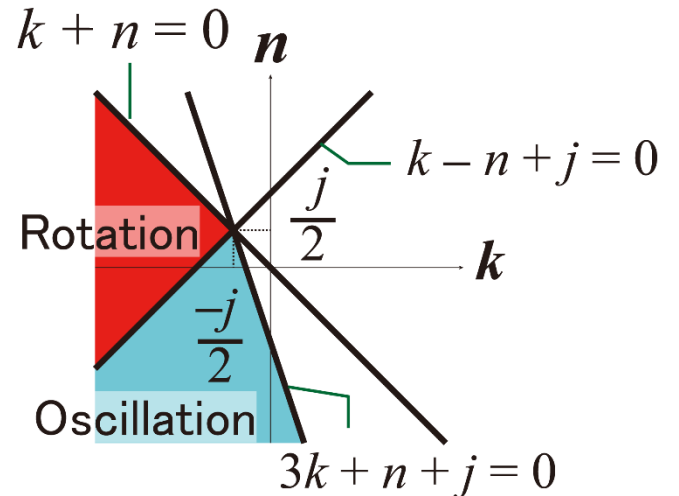
$$(m - g(R))\ddot{\boldsymbol{\rho}} = a(R)\boldsymbol{\rho} + (b(R) - \eta)\dot{\boldsymbol{\rho}} + c(R)|\boldsymbol{\rho}|^2\boldsymbol{\rho} + k(R)|\dot{\boldsymbol{\rho}}|^2\dot{\boldsymbol{\rho}} \\ n(R)|\boldsymbol{\rho}|^2\dot{\boldsymbol{\rho}} + h(R)|\dot{\boldsymbol{\rho}}|^2\boldsymbol{\rho} + j(R)(\boldsymbol{\rho} \cdot \dot{\boldsymbol{\rho}})\boldsymbol{\rho} + p(R)(\boldsymbol{\rho} \cdot \dot{\boldsymbol{\rho}})\dot{\boldsymbol{\rho}}$$

Koyano, Suematsu, HK *PRE* (2019)

Stable oscillation :  $\begin{cases} k - n + j > 0 \\ 3k + n + j < 0 \end{cases}$

Stable rotation :  $\begin{cases} k - n + j < 0 \\ k + n < 0 \end{cases}$

Koyano, Yoshinaga, HK *JCP* (2015)



# Explicit form of each term

$$a(R) = \frac{\mathcal{K}_0'(R)}{4\pi\mathcal{I}_0'(R)} + \frac{\mathcal{K}_1'(R)}{4\pi\mathcal{I}_1'(R)}$$

$\mathcal{I}_\nu(x)$ : the first-kind modified Bessel function  
 $\mathcal{K}_\nu(x)$ : the second-kind modified Bessel function

$$b(R) = \frac{1}{4\pi}(-\gamma_{\text{Euler}} + \log 2 - \log \epsilon) + \frac{1+R^2}{8\pi R^2\mathcal{I}_1'(R)^2} + \frac{\mathcal{K}_1'(R)}{4\pi\mathcal{I}_1'(R)}$$

$$g(R) = -\frac{1}{16\pi} + \frac{1}{16\pi\mathcal{I}_1'(R)^2} - \frac{(1+R^2)\mathcal{I}_1''(R)}{16\pi R\mathcal{I}_1'(R)^3} \quad c(R) = \frac{3\mathcal{K}_0'(R)}{32\pi\mathcal{I}_0'(R)} + \frac{\mathcal{K}_1'(R)}{8\pi\mathcal{I}_1'(R)} + \frac{\mathcal{K}_2'(R)}{32\pi\mathcal{I}_2'(R)}$$

$$k(R) = \frac{7-R^2}{256\pi\mathcal{I}_1(R)^2} - \frac{(3+7R^2)\mathcal{I}_1''(R)}{128\pi R\mathcal{I}_1'(R)^3} - \frac{(1+R^2)\mathcal{I}_2''(R)}{256\pi\mathcal{I}_1'(R)^3} + \frac{3(1+R^2)\mathcal{I}_1''(R)^2}{128\pi\mathcal{I}_1'(R)^4} - \frac{1}{32\pi}$$

$$n(R) = -\frac{1+R^2}{32\pi R^2\mathcal{I}_1'(R)^2} - \frac{4+R^2}{32\pi R^2\mathcal{I}_2'(R)^2} - \frac{\mathcal{K}_1'(R)}{8\pi\mathcal{I}_1'(R)} - \frac{\mathcal{K}_2'(R)}{8\pi\mathcal{I}_2'(R)}$$

$$h(R) = -\frac{R\mathcal{I}_1'(R)}{64\pi\mathcal{I}_1(R)^3} - \frac{1}{64\pi\mathcal{I}_1(R)^2} - \frac{\mathcal{K}_1(R)}{16\pi\mathcal{I}_1(R)} + \frac{9\mathcal{K}_1'(R)}{128\pi\mathcal{I}_1'(R)} + \frac{\mathcal{K}_2'(R)}{32\pi\mathcal{I}_2'(R)} + \frac{3\mathcal{K}_3'(R)}{128\pi\mathcal{I}_3'(R)} - \frac{67R^2+20}{1536\pi R^2\mathcal{I}_1'(R)^2}$$

$$-\frac{7R^2+8}{384\pi R^2\mathcal{I}_2'(R)^2} + \frac{5R^2+36}{512\pi R^2\mathcal{I}_3'(R)^2} + \frac{R\mathcal{I}_1'(R)}{32\pi\mathcal{I}_1(R)^3} + \frac{47(1+R^2)\mathcal{I}_1''(R)}{1536\pi R\mathcal{I}_1'(R)^3} + \frac{5(4+R^2)\mathcal{I}_2''(R)}{384\pi R\mathcal{I}_2'(R)^3} - \frac{(9+R^2)\mathcal{I}_3''(R)}{512\pi R\mathcal{I}_3'(R)^3}$$

$$j(R) = -\frac{1}{16\pi\mathcal{I}_1(R)^2} + \frac{\mathcal{K}_1(R)}{4\pi\mathcal{I}_1(R)} - \frac{1+R^2}{16\pi R^2\mathcal{I}_1'(R)^2} - \frac{\mathcal{K}_1'(R)}{4\pi\mathcal{I}_1'(R)}$$

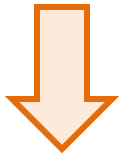
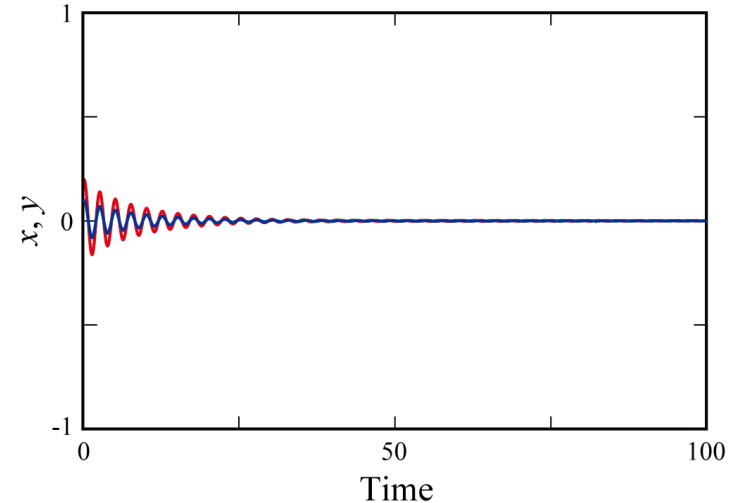
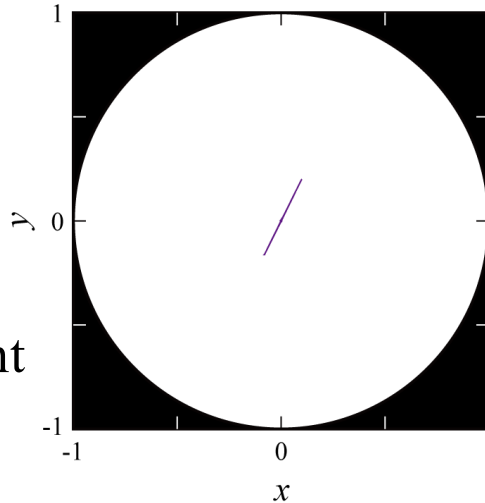
$$p(R) = -\frac{R\mathcal{I}_1'(R)}{64\pi\mathcal{I}_1(R)^3} + \frac{5}{64\pi\mathcal{I}_1(R)^2} - \frac{3\mathcal{K}_1(R)}{16\pi\mathcal{I}_1(R)} + \frac{33\mathcal{K}_1'(R)}{128\pi\mathcal{I}_1'(R)} + \frac{3\mathcal{K}_2'(R)}{32\pi\mathcal{I}_2'(R)} + \frac{3\mathcal{K}_3'(R)}{128\pi\mathcal{I}_3'(R)} + \frac{149R^2+124}{1536\pi R^2\mathcal{I}_1'(R)^2}$$

$$+\frac{11R^2+40}{384\pi R^2\mathcal{I}_2'(R)^2} + \frac{5R^2+36}{512\pi R^2\mathcal{I}_3'(R)^2} - \frac{25(1+R^2)\mathcal{I}_1''(R)}{1536\pi R\mathcal{I}_1'(R)^3} - \frac{(4+R^2)\mathcal{I}_2''(R)}{384\pi R\mathcal{I}_2'(R)^3} - \frac{(9+R^2)\mathcal{I}_3''(R)}{512\pi R\mathcal{I}_3'(R)^3}$$

# Comparison with simulation results

## Rest state

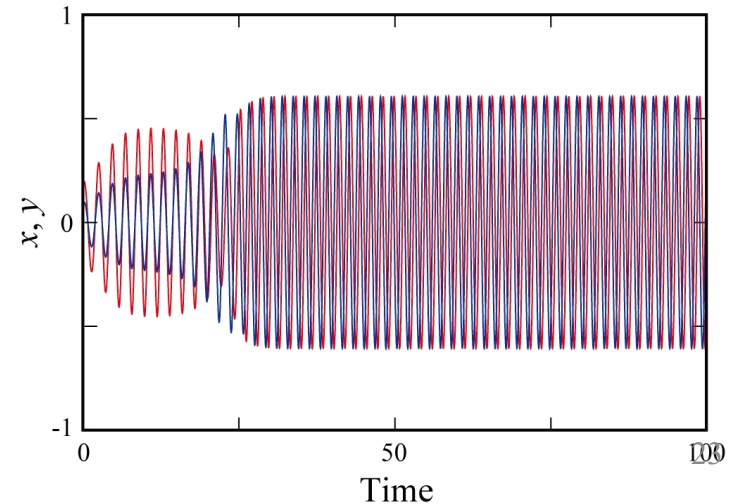
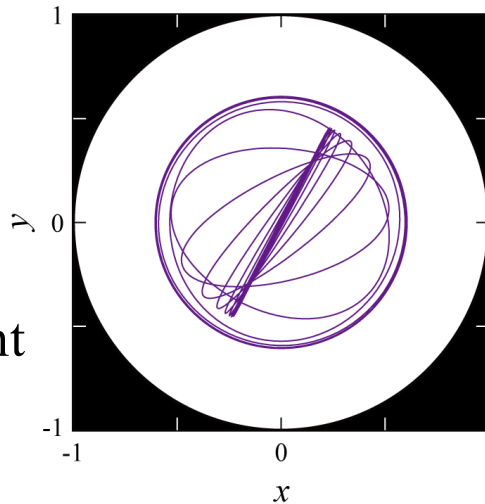
Resistance coefficient  
 $\eta = 0.2$



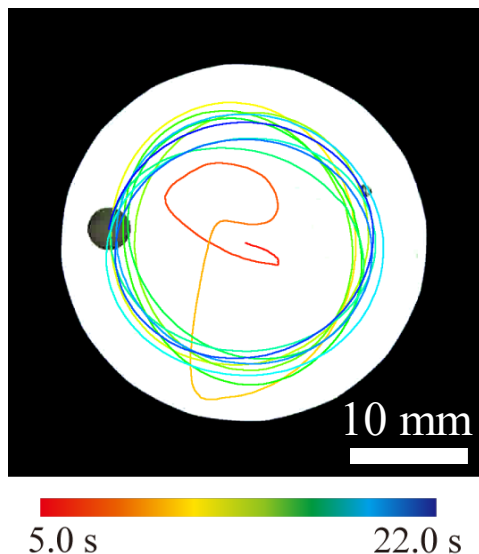
Instabilization of the rest state (Hopf bifurcation)

## Rotation

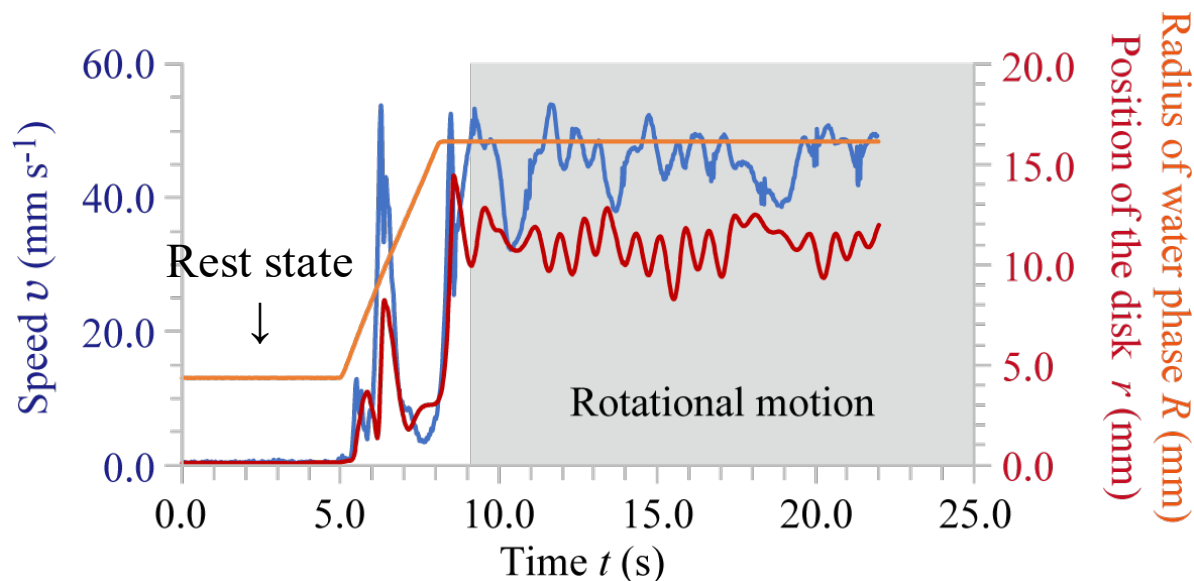
Resistance coefficient  
 $\eta = 0.18$



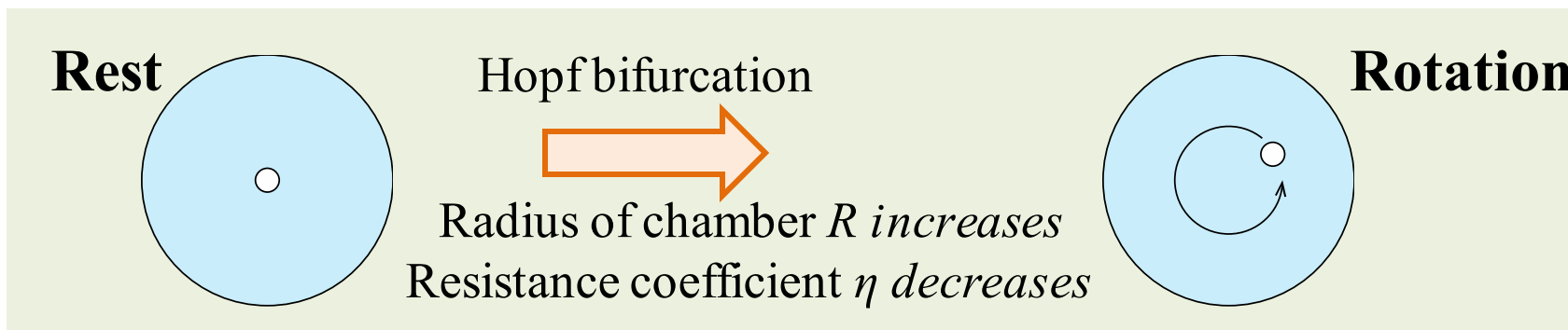
# Comparison with experimental results



Trajectory of  
a camphor disk



Time change in radius and speed of a camphor disk



Koyano, Yoshinaga, and Kitahata, *J. Chem. Phys.* **143**, 014117 (2015).

Koyano, Suematsu, and Kitahata, *Phys. Rev. E* **99**, 022211 (2019).<sup>24</sup>



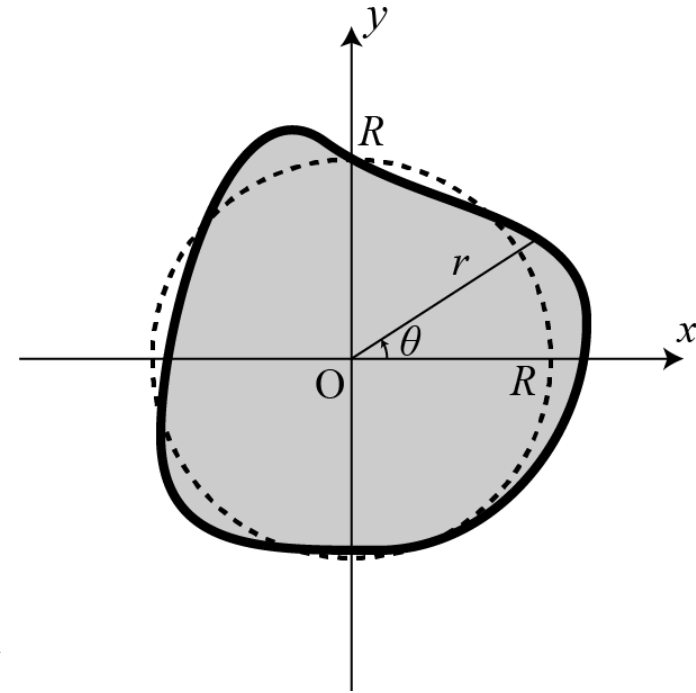
# Contents

- 1) Experimental and theoretical approach for Maranogni surfer (camphor disk)
- 2) Effect of the shape on the motion of a camphor particle
- 3) Interaction between the motion and deformation of an alcohol droplet
- 4) Interaction between the motion and deformation of an alcohol (hexanol) droplet

# How to describe the shape

In the 2D polar coordinates:

$$\begin{aligned} r &= R(1 + \epsilon f(\theta)) \\ &= R \left( 1 + \sum_{k=2}^{\infty} \{a_k \cos k\theta + b_k \sin k\theta\} \right) \end{aligned}$$



- Small deformation from a circular shape
- $a_k, b_k$  : Coefficients of the Fourier expansion
- Only valid when  $|a_k|, |b_k| \ll 1$

$$S_{ij} \Leftrightarrow a_2, b_2$$

$$U_{ijk} \Leftrightarrow a_3, b_3$$

# Theoretical model for the coupling between Motion and Deformation

## Ohta-Ohkuma model (2-mode deformation)

$$\begin{aligned}\frac{d}{dt}v_\alpha &= \gamma v_\alpha - |\mathbf{v}|^2 v_\alpha - a S_{\alpha\beta} v_\beta \\ \frac{d}{dt}S_{\alpha\beta} &= -\kappa S_{\alpha\beta} + b \left( v_\alpha v_\beta - \frac{1}{2} |\mathbf{v}|^2 \delta_{\alpha\beta} \right)\end{aligned}$$

$$S_{ij} \Leftrightarrow a_2, b_2$$

$$U_{ijk} \Leftrightarrow a_3, b_3$$

Ohta and Ohkuma, *Phys. Rev. Lett.* (2009)

## Tarama-Ohta model (2- and 3-mode deformation)

$$\begin{aligned}\frac{dv_i}{dt} &= -\kappa_1 v_i - a_0 v^2 v_i + a_1 S_{im} v_m + a_2 U_{imn} S_{mn} \\ \frac{dS_{ij}}{dt} &= -\kappa_2 S_{ij} - b_0 (S_{mn} S_{mn}) + b_1 \left[ v_i v_j - \frac{v^2}{2} \delta_{ij} \right] + b_2 U_{ijm} v_m \\ \frac{dU_{ijk}}{dt} &= -\kappa_3 U_{ijk} - c_0 (U_{mnp} U_{mnp}) U_{ijk} \\ &\quad + c_1 \left[ v_i S_{jk} + v_j S_{ki} + v_k S_{ij} - \frac{v_m}{2} (\delta_{ij} S_{km} + \delta_{jk} S_{im} + \delta_{ki} S_{jm}) \right]\end{aligned}$$

Tarama and Ohta, *EPL* (2016)

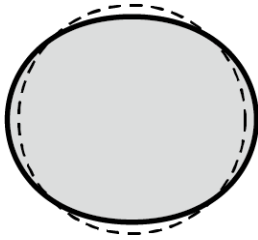
These models only reflect the symmetric properties of the system.

# Example of the deformed droplet

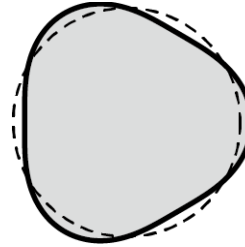
"2 mode" deformation  $a_2$

"3 mode" deformation  $a_3$

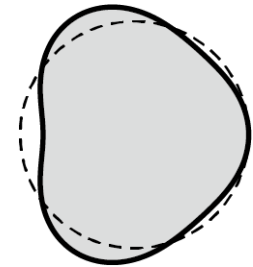
combined shape  $a_2, a_3$



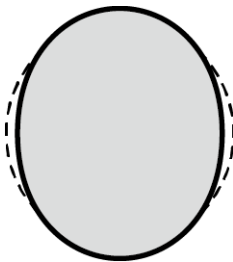
$$r = R(1 + 0.1 \cos 2\theta)$$



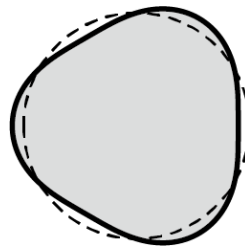
$$r = R(1 + 0.1 \cos 3\theta)$$



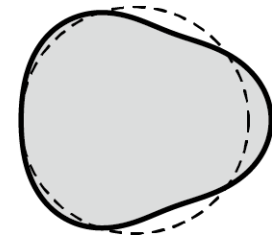
$$r = R(1 - 0.1 \cos 2\theta + 0.1 \cos 3\theta)$$



$$r = R(1 - 0.1 \cos 2\theta)$$



$$r = R(1 - 0.1 \cos 3\theta)$$

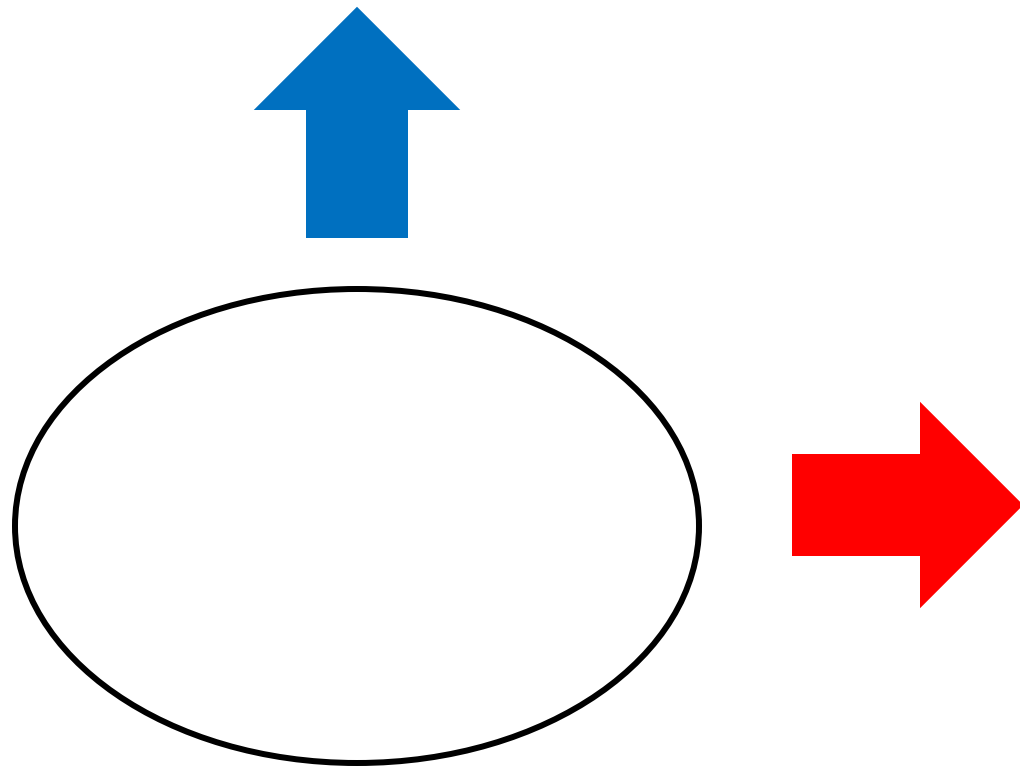


$$r = R(1 + 0.1 \cos 2\theta + 0.1 \cos 3\theta)$$

$$r = R \left( 1 + \sum_{k=2}^{\infty} \{a_k \cos k\theta + b_k \sin k\theta\} \right)$$



# Motion of an elliptic camphor particle (2-mode deformation)



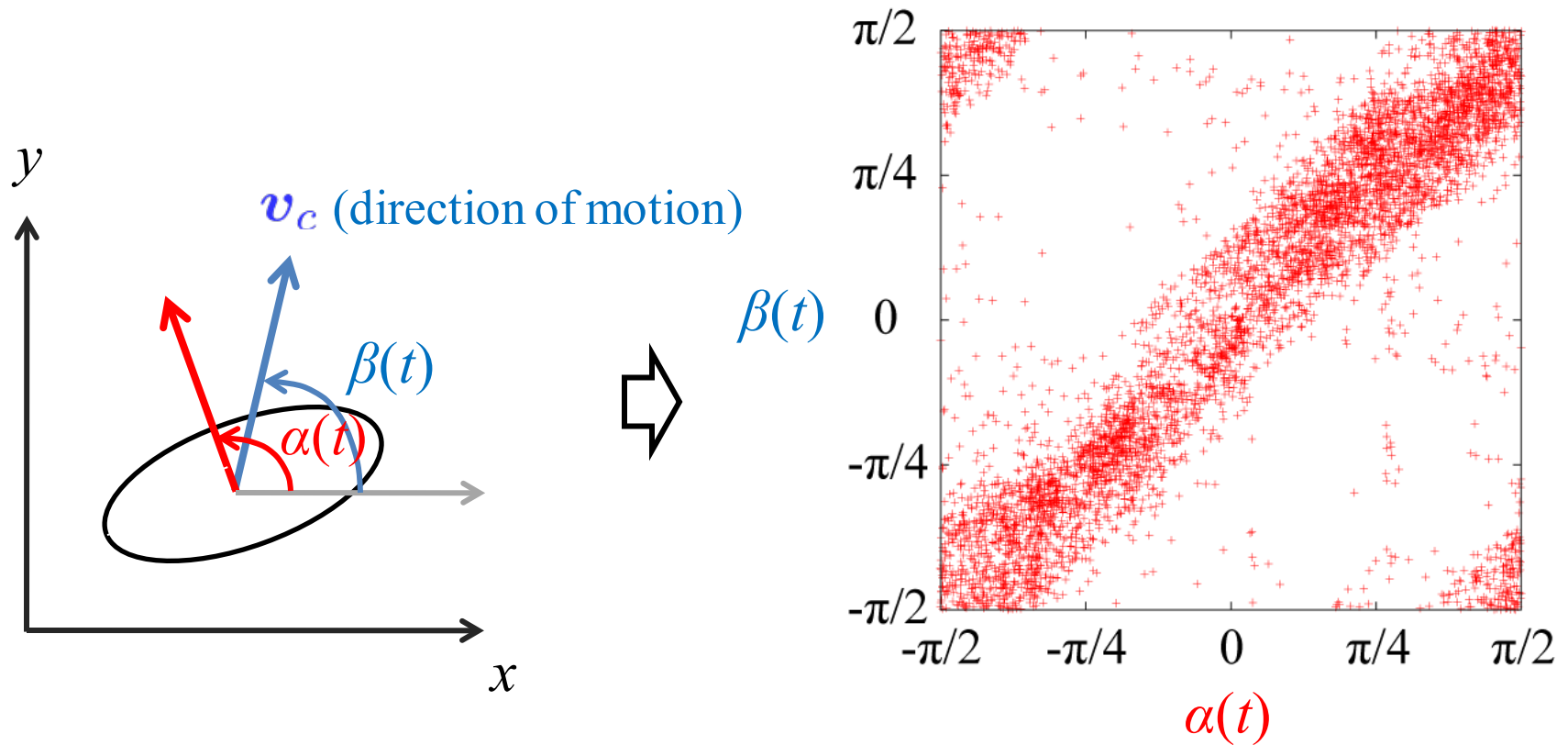
In which direction does the camphor particle move ?

# Motion of an elliptic camphor particle (2-mode deformation)



(real speed)

10 cm



An elliptic camphor disk moves in the minor-axis direction in experiments.

# Modelling (Dimensionless form)

Dynamics of camphor concentration field  $u$

$$\frac{\partial u}{\partial t} = \nabla^2 u - u + S(\mathbf{r}; \mathbf{r}_c, \theta_c)$$

$\mathbf{r}_c$  : COM of the camphor particle

$\theta_c$  : Characteristic angle of the camphor particle

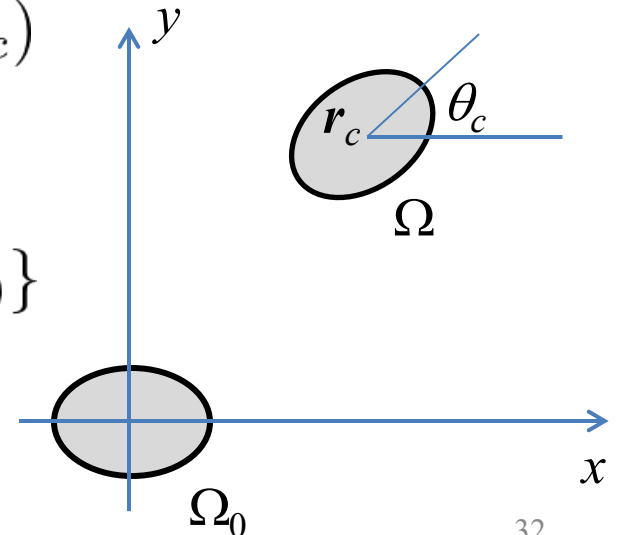
Supply:

$$S(\mathbf{r}; \mathbf{r}_c, \theta_c) = \begin{cases} 1/A, & \mathbf{r} \in \Omega(\mathbf{r}_c, \theta_c) \\ 0, & \mathbf{r} \notin \Omega(\mathbf{r}_c, \theta_c) \end{cases}$$

Shape of the camphor particle

$$\Omega(\mathbf{r}_c, \theta_c) = \{\mathbf{r} | \mathcal{R}(-\theta_c)(\mathbf{r} - \mathbf{r}_c) \in \Omega_0\}$$

$$\mathcal{R}(\phi) = \begin{pmatrix} \cos \phi & -\sin \phi \\ \sin \phi & \cos \phi \end{pmatrix}$$





## Dynamics of Center of mass $\mathbf{r}_c$ and characteristic angle $\theta_c$

$$m \frac{d^2 \mathbf{r}_c}{dt^2} = -\eta_t \frac{d\mathbf{r}_c}{dt} + \mathbf{F}$$

$m$  : Mass

$I$  : Moment of inertia

$$I \frac{d^2 \theta_c}{dt^2} = -\eta_r \frac{d\theta_c}{dt} + N$$

$\eta_t$  : Resistance coefficient for translational motion

$\eta_r$  : Resistance coefficient for rotational motion

## Explicit representation of force $\mathbf{F}$ and torque $N$

$$\mathbf{F} \{u(\mathbf{r}); \mathbf{r}_c, \theta_c\} = \oint_{\partial\Omega(\mathbf{r}_c, \theta_c)} \gamma(u(\boldsymbol{\ell})) \mathbf{n}(\boldsymbol{\ell}) d\ell$$

$$= \int_{\Omega(\mathbf{r}_c, \theta_c)} \nabla \gamma(u(\boldsymbol{\ell})) \mathbf{n}(\boldsymbol{\ell}) dA$$

$$N \{u(\mathbf{r}); \mathbf{r}_c, \theta_c\} = \oint_{\partial\Omega(\mathbf{r}_c, \theta_c)} (\boldsymbol{\ell} - \mathbf{r}_c) \times \gamma(\boldsymbol{\ell}) \mathbf{n}(\boldsymbol{\ell}) d\ell$$

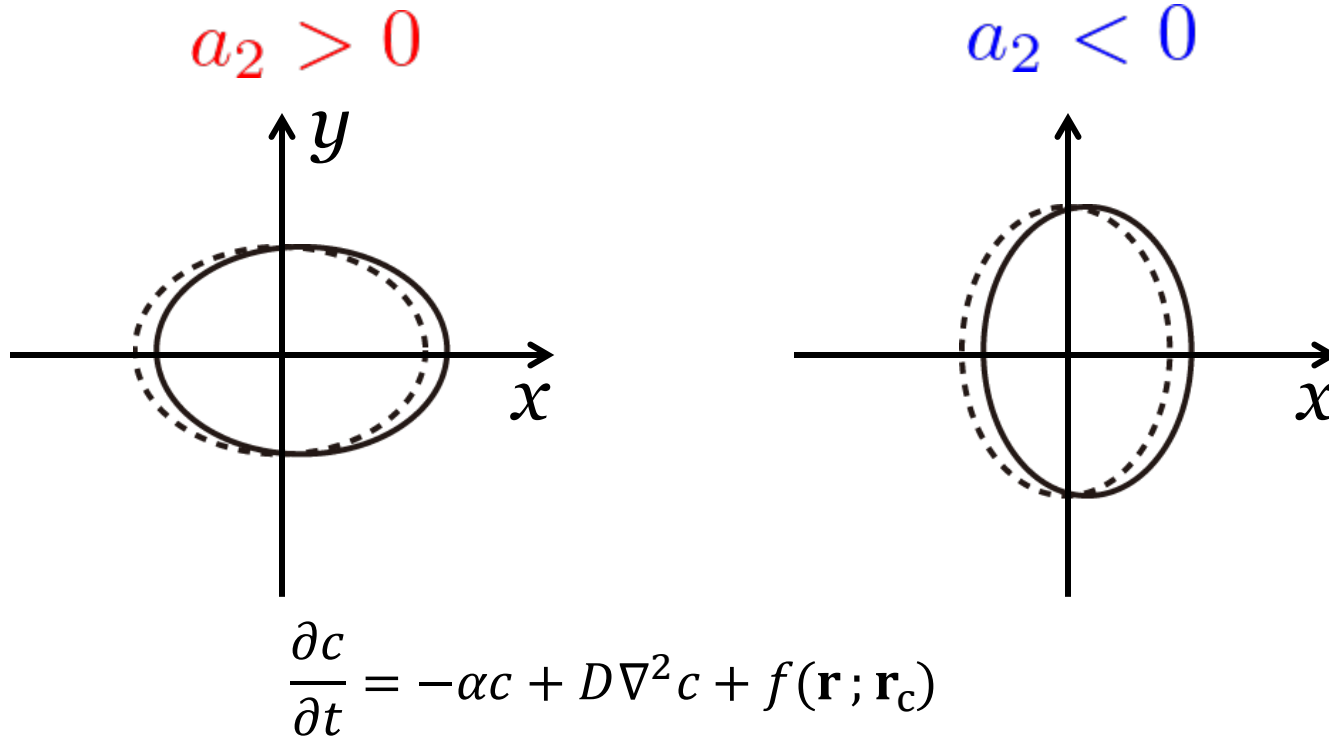
$$= \int_{\Omega(\mathbf{r}_c, \theta_c)} (\boldsymbol{\ell} - \mathbf{r}_c) \times \nabla \gamma(\boldsymbol{\ell}) \mathbf{n}(\boldsymbol{\ell}) dA$$

## Surface tension $\gamma$ depending on camphor concentration $u$

$$\gamma = \gamma(u) = \gamma_0 - ku \quad (\text{M. Nagayama } et al., \textit{Physica D}, 2004)$$

# Analysis for an elliptic particle

We calculated the force when the elliptic camphor particle is moving in the  $x$ -axis direction.



In the co-moving coordinates

$$-v \frac{\partial c}{\partial x} = -\alpha c + D\nabla^2 c + f(\mathbf{r}; \mathbf{0})$$

( $v$  is an infinitesimally small parameter.)

$$-v \frac{\partial c}{\partial x} = -\alpha c + D \nabla^2 c + f(\mathbf{r}; \mathbf{0})$$

$$-v \frac{\partial}{\partial x} (c_0 + v c_1 + v^2 c_2 + \dots) = (-\alpha + D \nabla^2) (c_0 + v c_1 + v^2 c_2 + \dots) + f(\mathbf{r}; \mathbf{0})$$

The perturbation method was used:

$$0 = -\alpha c_0 + D \nabla^2 c_0 + f(\mathbf{r}, 0)$$

$$c_0(r, \theta) = \begin{cases} \frac{f_0}{\alpha} \left[ 1 - \frac{R}{\lambda} \mathcal{K}_1 \left( \frac{R}{\lambda} \right) \mathcal{I}_0 \left( \frac{R}{\lambda} \right) + \epsilon \left( \frac{R}{\lambda} \right)^2 \mathcal{K}_2 \left( \frac{R}{\lambda} \right) \mathcal{I}_2 \left( \frac{r}{\lambda} \right) \cos 2\theta \right] & \text{if } r < R(1 + \epsilon \cos 2\theta) \\ \frac{f_0}{\alpha} \left[ \frac{R}{\lambda} \mathcal{I}_1 \left( \frac{R}{\lambda} \right) \mathcal{K}_0 \left( \frac{R}{\lambda} \right) + \epsilon \left( \frac{R}{\lambda} \right)^2 \mathcal{I}_2 \left( \frac{R}{\lambda} \right) \mathcal{K}_2 \left( \frac{r}{\lambda} \right) \cos 2\theta \right] & \text{if } r \geq R(1 + \epsilon \cos 2\theta) \end{cases}$$

$$-\frac{\partial c_{n-1}}{\partial x} = -\alpha c_n + D \nabla^2 c_n$$

$$c_1(r, \theta) = \dots$$

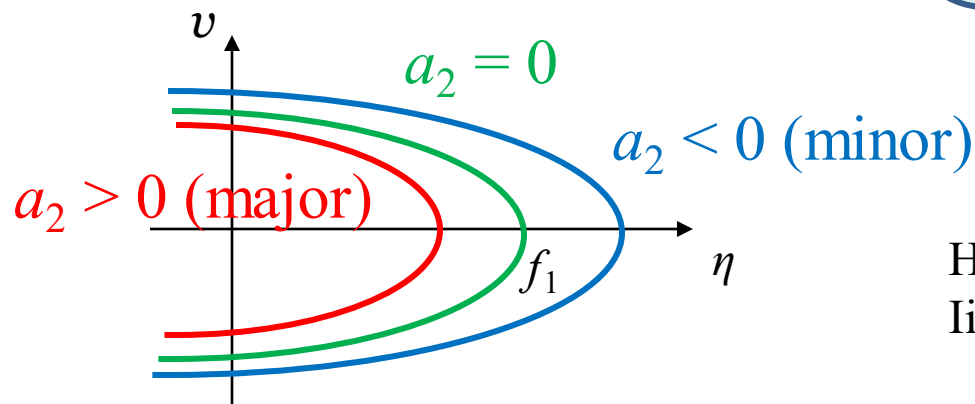
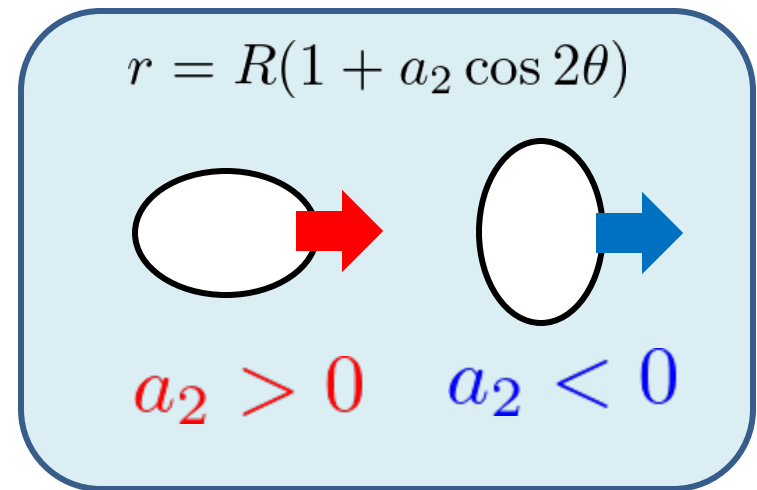
# Result of analysis

$$m \frac{dv}{dt} = -\eta v + \left( f_1^{(0)} + \tilde{f}_1 a_2 \right) v - \left( f_3^{(0)} + \tilde{f}_3 a_2 \right) v^3$$

$$\tilde{f}_1 = -\frac{R^2}{2} [\mathcal{I}_1(R)\mathcal{K}_1(R) - \mathcal{I}_2(R)\mathcal{K}_2(R)] < 0$$

If an elliptic camphor particle is moving in its minor-axis direction, the force originating from surface tension gradient is stronger.

An elliptic particle moves in its minor-axis direction.



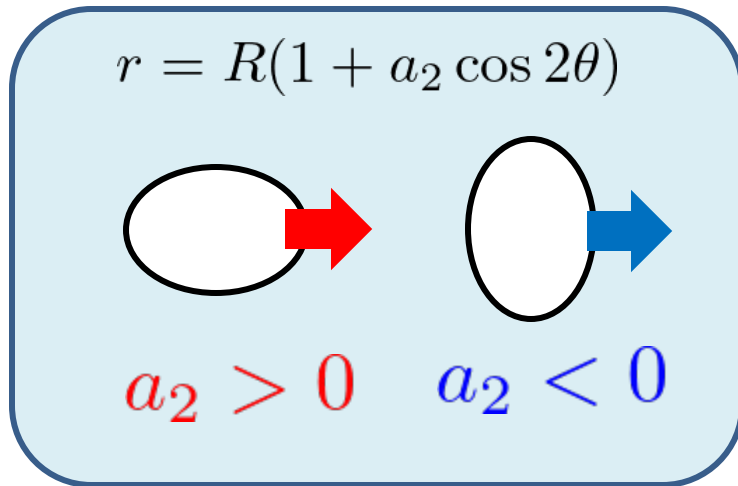
HK, Iida, Nagayama, *PRE* (2013)  
Iida, HK, Nagayama, *Physica D* (2014)



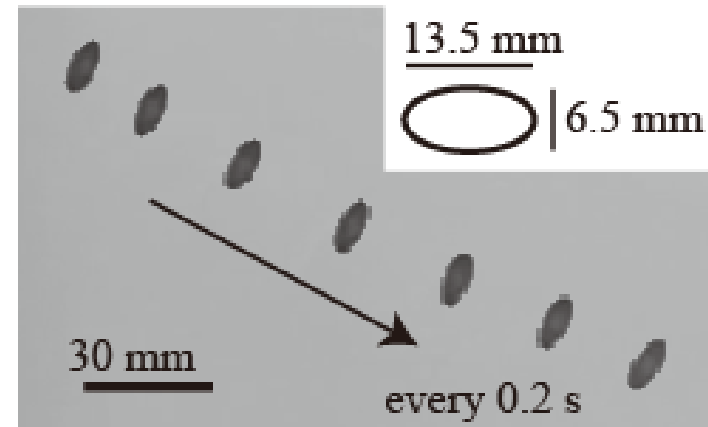
# Comparison with experiments

## Analyses

$$m \frac{dv}{dt} = -\eta v + \left( f_1^{(0)} + \tilde{f}_1 a_2 \right) v - \left( f_3^{(0)} + \tilde{f}_3 a_2 \right) v^3$$
$$\tilde{f}_1 < 0$$



## Experiments



An elliptic particle moves in its minor-axis direction.

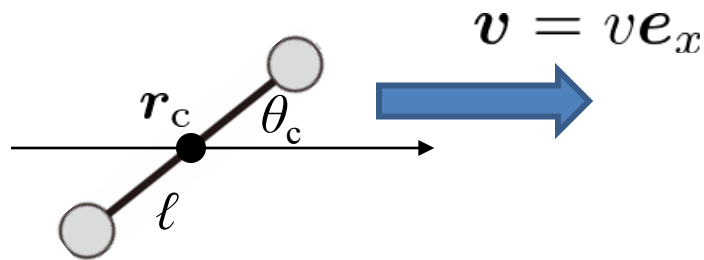
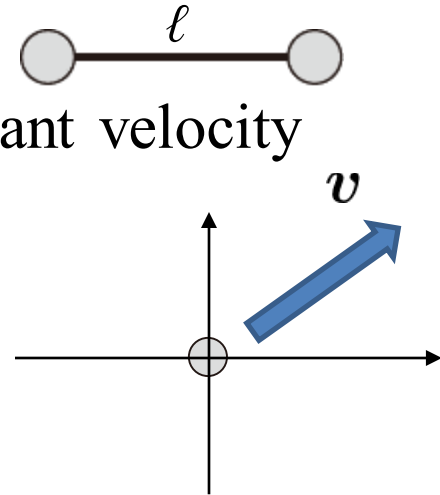
HK, K. Iida, M. Nagayama, *Phys. Rev. E* **84**, 015101 (2013).

K. Iida, HK, M. Nagayama, *Physica D* **272**, 39 (2014).

# Combination of point particles

Concentration field by one particle moving at a constant velocity

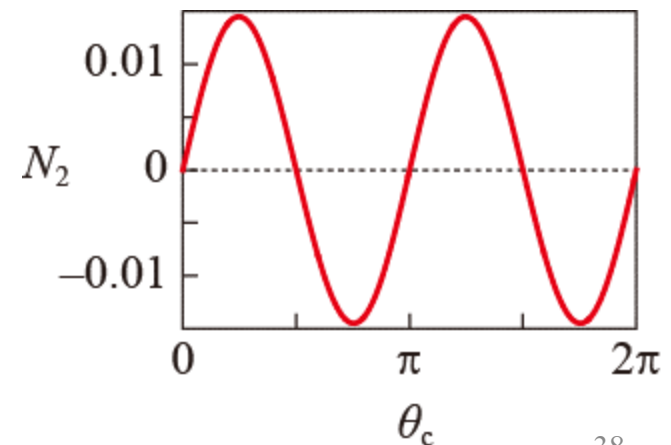
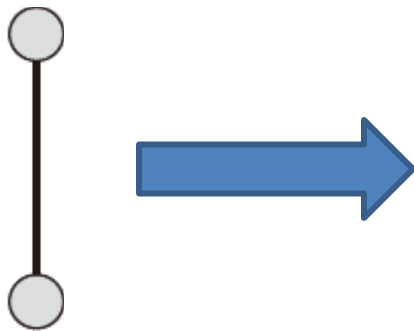
$$u(\mathbf{r}) = \frac{1}{2\pi} \mathcal{K}_0 \left( \left( 1 + \frac{|\mathbf{v}|^2}{4} \right)^{1/2} |\mathbf{r}| \right) \exp \left( -\frac{1}{2} \mathbf{v} \cdot \mathbf{r} \right)$$



Torque:

$$N_2 \simeq \frac{k}{8\pi} \mathcal{K}_0(\ell) \ell v^2 \sin 2\theta_c + \mathcal{O}(v^3)$$

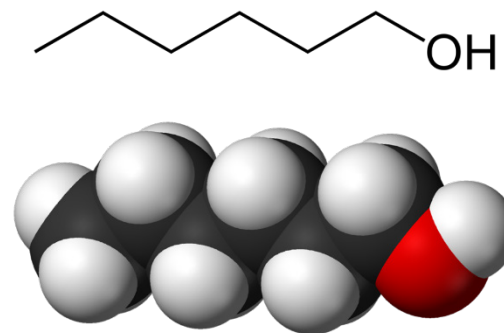
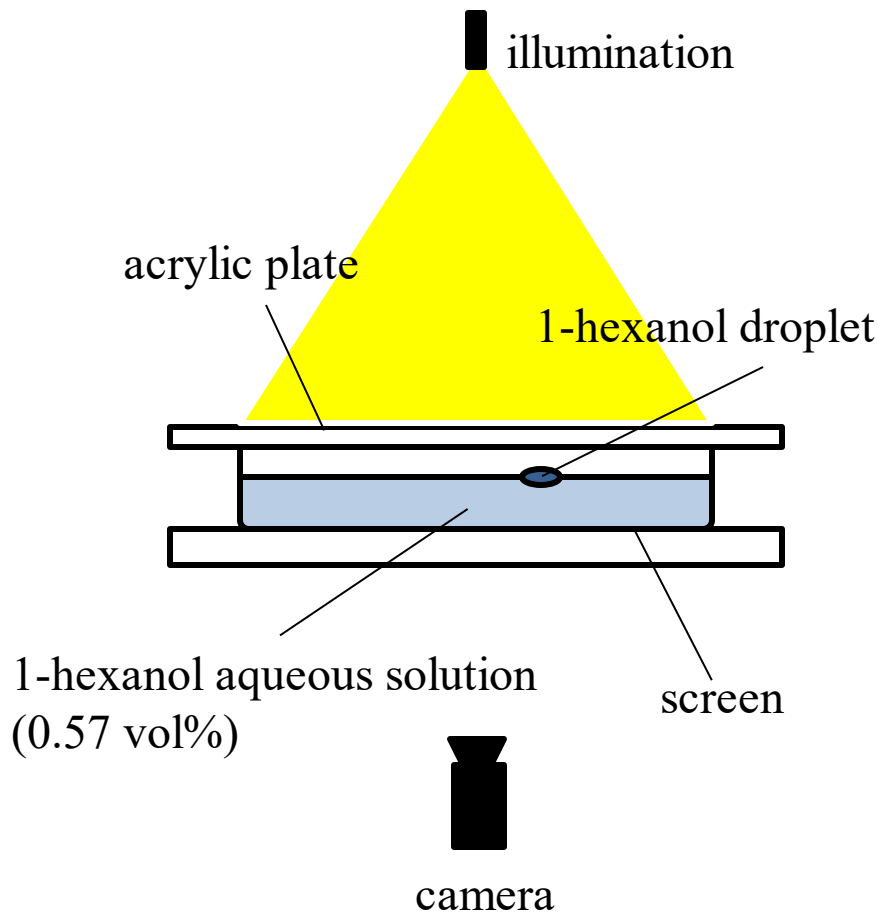
The fixed point at  $\theta_c = \pm \frac{\pi}{2}$  is stable.



# Contents

- 1) Experimental and theoretical approach for Maranogni surfer (camphor disk)
- 2) Effect of the shape on the motion of a camphor particle
- 3) Interaction between the motion and deformation of an alcohol droplet
- 4) Large deformation coupled with motion of an oil droplet with oil red O

# Deformation of the hexanol droplet



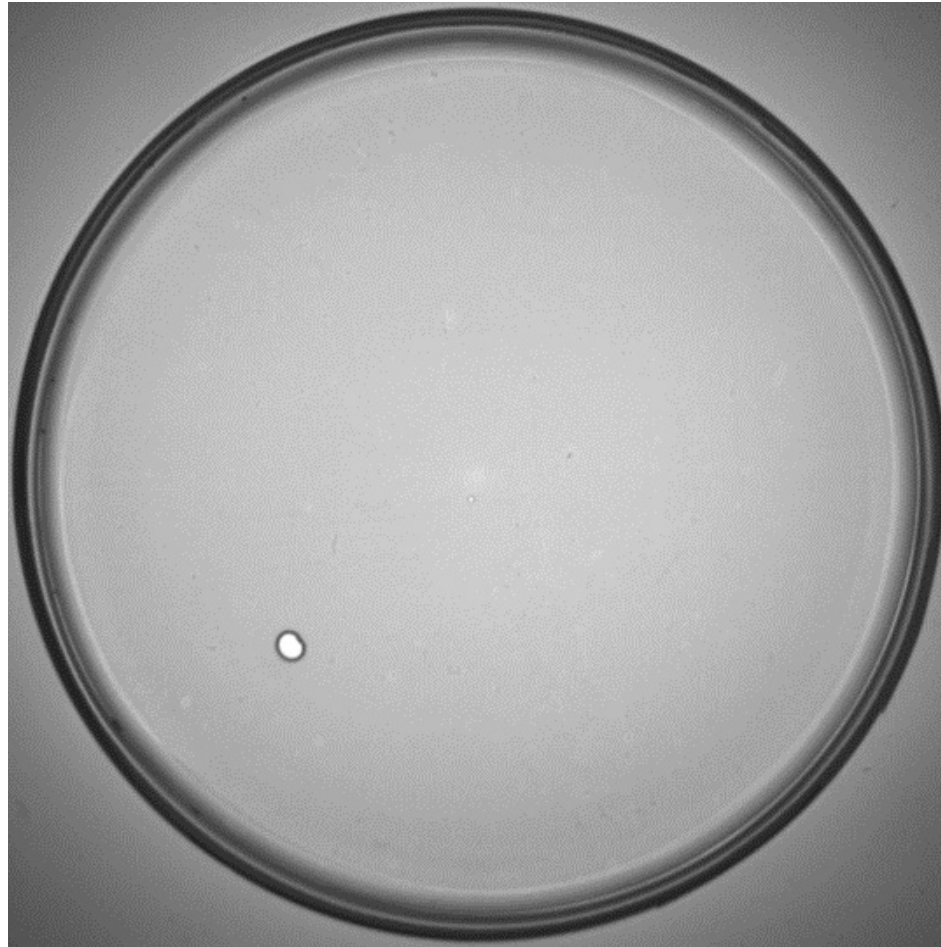
1-hexanol (Wikipedia)

Hexanol droplet on  
0.57 vol% hexanol aqueous solution  
(saturated solubility: 0.59 vol%)


Yalkowsky, S.H., He, Yan., Handbook of Aqueous Solubility Data: An Extensive Compilation of Aqueous Solubility Data for Organic Compounds Extracted from the AQUASOL dATABASE. CRC Press LLC, Boca Raton, FL. 2003., p. 326



# Experimental results



real speed

  
50 mm

# Measurement of droplet shape

From the video, we obtained the droplet shape and calculated the moments.

area:  $A = \iint_{\Omega} dS$

COM:  $\langle x_c \rangle = \frac{\iint_{\Omega} x dS}{A} \quad \langle y_c \rangle = \frac{\iint_{\Omega} y dS}{A}$

Moment:  $\langle X^i Y^j \rangle = \frac{\iint_{\Omega} (x - x_c)^i (y - y_c)^j dS}{A}$

$$a_2 = \frac{\pi}{A} (\langle X^2 \rangle - \langle Y^2 \rangle)$$

$$b_2 = \frac{\pi}{A} \langle 2XY \rangle$$

$$a_3 = \left(\frac{\pi}{A}\right)^{3/2} (2 \langle X^3 \rangle - 2 \langle XY^2 \rangle)$$

$$b_3 = \left(\frac{\pi}{A}\right)^{3/2} (2 \langle X^2 Y \rangle - 2 \langle Y^3 \rangle)$$

$$\text{cf) } r = R \left( 1 + \sum_{k=2}^{\infty} \{a_k \cos k\theta + b_k \sin k\theta\} \right)$$

# Relationship between motion and deformation

We consider the angle from the direction of the motion.

$\theta_v$  : direction of the droplet velocity

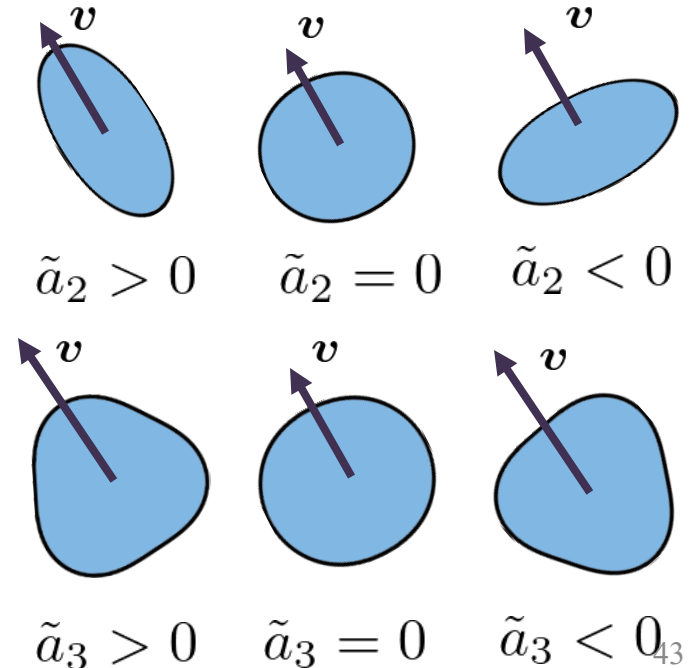
$$\mathbf{v} = \frac{dx_c}{dt} \mathbf{e}_x + \frac{dy_c}{dt} \mathbf{e}_y = v (\cos \theta_v \mathbf{e}_x + \sin \theta_v \mathbf{e}_y)$$

$$r = R \left( 1 + \sum_{k=2}^{\infty} \left\{ \tilde{a}_k \cos k(\theta - \theta_v) + \tilde{b}_k \sin k(\theta - \theta_v) \right\} \right)$$

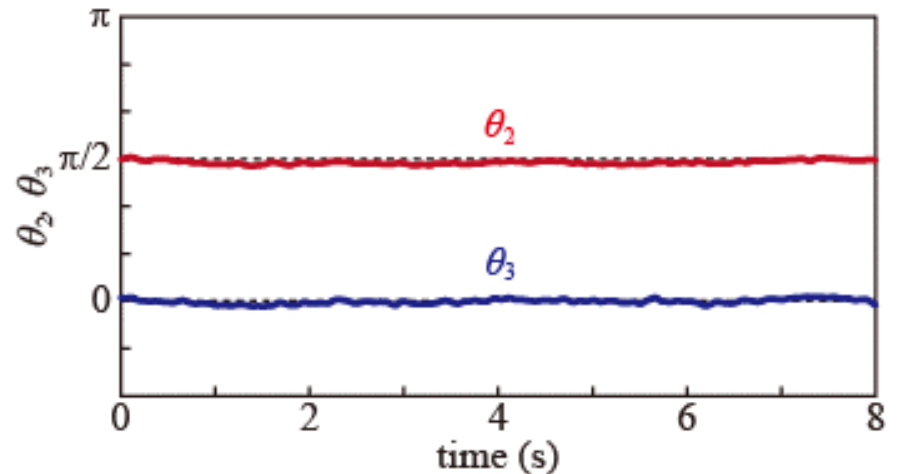
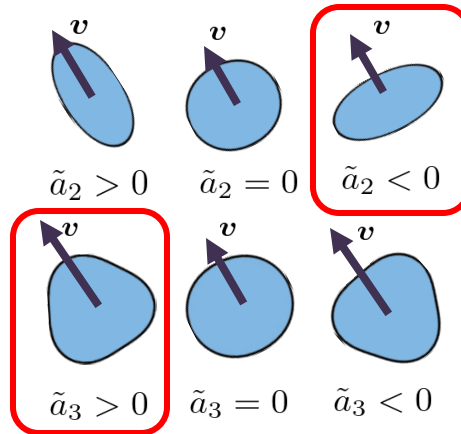
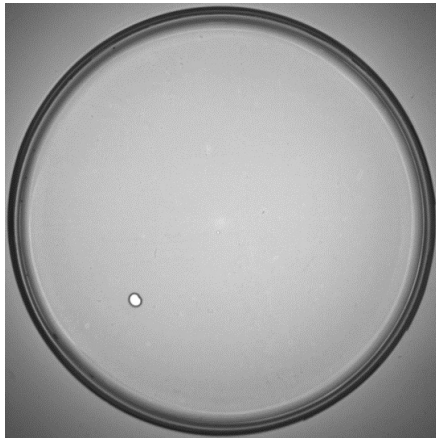
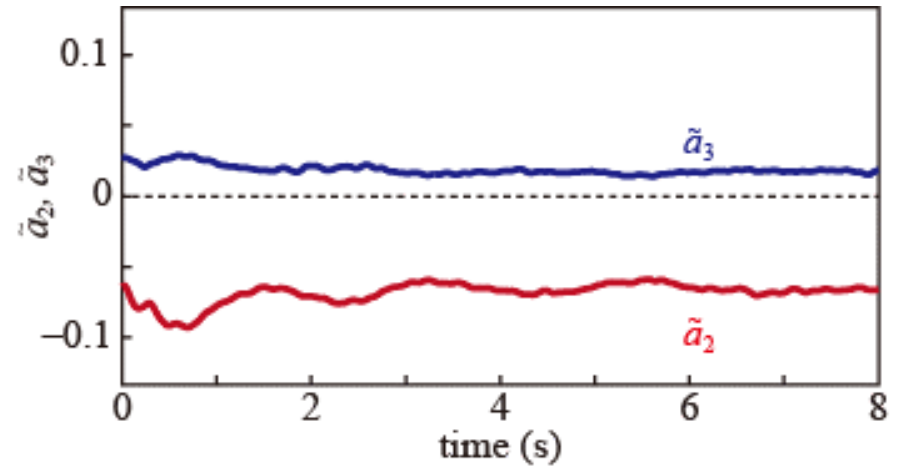
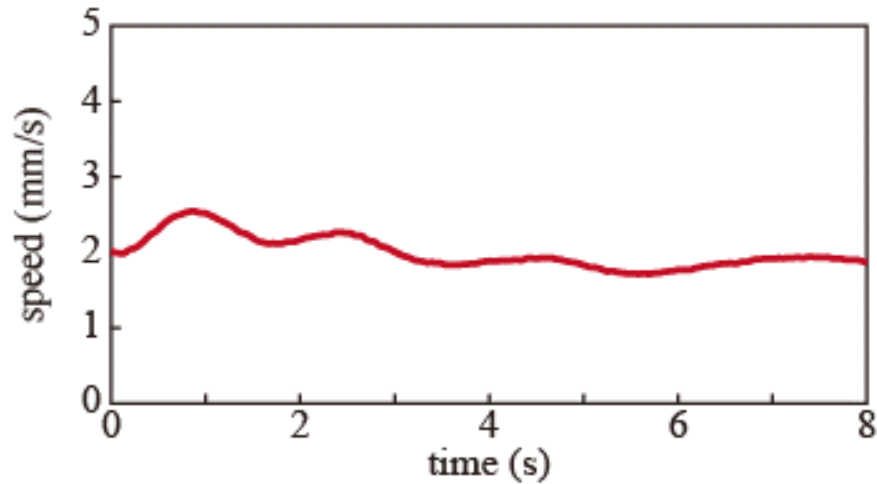
$$\begin{aligned} \tilde{a}_k &= a_k \cos k\theta_v + b_k \sin k\theta_v \\ &= \sqrt{a_k^2 + b_k^2} \cos k(\theta_k - \theta_v) \end{aligned}$$

$$\begin{aligned} \tilde{b}_k &= -a_k \sin k\theta_v + b_k \cos k\theta_v \\ &= \sqrt{a_k^2 + b_k^2} \sin k(\theta_k - \theta_v) \end{aligned}$$

$$\theta_k = \frac{1}{k} \tan^{-1} \frac{b_k}{a_k}$$



# Motion and deformation for translational motion

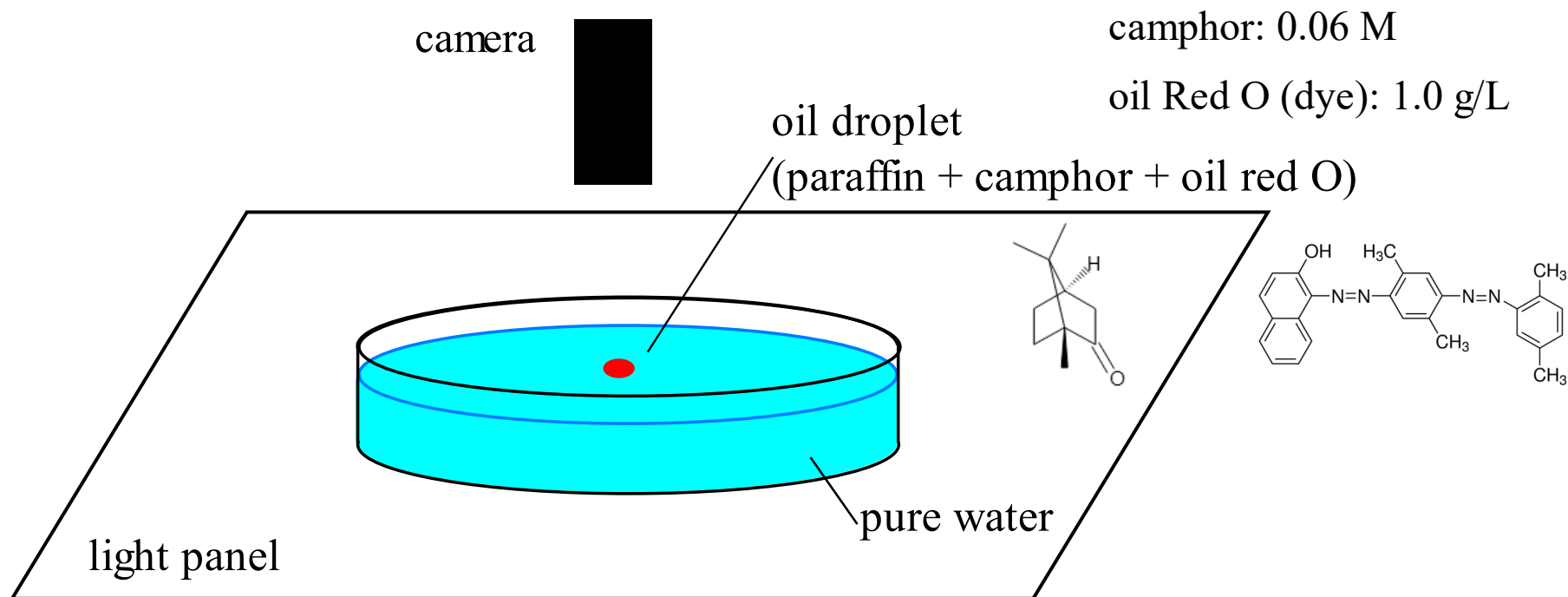




# Contents

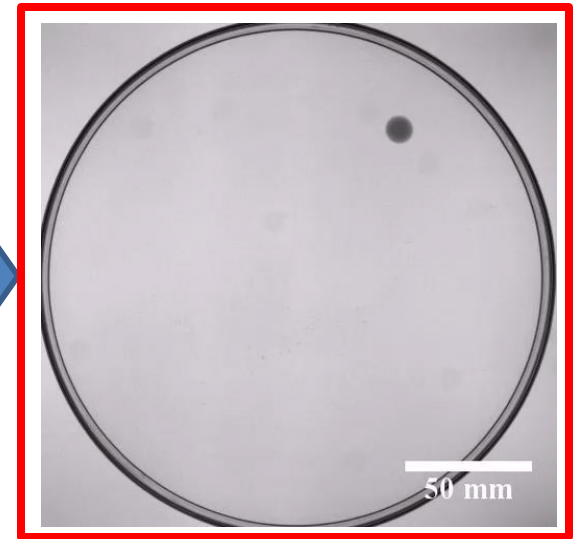
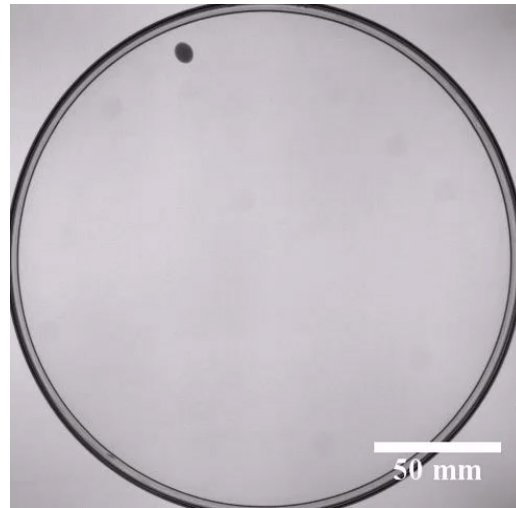
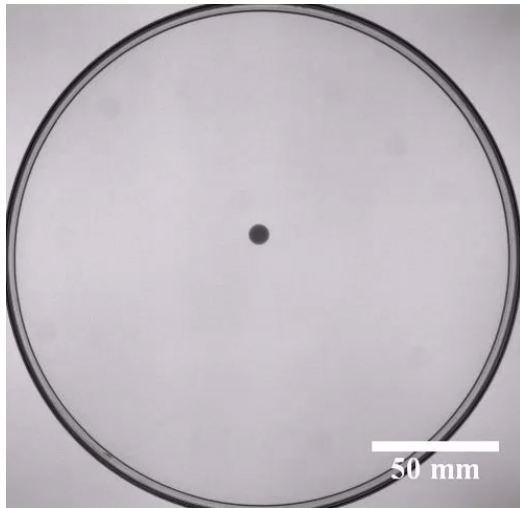
- 1) Experimental and theoretical approach for Maranogni surfer (camphor disk)
- 2) Effect of the shape on the motion of a camphor particle
- 3) Interaction between the motion and deformation of an alcohol droplet
- 4) Large deformation coupled with motion of an oil droplet with oil red O

# Large deformation of an oil droplet



Put a paraffin droplet containing camphor and oil red O on the water surface and record the video from above for an hour.

# Time evolution of the system

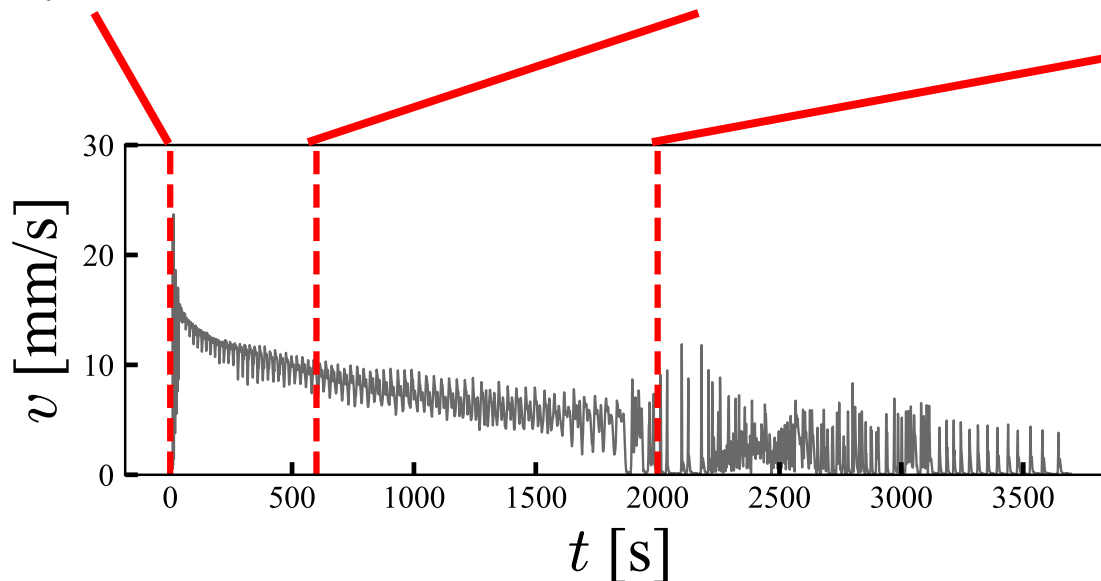


Straight motion with reflection by the dish wall

Motion along the dish wall

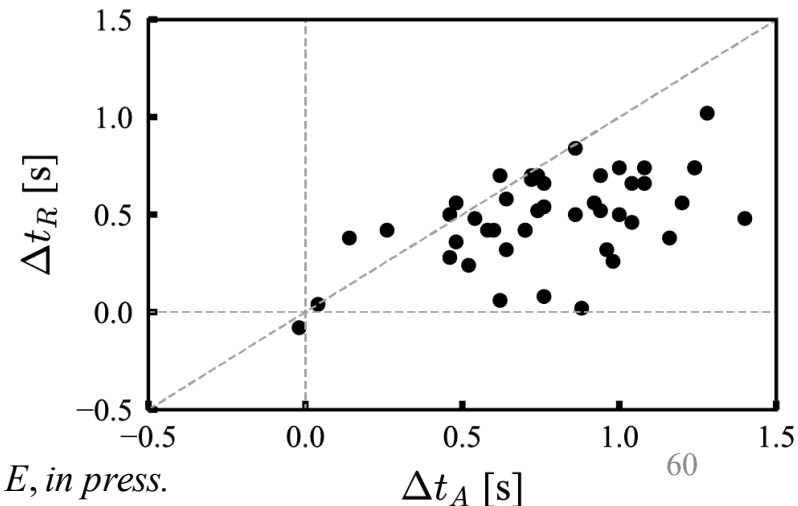
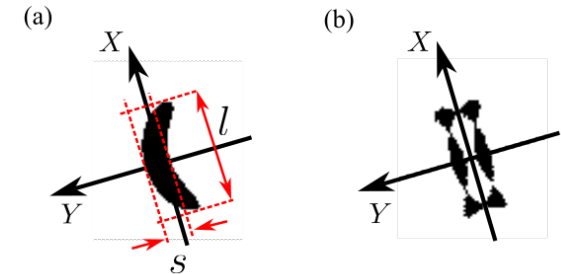
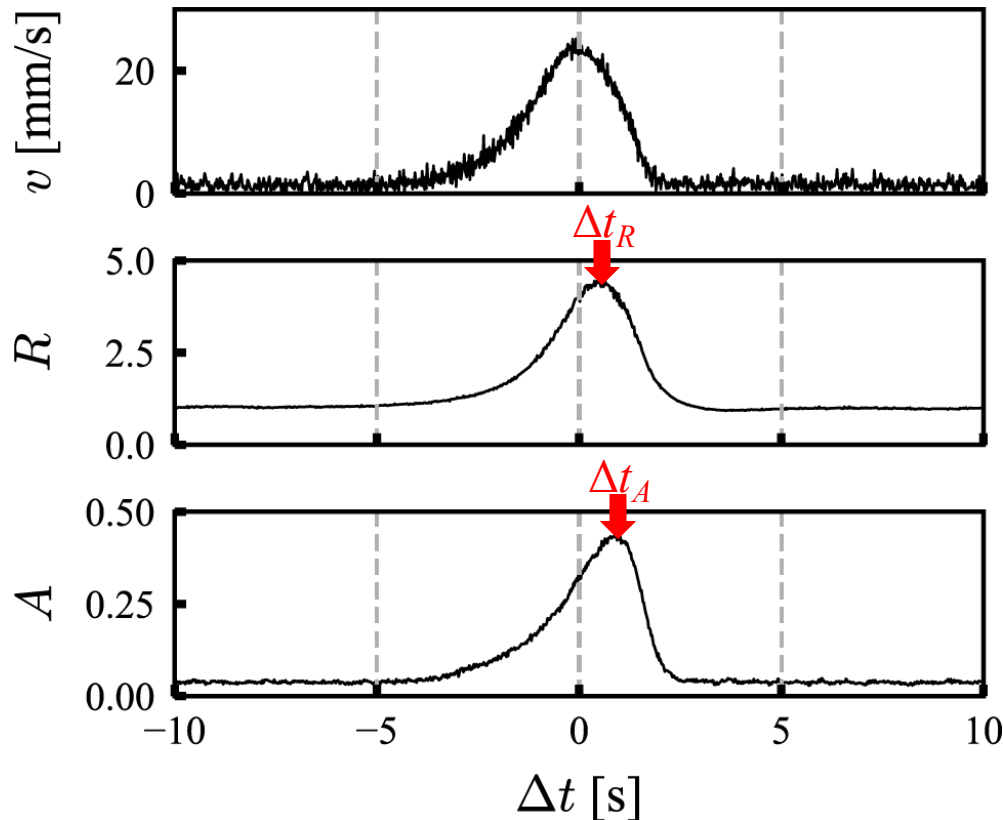
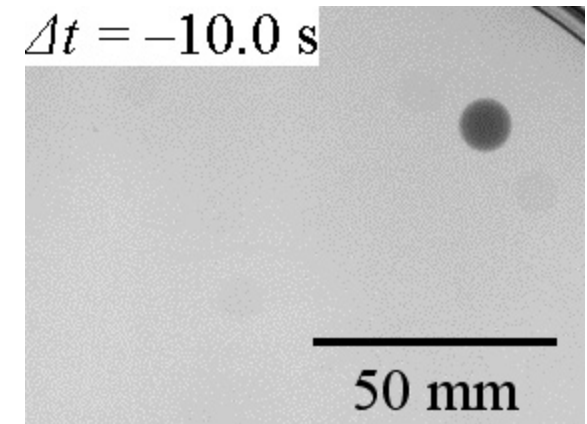
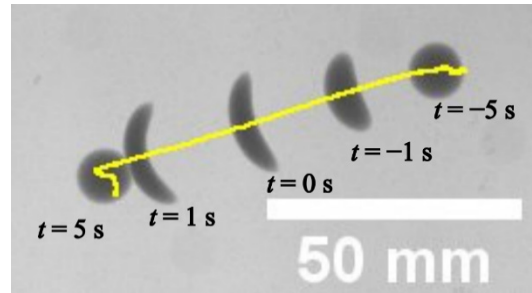
Dynamic deformation with intermittent motion

(real time)



# Time series of intermittent motion

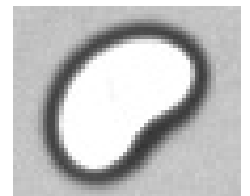
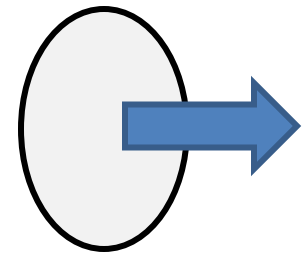
- Deformation and motion began almost at the same time.
- Deformation became even greater after its speed has a peak.





# Conclusion

- We investigated the effect of the shape on the motion in the system where a particle is moving due to the surface tension gradient generated by the diffusion of the surface-active compounds.
- Experiments and theoretical analysis show that an elliptic (2-mode) particle moves in its minor-axis direction.
- In the system with a self-propelled alcohol droplet, we succeeded in characterizing the time change in the droplet shape, and discussed the mechanism of the coupling between motion and deformation.



# Acknowledgments



JSPS-PAN Bilateral program  
(between Japan and Poland)

Kenichi Yoshikawa (Doshisha Univ.)  
Satoshi Nakata (Hiroshima Univ.)  
Jerzy Gorecki (Polish Academy of Sciences)  
Masaharu Nagayama (Hokkaido Univ.)  
Tatsunari Sakurai (Musashino Univ.)  
Natsuhiko Yoshinaga (Tohoku Univ.)  
Nobuhiko Suematsu (Meiji Univ.)  
Yutaka Sumino (Tokyo Univ. of Science)  
Ken Nagai (JAIST)  
Keita Iida (Osaka Univ.)  
Hiroyuki Ebata (Kyushu Univ.)  
Mitsusuke Tarama (Kyushu Univ.)  
Yuki Koyano (Kobe Univ.)  
Hiroaki Ito (Chiba Univ.)  
Shin Kojima (Chiba Univ.)  
Sayaka Otani (Chiba Univ.)



Active Matter c2c



物質・デバイス領域共同研究拠点



# Poster Presentation

\* Poster Award of ICMMA 2024

No.	POSTER TITLE	AUTHOR(S) NAME
1	“A design principle for slow-wave sleep firing pattern with Na <sup>+</sup> dynamics”	Tomohide Sato (Univ. Tokyo), Koji L. Ode (Univ. Tokyo), Fukuaki L. Kinoshita (RIKEN BDR), and Hiroki R. Ueda (Univ. Tokyo, RIKEN BDR)
2	“Optimal setting of a Poincaré section for calculating the phase of rhythmic spatiotemporal dynamics”	Takahiro Arai (JAMSTEC), Yoji Kawamura (JAMSTEC), and Toshio Aoyagi (Kyoto Univ.)
3	*Poster Award “Molecularly Designed Self-Propelled Motion of Perylenediimide Dianions”	Lara Rae Holstein (NIMS, Tsukuba Univ.), Nobuhiko J. Suematsu (Meiji Univ.), Masayuki Takeuchi (NIMS, Tsukuba Univ.), Atsuro Takai (NIMS)
4	“Collective Dynamics of Self-propelled BZ Droplets”	Nobuhiko J. Suematsu (Meiji Univ.)
5	“Towards molecular robots: far-from-equilibrium motion of molecular assembly”	Yoshiyuki Kageyama (Hokkaido Univ.)
6	“Reaction period and its fluctuation of Belousov-Zhabotinsky rection in microscale”	Hiroki Emmei (Kindai Univ.) and Takatoshi Ichino (Kindai Univ.)
7	“Movement of camphor boat with flow”	Takatoshi Ichino (Kindai Univ.)
8	“Objective assessment of sleep-wake rhythms using a wearable device in healthy adults”	Mitsuki Umino (Meiji Univ.), Sho Tachimoto (Meiji Univ.), and Takahiro J. Nakamura (Meiji Univ.)
9	“Characterizing two transitions in a population of Kuramoto oscillators with stochastic resetting”	Ayumi Ozawa (JAMSTEC) and Hiroshi Kori (Univ. Tokyo)
10	“Identifying the interaction type in phase oscillator networks from time series”	Weiwei Su (Univ. of Tokyo)



## Poster Presentation

✧ Poster Award of ICMMA 2024

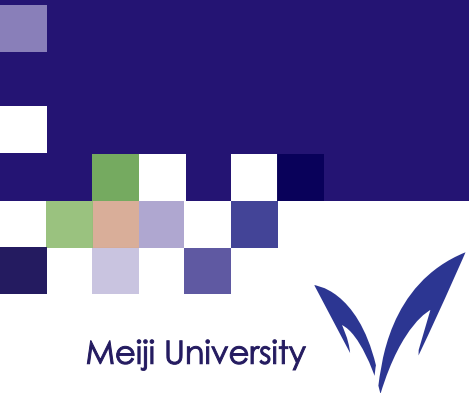
NO.	POSTER TITLE	AUTHOR(S) NAME
11	<b>*Best Poster Award</b> “Roles of suprachiasmatic AVP neurons on female reproductive functions”	Mizuki Sugiyama (Meiji Univ.), Jiaxu Chen (Meiji Univ.), Michihiro Mieda (Kanazawa Univ.), and Takahiro J. Nakamura (Meiji Univ.)
12	“Propagation properties of precipitation bands induced by precipitation and redissolution reactions”	Yuhei Onishi (Meiji Univ.) and Nobuhiko J. Suematsu (Meiji Univ.)
13	“Phase control of the high-dimensional Kuramoto model using dynamical reduction approaches”	Narumi Fujii (Tokyo Tech) and Hiroya Nakao (Tokyo Tech)
14	“Hydrodynamic simulation of synchronized flow pattern in two coupled collapsible tubes”	Yuki Araya (Chiba Univ.), Hiroaki Ito (Chiba Univ.), and Hiroyuki Kitahata (Chiba Univ.)
15	“The oscillatory phenomenon of glycolysis in astrocytes related to brain diseases.”	Li Xianghui (Yokohama Nat. Univ.), Amemiya Takashi (Yokohama Nat. Univ.), and Shibata Kenichi (Yokohama Nat. Univ.)
16	“Excessive synchronisation of cortical networks causes sensory processing disorders in human”	Osamu Inomoto (Kyusyu Sangyo Univ.)
17	<b>*Excellent Poster Presentation Award</b> “Analysis of bifurcation structure in the non-reciprocal Swift-Hohenberg model”	Yuta Tateyama (Chiba Univ.), Hiroaki Ito (Chiba Univ.), Shigeyuki Komura (WIUCAS), and Hiroyuki Kitahata (Chiba Univ.)
18	“Analysis of the bifurcation in thermal convection patterns in immiscible liquid bilayer with an undeformed interface”	Mizuki Nakamura (Chiba Univ.), Hiroaki Ito (Chiba Univ.), and Hiroyuki Kitahata (Chiba Univ.)
19	<b>*Poster Award</b> “Phase autoencoder: data-driven phase reduction for limit-cycle oscillators”	Koichiro Yawata (Tokyo Tech. Univ.) and Hiroya Nakao (Tokyo Tech. Univ.)
20	“Mode-switching of Self-propelled Camphor Disks depending on the Number Density”	Koki Shinoda (Meiji Univ.) and Nobuhiko. J. Suematsu (Meiji Univ.)



## Poster Presentation

\* Poster Award of ICMMA 2024

No.	POSTER TITLE	AUTHOR(S) NAME
21	“Bifurcation of the Belousov-Zhabotinsky Reaction in a Droplet depending on the Droplet Size and Light Intensity”	Keigo Takeda (Meiji Univ.) and Nobuhiko J. Suematsu (Meiji Univ.)
22	“Spatially locked chimera states”	Petar Mircheski (Tokyo Tech) and Hiroya Nakao (Tokyo Tech)
23	“GPPI: Gaussian Process Phase Interpolation for estimating the asymptotic phase of a limit cycle oscillator from time series”	Ryota Kobayashi (Univ. Tokyo), Taichi Yamamoto (Univ. Tokyo), and Hiroya Nakao (Tokyo Tech)
24	“Sharp interface limit of porous medium Allen-Cahn equation”	Hyunjoon Park (Meiji Univ.), Hiroshi Matano (Meiji Univ.), and Mori Ryunosuke (Meiji Univ.)
25	*Excellent Poster Presentation Award “The rate of photosynthesis of Euglena under periodic light”	Kosuke Harada (Meiji Univ.) and Nobuhiko J. Suematsu (Meiji Univ.)
26	“Bioconvection of Euglena in Response to Light from Above and Below”	Naoyasu Morino (Meiji Univ.) and Nobuhiko J. Suematsu (Meiji Univ.)
27	“On the synchronized intermittent motion of camphor disks”	Hiraku Nishimori (Meiji Univ.), Masashi Shiraishi (Meiji Univ.), and Nobuhiko J. Suematsu (Meiji Univ.)
28	“A Foldable Stylish Origami Hat/Helmet”	Toshie Sasaki (Meiji Univ.)



Meiji University

MEXT Joint Usage / Research Center  
"Center for Mathematical Modeling and Applications (CMMA)  
<http://cmma.mims.meiji.ac.jp/eng/>



Meiji Institute for Advanced Study of Mathematical Sciences (MIMS)  
8F High-Rise Wing, Nakano Campus, Meiji University,  
4-21-1 Nakano, Nakanoku, Tokyo, Japan, 164-8525

